CREGE/CHYN-UNINe

List of publications

André L., Rabemanana V. and Vuataz F.-D., 2006. Geochemical modelling of water-rock interactions and implications on the properties of the Soultz fractured reservoir. Geothermics, 35, 507-531.

André L., Spycher N., Xu T., Pruess K. and Vuataz F.-D., 2006. Modelling brine-rock interactions in an Enhanced Geothermal System deep fractured reservoir at Soultz-sous-Forêts (France): a joint approach from two geochemical codes: FRACHEM and TOUGHREACT. Lawrence Berkeley National Laboratory, Berkeley. LBNL Collaboration Report, LBNL-62357, 71 pp.

André L., Spycher N., Xu T., Pruess K. and Vuataz F.-D., 2006. Comparing FRACHEM and TOUGHREACT for reactive transport modeling of brine-rock interactions in Enhanced Geothermal Systems (EGS). Proc. 31st Workshop on Geothermal Reservoir Engineering, Jan. 30-Febr. 1, 2006, Stanford University, Stanford, California.

André L., Rabemanana V. and Vuataz F.-D., 2005. Geochemical modelling of water-rock interactions and implications on the properties of the Soultz fractured reservoir. Proc. EHDRA Scientific Conference, March 17-18, 2005, Soultz-sous-Forêts, France.

André L. and Vuataz F.-D., 2005. Simulated evolution of reservoir properties for the Enhanced Geothermal System at Soultz-sous-Forêts: the role of hot brine-rock interactions. Proceedings, 30th Workshop on Geothermal Reservoir Engineering. Stanford University, Stanford, California, January 31 - February 2, 2005.

Portier S., Vuataz F.-D., Nami P., Sanjuan B. and Gérard A., 2009. Chemical stimulation techniques for geothermal wells: experiments on the three-well EGS system at Soultz-sous-Forêts, France. Geothermics, in press.

Portier S., André L. and Vuataz F.-D., 2008. Reactive transport modelling of forced fluid circulation and scaling tendencies in fractured granite at Soultz-sous-Forêts EGS geothermal site. Proc. EHDRA Scientific Conference, Soultz-sous-Forêts, France, September 24-25, 2008.

Portier S., André L. and Vuataz F.-D., 2008. Review on chemical stimulation techniques in oil industry and applications to geothermal systems. Technical Report ENGINE, WP4, ENhanced Geothermal Innovative Network for Europe, 39 pp.

Portier S., André L. and Vuataz F.-D., 2007. Evolution of an EGS reservoir simulated by modelling the geochemical effects of forced fluid circulation at Soultz-sous-Forêts. Proc. EHDRA Scientific Conference, Soultz-sous-Forêts, France, June 28-29, 2007.

Portier S., André L., Vuataz F.-D. and Kohl T., 2007. Modelling the impact of forced fluid-rock interactions on reservoir properties at Soultz-sous-Forêts EGS geothermal site. Proc. European Geothermal Congress 2007, Unterhaching, Germany, 30 May - 1 June 2007.

Portier S., Kühn M. and Vuataz F.-D., 2007. Comparing FRACHEM and SHEMAT for the modelling of brine-rock interactions in Enhanced Geothermal Systems. Proc. European Geothermal Congress 2007, Unterhaching, Germany. 30 May - 1 June 2007.

Portier S., André L., Vuataz F.-D., 2006. Modelling geochemical effects of acid treatments and comparison with field observations at Soultz-sous-Forets geothermal site. Proc. ENGINE Scientific Workshop 3, « Stimulation of reservoir and microseismicity », Kartause Ittingen, Zürich, Switzerland, June 29-July 1, 2006.

Portier S., André L. and Vuataz F.-D., 2006. Review of chemical stimulation techniques and results of acid injection experiments at Soultz-sous-Forets. Proc. EHDRA Scientific Conference, Soultz-sous-Forêts, France, June 15-16, 2006.

Rabemanana V., Vuataz F.-D., Kohl Th. & André L., 2005. Simulation of mineral precipitation and dissolution in the 5-km deep enhanced geothermal reservoir at Soultz-sous-Forêts , France. Proc. World Geothermal Congress WGC2005, 24-29 April 2005, Antalya, Turkey.

Available online at www.sciencedirect.com
ScienceDirect
Geothermics 35 (2006) 507–531
GEOTHERMICS
www.elsevier.com/locate/geothermics

Influence of water–rock interactions on fracture permeability of the deep reservoir at Soultz-sous-Forêts, France

Laurent André [a,b,*], Vero Rabemanana [a,1], François-D. Vuataz [b]

[a] *Centre of Hydrogeology, University of Neuchâtel, E.-Argand 11, CH-2009 Neuchâtel, Switzerland*
[b] *CREGE, Centre for Geothermal Research, c/o CHYN, University of Neuchâtel, E.-Argand 11, CH-2009 Neuchâtel, Switzerland*

Received 3 January 2006; accepted 28 September 2006
Available online 8 December 2006

Abstract

Circulation of geothermal fluids through granitic fractured reservoirs leads to chemical reactions, modifying the porosity and permeability of the rock mass. FRACHEM, a thermo-hydraulic-chemical coupled computer code, was developed specifically to predict changes in the geothermal reservoir of the Soultz-sous-Forêts Enhanced Geothermal System (EGS) located in Alsace, France. This code can simulate fluid–rock interactions and determine the dissolution/precipitation reactions of eight minerals in the Soultz granite (i.e. carbonates, pyrite, silicates and aluminosilicates). Numerical simulation results of long-term fluid circulation through the 5000-m deep Soultz reservoir are comparable to those determined for the shallow reservoir and confirm the role played by carbonates in the evolution of reservoir porosity and permeability. Moreover, experiments with FRACHEM in simulating short-term fluid flow during hydraulic and/or chemical stimulations have demonstrated that the code could prove an efficient tool in reservoir engineering and management.

Keywords: Geothermal brine; Enhanced Geothermal System; Thermo-hydraulic-chemical modelling; Reservoir stimulation; Soultz-sous-Forêts; France

* Corresponding author. Present address: BRGM, Water Division, 3 Avenue C. Guillemin, BP 6009, F-45060 Orléans Cedex 2, France. Tel.: +33 238 64 31 68; fax: +33 238 64 37 19.
E-mail addresses: l.andre@brgm.fr (L. André), vero.rabemanana@fondex.ca (V. Rabemanana).
[1] Present address: Fondex Outaouais, 170 rue Deveault, J8Y 1S6 Gatineau, Québec, Canada.

0375-6505/$30.00 © 2006 CNR. Published by Elsevier Ltd. All rights reserved.
doi:10.1016/j.geothermics.2006.09.006

Nomenclature

a_i	activity of ionic species i (mol kg^{-1})
A_m	total reactive surface area of mineral m (m^2)
B_i	polynomial coefficients for activity coefficient calculations
$D_{f,i}$	fractal exponent dependent on rock porosity
k	total permeability (m^2)
k_F	fracture permeability based on fracture-type model (m^2)
k_G	porous-media permeability based on porous media-type model (m^2)
k_m	rate constant (mol s^{-1} m^{-2})
k_0	initial permeability (m^2)
K	equilibrium constant of reaction
M_i	molality of ionic species i (mol kg^{-1})
n_F	fracture frequency (m^{-1})
P	pressure (Pa)
q_{inj}	fluid injection rate into individual fractured zone (L s^{-1})
q_{total}	total fluid injection rate (L s^{-1})
Q	ionic activity product
r_d	dissolution rate (mol m^{-2} s^{-1})
r_p	precipitation rate (mol m^{-2} s^{-1})
R	gas constant (=8.314 J mol^{-1} K^{-1})
R_0	initial radius of closed pack spherical grains (m)
s	reactive mineral surface area (m^2)
T	temperature (K)
v	reaction rate (mol s^{-1})

Greek letters

α	ratio between fracture porosity and porous media porosity
γ_i	activity coefficient of ionic species i
μ, η	positive empirical parameters
Φ	total porosity
Φ_F	fracture porosity
Φ_G	porous-media porosity
Φ_0	initial porosity

1. Introduction

The research program for the extraction of thermal energy from the Enhanced Geothermal System at the Soultz-sous-Forêts site began in 1987 (Gérard and Kappelmeyer, 1991). The objective of the project is to convert to electricity the heat extracted from a deep reservoir hosted in fractured granite. The site was selected because of the large temperature gradient within the sedimentary cover (100 °C km^{-1}) and high heat flow, which locally reaches up to 0.15 W m^{-2} (Kohl and Rybach, 2001).

In order to extract heat from the fractured reservoir, three deviated wells were drilled to 5000 m depth, with 650 m between each bottom hole. At that depth the temperature of the reservoir reaches

200 °C. The cold water is injected into the reservoir through one of the wells (GPK3, the injector), while the other two (GPK2 and GPK4), located on either side of the injector, are used to extract the hot fluid from the subsurface. The injection-production system at Soultz is a "closed loop" and the fluid used is the formation brine existing in the fractured granite at the depths of the open-hole sections of the wells.

Forced injection in GPK3 and pumping of the production wells accelerate the natural flow of hot brine through the fractured reservoir; the consequent disturbance to the chemical and thermodynamic equilibria change reservoir properties. Scaling in the reservoir, for example, which causes serious problems, is usually the result of the deposition of carbonates or silicates such as amorphous silica, and leads to a reduction in the injectivity and productivity of the wells. This phenomenon has been observed in many geothermal fields, such as Bacman, Leyte, and Tiwi in the Philippines (Buning et al., 1995; Malate et al., 1999; Amistoso et al., 2005), Berlin in El Salvador (Barrios et al., 2002), Coso in the USA (Evanoff et al., 1995), and Latera in Italy (Barelli et al., 1985). Increasingly, geochemical modelling has been helping in the management of geothermal fields by predicting such scaling problems and designing solutions for maintaining well injectivity (Xu et al., 2004).

In the case of the Soultz project, scaling and other chemical processes are being modelled by means of the thermo-hydraulic and chemical coupled code FRACHEM (Durst, 2002; Bächler, 2003), specifically built to study the behaviour of fractured reservoirs through which there is flow of fluids of different composition, temperature and pressure. One of the objectives of the code is to simulate the evolution of reservoir porosity and permeability as the fluids circulate by taking into account thermal, hydraulic and chemical processes.

FRACHEM consists of two main parts, the first of which considers the thermal and hydraulic processes taking place in the system and simulates reactive transport, while the second models the chemical processes of dissolution and precipitation and calculates their impact on reservoir porosity and permeability.

The FRACHEM code has already been validated through sensitivity analyses with respect to time steps and mesh discretization and a benchmark with another geochemical code (SHEMAT; Bächler, 2003). It was also successfully applied to the shallower (3500-m deep) reservoir at Soultz, highlighting the strong reactivity of carbonates present in the reservoir during long-term circulation periods (Bächler and Kohl, 2005). The aim of our study is to demonstrate that FRACHEM is also an adequate tool for investigating chemical processes and the resulting permeability changes within the 5000-m deep Soultz reservoir during long and short periods of fluid re-injection.

In the first part of the paper, we briefly summarize our modelling approach and discuss the most recent modifications to the code. In the second part, we describe how the code can be applied to predicting changes in reservoir porosity and permeability during a long-term production/injection operation. Water–rock interactions and mineral behaviour have been investigated. The impact of chemical processes on fracture permeability was evaluated by modelling three examples of changes in porosity and permeability. Finally, we discuss the results of a series of assumed short-term injection cases. The four scenarios presented demonstrate that the code could prove very useful in reservoir engineering and field management.

2. Numerical modelling approach

Thermo-hydraulic and chemical (THC) coupled codes have been used in Enhanced Geothermal Systems to predict permeability evolution by modelling the behaviour of hot, hypersaline brines and their interactions with reservoir minerals. A new THC code has been developed specif-

ically for use in the conditions found in the Soultz reservoir. Two existing codes, FRACTure and CHEMTOUGH2, were combined in a new code called FRACHEM (Durst, 2002; Bächler, 2003; Rabemanana et al., 2003; André and Vuataz, 2005). FRACTure is a 3D finite element code that models thermal and hydraulic processes in fractured and porous rocks (Kohl and Hopkirk, 1995). The finite element approach was chosen because it is better suited to model the geometry of the fractured reservoir. FRACTure models thermal and hydraulic processes in order to predict temperature and pressure distributions, as well as fluid flow velocities. Details on these thermal and hydraulic models and their coupling are presented in Bächler (2003) and Bächler and Kohl (2005).

CHEMTOUGH2 is a 3D finite volume code (White, 1995) that simulates reactive transport while allowing for permeability variations resulting from chemical reactions between fluids and rocks occurring in the reservoir. This chemical code was initially developed for modelling diluted solutions. Due to the high salinity of the Soultz reservoir fluid, however, the original version of CHEMTOUGH2 cannot be directly implemented in FRACHEM without some modifications. Consequently, the chemical part of the FRACHEM code is based on the CHEMTOUGH2 program to which is added a thermodynamic model that uses the Pitzer formalism (Pitzer, 1973) to calculate the activity coefficients of selected chemical species, and a kinetic model to determine the reaction rates of precipitation/dissolution of major minerals; the added modules are described in detail by Durst (2002). Below, we describe the new features that were implemented in the code.

2.1. The thermodynamic model

The thermodynamic model establishes the state of the fluid with regard to the mineral phases present in the granitic rocks, i.e. the under- or over-saturation of the fluid with respect to these minerals. To this end, the ionic activity product Q is compared to the equilibrium constant of the reaction, K. If $Q < K$, the solution is undersaturated and the mineral has a tendency to dissolve. If $Q = K$, the system is at equilibrium, but if $Q > K$, the solution is oversaturated and the mineral tends to precipitate. In order to calculate these factors, we must determine the activity coefficients of each species in solution. In CHEMTOUGH2, the Debye-Hückel model (Debye and Hückel, 1923a,b) is used to calculate these coefficients, but it only applies to dilute solutions. Given the high salinity of the Soultz brine, this model was replaced by the Pitzer formalism (Pitzer, 1973). The Pitzer equations take into account more types of ionic interactions than the Debye-Hückel model. The activity coefficient calculations in the FRACHEM code are carried out indirectly by means of another code, TEQUIL (Moller et al., 1998). For a given fluid composition (i.e. constant ionic strength), the activity coefficients are determined at different temperatures in the range 50–200 °C using TEQUIL before running FRACHEM. The coefficients computed for each temperature are regressed as a function of temperature using a polynomial fit. Next, the coefficients are entered in the chemical input file. This approach works well for the Soultz simulations because the ionic strength of the re-circulated fluid remains more or less constant with time.

Based on this assumption, the activity coefficients of ionic species can be defined as functions of only two parameters, temperature and pressure:

$$\gamma_i(T, P) = (B_0 + B_1 T + B_2 T^2 + B_3 T^3 + B_4 T^4)\, f(P) \tag{1}$$

where B_i are coefficients calculated for each mineral and $f(P)$ is a factor dependent on pressure that takes into account the variation with pressure of molal volumes of the ionic species (Monnin,

1989). The activity of species i is then expressed as a function of molality so that:

$$a_i = \gamma_i(T, P)M_i \tag{2}$$

Although there are well known Pitzer interaction coefficients for many ions, this is not so for aqueous species such as aluminium. In this study, Al is assumed to be in the form of Al^{3+}. Considering the temperature and hydrostatic pressure in the reservoir, the species $Al(OH)_3{}^0$ and $Al(OH)_4{}^-$ could be assumed to be present (Pokrovskii and Helgeson, 1995). As there is, however, some uncertainty with regard to the activity coefficients of these species under Soultz conditions, we chose the species Al^{3+}. The activity coefficient of this ion was calculated using the computer program EQ3nr (Wolery, 1992) and by the method presented by Barrett and Anderson (1988).

Finally, and to simplify the system, some assumptions were made concerning the reservoir fluid, such as no boiling, no degassing, no condensation, and no mixing with a different fluid. All these assumptions are compatible with the constant composition of the fluid produced from the shallower reservoir during the first circulation test performed in 1997.

2.2. Kinetic model

The thermodynamic model allows us to determine the equilibrium or non-equilibrium state of the circulating fluid with regards to the reservoir rock. However, thermodynamic disequilibrium involves chemical reactions with variable kinetics that are a function of mineral composition.

A general kinetic model was adopted for the dissolution/precipitation reactions of minerals. Its overall form is expressed as (Lasaga et al., 1994):

$$v = k_{\mathrm{m}} A_{\mathrm{m}} \left(1 - \left(\frac{Q}{K}\right)^{\mu}\right)^{\eta} \tag{3}$$

Positive values of the reaction rate (v) correspond to dissolution rates and negative values to precipitation rates. Eq. (3) is adapted to each mineral, and parameters k_{m}, μ and η are computed on the basis of published results on high-temperature NaCl brine experiments.

The behaviour of eight minerals is investigated here. It is assumed that all dissolution reactions are congruent. Detailed kinetic data, including k_m values for calcite, dolomite, pyrite and quartz, can be found in Durst (2002). Rate equations for the newly added minerals (amorphous silica, K-feldspar, albite and illite) are presented in Table 1.

2.3. Porosity/permeability relationships

One option within the FRACHEM code allows us to choose from three possible porosity/permeability models.

2.3.1. Case 1a: fracture-type and porous media-type models

A combination of a fracture model and a porous media model is proposed for determining permeability of the fractured zone. The fracture-type model is based on the work of Norton and Knapp (1977), and modified by Steefel and Lasaga (1994), who consider the case of three sets of mutually orthogonal fractures that produce an isotropic permeability, where all the fractures have

Table 1
Kinetic equations for the dissolution and precipitation of amorphous silica, K-feldspar, albite and illite

Reaction rate laws	Sources
Amorphous silica dissolution rate $r_d = 10^{(0.82191-(3892.3/T))}(a_{SiO_2})(a_{H_2O})^2 s\left(1-\frac{Q}{K}\right)$	Rimstidt and Barnes (1980), Icenhower and Dove (2000)
Amorphous silica precipitation rate $r_p = 3.8\times10^{-10}\exp\left(\frac{-50\ 000}{8.314}\left(\frac{1}{T}-\frac{1}{298.15}\right)\right)s\left(\left(\frac{Q}{K}\right)^{4.4}-\frac{1}{(Q/K)^{8.8}}\right)$	Rimstidt and Barnes (1980), Carroll et al. (1998), and Xu et al. (2004)
K-feldspar dissolution rate $r_d = 5.25\times10^{-6}\exp\left(\frac{-51\ 700}{RT}\right)\left[\frac{10^{-0.97}a_{H^+}}{1+10^{-0.97}a_{H^+}+10^{3.04}a_{Na^+}}\right]^{0.5}s\left(1-\frac{Q}{K}\right)$	Blum and Stillings (1995) and Stillings and Brantley (1995)
K-feldspar precipitation rate $r_p = 10^{-12}\exp\left(\frac{-67\ 830}{R}\left(\frac{1}{T}-\frac{1}{298.15}\right)\right)s\left(\frac{Q}{K}-1\right)$	Blum and Stillings (1995)
Albite dissolution rate $r_d = 0.35\ \exp\left(\frac{-89\ 000}{RT}\right)\left[\frac{10^{-0.97}a_{H^+}}{1+10^{-0.97}a_{H^+}+10^{3.04}a_{Na^+}}\right]^{0.5}s\left(1-\frac{Q}{K}\right)$	Hellmann (1994) and Stillings and Brantley (1995)
Albite precipitation rate $r_p = 10^{-12}\exp\left(\frac{-67\ 830}{R}\left(\frac{1}{T}-\frac{1}{298.15}\right)\right)s\left(\frac{Q}{K}-1\right)$	Blum and Stillings (1995)
Illite dissolution rate $r_d = \left[2.2\times10^{-4}\ \exp\left(\frac{-46\ 000}{RT}\right)a_{H^+}^{0.6}+2.5\times10^{-13}\exp\left(\frac{-14000}{RT}\right)\right]s\left(1-\frac{Q}{K}\right)$	Köhler et al. (2003)
Illite precipitation rate $r_p = 1.1638T\ \exp\left(\frac{-117\ 000}{8.314T}\right)s\left(\frac{Q}{K}-1\right)^2$	Nagy et al. (1991)

the same spacing and fracture apertures. The fracture permeability k_F is:

$$k_F = \frac{\Phi_F^3}{324 n_F^2} \tag{4}$$

The porous media-type model is based on that of Kozeny-Carman, which was modified by Bolton et al. (1996):

$$k_G = \frac{R_0^2}{45} \frac{\Phi_G^3}{(1-\Phi_G)^2} \tag{5}$$

The global permeability of the fractured zone is given by

$$k = (1-\alpha)k_F + \alpha k_G \tag{6}$$

In this model, we assume that the fracture aperture and the thickness of the mineral layer follow Gaussian distributions (Durst, 2002).

2.3.2. Case 1b: modified porous media-type and fracture-type models

An alternative to the previous models is not to assume a Gaussian distribution of the fracture aperture and of the thickness of the mineral layer. This modification entails a different approach to calculating mineral-surface contact areas.

2.3.3. Case 2: a fracture-type model

In this model, the permeability changes can be approximated using the porosity change of planar parallel fractures of uniform aperture; that is, assuming the "cubic law" (e.g. Steefel and Lasaga, 1994). The permeability can be adjusted to porosity changes brought about by the precipitation or dissolution of minerals, i.e.

$$k = k_0 \left(\frac{\Phi}{\Phi_0} \right)^{D_{f,i}} \tag{7}$$

One of the disadvantages of this law is that zero permeability is only reached under the condition of zero fracture porosity. The fractal exponent $D_{f,i}$ depends on porosity. For porosities ranging from 0.01 to 1, which is supposed to be the case for the fractured zone of the Soultz granite, it is assumed that the permeability variations are calculated from changes in porosity, based on a square law (Clauser, 2003). Thus, permeability values are updated according to Eq. (8):

$$k = k_0 \left(\frac{\Phi}{\Phi_0} \right)^2 \tag{8}$$

2.4. Geometrical model set-up

All the FRACHEM code simulations described below were performed with the same 2D simplified model with a geometry that is close to that of the Soultz system. Injection and production wells are linked by 650 m long fractured zones in the granite rock mass. If we consider that the granitic Soultz reservoir can be represented by a series of alternating fractured and impermeable matrix zones (Dezayes et al., 2005), only one of these fractured zones needs to be modelled; it would be 10 cm thick, have a horizontal width of 10 m (Fig. 1a) and a mean porosity of 10%. The fractured zones are separated by 100-m thick rock matrix zones, this being the distance required

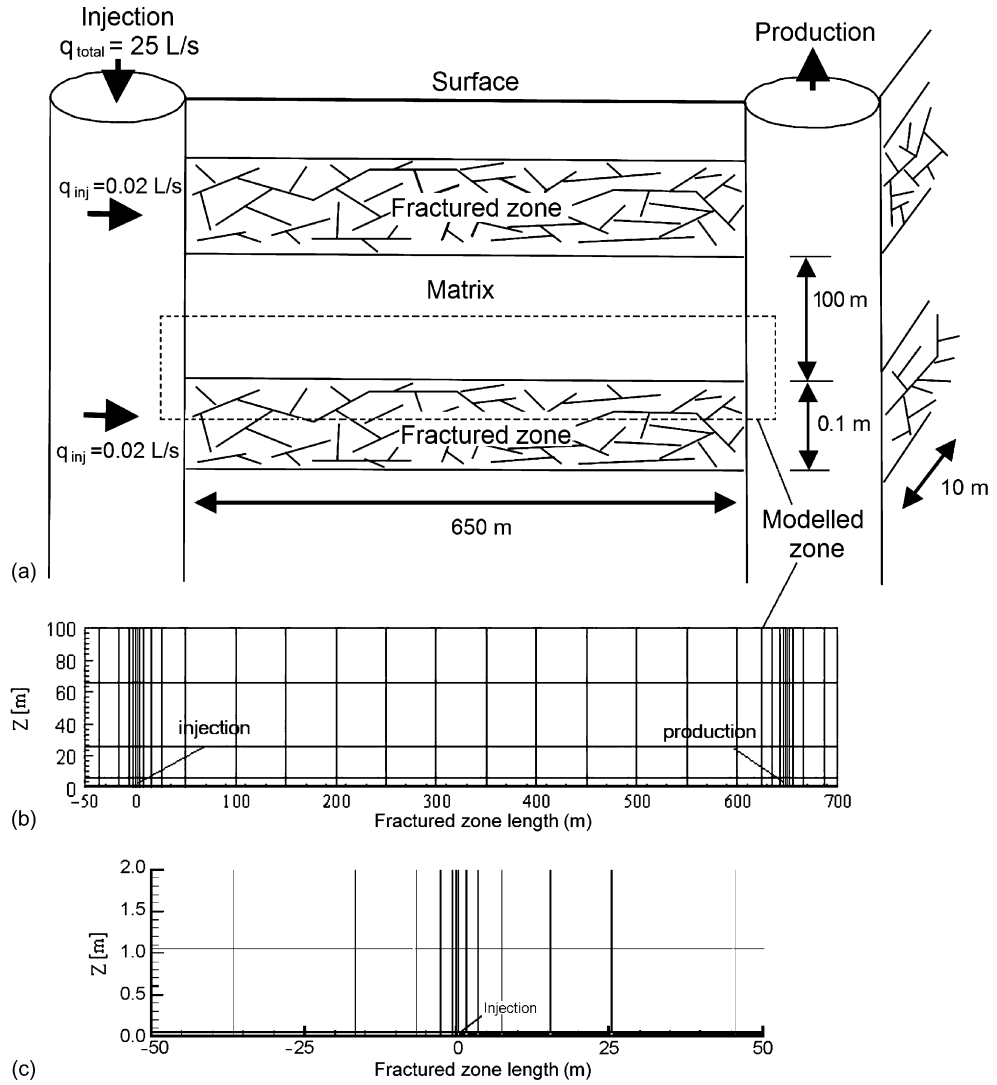

Fig. 1. (a) Simplified two-dimensional model of the Soultz system (dimensions are not shown to scale); (b) spatial discretization of the model; (c) finer mesh discretization near the injection zone. The black bar near the bottom corresponds to the fractured zone.

to assume a semi-infinite matrix for heat transfer purposes. We consider that the fluid exchange between fractured zones and the surrounding low-permeability matrix is insignificant and thus can be neglected. Only heat transfer between the matrix and the fractured zones is allowed, following the model of Sauty (1981).

Because of symmetry, only half (the upper part) of a fractured zone and of the adjacent porous matrix is modelled, by subdividing them into 222 two-dimensional elements (Fig. 1b). The size of the elements ranges from a minimum of 0.5 m × 0.05 m near the injection and the production wells to a maximum of 50 m × 35 m. The fractured zone is located between 0 and 650 m; injection is made at 0 m and production occurs at point 650 m (Fig. 1c). It should be noted that, in Fig. 3

Table 2
Values of the thermo-hydraulic parameters used in the FRACHEM simulations

Parameter	Fracture	Matrix	Fluid
Hydraulic conductivity ($m\,s^{-1)}$)	7.03×10^{-4}	9.5×10^{-12}	–
Thermal conductivity ($W\,m^{-1}\,K^{-1}$)	2.9	3	0.6
Density ($kg\,m^{-3}$)	–	2650	1000
Heat capacity ($J\,kg^{-1}\,K^{-1}$)	–	1000	4200
Porosity (%)	10	0	–

and Figs. 5–13, all the variables (porosity, permeability, reaction rates) are calculated at the centre of the elements of the fractured zone.

The initial temperature throughout the modelled area was set at 200 °C, the natural-state reservoir temperature. During the simulations, the fluid was injected into the modelled fractured zone at a constant 65 °C temperature. Hydrostatic pressure distribution was assumed in the production well, while a constant overpressure of 8 MPa was set at the injection well. The pressure gradient between the two wells does not change during the injection period, resulting in an initial flow of $0.02\,L\,s^{-1}$ into the modelled fractured zone. Mineral dissolution and precipitation bring about changes in the porosity and permeability of the modelled fractured zone affecting the flow rates through the mesh elements; they are therefore updated/recalculated at each time step.

Dirichlet boundary conditions (i.e. constant temperature and pressure conditions) were applied to the upper, left and right boundaries of the modelled zone. The values of the thermo-hydraulic parameters considered in the simulations are listed in Table 2.

2.5. *Mineral assemblages*

The geothermal reservoir at Soultz is made up of three types of granite (Jacquot, 2000; Hooijkaas et al., this issue) (Table 3). The first is non-altered (fresh) granite that is characterized by a predominance of feldspar, plagioclase and quartz, and by an extremely low fracture density. Consequently, its porosity is close to zero and does not contain significant amounts of water. The properties of this granite are that of the impermeable rock matrix. Fluid exchange, by advection or diffusion processes, will be disregarded for this granite; it will only act as a good heat convector.

Table 3
Mean composition (in %) of the different types of granite in the Soultz reservoir (Jacquot, 2000)

	Fresh granite	Hydrothermally altered granite	Alteration veins
Quartz	24.2	40.9	43.9
K-feldspar	23.6	13.9	
Plagioclase	42.5		
Illite		24.6	40.2
Smectite		9.7	9.6
Mica	9.4		
Calcite	0.3	3.3	4.3
Dolomite		0.8	0.7
Pyrite		0.7	1.0
Galena		1.3	0.3
Chlorite		4.8	

Table 4
Representative chemical analysis of the fluid sampled at the wellhead of GPK2 after being deepened to 5 km in 1999 (Durst, 2002)

Species	Concentration (mmol/kg)
Na^+	1148.00
K^+	73.40
Ca^{2+}	169.50
Mg^{2+}	3.21
Cl^-	1648.00
S	1.77
C	42.76
Fe^{2+}	2.61
SiO_2	6.06
Al^{3+}	3.7×10^{-3}

The second rock facies is a fractured, hydrothermally altered granite, with quartz as the major mineral component; because of alteration the amount of feldspar decreases and some secondary minerals such as galena, pyrite, smectite or illite are present. This facies is the most porous (porosity ranging from 5 to 10%) and contains most of the formation fluid.

The third rock facies is the most altered; it corresponds to alteration veins that present minerals such as illite, smectite and quartz. Precipitated secondary minerals (clays, carbonates) fully cement the fractures, resulting in a decrease of porosity and permeability. As a consequence, fluid circulation within the rock mass takes place through the second facies only (Genter et al., 1998).

2.6. Fluid composition

The formation fluid circulating through the fracture network is a sodium-chloride brine with a total mineralization close to 100 g L^{-1}. Its pH is approximately 4.9 and its temperature (200 °C) is in equilibrium with that of the rock at 5000-m depth. The composition of the formation brine extracted during a 1999 production test is given in Table 4. The chemistry of the deep fluid is not very different from that of the fluid produced from the shallower reservoir (Durst, 2002). Its silica and carbon concentrations are higher because of the elevated temperatures and CO_2 partial pressures.

3. Simulation of long-term fluid circulation using FRACHEM

3.1. Reservoir temperature

Before the start of forced fluid circulation in the fractured zone, the system (rock and brine) is in chemical and thermal equilibrium at 200 °C. Injection of colder (65 °C) fluid into the reservoir disturbs the system and the rock begins to cool down (Fig. 2).

In the model the fractured zone connects the injection and production wells along a horizontal plane at 5000 m depth. A decrease in temperature can be observed in this zone, especially near the injection well, due to the effect of the cooler (65 °C) injected fluid. After 1800 days of fluid circulation, the temperature in the vicinity of the production well is close to 160 °C (Fig. 2).

The decrease in the temperature of the produced fluid is particularly important for the EGS project, but it must be remembered that it greatly depends on the assumed geometry of the

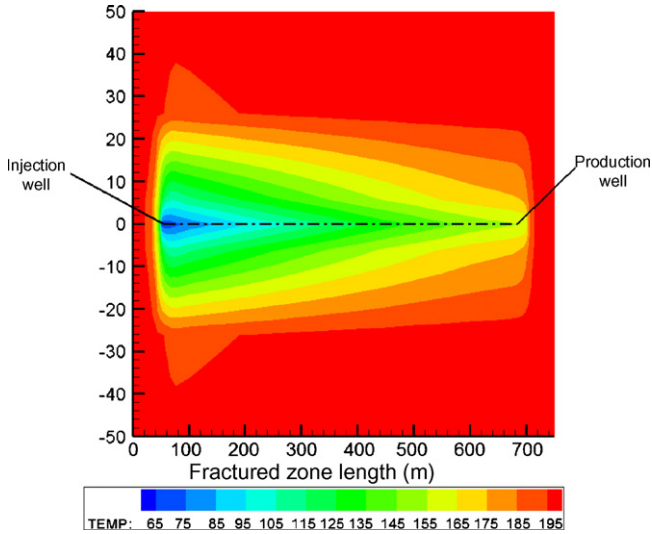

Fig. 2. Horizontal cross-section at 5000-m depth of computed reservoir temperature around the fractured zone after 1800 days of forced fluid circulation (temperatures in °C; dimension in metres).

model. In this case, we consider a direct, straight-line flow path between the injection and production wells, without considering possible parallel pathways. As a consequence, it is very likely that the model overestimates the cooling effect; in the actual EGS reservoir it would be smaller.

3.2. Mineral–brine interactions

Circulation of colder fluids through the fractured zone disturbs the chemical equilibrium of the rock–brine system, resulting in mineral precipitation and/or dissolution. As no diffusion is assumed between the fractured zone and matrix, all the chemical reactions occur in the fractured zone.

Calcite, deposited in the fractures of the granite in relatively small proportions, represents the most reactive mineral in the system. As shown in Fig. 3, calcite reacts mainly in the first metres of the fracture. The predominantly positive reaction rates indicate that calcite dissolution predominates. But, if calcite dissolves in the vicinity of the injection well, it precipitates further down the fracture (between 30 and 400 m) because calcite solubility decreases with temperature. Initially, at the start of forced fluid circulation, calcite dissolution occurs mainly in the first 40 m of the fracture and a maximum dissolution rate is reached during the first year. This dissolution leads to an enrichment of Ca^{2+} in the solution. Later, as the temperature increases along the fracture, calcite begins precipitating in the next 300 m of the flow path. In a given part of the fracture, calcite dissolves until all has been consumed. Fig. 4 shows that, in the vicinity of the injection well, it takes about 300 days to dissolve all the calcite present in the fracture. With time, the rock temperature decreases and the calcite dissolution zone extends towards the production well.

Dolomite is also present in the Soultz granite, but is less reactive than calcite. Figure 5 shows that dolomite dissolves in all parts of the fracture, but its reaction rate is an order of magnitude

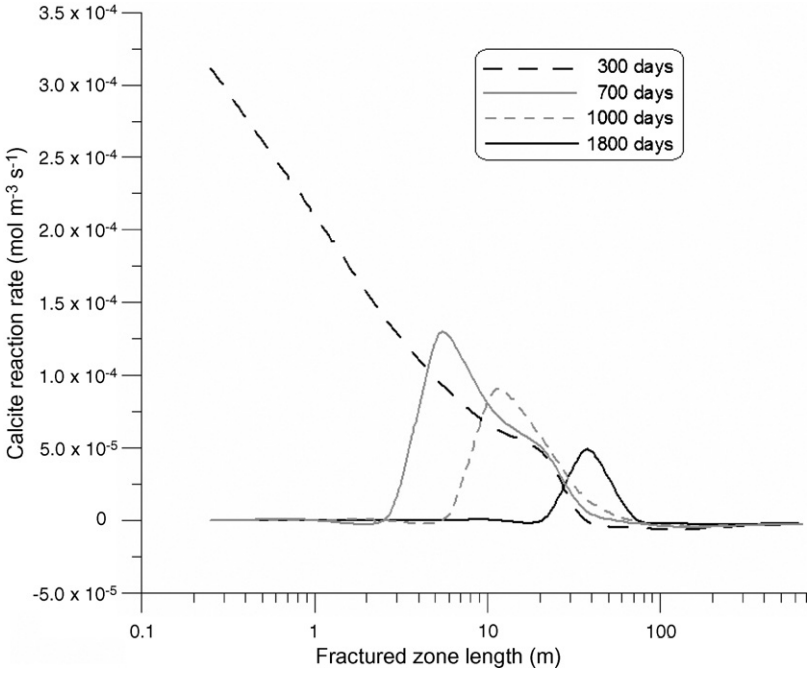

Fig. 3. Calcite reaction rate along the fractured zone at different times (positive values indicate dissolution).

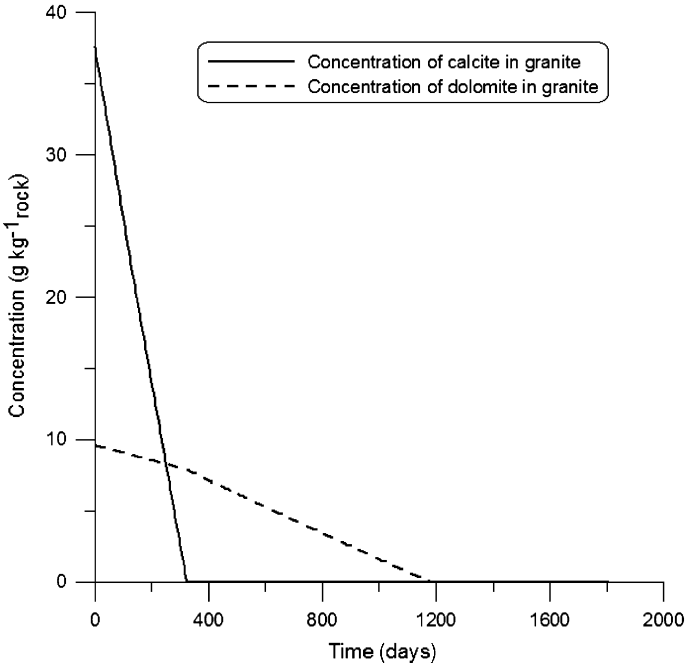

Fig. 4. Changes with time of calcite and dolomite concentrations in the granitic rock within the fractured zone, close to the injection point (first metre around the injection well).

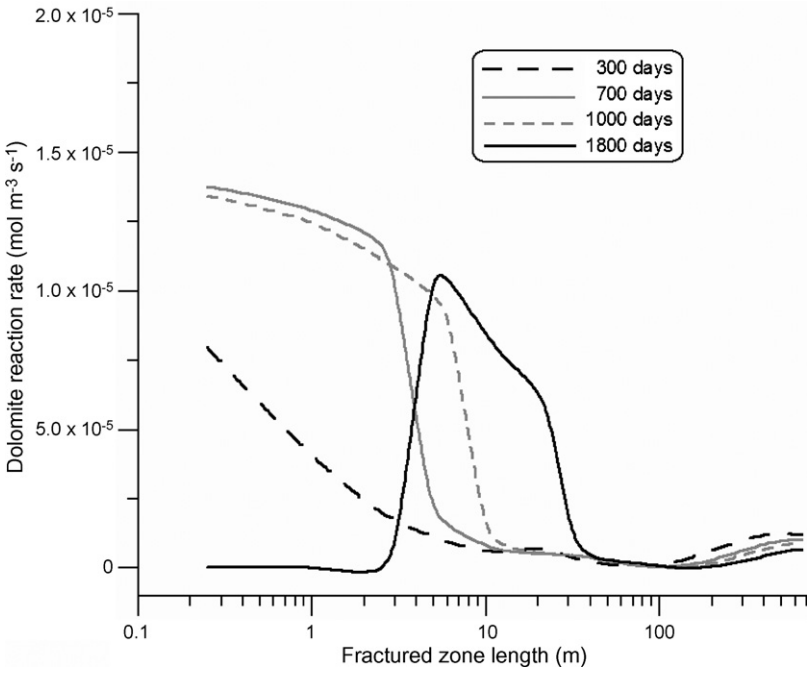

Fig. 5. Dolomite reaction rate along the fractured zone at different times (positive values indicate dissolution).

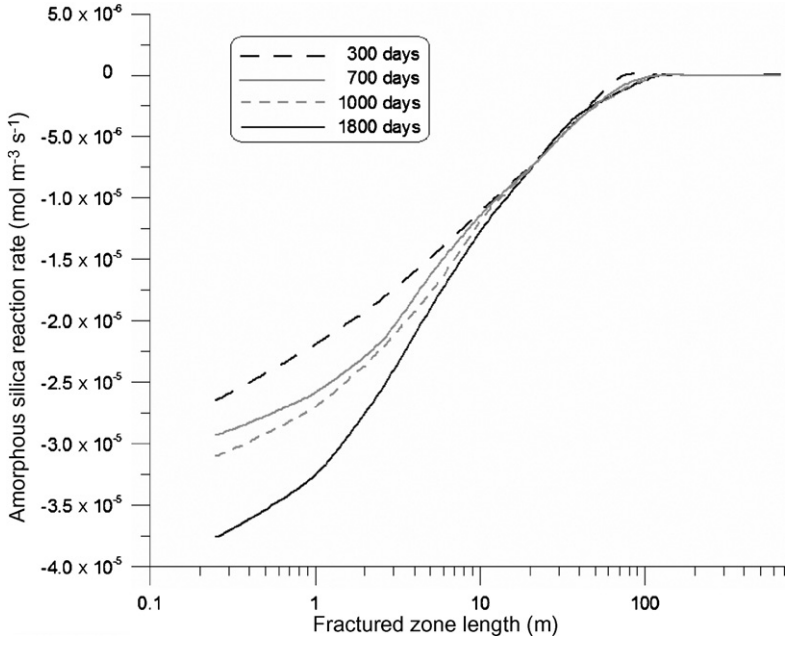

Fig. 6. Amorphous silica reaction rate along the fractured zone at different times (positive values indicate dissolution).

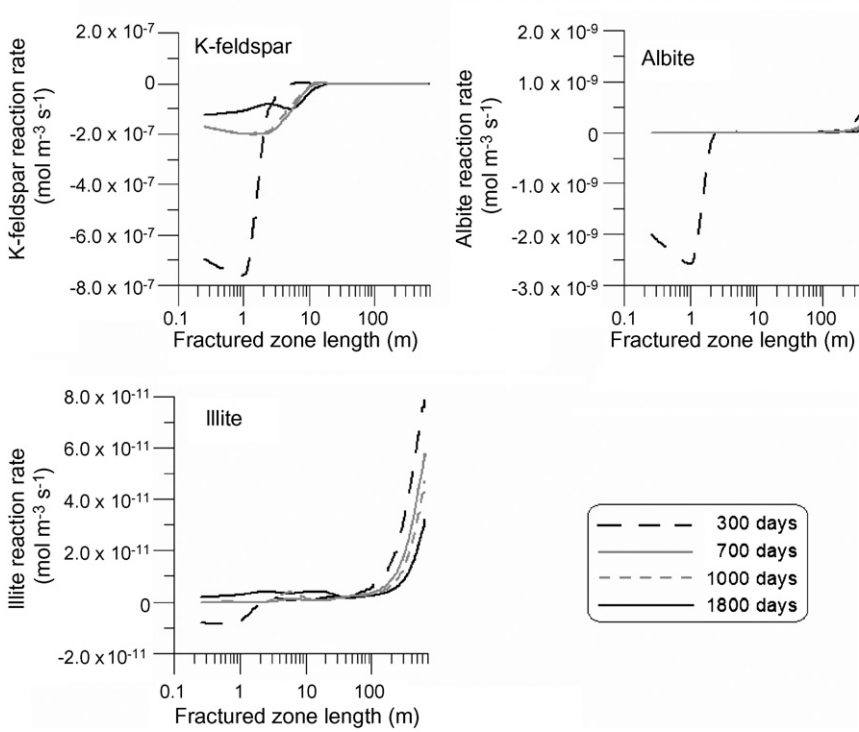

Fig. 7. Reaction rates of K-feldspar, albite and illite along the fractured zone at different times (positive values indicate dissolution).

smaller than that of calcite. Dolomite dissolution stops around the injection well after 1200 days because by then all of it has been consumed (Fig. 4).

The most reactive of the silicates is amorphous silica. Its reaction rate is three orders of magnitude larger than that of quartz. In contrast to calcite, the solubility of amorphous silica increases with temperature. As a consequence, it precipitates near the injection well (Fig. 6). With increasing circulation time, the zone of amorphous silica precipitation spreads towards the production well; the model shows that after 1800 days it extends over the first hundred metres of the fracture. However, the reaction rate of amorphous silica is one or two orders of magnitude smaller than calcite.

Pyrite precipitates all along the fracture, but as with quartz, its reaction rate is negligible in comparison to that of calcite.

K-feldspar seems to be the most reactive of the aluminosilicates (Fig. 7). Because its solubility increases with temperature, the precipitation of this feldspar occurs close to the injection point but drops off away from it.

It is interesting to note how small the dissolution of albite and illite is close to the production well. It is also clear that the main phase of aluminosilicate precipitation occurs at the start of forced fluid circulation, and that it decrease with time. The weak dissolution of aluminosilicates in the fracture keeps the aluminium concentrations low in the circulating fluid, thus preventing the precipitation of these minerals.

Table 5
Amount of precipitated and dissolved minerals within the entire fractured zone, after 1800 days of forced fluid circulation assuming two different injection temperatures

Mineral	Amount of mineral: precipitated/dissolved (kg)		
	Injection temperature (65 °C)	Injection temperature (50 °C)	Change (%)
Calcite	1530/1330	1630/1470	+6.54/+10.5
Dolomite	0.0/657	0.0/612	0.0/−6.8
Quartz	0.08/0.0	0.04/0.17	−50/+170
Amorphous silica	203/1.0	243/0.93	+19.7/−7.0
Pyrite	5.15/0.01	12.5/0.01	+143/0.0
K-feldspar	2.87/0.0	2.7/0.0	−6.7/0.0
Albite	0.0/0.35	0.0/0.35	0.0/0.0
Illite	0.0/0.04	0.0/0.04	0.0/0.0

3.3. Amount of precipitated and dissolved minerals

Once we have determined the reaction rates for the minerals, we can estimate the amounts that have precipitated or dissolved during each time step and in each fracture element of the model; Table 5 shows the total amounts after 1800 days of forced fluid circulation. During this period, about 2000 kg of carbonates (including calcite and dolomite) are dissolved and about 1500 kg are deposited in the investigated fractured zone. One can also observe that the amounts involved for the other reactive minerals are far smaller than those for the carbonates. The only other significant quantity is that of amorphous silica, with about 200 kg precipitating close to the injection well. After 1800 days of forced circulation, the amounts of pyrite and K-feldspar that have deposited are low, while those for quartz, albite and illite are negligible.

3.4. Effects on porosity and permeability

Mineral dissolution and precipitation affect reservoir properties, especially fracture porosity and permeability. Figure 8 illustrates, for Case 1a, how dissolution increases porosity close to the injection well; the process is dominated by the carbonates due to their large reactivities.

The average initial porosity in the fractured zone, before forced fluid circulation, was 10%. The total amount of dissolved calcite and dolomite implies a reservoir porosity of about 13.5–14% in the first 10 m of the fractured zone after 1000 days of brine circulation (Fig. 8). After 1800 days, this value goes from 12.5 to 13% between 0 and 2 m, and from 13 to 13.5% between 2 and 20 m. This slight decrease in porosity (from 13.5 to 12.5%) during the last 800 days of simulation is due to the precipitation of amorphous silica combined with aluminosilicates in the first 10 m.

Further into the fractured zone, between 30 and 600 m, calcite precipitation causes a reduction in fracture porosity of about 2.5% (from 10 to 9.75%) after 1800 days of fluid circulation whereas the decrease is negligible near the production well (at 650 m). Considering the relationship between porosity and permeability used in the Case 1a model, the same tendency is observed for reservoir permeability.

The changes in reservoir porosity and permeability estimated by the models of Cases 1a, 1b and 2 are given in Figs. 9 and 10, respectively. Both figures show more or less the same results, with most, albeit small, differences near the injection well (located on the left side of the figures) and in the first 30 m of the fractured zone. Consequently, the permeability changes for these cases

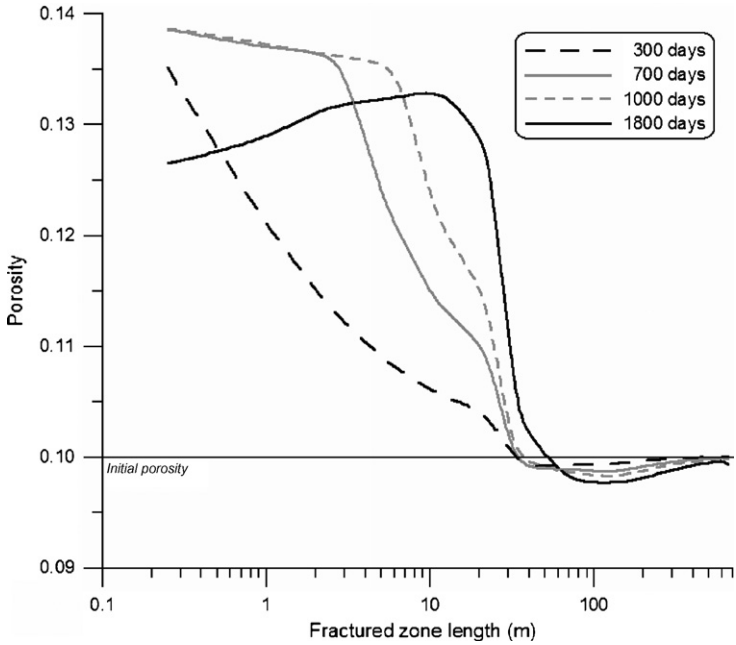

Fig. 8. Distribution of porosity along the fractured zone at different times, showing the effects of mineral dissolution and precipitation.

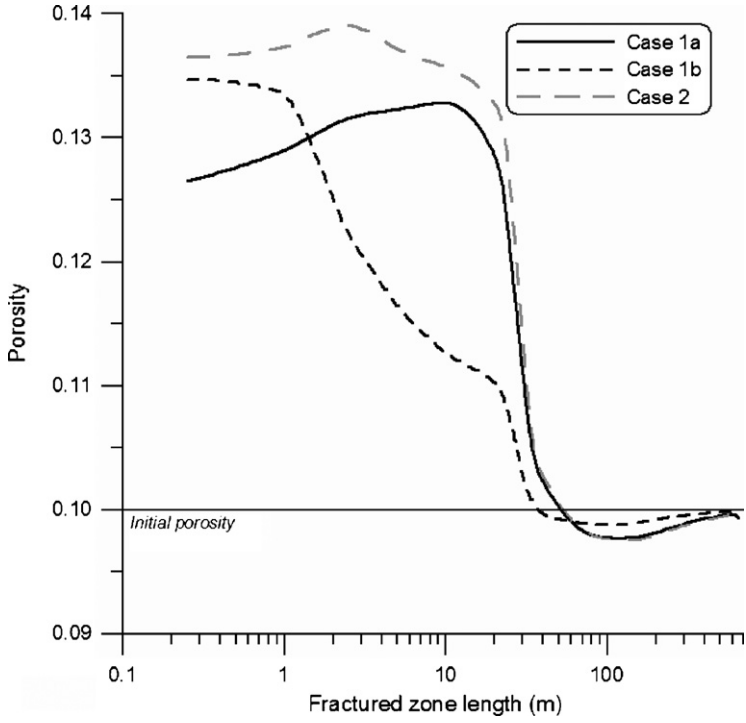

Fig. 9. Porosity along the fractured zone after 1800 days of forced fluid circulation according to the different models.

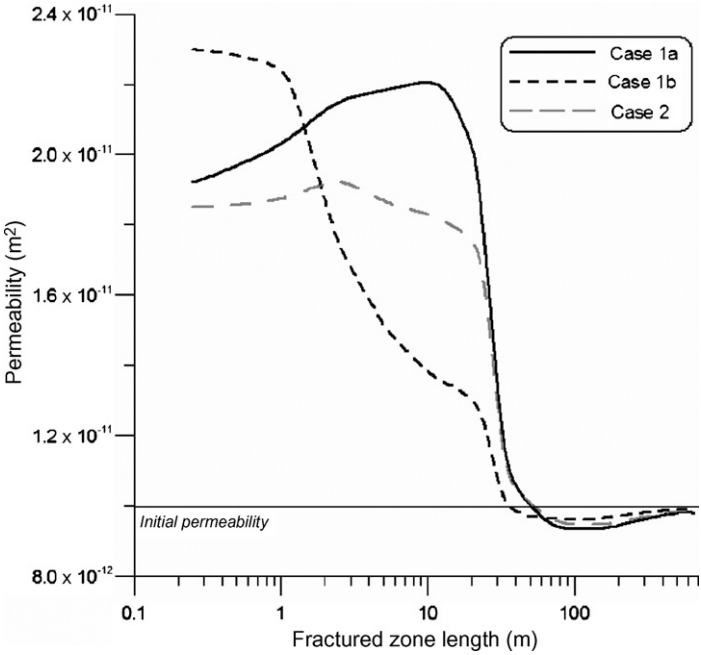

Fig. 10. Permeability along the fractured zone after 1800 days of forced fluid circulation according to the different models.

are also different, particularly near the injection well (Fig. 10). The trends and global changes in permeability given by the three models are similar, even though the permeability increase is smaller in Case 2 than in Cases 1a and 1b.

Summarizing, the three models show the same global changes in reservoir properties with an increase of porosity and permeability close to the injection well and a decrease in the second half (near the production well) of the fractured zone. Only field data will establish which of the proposed models is the most appropriate for the Soultz reservoir.

Field tests at Soultz-sous-Forêts have confirmed the results of these FRACHEM simulations. During the 140-day circulation test in 1997 involving the shallower (3500-m deep) reservoir, the pressure at the injection well decreased, indicating a rise in injectivity (Bächler and Kohl, 2005), probably caused by the dissolution of carbonates around the injector. This scenario is supported by FRACHEM simulations as well as by the results of other numerical codes (André et al., 2006).

4. Simulation of short-term circulations using FRACHEM

4.1. Simulation of acid injection

Techniques to improve or maintain injectivity during the period of exploitation of a geothermal well have advanced significantly over the last few years. One of these methods consists of pumping acid/mud acids into the wells to dissolve any mineral scales deposited in and around the boreholes. Similarly, injection of acid solutions is also being adopted to develop reservoir permeability around the geothermal producers and injectors.

In February 2003, an acid injection test was carried out at Soultz to observe its effects on the calcite deposited in fractures, and on pressure communication between wells GPK2 and

GPK3 (Hettkamp et al., 2004). The experiment consisted of successive injections of fresh water followed by that of a diluted acidified brine, using different injection rates. The results were positive, leading to a decrease of injection pressure, as calcite was presumably dissolved in the vicinity of the injection well and gradually carried away (Gérard et al., 2005).

The FRACHEM code was used to simulate this acidification test and to estimate the actual impact on reservoir porosity of adding HCl. In the model, the HCl solution was simulated by mixing one part of formation brine with two parts fresh water, followed by the addition of 2 g L^{-1} of concentrated HCl. The pH of the modelled injected solution was close to 1.4. The estimates that follow were obtained using the Case 1a porosity/permeability relationship (i.e. Eqs. (4)–(6)).

The simulation results indicate that the acid solution tends to dissolve carbonates in the first few metres of the fractured zone. After injecting the acidified brine for 1 day, the HCl affects only the first metre, with a decrease of about 10% of the initial calcite present in the fractured zone. After 3 days, the acid has dissolved some of the mineral deposits in a 2-m radius zone around the injection well. The first 0.5 m are the most affected by the acid, with dissolution of about 30% of the calcite and about 9% of the dolomite initially present. Due to differences in reaction rates, dolomite is dissolved only near the injection well and not farther into the fractured zone.

After 1 day of acid stimulation the porosity of the rock around the injection well (i.e. up to a radial distance of 0.5 m) increases by about 10%. After 3 days, it increases 0.2% between 0.5 and 1.5 m from the well.

4.2. Effects of a reverse circulation period

In another reservoir stimulation scenario, it is assumed that there is a temporary reverse fluid circulation after a given exploitation period. As mentioned earlier, higher temperature causes calcite deposition in the fractured zone near the production well. In order to improve porosity and permeability around the producer, we studied the effect of reversing the circulation of fluids in the zone during a 90-day period after 300 days of exploitation. That is, during that period, the production well becomes an injector, and vice versa. Fluid chemistry and mineral components in the fractured zone were updated after 300 days of circulation and the boundary conditions were inverted. Figure 11 shows the porosity distribution after 300 days of exploitation and after the period of reverse circulation.

By reversing circulation a slight change takes place in fracture porosity, due to mineral (mainly carbonates) dissolution and precipitation. After 300 days of circulation (solid line in Fig. 11), porosity increased by about 35% near the injection well (located towards the left in the figure) and decreased by about 0.2% near the production well. By reversing the circulation for 3 months (dashed line in Fig. 11), minerals (mainly carbonates) dissolved near the injection well (now located towards the right in the figure). As a consequence, a porosity increase was observed within the first 25 m of the fractured zone, between 625 and 650 m (see inset in Fig. 11). The dissolution of carbonates results in an increase of calcium in the fluid and the re-precipitation of calcite further away from the “new injector”, i.e. between 425 and 625 m.

These modelling results suggest that a period of reverse circulation in the injection/production doublet could improve reservoir properties, particularly in the vicinity of the production well.

4.3. Change in injection temperature

In order to estimate the sensitivity of the model to the temperature of the injected fluid, it was lowered in the model from 65 to 50 °C. Table 5 compares the amount of minerals precipitated

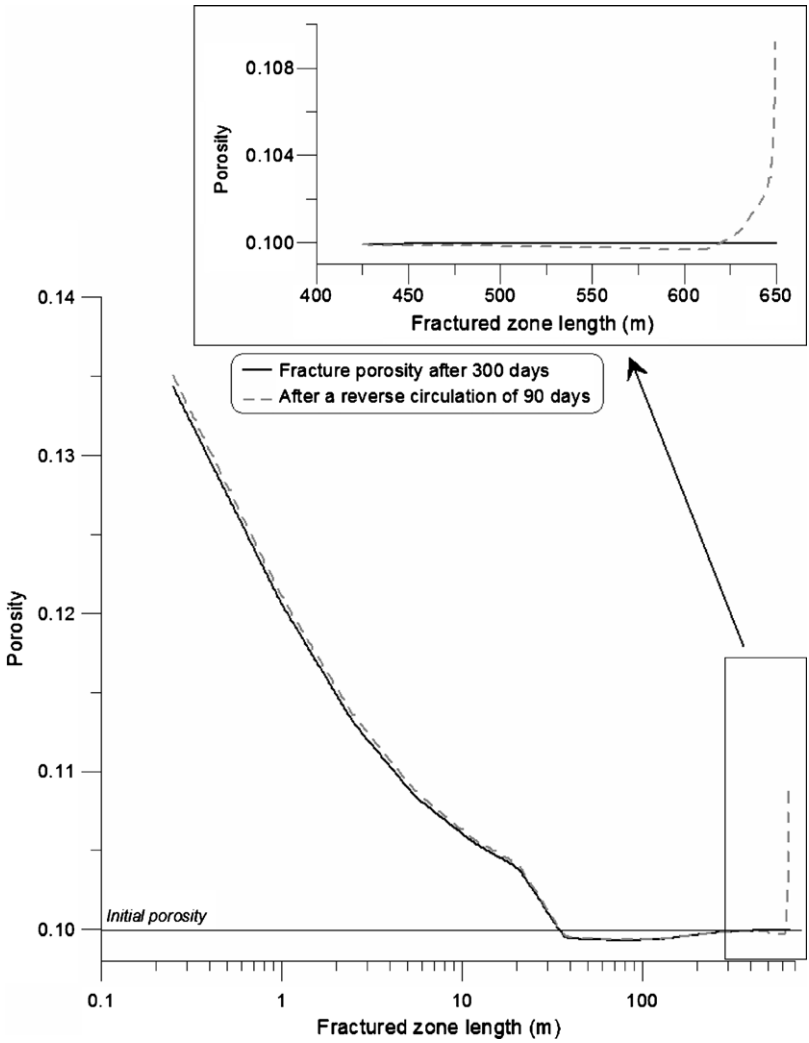

Fig. 11. Porosity along the fractured zone after 300 days of forced fluid circulation and after 90 days of reverse circulation according to the model of Case 1a.

and dissolved under these two assumed injectate temperatures. The most important changes only affect the less reactive minerals, so the effect of injection temperature on reservoir properties is negligible.

We mentioned beforehand that the solubility of calcite, the most reactive mineral in the system, changes with temperature. A drop of 15 °C in injectate temperature, however, does not have a significant impact on reservoir performance. Because of the small solubility of amorphous silica at low temperatures, this 15 °C decrease does, however, result in an increase in precipitation by about 20% (Table 5). This result is in line with research by Xu et al. (2004), which indicates that in many geothermal reservoirs silica precipitation is a major phenomenon and re-injection temperature a key parameter.

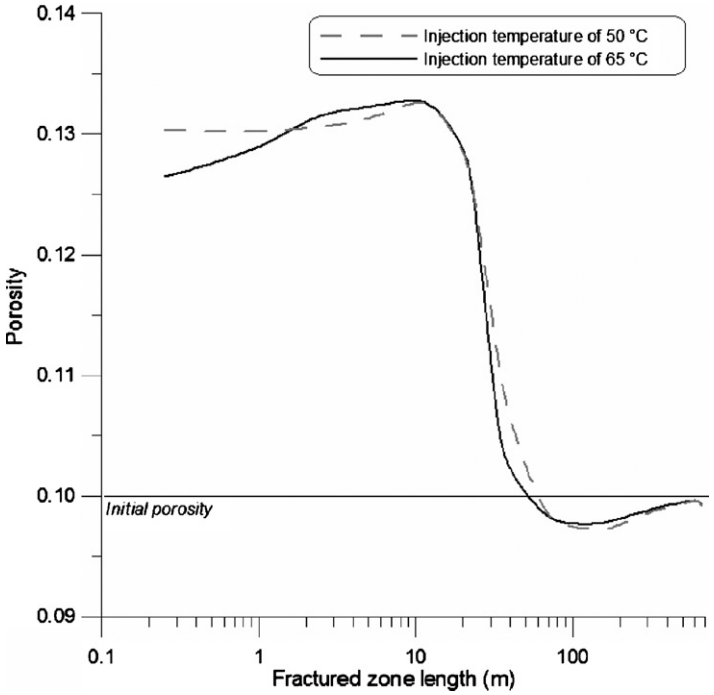

Fig. 12. Porosity along the fractured zone after 1800 days of forced fluid circulation assuming two different injection fluid temperatures. Results according to the model of Case 1a.

Considering the entire fractured zone, porosity differences between the 65 and 50 °C fluid injection cases do not exceed 2%. In the vicinity of the injection well, however, the differences range from 3 to 5% (Fig. 12).

4.4. Injection of fresh water into the reservoir

During the acidizing tests and the hydraulic stimulations performed in wells GPK2 and GPK3 in 2003, many thousands of cubic metres of fresh water were pumped into the reservoir. In both cases, the injected fluid had a chemical composition different from that of the initial brine in the reservoir.

To investigate the impact of fresh water injection on reservoir behaviour, a 300-day circulation test simulating the injection of a diluted brine was modelled utilizing the FRACHEM code. To this end, the injected solution was simulated by diluting the initial reservoir brine with fresh water so that it was a mixture of 90% original brine and 10% fresh water; the injection temperature and rate were maintained at 65 °C and 0.02 L s^{-1}, respectively. The dilution of the brine did not significantly affect the amounts of dolomite, quartz, amorphous silica and aluminosilicates that were precipitated and dissolved (Table 6). However, there was a difference in calcite behaviour, as brine dilution led to a reduction in calcite reactivity, in that it decreased by about 50% after 300 days of forced fluid circulation. As a consequence, the flow properties of the fractured zone were slightly varied, as shown in Fig. 13. The changes occurred mainly in the vicinity of the injection well, where reaction rates of calcite and dolomite are highest in the fractured zone.

Table 6
Comparison of amounts of mineral transferred after 300 days of forced fluid circulation assuming injection of original reservoir brine or diluted brine

Mineral	Amount (kg)	Original brine	Diluted brine
Calcite	Precipitated	362	356
	Dissolved	258	121
Dolomite	Precipitated	0.0	0.0
	Dissolved	170	143
Quartz	Precipitated	0.02	0.0
	Dissolved	0.0	0.07
Amorphous silica	Precipitated	26.2	16.7
	Dissolved	0.5	0.5
Pyrite	Precipitated	0.3	0.0
	Dissolved	0.0	0.02
K-feldspar	Precipitated	0.7	0.5
	Dissolved	0.0	0.0
Albite	Precipitated	0.0	0.0
	Dissolved	0.18	0.18
Illite	Precipitated	0.0	0.1
	Dissolved	0.0	0.0

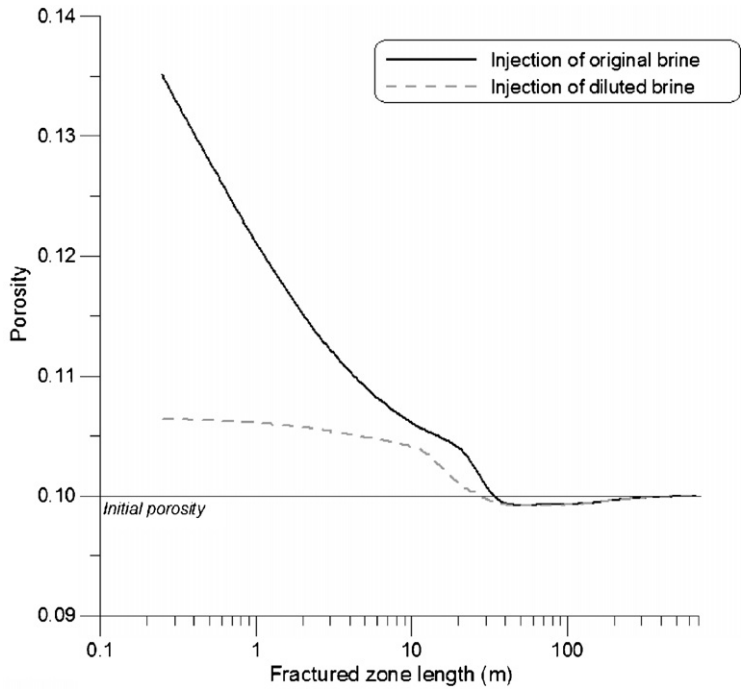

Fig. 13. Porosity along the fractured zone after 300 days of forced fluid circulation assuming two different injection fluids. Results according to the model of Case 1a. Diluted brine: 90% of original brine + 10% fresh water.

The modelling results suggest that the injection of a diluted brine can be used in the same way as the original brine to promote mineral dissolution near the injector in the fractured reservoir. However, the percentage of fresh water in the injection fluid should be accurately determined. The addition of fresh water will decrease the ionic strength of the injectate and may cause swelling of the clays present in the granite. Tchistiakov (2000) indicates that the injection of distilled water instead of a 1 M-NaCl solution through sandstones induces a decrease of 20% in permeability, due to clay swelling. In other words, the use of fresh water in reservoir stimulation has to be studied carefully before it is implemented in an EGS project.

5. Conclusions

The circulation of injected cold brine in the 5000-m deep Soultz reservoir was modelled using FRACHEM, a code that couples thermo-hydraulic and chemical processes. The flow of fluids through the granitic reservoir modifies the chemical and thermal equilibrium in the system, resulting in mineral dissolution and precipitation.

After circulating brine through the system for 1800 days, the model confirmed that calcite was the most reactive mineral in the system, with about 1300 kg dissolved within the first 50 m of the fractured zone around the injector and about 1500 kg precipitated in the second half of the fracture (i.e. towards the production well). Silicates and aluminosilicates tended to precipitate near the injection well, albeit in small quantities.

As a consequence of these mineral reactions there was a change in reservoir porosity and permeability. In the vicinity of the injection well, porosity increased by about 30%, mainly due to calcite dissolution, while porosity decreased by about 5% near the production well. Carbonate dissolution and precipitation seemed to control the porosity of the reservoir, at least during the first 1800 days of simulated forced fluid circulation. The chemical behaviour of the carbonates in the deep Soultz reservoir seemed to reflect what was observed in the shallower reservoir, an encouraging result for the EGS project.

Although silicates and aluminosilicates played a secondary role, their impact on fracture porosity and permeability was detected, particularly in the first 10 m of the fractured zone around the injection well.

We should emphasise that our modelling results as regards porosity and permeability depend on the assumed relationship between these two parameters. For the time being, our limited knowledge of the behaviour of the Soultz reservoir precludes any definition of the actual porosity/permeability relationship at this site. Only a comparison between simulation results and field data obtained from future tests and production periods will allow us to determine which model or models best reflect reality.

Another challenge for the FRACHEM code is to predict the effectiveness of chemical stimulations in enhancing the porosity and permeability of EGS reservoirs. Our study suggests that this numerical code will prove a good tool for investigating the effects of geochemical processes on reservoir properties.

Based on the scenarios presented here, brine dilution seems to be an efficient method for maintaining the hydraulic properties of the fractured reservoir. Although a relatively simple technique, it does require large volumes of make-up water and should not be adopted without thoroughly investigating the risk of clay swelling in the reservoir. Although technically more complex, a period of reverse fluid circulation is also an interesting option.

At this time, we can conclude that injection of diluted brines combined with periods of reverse circulation in the reservoir could help maintain the long-term productivity of fractured reservoirs

in granitic rocks. Finally, various acidification methods can be applied to enhance fracture permeability in the vicinity of the wells; the FRACHEM code could be used to identify the most efficient acid-treatment methods for EGS projects.

Acknowledgements

Thanks are due to Peter Rose for his careful review of the article and to the two anonymous reviewers for their comments and corrections, which have contributed significantly to improving the article. The authors would also like to thank the Swiss State Secretariat for Education and Research and the Swiss Federal Office of Energy for funding this project (OFES-No. 00.0453 and OFES-No. 03.04.60). The authors are also grateful to Thomas Kohl of Geowatt AG (Zürich) for his help in building and improving the thermo-hydraulic model and for numerous fruitful discussions.

References

Amistoso, A.E., Aqui, A.R., Yglopaz, D.M., Malate, R.C.M., 2005. Sustaining steam supply in Palinpinon 1 production field, Southern Negros Geothermal Project, Philippines. In: Proceedings of the World Geothermal Congress 2005, Antalya, Turkey.

André, L., Vuataz, F.-D., 2005. Simulated evolution of reservoir properties for the Enhanced Geothermal System at Soultz-sous-Forêts: the role of hot brine-rock interactions. In: Proceedings of the 30th Workshop on Geothermal Reservoir Engineering. Stanford University, pp. 283–290.

André, L., Spycher, N., Xu, T., Pruess, K., Vuataz, F.-D., 2006. Comparing FRACHEM and TOUGHREACT for reactive transport modeling of brine-rock interactions in Enhanced Geothermal Systems (EGS). In: Proceedings of the 31st Workshop on Geothermal Reservoir Engineering. Stanford University, pp. 350–358.

Bächler, D., 2003. Coupled Thermal-Hydraulic-Chemical Modelling at the Soultz-sous-Forêts HDR reservoir (France). PhD thesis, ETH-Zürich, Switzerland, 151 pp.

Bächler, D., Kohl, T., 2005. Coupled thermal-hydraulic-chemical modelling of enhanced geothermal systems. Geophys. J. Int. 161 (2), 533–548.

Barelli, A., Cappetti, G., Manetti, G., Peano, A., 1985. Well stimulation in Latera field. Geother. Resourc. Council Trans. 9 II, 213–219.

Barrett, T.J., Anderson, G.M., 1988. The solubility of sphalerite and galena in 1–5 m NaCl solutions to 300 °C. Geochim. Cosmochim. Acta 52 (4), 813–820.

Barrios, L.A., Quijano, J.E., Romero, R.E., Mayorga, H., Castro, M., Caldera, J., 2002. Enhanced permeability by chemical stimulation at the Berlin Geothermal Field, El Salvador. Geother. Resourc. Council Trans. 26, 73–78.

Blum, A.E., Stillings, L.L., 1995. Feldspar dissolution kinetics. In: White, A.F., Brantley, S.L. (Eds.), Chemical Weathering Rates of Silicate Minerals, 31. Mineralogical Society of America, pp. 291–351, Reviews in Mineralogy.

Bolton, E.W., Lasaga, A.C., Rye, D.M., 1996. A model for the kinetic control of quartz dissolution and precipitation in porous media flow with spatially variable permeability; formulation and examples of thermal convection. J. Geophys. Res. Part B. Solid Earth Planets 101 (10), 22157–22187.

Buning, B.C., Malate, R.C.M., Lacanilao, A.M., Sta Ana, F.X.M., Sarmiento, Z.F., 1995. Recent experiments in acid stimulation technology by PNOC-Energy Development Corporation, Philippines. In: Proceedings of the World Geothermal Congress '95, Florence, Italy, pp. 1807–1812.

Carroll, S., Mroczek, E., Alai, M., Ebert, M., 1998. Amorphous silica precipitation (60 to 120 °C): comparison of laboratory and field rates. Geochim. Cosmochim. Acta 62 (8), 1379–1396.

Clauser, C. (Ed.), 2003. Numerical simulation of reactive flow in hot aquifers. SHEMAT and Processing SHEMAT. Springer Verlag, Heidelberg, p. 332.

Debye, P., Hückel, E., 1923a. Zur Theorie der Elektrolyte I: Gefrierpunktserniedrigung und verwandte Erscheinungen. Phys. Zeitsch. 24, 185–207.

Debye, P., Hückel, E., 1923b. Zur Theorie der Elektrolyte II: das Grensgesetz für die elektrische Leitfähigkeit. Phys. Zeitsch. 24, 305–325.

Dezayes, C., Valley, B., Maqua, E., Sysen, G., Genter, A., 2005. Natural fracture system of the Soultz granite based on UBI data in the GPK3 and GPK4 wells. In: Proceedings of the EHDRA Scientific Meeting. Soultz-sous-Forêts, France.

Durst, P., 2002. Geochemical modelling of the Soultz-sous-Forêts Hot Dry Rock test site: coupling fluid-rock interactions to heat and fluid transport. PhD thesis, University of Neuchâtel, Switzerland, 127 pp.

Evanoff, J., Yeager, V., Spielman, P., 1995. Stimulation and damage removal of calcium carbonate scaling in geothermal wells: a case study. In: Proceedings of the World Geothermal Congress '95, Florence, Italy, pp. 2481–2485.

Genter, A., Dezayes, C., Gentier, S., Ledésert, B., Sausse, J., 1998. Conceptual fracture model at Soultz based on geological data. In: Proceedings of the 4th HDR Forum. Strasbourg, France.

Gérard A., Kappelmeyer O., 1991. European HDR Project at Soultz-sous-Forêts, Geothermal Sc. & Tech. 3(1–4), Gordon & Breach Science Publishers, New York, USA, 308 pp.

Gérard, A., Fritz, B., Vuataz, F.-D., 2005. Results of soft acid injection tests performed at Soultz in wells GPK2, GPK3 and GPK4—extended summary: revised status on 14 March 2005. In: Proceedings of the EHDRA Scientific Conference, Soultz-sous-Forêts, France.

Hellmann, R., 1994. The albite-water system. Part I. The kinetics of dissolution as a function of pH at 100, 200 and 300 °C. Geochim. Cosmochim. Acta 58 (2), 595–611.

Hettkamp, T., Baumgärtner, J., Baria, R., Gérard, A., Gandy, T., Michelet, S., Teza, D., 2004. Electricity production from hot rocks. In: Proceedings of the 29th Workshop on Geothermal Reservoir Engineering. Stanford University, pp. 184–193.

Hooijkaas, G.R., Genter, A., Dezayes, C., this issue. Deep-seated geology of the granite intrusions at the Soultz EGS site based on data from 5 km-deep boreholes. Geothermics.

Icenhower, J.P., Dove, P.M., 2000. The dissolution kinetics of amorphous silica into sodium chloride solutions: effects of temperature and ionic strength. Geochim. Cosmochim. Acta 64 (24), 4193–4203.

Jacquot, E., 2000. Modélisation thermodynamique et cinétique des réactions géochimiques entre fluides de bassin et socle cristallin: application au site expérimental du programme européen de recherche en géothermie profonde (Soultz-sous-Forêts, Bas-Rhin, France). PhD thesis, Université Louis Pasteur—Strasbourg I, France, 202 pp.

Kohl, T., Hopkirk, R.J., 1995. "FRACTure" – a simulation code for forced fluid flow and transport in fractured, porous rock. Geothermics 24 (3), 333–343.

Kohl, T., Rybach, L., 2001. Assessment of HDR reservoir geometry by inverse modelling of non-laminar hydraulic flow. In: Proceedings of the 26th Workshop on Geothermal Reservoir Engineering. Stanford University, pp. 259–265.

Köhler, S.J., Dufaud, F., Oelkers, E.H., 2003. An experimental study of illite dissolution kinetics as a function of pH from 1.4 to 12.4 and temperature from 5 to 50 °C. Geochim. Cosmochim. Acta 67 (19), 3583–3594.

Lasaga, A.C., Soler, J.M., Ganor, J., Burch, T.E., Nagy, K.L., 1994. Chemical weathering rate laws and global geochemical cycles. Geochim. Cosmochim. Acta 58, 2361–2386.

Malate, R.C.M., Austria, J.J.C., Sarmiento, Z.F., Sookprasong, P.A., Francia, E.S., 1999. Wellbore soaking: a novel acid treatment of geothermal injection wells. In: Proceedings of the 24th Workshop on Geothermal Reservoir Engineering. Stanford University, pp. 336–339.

Moller, N., Greenberg, J.P., Weare, J.H., 1998. Computer modeling for geothermal systems: predicting carbonate and silica scale formation, CO_2 breakout and H_2S exchange. Transp. Porous Media 33, 173–204.

Monnin, C., 1989. An ion interaction model for the volumetric properties of natural waters: density of the solution and partial molal volume of electrolytes to high concentrations at 25 °C. Geochim. Cosmochim. Acta 53, 1177–1188.

Nagy, K.L., Blum, A.E., Lasaga, A.C., 1991. Dissolution and precipitation kinetics of kaolinite at 80 °C and pH 3: the dependence on solution saturation state. Am. J. Sci. 291 (7), 649–686.

Norton, D., Knapp, R., 1977. Transport phenomena in hydrothermal systems; the nature of porosity. Am. J. Sci. 277 (8), 913–936.

Pitzer, K.S., 1973. Thermodynamic of electrolytes. I. Theoretical basis and general equations. J. Phys. Chem. 12, 268–277.

Pokrovskii, V.A., Helgeson, H.C., 1995. Thermodynamic properties of aqueous species and the solubilities of minerals at high pressures and temperatures: the system Al_2O_3-H_2O-NaCl. Am. J. Sci. 295, 1255–1342.

Rabemanana, V., Durst, P., Bächler, D., Vuataz, F.-D., Kohl, T., 2003. Geochemical modelling of the Soultz-sous-Forêts Hot Fractured Rock system: comparison of two reservoirs at 3.8 and 5 km depth. Geothermics 32 (4–6), 645–653.

Rimstidt, J.D., Barnes, H.L., 1980. The kinetics of silica-water reactions. Geochim. Cosmochim. Acta 44 (11), 1683–1699.

Sauty, J.P., 1981. Du comportement thermique des réservoirs aquifères exploités pour le stockage d'eau chaude ou la géothermie basse enthalpie. Thèse d'état, Grenoble, 207 pp.

Steefel, C.I., Lasaga, A.C., 1994. A coupled model for transport of multiple chemical species and kinetic precipitation/dissolution reactions with application to reactive flow in single-phase hydrothermal system. Am. J. Sci. 294 (5), 529–592.

Stillings, L.L., Brantley, S.L., 1995. Feldspar dissolution at 25 °C and pH 3: reaction stoichiometry and the effect of cations. Geochim. Cosmochim. Acta 59 (8), 1483–1496.

Tchistiakov, A.A., 2000. Physico-chemical aspects of clay migration and injectivity decrease of geothermal clastic reservoir. In: Proceedings of the World Geothermal Congress 2000, Kyushu-Tohoku, Japan, pp. 3087–3095.

White, S.P., 1995. Multiphase nonisothermal transport of systems of reacting chemicals. Water Resour. Res. 31 (7), 1761–1772.

Wolery, T.J., 1992. EQ3nr, a computer program for geochemical aqueous speciation solubility calculations: theoretical manual, user's guide and related documentation (Version 7.0). Report, UCRL-MA-110662 PT III, Lawrence Livermore National Laboratory, Livermore, California, USA, 246 pp.

Xu, T., Ontoy, Y., Molling, P., Spycher, N., Parini, M., Pruess, K., 2004. Reactive transport modeling of injection well scaling and acidizing at Tiwi field, Philippines. Geothermics 33 (4), 477–491.

LBNL-62357

MODELING BRINE-ROCK INTERACTIONS IN AN ENHANCED GEOTHERMAL SYSTEM DEEP FRACTURED RESERVOIR AT SOULTZ-SOUS-FORETS (FRANCE): A JOINT APPROACH USING TWO GEOCHEMICAL CODES: FRACHEM AND TOUGHREACT

Laurent André[(1)*], *Nicolas Spycher*[(2)], *Tianfu Xu*[(2)], *François-D. Vuataz*[(1)] *and Karsten Pruess*[(2)]

(1) Centre of Geothermal Research – c/o Centre of Hydrogeology - Emile Argand 11, CH-2009 Neuchâtel, Switzerland
(2) Earth Sciences Division - Lawrence Berkeley National Laboratory - Berkeley, CA 94720, USA

December 2006

* Current address: BRGM - Water Division, 3 avenue C. Guillemin, BP 6009, 45060 Orléans Cedex 2, France; l.andre@brgm.fr

DECEMBER 2006

This work was supported by the Swiss State Secretariat for Education and Research (SER) under contract OFES-N° 03.04.60 and by the Swiss Federal Office of Energy under contract OFEN-N° 100'528, as well as by the Assistant Secretary for Energy Efficiency and Renewable Energy, Office of Geothermal Technologies, of the U.S. department of Energy, under Contract No. DE-AC02-05CH11231.

EXECUTIVE SUMMARY

The modeling of coupled thermal, hydrological, and chemical (THC) processes in geothermal systems is complicated by reservoir conditions such as high temperatures, elevated pressures and sometimes the high salinity of the formation fluid. Coupled THC models have been developed and applied to the study of enhanced geothermal systems (EGS) to forecast the long-term evolution of reservoir properties and to determine how fluid circulation within a fractured reservoir can modify its rock properties. In this study, two simulators, FRACHEM and TOUGHREACT, specifically developed to investigate EGS, were applied to model the same geothermal reservoir and to forecast reservoir evolution using their respective thermodynamic and kinetic input data. First, we report the specifics of each of these two codes regarding the calculation of activity coefficients, equilibrium constants and mineral reaction rates. Comparisons of simulation results are then made for a Soultz-type geothermal fluid (ionic strength ~1.8 molal), with a recent (unreleased) version of TOUGHREACT using either an extended Debye-Hückel or Pitzer model for calculating activity coefficients, and FRACHEM using the Pitzer model as well.

Despite somewhat different calculation approaches and methodologies, we observe a reasonably good agreement for most of the investigated factors. Differences in the calculation schemes typically produce less difference in model outputs than differences in input thermodynamic and kinetic data, with model results being particularly sensitive to differences in ion-interaction parameters for activity coefficient models. Differences in input thermodynamic equilibrium constants, activity coefficients, and kinetics data yield differences in calculated pH and in predicted mineral precipitation behavior and reservoir-porosity evolution. When numerically cooling a Soultz-type geothermal fluid from 200°C (initially equilibrated with calcite at pH 4.9) to 20°C and suppressing mineral precipitation, pH values calculated with FRACHEM and TOUGHREACT/ Debye-Hückel decrease by up to half a pH unit, whereas pH values calculated with TOUGHREACT/Pitzer increase by a similar amount. As a result of these differences, calcite solubilities computed using the Pitzer formalism (the more accurate approach) are up to about 1.5 orders of magnitude lower. Because of differences in Pitzer ion-interaction parameters, the calcite solubility computed with TOUGHREACT/Pitzer is also typically about 0.5 orders of magnitude lower than that computed with FRACHEM, with the latter expected to be most accurate.

In a second part of this investigation, both models were applied to model the evolution of a Soultz-type geothermal reservoir under high pressure and temperature conditions. By specifying initial conditions reflecting a reservoir fluid saturated with respect to calcite (a reasonable assumption based on field data), we found that THC reservoir simulations with the three models yield similar results, including similar trends and amounts of reservoir porosity decrease over time, thus pointing to the importance of model conceptualization. This study also highlights the critical effect of input thermodynamic data on the results of reactive transport simulations, most particularly for systems involving brines.

Keywords: Geothermal reservoir, brine, granite, secondary minerals, numerical codes, simulation, Pitzer, activity coefficients, mineral reaction rate, porosity, Enhanced Geothermal System (EGS), Soultz-sous-Forêts.

INTENTIONALLY LEFT BLANK

TABLE OF CONTENTS

LIST OF FIGURES

LIST OF TABLES

INTENTIONALLY LEFT BLANK

1 INTRODUCTION

This work was initiated through the collaboration between the Centre of Geothermal Research, Neuchâtel, Switzerland (CREGE) and the Earth Sciences Division at Lawrence Berkeley National Laboratory (LBNL), Berkeley, California, USA. During the last several years, these two institutions have been developing reactive transport simulators applicable to the study of coupled thermal, hydrological, and chemical (THC) processes in geothermal systems. The Centre of Hydrogeology of Neuchâtel and then CREGE have been involved since 1998 in the European enhanced geothermal system (EGS) project at Soultz-sous-Forêts, France. The main objective of this project is to build a pilot plant for power production, based on the circulation of a geothermal fluid through a deep fractured reservoir.

The Soultz-sous-Forêts EGS is located in Alsace, about 50 km north of Strasbourg (France). The Soultz area was selected as the European EGS pilot site because of its strong temperature gradient in the sedimentary cover (up to 100°C/km) and its high heat flow, locally reaching 0.15 W/m^2 (Kohl and Rybach, 2001). The geology of the Soultz region is characterized by a graben structure affected by several N-S striking faults. The crystalline basement, covered by 1400 m of Triassic and Tertiary sediments, is composed of three facies in granitic rocks: (1) an unaltered granite in which fracture density is close to zero; (2) a hydrothermally altered granite facies and (3) altered veins within the hydrothermally altered granite (Jacquot, 2000). The hydrothermally altered granite is the most porous facies (Genter et al., 1997) and altered veins are highly fractured. Natural circulation of formation fluid and fluid-rock interaction processes take place mainly within the hydrothermally altered granite, and to a lesser extent within altered veins. Flow in the unaltered granite is essentially nil.

To extract the heat from the Soultz reservoir, three deviated wells have been installed to a depth of 5,000 m, with lower ends separated by 600 m (Figure 1-1). The reservoir encountered at this depth presents an initial temperature of 200°C. One well (GPK3) will be dedicated to the injection of cold water in the granitic reservoir at a rate of about 100 L/s, whereas the two other wells (GPK2 and GPK4), located on both sides of the injector, will be used to produce the formation fluid. At Soultz, the injection–production system has been designed as a closed loop. The fluid used is a formation fluid existing in the altered granite, namely a brine with a total dissolved solids value of around 100,000 ppm. Injection of cooled brine disturbs the equilibrium between the formation fluid and reactive minerals. The resulting change in temperature and pressure in the reservoir, and the forced circulation in fractured granite, will drive geochemical reactions able to affect the physical properties of the reservoir through mineral precipitation and dissolution. The main task of the research on THC coupled modeling for this site has been to forecast the evolution of reservoir porosity and permeability. Different researchers (Durst, 2002, Bächler, 2003, Rabemanana et al. 2003, André et al., 2005) have incrementally built a reactive transport simulator, FRACHEM, able to simulate the main characteristics of the Soultz reservoir at 5 km below the surface, 200°C, 500 bar, and a fluid salinity of around 100,000 ppm.

The reactive transport simulator developed at LBNL, TOUGHREACT (Xu and Pruess, 2001; Xu et al., 2001, 2004a, 2004b, and 2006) was based on introducing reactive chemistry into the code TOUGH2 (Pruess 1991). TOUGHREACT has been applied to different problems, such as CO_2 sequestration in deep saline aquifers and the evolution of water-rock interactions around nuclear

waste disposal sites. A recent upgrade of this code (Zhang et al., 2006a, 2006b) includes the implementation of a Pitzer ion-activity model, allowing model applications involving highly saline brines.

The aim of this study is to investigate the chemical reactions (currently not well known) that take place within the Soultz reservoir at high temperature, elevated pressure, and strong salinity. The main objectives are to determine, as accurately as possible, activity coefficients of dissolved species as well as mineral solubility and dissolution/precipitation rates, to forecast reservoir evolution and porosity variations with time.

Consequently, the first part of this report focuses on comparing values of different computed parameters (activity coefficients, saturation indices, dissolution/precipitation rates), as they are computed by each code according to different methods and/or input thermodynamic data.

The second part of this work relates directly to the enhanced geothermal system of Soultz. Simulations of this reservoir were carried out with FRACHEM to predict the evolution of the reservoir properties. The results obtained with FRACHEM are then compared with the results obtained with TOUGHREACT. Because the TOUGHREACT version used in this report allows selection between an extended Debye-Hückel model and the Pitzer formalism for the calculation of activity coefficients, the two methods have been applied and the predicted respective reservoir evolution then discussed.

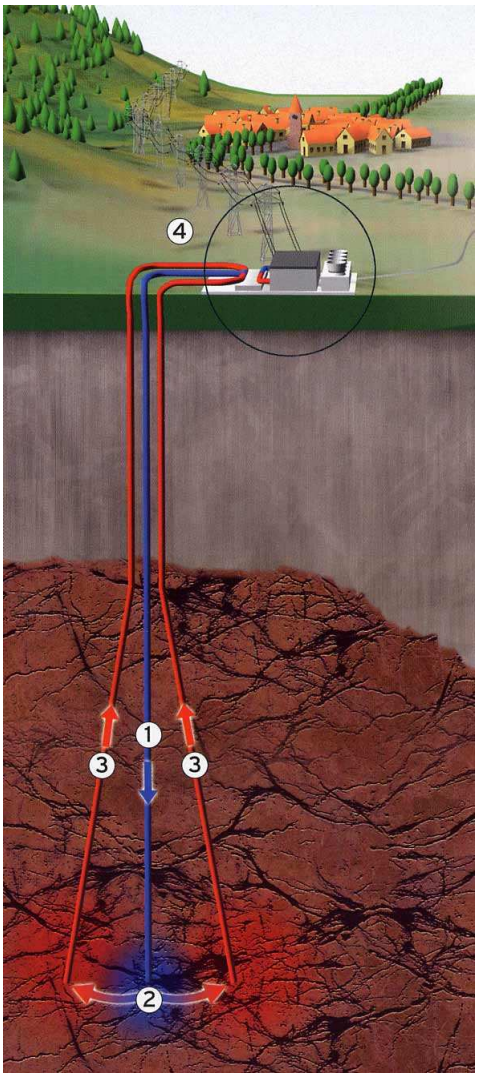

Figure 1-1. Initial conceptual diagram of the Soultz EGS pilot plant: (1) injection well ; (2) fractured reservoir ; (3) production wells ; (4) power plant.

INTENTIONALLY LEFT BLANK

2 DESCRIPTION OF CODES

This description of the codes is general overview of the computation capabilities of the two simulators. For more details, the reader can consult the TOUGHREACT User's Guide (Xu et al., 2004a) and Xu et al. (2006), as well as the different FRACHEM studies on the Soultz system (Durst, 2002, Bächler et al., 2005).

2.1 FRACHEM

FRACHEM is a THC simulator issued from the combination of two existing codes: FRACTure and CHEMTOUGH2. FRACTure is a 3-D finite-element code for modeling hydrological, transport and elastic processes. It was developed originally for the study of flow-driven interactions in fractured rock (Kohl & Hopkirk, 1995). CHEMTOUGH2 (White, 1995) is a THC code developed after the TOUGH2 simulator (Pruess, 1991), a 3-D numerical model for simulating the coupled transport of water, vapor, noncondensable gas, and heat in porous and fractured media. CHEMTOUGH2 presents the possibility to transport chemical species and to model the chemical water-rock interactions as well as the chemical reactions driven by pressure and temperature changes. The transport and reaction are coupled using a one-step approach.

FRACHEM has been built by introducing geochemical subroutines from CHEMTOUGH2 (White, 1995) into the framework of the code FRACTure (Bächler, 2003; Bächler and Kohl, 2005). After an initialization phase, FRACTure calculates, over each time step, the thermal and hydrological conditions within each element volume and determines the advective flow between each of them. Resulting thermal and hydrological variables are stored in arrays common to FRACTure and the geochemical modules. At this point, the program calculates the chemical reactions using a mass balance/mass action approach, the advective transport of chemical species, and the variations of porosity and permeability. Once this calculation is performed, the porosity and permeability are updated and fed into the FRACTure part of the code. The program then returns to the start of the loop until the end of the simulation time (sequential noniterative approach, SNIA) (Figure 2-1).

FRACHEM has been developed specially for the granitic reservoir of Soultz-sous-Forêts and consequently, specific implementations have been added to the chemical part of this code. The reservoir, at a depth of 5,000 m, contains a brine with about 100,000 ppm total dissolved solids (TDS) and a temperature of 200°C. Considering the high salinity of the geofluid, the Debye-Hückel model, initially implemented in the CHEMTOUGH2 routines to determine the activity coefficients, has been replaced by a Pitzer activity model. It should be mentioned here that the activity coefficients calculations are carried out in an indirect manner by means of another code, TEQUIL (Moller et al., 1998). For a given fluid composition (constant ionic strength), the activity coefficients are determined at different temperatures in the range 50– 200°C using TEQUIL before running FRACHEM. The activity coefficient values obtained at each temperature are regressed as a function of temperature using a polynomial fit, with coefficients then entered into the chemical input file. This approach works well for the case of Soultz simulations because the ionic strength of the circulated fluid remains more or less constant.

Presently, a limited number of minerals are considered, which correspond to the minerals constituting the Soultz granite. The precipitation/dissolution reactions of carbonates (calcite,

dolomite), quartz, amorphous silica, pyrite, and some aluminosilicates (K-feldspar, albite, illite) can be modeled under kinetic constraints. The implemented kinetic-rate laws are specific to each mineral and taken from published experiments conducted at high temperature in NaCl brines. Thermodynamic data (equilibrium constants) are taken mostly from SUPCRT92 (Johnson et al., 1992) and Helgeson et al. (1978) and are functions of temperature and pressure.

Finally, a supplementary module allows the determination of porosity and permeability variations linked with chemical processes occurring in the reservoir. Considering the alteration of the Soultz granite, the flow is assumed to circulate in a medium composed of fractures and grains. Therefore, a combination of fracture model (Norton and Knapp, 1977; Steefel and Lasaga, 1994) and grain model (Bolton et al., 1996) is used to determine the permeability evolution.

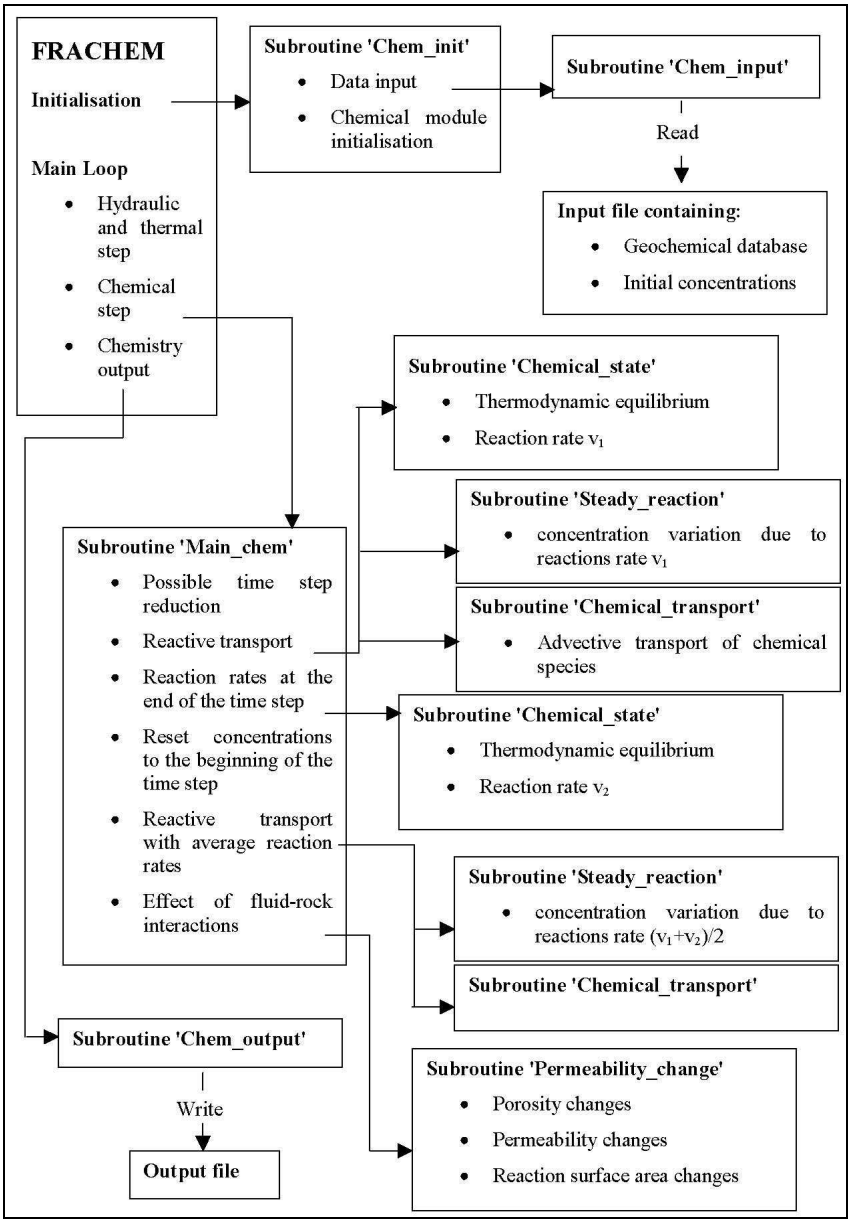

Figure 2-1. Flow chart of the FRACHEM code (Durst, 2002).

2.2 TOUGHREACT

TOUGHREACT (Xu and Pruess, 2001; Xu et al., 2004a; Xu et al., 2006) was developed by introducing multicomponent reactive transport into the framework of the existing multiphase 3-D finite volume fluid and heat flow code TOUGH2 (Pruess, 1991). It is a THC simulator applicable to a wide range of subsurface conditions and to a variety of reactive fluid and geochemical transport problems. Flow, transport, and chemistry are coupled in a sequential manner (Figure 2-2). Here, a sequential noniterative approach was applied for consistency with the FRACHEM simulations.

TOUGHREACT takes into consideration many processes, such as (1) fluid flow in both liquid and gas phases occurring under pressure, viscous, and gravity forces; (2) heat flow by conduction and convection; (3) diffusion of water vapor and air; (4) thermophysical and geochemical reactions as a function of temperature, such as fluid (gas and liquid) density and viscosity, and thermodynamic and kinetic data for mineral-water-gas reactions; (5) transport of aqueous and gaseous species by advection and molecular diffusion in liquid and gas phases, respectively; (6) temporal changes in porosity, permeability, and unsaturated hydrologic properties owing to mineral dissolution, precipitation and clay swelling. The primary governing equations for multiphase fluid and heat flow, and chemical transport are derived from the principle of mass (or energy) conservation (Pruess, 1987; Pruess et al., 1999). The chemistry computations are based on a mass-balance/mass-action approach (e.g., Reed, 1982). Mass conservation is written in terms of basis species, with distributions governed by the total concentrations of the components.

The code makes use of an input thermodynamic database incorporating equilibrium constants for mass-action equations and parameters for the calculation of activity coefficients. Temperature and pressure ranges are controlled by the applicable range of this thermodynamic database, and the range of the equation of state (EOS) module employed in the multiphase flow computations. For this study, equilibrium constants in the database are given for temperatures ranging from 0 to 300ºC, and pressures of 1 bar up to 100ºC and water saturation pressures above 100ºC. These data come mostly from SUPCRT92 (Johnson et al., 1992). Other thermodynamic and kinetic data are also functions of temperature. The currently released version of the code incorporates an extended Debye-Hückel equation (Helgeson et al., 1981) to compute activity coefficients of charged species and water activity for dilute to moderately saline water (up to ~4 molal for an NaCl-dominant solution). Activity coefficients for dissolved gases such as CO_2(aq) are computed from equations developed by Drummond (1981). Recently, a full Pitzer ion-interaction model was implemented as an option, using the formulation of Harvie et al. (1984) (Zhang et al., 2006a,b; see also Zhang et al., 2004) and ion-interaction parameters re-evaluated and fitted as a function of temperature by Wolery et al. (2004) (as published by Alai et al., 2005). Note that the latter data were modified to incorporate more suitable high-temperature data for $CO_{2(aq)}$ from Rumpf et al. (1994) and Rumpf and Maurer (1993), as discussed later.

Mineral dissolution and precipitation can proceed either subject to local equilibrium or kinetic conditions. For kinetically controlled mineral dissolution and precipitation, a general form of transition-state-theory (TST) rate law is used (Lasaga, 1984; Steefel and Lasaga, 1994; Palandri and Kharaka, 2004). Changes in porosity during the simulation are calculated from changes in mineral volume fractions. Several porosity-permeability and fracture aperture-permeability

relationships are included in the model. Here, fracture porosity is related to permeability using the relationship proposed by Verma and Pruess (1988) and described in Xu et al. (2004a).

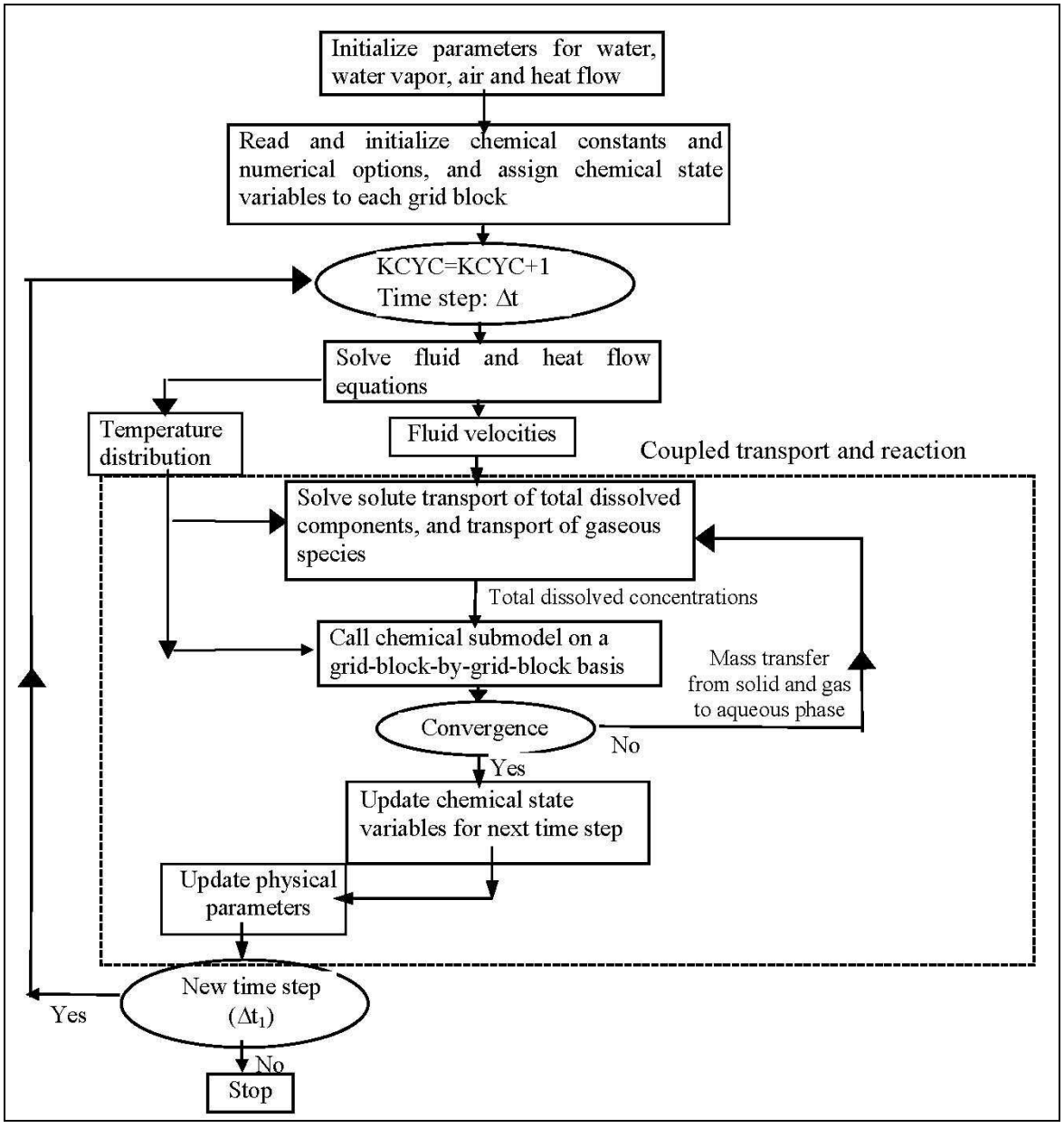

Figure 2-2. Flow chart of the TOUGHREACT simulator (Xu et al., 2004a).

3 CALCULATION OF ACTIVITY COEFFICIENTS

The methods for calculating activity coefficients are described for each code below. An application of these two methods is then presented using a Soultz-type high-salinity geothermal fluid.

3.1 FRACHEM SIMULATIONS

Activity coefficients in FRACHEM simulations are determined in an indirect way using TEQUIL (Moller et al., 1998; http://geotherm.ucsd.edu/tequil/run.html). The latter is used before running FRACHEM to compute aqueous speciation and values of activity coefficients for a given fluid composition and temperature. The activity coefficients for each dissolved species are then entered in a database as regression functions of temperature that are then read by FRACHEM on input.

The TEQUIL application package includes chemical models based on the Pitzer formalism, and calculates liquid-solid-gas equilibria in complex brine systems by globally minimizing the free energy of a system at constant temperature and pressure. Currently, three different models are available in TEQUIL. They are:

- A model of the Na-K-H-Ca-Cl-SO_4-HCO_3-CO_3 -CO_2-H_2 system for 0 to 250^{o}C (Moller et al., 1998).
- A 25^{o}C model for the Na-K-Ca-Mg-H-Cl-OH-SO_4-HCO_3-CO_3-CO_2-H_2O system (Harvie et al., 1984).
- A low temperature (-54^{o}C $\leq$ T $\leq$ 25^{o}C) model for the Na-K-Ca-Mg-Cl-SO_4-H_2O system (Spencer et al., 1990).

In this study, we applied the first model listed above. Using this model, total concentrations obtained from chemical analyses (Table 3-1) were input into TEQUIL, which then computed speciation (Table 3-1) and corresponding activity coefficients. Computations were done using a typical Soultz fluid at a temperature of 200°C. This fluid was initially equilibrated with calcite and anhydrite at 200°C, which resulted in a decrease of Ca^{+2} and SO_4^{-2} concentrations (compared to input concentrations) due to precipitation of calcite and anhydrite. The pH value of 4.9 at 200°C was calculated from the equilibration with calcite and input total aqueous carbonate concentration. Using the fluid composition at 200°C, TEQUIL was then used to numerically cool the solution, recompute pH, and determine activity coefficients at temperatures down to 20°C. It should be noted that the cooling simulation was performed without allowing reactions with gases or minerals.

Mg, Fe, and Al are not included in the TEQUIL database. For this reason, the geochemical program EQ3nr (Wolery, 1992) was applied to determine the activity coefficients of Mg^{2+}, Fe^{2+} and Al^{3+} by using the Pitzer model and the EQ3nr thermodynamic database *data0.hmw* (Harvie et al. 1984).

Activity coefficients determined in this way were then input into FRACHEM as polynomial functions of temperature, for the specific ionic strength of the fluid (nearly constant in our case).

Activity coefficients were then compared with activity coefficients computed with TOUGHREACT as discussed below (Table 3-2).

Activity coefficients by themselves do not provide a means to evaluate differences in chemical behavior predicted by the various codes. Activity coefficients need to be considered together with results of speciation calculations, as expressed by the computed activities of dissolved species (i.e., the product of individual molalities and activity coefficients). This is because ion association and complexation may be implicitly accounted for by activity coefficients (e.g., as done typically with Pitzer models), or explicitly computed with the use of secondary species (e.g., as done with Debye-Hückel models). Therefore, two codes could compute quite different activity coefficients for a given primary aqueous species, but quite similar activities (and thus similar chemical behavior). For this reason, activities of aqueous species computed with FRACHEM are also presented (Table 3-3), for direct comparison with the results of TOUGHREACT.

Table 3-1. Fluid composition from field data (circulation test of 03/12/1999) and modeled composition of the same fluid after equilibration with calcite and anhydrite at 200°C using TEQUIL (Na-K-H-Ca-Cl-SO_4-HCO_3-CO_3-CO_2-SiO_2-H_2O system).

Analyte	**Total concentrations (molal)**	**Species**	**Concentrations of individual species computed by TEQUIL (molal)**
		pH	4.9 (at 200°C)
Σ Na	1.148	**Na^+**	1.148
Σ K	73.40×10^{-3}	**K^+**	$73.4\ 10^{-3}$
Σ Ca	0.1695 / 0.1193**	**Ca^{++}**	0.1190
Σ Cl	1.648	**Cl^-**	1.64800
Σ $S^{(VI)}$	1.771×10^{-3} / 0.9817×10^{-3} **	**SO_4^{--}**	$0.711\ 10^{-3}$
Σ Si	6.060×10^{-3}	**H_4SiO_4**	$6.060\ 10^{-3}$
Σ C	4.250×10^{-2} / 4.277×10^{-2} **	**OH^-**	$1.908\ 10^{-6}$
Σ Mg	3.210×10^{-3}	**HCO_3^-**	$1.539\ 10^{-3}$
Σ Fe	2.614×10^{-3}	**CO_3^{--}**	$2.038\ 10^{-7}$
Σ Al	3.700×10^{-5}	**$CaCO_{3(aq)}$**	$7.026\ 10^{-7}$
		$CO_{2(aq)}$	$4.123\ 10^{-2}$
		$CaHCO_3^+$	$1.111\ 10^{-18}$
		$CaSO_{4(aq)}$	$2.707\ 10^{-4}$

** After equilibration with calcite and anhydrite

3.2 TOUGHREACT SIMULATIONS

In TOUGHREACT, activity coefficients are computed in the code as a function of the current (true) ionic strength. In the version used for his study (V3.2ymp), the user has the choice of an extended Debye-Hückel model (Helgeson et al., 1981) for solution of moderate ionic strengths, or a Pitzer model following Harvie et al. (1984) for more saline solutions (Zhang et al., 2006a,b; see also Zhang et al., 2004). Here, we compare the results of these two models with the FRACHEM/TEQUIL results discussed earlier.

3.2.1 TOUGHREACT with Extended Debye-Hückel model (Tr-DH)

The Debye-Hückel model with TOUGHREACT was selected by setting the input flag MOPR(9) equal to 0. The computation was carried out with the *ThermXu4.dat* database, which consists

essentially of thermodynamic data from the SUPCRT92 package (Johnson et al., 1992) (see also Section 5). For consistency with the TEQUIL simulation, a TOUGHREACT speciation calculation was first run at 200°C using the fluid composition in Table 3-1 and fixing the pH at a value of 4.9, as determined earlier from the TEQUIL simulation. As previously, the resulting fluid was then numerically cooled without allowing reaction with minerals, yielding activity coefficients and activities at different temperatures down to 20°C (Tables 3-2 and 3-3).

3.2.2 TOUGHREACT with Pitzer model (Tr-Pitzer)

The Pitzer model with TOUGHREACT was selected by setting the input flag MOPR(9) equal to 2. As previously, the computation was carried out using the database *ThemXu4.dat* for equilibrium constants of minerals and secondary species. The EQ3/6 *data0.ypf* database (Wolery et al., 2004, as published by Alai et al., 2005) is used for all Pitzer ion-interaction parameters, except for the $CO_{2(aq)}$ parameters, which had to be revised for this study. Earlier simulations using the original *data0.ypf* database (André et al., 2006) showed that this database could not reasonably reproduce the solubility of calcite at temperatures above about 100°C. This discrepancy was eventually traced to the Pitzer ion-interaction parameters for $CO_{2(aq)}$ in the database. These parameters (after He and Morse, 1993) were found to yield erroneous activity coefficients for $CO_{2(aq)}$ when extrapolated at temperatures above about 100°C, in large part because these authors fitted their data (up to 90°C) to a polynomial as a function of temperature, using the same number of data points as the number of fit coefficients. For this reason, we replaced the $CO_{2(aq)}$ data in the *data0.ypf* database with values refitted from ion-interaction parameters reported by Rumpf et al. (1994) and Rumpf and Maurer (1993) for temperatures up to 160°C, which extrapolate smoothly and with reasonable accuracy up to 200°C. The *data0.ypf* database revised with these data was used for all Tr-Pitzer simulations presented in this report.

Secondary species used in the calculations were selected specifically to be consistent with the secondary species in use with the *data0.ypf* Pitzer database. The input flags MOPR(10) and MOPR(11) were set to 3 and 1, respectively, for a fluid ionic strength less than 5 (Zhang et al., 2006a). TOUGHREACT was then run with the same fluid composition as previously (Table 3-1), starting with a pH of 4.9 at 200°C and cooling the solution down to 20°C without allowing mineral reaction. The computed activity coefficients and activities were then compared with the data from the other models (Tables 3-2 and 3-3).

Table 3-2. Computed activity coefficients (molal scale) as a function of temperature, using the fluid composition given in Table 3-1.

Species	Model	20°C	50°C	80°C	110°C	140°C	170°C	200°C
Al^{+++}	FRACHEM[1]	0.3540	0.2400	0.1310	0.0590	0.0209	0.0006	0.0001
	Tr-DH	0.0315	0.0159	0.0073	0.0032	0.0014	0.0006	0.0003
	Tr-Pitzer	0.0007	0.0003	0.0001	0.0001	0.0000	0.0000	0.0000
AlO_2^-	FRACHEM [2]	/	/	/	/	/	/	/
	Tr-DH	0.675	0.685	0.662	0.623	0.577	0.528	0.475
	Tr-Pitzer	0.570	0.534	0.485	0.441	0.403	0.370	0.341
Ca^{++}	FRACHEM	0.296	0.285	0.257	0.222	0.182	0.142	0.104
	Tr-DH	0.191	0.149	0.108	0.077	0.054	0.037	0.025
	Tr-Pitzer	0.041	0.100	0.178	0.256	0.301	0.289	0.224
$CaCO_{3(aq)}$	FRACHEM	1.000	1.000	1.000	1.000	1.000	1.000	1.000
	Tr-DH	1.000	1.000	1.000	1.000	1.000	1.000	1.000
	Tr-Pitzer	1.000	1.000	1.000	1.000	1.000	1.000	1.000
$CaHCO_3^+$	FRACHEM	0.490	0.488	0.471	0.444	0.411	0.372	0.329
	Tr-DH	0.613	0.642	0.640	0.620	0.591	0.555	0.512
	Tr-Pitzer	0.445	0.405	0.368	0.336	0.305	0.272	0.237
$CaSO_{4(aq)}$	FRACHEM	1.000	1.000	1.000	1.000	1.000	1.000	1.000
	Tr-DH	1.000	1.000	1.000	1.000	1.000	1.000	1.000
	Tr-Pitzer	1.000	1.000	1.000	1.000	1.000	1.000	1.000
Cl^-	FRACHEM	0.585	0.559	0.528	0.492	0.453	0.409	0.363
	Tr-DH	0.675	0.685	0.662	0.623	0.577	0.528	0.475
	Tr-Pitzer	0.613	0.644	0.646	0.630	0.599	0.554	0.494
$CO_{2(aq)}$	FRACHEM	1.371	1.356	1.344	1.334	1.325	1.318	1.311
	Tr-DH	1.420	1.363	1.336	1.332	1.343	1.365	1.394
	Tr-Pitzer	1.418	1.346	1.316	1.310	1.318	1.335	1.355
CO_3^{--}	FRACHEM	0.038	0.030	0.022	0.016	0.010	0.006	0.004
	Tr-DH	0.203	0.157	0.114	0.080	0.056	0.039	0.026
	Tr-Pitzer	0.095	0.070	0.044	0.024	0.011	0.004	0.001
Fe^{++}	FRACHEM[1]	0.347	0.294	0.224	0.154	0.093	0.049	0.022
	Tr-DH	0.210	0.157	0.110	0.076	0.051	0.035	0.023
	Tr-Pitzer	0.039	0.027	0.018	0.013	0.009	0.006	0.003
H^+	FRACHEM	1.084	1.051	0.997	0.934	0.865	0.792	0.716
	Tr-DH	0.575	0.621	0.638	0.637	0.623	0.600	0.568
	Tr-Pitzer	0.990	0.874	0.779	0.696	0.615	0.529	0.438
HCO_3^-	FRACHEM	0.389	0.374	0.347	0.310	0.267	0.222	0.178
	Tr-DH	0.637	0.660	0.651	0.624	0.588	0.547	0.501
	Tr-Pitzer	0.613	0.592	0.531	0.446	0.350	0.255	0.172
K^+	FRACHEM	0.653	0.689	0.689	0.667	0.630	0.581	0.523
	Tr-DH	0.616	0.644	0.641	0.620	0.589	0.552	0.509
	Tr-Pitzer	0.603	0.589	0.563	0.531	0.495	0.452	0.402

Species	Model	20°C	50°C	80°C	110°C	140°C	170°C	200°C
Mg^{++}	**FRACHEM** [1]	0.371	0.296	0.221	0.154	0.100	0.060	0.032
	Tr-DH	0.218	0.161	0.112	0.076	0.051	0.034	0.022
	Tr-Pitzer	0.417	0.301	0.224	0.175	0.140	0.110	0.080
Na^{+}	**FRACHEM**	0.741	0.784	0.783	0.754	0.706	0.645	0.574
	Tr-DH	0.654	0.669	0.651	0.616	0.574	0.528	0.478
	Tr-Pitzer	0.691	0.675	0.639	0.597	0.548	0.494	0.433
OH^{-}	**FRACHEM**	0.431	0.411	0.380	0.340	0.293	0.244	0.197
	Tr-DH	0.774	0.753	0.698	0.631	0.564	0.498	0.434
	Tr-Pitzer	0.633	0.600	0.557	0.513	0.468	0.420	0.369
$SiO_{2(aq)}$	**FRACHEM**	1.315	1.272	1.236	1.208	1.183	1.163	1.145
	Tr-DH	1.000	1.000	1.000	1.000	1.000	1.000	1.000
	Tr-Pitzer	1.333	1.332	1.313	1.277	1.226	1.163	1.091
SO_4^{--}	**FRACHEM**	0.048	0.043	0.034	0.025	0.017	0.010	0.006
	Tr-DH	0.183	0.148	0.111	0.082	0.059	0.042	0.030
	Tr-Pitzer	0.092	0.079	0.060	0.044	0.031	0.021	0.013

[1] Activity coefficients calculated with EQ3nr (Wolery 1992) using with the Pitzer model – this species is not included in the Tequil database.
[2] In FRACHEM, aluminium is only considered under the form Al^{+3}.

Table 3-3. Computed activities (in log molal except for H_2O) as a function of temperature, using the fluid composition given in Table 3-1.

Species	Model	20°C	50°C	80°C	110°C	140°C	170°C	200°C
H_2O	FRACHEM	0.952	0.952	0.952	0.953	0.954	0.955	0.957
	Tr-DH	0.950	0.952	0.954	0.956	0.959	0.962	0.966
	Tr-Pitzer	0.949	0.949	0.948	0.949	0.950	0.951	0.953
Al^{+++}	FRACHEM [1]	-4.88	-5.05	-5.31	-5.66	-6.11	-6.67	-7.36
	Tr-DH	-5.94	-6.27	-6.76	-8.02	-9.94	-11.84	-13.71
	Tr-Pitzer	-7.60	-7.96	-8.35	-9.00	-10.20	-11.58	-13.04
AlO_2^-	Frachem[2]	/	/	/	/	/	/	/
	Tr-DH	-12.65	-9.97	-7.69	-6.50	-6.08	-5.78	-5.57
	Tr-Pitzer	-9.74	-7.74	-6.09	-5.08	-4.86	-4.87	-4.90
Ca^{++}	FRACHEM	-1.45	-1.47	-1.51	-1.58	-1.66	-1.77	-1.91
	Tr-DH	-1.69	-1.79	-1.93	-2.08	-2.24	-2.41	-2.60
	Tr-Pitzer	-2.31	-1.93	-1.68	-1.53	-1.47	-1.49	-1.60
$CaCO_{3(aq)}$	FRACHEM	-5.99	-6.04	-6.06	-6.08	-6.10	-6.13	-6.15
	Tr-DH	-8.04	-7.53	-7.15	-6.90	-6.67	-6.46	-6.28
	Tr-Pitzer	-6.45	-5.79	-5.39	-5.24	-5.24	-5.29	-5.37
$CaHCO_3^+$	FRACHEM	-18.26	-18.27	-18.28	-18.31	-18.34	-18.38	-18.44
	Tr-DH	-4.08	-4.02	-3.96	-3.92	-3.87	-3.81	-3.75
	Tr-Pitzer	-3.64	-3.26	-3.00	-2.86	-2.81	-2.81	-2.84
$CaSO_{4(aq)}$	FRACHEM	-4.24	-3.89	-3.70	-3.61	-3.60	-3.62	-3.57
	Tr-DH	-3.79	-3.84	-3.89	-3.93	-3.96	-3.98	-3.99
	Tr-Pitzer	-4.29	-3.89	-3.64	-3.48	-3.40	-3.35	-3.34
Cl^-	FRACHEM	-0.07	-0.09	-0.11	-0.15	-0.18	-0.23	-0.28
	Tr-DH	0.01	0.01	-0.02	-0.05	-0.10	-0.15	-0.21
	Tr-Pitzer	0.00	0.03	0.03	0.02	-0.01	-0.04	-0.09
$CO_{2(aq)}$	FRACHEM	-1.25	-1.25	-1.26	-1.26	-1.26	-1.27	-1.27
	Tr-DH	-1.23	-1.25	-1.26	-1.26	-1.25	-1.24	-1.24
	Tr-Pitzer	-1.30	-1.32	-1.33	-1.34	-1.33	-1.33	-1.32
CO_3^{--}	FRACHEM	-9.17	-9.09	-9.05	-9.04	-9.07	-9.11	-9.15
	Tr-DH	-9.62	-9.31	-9.13	-9.07	-9.03	-9.04	-9.11
	Tr-Pitzer	-7.41	-7.43	-7.61	-7.95	-8.37	-8.80	-9.20
Fe^{++}	FRACHEM [1]	-3.05	-3.11	-3.23	-3.40	-3.62	-3.89	-4.24
	Tr-DH	-3.36	-3.48	-3.64	-3.84	-4.11	-4.52	-5.10
	Tr-Pitzer	-3.99	-4.15	-4.32	-4.48	-4.64	-4.84	-5.08
H^+	FRACHEM	-4.44	-4.34	-4.34	-4.41	-4.54	-4.70	-4.90
	Tr-DH	-4.19	-4.20	-4.28	-4.37	-4.52	-4.70	-4.90
	Tr-Pitzer	-5.33	-5.18	-5.07	-4.97	-4.90	-4.86	-4.90
HCO_3^-	FRACHEM	-3.22	-3.23	-3.27	-3.32	-3.38	-3.47	-3.56
	Tr-DH	-3.44	-3.34	-3.31	-3.34	-3.39	-3.46	-3.55
	Tr-Pitzer	-2.37	-2.44	-2.59	-2.83	-3.10	-3.38	-3.64

Species	Model	20°C	50°C	80°C	110°C	140°C	170°C	200°C
K^+	**FRACHEM**	-1.32	-1.30	-1.30	-1.31	-1.34	-1.37	-1.42
	Tr-DH	-1.35	-1.34	-1.35	-1.38	-1.41	-1.45	-1.50
	Tr-Pitzer	-1.35	-1.36	-1.38	-1.41	-1.44	-1.48	-1.53
Mg^{++}	**FRACHEM** [1]	-2.92	-3.02	-3.15	-3.31	-3.49	-3.72	-3.99
	Tr-DH	-3.26	-3.37	-3.53	-3.70	-3.88	-4.08	-4.30
	Tr-Pitzer	-2.87	-3.02	-3.14	-3.25	-3.35	-3.45	-3.59
Na^+	**FRACHEM**	-0.07	-0.05	-0.05	-0.06	-0.09	-0.13	-0.18
	Tr-DH	-0.17	-0.17	-0.20	-0.23	-0.28	-0.33	-0.40
	Tr-Pitzer	-0.10	-0.11	-0.14	-0.17	-0.20	-0.25	-0.30
OH^-	**FRACHEM**	-9.74	-8.96	-8.29	-7.72	-7.23	-6.80	-6.43
	Tr-DH	-9.99	-9.10	-8.35	-7.75	-7.23	-6.78	-6.40
	Tr-Pitzer	-8.85	-8.12	-7.56	-7.16	-6.86	-6.62	-6.41
$SiO_{2(aq)}$	**FRACHEM**	-2.10	-2.11	-2.13	-2.14	-2.15	-2.15	-2.16
	Tr-DH	-2.22	-2.22	-2.22	-2.22	-2.22	-2.22	-2.22
	Tr-Pitzer	-2.09	-2.09	-2.10	-2.11	-2.13	-2.15	-2.18
SO_4^{--}	**FRACHEM**	-4.36	-4.44	-4.58	-4.74	-4.91	-5.13	-5.39
	Tr-DH	-4.18	-4.26	-4.35	-4.44	-4.54	-4.66	-4.81
	Tr-Pitzer	-4.07	-4.17	-4.35	-4.54	-4.75	-4.95	-5.17

[1] Activity coefficients calculated with EQ3nr (Wolery 1992) using with the Pitzer model – this species is not included in the Tequil database.
[2] In FRACHEM, aluminium is only considered under the form Al^{+3}.

3.3 DISCUSSION

The activity coefficients and the activities of dissolved species computed with the three models (FRACHEM, Tr-DH and Tr-Pitzer) are compared in Tables 3-2 and 3-3, and also plotted in Figures 3-1 and 3-2. The agreement is reasonably good for Na^+, K^+ and SiO_2; however, important divergences occur with Ca^{2+} and Mg^{2+}, primarily between simulations making use of the Pitzer formalism (FRACHEM and Tr-Pitzer) and the extended Debye-Hückel model (Tr-DH). As mentioned earlier, activities (and not activity coefficients) drive the chemical reactions. Therefore, comparing activities rather than activity coefficients is generally more instructive. However, differences in computed activities for a given species may not necessarily indicate differences in simulated chemical behavior, if the species is not a dominant one. For example, in our case, computed activities of Al^{+++} are quite different (Table 3-3) but the dominant species in the simulation is AlO_2^-, for which computed activities do not differ significantly between models (thus not significantly affecting simulation results).

Starting at pH 4.9 at 200°C, all three models predict an initial pH decrease with decreasing temperature (see the log activity of H+ in Table 3-3). However, pH values predicted with Tr-Pitzer start to increase as the temperature decreases below 150°C, and reach about 5.3 at 20°C. In contrast, pH values predicted with FRACHEM decrease to a minimum of around 4.3 at 80°C, then slightly increase to end up around 4.4 at 20°C. With the Tr-DH model, no trend reversal is observed, and the pH keeps decreasing with temperature to about 4.2 at 20°C (Table 3-3). Note that during the circulation test occurring in 1997 in Soultz, a pH of 4.8 was measured on line, after the heat exchanger outlet, at a temperature of 60–65°C (Durst, 2002). This value is within

the range of the calculated pH values, but not much below the initial pH of 4.9 at 200°C. In the real system, precipitation of aluminum silicates by cooling could take place, which would then have a tendency to drive pH up. Therefore, these simple cooling simulations are likely to underestimate pH. It should be kept in mind that mineral precipitation during cooling was intentionally suppressed, here, such that model comparisons with respect to activity coefficients could be made for identical fluid compositions. More realistic simulations of field conditions are discussed in Section 5.

At the same initial pH of 4.9 at 200°C, the range of calcite saturation indices predicted by the three models spans about 0.9 log(Q/K) units (Table 3-4), representing the difference between the Tr-Pitzer and Tr-DH models. This difference is primarily attributed to the activity coefficient of Ca^{++} (Table 3-2). The larger Ca^{++} activity coefficient (by up to one order of magnitude) computed using the Pitzer formalism, compared to the extended Debye-Hückel equation, translate to about the same range in Ca^{++} activity increase (Table 3-3), and thus to a solubility decrease of close to 1 log(Q/K) unit at 200°C. The difference in calcite saturation index computed by TR-Pitzer and FRACHEM is only about 0.3 log(Q/K) units at 200°C. These differences at 200°C increase at lower temperatures (Table 3-3), as a result of the pH differences discussed above, which are themselves also the result of activity coefficient effects. For all three models, however, a similar trend of decreasing calcite log(Q/K) values (increasing solubility) with decreasing temperature is observed (Table 3-4, see also Figure 3-3). This is consistent with literature data (e.g., Ellis, 1963; Newton and Manning, 2002) indicating retrograde calcite solubility in pure water and NaCl solutions.

The fluid saturation with respect to quartz was also investigated (Table 3-4). Results show minor differences in the quartz solubilities computed by Tr-Pitzer and Tr-DH at all temperatures, even though Tr-DH assumes a unit activity coefficient for $SiO_{2(aq)}$. These two models, however, predict significantly lower solubility than FRACHEM at low temperature, the result of differences in input solubility data (Section 5). Note that quartz precipitation at temperatures below about 150°C becomes increasingly kinetically retarded, such that the variability of solubility data at low temperature has not much bearing on the results of THC simulations such as those presented later in Section 6.

Table 3-4. Saturation Index of quartz and calcite minerals computed as a function of temperature, using the fluid composition given in Table 3-1.

		Log (Q/K)					
		50°C	**80°C**	**110°C**	**140°C**	**170°C**	**200°C**
Calcite	**Tr-DH**	-2.41	-2.00	-1.68	-1.34	-1.000	-0.672
	Tr-Pitzer	-0.670	-0.250	-0.020	0.093	0.165	0.237
	FRACHEM	-1.66	-1.32	-0.960	-0.611	-0.287	0.000
Quartz	**Tr-DH**	1.23	0.937	0.689	0.483	0.311	0.166
	Tr-Pitzer	1.36	1.056	0.796	0.572	0.377	0.204
	FRACHEM	0.355	0.166	0.008	-0.125	-0.241	-0.343

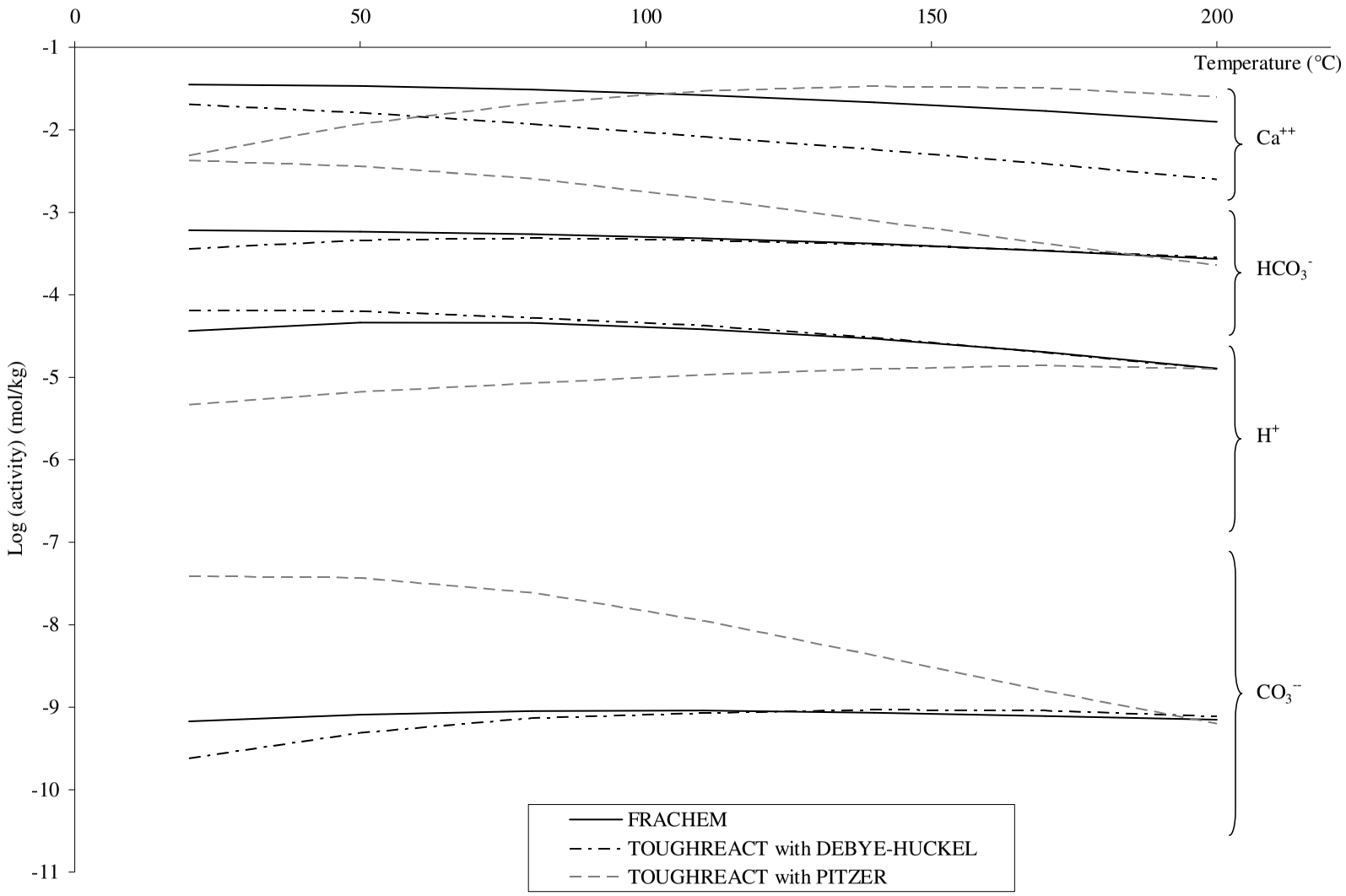

Figure 3-1. Evolution of logarithm of activities with temperature for selected dissolved species: Ca^{++}, HCO_3^-, H^+ and CO_3^{--}. For each species, activities have been computed with FRACHEM (black continuous lines), Tr-DH (black dashed lines) and Tr-Pitzer (grey dashed lines).

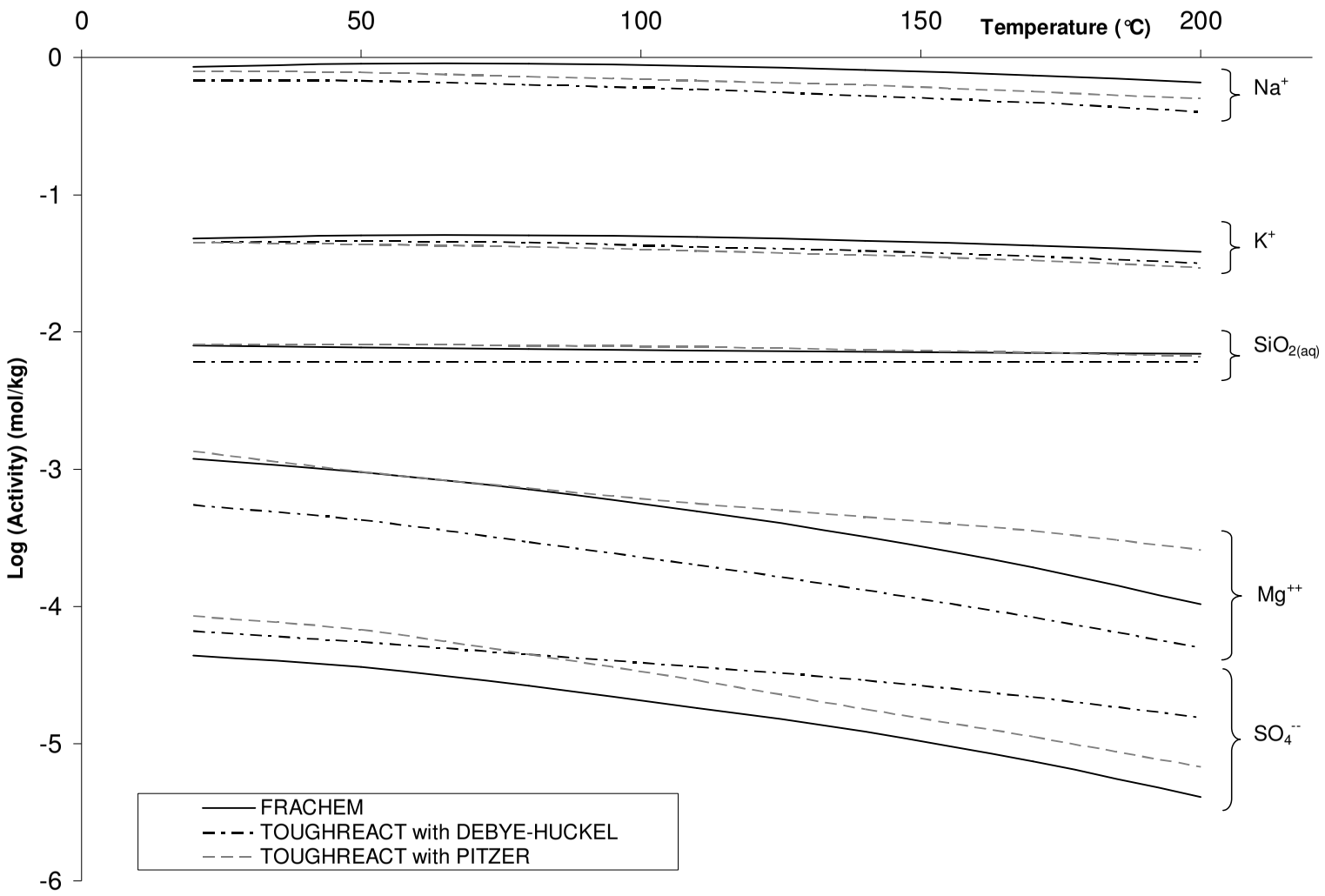

Figure 3-2. Evolution of logarithm of activities with temperature for selected dissolved species: Na+, K+, SiO2, Mg++ and SO4--. For each species, activities have been computed with FRACHEM (black continuous lines), Tr-DH (black dashed lines) and Tr-Pitzer (grey dashed lines).

To further investigate the predicted trends of pH and calcite saturation with temperature, the same simple cooling simulation (without mass transfer to minerals or gases) was repeated with several other popular geochemical codes, with thermodynamic databases and activity coefficient models as follows:

- PHREEQC 2.12 (Parkhurst and Appelo, 1999) with the following databases (as released with version 2.12): *phreeqc.*dat *431 2005-08-23* with the Davies equation; *llnl.dat 85 2005-02-0* with the extended Debye-Hückel equation; and the Pitzer model implemented with database *pitzer.dat 2005-11-16*.
- EQ3/6 8.0 (Wolery and Jareck, 2003) with (1) the "b-dot" extended Debye-Hückel model of Helgeson (1969) and database *data0.ymp*; (2) the Pitzer model and database *data0.hmw* (after Harvie et al., 1984); and (3) the Pitzer model and the same revised *data0.ypf* database as used with Tr-Pitzer (Wolery et al., 2004, as published in Alai et al. (2005) except for revisions to $CO_{2(aq)}$ ion interaction parameter after Rumpf et al. 1994 and Rumpf and Maurer 1993).
- SOLVEQ/CHILLER (Reed, 1998; Reed and Spycher, 1998), which incorporates the extended Debye-Hückel model of Helgeson et al. (1981) and the same equilibrium constants as used with Tr-DH (SUPCRT92, Johnson et al., 1992).

These codes were applied to the same fluid composition as used with the three other models (FRACHEM, Tr-DH and Tr-Pitzer) (Table 3-1) with an input brine pH of 4.9 at 200ºC. However, in this case, the minor components Al, Fe, and Mg were excluded from the system, such that TEQUIL could be used directly (in place of FRACHEM). Note that the calcite equilibrium constant is nearly the same in all the databases considered (Section 5). It was also verified that only those secondary aqueous species called for by the different activity coefficient models were included in simulations.

The most remarkable parameters, pH and calcite saturation index (Figure 3-3) show significant variations. Using the Pitzer formalism, some divergences appear with the use of different ion-interaction parameters. The results of EQ3/6 with the revised *data0.ypf* Pitzer database closely match the TR-Pitzer results, as expected because both models make use of the same database. Therefore, the trend of mostly increasing pH with decreasing temperature computed with Tr-Pitzer is confirmed by the EQ3/6 results. Both models also predict lower calcite solubilities than TEQUIL (typically by about 0.5 log(Q/K) units) (Figure 3-3). Nevertheless, all models yield a consistent trend of calcite retrograde solubility. Because of similarities between databases, EQ3/6 with the Harvie et al. (1984) Pitzer database yield results fairly close to those of TEQUIL. EQ3/6 with the "b-dot" model also matches surprisingly well the results of TEQUIL. The same extended Debye-Hückel equation and parameters are implemented in Tr-DH and SOLVEQ/CHILLER, and therefore the results of both these models match closely. Note that the results from the PHREEQC-Pitzer model are more in line with the Debye-Hückel models, whereas the standard PHREEQC model (Davies equation) matches somewhat more closely the TR-Pitzer results (Figure 3-3). Although this may seem counterintuitive, these differences result from the fact that the Davies equation typically predicts a sharper rise in activity coefficient values at elevated ionic strength compared to the other extended Debye-Hückel models (e.g., Langmuir 1997). Also, the Pitzer ion-interaction parameters in the PHREEQC Pitzer database are temperature-independent and therefore not really applicable here.

These results illustrate the importance of activity coefficients when dealing with concentrated solutions. The variation of activity coefficients with temperature is critical and often the weak point of Pitzer databases available from the literature. For example, in some databases, ion-interaction parameters may be set to 0 or fixed values for different temperatures. Avoiding "double counting" between interaction parameters and secondary species is also critical. Even with the simpler Debye-Hückel model, it is important to keep consistency between the data used to compute activity coefficients and the types of secondary aqueous species and their dissociation constants. For application to Soultz-type concentrated fluids at elevated temperatures, a Pitzer approach is definitely favored, with preference given to the TEQUIL database because it was developed specifically for geothermal applications at moderate ionic strengths. The relatively recent EQ3/6 database *data0.ypf*, as revised in this study, is expected to be most accurate for applications below 150°C and very high ionic strengths. As shown later, for reactive transport simulations of the Soultz system, differences in computed calcite solubility using these different databases can be partly offset by specifying initial conditions of fluid saturation with respect to calcite in the reservoir. This is accomplished by adjusting pH, bicarbonate, and/or calcium concentrations, whichever has highest uncertainty, to reflect initial saturation of the fluid with respect to calcite. In this respect, the conceptual model is just as important as the thermodynamic data input into the numerical model.

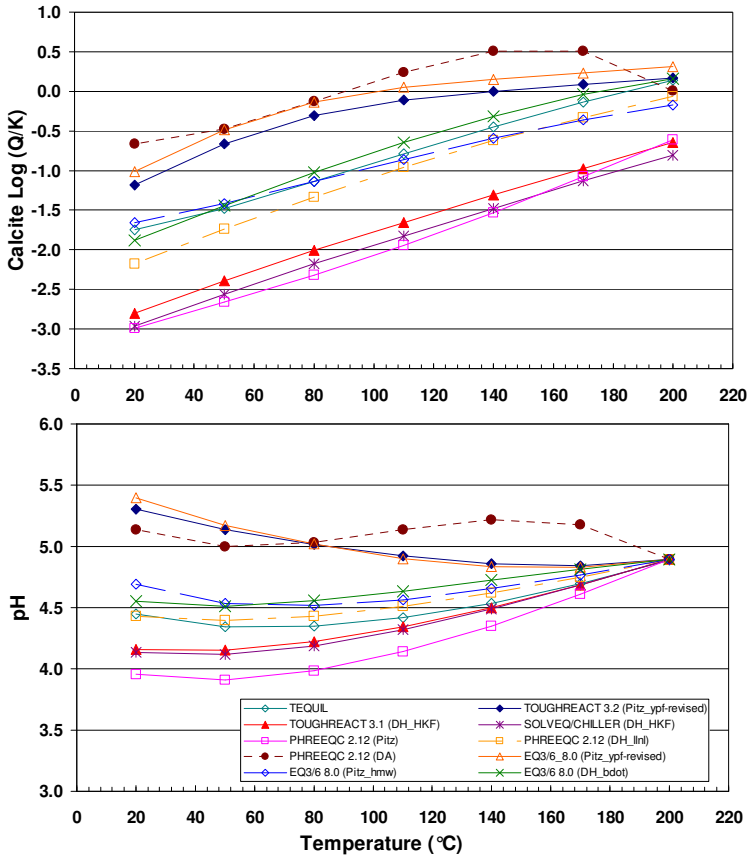

Figure 3-3. Cooling simulation of a Soultz-type fluid (Table 3-1): calcite saturation index and pH predicted as a function of temperature, using various codes and thermodynamic databases (see text). To keep the fluid composition identical in all cases (except for H+, which is set by specifying a pH of 4.9 at 200°C), no minerals are allowed to form during cooling.

4 THE KINETIC RATE LAWS

4.1 FRACHEM

A general kinetic model has been adopted to explain the dissolution/precipitation reactions of minerals. Its overall form is the transition state theory (TST)-derived equation (e.g., Lasaga et al., 1994) expressed as

$$v = k_m s_m \left(1 - \left(\frac{Q_m}{K_m} \right)^{\mu} \right)^{n} \qquad \text{Eq. 1}$$

where v is the reaction rate (mol s^{-1} kg_{water}^{-1}), k_m is the rate constant (mol s^{-1} m^{-2}), s_m is the surface area of mineral in contact with fluid (m^2 kg_{water}^{-1}), μ and η are positive empirical parameters, and Q_m and K_m are the ion activity product and equilibrium constant for the mineral reaction, respectively. Positive values of v correspond to dissolution rates, whereas negative values refer to precipitation rates. In FRACHEM, rate laws more or less following Equation 1 were specifically coded for each mineral, using published parameters (k_m, μ and η) determined from experimental data obtained at high temperature in NaCl brines (Table 4-1).

Table 4-1. Mineral dissolution and precipitation rates used in FRACHEM

Reaction rates laws	**sources**
Calcite dissolution rate $r_d = \left(1.643 \times 10^{-1}\ a_{H^+} + 1.11 \times 10^{-5}\right) \frac{T}{321.15} \left[\exp\left(\frac{(T - 321.15)(-151.94 \ln(a_{H^+}) + 545.91)}{321.15\, T} \right) \right] s \left(1 - \frac{Q}{K}\right)$ Eq. 2	Sjöberg & Rickard (1984)
Calcite precipitation rate $r_p = 1.927 \times 10^{-2}\ T \exp\left(\frac{-41840}{RT}\right) s \left(\frac{Q}{K} - 1\right)^{1.93}$ *for* $\frac{Q}{K} < 1.72$ Eq. 3 $r_p = 1.011\, T \exp\left(\frac{-41840}{RT}\right) s \exp\left(-\frac{2.36}{\ln\left(\frac{Q}{K}\right)}\right)$ *for* $\frac{Q}{K} > 1.72$ Eq. 4	Shiraki & Brantley (1995)
Dolomite dissolution rate $r_d = 10^{(-0.0436\ pH^2 - 0.5948\ pH - 2.0509)} \frac{T}{353.15} \left[\exp\left(\frac{(972\ pH - 5951)(353.15 - T)}{353.15\ T} \right) \right] s \left(1 - \frac{Q}{K}\right)$ Eq. 5	Gautelier et al. (1999)
Dolomite precipitation rate $r_p = 1.122 \times 10^{5} \exp\left(\frac{-16060}{T}\right) s \left(\frac{Q}{K} - 1\right)^{2.26}$ Eq. 6	Arvidson & Mackenzie (1999)

Reaction rates laws		**sources**
Quartz dissolution rate $r_d = \left[\begin{array}{l} \exp(-10.7)\ T \exp\left(\frac{-66000}{RT}\right)\theta_{>SiOH} + \\ \exp(4.7)\ T \exp\left(\frac{-82700}{RT}\right)\left(\theta_{>SiO^-_{tot}}\right)^{1.1} \end{array} \right] s\left(1-\frac{Q}{K}\right)$ with $\theta_{>SiOH} = 1.055768 - 4.464707\times10^{-2}\,pH + 1.224392\times10^{-2}\,pH^2 - 1.168033\times10^{-3}\,pH^3$ $\theta_{>SiO^-_{tot}} = 1-\theta_{>SiOH}$	Eq. 7	Dove & Rimstidt (1994)
Quartz precipitation rate $r_p = \left[a^2_{H_2O} \exp\left(\left(1.174 - 2.028\text{x}10^{-3}\ T - \frac{4158}{T}\right)\ln 10\right)\right] s\left(\frac{Q}{K}-1\right)$	Eq. 8	Rimstidt & Barnes (1980)
Pyrite dissolution rate $r_d = 3.23\text{x}10^{6} \exp(-0.0455\ T)\exp\left(\frac{-65000}{RT}\right) s\left(1-\frac{Q}{K}\right)$	Eq. 9	Williamson & Rimstidt (1994)
Pyrite precipitation rate $r_p = \frac{K_{FeS}}{K_{H_2S}} a_{Fe}\ a^2_{HS} \left(\frac{256.797}{T} - 0.534\right)\exp\left(\frac{-34140}{RT}\right)\ s\left(\frac{Q}{K}-1\right)$	Eq. 10	Rickard (1997) Rickard & Luther (1997)
Amorphous silica dissolution rate $r_d = 10^{\left(0.82191-\frac{3892.3}{T}\right)}\ a_{SiO_2}\ a^2_{H_2O}\ s\left(1-\frac{Q}{K}\right)$	Eq. 11	Rimstidt & Barnes (1980) Icenhower & Dove (2000)
Amorphous silica precipitation rate $r_p = 3.8\text{x}10^{-10} \exp\left(\frac{-50000}{R}\left(\frac{1}{T}-\frac{1}{298.15}\right)\right) s\left(\left(\frac{Q}{K}\right)^{4.4} - \frac{1}{\left(\frac{Q}{K}\right)^{8.8}}\right)$	Eq. 12	Rimstidt & Barnes (1980) Xu et al. (2004b) Carroll et al. (1998)
K-Feldspar dissolution rate $r_d = 5.25\text{x}10^{-6} \exp\left(\frac{-51700}{RT}\right)\left[\frac{10^{-0.97} a_{H^+}}{1+10^{-0.97} a_{H^+} + 10^{3.04} a_{Na^+}}\right]^{0.5} s\left(1-\frac{Q}{K}\right)$	Eq. 13	Stillings & Brantley (1995) Blum & Stillings (1995)
K-Feldspar precipitation rate $r_p = 10^{-12} \exp\left(\frac{-67830}{R}\left(\frac{1}{T}-\frac{1}{298.15}\right)\right) s\left(\frac{Q}{K}-1\right)$	Eq. 14	Blum & Stillings (1995)
Albite dissolution rate $r_d = 0.35 \exp\left(\frac{-89000}{RT}\right)\left[\frac{10^{-0.97} a_{H^+}}{1+10^{-0.97} a_{H^+} + 10^{3.04} a_{Na^+}}\right]^{0.5} s\left(1-\frac{Q}{K}\right)$	Eq. 15	Stillings & Brantley (1995) Hellmann (1994)

Reaction rates laws	sources
Albite precipitation rate $r_p = 10^{-12} \exp\left(\frac{-67830}{R}\left(\frac{1}{T} - \frac{1}{298.15}\right)\right) s\left(\frac{Q}{K} - 1\right)$ Eq. 16	Blum & Stillings (1995)
Illite dissolution rate $r_d = \left[2.2\text{x}10^{-4} \exp\left(\frac{-46000}{RT}\right) a_{H^+}^{0.6} + 2.5\text{x}10^{-13} \exp\left(\frac{-14000}{RT}\right)\right] s\left(1 - \frac{Q}{K}\right)$ Eq. 17	Köhler et al. (2003)
Illite precipitation rate $r_p = 1.1638\ T \exp\left(\frac{-117000}{RT}\right) s\left(\frac{Q}{K} - 1\right)^2$ Eq. 18	Nagy et al. (1991)

* R is the gas constant (= 8.314 J mol^{-1} K^{-1}) and T the temperature in Kelvin

4.2 TOUGHREACT

Equation 1 (TST kinetic rate law) is implemented into TOUGHREACT in a generic form, and rate parameters are input into the model for each mineral. The variation of the rate constant with temperature is implemented through the Arrhenius equation:

$$k = k_{298.15} \exp\left[\frac{-E_a}{R}\left(\frac{1}{T} - \frac{1}{298.15}\right)\right] \qquad \text{Eq. 19}$$

where E_a is the activation energy, $k_{298.15}$ is the rate constant at 25°C, R is the gas constant and T is the absolute temperature in Kelvin. Equation 19 does not consider pH effects, and is generally applied at neutral pH (neutral mechanism). Because dissolution and precipitation processes can be affected by H^+ (acid mechanism) or OH^- (base mechanism), the full rate law expression for these cases is implemented as

$$k = k_{25}^{nu} \exp\left[\frac{-E_a^{nu}}{R}\left(\frac{1}{T} - \frac{1}{298.15}\right)\right] + k_{25}^{ac} \exp\left[\frac{-E_a^{ac}}{R}\left(\frac{1}{T} - \frac{1}{298.15}\right)\right] a_{H+}^{n_{ac}} + k_{25}^{ba} \exp\left[\frac{-E_a^{ba}}{R}\left(\frac{1}{T} - \frac{1}{298.15}\right)\right] a_{H^+}^{n_{ba}} \qquad \text{Eq. 20}$$

where the subscripts *nu*, *ac* and *ba* indicate neutral, acid and base mechanisms, respectively and a_{H+} is the activity of hydrogen ion. The values of the different parameters have been compiled for many minerals by Palandri and Kharaka (2004), using the data sources shown in Table 4-2.

Table 4-2. Mineral dissolution rate parameters used in TOUGHREACT simulations. Parameters for the neutral mechanism are also used to describe mineral precipitation rates.

	Acid mechanism				Neutral mechanism			Base mechanism		
	Log *k*	*E*	*n*	*m*	Log *k*	*E*	*p*	Log *k*	*E*	*n*
Calcite[1]	-0.30	14.4	1.000	--	-5.81	23.5	--	-3.48	35.4	1.000
Sedimentary dolomite[2]	-3.19	36.1	0.500	--	-7.53	52.2	--	-5.11	34.8	0.500
Hydrothermal dolomite[2]	-3.76	56.7	0.500	--	-8.60	95.3	--	-5.37	45.7	0.500
Pyrite[3]	-7.52	56.9	-0.500	0.500	-4.55	56.9	0.500	--	--	--
Quartz[4]	--	--	--	--	-13.99	87.7	--	--	--	--
Amorphous silica[4]	--	--	--	--	-12.14	62.9	--	--	--	--
K-feldspar[5]	-10.06	51.7	0.500	--	-12.41	38.0	--	-21.20	94.1	-0.823
Albite[6]	-10.16	65.0	0.457	--	-12.56	69.8	--	-15.60	71.0	-0.572
Illite[7]	-10.98	23.6	0.340	--	-12.78	35.0	--	-16.52	58.9	-0.400

Log_{10} rate constant *k* fitted to Eq. 20 at 25°C (assuming $a_{H+} = 1$) expressed in mol m^{-2} s^{-1} (Palandri and Kharaka, 2004)
E = Arrhenius activation energy ($kJ.mol^{-1}$)
n = Reaction order with respect to H^+
m = Reaction order with respect to Fe^{+++}
p = Reaction order with respect to O_2
[1] Plummer et al. (1978) and Talman et al. (1990); [2]Busenberg and Plummer (1982); [3]McKibben and Barnes (1986); [4]Icenhower and Dove (2000); [5]Blum and Stillings (1995), Helgeson et al. (1984), Bevan and Savage (1989), Gautier et al. (1994), and Knauss and Copenhaver (1995); [6]Chou and Wollast (1985), Hellman (1994); [7]Bauer and Berger (1998), Huertas et al. (2001), Sverdrup (1990) and Zysset and Schindler (1996).

4.3 COMPARISON AND INTERPRETATION

As presented above, FRACHEM and TOUGHREACT make use of TST-type rate laws, but these laws do not take exactly the same form in both codes. Most often, the rate laws and parameters implemented into FRACHEM were established specifically for high-salinity and/or high-temperature fluids most relevant to the reservoir conditions at Soultz. Rate laws for all minerals incorporate a dependence on temperature. Other specific dependencies are implemented for certain minerals. For the carbonates, the dissolution equation depends on pH, whereas for quartz, we note the influence of salinity through the water activity. For the feldspars group, dissolution rates are a function of Na^+, which plays an inhibitor role in the dissolution of these minerals (Stillings and Brantley, 1995). In TOUGHREACT, one generic equation is used incorporating different mechanisms which are activated or not depending on the mineral considered. In this study, no dependencies on the concentration of species other than H^+ (Equation 20) are applied (Table 4-2).

Rates computed according to these different rate laws as a function of temperature are compared in Figures 4-1 through 4-8, and discussed in separate subsections below. The comparisons were done for pH 5, assuming unit surface areas and no limitation from the affinity term (i.e., $[1- Q/K] \approx 1$). Concentrations of species required in some rate laws were fixed at values representative of field conditions, as discussed below. For each mineral, both the precipitation and dissolution rates are shown on the same plot, using opposite directions on the Y axis. The FRACHEM

results are shown by continuous lines; the TOUGHREACT results are displayed with dashed lines.

4.3.1 Calcite – Quartz – Amorphous silica

For these three minerals, the two codes give results that are in fairly good agreement (Figures 4-1, 4-2 and 4-3). The differences in rates do not exceed 1.5 orders of magnitude, except for the case of the calcite precipitation rate if a saturation index exceeding 1.72 is supposed. In this case, an alternative precipitation rate is applied with FRACHEM (Eq. 4, Table 4-1), yielding a rate about 3 orders of magnitude larger (Figure 4-1) than when the saturation index is < 1.72.

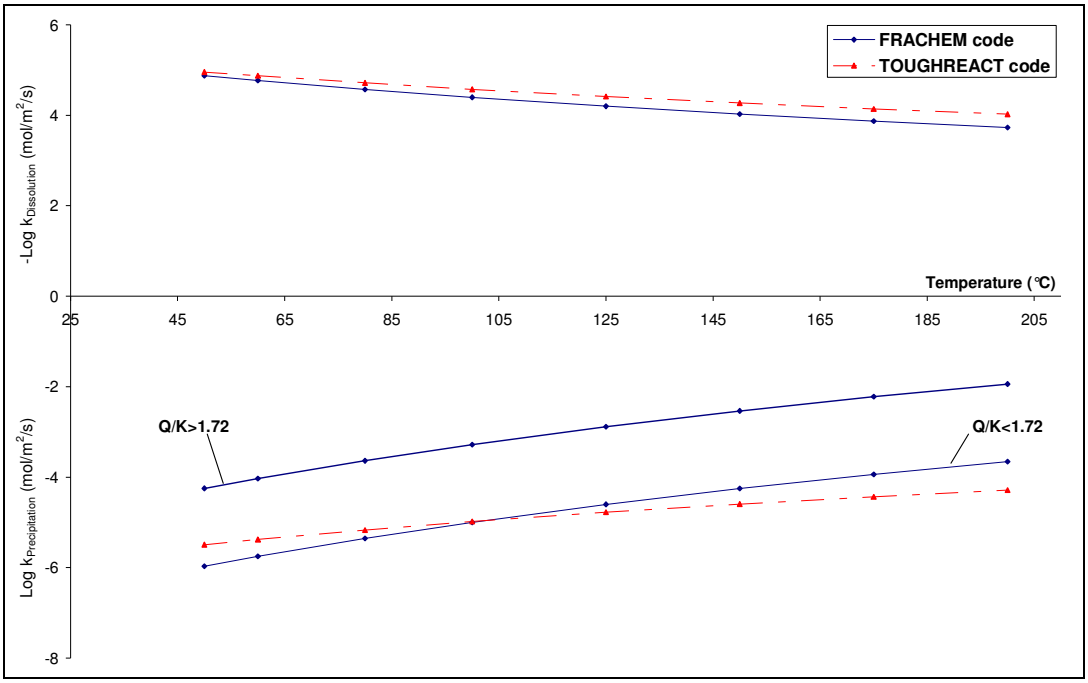

Figure 4-1. Calcite precipitation rate (bottom) and dissolution rate (top) at pH 5 (see text).

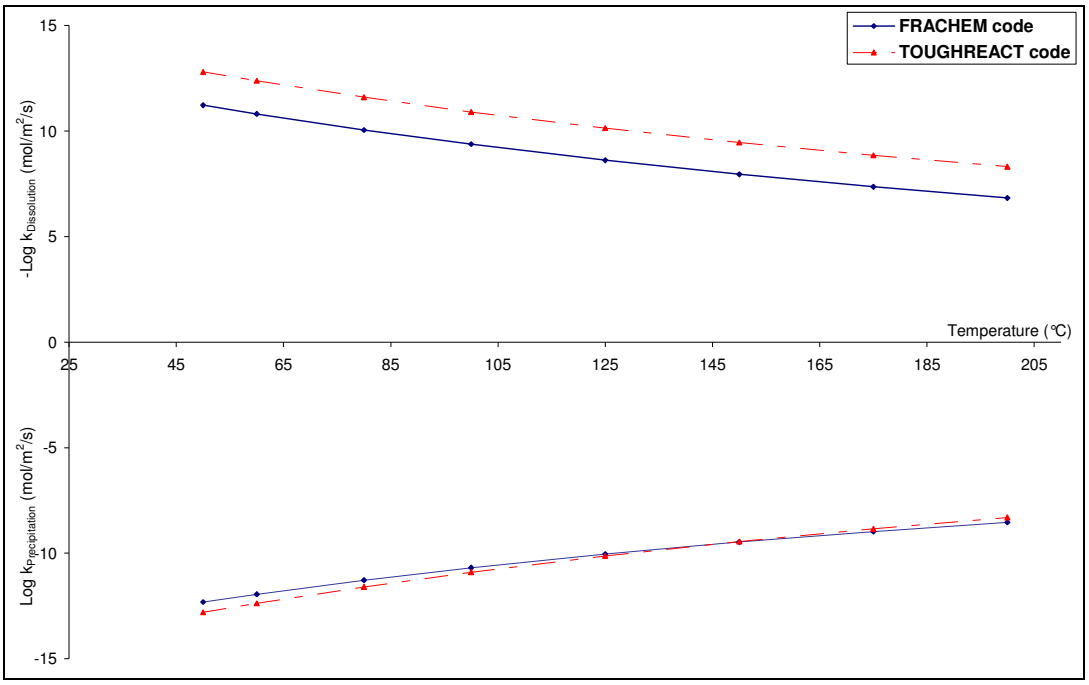

Figure 4-2. Quartz precipitation rate (bottom) and dissolution rate (top) at pH 5 (see text).

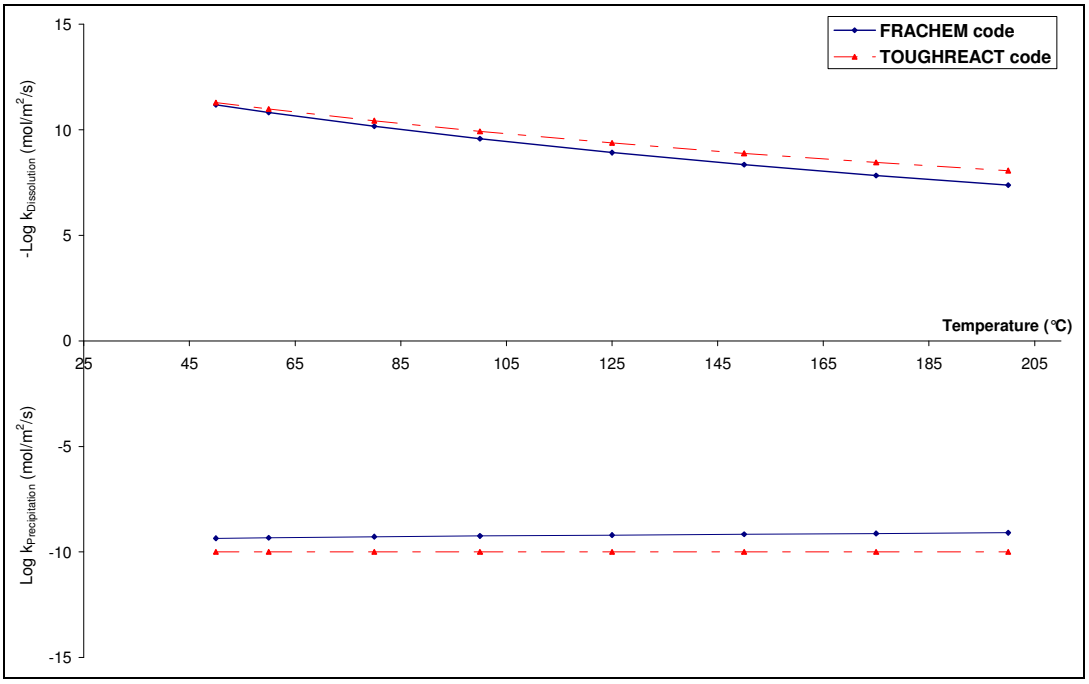

Figure 4-3. Amorphous silica precipitation rate (bottom) and dissolution rate (top) at pH 5 (see text).

4.3.2 Aluminosilicates

For K-feldspar (Figure 4-4) the precipitation and dissolution rates computed by both codes differ by 2–3 orders of magnitude. This difference is explained in part by the different activation energies used in the two codes (67.83 $kJ.mol^{-1}$ with FRACHEM and 38 $kJ.mol^{-1}$ with TOUGHREACT). The albite precipitation rates are in good agreement (Figure 4-5); however, the albite dissolution rates differ by about 2 orders of magnitude. This discrepancy can be explained by the fact that, with FRACHEM, the inhibitor effect of Na^+ is taken into consideration (concentration of 1.2 molal assumed here), whereas it is not with TOUGHREACT. Differences in pH dependence also affect model results. For illite (Figure 4-6), similar differences around 2–3 orders of magnitude are mainly caused by differences in activation energies, as well as in the exponent applied to H^+ activity (0.6 with FRACHEM, 0.34 with TOUGHREACT).

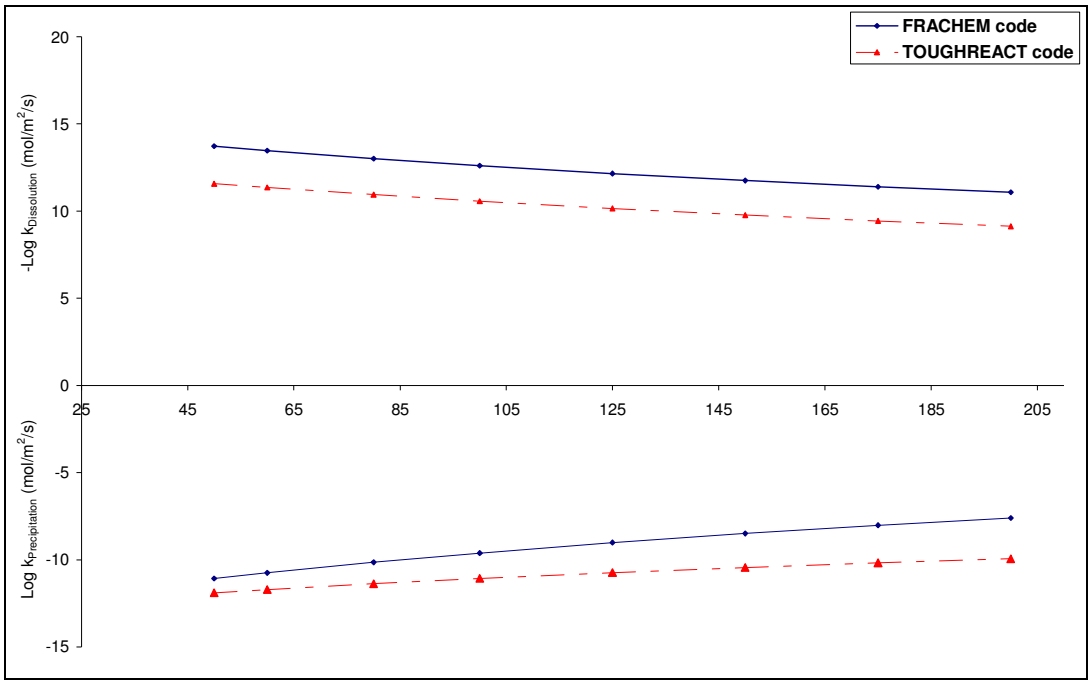

Figure 4-4. K-feldspar precipitation rate (bottom) and dissolution rate (top) at pH 5 (see text).

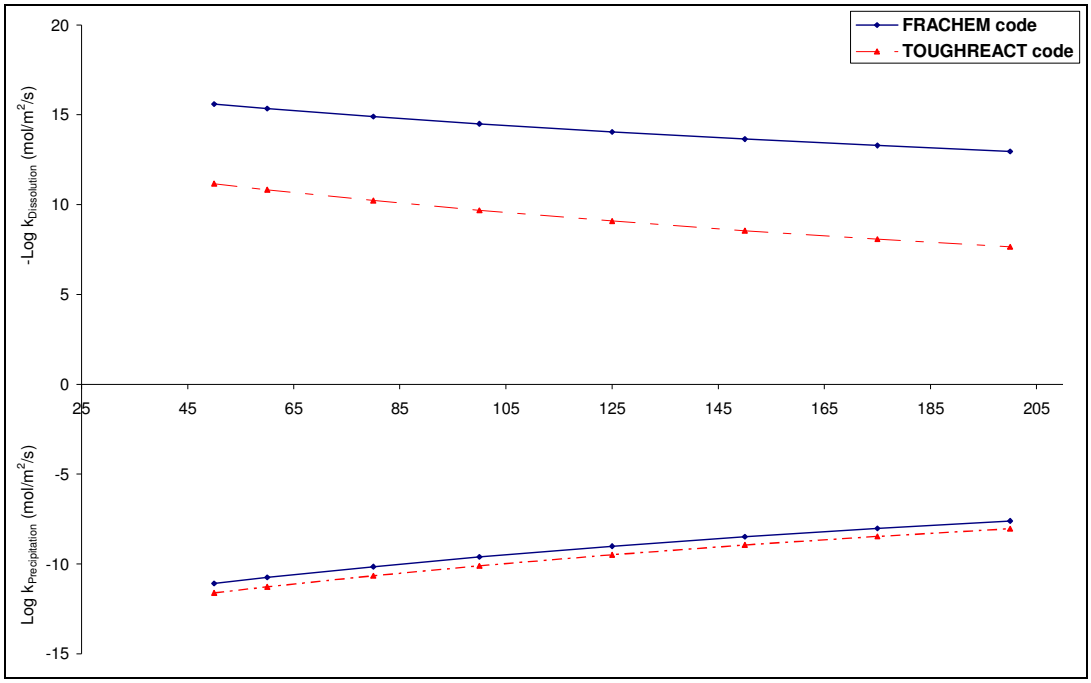

Figure 4-5. Albite precipitation rate (bottom) and dissolution rate (top) at pH 5 and Na^+ concentration of 1.2 molal (see text).

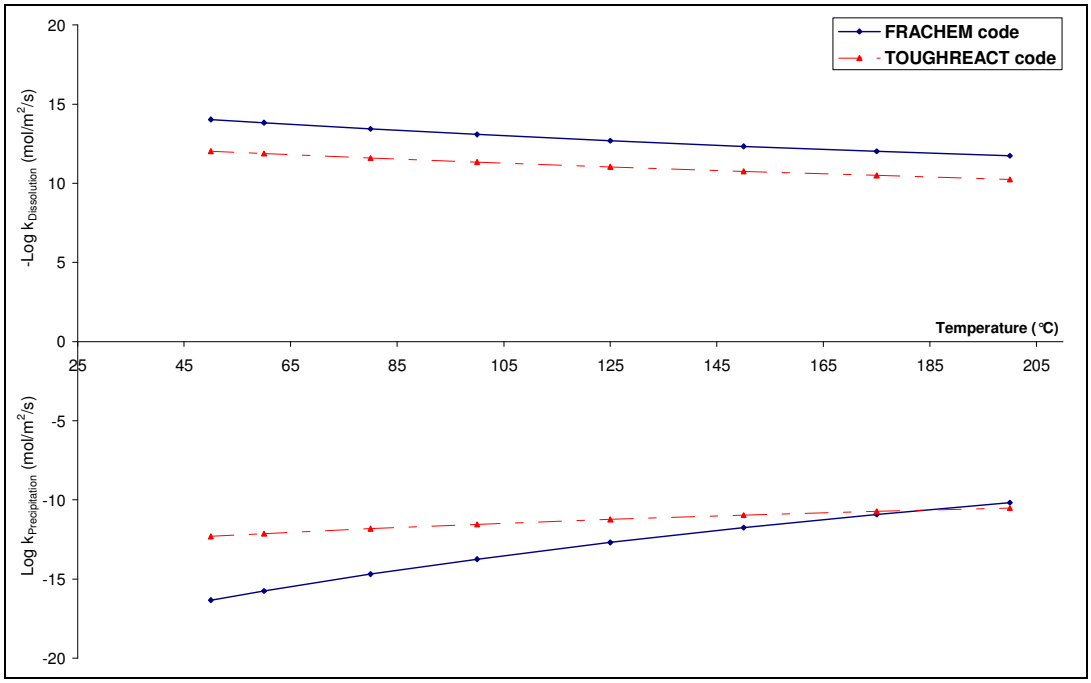

Figure 4-6. Illite precipitation rate (bottom) and dissolution rate (top) at pH 5 (see text).

4.3.3 Dolomite – Pyrite

These two minerals show the most marked differences. For dolomite, the spread between models can reach 4 and 10 orders of magnitude, for dissolution and precipitation, respectively, regardless of the type of dolomite considered (hydrothermal or sedimentary, Table 4-2). The dolomite dissolution-rate parameters used in FRACHEM were extrapolated from experimental results reported by Gautelier et al. (1999) at pH -0.39 to 4.4 and temperatures between 25 and 80°C. The dissolution rates obtained with these parameters are in good agreement with the TOUGHREACT results at low temperatures (Figure 4-7). However, large differences appear at high temperatures, which seems to indicate an inappropriate extrapolation method. The very large differences in precipitation rates are more puzzling. The dolomite precipitation-rate law implemented in FRACHEM comes from Arvidson and Mackenzie (1999), who experimentally determined rates between 100 and 200°C and for pH ranging from 4.8 to 7. Nevertheless, the accuracy of this rate is apparently questionable because of dolomite precipitation competing with magnesian calcite formation. This could explain why this reaction rate was quite underestimated when compared to the rates used with TOUGHREACT.

Dissolution and precipitation reactions of pyrite (Figure 4-8) are governed by many processes and factors including pH, O_2/sulfide levels and Fe^{++} concentration. The pyrite precipitation rate law implemented into FRACHEM (Table 4-1) incorporates HS^- and Fe^{++} concentrations (assumed here at 1 and 2.5 millimolal at pH 5, respectively), whereas a simpler rate law is applied for dissolution (Table 4-1). In contrast, the rate law used with TOUGHREACT (McKibben and Barnes, 1986) is the same for precipitation and dissolution, and was determined for pyrite dissolution at pH 1–2 and temperature of 30°C.

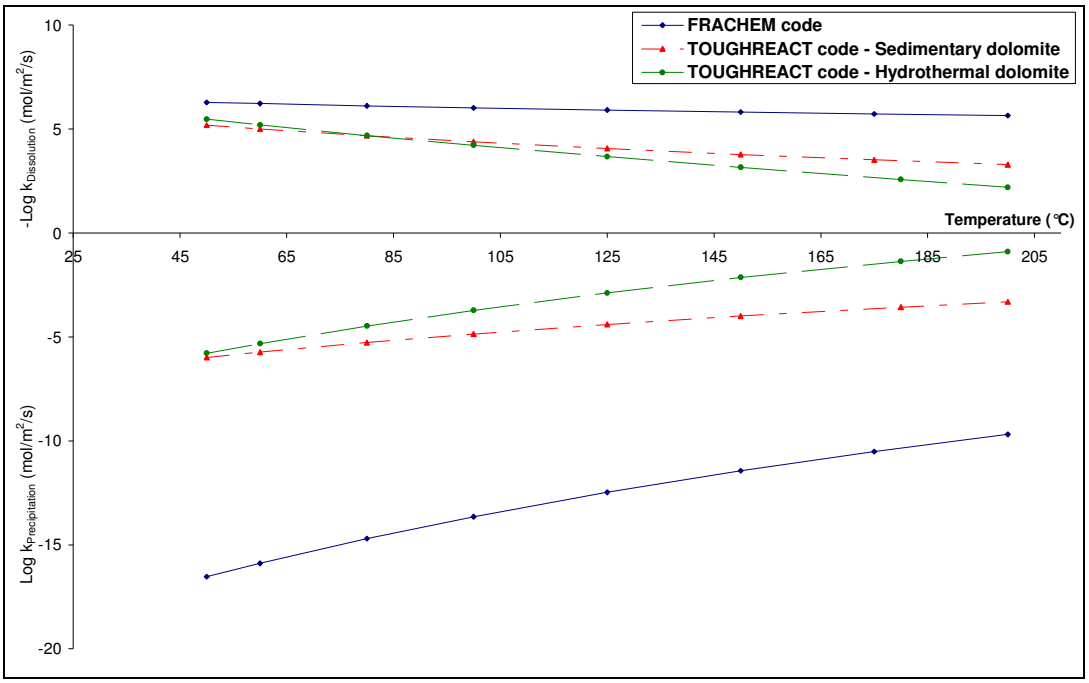

Figure 4-7. Dolomite precipitation rate (bottom) and dissolution rate (top) at pH 5 (see text).

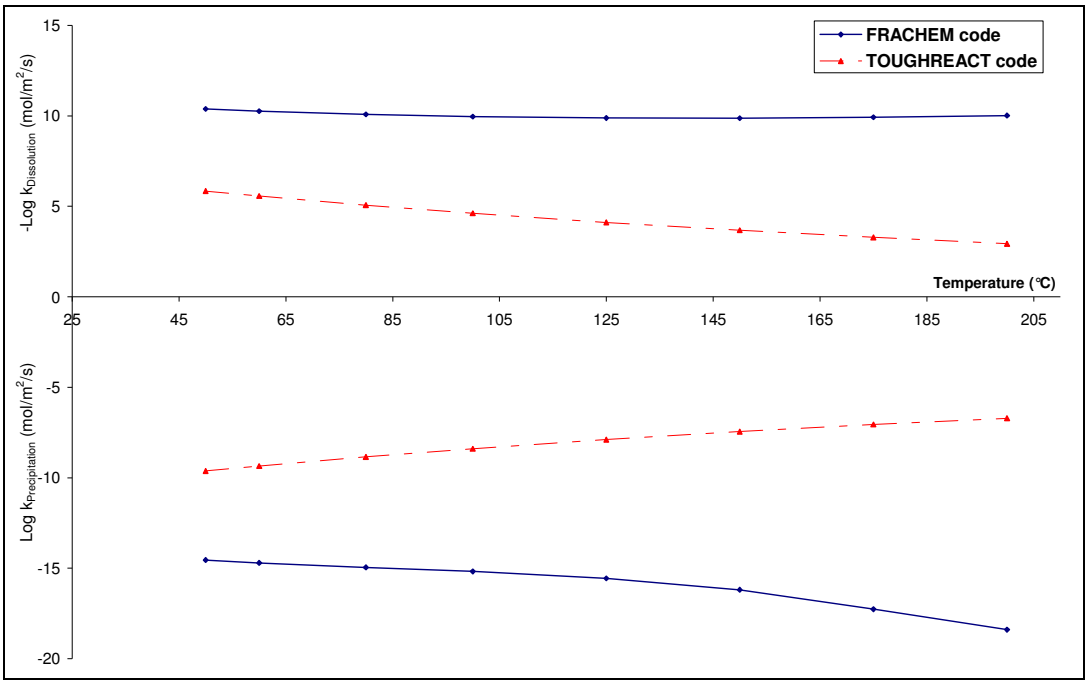

Figure 4-8. Pyrite precipitation rate (bottom) and dissolution rate (top) at pH 5, 2.5×10^{-3} molal Fe^{++}, and 10^{-3} molal HS^- (see text).

.

5 EQUILIBRIUM CONSTANTS

In this section, we compare the equilibrium constants used in the FRACHEM and TOUGHREACT simulations. It should be recalled here that for the case of TOUGHREACT, these equilibrium constants are read from a separate (code-independent) thermodynamic database. Comparisons of all thermodynamic data in this database with corresponding data implemented into FRACHEM are beyond the scope of this study. For this reason, only data for key minerals are compared here. The full TOUGHREACT database used in the present study (*thermXu4-ns.dat*) consists primarily of equilibrium constants derived using SUPCRT92 (Johnson et al., 1992) with input thermodynamic properties in the SUPCRT92 database *sprons96.dat*. Essentially the same data are used in FRACHEM, except as discussed below. One main difference between the codes is that the effect of pressure on equilibrium constants is explicitly taken into account with FRACHEM. With TOUGHREACT, the thermodynamic database is created for a given pressure (or pressure curve), and only the temperature effect is considered in the course of a simulation. In the present case, the thermodynamic data were derived for pressures along the water-pressure saturation curve at temperatures above 100°C, and at 1 bar at temperatures below 100°C. The equilibrium constants input into FRACHEM were initially computed along the same water-saturation pressure curve, however, these constants are recomputed with changes in pressure during run time as discussed further below.

5.1 COMPARISONS FOR SELECTED MINERALS

Equilibrium constants (as log(K) values) for key minerals are compared in Table 5-1. For each mineral, the first record in this table corresponds to the reactants (negative stoichiometric coefficients) and products (positive stoichiometric coefficients) of the mineral dissolution reaction. The second and third records give the logarithmic values (base 10) of the equilibrium constants used with FRACHEM and TOUGHREACT, respectively, for the dissolution reaction shown. Data sources are also included in Table 5-1.

It should be noted that, in the TOUGHREACT database, aqueous silica is considered in the form of $SiO_{2(aq)}$. With FRACHEM, it is considered in the form of H_4SiO_4. By convention, the log(K) for the reaction $H_4SiO_4 = 2H_2O + SiO_{2(aq)}$ is zero, such that the log(K) values for quartz and amorphous silica reported in Table 5-1 for both codes correspond to equivalent (effectively the same) reactions.

The equilibrium constants of aluminium silicate minerals in the TOUGHREACT database are expressed in terms of AlO_2^- and $SiO_{2(aq)}$, whereas reactions in terms of Al^{3+} and H_4SiO_4 are used in FRACHEM. To better compare the equilibrium constants between both codes, we converted the TOUGHREACT data to reactions in terms of Al^{3+} and H_4SiO_4, using the convention discussed above for silica and log(K) data used by TOUGHREACT for the reaction $Al^{3+} + 2H_2O = 4H^+ + AlO_2^-$ (from SUPCRT92).

Table 5-1. Comparison of equilibrium constant values for selected minerals used in FRACHEM and TOUGHREACT simulations. The dissolution reaction is placed in front of each mineral, with negative coefficients corresponding to the reactants, and positive coefficients corresponding to products. The calculations are made at 1 bar up to 100°C, and at saturation vapor pressure for T > 100°C.

Temperature (°C)	**0**	**25**	**60**	**100**	**150**	**200**	**250**
Calcite	-1.00 H^+	1.00 Ca^{2+}	1.00 HCO_3^-				
Log K (FRACHEM)[a]	2.227	1.847	1.334	0.775	0.099	-0.583	-1.326
Log K (TREACT)[a]	2.226	1.849	1.333	0.774	0.100	-0.584	-1.326
Dolomite	-2.00 H^+	1.00 Ca^{2+}	1.00 Mg^{2+}	2.00 HCO_3^-			
Log K (FRACHEM)[a]	3.408	2.509	1.334	0.095	-1.351	-2.773	-4.297
Log K (TREACT)[a]	3.406	2.514	1.331	0.094	-1.349	-2.774	-4.297
Quartz	-2.00 H_2O	1.00 H_4SiO_4					
Log K (FRACHEM)[b]	-4.501	-4.001	-3.500	-3.097	-2.717	-2.427	-2.312
Log K (TREACT)[a,e]	-4.079	-3.739	-3.349	-2.992	-2.642	-2.365	-2.206
Amorphous silica	-2.00 H_2O	1.00 H_4SiO_4					
Log K (FRACHEM)[c]	-2.967	-2.738	-2.465	-2.215	-1.979	-1.813	-1.700
Log K (TREACT)[a,e]	-3.124	-2.714	-2.407	-2.184	-1.98	-1.819	-1.693
Pyrite	-1.00 H_2O	1.00 Fe^{2+}	1.75 HS^-	0.25 H^+	0.25 SO_4^{2-}		
Log K (FRACHEM)[a]	-26.500	-24.656	-22.748	-21.238	-20.019	-19.428	-19.694
Log K (TREACT)[a,f]	-26.504	-24.653	-22.753	-21.235	-20.024	-19.396	-19.278
K-feldspar	-4.00 H_2O	-4.00 H^+	1.00 K^+	1.00 Al^{3+}	3.00 H_4SiO_4		
Log K (FRACHEM)[d]	0.455	0.068	-0.503	-1.105	-1.701	-2.154	-2.651
Log K (TREACT)[a,g]	0.934	-0.027	-1.048	-1.944	-2.873	-3.745	-4.574
Albite (High temperature)	-4.00 H_2O	-4.00 H^+	1.00 Na^+	1.00 Al^{3+}	3.00 H_4SiO_4		
Log K (FRACHEM)[d]	5.416	4.405	3.118	1.878	0.685	-0.211	-1.052
Log K (TREACT)[a,g]	3.731	3.228	2.038	0.7	-0.722	-1.902	-2.939
Illite	-8.00 H^+	-2.00 H_2O	0.60 K^+	2.30 Al^{3+}	0.25 Mg^{2+}	3.50 H_4SiO_4	
Log K (FRACHEM)[d]	13.450	10.340	6.850	3.820	0.810	-1.230	-2.870
Log K (TREACT)[a,g]	11.386	9.026	5.555	2.047	-1.59	-4.612	-7.253

[a]SUPCRT92 (Johnston et al., 1992); [b]Walther & Helgeson (1977); [c]Gunnarsson and Arnorson (2000); [d]Helgeson et al. (1978); [e]Originally expressed in terms of $SiO_{2(aq)}$ instead of H_4SiO_4, see text; [f]Converted from original reaction in terms of $O_{2(aq)}$ using the log(K) data for the reaction $HS^- + 2O_{2(aq)} = H^+ + SO_4^{2-}$ in the same database (from SUPCRT92); [g]Converted from original reaction in terms of AlO_2^- and $SiO_{2(aq)}$ as discussed in text.

5.2 REMARKS

A reasonably good agreement is observed between the log(K) values used here with FRACHEM and TOUGHREACT for carbonates (calcite and dolomite) and silica phases (quartz and amorphous silica). The differences in quartz solubilities reflect more recent data implemented in FRACHEM consistent with new measurements by Rimstidt (1997). Significant divergences appear with aluminosilicates. Note that log(K) values for reactions expressed in terms of $Al(OH)_3$ or $Al(OH)_4^-$ (also corresponding to $HAlO_2$ and AlO_2^-, respectively) instead of Al^{3+} would yield smaller differences, because differences in the first hydrolysis constant of Al^{3+} reported in the literature are larger than for the second and higher hydrolysis constants. It should also be noted that in the Soultz fluids considered here (pH 4.5 to 5.5 range), Al^{3+} dominates the aluminium species only at temperatures below about 100°C. At temperatures above 100°C, the other two complexes start to dominate.

5.3 VARIATION OF MINERAL SOLUBILITY WITH PRESSURE

In the Soultz reservoir, at a depth of 5,000 m, the pressure is estimated to be about 500 bar. Under these conditions, pressure plays a significant role in mineral solubility, particularly for the carbonates, as discussed below.

The pressure effect on the solubility of minerals has been implemented in FRACHEM for some minerals. The effect of pressure (P) on the solubility of minerals in water can be estimated from:

$$\ln\left(\frac{K_{P,T}}{K_{P_0,T}}\right)=\left(\frac{-P\Delta V+0.5\Delta\kappa P^2}{RT}\right) \qquad \text{Eq. 21}$$

where K is the equilibrium constant, P_0 is the reference pressure (here taken as 1 bar below 100°C and the water saturation pressure above 100°C), R is the gas constant (83.15 cm^3 bar K^{-1} mol^{-1}) and T is the absolute temperature (°K). The volume (ΔV) and compressibility ($\Delta\kappa$) changes at atmospheric pressure are given by:

$$\Delta V=\sum\overline{V_i}(products)-\sum\overline{V_i}(\text{reactants})$$
$$\Delta\kappa=\sum\overline{\kappa_i}(products)-\sum\overline{\kappa_i}(\text{reactants})$$

V_i and κ_i are the partial volume and compressibility of species i. Standard partial molar volume of aqueous cations and anions at vapor-liquid saturation pressures for H_2O and temperature from 0° to 350 °C are given by Millero (1982) and Tanger and Helgeson (1988).

The variations in solubility products of calcite (Table 5-2) and dolomite (Table 5-3) were estimated between 1 and 1000 bars using Equation 21. The effect of pressure on equilibrium constants for these minerals is quite important, showing significant solubility increase with pressure at all temperatures. From these data, the following two correlations were established with temperature T in °C, and pressure P in bar:

- For calcite:

$$K_{T,P} = K_{T,P_0} \exp\left[-\left(\frac{-1.5155\times10^{-3}T^2 + 0.1811T - 34.477}{83.14(273.15+T)} \right) P \right] \qquad \text{Eq. 22}$$

- For dolomite:

$$K_{T,P} = K_{T,P_0} \exp\left[-\left(\frac{-3.0751\times10^{-3}T^2 + 0.3405T - 62.0860}{83.14(273.15+T)} \right) P \right] \qquad \text{Eq. 23}$$

Table 5-2. Evolution of $K_{T,P}/K_{T,P0}$ with temperature and pressure for calcite.

		Pressure (bars)									
		100	**200**	**300**	**400**	**500**	**600**	**700**	**800**	**900**	**1000**
Temperature (°C)	**0**	1.159	1.337	1.534	1.750	1.986	2.240	2.514	2.805	3.112	3.433
	10	1.145	1.307	1.483	1.676	1.883	2.107	2.344	2.596	2.861	3.136
	25	1.127	1.266	1.416	1.577	1.750	1.933	2.127	2.330	2.542	2.762
	50	1.113	1.236	1.368	1.510	1.662	1.823	1.993	2.172	2.360	2.557
	75	1.107	1.224	1.350	1.485	1.630	1.785	1.951	2.126	2.312	2.508
	100	1.106	1.223	1.349	1.486	1.634	1.793	1.964	2.147	2.343	2.553
	125	1.110	1.232	1.365	1.511	1.669	1.842	2.029	2.232	2.452	2.689
	150	1.120	1.253	1.401	1.564	1.745	1.943	2.161	2.401	2.664	2.952
	175	1.139	1.297	1.476	1.677	1.903	2.158	2.443	2.763	3.120	3.520
	200	1.161	1.347	1.562	1.809	2.092	2.417	2.789	3.214	3.699	4.252

Table 5-3. Evolution of $K_{T,P}/K_{T,P0}$ with temperature and pressure for dolomite.

		Pressure (bars)									
		100	**200**	**300**	**400**	**500**	**600**	**700**	**800**	**900**	**1000**
Temperature (°C)	**0**	1.302	1.685	2.160	2.745	3.456	4.313	5.334	6.536	7.938	9.553
	10	1.276	1.619	2.036	2.540	3.142	3.853	4.686	5.652	6.759	8.015
	25	1.240	1.529	1.871	2.272	2.738	3.275	3.888	4.580	5.354	6.212
	50	1.214	1.468	1.762	2.103	2.492	2.935	3.434	3.991	4.610	5.289
	75	1.205	1.446	1.726	2.048	2.416	2.835	3.307	3.837	4.425	5.075
	10	1.206	1.450	1.735	2.066	2.446	2.882	3.379	3.942	4.574	5.282
	125	1.218	1.480	1.789	2.154	2.580	3.077	3.652	4.315	5.074	5.940
	150	1.242	1.539	1.899	2.334	2.855	3.477	4.217	5.092	6.122	7.328
	175	1.290	1.662	2.132	2.723	3.465	4.389	5.537	6.957	8.703	10.843
	200	1.344	1.804	2.412	3.212	4.259	5.624	7.397	9.688	12.638	16.419

The variations in the solubility of quartz with pressure (Table 5-4) are given by Fritz (1981), whereas Fournier and Rowe (1977) presents the variation of solubility of amorphous silica in water at high temperatures and an elevated pressure of 1034 bar (Table 5-5). As shown by these data, the solubility increase in quartz and amorphous silica with pressure is not negligible, although it is much less than for the carbonates.

Table 5-4. Solubility of quartz (mg SiO_2/kg water) as a function of temperature and pressure.

T (°C)	0	25	50	100	150	200	250	300
P_{sat}	1 bar	1 bar	1 bar	1 bar	4.8 bar	15.5 bar	39.7 bar	85.8 bar
	1.89	6.00	12.2	48.3	115	225	384	586
500 bars	1.97	7.12	17.5	60.6	144	278	473	730
1000 bars	1.99	8.20	21.0	74.6	177	340	576	895

Table 5-5. Change in amorphous silica equilibrium constant with pressure.

T(°C)	25	50	75	100	125	150	175	200
$K_{T,1034}/K_{T,1}$	1.084	1.136	1.183	1.225	1.263	1.298	1.330	1.358

$K_{T,1034}$ and $K_{T,1}$ refer to the values of amorphous silica solubility at 1034 and 1 bar, respectively.

From these data, the following two correlations were established with temperature T in °C, and pressure P in bar:

- For quartz:

$$K(T,P) = K(T,P_0)\exp\left[\begin{array}{r} 7\times10^{-10}T^4 - 5.25\times10^{-7}T^3 + 1.45\times10^{-4}T^2 \\ -1.74\times10^{-2}T + 5.74\times10^{-4}P + 1.713 \end{array}\right] \quad \text{Eq. 24}$$

- For amorphous silica:

$$\frac{K_{T,1034\,bar}}{K_{T,P_{sat}}} = 10^{-\frac{79}{T}+0.3} \quad \text{Eq. 25}$$

To gain confidence in the correlations established above, the equilibrium constants calculated with FRACHEM using Equations 22 to 25 were compared with values computed directly with SUPCRT92 (Johnston et al., 1992). The results (Table 5-6) show reasonably good agreement.

Table 5-6: Comparison of the equilibrium constants computed with FRACHEM and SUPCRT92 as a function of temperature and pressure

Temperature (°C)		0	25	50	100	150	200	250
Calcite	Log K (FRACHEM) – 500 bars	2.555	2.117	1.715	1.000	0.365	-0.241	-0.883
	Log K (SUPCRT) – 500 bars	2.535	2.100	1.701	0.979	0.314	-0.334	-0.997
	Log K (FRACHEM) – 1000 bars	2.883	2.386	1.942	1.226	0.631	0.101	-0.440
	Log K (SUPCRT) – 1000 bars	2.797	2.317	1.896	1.158	0.498	-0.125	-0.738
Dolomite	Log K (FRACHEM) – 500 bars	4.001	2.995	2.087	0.506	-0.856	-2.127	-3.453
	Log K (SUPCRT) – 500 bars	3.955	2.962	2.062	0.473	-0.942	-2.285	-3.638
	Log K (FRACHEM) – 1000 bars	4.595	3.481	2.513	0.918	-0.361	-1.481	-2.608
	Log K (SUPCRT) – 1000 bars	4.406	3.339	2.404	0.793	-0.602	-1.886	-3.128
Quartz	Log K (FRACHEM) – 500 bars	-4.200	-3.683	-3.138	-2.621	-2.132	-1.753	-1.565
	Log K (SUPCRT) – 500 bars	-3.966	-3.367	-3.011	-2.571	-2.279	-2.052	-1.872
	Log K (FRACHEM) – 1000 bars	-4.142	-3.627	-3.087	-2.581	-2.101	-1.728	-1.543
	Log K (SUPCRT) – 1000 bars	-3.919	-3.290	-2.924	-2.482	-2.194	1.970	-1.782
Amorphous Silica	Log K (FRACHEM) – 1000 bars	-2.956	-2.703	-2.410	-2.127	-1.866	-1.680	-1.551
	Log K (SUPCRT) – 1000 bars	-2.959	-2.497	-2.250	-1.960	-1.769	-1.621	-1.504

6 APPLICATION – SIMULATION OF INJECTION

6.1 MODEL CONCEPTUALISATION AND INPUT DATA

The two codes were applied to a geometrical model representing the granitic reservoir in Soultz. Injection and production wells were linked by fractures zones surrounded by a low-permeability granite matrix. The model is composed of 1,250 fractured zones. Each fracture zone has an aperture of 0.1 m, a fixed horizontal depth of 10 m, and a porosity of 10%. Here, reactive transport is simulated into one of these fractured zones, with the assumption that the fluid exchange with the surrounding low-permeability matrix is insignificant. Due to the symmetrical shape of the geometrical model, only the upper half of the fractured zone is considered in the simulation. It should be noted that, with FRACHEM, matrix gridblocks are added above the fracture blocks for proper thermal behavior. The area is discretized into 222 two-dimensional gridblocks (Figure 6-1): 25 for the fracture zone and 197 for the matrix. The size of the gridblocks ranges from a minimum of 0.5 m x 0.05 m near the injection and the production wells to a maximum of 50 m x 35 m. With TOUGHREACT, however, only the fracture zone is modeled, without adjacent matrix gridblocks. Heat loss in the impermeable matrix is modeled by a semi-analytical solution (Vinsome and Westerveld, 1980) built into the code. As a result, the model contains only 25 gridblocks.

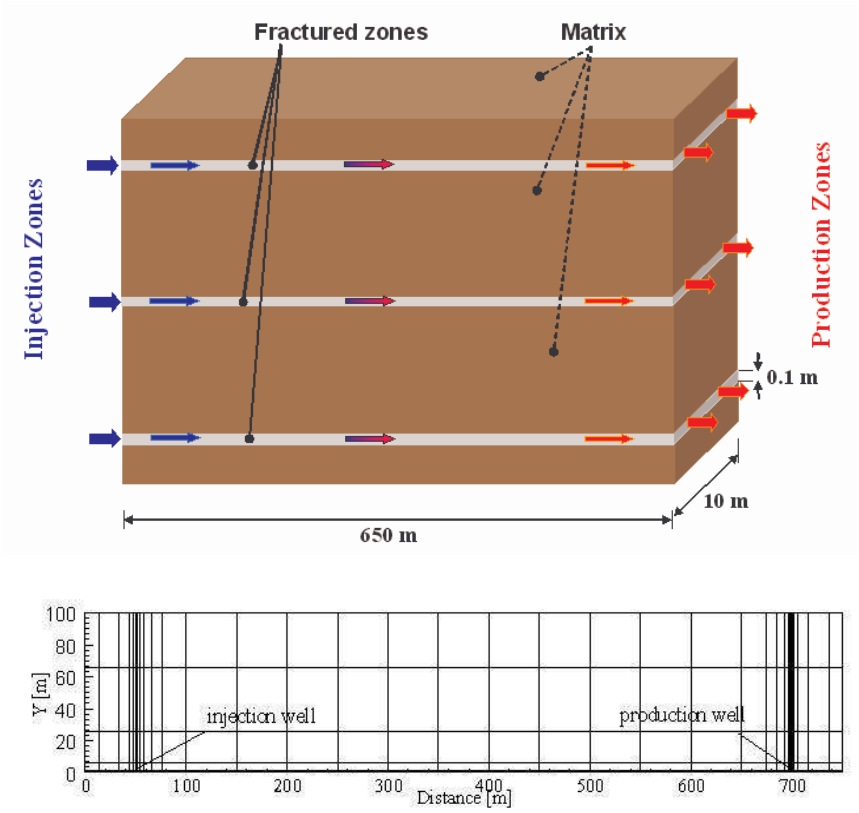

Figure 6-1: Simplified model and spatial discretization.

Initially, the system temperature was set to the reservoir temperature of 200°C. The geothermal fluid (Table 3-1) was injected in the modeled fractured zone at a rate of $2x10^{-2}$ L s^{-1} (corresponding to a total production rate of 50 L s^{-1} for the full geometric model) and constant temperature of 65°C. During this simulation, a constant overpressure of 8 MPa was assumed at the injection well, and a hydrostatic pressure was assumed at the production well. With FRACHEM, Dirichlet boundary conditions were applied to the upper, left, and right side of the model. The fluid was continuously recirculated from the production well to the injection well. With TOUGHREACT, the fluid was not recirculated (continuous injection of the same fluid composition), and constant boundary conditions were simulated by connecting gridblocks of infinite dimensions to the injection well (constant chemical composition, temperature, and pressure) and to the production well (constant temperature and pressure).

The values of thermal and hydrological parameters considered in the simulation are listed in Table 6-1. The assumed initial fluid composition is the same as that used for the cooling simulations presented in Section 3 (Table 3-1). However, in this case, the pH of the initial fluid was adjusted to reflect equilibrium of this fluid with calcite in all simulations (i.e., FRACHEM, Tr-DH, and Tr-Pitzer). In this way, simulations with the three codes reflected the same model conceptualization, i.e., that the reservoir fluid is at equilibrium with calcite, which is anticipated to be the case in the field. Making this same assumption for all three models also resulted in minimizing differences in model results caused by the differences in calcite solubilities computed using the different activity coefficient models (see Section 3). The initial fluid pH computed with the three codes, assuming saturation with respect to calcite, was 4.95 using FRACHEM, 4.76 using Tr-Pitzer, and 5.24 using Tr-DH.

The following minerals were included in the simulation: dolomite, calcite, quartz and potassium feldspar. These minerals are the main phases observed in the reservoir rocks at Soultz. Secondary precipitation of amorphous silica was initially considered. However, because silica concentrations remained below the solubility of amorphous silica in the temperature range considered, amorphous silica was not included in the final simulations. Input kinetic and thermodynamic data were discussed in Sections 4 and 5, respectively. A sequential non-iterative approach (SNIA) to reactive transport was implemented. Owing to the sensitivity of the SNIA method on the time discretization, the time step used for the simulations was limited to 10^2 s.

Table 6-1. Thermohydraulic model parameters.

Parameters		**Fracture**	**Matrix**	**Fluid**
Permeability	[m^2]	$5\ 10^{-13}$	10^{-18}	-
Thermal conductivity	[W/m K]	2.9	3	0.6
Density	[kg/m^3]	-	2650	1000
Heat capacity	[J/kg K]	-	1000	4200
Porosity	[%]	10	2	-

6.2 SIMULATIONS WITH FRACHEM

The observation of the mineral behavior (Figure 6-2) shows that all the reactions occur in the first 20 m of the injection zone. Calcite, a secondary mineral present within granite fractures in relatively small proportions, is the most reactive. In the vicinity of the injection well, calcite dissolves, whereas it precipitates from about 2 to 20 m, because of the retrograde solubility of

calcite (solubility decrease with temperature increase). At the onset of fluid circulation within the reservoir, calcite dissolves mainly within the first two meters of the injection well. This dissolution releases calcium in solution, which is then available for calcite precipitation further away from the injection well, where the temperature increases. With increasing simulation times and decreasing rock temperatures, the dissolution of calcite extends towards the production well and ends when this mineral becomes depleted.

Figure 6-2 shows that dolomite dissolves within the first ten meters from the injection well. Similarly to calcite, dolomite dissolution stops when this mineral becomes depleted. Among silicates, quartz and K-feldspar are major minerals in granite. Contrary to calcite, the solubility of these minerals decreases with cooling. As a consequence, these minerals precipitate near the injection well, but less so further away as temperature increases. As mentioned earlier, the fluid always remains undersaturated with respect to amorphous silica. After 25–30 m along the fracture, the fluid becomes essentially unreactive with all the minerals shown in Figure 6-2 because the injected brine becomes close to equilibrium with these minerals.

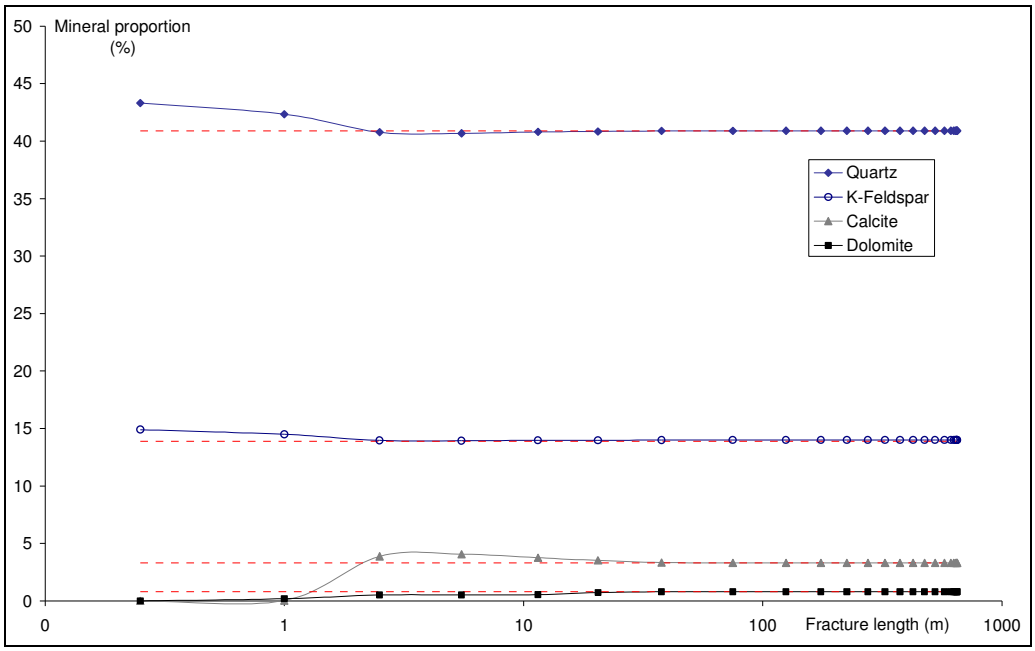

Figure 6-2. Evolution of the rock composition in the fracture zone (volume %) after 5 years of circulation simulated with FRACHEM. The dashed lines correspond to initial concentrations.

6.3 SIMULATIONS WITH TR-DH

The carbonates are the most reactive minerals. As presented in the case of the FRACHEM simulation, calcite and dolomite dissolve near the injection well (Figure 6-3). These minerals are predicted to dissolve faster than in the FRACHEM simulations because of small differences in reaction rates. Calcite dissolves for the first 10 m (when temperature is below 145°C), then precipitates between 10 and 100 m from the injection well. Dolomite dissolves within the first 100 m and remains unaffected further out. Quartz precipitation is negligible, whereas feldspars precipitate in the close vicinity of the injection well.

6.4 SIMULATIONS WITH TR-PITZER

The predicted behavior of quartz, K-feldspars and carbonates (calcite, dolomite) is similar to the behavior predicted with FRACHEM and Tr-DH. As shown in Figure 6-4, calcite dissolution is predicted along the fracture zone in the first 3 m from the injection well, and then significant precipitation is predicted further away from the injection well, between 5 and 200 m.

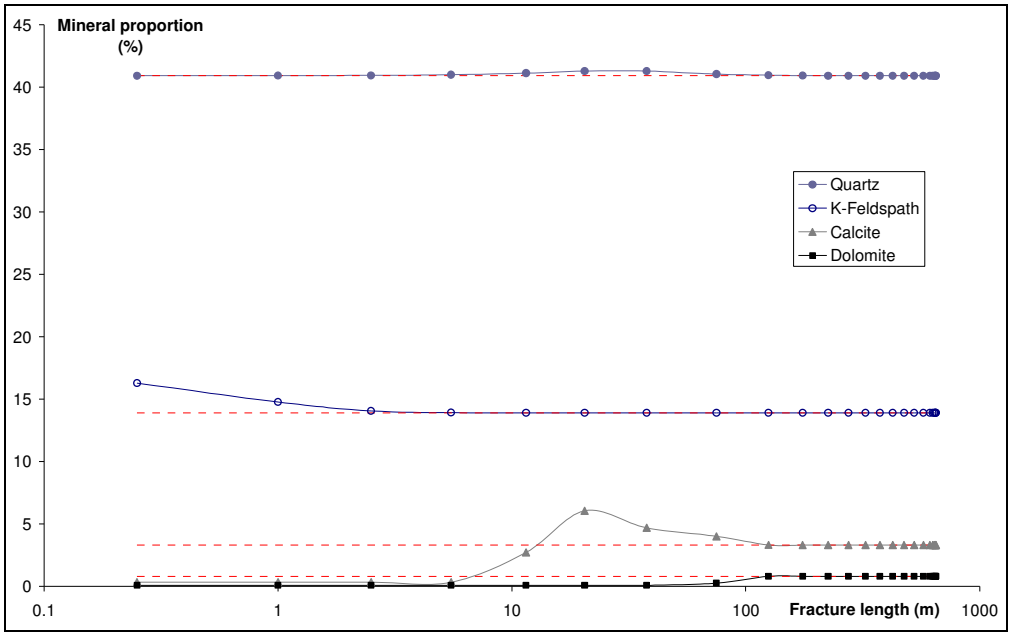

Figure 6-3. Evolution of the rock composition in the porous zone after 5 years of circulation simulated with Tr-DH. The dashed lines correspond to the initial concentrations.

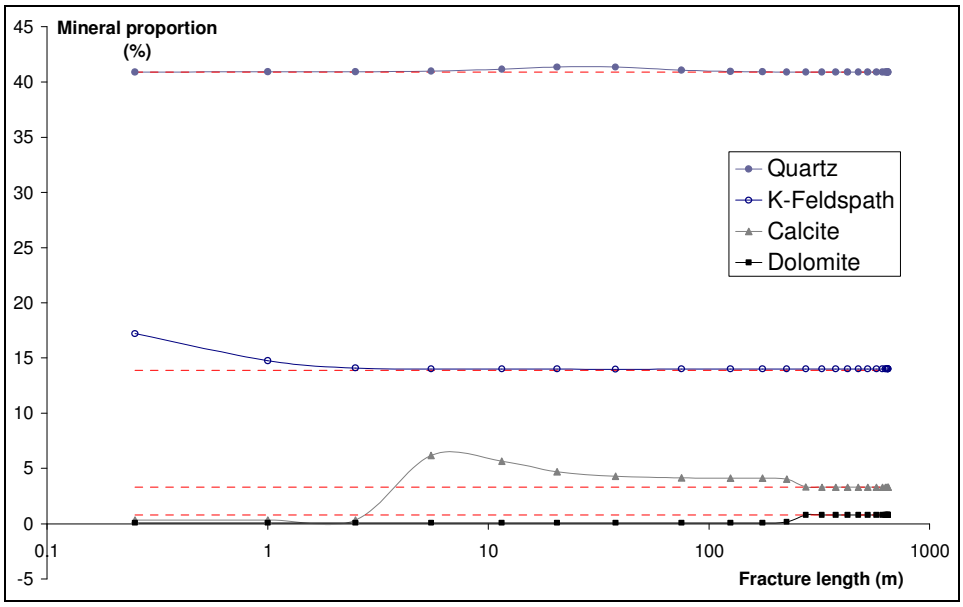

Figure 6-4. Evolution of the rock composition in the porous zone after 5 years of circulation simulated with Tr-Pitzer. The dashed lines correspond to initial concentrations.

6.5 IMPLICATIONS ON RESERVOIR PROPERTIES

The circulation of cooled fluid in the fracture zone affects the temperature of the reservoir within a distance of about 100 m from the injection well (Figure 6-5). Obviously, the temperature is lowest near the injection well (around 65°C), then increases to ambient reservoir temperatures (around 200°C) further away from the injection well. The predicted general trend of temperature with distance is similar for the three simulations. Temperature profiles take the shape of a front, which reaches mid-point temperatures (~132°C) somewhat closer to the injection well in the TOUGHREACT simulations compared to the FRACHEM simulation (Figure 6-5). The steeper front predicted with TOUGHREACT give rise to temperatures up to 30°C higher than FRACHEM-predicted temperatures at 20 to 50 m from the injection well. These differences diminish further away from the injection well and are attributed to the different model conceptualizations regarding heat transport.

Evolution of the reservoir porosity (Figure 6-6) is determined by the mineral reactions occurring in the reservoir. The three models give generally similar trends, although absolute changes in porosity vary significantly between models. With FRACHEM, the porosity is predicted to increase near the injection well because of the dissolution of calcite and dolomite. The porosity is enhanced by more than 50% at the injection well, but then decreases away from the well. Within a couple of meters from the injection well, the overall porosity change becomes negative because of calcite reprecipitation, resulting in a maximum overall porosity decrease close to 6%. At distances about 10 to 20 m away from the injection well, the porosity is predicted to remain essentially unaffected.

With Tr-DH, as with FRACHEM, the porosity is enhanced in the first 10 m from the injection well, due to the dissolution of carbonates. Calcite then precipitates between about 10 and 100 m, yielding a maximum porosity decrease of about 25% in this zone. However, the TOUGHREACT simulations show a trend of increasing porosity with distance along the fracture zone for the first several meters from the injection well (Figure 6-6). This increase results from feldspar precipitation near the injection well, impeding the porosity increase near the well. This precipitation is less prevalent in the FRACHEM simulations because the reservoir fluid is continuously recirculated in these simulations. In contrast, injection of the same initial fluid composition (Table 3-1, with pH 5.24) is simulated with TOUGHREACT. Simulations with Tr-Pitzer show a trend of porosity change with distance similar to that predicted with Tr-DH (Figure 6-6), except that calcite reprecipitation occurs closer to the injection well, which is more consistent with the FRACHEM results. This is expected, given that the solubility of calcite is overpredicted when activity coefficients are calculated using the Debye-Hückel model (Section 3). Again, calcite dissolution is the primary cause of porosity enhancement near the injection well.

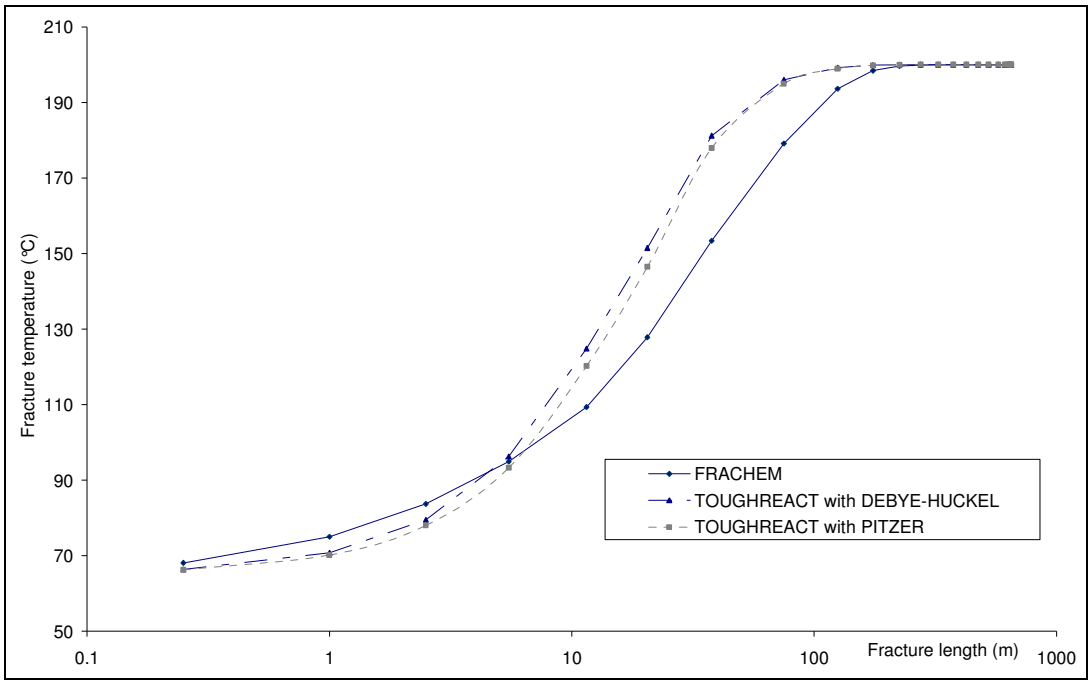

Figure 6-5. Evolution of the reservoir temperature after 5 years of circulation.

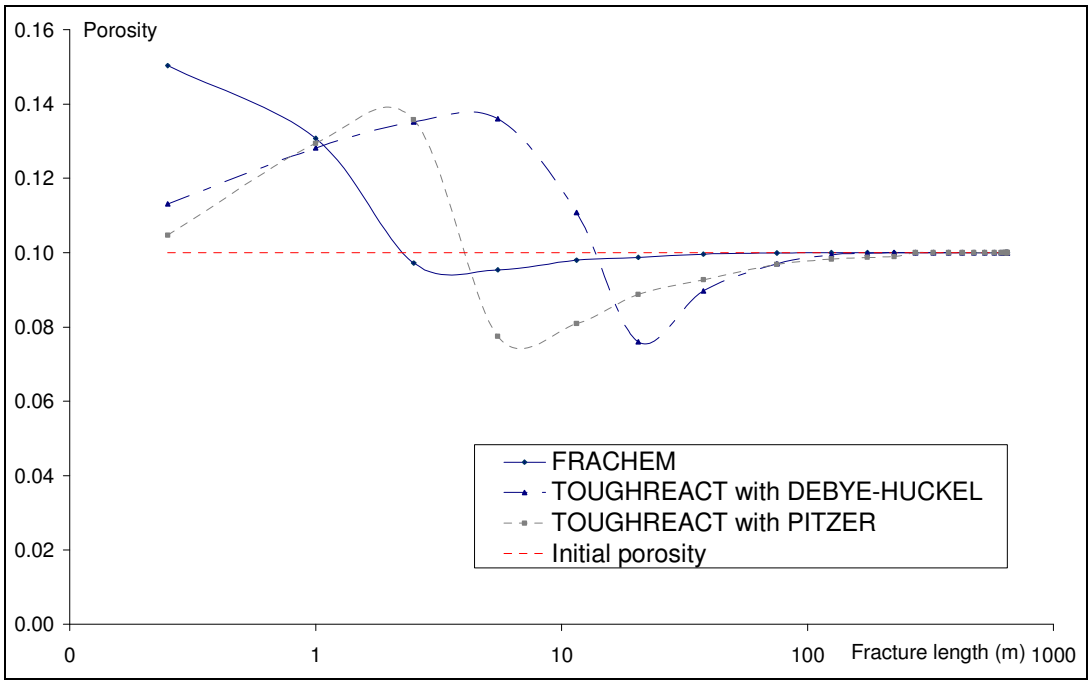

Figure 6-6. Evolution of the reservoir porosity after 5 years of circulation.

7 CONCLUSIONS

The goals of this work were to compare two multicomponent reactive transport codes, FRACHEM (Durst, 2002; Bächler, 2003, Rabemanana et al. 2003; André et al., 2005; Bächler and Kohl, 2005) and TOUGHREACT (Xu and Pruess, 2001; Xu et al., 2004; Xu et al., 2006), to model complex water-rock interactions such as at the enhanced geothermal system at Soultz. In a first phase, different aspects of each code and input data were evaluated, including the methods to calculate activity coefficients, the mineral reaction rates, and the equilibrium constants of key minerals. The second phase of this study involved simulating the Soultz system.

TOUGHREACT offers the choice of either an extended Debye-Hückel (Tr-DH) model or the Pitzer formalism (Tr-Pitzer) to compute activity coefficients of dissolved species and water activity. FRACHEM uses activity coefficients externally calculated using TEQUIL (Moller et al., 1998). Activities of dissolved species computed with these codes for a typical Soultz fluid (ionic strength around 2 molal) were compared. Key differences were found in the activity coefficients of Ca^{2+} and Mg^{2+}, yielding calcite saturation indices lower by up to 1.5 log(Q/K) units when computed with Tr-DH instead of FRACHEM or Tr-Pitzer. However, the effect of increased calcite solubility in the Tr-DH simulations is minimal, because the model assumes an initial reservoir fluid composition reflecting saturation with respect to calcite. This shows that the model conceptualization is as important as the model input data. The Pitzer ion-interaction parameters implemented in TEQUIL are expected to provide more accurate calcite solubilities for applications with Soultz-type fluids, because these parameters were developed specifically for high-temperature geothermal applications at moderate ionic strengths. The relatively recent EQ3/6 Pitzer database *data0.ypf*, revised and used with TOUGHREACT in this study, is expected to be most accurate for applications below 150°C and very high ionic strengths.

Concerning the minerals reaction rates, a good agreement was observed for calcite, quartz and amorphous silica. For aluminosilicates (K-feldspar, albite and illite), differences in rates reach about two orders of magnitude, but can be explained easily by the fact that FRACHEM takes into consideration the inhibitor effect of Na^{+}, whereas TOUGHREACT does not. The largest differences in reaction rates were observed with dolomite and pyrite. In FRACHEM, kinetic data for these two minerals were determined from extrapolations that may be questionable. As a result some modifications to the future FRACHEM database should be considered.

The equilibrium constants for minerals used with FRACHEM and TOUGHREACT are mostly issued from the same sources. A good agreement is observed for the carbonates (calcite and dolomite) and for silicates (quartz and amorphous silica). The most important differences are observed for aluminosilicates, and these differences mainly result from the assumed form of aluminium in solution. Because reservoir pressures at Soultz are high (estimated to about 500 bar), pressure corrections to the equilibrium constants of carbonates and silica phases were investigated. For these minerals, the variation of equilibrium constants with pressure was implemented in FRACHEM using simple correlations. These correlations show that the equilibrium constants of carbonates increase significantly with pressure. For this reason, consideration should be given to implementing similar correlations into TOUGHREACT.

The codes were applied to simulate reactive transport processes in the Soultz reservoir, using essentially identical model conceptualizations and input chemical and hydrological data. Three

main processes were investigated for a fluid-injection period of 5 years: the evolution of reservoir temperature, the mineral precipitation/dissolution behavior, and the evolution of reservoir porosity. The three codes (FRACHEM, Tr-Pitzer, and Tr-DH) produced similar results. The circulation of cooled fluid in the fracture zone is predicted to affect the temperature of the reservoir within the first 100 m from the injection well. The injection of cooled fluid results in chemical disequilibrium and dissolution/precipitation reactions of several minerals. Carbonates dissolve at the injection well head (because of their retrograde solubility), whereas quartz and K-feldspar precipitate. The dissolved calcite eventually reprecipitates away from the well, leading to an overall permeability decrease, which is predicted to range between 6% (with FRACHEM) and 25% (with Tr-DH and Tr-Pitzer). However, water-rock interactions occur mostly within the first 20 m from the injection well, and the porosity of the reservoir remains essentially unchanged at distances greater than about 100 m from the injection well. These results are consistent with a circulation test performed in 1997 within the shallow reservoir at 3,500 m at Soultz-sous-Forêts. The initial reservoir temperature was only 165°C, but the mineral composition of the granite was very similar to that in the deep reservoir (5000 m). During this circulation of 140 days, the pressure at the injection well decreased, indicating an increase of the injectivity around the injection well. According to the simulation presented in this report, this process is likely caused by the dissolution of carbonates, the most reactive minerals. It should also be noted that concentrations of dissolved silica in the injected fluid remain below the solubility of amorphous silica, even at a temperature of 65°C, and therefore porosity reduction from silica precipitation is avoided. This occurs because the reservoir temperature is relatively low (200°C), precluding the dissolution of silica at concentrations exceeding the 65°C solubility of amorphous silica (i.e., temperature remaining within a silica precipitation "gap"). Should injection occur in hotter intervals, amorphous silica precipitation in the injection well could be significant.

Although the three codes yield similar results, in a qualitative sense, quantitative results differ significantly (e.g., 6% versus 25% predicted porosity decrease at distances varying from about 2 to 20 m from the injection well, depending on the code). These differences are primarily caused by differences in implemented activity coefficient models and their input parameters, as well as other model input thermodynamic and kinetic data. This study, therefore, highlights the importance of these data in reactive transport simulations, in particular for systems involving brines.

Reactive transport simulations are of enormous value in helping understanding processes at play, especially the various feedbacks between strongly coupled mechanisms. However this study clearly shows that the predictive value of complex coupled THC simulations is mostly qualitative. Unless these simulations are closely integrated with field and laboratory experiments, their predictive ability should be asserted with much caution. Therefore, if THC simulations such as those presented here are to be used in a quantitative manner to plan the design and operation of the Soultz EGS (or any other geothermal system), integration of these simulations with laboratory experiments and field tests is highly recommended.

8 ACKNOWLEDGMENTS

We are grateful to the geochemistry and hydrogeology teams of LBNL, and we want to thank especially Guoxiang Zhang for his valuable support during this work. This study was supported by the Swiss State Secretariat for Education and Research and by the Swiss Federal Office of Energy (OFES-N° 03.04.60 and OFEN-N° 100'528), as well as by the Assistant Secretary for Energy Efficiency and Renewable Energy, Office of Geothermal Technologies, of the U.S. Department of Energy, under Contract No. DE-AC02-05CH1123.

INTENTIONALLY LEFT BLANK

9 REFERENCES

Alai, M., Sutton, M. and Carroll, S. (2005). Evaporative evolution of a Na-Cl-NO3-K-Ca-SO4-Mg-Si brine at 95 degrees C: Experiments and modeling relevant to Yucca Mountain, Nevada. *Geochem. Transactions*, 6(2), 31-45.

André, L., Rabemanana, V. and Vuataz, F.-D., (2005). Geochemical modelling of water-rock interactions and implications on the properties of the Soultz fractured reservoir. *Proceedings EHDRA Scientific Conference*, March 17-18, 2005, Soultz-sous-Forêts, France.

André, L., Spycher, N., Xu, T., Pruess, K. and Vuataz F.-D. (2006). Comparing FRACHEM and TOUGHREACT for reactive transport modelling of brine-rock interactions in enhanced geothermal systems (EGS). *Proceedings 31th Workshop on Geothermal Reservoir Engineering*, 30 Janvier – 1er Février, 2006, Stanford University, Stanford, California.

Arvidson, R.S. and Mackenzie, F.T., (1999). The dolomite problem: control of precipitation kinetics by temperature and saturation state. *Am. J. Sci.*, 299: 257-288.

Bächler, D., (2003), Coupled Thermal-Hydraulic-Chemical Modelling at the Soultz-sous-Forêts HDR reservoir (France). PhD thesis, ETH-Zürich, Switzerland, 150 p.

Bächler, D., Durst, P., Evans, K., Hopkirk, R., Kohl, Th., Megel, Th., Rabemanana, V. and Vuataz, F.-D., (2005). Studies and support for the Hot Fractured Rock reservoirs at Soultz-sous-Forêts. Final report for the Federal Office for Education and Science Project – OFES N° 00.0453.

Bauer, A. and Berger, G., (1998). Kaolinite and smectite dissolution rate in high molar KCl solutions at 35° and 80°C. *Appl. Geochem.*, 13: 905-916.

Bevan, J. and Savage, D., (1989). The effect of organic acids on the dissolution of K-feldspar under conditions relevant to burial diagenesis. *Mineralogical Magazine*, 53: 415-425.

Blum, A.E. and Stillings, L.L., (1995). Feldspar dissolution kinetics. In: A.F. White & S.L. Brantley (eds.), Chemical weathering rates of silicate minerals. *Mineralogical Society of America, Reviews in Mineralogy*, 31: 291-351.

Bolton, E.W., Lasaga, A.C. and Rye, D.M.,(1996). A model for the kinetic control of quartz dissolution and precipitation in porous media flow with spatially variable permeability; formulation and examples of thermal convection, *J. Geophys. Res., B, Solid Earth and Planets,* 101(10), 22157-22187.

Busenberg, E. and Plummer, L.N., (1982). The kinetics of dissolution of dolomite in CO_2-H_2O system at 1.5 to 65°C and 0 to 1 atm P(CO_2). *Am. J. Sci*., 282: 45-78.

Carroll, S., Mroczek, E., Alai, M. and Ebert, M., (1998). Amorphous silica precipitation (60 to 120°C): Comparison of laboratory and field rates. *Geochim. Cosmochim. Acta*, 62(8): 1379-1396.

Chou, L. and Wollast, R. (1985). Steady-state kinetics and dissolution mechanism of albite. *Am. J. Sci.*, 285: 963-993.

Dove, P. M. and Rimstidt, J. D., (1994). Silica-water interaction. In: P.J. Heaney, C.T. Prewitt & G.V. Gibbs (eds.), Silica: Physical behavior, geochemistry and materials applications. *Mineralogical Society of America, Reviews in Mineralogy*, 29: 259-308.

Durst, P., (2002). Geochemical modelling of the Soultz-sous-Forêts Hot Dry Rock test site: coupling fluid-rock interactions to heat and fluid transport. PhD Thesis, Neuchâtel, 127 pp.

Drummond, J. M., Jr. (1981). Boiling and mixing of hydrothermal fluids: Chemical effects on mineral precipitation, Ph.D. thesis, The Pennsylvania State University, University Park, Pennsylvania.

Ellis, A.J., (1963). The solubility of calcite in sodium chloride solutions at high temperature. *Am. J. Sci*., 261: 259-267.

Fournier, R.O. and Rowe, J., (1977). The solubility of amorphous silica in water at high temperatures and high pressures. *American Mineralogist*, 62: 1052-1056.

Fritz, B., (1981). Etude thermodynamique et modélisation des réactions hydrothermales et diagénétiques. *Sciences Géologiques*, *Mémoire*, 197 p.

Gautelier, M., Oelkers, E.H. and Schott, J., (1999). An experimental study of dolomite dissolution rates as a function of pH from -0.5 to 5 and temperature from 25 to 80ºC. *Chem. Geol.*, 157(1-2): 13-26.

Gautier, J.-M., Oelkers, E.H. and Schott, J., (1994). Experimental studies of K-feldspar dissolution rates as a fonction of chemical affinity at 150° and pH 9. *Geochim. Cosmochim. Acta*, 58(21): 4549-4560.

Genter, A., Traineau, H. and Artignan, D., (1997). Synthesis of geological and geophysical data at Soultz-sous-Forêts (France), *BRGM Report*, R 39440.

Gunnarsson, I. and Arnorsson, S., (2000). Amorphous silica solubility and the thermodynamic properties of H_4SiO_4 in the range of 0° to 350°C at P_{sat}. *Geochim. Cosmochim. Acta*, 64(13): 2295-2307.

Harvie, C.E., Moller, N. and Weare, J.H., (1984). The prediction of mineral solubilities in natural waters: The Na-K-Mg-Ca-H-Cl-SO_4-OH-HCO_3-CO_3-CO_2-H_2O system to high ionic strengths at 25°C. *Geochim. Cosmochim. Acta*, 48(4): 723-751.

He, S.L. and Morse, J.W. (1993). The carbonic-acid system and calcite solubility in aqueous Na-K-Ca-Mg-Cl-SO_4 solutions from 0 to 90-degrees-C. *Geochim. Cosmochim. Acta*, 57(15) 3533-3554

Helgeson, H.C. (1969). Thermodynamics of hydrothermal systems at elevated temperatures and pressures. *Am. J. Science*, 267, 729-804.

Helgeson, H.C., Delany, J.M., Nesbitt, H.W. and Bird, D.K., (1978). Summary and critique of the thermodynamic properties of rock-forming minerals. *Am. J. Sci.*, 278-A: 1-229.

Helgeson, H. C., Kirkham, D. H., Flowers, D. C. (1981). Theoretical prediction of the thermodynamic behavior of aqueous electrolytes at high pressures and temperatures: IV. Calculation of activity coefficients, osmotic coefficients, and apparent molal and standard and relative partial molal properties to 600 C and 5 kb. Am. J. Sci., v. 281, p. 1249–1516.

Helgeson, H.C., Murphy, W.M. and Aagaard, P., (1984). Thermodynamic and kinetic constraints on reaction rates among minerals and aqueous solutions. II. Rate constants, effective surface area, and the hydrolysis of feldspar. *Geochim. Cosmochim. Acta*, 48(12): 2405-2432.

Hellmann, R., (1994). The albite-water system: Part I. The kinetics of dissolution as a function of pH at 100, 200 and 300°C. *Geochim. Cosmochim. Acta*, 58(2): 595-611.

Huertas, F.J., Caballero, E., Jimenez de Cisneros, C., Huertas, F. and Linares, J., (2001). Kinetics of Montmorillonite dissolution in granitic solutions. *Appl. Geochem.*, 16: 397-407.

Icenhower, J.P. and Dove, P.M., (2000). The dissolution kinetics of amorphous silica into sodium chloride solutions: effects of temperature and ionic strength. *Geochim. Cosmochim. Acta*, 64(24): 4193-4203.

Jacquot, E., (2000). Modélisation thermodynamique et cinétique des réactions géochimiques entre fluides de bassin et socle cristallin: application au site expérimental du programme européen de recherche en géothermie profonde (Soultz-sous-Forêts, Bas-Rhin, France), PhD thesis, Université Louis Pasteur-Strasbourg I, France.

Johnson, J.W., Oelkers, E.H. and Helgeson, H.C., (1992). SUPCRT92: A software package for calculating the standard molal thermodynamic properties of minerals, gases, aqueous species, and reactions from 1 to 5000 bar and 0 to 1000°C. *Computers & Geosciences*, 18(7): 899-947.

Knauss, K.G. and Copenhaver, S.A., (1995). The effect of malonate on the dissolution kinetics of albite, quartz, and microcline as a fonction of pH at 70°C. *Appl. Geochem.*, 10: 17-33.

Kohl, T. and Hopkirk, R.J., (1995). "FRACTure" – A simulation code for forced fluid flow and transport in fractured, porous rock. *Geothermics*, 24(3), 333-343.

Kohl, T. and Rybach, L., (2001). Assessment of HDR reservoir geometry by inverse modelling of non-laminar hydraulic flow, *Proceedings, 26th Workshop on Geothermal Reservoir Engineering,* Stanford University, Stanford, California, January 29-31, 2001, 259-265.

Kohler, S.J., Dufaud, F. and Oelkers, E.H., (2003). An experimental study of illite dissolution kinetics as a function of pH from 1.4 to 12.4 and temperature from 5 to 50°C. *Geochim. Cosmochim. Acta*, 67(19): 3583-3594.

Langmuir, D. (1997). Aqueous Environmental Geochemistry, Prentice Hall, Upper Saddle River, New Jersey, 600pp.

Lasaga, A. C., (1984). Chemical kinetics of water-rock interactions. *J. Geophys. Res*., 89: 4009-4025.

Lasaga, A.C., Soler, J.M., Ganor, J., Burch, T.E. and Nagy, K.L., (1994). Chemical weathering rate laws and global geochemical cycles. *Geochim. Cosmochim. Acta*, 58: 2361-2386.

McKibben, M.A. and Barnes, H.L., (1986). Oxidation of pyrite in low temperature acidic solutions: Rate laws and surface textures. *Geochim. Cosmochim. Acta*, 50: 1509-1520.

Millero, F.J., (1982). The effect of pressure on the solubility of minerals in water and seawater. *Geochim. Cosmochim. Acta*, 46(1): 11-22.

Moller, N., Greenberg, J.P. and Weare, J.H., (1998). Computer modeling for geothermal systems: predicting carbonate and silica scale formation, CO_2 breakout and H_2S exchange. *Transp. porous media*, 33: 173-204.

Nagy, K.L., Blum, A.E. and Lasaga, A.C., (1991). Dissolution and precipitation kinetics of kaolinite at 80°C and pH 3: The dependence on solution saturation state. *Am. J. Sci.*, 291(7): 649-686.

Newton, R.C. and Manning, C.E., (2002). Experimental determination of calcite solubility in H_2O-NaCl solutions at deep crust/upper mantle pressures and temperature: Implications for metasomatic processes in shear zones. *American Mineralogist*, 87: 1401-1409.

Norton, D. and Knapp, R., (1977). Transport phenomena in hydrothermal systems; the nature of porosity, *Am. J. Sci.*, 277(8), 913-936.

Palandri, J.L. and Kharaka, Y.K., (2004). A compilation of rate parameters of water-mineral interaction kinetics for application of geochemical modelling. U.S. Geological Survey, Report 2004-1068.

Parkhurst, D.L. and Appelo, C.A.J. (1999). User's guide to PHREEQC (Version2) - A computer program for speciation, batch-reaction, one dimensional transport, and inverse

geochemical calculations. *U.S.Geological Survey Water-Resources Investigations,* Report 99-4259, 310 p.

Plummer, L.N., Wigley, T.M.L. and Parkhurst, D.L., (1978). The kinetics of calcite dissolution in CO_2-water systems at 5° to 60°C and 0.0 to 1.0 atm CO_2. *Am. J. Sci*., 278: 179-216.

Pruess, K., (1987). TOUGH user's guide, Nuclear Regulatory Commission, report NUREG/CR-4645 (also Lawrence Berkeley Laboratory Report LBL-20700, Berkeley, California), 1987.

Pruess, K., (1991). TOUGH2: A general numerical simulator for multiphase fluid and heat flow. Lawrence Berkeley Laboratory Report LBL-29400, Berkeley, California, 1991.

Pruess, K., Oldenburg, C. and Moridis, G., (1999). TOUGH2 user's guide, Version 2.0. Lawrence Berkeley Laboratory Report LBL-43134, Berkeley, California, 1999.

Rabemanana, V., Durst, P., Bächler, D., Vuataz, F.-D. and Kohl, Th., (2003). Geochemical modelling of the Soultz-sous-Forêts Hot Fractured Rock system: comparison of two reservoirs at 3.8 and 5 km depth. *Geothermics*, 32(4-6), 645-653.

Reed, M.H. (1982) Calculation of multicomponent chemical equilibria and reaction processes in systems involving minerals, gases and aqueous phase. *Geochim. Cosmochim. Acta*, 46: 513-528.

Reed, M.H. (1998). Calculation of simultaneous chemical equilibria in aqueous-mineral-gas systems and its application to modeling hydrothermal processes. In: *Techniques in Hydrothermal Ore Deposits Geology*, J. Richards and P. Larson (Eds), *Reviews in Economic Geology*, 10, 109-124.

Reed, M.H. and Spycher, N.F. (1998). User's guide for CHILLER: A program for computing water-rock reactions, boiling, mixing and other reaction processes in aqueous-mineral-gas systems and minplot guide, 3rd edition. Department of Geological Sciences, University of Oregon, Eugene, Or, USA.

Rickard, D., (1997). Kinetics of pyrite formation by the H_2S oxidation of iron (II) monosulfide in aqueous solutions between 25 and 125°C: The rate equation. *Geochim. Cosmochim. Acta*, 61(1): 115-134.

Rickard, D. and Luther, G. W., (1997). Kinetics of pyrite formation by the H_2S oxidation of iron (II) monosulfide in aqueous solutions between 25 and 125°C: The mechanism. *Geochim. Cosmochim. Acta*, 61(1): 135-147.

Rimstidt, J. D. and Barnes, H. L., (1980). The kinetics of silica-water reactions. *Geochim. Cosmochim. Acta*, 44(11): 1683-1699.

Rimstidt, J.D. (1997). Quartz solubility at low temperatures. *Geochim.Cosmochim. Acta*, 61(13): 2553-2558.

Rumpf, B. and Maurer, G. (1993). An experimental and theoretical investigation of the solubility of carbon-dioxide in aqueous solutions of strong electrolytes . Phys. Chem. Chem. Phys. 97(1): 85-97.

Rumpf, B. Nicolaisen, H, Ocal, C. and Maurer, G. (1994). Solubility of carbon-dioxyde in aqueous solutions of sodium chloride – Experimental results and correlation. *J Sol. Chem*., 23(3): 431-448.

Shiraki, R. and Brantley, S. L., (1995). Kinetics of near-equilibrium calcite precipitation at 100°C: An evaluation of elementary reaction-based and affinity-based rate laws. *Geochim. Cosmochim. Acta*, 59(8): 1457-1471.

Sjoberg, E. L. and Rickard, D. T., (1984). Temperature dependence of calcite dissolution kinetics between 1 and 62°C at pH 2.7 to 8.4 in aqueous solutions. *Geochim. Cosmochim. Acta*, 48(3): 485-493.

Spencer, R.J., Moller, N. and Weare, J.H., (1990). The predictions of mineral solubilities in natural waters: A chemical equilibrium model for the Na-K-Ca-Mg-Cl-SO_4-H_2O system at temperatures below 25°C. *Geochim. Cosmochim. Acta*, 54: 575-590.

Steefel, C.I., and Lasaga, A.C., (1994). A coupled model for transport of multiple chemical species and kinetic precipitation/dissolution reactions with applications to reactive flow in single phase hydrothermal system. *Am. J. Sci.*, 294: 529-592.

Stillings, L.L. and Brantley, S.L., (1995). Feldspar dissolution at 25°C and pH 3: Reaction stoichiometry and the effect of cations. *Geochim. Cosmochim. Acta*, 59(8): 1483-1496.

Sverdrup, H., (1990). The kinetics of base cation release due to chemical weathering, Lund University Press, Lund, Sweden.

Talman, S.J., Wiwchar, B. and Gunter, W.D., (1990). Dissolution kinetics in the H_2O-CO_2 system along the steam saturation curve to 210°C. In Fluid-Mineral Interactions. Lancaster Press, Inc, San Antonio, Texas, pp. 41-55.

Tanger, J.C. and Helgeson, H.C., (1988). Calculations of the thermodynamic and transport properties of aqueous species at high pressures and temperatures: revised equations of state for the standard partial molal properties of ions and electrolytes. *Am. J. Sci.*, 288: 19-98.

Verma, A. and Pruess, K., (1988). Thermohydrological conditions and silica redistribution near high-level nuclear wastes emplaced in saturated geological formations. *J. Geophys. Res*., 93: 1159-1173.

Vinsome, P. K. W. and Westerveld, J. (1980), A simple method for predicting cap and base rock heat losses in thermal reservoir simulators. *J. Canadian Pet. Tech*., 19(3), 87–90.

Walther, J.V. and Helgeson, H.C., (1977). Calculation of the thermodynamic properties of aqueous silia and the solubility of quartz and its polymorphs at high pressures and temperatures. *Am. J. Sci.*, 277(10): 1315-1351.

White, S.P., (1995). Multiphase nonisothermal transport of systems of reacting chemicals. *Water Resour. Res.*, 31(7), 1761-1772.

Williamson, M. A. and Rimstidt, J. D., (1994). The kinetics and electrochemical rate-determining step of aqueous pyrite oxidation. *Geochim. Cosmochim. Acta*, 58(24): 5443-5454.

Wolery, T.J., (1992). A computer program for geochemical aqueous speciation solubility calculations: theoretical manual user's guide, and related documentation (Version 7.0). Lawrence Livermore Nat. Lab. Report, UCRL-MA-110662 PT III. 246 p.

Wolery, T.J. and Jarek, R.L. (2003). EQ3/6, Version 8.0, Software User's Manual, Software Document Number 10813-UM-8.0-00, *U.S. Department of Energy*, Office of Civilian Radioactive Waste Management, Office of Repository Development, 1261 Town Center Drive, Las Vegas, Nevada 89144, 2003.

Wolery, T.J., Jove-Colon, C., Rard, J. and Wijesinghe, A. (2004). Pitzer Database Development: Description of the Pitzer Geochemical Thermodynamic Database data0.ypf. Appendix I in *In-Drift Precipitates/Salts Model (P. Mariner)* Report ANL-EBS-MD-000045 REV 02. Las Vegas, Nevada: Bechtel SAIC Company.

Xu, T., Sonnenthal E., Spycher N., and Pruess, K., (2006). TOUGHREACT - A simulation program for non-isothermal multiphase reactive geochemical transport in variably saturated geologic Media: applications for geothermal injectivity and CO2 geologic sequestration. Computers and Geosciences, 32, 145-165.

Xu, T., Sonnenthal, E., Spycher, N. and Pruess, K. (2004). TOUGHREACT user's guide: a simulation program for non-isothermal multiphase reactive geochemical transport in variably saturated geologic media. Report LBNL-55460, Lawrence Berkeley National Laboratory, Berkeley, California.

Xu, T. and Pruess, K., (2001). Modeling multiphase fluid flow and reactive geochemical transport in variably saturated fractured rocks: 1. Methodology. *Am. J. Sci.*, 301: 16-33.

Xu, T., Sonnenthal, E., Spycher, N., Pruess, K., and Brimhall, G. (2001). Modeling multiphase fluid flow and reactive geochemical transport in variably saturated fractured rocks: 2. Applications to supergene copper enrichment and hydrothermal flows. *Am. J. Sci.*, 301: 34-59.

Xu, H., Sonnenthal, E.L., Spycher, N. and Pruess, K., (2004a). TOUGHREACT user's guide: a simulation program for nonisothermal multiphase reactive geochemical transport in variably saturated geologic media, Lawrence Berkeley National Laboratory, Berkeley, California, Report LBNL-55460, September 2004.

Xu, T., Ontoy, Y., Molling, P., Spycher, N., Parini, M. and Pruess, K., (2004b). Reactive transport modeling of injection well scaling and acidizing at Tiwi field, Philippines. Geothermics, 33(4): 477-491.

Zhang, G., Spycher, N., Xu, T., Sonnenthal, E., and Steefel, C., (2006a). Reactive geochemical transport modeling of concentrated aqueous solutions with TOUGHREACT — Supplement to TOUGHREACT users' guide for the Pitzer ion-interaction model. Report LBNL-57873, Lawrence Berkley National Laboratory, Berkeley, California (in review).

Zhang, G., Spycher, N., Sonnenthal, E., and Steefel, C. 2006, Implementation of a Pitzer activity model into TOUGHREACT for modeling concentrated solutions. Proceedings, *TOUGH Symposium 2006*, Lawrence Berkeley National Laboratory, Berkeley, California, May 15–17 (Report LBNL-60016).

Zhang, G., Zheng, Z. and Wan, J. (2004). Modeling reactive geochemical transport of concentrated aqueous solutions. *Water Resour. Res*., 41(2), W02018.

Zysset, M. and Schindler, P.W., (1996). The proton promoted dissolution of K-montmorillonite. *Geochim. Cosmochim. Acta*, 60: 921-931.

APPENDIX 1: DISSOLUTION AND PRECIPITATION RATES

	Temperature	50	60	80	100	125	150	175	200
Calcite	**-Log k_{diss}**	4.873	4.767	4.572	4.397	4.201	4.027	3.870	3.729
	Log $k_{prec.}$ (Q/K<1.72)	-5.968	-5.752	-5.355	-5.000	-4.604	-4.253	-3.940	-3.659
	Log $k_{prec.}$ (Q/K>1.72)	-4.249	-4.033	-3.636	-3.280	-2.885	-2.534	-2.221	-1.939
Dolomite	**-Log k_{diss}**	6.278	6.221	6.115	6.019	5.911	5.814	5.727	5.648
	Log k_{prec}	-16.534	-15.886	-14.700	-13.642	-12.468	-11.433	-10.513	-9.691
Quartz	**-Log k_{diss}**	11.216	10.804	10.047	9.369	8.615	7.949	7.355	6.822
	Log k_{prec}	-12.314	-11.948	-11.282	-10.691	-10.042	-9.476	-8.978	-8.539
Amorphous silica	**-Log k_{diss}**	11.188	10.827	10.165	9.574	8.919	8.342	7.829	7.370
	Log k_{prec}	-9.352	-9.328	-9.284	-9.244	-9.200	-9.161	-9.127	-9.096
Pyrite	**-Log k_{diss}**	10.383	10.266	10.084	9.964	9.886	9.876	9.923	10.017
	Log k_{prec}	-14.550	-14.709	-14.949	-15.177	-15.561	-16.187	-17.268	-18.393
K-feldspar	**-Log k_{diss}**	13.726	13.475	13.016	12.606	12.152	11.751	11.395	11.076
	Log k_{prec}	-11.081	-10.751	-10.149	-9.611	-9.015	-8.489	-8.022	-7.605
Albite	**-Log k_{diss}**	15.601	15.354	14.901	14.496	14.044	13.645	13.288	12.966
	Log k_{prec}	-11.081	-10.751	-10.149	-9.611	-9.015	-8.489	-8.022	-7.605
Illite	**-Log k_{diss}**	14.026	13.822	13.436	13.082	12.685	12.332	12.017	11.734
	Log k_{prec}	-16.338	-15.757	-14.692	-13.741	-12.684	-11.751	-10.920	-10.176

Logarithm of dissolution and precipitation reaction rate (in mol.m^2.s^{-1}) as determined in FRACHEM code

	Temperature	50	60	80	100	125	150	175	200
Calcite	**-Log k_{diss}**	4.955	4.872	4.717	4.576	4.417	4.273	4.143	4.024
	Log k_{prec}	-5.491	-5.377	-5.168	-4.982	-4.776	-4.593	-4.432	-4.287
Sedimentary dolomite	**-Log k_{diss}**	5.186	5.009	4.683	4.392	4.066	3.777	3.517	3.283
	Log k_{prec}	-5.985	-5.732	-5.269	-4.855	-4.396	-3.991	-3.565	-3.310
Hydrothermal dolomite	**-Log k_{diss}**	5.478	5.200	4.686	4.216	3.673	3.161	2.573	2.196
	Log k_{prec}	-5.780	-5.318	-4.471	-3.716	-2.878	-2.140	-1.361	-0.896
Quartz	**-Log k_{diss}**	12.801	12.376	11.597	10.902	10.131	9.451	8.847	8.307
	Log k_{prec}	-12.801	-12.376	-11.597	-10.902	-10.131	-9.451	-8.847	-8.307
Amorphous silica	**-Log k_{diss}**	11.287	10.982	10.424	9.925	9.372	8.885	8.451	8.064
	Log k_{prec}	-10.000	-10.000	-10.000	-10.000	-10.000	-10.000	-10.000	-10.000
Pyrite	**-Log k_{diss}**	5.851	5.575	5.069	4.618	4.118	3.677	3.285	2.935
	Log k_{prec}	-9.627	-9.351	-8.845	-8.394	-7.894	-7.453	-7.061	-6.711
K-feldspar	**-Log k_{diss}**	11.576	11.355	10.946	10.573	10.153	9.777	9.437	9.130
	Log k_{prec}	-11.895	-11.711	-11.373	-11.072	-10.738	-10.443	-10.182	-9.948
Albite	**-Log k_{diss}**	11.166	10.835	10.228	9.685	9.082	8.550	8.076	7.652
	Log k_{prec}	-11.614	-11.275	-10.655	-10.102	-9.489	-8.947	-8.467	-8.037
Illite	**-Log k_{diss}**	12.022	11.874	11.595	11.336	11.035	10.754	10.490	10.239
	Log k_{prec}	-12.306	-12.136	-11.825	-11.548	-11.240	-10.969	-10.728	-10.512

Logarithm of dissolution and precipitation reaction rate (in mol.m^2.s^{-1}) as determined in TOUGHREACT code

INTENTIONALLY LEFT BLANK

APPENDIX 2: INPUT FILES

Chemical input files of FRACHEM: chem.dat

```
CHEM
 10.0  5000. .T.
 14 27  0
H2O          0.00 L  5.5515E+01      1.80000E+01  0.00000E+00
  0.938758E+00  0.531202E-03 -0.714763E-05  0.402949E-07 -0.771605E-10
Na+          1.00 L  1.1480E+00      23.0000E+00  0.00000E+00
  0.690774E+00  0.342080E-02 -0.368776E-04  0.114883E-06 -0.154321E-09
K+           1.00 L  7.3400E-02      39.0000E+00  0.00000E+00
  0.620091E+00  0.256082E-02 -0.264300E-04  0.768176E-07 -0.102881E-09
Ca++         2.00 L  0.1539E+00      40.0000E+00  0.00000E+00
  0.306380E+00 -0.198016E-03 -0.662294E-05  0.737311E-08  0.257202E-10
H+           1.00 L  1.2679E-05      1.00000E+00  0.00000E+00
  0.107989E+01  0.439006E-04 -0.205684E-04  0.811043E-07 -0.128601E-09
Cl-         -1.00 L  1.5269E+00      35.45000E+00  0.00000E+00
  0.601199E+00 -0.810744E-03 -0.102623E-05 -0.977366E-08  0.257202E-10
HCO3-       -1.00 L  9.4267E-04      61.0000E+00  0.00000E+00
  0.360300E+00  0.389609E-03 -0.135957E-04  0.442387E-07 -0.514403E-10
SO4--       -2.00 L  6.5974E-04      96.0000E+00  0.00000E+00
  0.522115E-01 -0.150909E-03 -0.197436E-05  0.997771E-08 -0.110597E-10
H4SiO4       0.00 L  6.0600E-03      96.0000E+00  0.00000E+00
  0.143047E+01 -0.594297E-02  0.599280E-04 -0.291495E-06  0.514403E-09
FE++         2.00 L  2.4000E-03      55.8500E+00  0.00000E+00
  0.126180E+00 -0.210151E-02  0.162531E-04  0.000000E+00  0.000000E+00
MG++         2.00 L  4.6050E-03      24.3000E+00  0.00000E+00
  0.314857E+00 -0.283000E-02  0.942857E-05 0.000000E+00  0.000000E+00
HS-         -1.00 L  9.8500E-04      33.0000E+00  0.00000E+00
  0.210969E-03 -0.507186E-05  0.877067E-07 -0.609429E-09  0.136579E-11
Al+++        3.00 L  3.7000E-06      26.9815E+00  0.00000E+00
  0.102442E-01 -0.213274E-03  0.169612E-05 -0.609318E-08  0.832131E-11
CO3--       -2.00 L  3.0182E-07      60.0000E+00  0.00000E+00
  0.382177E-01 -0.245813E-03 -0.143158E-06  0.378258E-08 -0.668724E-11
OH-         -1.00 L  2.8449E-06      17.0000E+00  0.00000E+00
  0.406520E+00  0.860523E-04 -0.101955E-04  0.212620E-07 -0.174868E-21
Ca(HCO3)+    1.00 L  1.1105E-18      101.000E+00  0.00000E+00
  0.486211E+00  0.539741E-03 -0.109594E-04  0.269204E-07 -0.257202E-10
CO2(aq)      0.00 L  1.6524E-02      44.0000E+00  0.00000E+00
  0.139083E+01 -0.142460E-02  0.171039E-04 -0.111454E-06  0.257202E-09
CaCO3(aq)    0.00 L  7.0223E-07      100.000E+00  0.00000E+00
  0.100000E+01  0.000000E+00  0.000000E+00  0.000000E+00  0.000000E+00
CASO4(AQ)    0.00 L  2.7056E-04      136.000E+00  0.00000E+00
  0.100000E+01  0.000000E+00  0.000000E+00  0.000000E+00  0.000000E+00
QUARTZ       0.00 S  8.18E+00       60.0000E+00  2.65000E+03
  0.100000E+01  0.000000E+00  0.000000E+00  0.000000E+00  0.000000E+00
CALCITE      0.00 S  8.30E00         100.000E+00  2.71000E+03
  0.100000E+01  0.000000E+00  0.000000E+00  0.000000E+00  0.000000E+00
DOLOMITE     0.00 S   1.15E+00       184.300E+00  2.71000E+03
  0.100000E+01  0.000000E+00  0.000000E+00  0.000000E+00  0.000000E+00
PYRITE       0.00 S  2.72E+00        119.850E+00  5.00000E+03
  0.100000E+01  0.000000E+00  0.000000E+00  0.000000E+00  0.000000E+00
SILICAM      0.00 S  159.2E+00       60.0000E+00  2.07000E+03
  0.100000E+01  0.000000E+00  0.000000E+00  0.000000E+00  0.000000E+00
KFELDS       0.00 S  11.54E+00       278.330E+00  2.50000E+03
  0.100000E+01  0.000000E+00  0.000000E+00  0.000000E+00  0.000000E+00
ALBITE       0.00 S  13.45E+00       262.220E+00  2.61000E+03
  0.100000E+01  0.000000E+00  0.000000E+00  0.000000E+00  0.000000E+00
ILLITE       0.00 S  13.12E+00       389.340E+00  2.75000E+03
```

```
 0.100000E+01  0.000000E+00  0.000000E+00  0.000000E+00  0.000000E+00
CO3--
  0.00  0.00  0.00  0.00 -1.00  0.00  1.00  0.00  0.00  0.00  0.00  0.00  0.00 1
 0.106210E+02 -0.141799E-01  0.119948E-03 -0.377598E-06  0.563170E-09
OH-
  1.00  0.00  0.00  0.00 -1.00  0.00  0.00  0.00  0.00  0.00  0.00  0.00  0.00 1
 0.149397E+02 -0.427928E-01  0.221928E-03 -0.752711E-06  0.129450E-08
Ca(HCO3)+
  0.00  0.00  0.00  1.00  0.00  0.00  1.00  0.00  0.00  0.00  0.00  0.00  0.00 1
-0.009172E+01  0.377718E-02 -0.100084E-03  0.355916E-06 -0.566154E-09
CO2(aq)
 -1.00  0.00  0.00  0.00  1.00  0.00  1.00  0.00  0.00  0.00  0.00  0.00  0.00 1
-0.657655E+01  0.122524E-01 -0.143343E-03  0.466424E-06 -0.666853E-09
CaCO3(aq)
  0.00  0.00  0.00  1.00 -1.00  0.00  1.00  0.00  0.00  0.00  0.00  0.00  0.00 1
 0.750075E+01 -0.218770E-01  0.865748E-04 -0.237638E-06  0.206620E-09
CASO4(AQ)
  0.00  0.00  0.00  1.00  0.00  0.00  0.00  1.00  0.00  0.00  0.00  0.00  0.00 1
-0.207040E+01 -0.255960E-03 -0.654052E-04  0.314719E-06 -0.770838E-09
QUARTZ
 -2.00  0.00  0.00  0.00  0.00  0.00  0.00  0.00  1.00  0.00  0.00  0.00  0.00 5
-0.450127E+01  0.230740E-01 -0.136254E-03  0.554763E-06 -0.955384E-09
0 .1 .1 1 0
CALCITE
  0.00  0.00  0.00  1.00 -1.00  0.00  1.00  0.00  0.00  0.00  0.00  0.00  0.00 5
 0.222690E+01 -0.154277E-01  0.866480E-05  0.164848E-07 -0.126807E-09
0 .1 .1 2 0
DOLOMITE
  0.00  0.00  0.00  1.00 -2.00  0.00  2.00  0.00  0.00  0.00  1.00  0.00  0.00 5
 0.340778E+01 -0.370318E-01  0.430942E-04 -0.191080E-07 -0.215571E-09
0 .1 .1 3 0
PYRITE
 -1.00  0.00  0.00  0.00  0.25  0.00  0.00  0.25  0.00  1.00  0.00  1.75  0.00 5
-0.265025E+02  0.836345E-01 -0.427566E-03  0.142557E-05 -0.247958E-08
0 .1 .1 4 0
SILICAM
 -2.00  0.00  0.00  0.00  0.00  0.00  0.00  0.00  1.00  0.00  0.00  0.00  0.00 5
-0.296646E+01  0.976023E-02 -0.251011E-04  0.273648E-07 -0.822790E-11
0 .1 .1 5 0
KFELDS
 -4.00  0.00  1.00  0.00 -4.00  0.00  0.00  0.00  3.00  0.00  0.00  0.00  1.00 5
 0.454871E+00 -0.144933E-01 -0.509821E-04  0.507837E-06 -0.109326E-08
0 .1 .1 6 0
ALBITE
 -4.00  1.00  0.00  0.00 -4.00  0.00  0.00  0.00  3.00  0.00  0.00  0.00  1.00 5
 0.541616E+01 -0.415801E-01 +0.381644E-04  0.331536E-06 -0.931468E-09
0 .1 .1 7 0
ILLITE
 -2.00  0.00  0.60  0.00 -8.00  0.00  0.00  0.00  3.50  0.00  0.25  0.00  2.30 5
 0.134375E+02 -0.133928E+00  0.461581E-03 -0.999223E-06  0.100997E-08
0 .1 .1 8 0
INJ
1
3  -1
PROD
1
15  -1
SURF
2000.0  65.0d0  0.0e6
ENDFI
```

Chemical input files of TOUGHREACT and DEBYE-HUCKEL: chemical.inp

```
'Soultz - Febr-18-05
'--------------------------------------------------------------------------'
'DEFINITION OF THE GEOCHEMICAL SYSTEM'
'PRIMARY AQUEOUS SPECIES'
'h2o'
'h+'
'ca+2'
'mg+2'
'na+'
'k+'
'cl-'
'sio2(aq)'
'hco3-'
'so4-2'
'alo2-'
'*'
'AQUEOUS COMPLEXES'
'al+3'
'caco3(aq)'
'cahco3+'
'caso4(aq)'
'co3-2'
'co2(aq)'
'oh-'
'*'
'MINERALS'
'quartz'          1    3     0    0
          1.2589e-14 0 1.0 1.0 87.5 0.0 0.0 0.0    ! prec.
          1.2589e-14 0 1.0 1.0 87.5 0.0 0.0 0.0  1.e-6   0    1.0000e+02 0 1.0 1.0 00.0  1.174  -0.002028  -4158.0  1.e-6
0
0.0   0.0    000.00
'k-feldspar'     1      3     0    0
          3.8905e-13    2   1.0  1.0  38.00  0.0  0.0  0.0
                    2
                    8.7096e-11   51.7    1   'h+'   0.5      ! acid mechanism
                    6.3096e-22   94.1    1   'h+'  -0.823    ! base
          3.8905e-13  0  1.0  1.0  38.00  0.0  0.0  0.0  1.e-6   0
0.0   0.    000.00
'calcite'        1      3     0    0
          1.5488e-06    2   1.0  1.0  23.50  0.0  0.0  0.0
                    1
                    5.0119e-01  14.40   1  'h+'  1.0
          1.5488e-6     0   1.0  1.0  23.50  0.0  0.0  0.0  1.e-6   0
0.0   0.    000.00
'dolomite'       1      3     0    0
          2.9512e-08    2   1.0  1.0  52.20  0.0  0.0  0.0
                    1
                    6.4565e-04  36.1    1   'h+'   0.5
          2.9512e-08    0   1.0  1.0  52.20  0.0  0.0  0.0  1.e-6   0
0.0   0.    000.00
'*'   0  0   0           0
'GASES'
'*'
'SURFACE COMPLEXES'
'*'
'species with Kd and decay    decay constant(1/s)'
'*'                  0.0d0
'EXCHANGEABLE CATIONS'
'               master     convention     ex. coef.'
'*'               0           0           0.0
```

```
'-------------------------------------------------------------------------'
'INITIAL AND BOUNDARY WATER TYPES'
2   0   0   !niwtype, nbwtype, nrwtype= number of ini, bound, rech waters
1     200.0    0                    !iwtype initial, temp (C)
'       icon        guess         ctot          constrain'         ! Vein alteration
h2o         1    0.1000E+01    0.10000E+01
h+          1    0.1000E-04    0.15617E+00
ca+2        1    0.1000E-00    0.16950E+00
mg+2        1    0.5000E-02    0.32100E-02
na+         1    0.1150E+01    0.11480E+01
k+          1    0.7000E-01    0.73400E-01
fe+2        1    0.2000E-02    0.26140E-02
cl-         1    0.1500E+01    0.16480E+01
sio2(aq)    1    0.6000E-02    0.60600E-02
hco3-       1    0.9000E-03    0.16002E+00
so4-2       1    0.6500E-03    0.17714E-02
alo2-       1    0.3700E-05    0.37000E-04
'*'         0         0.0           0.0           ' '      0
2      65.0    0                    !iwtype initial, temp (C)
'       icon        guess         ctot          constrain'         ! Vein alteration
h2o         1    0.1000E+01    0.10000E+01
h+          1    0.1000E-04    0.15617E+00
ca+2        1    0.1000E-00    0.16950E+00
mg+2        1    0.5000E-02    0.32100E-02
na+         1    0.1150E+01    0.11480E+01
k+          1    0.7000E-01    0.73400E-01
fe+2        1    0.2000E-02    0.26140E-02
cl-         1    0.1500E+01    0.16480E+01
sio2(aq)    1    0.6000E-02    0.60600E-02
hco3-       1    0.9000E-03    0.16002E+00
so4-2       1    0.6500E-03    0.17714E-02
alo2-       1    0.3700E-05    0.37000E-04
'*'         0         0.0           0.0           ' '      0
'-------------------------------------------------------------------------'
'INITIAL MINERAL ZONES'
 1
 1
'mineral         vol.frac. '                !  Vein alteration
'quartz'          0.409        1
1.0e-5            98.0e-1            0
'k-feldspar'      0.139         1
1.0e-5            98.0e-1            0
'calcite'         0.033       1
1.0e-5            98.0e-1            0
'dolomite'        0.008          1
1.0e-5            98.0e-1            0
'*'               0.0            0
'-------------------------------------------------------------------------'
'INITIAL gas ZONES'
1                                !ngtype= number of gas zones
1                                !igtype
'gas      partial pressure'    !at 25 C equil w/ water
'*'                0.0
'-------------------------------------------------------------------------'
'Permeability-Porosity Zones'
 1
 1
'perm law   a-par   b-par tcwM1'          ! Fractured vein
    5        0.16     2.0               ! PHIc=0.16, n(power term)=2
'-------------------------------------------------------------------------'
'INITIAL SURFACE ADSORPTION ZONES'
0                                !ndtype= number of sorption zones
```

```
'zone       ad.surf.(m2/kg)  total ad.sites (mol/l)'
'----------------------------------------if Sden=0 Kd store retardation factor'
'INITIAL LINEAR EQUILIBRIUM Kd ZONE'
1                                          !kdtpye=number of Kd zones
1                                          !idtype
'species   solid-density(Sden,kg/dm**3)  Kd(l/kg=mass/kg solid / mass/l'
'*'              0.0                0.0
'----------------------------------------if Sden=0 Kd store retardation factor'
'INITIAL ZONES OF CATION EXCHANGE'
0                            !nxtype= number of exchange zones
'zone           ex. capacity'
'-------------------------------------------------------------------------------'
'end'
```

Chemical input files of TOUGHREACT and PITZER: extract from chemical.inp

The only difference with the file presented above concerns the water composition

```
/……
'-------------------------------------------------------------------------------'
'INITIAL AND BOUNDARY WATER TYPES'
2   0   0   !niwtype, nbwtype, nrwtype= number of ini, bound, rech waters
1     200.0    0                      !iwtype initial, temp (C)
'       icon        guess         ctot         constrain'        ! Vein alteration
h2o        1    0.1000E+01    0.10000E+01
h+         1    0.1000E-04    0.32305E-02
ca+2       1    0.1000E-00    0.16950E+00
mg+2       1    0.5000E-02    0.32100E-02
na+        1    0.1150E+01    0.11480E+01
k+         1    0.7000E-01    0.73400E-01
fe+2       1    0.2000E-02    0.26140E-02
cl-        1    0.1500E+01    0.16480E+01
sio2(aq)   1    0.6000E-02    0.60600E-02
hco3-      1    0.9000E-03    0.74998E-02
so4-2      1    0.6500E-03    0.17710E-02
alo2-      1    0.3700E-05    0.37000E-04
'*'        0        0.0           0.0           ' '      0
2      65.0    0                      !iwtype initial, temp (C)
'       icon        guess         ctot         constrain'        ! Vein alteration
h2o        1    0.1000E+01    0.1000E+01
h+         1    0.1000E-04    0.32305E-02
ca+2       1    0.1000E-00    0.16950E+00
mg+2       1    0.5000E-02    0.32100E-02
na+        1    0.1150E+01    0.11480E+01
k+         1    0.7000E-01    0.73400E-01
fe+2       1    0.2000E-02    0.26140E-02
cl-        1    0.1500E+01    0.16480E+01
sio2(aq)   1    0.6000E-02    0.60600E-02
hco3-      1    0.9000E-03    0.74998E-02
so4-2      1    0.6500E-03    0.17710E-02
alo2-      1    0.3700E-05    0.37000E-04
'*'        0        0.0           0.0           ' '      0
/.........
```

Flow input files of TOUGHREACT: flow.inp

```
# Batch model for initializing water chemistry, Soultz site
ROCKS----1----*----2----*----3----*----4----*----5----*----6----*----7----*----8
VEINA    1     2650.      0.10  0.55E-12  0.55E-12  0.55E-12       2.9        0.
                                    0.3
CONBD    1     2650.      0.02   1.0E-18   1.0E-18   1.0E-18       3.0     1000.
                                   0.05

START
REACT----1MOPR(20)-2----*----3----*----4----*----5----*----6----*----7----*----8
00020000231000                            ! 5(1, HMW)1(0)0
PARAM----1 MOP: 123456789*123456789*1234 ---*----5----*----6----*----7----*----8
   29999    900000000010002000140000500 0
          1.5768E08      -1.0   8.64E02                9.81
     1.E00     1.E00     1.E00     1.E00     1.E00     1.E00     1.E00     1.E00
     1.E-7        1.        0.1        1.        1.     1.E-8
 0.5000000000000E+08 0.2000000000000E+03
RPCAP----1----*----2----*----3----*----4----*----5----*----6----*----7----*----8
    1        0.33333      0.05        1.        1.
    1             0.        1.
TIMES----1----*----2----*----3----*----4----*----5----*----6----*----7----*----8
    9
   8.64E048.6400E+052.5920E+061.55520E07 3.1104E07 6.3072E07 9.4608E071.26144E08
 1.5768E08
ELEME----1----*----2----*----3----*----4----*----5----*----6----*----7----*----8
    1             10.2500E+000.1000E+02          0.2500E+000.5000E+01-.2500E-01
    2             10.5000E+000.2000E+02          0.1000E+010.5000E+01-.2500E-01
    3             10.1000E+010.4000E+02          0.2500E+010.5000E+01-.2500E-01
    4             10.2000E+010.8000E+02          0.5500E+010.5000E+01-.2500E-01
    5             10.4000E+010.1600E+03          0.1150E+020.5000E+01-.2500E-01
    6             10.5000E+010.2000E+03          0.2050E+020.5000E+01-.2500E-01
    7             10.1225E+020.4900E+03          0.3775E+020.5000E+01-.2500E-01
    8             10.2500E+020.1000E+04          0.7500E+020.5000E+01-.2500E-01
    9             10.2500E+020.1000E+04          0.1250E+030.5000E+01-.2500E-01
   10             10.2500E+020.1000E+04          0.1750E+030.5000E+01-.2500E-01
   11             10.2500E+020.1000E+04          0.2250E+030.5000E+01-.2500E-01
   12             10.2500E+020.1000E+04          0.2750E+030.5000E+01-.2500E-01
   13             10.2500E+020.1000E+04          0.3250E+030.5000E+01-.2500E-01
   14             10.2500E+020.1000E+04          0.3750E+030.5000E+01-.2500E-01
   15             10.2500E+020.1000E+04          0.4250E+030.5000E+01-.2500E-01
   16             10.2500E+020.1000E+04          0.4750E+030.5000E+01-.2500E-01
   17             10.2500E+020.1000E+04          0.5250E+030.5000E+01-.2500E-01
   18             10.2500E+020.1000E+04          0.5750E+030.5000E+01-.2500E-01
   19             10.1225E+020.4900E+03          0.6122E+030.5000E+01-.2500E-01
   20             10.5000E+010.2000E+03          0.6295E+030.5000E+01-.2500E-01
   21             10.4000E+010.1600E+03          0.6385E+030.5000E+01-.2500E-01
   22             10.2000E+010.8000E+02          0.6445E+030.5000E+01-.2500E-01
   23             10.1000E+010.4000E+02          0.6475E+030.5000E+01-.2500E-01
   24             10.5000E+000.2000E+02          0.6490E+030.5000E+01-.2500E-01
   25             10.2500E+000.1000E+02          0.6498E+030.5000E+01-.2500E-01
L   1             10.2000E+310.0000E+00          0.0000E+000.0000E+000.0000E+00
   30             10.2000E+310.0000E+00          0.6510E+030.0000E+000.0000E+00
con00          CONBD

CONNE----1----*----2----*----3----*----4----*----5----*----6----*----7----*----8
    1    2                  10.2500E+000.5000E+000.5000E+00
    2    3                  10.5000E+000.1000E+010.5000E+00
    3    4                  10.1000E+010.2000E+010.5000E+00
    4    5                  10.2000E+010.4000E+010.5000E+00
    5    6                  10.4000E+010.5000E+010.5000E+00
    6    7                  10.5000E+010.1225E+020.5000E+00
```

```
    7    8                   10.1225E+020.2500E+020.5000E+00
    8    9                   10.2500E+020.2500E+020.5000E+00
    9   10                   10.2500E+020.2500E+020.5000E+00
   10   11                   10.2500E+020.2500E+020.5000E+00
   11   12                   10.2500E+020.2500E+020.5000E+00
   12   13                   10.2500E+020.2500E+020.5000E+00
   13   14                   10.2500E+020.2500E+020.5000E+00
   14   15                   10.2500E+020.2500E+020.5000E+00
   15   16                   10.2500E+020.2500E+020.5000E+00
   16   17                   10.2500E+020.2500E+020.5000E+00
   17   18                   10.2500E+020.2500E+020.5000E+00
   18   19                   10.2500E+020.1225E+020.5000E+00
   19   20                   10.1225E+020.5000E+010.5000E+00
   20   21                   10.5000E+010.4000E+010.5000E+00
   21   22                   10.4000E+010.2000E+010.5000E+00
   22   23                   10.2000E+010.1000E+010.5000E+00
   23   24                   10.1000E+010.5000E+000.5000E+00
   24   25                   10.5000E+000.2500E+000.5000E+00
L   1    1                   10.1000E-030.5000E-010.1000E+010.0000E+00
   25   30                   10.1000E+020.1000E+010.1000E+010.0000E+00

INCON----1----*----2----*----3----*----4----*----5----*----6----*----7----*----8
L   1                     0.1
           0.58E+08            0.65E+02

ENDCY

MESHMAKER1----*----2----*----3----*----4----*----5----*----6----*----7----*----8
XYZ

NX      25        0.
5.0000e-011.0000e-002.0000e-004.0000E-008.0000E-001.0000E+012.4500E+015.0000E+01
5.0000E+015.0000E+015.0000E+015.0000E+015.0000E+015.0000E+015.0000E+015.0000E+01
5.0000E+015.0000E+012.4500E+011.0000E+018.0000E+004.0000E+002.0000E+001.0000E+00
5.0000E-01
NY       11.0000E+01
NZ       15.0000E-02


ENDFI----1----*----2----*----3----*----4----*----5----*----6----*----7----*----8
```

PROCEEDINGS, Thirty-First Workshop on Geothermal Reservoir Engineering
Stanford University, Stanford, California, January 30-February 1, 2006
SGP-TR-179

COMPARING FRACHEM AND TOUGHREACT FOR REACTIVE TRANSPORT MODELING OF BRINE-ROCK INTERACTIONS IN ENHANCED GEOTHERMAL SYSTEMS (EGS)

Laurent André[(1)], Nicolas Spycher[(2)], Tianfu Xu[(2)], Karsten Pruess[(2)] & François-D. Vuataz[(1)]

[(1)] Centre for Geothermal Research – CREGE, c/o CHYN - Emile Argand 11, CH-2009 Neuchâtel, Switzerland
[(2)] Earth Sciences Division - Lawrence Berkeley National Laboratory - University of California - Berkeley, CA 94720, USA

laurent.andre@unine.ch, nspycher@lbl.gov, tianfu_xu@lbl.gov, k_pruess@lbl.gov, francois.vuataz@crege.ch

ABSTRACT

Coupled modelling of fluid flow and reactive transport in geothermal systems is challenging because of reservoir conditions such as high temperatures, elevated pressures and sometimes high salinities of the formation fluids. Thermal-hydrological-chemical (THC) codes, such as FRACHEM and TOUGHREACT, have been developed to evaluate the long-term hydrothermal and chemical evolution of exploited reservoirs. In this study, the two codes were applied to model the same geothermal reservoir, to forecast reservoir evolution using respective thermodynamic and kinetic input data. A recent (unreleased) TOUGHREACT version allows the use of either an extended Debye-Hückel or Pitzer activity model for calculating activity coefficients, while FRACHEM was designed to use the Pitzer formalism. Comparison of models results indicate that differences in thermodynamic equilibrium constants, activity coefficients and kinetics models can result in significant differences in predicted mineral precipitation behaviour and reservoir-porosity evolution. Differences in the calculation schemes typically produce less difference in model outputs than differences in input thermodynamic and kinetic data, with model results being particularly sensitive to differences in ion-interaction parameters for high-salinity systems.

INTRODUCTION

This work was initiated through the collaboration between the CREGE (Centre for Geothermal Research – Neuchâtel, Switzerland), and LBNL (Lawrence Berkeley National Laboratory – Earth Science Division – Berkeley, California, USA). These two institutions have developed reactive transport simulators applicable to geothermal systems.

The Centre of Hydrogeology of Neuchâtel and now the CREGE have been involved since 1998 in the European Soultz EGS project (Alsace, France), for which the main objective is to build a pilot plant for power production based on the circulation of a geothermal fluid through a deep fractured reservoir. Different studies (Durst, 2002; Bächler, 2003, Rabemanana et al. 2003; André et al., 2005; Bächler and Kohl, 2005) have progressively allowed the development of a geochemical code able to take into account the main characteristics of the Soultz reservoir at a depth of 5 km: 200°C, 500 bars and a fluid salinity of 100 g L^{-1} (ionic strength around 1.8 molal). The resulting code is called FRACHEM.

LBNL developed TOUGHREACT (Xu and Pruess, 2001; Xu et al., 2004) by introducing reactive transport into the existing code TOUGH2 (Pruess et al., 1999). TOUGHREACT has been applied to different problems such as CO_2 sequestration in deep saline aquifers and the prediction of the underground thermal, hydrological, and chemical evolution around nuclear waste geologic repositories. Recent developments of this code included the addition of the Pitzer formalism (Pitzer, 1973) for the computation of activity coefficients in highly saline brines (Zhang et al., in prep).

The aim of this collaboration between CREGE and LBNL, working in similar fields with similar tools, was both to exchange ideas between the two laboratories and to compare the characteristics of the two codes. For best comparison, the two codes were applied to the same geothermal problem: the circulation of cooled brine in a hot porous-equivalent reservoir similar to that at Soultz, between two wells spaced 650 m apart. However, the model conceptualisation was somewhat different with the two codes. Closed-loop injection of fluid under near-reservoir conditions was simulated with FRACHEM, whereas open injection of the same reservoir fluid was simulated with TOUGHREACT (constant fluid composition, without previous circulation in the reservoir). Simulated processes within the reservoir included mineral precipitation/dissolution and changes in reservoir porosity.

The circulation of cooled fluid in the reservoir affects its temperature and involves a thermodynamic disequilibrium between rocks and fluid, resulting in the dissolution and precipitation of several minerals. Mineral precipitation and dissolution have an impact on the evolution of reservoir porosity. The two codes and respective thermodynamic and kinetic input data, as well as activity coefficient models, yield significant divergences, most particularly with respect to the computed solubility of carbonate minerals (mainly calcite) and CO_2 partial pressure. Two reasons can be advanced to explain these differences. First and foremost, activity coefficients are computed using different formulations (Pitzer versus extended Debye-Hückel) and/or different sources of ion interaction parameters, thus generating differences in the predicted solubility and precipitation behaviour of calcite, underlining the importance of these data for reactive transport simulations involving saline reservoirs. Second, differences of model conceptualisation (i.e. simulation of closed-loop versus open injection with FRACHEM and TOUGHREACT, respectively) also affect model results, however to a much lesser extent.

THE CODES

FRACHEM

FRACHEM is a THC simulator issued from the combination of two existing codes: FRACTure and CHEMTOUGH2. FRACTure is a 3-D finite-element code for modelling hydrological, transport and elastic processes. It was developed originally for the study of flow-driven interactions in fractured rock (Kohl & Hopkirk, 1995). CHEMTOUGH2 (White, 1995) is a THC code developed after the TOUGH2 simulator (Pruess, 1991), a 3-D numerical model for simulating the coupled transport of water, vapor, non-condensable gas and heat in porous and fractured media. CHEMTOUGH2 presents the possibility to transport chemical species and to model the chemical water-rock interactions as well as the chemical reactions driven by pressure and temperature changes. The transport and reaction are coupled using a one-step approach.

FRACHEM has been built by introducing geochemical subroutines from CHEMTOUGH2 (White, 1995) into the framework of the code FRACTure (Bächler, 2003; Bächler and Kohl, 2005). After an initialisation phase, FRACTure calculates, over each time step, the thermal and hydrological conditions within each element volume and determines the advective flow between each of them. Resulting thermal and hydrological variables are stored in arrays common to FRACTure and the geochemical modules. At this point the program calculates the chemical reactions using a mass balance/mass action approach, the advective transport of chemical species and the variations of porosity and permeability. Once this calculation is performed, the porosity and permeability are updated and fed into the FRACTure part of the code. The program then returns to the start of the loop until the end of the simulation time (sequential non-iterative approach, SNIA).

FRACHEM has been developed specially for the granitic reservoir of Soultz-sous-Forêts and consequently, specific implementations have been added to the chemical part of this code. The reservoir, at a depth of 5000 m, contains a brine with total dissolved solids (TDS) about 100 g kg^{-1} and a temperature of 200°C. Considering the high salinity of the geofluid, the Debye-Hückel model, initially implemented in the CHEMTOUGH2 routines to determine the activity coefficients, has been replaced by a Pitzer activity model. It should be mentioned here that the activity coefficients calculations are carried out in an indirect manner by means of another code, TEQUIL (Moller et al., 1998). For a given fluid composition (constant ionic strength), the activity coefficients are determined at different temperatures in the range 50 - 200°C using TEQUIL before running FRACHEM. The activity coefficient values obtained at each temperature are regressed as a function of temperature using a polynomial fit, with coefficients then entered into the chemical input file. This approach works well for the case of Soultz simulations because the ionic strength of the circulated fluid remains more or less constant.

Presently, a limited number of minerals are considered, which correspond to the minerals constituting the Soultz granite. The precipitation/ dissolution reactions of carbonates (calcite, dolomite), quartz, amorphous silica, pyrite and some aluminosilicates (K-feldspar, albite, illite) can be modelled under kinetic constraints. The implemented kinetic rate laws are specific to each mineral and taken from published experiments conducted at high temperature in NaCl brines. Thermodynamic data (equilibrium constants) are taken mostly from SUPCRT92 (Johnson et al., 1992) and Helgeson et al. (1978) and are function of temperature and pressure.
At last, a supplementary module allows the determination of porosity and permeability variations linked with chemical processes occurring in the reservoir. Considering the alteration of the Soultz granite, the flow is assumed to circulate in a medium composed of fractures and grains. Therefore, a combination of fracture model (Norton and Knapp, 1977; Steefel and Lasaga, 1994) and grain model (Bolton et al., 1996) is used to determine the permeability evolution.

TOUGHREACT

TOUGHREACT (Xu and Pruess, 2001; Xu et al., 2004) was developed by introducing multi-

component reactive transport into the framework of the existing multi-phase 3-D finite volume fluid and heat flow code TOUGH2 (Pruess, 1991). It is a THC simulator applicable to a wide range of subsurface conditions and to a variety of reactive fluid and geochemical transport problems. Flow, transport, and chemistry are coupled in a sequential manner. Here, a sequential non-iterative approach was applied for consistency with the FRACHEM simulations.

TOUGHREACT takes into consideration many processes such as 1) fluid flow in both liquid and gas phases occurring under pressure, viscous, and gravity forces; 2) heat flow by conduction and convection; 3) diffusion of water vapor and air; 4) thermophysical and geochemical reactions as a function of temperature, such as fluid (gas and liquid) density and viscosity, and thermodynamic and kinetic data for mineral-water-gas reactions; 5) transport of aqueous and gaseous species by advection and molecular diffusion in liquid and gas phases, respectively; 6) temporal changes in porosity, permeability, and unsaturated hydrologic properties owing to mineral dissolution, precipitation and clay swelling.

Geochemical computations are carried out using a mass balance/mass action approach. By default, activity coefficients are computed using an extended Debye-Hückel model (Helgeson et al., 1981) applicable to NaCl-dominant, moderately saline solutions. Recently, a full Pitzer ion-interaction model was implemented as an option, using the formulation of Harvie et al. (1984) (Zhang et al., in prep; see also Zhang et al., 2004). The themodynamic database used for the TOUGHREACT simulations presented here makes use of equilibrium constants mostly from SUPCRT92 (Johnson et al., 1992) and ion-interaction parameters re-evaluated and fitted as a function of temperature by Wolery et al. (2004) (as published by Alai et al., 2005). Other thermodynamic and kinetic data are also functions of temperature.

Mineral dissolution and precipitation can proceed either subject to local equilibrium or kinetic conditions. For kinetically-controlled mineral dissolution and precipitation, a general form of rate law (Lasaga, 1984; Steefel and Lasaga, 1994; Palandri and Kharaka, 2004) is used.

Changes in porosity during the simulation are calculated from changes in mineral volume fractions. Several porosity-permeability and fracture aperture-permeability relationships are included in the model. Here, fracture porosity is related to permeability using the relationship proposed by Verma and Pruess (1988) and described in Xu et al. (2004).

APPLICATIONS

The two codes have been applied to a 2-D geometrical model representing the granitic reservoir at Soultz. Injection and production wells are linked by permeable fracture zones surrounded by low-permeability granite matrix. Each fracture zone has an aperture of 0.1 m, a fixed horizontal depth of 10 m and a porosity of 10% (Figure 1).

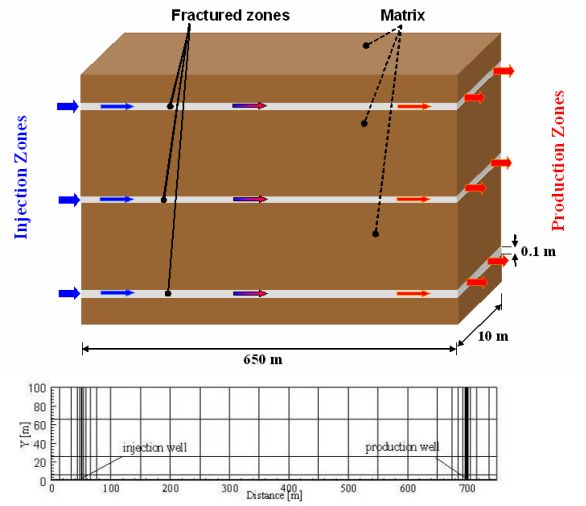

Figure 1: Simplified model and spatial discretization.

It is assumed that the fluid exchange with the surrounding low permeability matrix is insignificant. Because of symmetry, it is sufficient to consider only the upper part of one fracture zone in the simulation (Figure 1).

It should be noted that, with FRACHEM, matrix gridblocks are added above the fracture block for proper thermal behaviour. The modelled area is discretized into 222 2-D elements (Figure 1): 25 for the fracture zone and 197 for the matrix. The size of the element is ranging from a minimum of 0.5 m x 0.05 m near the injection and the production wells to a maximum of 50 m x 35 m. With TOUGHREACT, however, only the fracture zone is modelled, without adjacent matrix blocks. Heat loss in the impermeable matrix is modelled by a semi-analytical solution (Vinsome and Westerveld, 1980) built into the code. As a result, the model contains only 25 elements.

Initially the system temperature was set to the reservoir temperature of 200°C. The geothermal fluid (Table 1) was injected in the fracture zone at a rate of $2x10^{-2}$ L s^{-1} at a constant temperature of 65°C. A constant overpressure of 8 MPa was assumed at the injection well. With FRACHEM, Dirichlet boundary conditions were applied to the upper, left and right side of the model. The fluid was continuously recirculated from the production well to the injection well. With TOUGHREACT, the fluid was not

recirculated, and constant boundary conditions were simulated by connecting gridblocks of infinite dimensions to the injection well (constant chemical composition, temperature and pressure) and to the production well (constant temperature and pressure).

Table 1: Mean composition of fluid coming from the reservoir at a depth of 5 km.

Species	Concentration [mmol/kg_{H2O}]
Na^+	1148
K^+	73.4
Ca^{2+}	169.5
Mg^{2+}	3.2
Cl^-	1648
S	1.7
C	42.5
Fe^{2+}	2.6
SiO_2	6.1

Due to the sensitivity of the sequential non-iterative approach (SNIA) method to time discretization, the time step used for this simulation was limited to 10^2s. The values of thermo-hydraulic parameters considered in the simulation are listed in Table 2.

Table 2: Thermo-hydraulic model parameters.

Parameters		Fracture	Matrix	Fluid
Permeability	[m^2]	$5x10^{-13}$	10^{-18}	-
Thermal conductivity	[W/m.K]	2.9	3	0.6
Density	[kg/m^3]	-	2650	1000
Heat capacity	[J/kg.K]	-	1000	4200
Porosity	[%]	10	2	-

EFFECTS OF CHEMICAL PARAMETERS

Before presenting results of reactive transport simulations, we evaluate the factors most likely to affect chemistry results: the activity coefficients of dissolved species, the mineral equilibrium constants, and the minerals reaction rates.

The equilibrium constants used in the respective databases are not all derived from the same sources but a reasonably good agreement is observed for the minerals included in the simulations, including carbonates (calcite and dolomite) and silica phases (quartz and amorphous silica). Only small divergences are observed for aluminium silicates.

The reaction rates of calcite, quartz and amorphous silica present a good agreement. For aluminosilicates (K-feldspar, albite and illite), the differences can reach about two orders of magnitude, but this can be explained easily by the fact that, with FRACHEM, the inhibitor effect of Na^+ was taken into consideration, whereas it was not TOUGHREACT simulations.

Of greatest importance here, with a concentrated fluid, is the calculation of activity coefficients, which affect ion activities and consequently the saturation indices of minerals. The effect is most significant with minerals including divalent cations, such as calcium and magnesium carbonates, which have a strong effect on pH. Because we initially observed large differences in pH values computed with FRACHEM and TOUGHREACT (up to 1.5 pH units), we decided to run benchmark simulations for a case of simple cooling without mass transfer to minerals or gases (homogeneous equilibrium) and no transport. This allowed the results of several other popular geochemical codes and thermodynamic databases to be compared with one another for the exact same problem.

A Soultz-like brine, with pH = 4.9 at 200°C was numerically cooled from 200 to 20°C without considering reaction with minerals. The evolution of the brine pH and its saturation with respect to calcite was evaluated using the following different models and databases.

- PHREEQC 2.12 (Parkhurst and Appelo, 1999) with the "phreeqc" (Debye-Hückel) and "pitzer" databases (phreeqc.dat 431 2005-08-23 and pitzer.dat 2005-11-16, as released with version 2.12)

- TEQUIL, incorporating a Pitzer activity coefficient model and data for the Na-K-H-Ca-Cl-SO_4-HCO_3-CO_3-CO_2-H_2 system (Møller et al, 1998). As noted earlier, TEQUIL results are used by FRACHEM to compute activity coefficients, so FRACHEM was not used directly in this benchmarking exercise.

- TOUGHREACT, two versions including 1) the released version 1.0 (Xu et al., 2004), making use of the extended Debye-Hückel activity coefficient model of Helgeson et al. (1981) and thermodynamic data from the EQ3/6 database "data0.ymp", and 2) an unreleased version using the Pitzer activity coefficient model and the EQ3/6 database "data0.ypf" (Wolery et al., 2004, as published in Alai et al., 2005).

- EQ3/6 8.0 (Wolery and Jareck, 2003) with 1) the "b-dot" extended Debye-Hückel model of Helgeson (1969) and database "data0.ymp"; 2) the Pitzer model and database "data0.hmw" (after Harvie et al., 1984); and 3) the Pitzer model and "data0.ypf" database (Wolery et al., 2004, as published in Alai et al., 2005).

- SOLVEQ/CHILLER (Reed, 1998; Reed and Spycher, 1998), which incorporates the extended Debye-Hückel model of Helgeson et al. (1981) and the same equilibrium constants as used with TOUGHREACT.

All these codes were applied to the same fluid composition (ionic strength ~ 1.8 molal, Na-Cl dominated Soultz-like fluid), except for the total H^+ concentration which initially needs to be computed by each code from the input brine pH of 4.9 at 200ºC.

The cooling of the solution induces shifts in the equilibrium between aqueous species as a result of the temperature effect on equilibrium constants and activity coefficients. Note that the equilibrium constants for calcite were nearly the same in all the databases considered. It was also verified that only those secondary aqueous species called for by the different activity coefficient models were included in simulations.

Significantly different results were obtained. Figures 2 and 3 present the most remarkable parameters: pH and saturation index of calcite. Some variations were expected, in particular the differences between the simulations using the Debye-Hückel model and those using the Pitzer formalism. More surprising are differences between results of simulations making use of the same methodology for computing activity coefficients. Using the Pitzer formalism, major divergences appear with the use of different ion-interaction parameters. Upon cooling, a pH increase is predicted with EQ3/6 when the "data0.ypf" Pitzer database is used, but a decrease similar to that computed with TEQUIL is predicted when the "data0.hmw" is used. Because the TOUGHREACT Pitzer version was used with the EQ3/6 "data0.ypf" database, the two codes are in very close agreement when using this database.

In contrast, results from the other codes and databases all predict a pH decrease (at least initially), with differences reaching more than 2 pH units at 20°C (Figure 2). Consequently, computed saturation indices of minerals such as calcite vary tremendously (Figure 3), in three cases leading to supersaturation with respect to this mineral and a change from retrograde to prograde solubility above ~110ºC, and in most other cases yielding undersaturation and the usual retrograde solubility behaviour.

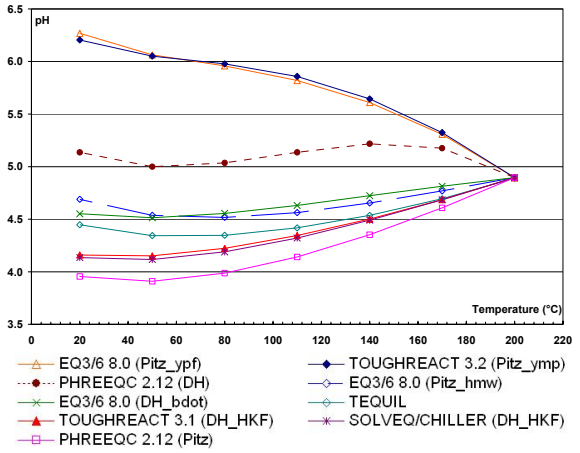

Figure 2: Calculated pH evolution of a brine with ionic strength of 1.8 during its cooling from 200 to 20°C. Variations are observed for different geochemical codes and databases (DH: Debye-Hückel; Pitz: Pitzer; see text)

These results illustrate the importance of input thermodynamic data in geochemical computations, and particularly those affecting activity coefficients when dealing with concentrated solutions. When using the Pitzer formalism, the types of ion-interaction parameters included in simulations (binary, ternary, cation-anion, etc.) and their variation with temperature are critical. When using simpler Debye-Hückel expressions, extrapolations to higher ionic strengths present significant risks. In the present case, differences shown in Figures 2 and 3 are still being investigated. In some databases, some of the ion-interaction parameters are set to 0, or fixed with temperature. "Double counting" between interaction parameters and secondary species is also a possibility. Even with the simpler Debye-Hückel model, consistency between the activity coefficient model and the types and dissociation constants of secondary aqueous species is critical. At this time, for this particular example, we tend to give preference to the results of TEQUIL and those of EQ3/6 (Pitzer version) with the "data0.hmw" database, although we cannot discard the other results until further study. Obviously, differences in calcite solubility behaviour such as those shown on Figure 3 have direct implications on evaluations of long-term reservoir productivity at Soultz, as described in the next sections.

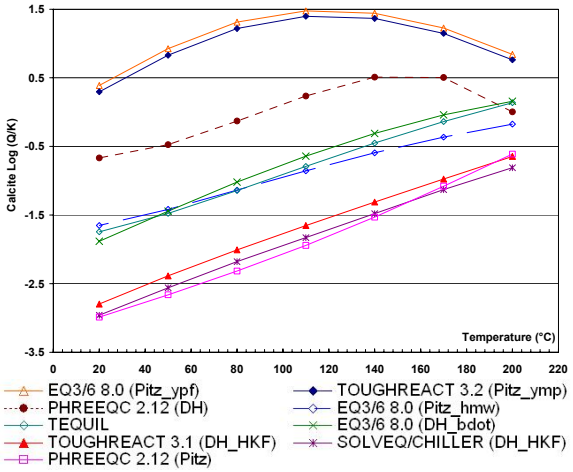

Figure 3: Predicted saturation index of calcite during the cooling from 200 to 20°C of a brine with ionic strength of 1.8.

REACTIVE TRANSPORT RESULTS

Simulations with FRACHEM (Pitzer model of TEQUIL)

The observation of the mineral behaviour shows that all the reactions occur in the first 20 metres of the injection zone. Calcite, a secondary mineral, present within granite fractures in relatively small proportions, is the most reactive.

In the vicinity of the injection well, calcite dissolves whereas it precipitates from about 2 to 20 m. This is due to the retrograde solubility of calcite (solubility decrease with temperature increase). At the onset of fluid circulation within the reservoir, calcite dissolves mainly within the first two metres of the injection well. This dissolution releases calcium in solution which is then available for calcite precipitation further away from the injection well where the temperature increases. With increasing simulation times and decreasing rock temperatures, the dissolution of calcite extends towards the production well and ends when this mineral becomes depleted.
Another carbonate has also been investigated. Figure 4 shows that dolomite dissolves within the first ten metres from the injection well. Similarly to calcite, dolomite dissolution stops when this mineral becomes depleted.

Among silicates, quartz and K-feldspar are major minerals in granite. Contrary to calcite, the solubility of these minerals decreases with cooling. As a consequence, these minerals precipitate near the injection well (note that the fluid always remains undersaturated with respect to amorphous silica in this case) and less so further away as temperature increases.

After 25–30 metres along the fracture, the fluid becomes essentially unreactive with all the minerals shown in Figure 4 as the injected brine becomes close to equilibrium with these minerals.

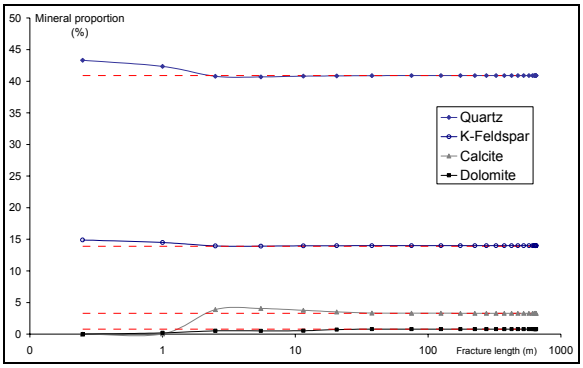

Figure 4: Predicted mineral precipitation and dissolution with FRACHEM after 5 years of circulation (volume percent). The dashed lines correspond to the initial amounts.

Simulations with TOUGHREACT and the Extended Debye-Hückel model

The carbonates are the most reactive minerals. As presented in the case of the FRACHEM simulations, calcite and dolomite dissolve near the injection well (Figure 5).

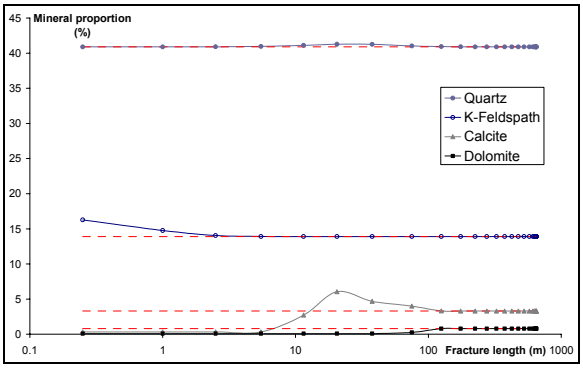

Figure 5: Predicted mineral precipitation and dissolution with TOUGHREACT and extended Debye-Hückel model, after 5 years of injection (volume percent). The dashed lines correspond to the initial amounts.

These minerals are predicted to dissolve faster than in the FRACHEM simulations because of small differences in reaction rates. Calcite dissolves for the first 10 metres (when temperature is below 145°C), then precipitates between 10 and 100 metres from the injection well. Dolomite dissolves within the first 100 metres and remains unaffected further out. Quartz precipitation is negligible, whereas feldspars precipitate in the close vicinity of the injection well.

Simulations with TOUGHREACT and the Pitzer model

The behaviour of silicates is mostly similar to preceding results obtained with the Debye-Hückel model and with FRACHEM. However, the behaviour of calcite is notably different. We showed earlier that cooling simulations using the extended Debye-Hückel model, and the FRACHEM simulations, yield a low pH at 65°C (4–4.5 range) (Figure 2) and consequently undersaturation with respect to calcite at this temperature (Figure 3). In contrast, the Pitzer database used here (Wolery et al., 2004) yields a significantly higher predicted pH (near 6.2) in the fluid cooled to 65°C and, as a result, significant supersaturation with respect to calcite (Figure 3). Consequently, the injection of this solution in the system leads to important calcite precipitation along the first 10 metres of the fracture zone and a more moderate precipitation between 10 and 400 metres from the injection well (Figure 6).

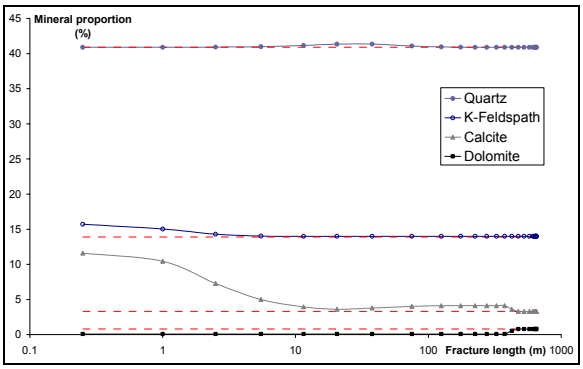

Figure 6: Predicted mineral precipitation and dissolution with TOUGHREACT and the Pitzer model, after 5 years of injection (volume percent). The dashed lines correspond to the initial amounts.

Implications on predicted reservoir porosity

The predicted evolution of reservoir porosity (Figure 7) is determined according to the mineral reactions occurring in the reservoir. As expected from the results presented above, the three models give rather different results.

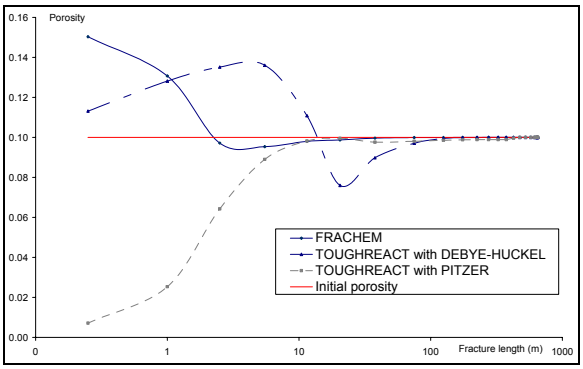

Figure 7: Evolution of the reservoir porosity after 5 years of circulation.

In the FRACHEM simulation, the porosity increases near the injection well due to the dissolution of carbonates (calcite and dolomite). It increases by 30% in the first metre from the injection well before decreasing quickly between 1 and 10 metres because of calcite reprecipitation. The predicted maximum porosity decrease is close to 6%.

With the Debye-Hückel TOUGHREACT model, the general trend is somewhat similar to that predicted with FRACHEM. The porosity increases near the injection well and in the first ten metres of the fracture zone, due to carbonates dissolution. Calcite precipitation between 10 and 100 metres decreases the porosity within this interval by a maximum of about 25%. Feldspar precipitation near the injection well (Figure 5) reduces the magnitude of porosity increase near the well. At first, porosity increases to ~0.14 due to carbonates dissolution and then, when carbonates have disappeared, silicates precipitate, resulting in a porosity decrease.

With the Pitzer TOUGHREACT model, the porosity evolves differently. Calcite precipitation leads to a large decrease of porosity within the first ten metres from the injection well. Because the same fluid (in this case supersaturated with respect to calcite at 65ºC) is continuously injected in the system, calcite precipitation never stops. The small amount of dolomite dissolution in this zone (Figure 5) cannot compensate for the porosity reduction caused by calcite precipitation and, after five years of circulation, the porosity at the injection well head becomes close to zero.

It should be noted that these respective evolutions of porosity are also affected by the simulated injection mode. In the FRACHEM simulation, the injected fluid circulates in a closed loop; the brine is heated in the system in contact with rock, and then cooled to 65°C before injection. In the TOUGHREACT simulations, the same fluid (initially equilibrated with the reservoir) is continuously injected. This difference in conceptualization affects the behaviour of silicates. These minerals precipitate near the injection well because of the temperature decrease. However, no significant dissolution of silicates occurs within the reservoir (slower dissolution than precipitation), such that the amounts of dissolved silica and aluminium initially deposited near the injection wells are never fully replenished when the brine circulates through the reservoir. Consequently, less silicate precipitate close to the injection well in the case of closed circulation, compared to open injection. This effect is most visible after injection periods longer than five years, and is negligible compared to the large difference in calcite precipitation behaviour between the models.

CONCLUSIONS

The goal of this work was to compare two geochemical transport codes, FRACHEM and TOUGHREACT, to model complex systems like geothermal reservoirs. Significant differences in model results were found to be caused primarily by differences in activity coefficient models and their parameters.

First, this study highlights the importance of the databases in the results of geochemical modelling in particular for brines. Depending on the implemented activity coefficient models and sources of input parameters for these models, variations reaching 2 units have been observed in the predicted brine pH. Such pH differences have a strong impact on saturation indices of minerals such as carbonates. In the FRACHEM simulations (implementing a Pitzer model) and those with an extended Debye-Hückel TOUGHREACT model, significant undersaturation

is predicted with respect to calcite. In contrast, the Pitzer TOUGHREACT model together with a newly acquired Pitzer database results in strong supersaturations. These differences have a tremendous influence on the predicted evolution of reservoir porosity. In the first case, the porosity is predicted to increase due to the dissolution of carbonates (calcite and dolomite) near the injection well, then slightly decrease further away because of calcite reprecipitation. In the other case, calcite is predicted to precipitate within the first ten metres of the injection well, to the point of nearly plugging off the injection zone.

It is difficult for the time being to forecast what will be the real evolution of the reservoir. A circulation test was performed in 1997 within the shallow reservoir at 3500 m at Soultz-sous-Forêts. The initial reservoir temperature was only 165 °C but the mineral composition of the granite was very similar to the one of the deep reservoir (5000 m). During this circulation of 140 days, the pressure at the injection well decreased, indicating an increase of the injectivity around the injection well. This process is probably due to the dissolution of carbonates, the most reactive minerals. This scenario is supported by FRACHEM simulations, as well as by simulations using the currently released TOUGHREACT version. Further work is underway to evaluate currently available ion interaction parameters required for implementing the Pitzer model with the codes discussed in this study.

Acknowledgements

We are grateful to the geochemistry and hydrogeology teams of LBNL and thank especially Guoxiang Zhang for his work on the TOUGHREACT Pitzer version and valuable help and support during this work. This study was partly (for L. André and F.-D. Vuataz) supported by the State Secretariat for Education and Research and the Swiss Federal Office of Energy, both funding this project (OFES-N° 00.0453 and OFES-N° 03.04.60); and also partly (For N. Spycher, T. Xu, K. Pruess) supported by the Assistant Secretary for Energy Efficiency and Renewable Energy, Office of Geothermal Technologies, of the U.S. department of Energy, under Contract No. DE-AC02-05CH11231.

REFERENCES

Alai, M., Sutton, M. and Carroll, S. (2005). Evaporative evolution of a Na-Cl-NO_3-K-Ca-SO_4-Mg-Si brine at 95 degrees C: Experiments and modeling relevant to Yucca Mountain, Nevada. *Geochem. Transactions*, **6**(2), 31-45.

André, L., Rabemanana, V. and Vuataz, F.-D. (2005). Geochemical modelling of water-rock interactions and implications on the properties of the Soultz fractured reservoir. *Proceedings EHDRA Scientific Conference*, March 17-18, 2005, Soultz-sous-Forêts, France.

Bächler, D. (2003). Coupled Thermal-Hydraulic-Chemical Modelling at the Soultz-sous-Forêts HDR reservoir (France). PhD thesis, ETH-Zürich, Switzerland, 150 p.

Bächler, D. and Kohl, Th. (2005). Coupled thermal-hydraulic-chemical modelling of enhanced geothermal systems. *Geophys. J. Int.*, **161**(2), 533-548.

Bolton, E.W., Lasaga, A.C. and Rye, D.M. (1996). A model for the kinetic control of quartz dissolution and precipitation in porous media flow with spatially variable permeability; formulation and examples of thermal convection. *J. Geophys. Res., B, Solid Earth and Planets,* **101**(10), 22157-22187.

Durst, P. (2002). Geochemical modelling of the Soultz-sous-Forêts Hot Dry Rock test site: coupling fluid-rock interactions to heat and fluid transport. PhD Thesis, Neuchâtel, 127 p.

Harvie, C.E., Møller, N. and Weare, J.H. (1984). The prediction of mineral solubilities in natural waters: the Na-K-Mg-Ca-H-Cl-SO4-OH-HCO_3-CO_3-CO_2-H_2O system to high ionic strengths at 25°C. *Geochim. Cosmochim. Acta*, **48**, 723-751.

Helgeson, H.C. (1969). Thermodynamics of hydrothermal systems at elevated temperatures and pressures. *Am. J. Science*, **267**, 729-804.

Helgeson, H.C., Delany, J.M., Nesbitt, H.W. and Bird, D.K. (1978). Summary and critique of the thermodynamic properties of rock-forming minerals. *Am. J. Sci.*, **278**-A, 1-229.

Helgeson, H.C., Kirkham, D.H. and Flowers, G.C. (1981). Thermodynamic prediction of the thermodynamic behaviour of aqueous electrolytes at high pressure and temperature: IV. Calculations of activity coefficients, osmotic coefficients and apparent molal and standard and relative partial molal properties to 600°C and 5 KB. *Am. J. Science*, **281**, 1249-1516.

Johnson, J.W., Oelkers, E.H. and Helgeson, H.C. (1992). SUPCRT92: A software package for calculating the standard molal thermodynamic properties of minerals, gases, aqueous species, and reactions from 1 to 5000 bars and 0 to 1000 degrees C. *Computers and Geosciences*, **18**, 899–948.

Kohl, T. and Hopkirk, R.J. (1995). "FRACTure" – A simulation code for forced fluid flow and transport in fractured, porous rock. *Geothermics*. **24**(3), 333-343.

Lasaga, A.C. (1984). Chemical kinetics of water-rock interactions. *J. Geophys. Res*., **89**, 4009-4025.

Møller, N., Greenberg, J.P. and Weare, J.H. (1998). Computer modeling for geothermal systems: predicting carbonate and silica scale formation, CO_2 breakout and H_2S exchange. *Transp. Porous Media*, **33**, 173-204.

Norton, D. and Knapp, R. (1977). Transport phenomena in hydrothermal systems; the nature of porosity. *Am. J. Sci.*, **277**(8), 913-936.

Palandri, J.L. and Kharaka, Y.K. (2004). A compilation of rate parameters of water-mineral interaction kinetics for application of geochemical modelling. *U.S. Geological Survey,* Report 2004-1068.

Parkhurst, D.L. and Appelo, C.A.J. (1999). User's guide to PHREEQC (Version2) - A computer program for speciation, batch-reaction, one-dimensional transport, and inverse geochemical calculations. *U.S.Geological Survey Water-Resources Investigations,* Report 99-4259, 310 p.

Pitzer, K.S. (1973). Thermodynamics of electrolytes. I. theoretical basis and general equations. *J Phys. Chem*., **12**, 268-277.

Pruess, K. (1991). TOUGH2: A general numerical simulator for multiphase fluid and heat flow. Lawrence Berkeley Laboratory Report LBL-29400, Berkeley, California, 1991.

Pruess, K., Oldenburg, C. and Moridis, G. (1999). TOUGH2 user's guide, Version 2.0. Lawrence Berkeley Laboratory Report LBL-43134, Berkeley, California, 1999.

Rabemanana, V., Durst, P., Bächler, D., Vuataz, F.-D. and Kohl, Th. (2003). Geochemical modelling of the Soultz-sous-Forêts Hot Fractured Rock system: comparison of two reservoirs at 3.8 and 5 km depth. *Geothermics*, **32**(4-6), 645-653.

Reed, M.H. (1998). Calculation of simultaneous chemical equilibria in aqueous-mineral-gas systems and its application to modeling hydrothermal processes. In: *Techniques in Hydrothermal Ore Deposits Geology*, J. Richards and P. Larson (Eds), *Reviews in Economic Geology*, **10**, 109-124.

Reed, M.H. and Spycher, N.F. (1998). User's guide for CHILLER: A program for computing water-rock reactions, boiling, mixing and other reaction processes in aqueous-mineral-gas systems and minplot guide, 3rd edition. Department of Geological Sciences, University of Oregon, Eugene, Or, USA.

Steefel, C.I. and Lasaga, A.C. (1994). A coupled model for transport of multiple chemical species and kinetic precipitation/dissolution reactions with applications to reactive flow in single phase hydrothermal system. *Am. J. Sci.*, **294**, 529-592.

Vinsome, P.K.W. and Westerveld, J. (1980). A simple method for predicting cap and base rock heat losses in thermal reservoir simulators. *J. Canadian Pet. Tech*., **19**(3), 87–90.

White, S.P. (1995). Multiphase nonisothermal transport of systems of reacting chemicals. *Water Resour. Res.*, **31**(7), 1761-1772.

Verma, A. and Pruess, K. (1988). Thermohydrological conditions and silica redistribution near high-level nuclear wastes emplaced in saturated geological formations. *J. Geophys. Res*., **93**, 1159-1173.

Wolery, T.J. and Jarek, R.L. (2003). EQ3/6, Version 8.0, Software User's Manual, Software Document Number 10813-UM-8.0-00, *U.S. Department of Energy*, Office of Civilian Radioactive Waste Management, Office of Repository Development, 1261 Town Center Drive, Las Vegas, Nevada 89144, 2003.

Wolery, T.J., Jove-Colon, C., Rard, J. and Wijesinghe, A. (2004). Pitzer Database Development: Description of the Pitzer Geochemical Thermodynamic Database data0.ypf. Appendix I in *In-Drift Precipitates/Salts Model (P. Mariner)* Report ANL-EBS-MD-000045 REV 02. Las Vegas, Nevada: Bechtel SAIC Company.

Xu, T. and Pruess, K., (2001). Modeling multiphase fluid flow and reactive geochemical transport in variably saturated fractured rocks: 1. Methodology. *Am. J. Sci.*, **301**, 16-33.

Xu, T., Sonnenthal, E., Spycher, N. and Pruess, K. (2004). TOUGHREACT user's guide: a simulation program for non-isothermal multiphase reactive geochemical transport in variably saturated geologic media. *Report LBNL-55460, Lawrence Berkeley National Laboratory, Berkeley, California*.

Zhang, G., Zheng, Z. and Wan, J. (2004). Modeling reactive geochemical transport of concentrated aqueous solutions. *Water Resour. Res*., **41**(2), W02018.

EC Contract ENK5-2000-00301

PARTICIPANT ORGANIZATION NAME: Centre of Hydrogeology, University of Neuchâtel, Switzerland

Synthetic final report

Related with Work Package 8 - Thermo-Hydro-Mechanical modelling of reservoir / heat exchanger

GEOCHEMICAL MODELLING OF WATER-ROCK INTERACTIONS AND IMPLICATIONS ON THE PROPERTIES OF THE SOULTZ FRACTURED RESERVOIR

Laurent André[1,2], Vero Rabemanana[1] and François-D. Vuataz[2]

[1] Centre of Hydrogeology – University of Neuchâtel, E.-Argand 11, CH-2007 Neuchâtel, Switzerland
[2] Centre of Geothermal Research – CHYN, University of Neuchâtel, E.-Argand 11, CH-2007 Neuchâtel, Switzerland

e-mail: laurent.andre@unine.ch; francois.vuataz@crege.ch

ABSTRACT

Rock porosity and permeability do not remain constant with time. In particular, the fluid circulation within the fractured reservoir involves chemical reactions between the brine and the altered granite, which modifies porosity and permeability. The FRACHEM code, a Thermo-Hydraulic-Chemical coupled code, has been developed especially to forecast the evolution of the Soultz system. For the time being, this code can simulate fluid-rock interactions and determine the dissolution/precipitation reactions of eight minerals (carbonates, pyrite, silicated minerals). The last simulations demonstrate an important dissolution of carbonates close to the injection well, whereas small amounts of silicates precipitation are inferred. Several relationships between porosity and permeability as well as comparisons of FRACHEM with other codes have been tested to forecast the long-term influence of chemical reactions on reservoir properties.

INTRODUCTION

The geothermal research programme for the extraction of energy from the Enhanced Geothermal System at the Soultz-sous-Forêts site began in 1987 (Hettkamp et al., 2004). The project aims to convert heat to electricity from a deep reservoir in fractured granite. This site has been selected because of its temperature gradient in the sedimentary cover (100°C.km^{-1}) and its high heat flow reaching locally 0.15 W.m^{-2} (Kohl and Rybach, 2001).

To extract the heat from the reservoir, three deviated wells have been installed at a depth of 5000 m and their bottoms are separated by 650 m. At this depth the reservoir encountered reaches a temperature of 200°C. One well (GPK3) is dedicated to the injection of cold water in the reservoir whereas the two others (GPK2 and GPK4), located on both sides of the injector, are used to produce hot water. At Soultz, the injection-production system is a "closed loop" and the fluid used is the formation brine existing in the fractured granite.

An accelerated flow of the hot brine takes place within the fractured reservoir, but chemical and thermodynamic equilibriums will be disturbed, involving chemical processes affecting the reservoir properties.

The aim of this study is to predict the long-term behaviour of this system under continuous production. To reach this objective, many aspects as heat, hydraulics, fluid transport and geochemical processes have to be taken into account, and their impact on porosity and permeability evolution has to be evaluated. We have examined in details the water-rock interactions on fluid flow, as well as the variations of reservoir properties during production.

Considering the strong mineralization of brine and the high temperature of the reservoir, a new Thermo-Hydraulic and Chemical coupled code, called FRACHEM, has been built for the Soultz reservoir conditions. It results from the combination of two existing codes, FRACTure and CHEMTOUGH2. FRACHEM code determines the thermal and hydraulic processes and simulates the reactive transport. The Pitzer formalism has also been implemented in FRACHEM code to calculate the activity coefficients of selected chemical species; then, the precipitation/dissolution reactions of some minerals, i.e carbonates, quartz, amorphous silica, pyrite and some aluminosilicates can be estimated. At last, a supplementary module allows the determination of porosity and permeability variations linked with chemical processes occurring in the reservoir.

MINERALOGICAL ASSEMBLAGE

The geothermal reservoir at Soultz is composed of three types of granite (Jacquot, 2000) (Table 1).

Table 1: Mean composition (in percent) of the different types of granite in the Soultz reservoir (Jacquot, 2000).

	Healthy granite	Hydrothermalised granite	Vein of alteration
Quartz	24.2	40.9	43.9
K-Feldspar	23.6	13.9	
Plagioclases	42.5		
Illite		24.6	40.2
Smectite		9.7	9.6
Micas	9.4		
Calcite	0.3	3.3	4.3
Dolomite		0.8	0.7
Pyrite		0.7	1.0
Galena		1.3	0.3
Chlorite		4.8	

The first one is a healthy granite, characterized by the predominance of feldspars, plagioclases and quartz. This granite is not altered and contains no water. The second facies is a fractured hydrothermalised granite. Its composition reveals the following alteration: quartz is the major mineral, the amount of feldspars decreases and some secondary minerals appear like galena, pyrite, smectite or illite. This rock facies is more porous than the first one. The last facies corresponds to the vein of alteration,

characterized by minerals such as illite, smectite and quartz. This facies is the most altered one but precipitation of these secondary minerals in the fractures network involves a decrease of porosity and permeability. As a result, the porosity of the second facies is the only one assuming fluid flow in the granitic rock.

FLUID COMPOSITION

The fluid circulating in the fractures network is the formation fluid, a sodium-chloride brine with a total mineralization close to 100 $g.L^{-1}$. pH value reaches 4.9 and its temperature is equilibrated with the rock at this depth i.e. 200 °C. The brine composition, analysed from the fluid extracted during the production test in 1999, is given in Table 2.

Table 2: Mean composition of fluid coming from the reservoir at a depth of 5 km.

Species	Concentration [mmol/kg]
Na^+	1079
K^+	68.5
Ca^{2+}	157
Mg^{2+}	3
Cl^-	1452
S	1.6
C	19
Fe^{2+}	2.4
SiO_2	5.7

NUMERICAL MODELLING

To predict the long-term evolution of the Enhanced Geothermal System, several Thermo-Hydraulic and Chemical (THC) coupled codes are available. They can model the behaviour of hot diluted fluids or cold brines, but are unable to deal with hot hypersaline brines. Consequently, a new THC code had to be built for the Soultz reservoir conditions. Instead of creating a totally new modelling programme, two existing codes, FRACTure and CHEMTOUGH2, have been combined in a new code called FRACHEM (Durst, 2002; Bächler, 2003; Rabemanana et al., 2003). FRACTure is a 3-D finite elements code and it determines thermal and hydraulic processes in fractured and porous rocks (Kohl and Hopkirk, 1995). CHEMTOUGH2 is a 3-D finite volumes code (White, 1995); it simulates the reactive transport and allows the variation of permeability according to chemical reactions occurring between fluid and rock of the reservoir. Due to the high fluid salinity of the Soultz reservoir, this last code has been modified by several implementations: thermodynamic model and computation of the activity coefficients of selected species in solution, kinetic model for dissolution and precipitation of minerals, as well as the relationship between porosity and permeability.

The thermodynamic model

The thermodynamic model has to determine the state of the fluid in regard to mineral phases present in granite i.e. the under- or over-saturation of the fluid towards these minerals. To reach this goal, the ionic activity product (Q) must be compared to the equilibrium constant of the reaction (K). If Q<K, the solution is undersaturated and the mineral has a tendency to dissolve. If Q=K, the system is at equilibrium, but if Q>K, the solution is oversaturated and the mineral precipitates.
In order to calculate these factors, the activity coefficients of each species in solution must be determined. In CHEMTOUGH2, the Debye-Huckel model is used to calculate these coefficients but this model can only be considered with dilute solutions.
Knowing the high salinity of the brine of the Soultz system, this model has been substituted by Pitzer formalism. The Pitzer equations have the advantage to take into account more types of ionic interactions than Debye-Huckel model.
To simplify the system, some assumptions have been made concerning the fluid, such as no boiling, no degassing, no condensing and no mixing with a different fluid.
Assuming these hypotheses, the activity coefficients of ionic species can be defined and only depend on two parameters, temperature and pressure.

$$\gamma_i(T,P) = (B_0 + B_1 T + B_2 T^2 + B_3 T^3 + B_4 T^4).f(P)$$

Where B_i are coefficients calculated for each mineral and f(P) is a factor depending on pressure.
Then, the activity of the species i is expressed in function of the molality m_i as:

$$a_i = \gamma_i(T,P).m_i$$

The kinetic model

The thermodynamic model allowed determining the equilibrium or non-equilibrium state of the fluid in regard to the rock. But a thermodynamic disequilibrium involves chemical reactions with variable kinetics according to the type of minerals.
A general kinetic model has been adopted to explain the dissolution/precipitation reactions of minerals. Its overall form is expressed as:

$$v = k_m.s_m.\left(1 - \left(\frac{Q_m}{K_m}\right)^{\mu}\right)^n$$

Where v is the reaction rate ($mol.s^{-1}$), k_m is the rate constant ($mol.s^{-1}.m^{-2}$), s_m is the surface of mineral in contact with fluid (m^2), μ and n are positive empirical parameters. Positive values of v correspond to dissolution rates, whereas negative values refer to precipitation rates.
This equation is adapted to each mineral and the determination of parameters k_m, μ and n are deduced from published experiments, conducted at high temperature in NaCl brines.
For the present time, the behaviour of eight minerals (calcite, dolomite, pyrite, quartz, amorphous silica, K-feldspars, albite and illite) is investigated. Detailed information on the determination of the reaction laws can be found in Durst (2002).

The porosity/permeability relationship

As mentioned before, many chemical processes can have an influence on porosity and permeability of the system. To assume this, the porosity variations are calculated and a combination of a fracture model and a grain model is used to determine the permeability evolution. This double model has been validated considering the structural characteristics of the altered granite crossed by the fluid.
The fracture model is based on the work of Norton and Knapp (1977) and modified by Steefel and Lasaga (1994), who consider the case of three sets of mutually orthogonal fractures, which produce an isotropic permeability and where all the fractures have the same spacing and fracture apertures. The permeability k_F (in m^2), in this case, is:

$$k_F = \frac{\Phi_F^3}{324.n_F^2}$$

Where Φ_F represents the fracture porosity and n_F the fracture frequency in m^{-1}.
The grain model is based on the model of Kozeny-Carman which has been modified by Bolton et al. (1996). The expression of the permeability k_G is:

$$k_G = \frac{R_0^2}{45} \cdot \frac{\Phi_G^3}{(1-\Phi_G)^2}$$

Where Φ_G and R_0 represent the grain porosity and the initial radius of closed pack spherical grains, respectively.

APPLICATION OF FRACHEM TO THE SOULTZ SYSTEM

Model set up

The present application of FRACHEM is the modelling of a 2-D simplified model with a geometry close to the Soultz system. Injection and production wells are linked by fractured zones and surrounded by the granite matrix. The model is composed of 1250 fractured zones. Each fractured zone has an aperture of 0.1 m, a depth of 10 m, a porosity of 10%, and contains 200 fractures. Initially the temperature was set to the reservoir temperature of 200°C. One of these fractured zones is modelled with the assumption that the fluid exchange with the surrounding low permeability matrix is insignificant. Due to the symmetrical shape of the model, only the upper part of the fractured zone is considered in the simulation. The area is discretized into 222 2D elements (Figure 1).

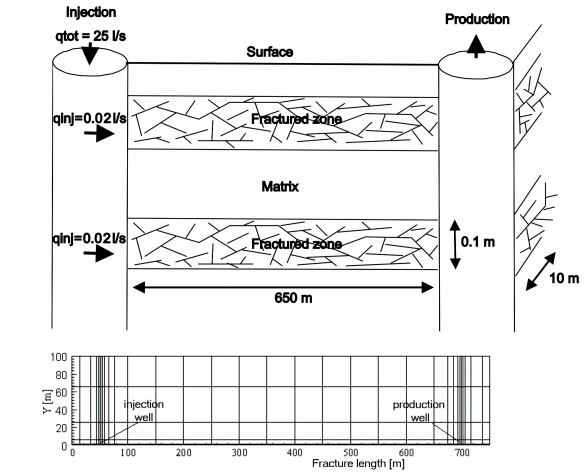

Figure 1: Simplified model and spatial discretization.

The size of the elements ranges from a minimum of 0.5 m x 0.05 m near the injection and the production wells to a maximum of 50 m x 35 m. Considering a production rate of 25 $l.s^{-1}$, the fluid was re-injected in each of the fractured zones at a rate of 2 x 10^{-2} $l.s^{-1}$ at a constant temperature of 65°C. During this simulation a constant overpressure of 8 MPa was assumed at the injection well and a hydrostatic pressure at the production well. Dirichlet boundary conditions were applied to the upper, left and right side of the model. Due to the sensitivity of the sequential non iterative approach (SNIA) method on the time discretization, the time step used for this simulation is limited to 10^2 s, meaning that several years of simulations take several days of computer time. The values of thermo-hydraulic parameters considered in the simulation are listed in Table 3.

Table 3: Thermo-hydraulic model parameters.

Parameters		Fracture	Matrix	Fluid
Hydraulic conductivity	[m^2/Pa]	7.4 10^{-8}	10^{-15}	-
Thermal conductivity	[W/m.K]	2.9	3	0.6
Density	[kg/m^3]	-	2650	1000
Heat capacity	[J/kg.K]	-	1000	4200
Porosity	[%]	10	0	-

Results

Reservoir temperature

Before fluid circulation in the fractured zone, all the system (rock and brine) is chemically and thermally at equilibrium. The brine is in chemical equilibrium with the granite and these two components are at a constant temperature of 200°C. But, during the injection of cold fluid at 65°C in the reservoir, the system is disturbed and the rock progressively cools down (Figure 2).

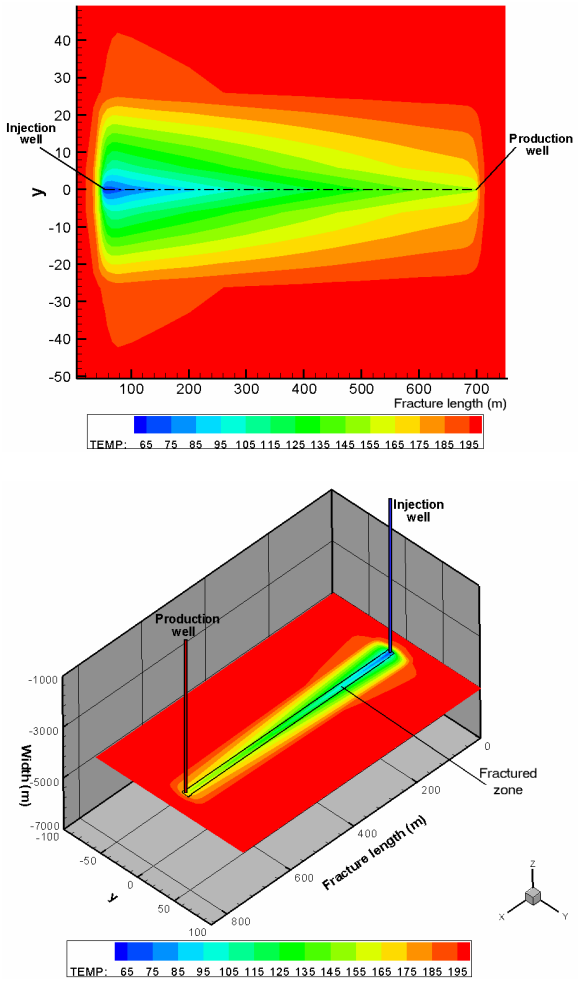

Figure 2: Temperature of rock around the fractured zone after 1800 days of fluid circulation.

The fractured zone is represented between injection and production wells, in a plane at - 5000 m from surface. All along the fractured zone, we observe a global decrease of temperature, especially near the injection well, due to the temperature of the re-injected fluid. After 1800 days of fluid circulation, the temperature in the vicinity of the production well is close to 160°C. The development of this thermal front due to the thermal diffusion from rock to fluid affects a zone

of 30 to 40 metres around the fractured zone (Figure 2). This temperature decrease of the produced fluid is particularly important but it is strongly dependent of the geometric model. In this case, we consider a direct flow, in straight line, between injection and production wells, without taking in consideration parallel pathways. As a consequence, the cooling effect modelled here is most probably overvalued compared to the real reservoir.

Minerals-brine interactions

The circulation of cold fluid in the fracture disturbs the chemical equilibrium of the rock-brine system involving chemical reactions such as minerals precipitation and dissolution.

If the properties of some minerals are well known, such as for carbonates, the application of the reactions of aluminosilicates in the model presents some difficulties. Some assumptions had to be done: dissolution reactions are considered as congruent and aluminium in solution is under the form of Al^{3+}. Considering the temperature and the hydrostatic pressure in the reservoir, $Al(OH)_3^0$ and $Al(OH)_4^-$ species must be used (Pokrovskii and Helgeson, 1995). Nevertheless, the determination of activity coefficients of these species in the Soultz conditions presents some uncertainties. Therefore, and with a brine pH close to 4.8-4.9, the species Al^{3+} has been chosen. The calculation of the activity coefficient of this ion has been carried out with the EQ3nr programme (Wolery, 1992) and by the method presented by Barrett and Anderson (1988). The aluminium concentration in solution is fixed to 0.1 ppm.

The calcite is a secondary mineral, crystallized in granite fractures in relative weak proportions, but it represents the most reactive mineral. As shown in figure 3, for every time period, the calcite reacts in the entire fracture. Positive values of the reaction rate indicate a dissolution and the negative ones, a precipitation process.

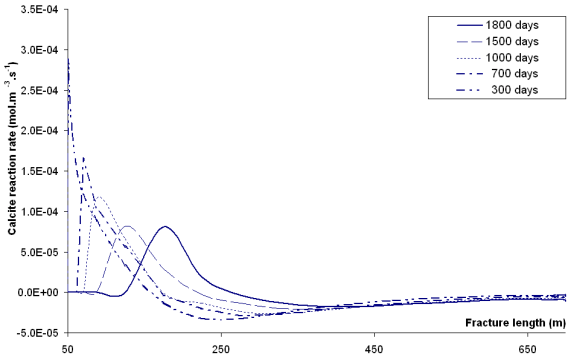

Figure 3: Calcite reaction rate along the fracture.

In the vicinity of the injection well, the calcite dissolves whereas it precipitates from the middle of the fracture up to the production well. This is due to the solubility of calcite, which decreases when temperature increases. At the beginning of the fluid circulation in the reservoir, the dissolution of calcite occurs mainly in the first 100 metres of the fracture and a maximum of dissolution rate is reached during the first year. This dissolution involves an enrichment of calcium Ca^{2+} in solution and later the temperature increase along the fracture causes calcite precipitation in the last 500 metres of the flow path. The dissolution of calcite goes on until all the mineral has been consumed. Figure 4 demonstrates that in the vicinity of the injection well, about 350 days are needed to dissolve all the calcite present in the fractured granite.

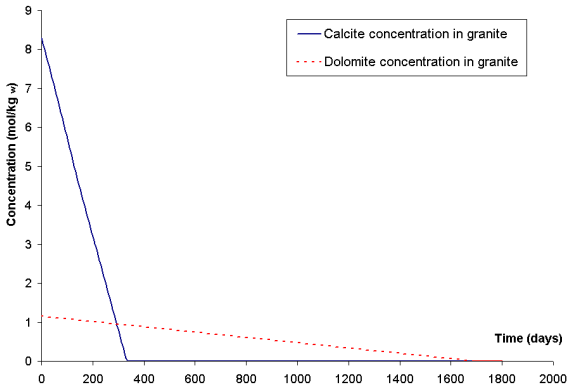

Figure 4: Evolution of calcite and dolomite concentration in the granite, close to the injection point.

When increasing simulation time and decrease of the rock temperature, the dissolution zone of calcite extends towards the production well.

Another carbonate has also been investigated. The dolomite, present in granite, is less reactive than calcite. Figure 5 shows that dolomite dissolves everywhere in the fracture, but the reaction rate is one order of magnitude smaller than for calcite. Similarly to calcite, dolomite dissolution is stopped by the lack of mineral but around the injection well, more than 1700 days are needed for the total disappearance of this mineral (Figure 4).

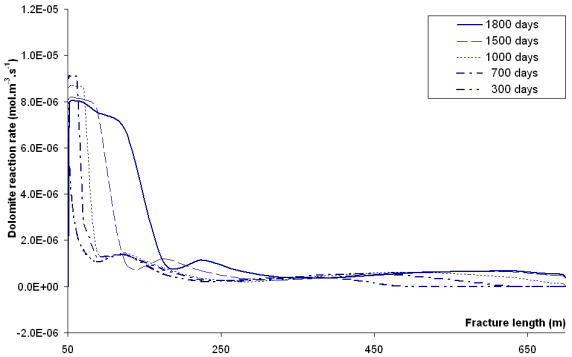

Figure 5: Dolomite reaction rate along the fracture.

Concerning the silicates, the most reactive one is amorphous silica. Quartz, which is a major mineral in granite, has a reaction rate three order of magnitude smaller than the one of amorphous silica. Contrary to calcite, the solubility of amorphous silica augments with temperature increase. As a consequence, this property involves the precipitation of this mineral near the injection well (Figure 6).

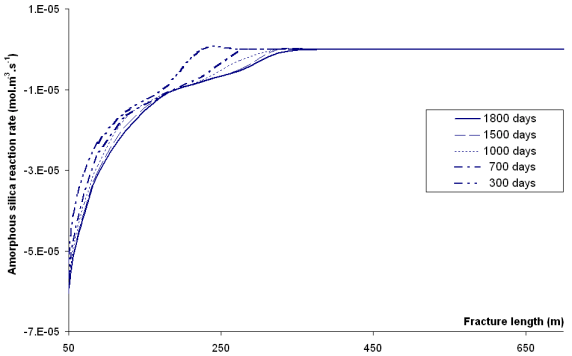

Figure 6: Amorphous silica reaction rate along the fracture.

When increasing circulation time, the precipitation zone of this mineral extends towards the production well and concerns, after 1800 days, the first half of the fracture. However, the reaction rate stays one or two orders of magnitude smaller than for calcite.
Concerning pyrite, this mineral precipitates all along the fracture but, similarly to quartz, the reaction rate stays negligible in comparison with calcite.

K-feldspars seem to be the most reactive of aluminosilicates (Figure 7). This mineral precipitates close to injection point and this process decreases when temperature increases. It is interesting to note the weak dissolution of albite and illite close to the production well.

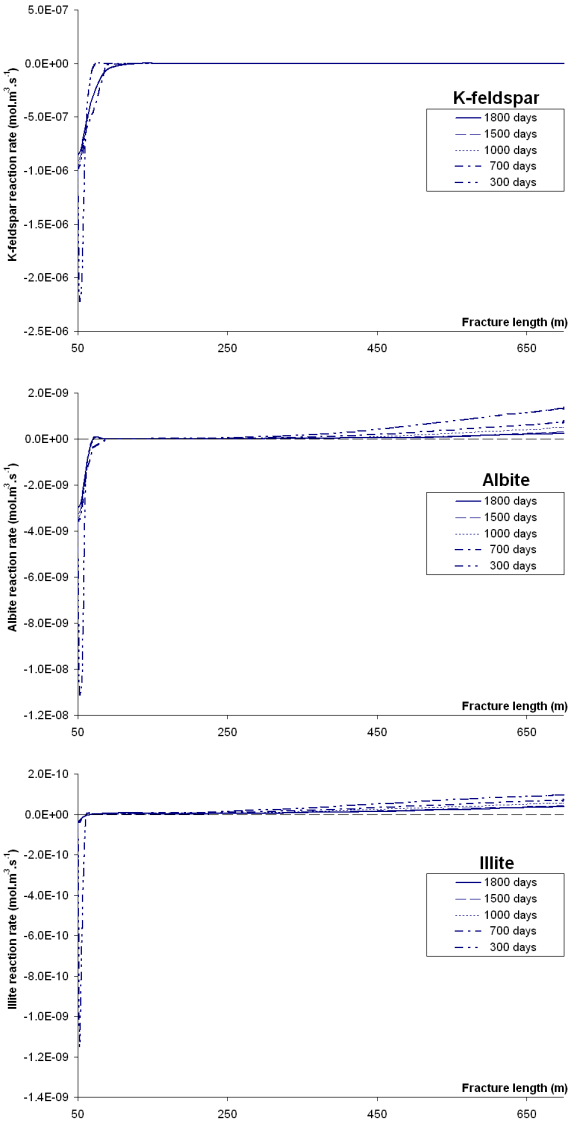

Figure 7: Aluminosilicates reaction rate along the fracture.

We can also notice that the main phase of aluminosilicates precipitation occurs at the beginning of the fluid flow and that the reaction rates decrease with increasing circulation time.

Amounts of precipitated and dissolved minerals

Knowing the reaction rates, the amount of each mineral, precipitated or dissolved, can be estimated at each time and in each fracture element of the model.

Table 4 presents the total amount of precipitated and dissolved mineral after 1800 days of fluid circulation.

Table 4: Amounts of precipitated and dissolved minerals including the aluminosilicates within the entire fractured zone, after 1800 days of fluid circulation.

Minerals	Total precipitation (kg)	Total dissolution (kg)
Calcite	-4971	5935
Dolomite	/	896
Quartz	-0.44	/
Amorphous silica	1880	0.67
Pyrite	-0.5	-
K-feldspar	-47	-
Albite	-0.15	0.34
Illite	-0.02	0.05

As calculated above by the reaction rates, calcite is the most reactive mineral. Including dolomite, more than 6000 kg of carbonates are dissolved in the fracture within 1800 days, whereas about 5000 kg precipitate. We can also observe that the amounts of other reactive minerals stay far below the carbonates. The only significant amount concerns the amorphous silica, with about 1900 kg, which precipitate close to the injection well.
After 1800 days of circulation, the precipitated amounts of K-feldspar are low and even negligible for albite and illite.

Influence on porosity and permeability

The amounts of dissolved and precipitated minerals have a direct consequence on the reservoir properties, mainly porosity and permeability.
As Figure 8 shows it, calcite dissolution, close to the injection well, involves a porosity increase until all the carbonates have disappeared.

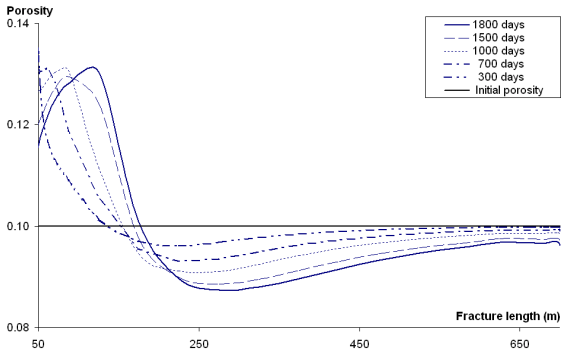

Figure 8: Influence of the reactions of aluminosilicates on the fracture porosity.

The total dissolution of calcite and dolomite implies a reservoir porosity of about 0.135; this value indicates an increase of 30-35 % compared to the initial porosity. After 1800 days of circulation, this increase of 30 % concerns only the first 100-150 m of fractured zone but, with an increase of circulation time, we can suppose that the porosity of the whole fracture will reach this value.
In the middle of the fractured zone, calcite precipitation causes a decrease of the fracture porosity of about 10-12 % after 1800 days of fluid circulation whereas this decrease reaches only about 5 % close to the production well.
The precipitation of amorphous silica combined with aluminosilicates has nevertheless an impact on porosity. This influence is more pronounced in the first 70 meters of the fracture and involves a porosity decrease from 0.135 to a value of 0.120 after 1800 days of circulation.

Considering the relationship between porosity and permeability used in this model, the same tendency is observed for reservoir permeability.

Porosity/permeability relationships

All the chemical reactions involved in this simulation have an influence on reservoir properties, but it is quite difficult to determine an adequate relationship between porosity and permeability considering that few field data are available and that the real structure of the Soultz granite is not well known. An estimation of the evolution of the reservoir porosity is proposed through two examples of relationships. The theoretical aspect of each model is first described and then a comparison of the results is presented.

A combination of grain and fracture models (Case 1a)

Considering the alteration of the Soultz granite, the flow can circulate in a medium composed of fractures and grains. Concerning the fracture medium, the permeability of fracture (k_F) is given by (Norton and Knapp, 1977; Steefel and Lasaga, 1994)

$$k_F = \frac{\Phi^3}{324.n_F^2}$$

Whereas the permeability around the grain is given by (Bolton et al., 1996)

$$k_G = \frac{R_0^2}{45}.\frac{\Phi^3}{(1-\Phi)^2}$$

Then, during fluid circulation in the system, mineral precipitation and dissolution imply porosity changes in the fracture directly tied to the volume changes

$$\Delta\Phi = \frac{\Delta V_{water}}{V_{tot}} = \frac{\Delta V_i}{V_{tot}}$$

As a consequence, permeability changes occur in the rock. In the fracture, the variations are given by

$$\frac{dk_F}{d\Phi} = \frac{\Phi^2}{108.n_F^2}$$

Whereas, around the grains

$$\frac{dk_G}{d\Phi} = \frac{R_0^2}{45}.\frac{\Phi^2.(3-\Phi)}{(1-\Phi)^3}$$

These variations are calculated for each time step and for each mineral. If α represents the ratio between the fracture porosity and the grain porosity, the new permeability k is given by

$$k(t+\Delta t) = k(t) + (1-\alpha).\Delta k_F + \alpha.\Delta k_G$$

Another parameter evolves during the fluid circulation: the reactive surface area of each mineral (A_i). At the beginning, the surface area ($A_{F,i}$) for a mineral i, in the fracture, can be calculated, considering that the surface occupied by this mineral is proportional to its volume fraction (f_i) in the rock

$$A_{F,i} = A_{F_0}.f_i = 6n_F f_i = 6.f_i\sqrt{\frac{\Phi^3}{324.k_{F,i}}}$$

Where A_{Fo} is the total reactive surface area (m^2).

As the same way, the surface area per rock volume around the grains is given by

$$A_{G,i} = A_{G_0}.f_i = \frac{\pi.\varepsilon.(6-5\varepsilon)}{\sqrt{2}.R_0}.f_i$$

With $$R_0 = \sqrt{45.\kappa_i.k_0.\frac{(1-\Phi)^2}{\Phi^3}}$$

And $$\varepsilon = -14.32.\Phi^3 + 7.215.\Phi^2 - 1.769.\Phi + 1.207$$

κ_i is the ratio between the fracture permeability and the grain permeability.

The total surface area of a mineral is the sum of the two systems:

$$A_i = (1-\alpha)\, A_{F,i} + \alpha\, A_{G,i}$$

Dissolution and precipitation reactions imply variations of the surface area of each mineral at each time step, in the fracture and around grains. If the fracture aperture and the thickness of the mineral layer follow a Gaussian distribution then the surface area of a mineral i can be expressed as

$$A_{F,i} = A_{F_0}.f_i.\exp\left(-\left((\Phi_t - \Phi_0)\sigma\right)^2\right)$$

And the variations are given by

$$\frac{dA_{F,i}}{d\Phi} = -A_{F_0}.\exp\left(-\left((\Phi_t - \Phi_0)\sigma\right)^2\right)\left[2.f_i.(\Phi_t - \Phi_0)\sigma^2 + 1\right]$$

With σ an empirical parameter defining the shape of the Gaussian distribution.

Around the grains, the variations are given by

$$\frac{dA_{G,i}}{d\Phi} = \frac{f_i}{1-\Phi}.\frac{\pi}{\sqrt{2}.R_0^1}.\left[\begin{array}{c}(1-\Phi).(6-10.\varepsilon)\\.\left(-42.96\Phi^2 + 14.43\Phi - 1.769\right)\\+\dfrac{6\varepsilon - 5\varepsilon^2}{\Phi}\end{array}\right]$$

These variations are calculated for each time step and for each mineral and the new surface area for each mineral is given by

$$A(t+\Delta t) = A(t) + (1-\alpha).\Delta A_{F,i} + \alpha.\Delta A_{G,i}$$

Modified grain and fracture models (Case 1b)

An alternative to this method is to give up with the Gaussian distribution of the area from fractures network. In this case (case 1b), the variation of the reactive area depends only on the fracture porosity

$$\frac{dA_{F,i}}{d\Phi} = A_{F_0}.f_i.\frac{1}{\Phi_i.(1-\Phi_i)}$$

The variation of area from grain porosity and the global surface area are calculated in the same way in cases 1a and 1b.

A fracture model (Case 2)

The Soultz reservoir can also be considered as a succession of fractured zones. Fracture permeability changes can be then approximated using the porosity change of plane parallel fractures of uniform aperture (cubic law; e.g., Steefel and Lasaga, 1994).
The modified permeability can be adjusted to porosity changes brought by precipitation or dissolution of minerals and is given by:

$$k = k_0 \left(\frac{\Phi}{\Phi_0} \right)^{D_{f,i}}$$

Where k_0 and Φ_0 represent the initial permeability and porosity, respectively. One of the disadvantages of this law is that zero permeability is only reached under the condition of zero fracture porosity. Three different fractal exponents $D_{f,i}$ can be specified for three different intervals of porosity (Clauser, 2003)

$0.01 < \Phi < 0.1$, $\quad k = 7463.\Phi^2 \quad (\text{in nm}^2)$

$\Phi > 0.1$, $\quad k = 191.(10\Phi)^{10} \quad (\text{in nm}^2)$

$\Phi < 0.01$, $\quad k = 31.\Phi \quad (\text{in nm}^2)$

The variation of porosity is determined like in case 1 and the new porosity is given by

$$\Phi = \Phi_0 + \sum_i \Delta\Phi_i$$

Considering the properties of Soultz granite, porosity is estimated to range between 0.01 and 0.1. Then, permeability is updated according to the following equation.

$$k = k_0 \left(\frac{\Phi}{\Phi_0} \right)^2$$

The variations of the reactive surface area of each mineral and the global surface area are determined such as defined in case 1a.

Results

The three relationships between porosity and permeability described above have been applied to the model presented in Figure 1. Concerning the minerals, only carbonates (calcite, dolomite), quartz, amorphous silica and pyrite have been integrated to the simulations. The variations of reservoir porosity and permeability forecasted by each method are presented in Figures 9 and 10, respectively.
The cases 1a and 1b give the same results about variations of reservoir porosity and permeability; only some differences are observed near the injection well but they can be neglected. However, concerning the case 2, the results present more divergences. The porosity evolution is similar near the injection well but differs slightly within the whole fractured zone: these variations are linked to the porosity update mode. The differences between the cases 1 and 2 are more pronounced for the permeability, mainly near the injection well. The tendency and the global evolution of this parameter are the same in the two cases but the permeability increase is less important in case 2 than in case 1.

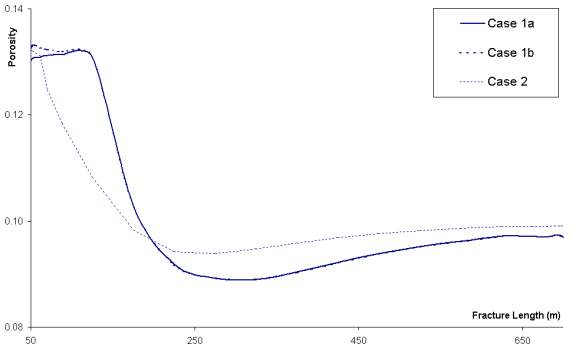

Figure 9: Variations of reservoir porosity according to different models.

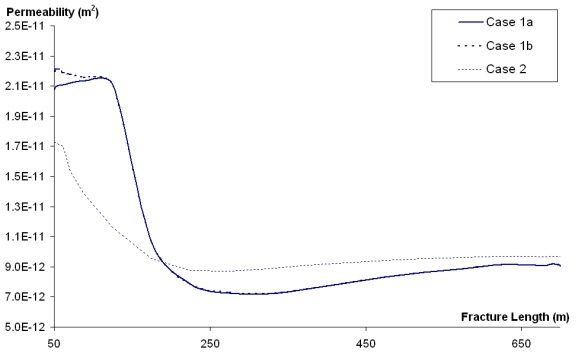

Figure 10: Variations of the reservoir permeability according to different models.

As a first conclusion, some hypothesis on the evolution of the reservoir properties can be forecasted. Each method gives the same global evolution of the reservoir properties with an increase of porosity and permeability close to the injection well and a decrease in the second half of the fractured zone. But only field data will be able to confirm which proposed scenario is the most adequate for the Soultz reservoir.

Scenarios proposed to manage the reservoir properties

Simulation of acid injection

Porosity and permeability are expected to evolve with time during the reservoir exploitation. A decrease of these parameters values is the result of calcite precipitation and it may alter the performance of the fluid circulation after a long-term exploitation. In February 2003, the impact of acid injection on calcite deposits in fractures and on the pressure transfer between GPK2 and GPK3 are tested (Hettkamp et al., 2004). This experiment consisted of a succession of injection of fresh water followed by diluted acidified brine at different injection rates. The results showed a decrease of the injection pressure in the vicinity of the injection well, as the calcite was dissolved and progressively carried away.
The response of the model to the HCl acid addition has been examined. This simulation was performed with the initial brine. Its pH was lowered to 3.7, whereas the injection rate within the fractured zone was maintained to 2 10^{-2} $l.s^{-1}$. The simulation results were consistent with those of the experiment. The additional H^+ ions significantly modify the calcite reaction rate around the injection well. The brine acidification increases the amount of dissolved calcite of about 70 % around the injection well.
As the reservoir permeability and porosity are controlled by the occurrence of mineral precipitation and dissolution, this increase of calcite dissolution implies an improvement of the

reservoir properties, namely the hydraulic impedance of the injection well.

Effect of a temporary reverse circulation

Another scenario of measures linked to reservoir management has been tested with a temporary reverse fluid circulation after a given period of exploitation. The simulation of fluid-rock interaction showed that calcite is more soluble around the injection well and that an increase of temperature favours calcite deposition towards the production zone. In order to improve porosity and permeability around the production well, the fluid circulation has been reversed during 3 months after 300 days of exploitation. It means that the production well was used for injection and vice versa during this period. The fluid chemistry and mineral components are updated to the situation after 300 days of circulation and the boundary conditions are inverted to this configuration. Figure 11 shows the evolution of the porosity after 300 days of exploitation with a reverse circulation of three months.

The reverse circulation modifies slightly the reservoir porosity. This parameter is mainly influenced by carbonates reactions. After 300 days of circulation (dashed line on figure 11), porosity has increased of about 30 % near the injection well and it has decreased of about 1 % near the production well. By reversing circulation during 3 months (continuous line on figure 11), carbonates dissolve near the "new" injection well. As a consequence, an increase of about 10 % of the porosity is observed in the first 50 meters of the fracture, between 650 and 700 m (see zoom on figure 11). This dissolution involves the augment of calcium in solution and the re-precipitation of calcite further in the fracture between 450 and 650 m. Porosity is not affected in the rest of the fracture.

Considering these results, it seems that a temporary reverse circulation could improve the reservoir properties, particularly in the vicinity of the production well.

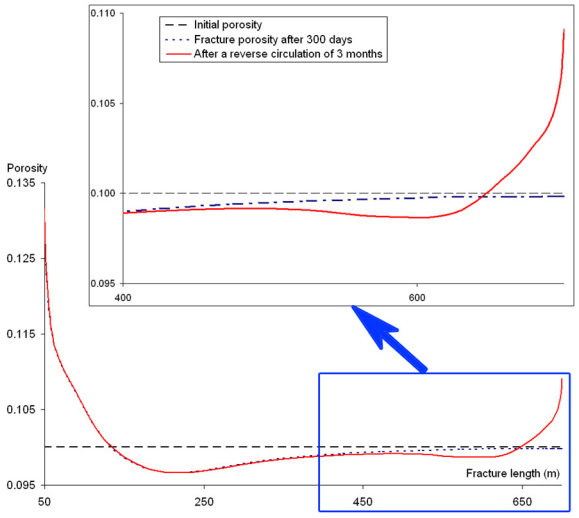

Figure 11: Evolution of porosity after 300 days of exploitation including reverse circulation (3 months)

Change in temperature injection

In order to estimate the sensitivity of the model to the re-injection temperature, it was modified from 65°C to 50°C. As shown in Table 5, the amounts of mineral precipitated and dissolved have been compared to the simulation carried out at 65°C.

Table 5: Amounts of minerals precipitated and dissolved after 5 years of circulation with a re-injection temperature of 50°C and comparison with a re-injection temperature of 65°C (cf Table 4)

Minerals		Amount (Kg)	Δ (%)
Calcite	Precipitation	-5229	+ 5.2
	Dissolution	6286	+ 5.9
Dolomite	Precipitation	-	-
	Dissolution	799	- 10.8
Quartz	Precipitation	- 0.25	- 43.2
	Dissolution	-	-
Amorphous silica	Precipitation	- 2190	+ 16.5
	Dissolution	0.67	0
Pyrite	Precipitation	- 1	+ 100
	Dissolution	-	-
K-feldspar	Precipitation	- 43.6	- 7.2
	Dissolution	-	-
Albite	Precipitation	- 0.1	- 33.3
	Dissolution	0.33	- 2.9
Illite	Precipitation	- 0.01	- 50
	Dissolution	0.05	0

The most important variations concern only the less reactive mineral but without influence on reservoir properties. Among the most reactive minerals, we can note that calcite behaviour is weakly affected by this variation of re-injection temperature. This is explained by the retrograde solubility of calcite, but a variation of 15°C of re-injection temperature does not influence the reservoir performance. Concerning the amorphous silica, its weak solubility at small temperature involves an increase of its precipitation of about 16 %. As a consequence, the porosity and the properties of reservoir are influenced by this increase of precipitation, mainly in the vicinity of the injection well (Figure 12). In the whole fracture, the porosity differences between the two simulations do not exceed 2 %. In the vicinity of the injection well however, variations of about 8-10 % are observed.

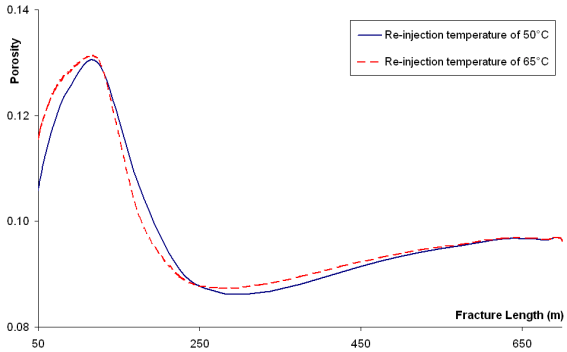

Figure12: Evolution of porosity after 5 years of exploitation according to the re-injection temperature

In many geothermal reservoirs silica precipitation is a major process and reinjection temperature is a key parameter (Xu et al., 2004).

Dilution by fresh water

During the soft acidizing test, 5814 m^3 of fresh water were injected into GPK2. To understand the impact of fresh water injection into the reservoir, a circulation test of one year was simulated using FRACHEM.

To this end, the brine was diluted by 10%, the injection temperature and rate were respectively maintained to 65°C and 2.10^{-2} L s^{-1} within the fractured zone. The amounts of precipitated and dissolved minerals were similar for quartz, amorphous silica and aluminosilicates (Table 6).

Table 6: Comparison of amounts of mineral transfer obtained from initial and diluted brine after 300 days of fluid circulation

Minerals	Amount (kg)	Original brine	Diluted brine
Calcite	Precipitated	- 951	- 632
	Dissolved	1078	759
Dolomite	Precipitated	-	-
	Dissolved	52.9	115
Quartz	Precipitated	- 0.09	-0.09
	Dissolved	-	-
Amorphous silica	Precipitated	- 173	- 159
	Dissolved	0.4	0.4
Pyrite	Precipitated	- 0.03	- 0.01
	Dissolved	-	-
K-feldspar	Precipitated	- 10.8	-10.4
	Dissolved	-	-
Albite	Precipitated	- 0.06	- 0.08
	Dissolved	0.19	0.16
Illite	Precipitated	- 0.02	- 0.04
	Dissolved	0.02	0.01

Nevertheless, the carbonates behaviour was different for the two fluids. The diluted brine mainly led to a decrease of the calcite reactivity and to an increase of that of dolomite. After 300 days of fluid circulation, the amount of dissolved dolomite doubles whereas the calcite reactivity decreases by 30 %.
To explain these computed variations, it appears that the brine dilution increases the under-saturation respectively to dolomite by 15 %. Consequently, the under-saturation improves the dissolution of this mineral, adding in solution cations such as Ca^{2+} and Mg^{2+}. Then, the increase of the calcium concentration can modify the equilibrium state respectively to calcite, decreasing its reactivity.
As a consequence, the reservoir properties are slightly modified, as shown in Figure 13.

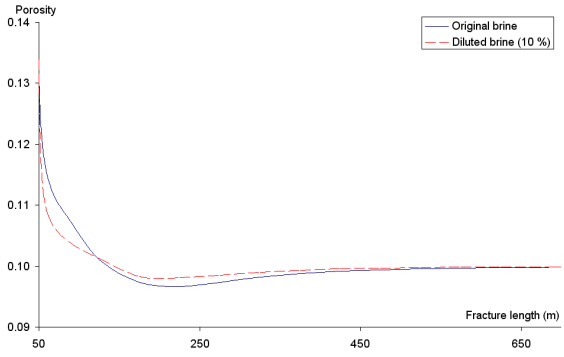

Figure 13: Evolution of porosity after dilution of brine with fresh water

These variations mainly occur in the vicinity of the injection well, where calcite and dolomite reactivities are the highest.

Conclusions

The circulation of injected cold brine in the Soultz reservoir is modelled using a Thermo-Hydraulic and Chemical coupled code. The fluid flow within the granitic reservoir modifies the chemical and thermal equilibrium of the system involving dissolution and precipitation of some minerals.
Calcite is the most reactive of them with about 6000 kg of mineral dissolved in the first 200 meters of the fractured zone and about 5000 kg precipitated in the second half of the fracture.
Silicates and aluminosilicates tend to precipitate near the injection well but in small quantities. A consequence of these reactions is the impact on porosity and permeability of the reservoir. In the vicinity of the injection well, the porosity increases of about 30 %, mainly due to calcite dissolution, while porosity decreases by 12% near the production well. Carbonates reactions seem to control the porosity of the reservoir, at least during the first 1800 days of circulation.
Silicates and aluminosilicates however play a secondary role. Their impact on porosity and permeability is visible, particularly in the first 50 meters of the fracture.
These porosity variations have an impact on properties of the Soultz Enhanced Geothermal System, with an increase of injectivity and, at the same time, a decrease of the productivity.
To improve these two parameters, different scenarios of reservoir management have been investigated. The dilution of brine seems to be the most efficient scenario to maintain the reservoir properties. This method is rather simple, but needs large volumes of make-up water. Although technically more complex, the temporary reverse circulation could also be an interesting method. Then, a combination of these methods could keep the reservoir properties during long-term production.
All these results are dependent on the relationship between porosity and permeability. For the time being, the limited knowledge of the Soultz reservoir behaviour precludes the choice of a porosity/permeability relationship. Only a comparison between simulation results and field data during the future circulation and production periods will allow selecting the proper relationship.

Acknowledgements

The authors thank the Swiss Federal Office for Education and Science and the Swiss Federal Office of Energy for funding this project (OFES-N° 00.0453 and OFES-N° 03.04.60). The authors are also grateful to Thomas Kohl of GEOWATT AG (Zürich) for his help in hydraulic modelling and numerous fruitful discussions.

REFERENCES

Bächler, D. (2003), Coupled Thermal-Hydraulic-Chemical Modelling at the Soultz-sous-Forêts HDR reservoir (France), PhD thesis, ETH-Zürich, Switzerland, 150 p.

Barrett, T. J. and Anderson, G. M. (1988), The solubility of sphalerite and galena in 1-5 m NaCl solutions to 300°C, *Geochimica et Cosmochimica Acta*, **52**(4): 813-820.

Bolton, E. W., Lasaga, A. C. and Rye, D. M. (1996), A model for the kinetic control of quartz dissolution and precipitation in porous media flow with spatially variable permeability; formulation and examples of thermal convection, *Journal of Geophysical Research, B, Solid Earth and Planets,* **101**(10), 22157-22187.

Clauser, C. (2003), Shemat and Processing SHEMAT - Numerical simulation of reactive flow in hot aquifers. Springer Verlag, Heidelberg, 332 p.

Durst, P. (2002), Geochemical modelling of the Soultz-sous-Forêts Hot Dry Rock test site: Coupling fluid-rock interactions to heat and fluid transport, PhD thesis, University of Neuchâtel, Switzerland, 127 p.

Hettkamp, T., Baumgärtner, J., Baria, R., Gérard, A., Gandy, T., Michelet, S. and Teza, D. (2004), Electricity production from hot rocks, *Proceedings, 29th Workshop on Geothermal Reservoir Engineering,* Stanford University, Stanford, California, January 26-28, 2004, 184-193.

Jacquot, E. (2000), Modélisation thermodynamique et cinétique des réactions géochimiques entre fluides de bassin et socle cristallin: application au site expérimental du programme européen de recherche en géothermie profonde (Soultz-sous-Forêts, Bas-Rhin, France), PhD thesis, Université Louis Pasteur-Strasbourg I, France, 202 p.

Kohl, T. and Hopkirk, R. J. (1995), "FRACTure" – A simulation code for forced fluid flow and transport in fractured, porous rock, *Geothermics*, **24**(3), 333-343.

Kohl, T. and Rybach, L. (2001), Assessment of HDR reservoir geometry by inverse modelling of non-laminar hydraulic flow, *Proceedings, 26th Workshop on Geothermal Reservoir Engineering,* Stanford University, Stanford, California, January 29-31, 2001, 259-265.

Norton, D. and Knapp, R. (1977), Transport phenomena in hydrothermal systems; the nature of porosity, *American Journal of Science*, **277**(8), 913-936.

Pokrovskii, V. A. and Helgeson, H. C. (1995), Thermodynamic properties of aqueous species and the solubilities of minerals at high pressures and temperatures: the system Al_2O_3-H_2O-NaCl, *American Journal of Science*, **295**, 1255-1342.

Rabemanana, V., Durst, P., Bächler, D., Vuataz, F.-D., and Kohl, T. (2003), Geochemical modelling of the Soultz-sous-Forêts Hot Fractured Rock system: comparison of two reservoirs at 3.8 and 5 km depth, *Geothermics*, **32**(4-6), 645-653.

Steefel, C. I. and Lasaga, A. C. (1994), A coupled model for transport of multiple chemical species and kinetic precipitation/dissolution reactions with application to reactive flow in single phase hydrothermal system, *American Journal of Science*, **294**(5), 529-592.

White, S. P. (1995), Multiphase nonisothermal transport of systems of reacting chemicals, *Water Resources Research*, **31**(7), 1761-1772.

Wolery, T. J. (1992), A computer program for geochemical aqueous speciation solubility calculations: theoretical manual user's guide, and related documentation (Version 7.0), Lawrence Livermore Nat. Lab. Report, UCRL-MA-110662 PT III. 246 p.

Xu, T., Ontoy, Y., Molling, P., Spycher, N., Parini, M. and Pruess, K. (2004), Reactive transport modeling of injection well scaling and acidizing at Tiwi field, Philippines. *Geothermics*, **33**(4): 477-491.

PROCEEDINGS, Thirtieth Workshop on Geothermal Reservoir Engineering
Stanford University, Stanford, California, January 31-February 2, 2005
SGP-TR-176

SIMULATED EVOLUTION OF RESERVOIR PROPERTIES FOR THE ENHANCED GEOTHERMAL SYSTEM AT SOULTZ-SOUS-FORÊTS: THE ROLE OF HOT BRINE-ROCK INTERACTIONS

Laurent André[1,2] and François-D. Vuataz[2]

[1] Centre of Hydrogeology – University of Neuchâtel, E.-Argand, 11, CH-2007 Neuchâtel, Switzerland
[2] Centre of Geothermal Research – CHYN, University of Neuchâtel, E.-Argand, 11, CH-2007 Neuchâtel, Switzerland

laurent.andre@unine.ch; francois.vuataz@unine.ch

ABSTRACT

Rock porosity and permeability do not remain constant with time. In particular, the fluid circulation within the fractured reservoir involves chemical reactions between the brine and the altered granite, which modify porosity and permeability. The FRACHEM code, a Thermo-Hydraulic-Chemical coupled code, has been developed especially to forecast the evolution of the Soultz system. For the time being, this code can simulate fluid-rock interactions and determine the dissolution/ precipitation reactions of eight minerals (carbonates, pyrite, silicated minerals). The last simulations demonstrate an important dissolution of carbonates close to the injection well, whereas small amounts of silicates precipitation are inferred.

INTRODUCTION

The geothermal research program for the extraction of energy from Hot Fractured Rock at the Soultz-sous-Forêts site began in 1987 (Hettkamp et al., 2004). The project aims to convert heat to electricity from a deep fractured and granitic reservoir. This site has been selected because of its temperature gradient in the sedimentary cover (100°C.km^{-1}) and its high heat flow reaching locally 0.15 W.m^{-2} (Kohl and Rybach, 2001).

To extract the heat from the reservoir, three deviated wells have been installed at a depth of 5000 m and their bottoms are separated by 650 m. The reservoir encountered at this depth presents a temperature of 200°C. One well (GPK3) is dedicated to the injection of cold water in the granitic reservoir whereas the two others (GPK2 and GPK4), located on both sides of injector, are used to pump hot water. At Soultz, the injection-production system is a closed loop and the fluid used is the formation brine existing in the fractured granite.

This accelerated circulation of hydrothermal brine takes place within the fractured reservoir, but chemical and thermodynamic equilibriums will be disturbed, involving chemical processes which can affect the properties of this reservoir.

The aim of this study is to predict the long-term behavior of this system under continuous production. To reach this objective, many aspects as heat, hydraulics, fluid transport and geochemical processes have to be taken into account, and their impact on porosity and permeability evolution has to be evaluated. We have examined in details the water-rock interactions on fluid flow, as well as the variations of reservoir properties with production time.

Considering the high mineralization of brine and the temperature of the reservoir, a new Thermo-Hydraulic and Chemical coupled code, called "FRACHEM", has been built for the Soultz reservoir conditions. It results from the combination of two existing codes, FRACTure and CHEMTOUGH 2. FRACHEM code determines the thermal and hydraulic processes and simulates the reactive transport. The Pitzer formalism has also been implemented in FRACHEM code to calculate the activity coefficients of selected chemical species; then, the precipitation/dissolution reactions of some minerals, i.e carbonates, quartz, amorphous silica, pyrite and some aluminosilicates can be estimated. At last, a supplementary module allows the determination of porosity and permeability variations linked to chemical processes occurring in the reservoir.

GEOLOGICAL SETTING

The Soultz-sous-Forêts Enhanced Geothermal System (EGS) is established in the Rhine Graben (Figure 1), 50 km in the North of Strasbourg (France). This graben runs along 300 km from south to north and is bordered by the Vosges to the West and the Black Forest to the East and it is affected by many faults and structures principally oriented N-S.

The granite basement is covered by 1400 m of Triassic, Jurassic and Oligocene sediments which permeability is weak. But the most interesting feature of this site is the temperature anomaly

observed within the sedimentary cover. The zone of Soultz presents a geothermal gradient which reaches 100 °C.km^{-1} down to a depth of 1000 m. Below this zone, the gradient decreases to values in the range 15-30 °C.km^{-1}, which allows a rock temperature close to 200°C at 5000 m deep (Schellschmidt and Pribnow, 2001).

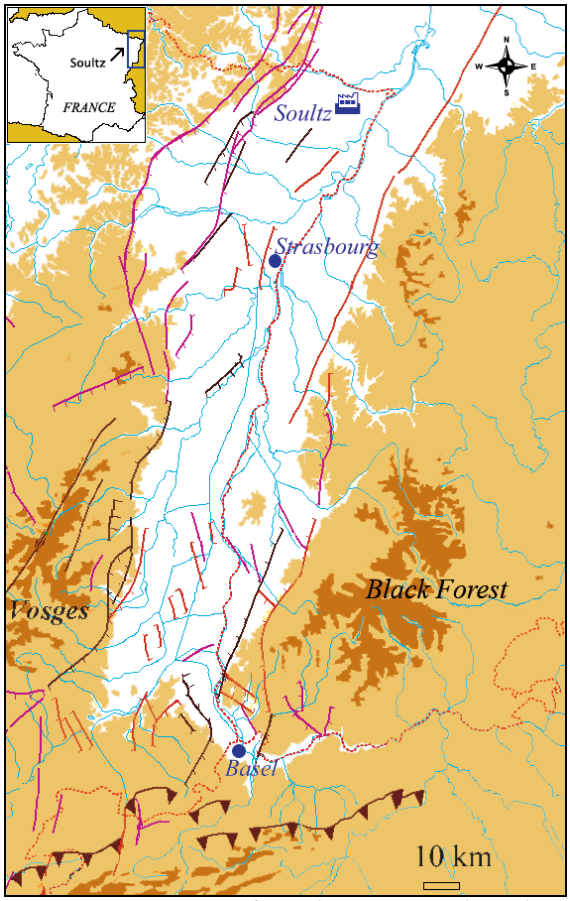

Figure 1. Location of Soultz site in the Rhine Graben.

MINERALOGICAL ASSEMBLAGE

The geothermal reservoir at Soultz is composed of three types of granite (Jacquot, 2000). The first one is a healthy granite (Table 1), characterized by the predominance of feldspars, plagioclases and quartz. This granite is not altered and contains no water. The second facies is a fractured hydrothermalised granite. Its composition revealed the following alteration: quartz is the major mineral, the amount of feldspars decreases and some secondary minerals appear like galena, pyrite, smectite or illite. This rock facies is more porous than the first one. The last facies corresponds to the vein of alteration, characterized by minerals such as illite, smectite and quartz. This facies is the most altered one but precipitation of these secondary minerals in the fractures network involves a decrease of porosity and permeability. As a result, the porosity of the second facies is the only one assuming fluid circulation in the granitic rock.

Table 1. Mean composition (in percent) of the different types of granite in the Soultz reservoir (Jacquot, 2000).

	Healthy granite	Hydrothermalised granite	Vein of alteration
Quartz	24.2	40.9	43.9
K-Feldspar	23.6	13.9	
Plagioclases	42.5		
Illite		24.6	40.2
Smectite		9.7	9.6
Micas	9.3		
Calcite	0.3	3.3	4.3
Dolomite		0.8	0.7
Pyrite		0.7	1.0
Galena		1.3	0.3
Chlorite		4.8	

FLUID COMPOSITION

The fluid circulating in the fractures network is the formation fluid, a sodium-chloride brine with total dissolved solids close to 100 g.L^{-1}. pH value reaches 4.9 and its temperature is equilibrated with the rock at this depth i.e. 200 °C. The brine composition, obtained from the fluid extracted during the production test in 1999, is given in Table 2.

Table 2. Mean composition of fluid coming from reservoir at a depth of 5 km.

Species	Concentration [mmol/kg]
Na^+	1079
K^+	68.5
Ca^{2+}	157
Mg^{2+}	3
Cl^-	1452
S	1.6
C	19
Fe^{2+}	2.4
SiO_2	5.7

NUMERICAL MODELLING

To predict the long-term evolution of the Enhanced Geothermal System, several Thermo-Hydraulic and Chemical (THC) coupled codes are available. They model the behavior of hot diluted fluids or cold brines, but not of hot hypersaline brines. Consequently, a new THC code had to be built for the Soultz reservoir conditions. Instead of creating a totally new modelling programme, two existing codes, FRACTure and CHEMTOUGH 2, have been combined in a new code called “FRACHEM” (Durst,

2002; Bächler, 2003; Rabemanana et al., 2003). FRACTure is a 3-D finite elements code and it determines thermal and hydraulic processes in fractured and porous rocks (Kohl and Hopkirk, 1995). CHEMTOUGH 2 is a 3-D finite volumes code (White, 1995); it simulates the reactive transport and allows the variation of permeability according to chemical reactions occurring between the fluid and the rock of the reservoir. This last code has been modified because of the high fluid salinity of the Soultz reservoir by several implementations: thermodynamic model and computation of the activity coefficients of selected species in solution; kinetic model for dissolution and precipitation of minerals as well as the relationship between porosity and permeability.

The thermodynamic model

The thermodynamic model has to determine the state of the fluid in regard to mineral phases present in granite i.e. the under- or over-saturation of the fluid towards these minerals. To reach this goal, the ionic activity product (Q) must be compared to the equilibrium constant of the reaction (K). If Q<K, the solution is undersaturated and the mineral has a tendency to dissolve. If Q=K, the system is at equilibrium, but if Q>K, the solution is oversaturated and the mineral precipitates.
In order to calculate these factors, the activity coefficients of each species in solution must be determined. In CHEMTOUGH2, the Debye-Huckel model is used to calculate these coefficients but this model can only be considered with dilute solutions.
Knowing the high salinity of the brine of the Soultz system, this model has been substituted by Pitzer formalism. The Pitzer equations have the advantage to take into account more types of ionic interactions than Debye-Huckel model.
To simplify the system, some assumptions have been made concerning the fluid, such as no boiling, no degassing, no condensing and no mixing with a different fluid.
Assuming these hypotheses, the activity coefficients of ionic species can be defined and only depend on two parameters, temperature and pressure.

$$\gamma_i(T,P) = (B_0 + B_1T + B_2T^2 + B_3T^3 + B_4T^4).f(P)$$

Where B_i are coefficients calculated for each mineral and f (P) is a factor depending on pressure.
Then, the activity of the species i is expressed in function of the molality m_i as:

$$a_i = \gamma_i(T,P).m_i$$

The kinetic model

The thermodynamic model allowed determining the equilibrium or non equilibrium state of the fluid in regard to the rock. But a thermodynamic disequilibrium involves chemical reactions with kinetics varying according to minerals.
A general kinetic model has been adopted to explain the dissolution/precipitation reactions of minerals. Its overall form is expressed as:

$$v = k_m.s_m.\left(1 - \left(\frac{Q_m}{K_m}\right)^{\mu}\right)^n$$

Where v is the reaction rate ($mol.s^{-1}$), k_m is the rate constant ($mol.s^{-1}.m^{-2}$), s_m is the surface of mineral in contact with fluid (m^2), μ and n are positive empirical parameters. Positive values of v correspond to dissolution rates, whereas negative values refer to precipitation rates.
This equation is adapted to each mineral and the determination of parameters k_m, μ and n are deduced from published experiments, conducted at high temperature in NaCl brines.
For the present time, the behavior of eight minerals (calcite, dolomite, pyrite, quartz, amorphous silica, K-feldspars, albite and illite) is investigated. Detailed information on the determination of the reaction laws can be found in Durst (2002).

The porosity/permeability relationship

As seen before, many chemical processes can have an influence on porosity and permeability of the system. To assume this, the porosity variations are calculated and a combination of a fracture model and a grain model is used to determine the evolution of permeability. This double model has been validated considering the structural characteristics of the altered granite crossed by the fluid.
The fracture model is based on the work of Norton and Knapp (1977) and modified by Steefel and Lasaga (1994), whose consider the case of three sets of mutually orthogonal fractures, which produce an isotropic permeability and where all the fractures have the same spacing and fracture apertures. The permeability k_F (in m^2), in this case, is:

$$k_F = \frac{\Phi_F^3}{324.n_F^2}$$

Where Φ_F represents the fracture porosity and n_F the fracture frequency in m^{-1}.
The grain model is based on the model of Kozeny-Carman which has been modified by Bolton et al. (1996). The expression of the permeability k_G is:

$$k_G = \frac{R_0^{I^2}}{45}.\frac{\Phi_G^3}{(1-\Phi_G)^2}$$

Where Φ_G and R_0^I represent the grain porosity and the initial radius of closed pack spherical grains, respectively.

APPLICATION OF FRACHEM TO THE SOULTZ SYSTEM

Model set up

The present application of FRACHEM is the modelling of a 2-D simplified model with a geometry close to the Soultz system. The injection and the production wells are linked by fractured zones and surrounded by the granite matrix. The model is composed of 1250 fractured zones. Each fractured zone has an aperture of 0.1 m, a depth of 10 m, a porosity of 10%, and contains 200 fractures. Initially the temperature was set to the reservoir temperature of 200°C. One of these fractured zones is modelled with the assumption that the fluid exchange with the surrounding low permeability matrix is insignificant. Due to the symmetrical shape of the model, only the upper part of the fractured zone is considered in the simulation. The area is discretized into 222 2D elements (Figure 2).

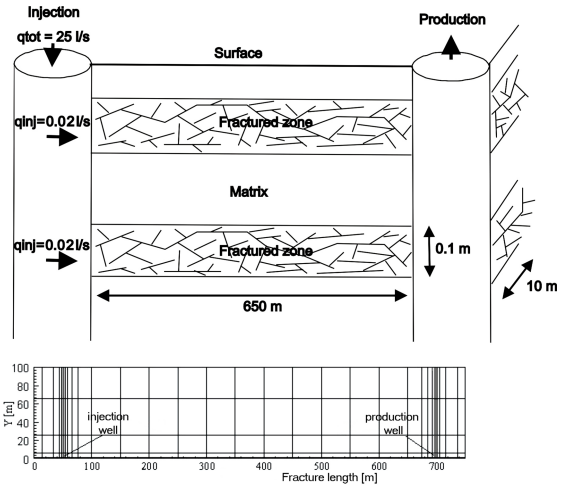

Figure 2. Simplified model and spatial discretization.

The size of the elements ranges from a minimum of 0.5 m x 0.05 m near the injection and the production wells to a maximum of 50 m x 35 m. Considering a production rate of 25 l s^{-1}, the fluid was re-injected in each of the fractured zones at a rate of 2 x 10^{-2} l s^{-1} and at a constant temperature of 65°C. During this simulation a constant overpressure of 8 MPa was assumed at the injection well and a hydrostatic pressure at the production well. Dirichlet boundary conditions were applied to the upper, left and right side of the model. Due to the sensitivity of the sequential non iterative approach (SNIA) method on the time discretization, the time step used for this simulation is limited to 10^2 s, meaning that several years of simulations take several days of computer time. The values of thermo-hydraulic parameters considered in the simulation are listed in Table 3.

Table 3. Thermo-hydraulic model parameters.

Parameters		Fracture	Matrix	Fluid
Hydraulic conductivity	[m^2/Pa]	7.4 10^{-8}	10^{-15}	-
Thermal conductivity	[W/m.K]	2.9	3	0.6
Density	[kg/m^3]	-	2650	1000
Heat capacity	[J/kg.K]	-	1000	4200
Porosity	[%]	10	0	-

Results

Reservoir temperature

Before fluid circulation in the fractured zone, all the system (rock and brine) is chemically and thermally at equilibrium. The brine is in chemical equilibrium with the granite and these two components are at a constant temperature of 200°C. But, during the injection of cold fluid at 65°C in the reservoir, the system is disturbed and the rock progressively cools down (Figure 3).

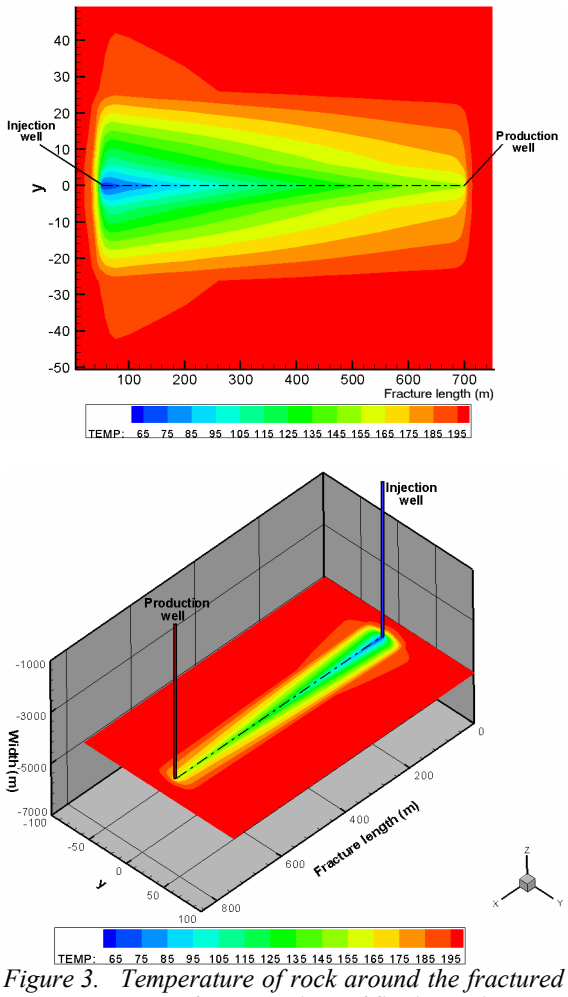

Figure 3. Temperature of rock around the fractured zone after 1500 days of fluid circulation.

The fracture is represented between the injection and the production wells, in a plane at -5000 m from surface. All along the fractured zone, we observe a global decrease of temperature, more important close to the injection well, due to the temperature of the re-injected fluid. After 1500 days of fluid circulation, the temperature in the vicinity of production well is close to 160°C. The development of this thermal front due to the thermal diffusion from rock to fluid affects a zone of 30 to 40 meters around the fractured zone (Figure 3). This temperature decrease of the produced fluid is particularly important but this value of 160°C is very dependent of the geometric model. In that case, we consider a direct circulation, in right line, between the injection and the production wells, without taking in consideration parallel paths. As a consequence, the cooling effect modelled here is probably more pronounced than in a real reservoir.

Minerals-brine interactions

The circulation of cold fluid in the fracture disturbs the chemical equilibrium of the rock-brine system involving chemical reactions such as minerals precipitation and dissolution. In this paragraph, the investigations only concern the behavior of five minerals: calcite, dolomite, quartz, amorphous silica and pyrite. For the aluminosilicates, their results will be presented later.

The calcite is a secondary mineral, crystallized in granite fractures in relative weak proportions, but it represents the most reactive mineral. As shown in figure 4, for every time period, the calcite reacts in the entire fracture. Positive values of the reaction rate indicate a dissolution and the negative ones, a precipitation process.

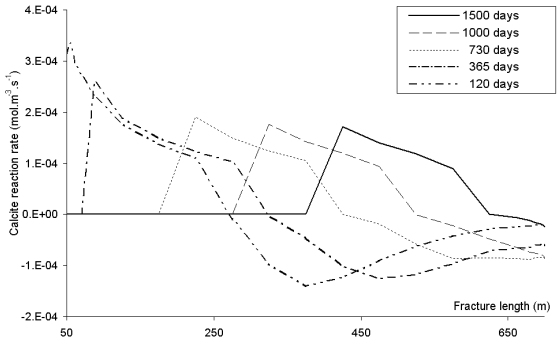

Figure 4. Calcite reaction rate along the fracture.

In the vicinity of the injection well, the calcite dissolves whereas it precipitates close to the production well. This is due to the solubility of calcite which decreases when temperature increases. At the beginning of the fluid circulation in the reservoir, the dissolution of calcite occurs mainly in the first 300 meters of fracture and a maximum of dissolution rate is reached after 120 days. This dissolution involves an enrichment of calcium Ca^{2+} in solution and later the temperature increase along the fracture causes the precipitation of calcite in the last 300 meters of fracture. The dissolution of calcite goes on until all the mineral has been consumed. Figure 5 demonstrates that in the vicinity of the injection well, about 300 days are needed to dissolve all the calcite present in the fractured granite.

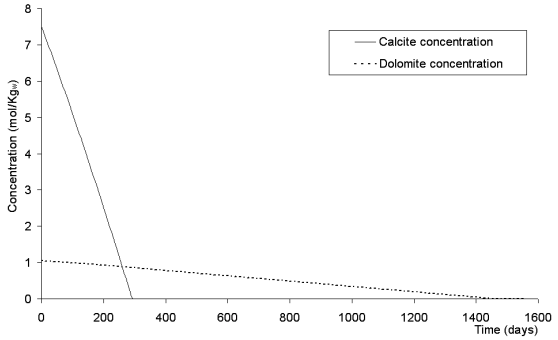

Figure 5. Evolution of dolomite and calcite concentration in the granite, close to the injection point.

With increasing simulation time, and with the decrease of the rock temperature, the dissolution zone of calcite extends towards the production well.

Another carbonate has also been investigated. The dolomite, present in granite, is less reactive than calcite. Figure 6 shows that dolomite dissolves everywhere in the fracture, but the reaction rate is one order of magnitude less than for calcite. Similarly to calcite, dolomite dissolution is stopped by the lack of mineral but, around the injection well, more than 1400 days are needed to the total disappearance of this mineral (Figure 5).

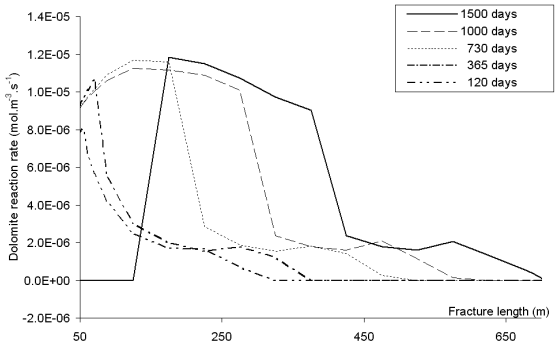

Figure 6. Dolomite reaction rate along the fracture.

Concerning the silicates, the most reactive one is amorphous silica. Quartz, which is a major mineral in granite, has a reaction rate three order of magnitude smaller than the one of amorphous silica. Contrary to calcite, the solubility of amorphous silica augments with temperature increase. As a consequence, this property involves the precipitation of this mineral near the injection well (Figure 7). With increasing the circulation time, the precipitation

zone of this mineral extends towards the production well and concerns, after 1500 days, the first half of the fracture. But, the reaction rate stays one to two orders of magnitude smaller than the one of calcite.

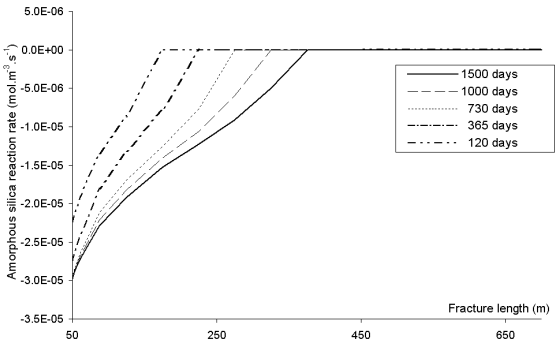

Figure 7. Amorphous silica reaction rate along the fracture.

Concerning pyrite, this mineral precipitates all along the fracture but, like in the case of quartz, the reaction rate stays negligible in comparison with calcite.

Amounts of precipitated and dissolved minerals

Knowing the reaction rate, the amount of each mineral, precipitated or dissolved, can be estimated at each time and in each fracture element of the model.
Table 4 presents the total amount of precipitated and dissolved mineral after 1500 days of fluid circulation.

Table 4. Amounts of precipitated and dissolved minerals within the entire fractured zone, after 1500 days of fluid circulation.

Minerals	Total precipitation (kg)	Total dissolution (kg)
Calcite	-534	1737
Dolomite	-	328
Quartz	-0.4	-
Amorphous silica	-153	0.05
Pyrite	-0.02	-

As calculated above by the reaction rates, calcite is the most reactive mineral. Including dolomite, more or less 2 tons of carbonates are dissolved in the fracture within 1500 days, whereas only 500 kg precipitate. We can also observe that the amounts of other reactive minerals stay far below the ones of carbonates. The only significant amount concerns the amorphous silica with about 150 kg, which precipitate close to the injection well.

Influence on porosity and permeability

The amounts of dissolved and precipitated minerals have a direct consequence on the reservoir properties, mainly porosity and permeability.

As Figure 8 shows it, calcite dissolution, close to the injection well, involves an increase of the porosity until all the carbonates have disappeared.

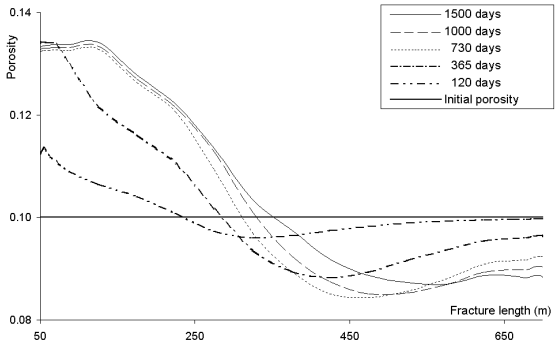

Figure 8. Evolution of porosity within the fracture according to time of circulation.

When calcite and dolomite have been dissolved, the reservoir porosity stabilizes at about 0.135; this value indicates an increase of 30-35 % compared to the initial porosity. The precipitation of amorphous silica within this zone has a limited influence on the porosity. After 1500 days of circulation, this increase of 30 % concerns only the first 100 m of fractured zone but, with an increase of circulation time, we can suppose that the porosity of all the fracture will reach this value.
Close to the production well, calcite precipitation causes a decrease of the fracture porosity of about 15 % after 1500 days of fluid circulation.
Considering the relationship between porosity and permeability used in this model, the same tendency is observed for reservoir permeability.

The case of aluminosilicates

As yet mentioned in the mineralogical description of the granite, aluminosilicates constitute an important part of the mineral assemblage.
However, taking into consideration their reactions in the model presents some difficulties. Some assumptions had to be done: the dissolution reactions are considered as congruent; aluminium in solution is under the form of Al^{3+}. Considering the temperature and the hydrostatic pressure in the reservoir, $Al(OH)_3^0$ and $Al(OH)_4^-$ species must be used (Pokrovskii and Lasaga, 1995). Nevertheless, the determination of activity coefficients of these species in the Soultz conditions presents some uncertainty and with the brine pH close to 4.8-4.9, the species Al^{3+} has been chosen. The calculation of the activity coefficient of this ion has been carried out with the EQ3nr programme (Wolery, 1992) and by the method presented by Barrett and Anderson (1988). The aluminium concentration in solution is fixed to 0.1 ppm.
From the hypothesis defined above, K-feldspars and illite seem to be more reactive than albite (Figure 9).

These two minerals precipitate close to the injection point and this process decreases when temperature increases.

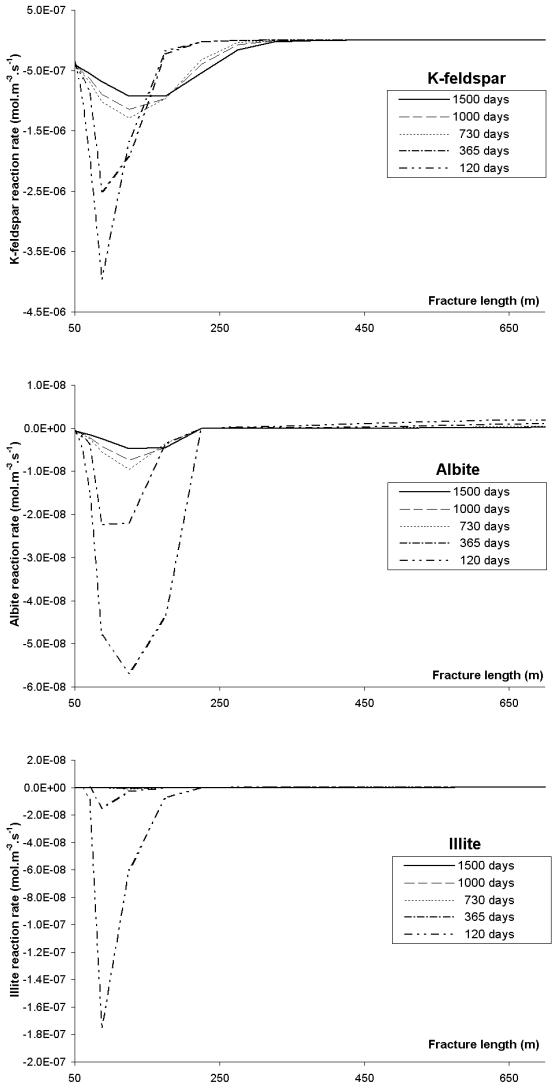

Figure 9. Aluminosilicates reaction rate along the fracture.

Above 110°C, the reaction rates of all the aluminosilicates could be considered as negligible. We can also note that the main precipitation of aluminosilicates occur at the beginning of the fluid circulation and that the reaction rates decrease with increasing circulation time, particularly in the case of illite.

After 1500 days of circulation, the precipitated amounts of K-feldspar and illite are relatively low and are negligible for albite (Table 5). Addition of aluminosilicates in the code involves small modifications of the reactive amounts of the other minerals which has some effects on the reservoir properties (Figure 10).

Table 5. Amounts of precipitated and dissolved minerals including the aluminosilicates within the entire fractured zone, after 1500 days of fluid circulation.

Minerals	Total precipitation (kg)	Total dissolution (kg)
Calcite	-453	1939
Dolomite	/	407
Quartz	-0.44	/
Amorphous silica	197	0.05
Pyrite	-0.078	-
K-feldspar	-48	-
Albite	-0.53	0.02
Illite	-0.95	0.003

Porosity of the reservoir increases until the complete dissolution of calcite and dolomite, reaching a maximum of 0.135 close to the injection zone. Following this step, the precipitation of amorphous silica and mainly K-feldspar involves a porosity decrease to a value of 0.125 after 1500 days of circulation.

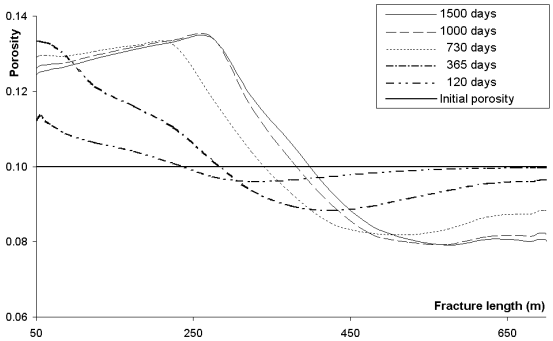

Figure 10. Influence of the reactions of aluminosilicates on the fracture porosity.

CONCLUSION

The circulation of injected cold brine in the Soultz reservoir is modelled using a Thermo-Hydraulic and Chemical coupled code. The fluid flow within the granitic reservoir modifies the chemical and thermal equilibrium of the system involving dissolution and precipitation of some minerals. Calcite is the most reactive of them with more than 1500 Kg of mineral dissolved in the first half of the fractured zone and 500 Kg precipitated close to the production well. Silicates and aluminosilicates tend to precipitate near the injection well but in small quantities. A consequence of these reactions is the impact on porosity and permeability of the reservoir. In the vicinity of the injection well, the porosity increases of about 30 %, mainly due to calcite dissolution, while it decreases of about 15% close to the production well. Carbonates reactions seem to control the porosity of the reservoir, at least during the first 1500 days of

circulation. Silicates and aluminosilicates however play a secondary role.
These porosity variations have an impact on injectivity and productivity of the EGS system with an increase of the first one and at the same time a decrease of the latter.

ACKNOWLEDGEMENTS

The authors thank the Swiss Federal Office for Education and Science for funding this project (OFES-N° 03.04.60).

REFERENCES

Bächler, D. (2003), "Coupled Thermal-Hydraulic-Chemical Modelling at the Soultz-sous-Forêts HDR reservoir (France)", PhD Thesis, ETH-Zürich, Switzerland, 150 p.

Barrett, T.J. and Anderson, G.M. (1988), "The solubility of sphalerite and galena in 1-5 m NaCl solutions to 300°C". *Geochimica et Cosmochimica Acta*, **52**(4): 813-820.

Bolton, E.W., Lasaga, A.C. and Rye, D.M. (1996). "A model for the kinetic control of quartz dissolution and precipitation in porous media flow with spatially variable permeability; formulation and examples of thermal convection", *Journal of Geophysical Research, B, Solid Earth and Planets,* **101**(10), 22157-22187.

Durst, P. (2002), "Geochemical modelling of the Soultz-sous-Forêts Hot dry Rock test site: Coupling fluid-rock interactions to heat and fluid transport", PhD thesis, University of Neuchâtel, Switzerland, 127 p.

Hettkamp, T., Baumgärtner, J., Baria, R., Gérard, A. Gandy, T., Michelet, S. and Teza, D. (2004), "Electricity production from hot rocks". *Proceedings, 29th Workshop on Geothermal Reservoir Engineering,* Stanford University, Stanford, California, January 26-28, 2004, 184-193.

Jacquot, E. (2000), "Modélisation thermodynamique et cinétique des réactions géochimiques entre fluides de bassin et socle cristallin: application au site expérimental du programme européen de recherche en géothermie profonde (Soultz-sous-Forêts, Bas-Rhin, France)", PhD thesis, Université Louis Pasteur-Strasbourg I, France.

Kohl, T. and Hopkirk, R. J. (1995), ""FRACTURE" – A simulation code for forced fluid flow and transport in fractured, porous rock", *Geothermics*, **24**, 333-343.

Kohl, T., and Rybach, L. (2001), "Assessment of HDR reservoir geometry by inverse modelling of non-laminar hydraulic flow", *Proceedings, 26th Workshop on Geothermal Reservoir Engineering,* Stanford University, Stanford, California, January 29-31, 2001, 259-265.

Norton, D. and Knapp, R. (1977), "Transport phenomena in hydrothermal systems; the nature of porosity", *American Journal of Science*, **277**, 913-936.

Pokrovskii, V.A. and Helgeson, H.C. (1995), "Thermodynamic properties of aqueous species and the solubilities of minerals at high pressures and temperatures: the system Al_2O_3-H_2O-NaCl", *American Journal of Science*, **295**, 1255-1342.

Rabemanana, V., Durst, P., Bächler, D., Vuataz, F.-D., and Kohl, T. (2003), "Geochemical modelling of the Soultz-sous-Forêts Hot Fractured Rock system: comparison of two reservoirs at 3.8 and 5 km depth", *Geothermics*, **32**(4-6), 645-653.

Schellschmidt, R. and Pribnow, D. (2001). "GGA Temperature Logs from the HDR site in Soutz-sous-Forêts". In: Baria, R., Baumgärtner, J., Gérard, A., Weidler, R. and Hopkirk, R. (Editors). European Hot Dry Rock Geothermal Research Programme 1998-2001. European Commission Final Report, contract no. JOR3-CT98-0313, Annex 7, 15p.

Steefel, C.I. and Lasaga, A.C. (1994), "A coupled model for transport of multiple chemical species and kinetic precipitation/dissolution reactions with application to reactive flow in single phase hydrothermal system", *American Journal of Science*, **294**, 529-592.

White, S.P. (1995), "Multiphase nonisothermal transport of systems of reacting chemicals", *Water Resources Research*, **31**, 1761-1772.

Wolery, T.J. (1992), "A computer program for geochemical aqueous speciation solubility calculations: theoretical manual user's guide, and related documentation (Version 7.0)", Lawrence Livermore Nat. Lab. Report, UCRL-MA-110662 PT III. 246 pp.

Geothermics xxx (2009) xxx–xxx

Contents lists available at ScienceDirect

Geothermics

journal homepage: www.elsevier.com/locate/geothermics

Chemical stimulation techniques for geothermal wells: experiments on the three-well EGS system at Soultz-sous-Forêts, France

Sandrine Portier[a,*], François-David Vuataz[a], Patrick Nami[b], Bernard Sanjuan[c], André Gérard[d]

[a] CREGE c/o CHYN, University of Neuchâtel, Emile-Argand 11, CP 158, CH-2009 Neuchâtel, Switzerland
[b] Leibniz Institute for Applied Geosciences (GGA-Institute), Stilleweg 2, D-30655 Hannover, Germany
[c] Bureau de Recherches Géologiques et Minières, 3 Av. Claude Guillemin, 45065 Orléans Cedex 02, France
[d] ESGéothermie, 3a Chemin du Gaz, 67500 Haguenau, France

ARTICLE INFO

Article history:
Received 9 July 2008
Accepted 1 July 2009
Available online xxx

Keywords:
Enhanced Geothermal Systems
Scaling
Chemical stimulation
Acid injection
Chelating agent
Well cleaning
Fractured granite
Soultz-sous-Forêts
France

ABSTRACT

Rock matrix stimulation is a method of enhancing well production or injection within a broad range of challenging environments, varying from naturally fractured limestones to sandstones with complex mineralogy. A common and often successful stimulation option, matrix acidizing, utilizes acids that react and remove mineral phases restricting fluid flow. Reviewed is the technology of chemical treatments available for oil, gas and geothermal wells and the key elements and results of the chemical reservoir stimulation program at the Soultz-sous-Forêts, France, Enhanced Geothermal System Project.

1. Introduction

The goal of Enhanced Geothermal System (EGS) projects is to harness the heat stored in deep, hot and very low permeability rocks. The economic success of the operation depends largely in opening existing fractures or creating new ones, and keeping the fracture network open to allow fluid circulation. EGS projects are at risk from natural or induced mineral precipitation in the fractures and the associated decrease in permeability. This may inhibit flow in the fractures (and in some extreme situations within the well itself), thereby lowering the rate at which heat can be extracted from the system.

A problem frequently observed in the exploration of geothermal reservoirs is the poor hydraulic connection between the production/injection wells and the fractured reservoir restricting considerably the possibility of extracting the thermal energy from the subsurface. The main reservoir lithologies currently being targeted in EGS projects tend to be crystalline igneous rocks with inherently very low natural porosity and permeability. In a given reservoir, some wells can be productive, and others not, or less so, due to a strong heterogeneity of the fracture networks. In such cases it is necessary to improve or create around the wells a permeable fracture network with a fluid–rock surface area large enough to be efficiently connected to the most permeable fractures draining the reservoir in the vicinity. Hydraulic and/or chemical stimulation methods can be used to increase the hydraulic connection between the wells and the reservoir fracture networks. Stimulation by thermal cracking is rarely used (Combs et al., 2004) but can be efficient in some high-temperature geothermal wells (Correia et al., 2000).

Chemical stimulation techniques consist mainly of acid injection into the formation at below fracturing pressures with the aim of removing near-wellbore permeability damage and material deposited in fractures through transport and precipitation processes. The oil industry has been developing these operations for more than a century in order to improve the productivity of oil and gas wells (Smith and Hendrickson, 1965; Economides and Nolte, 1989; Schechter, 1992). Acidizing may, in fact, be the oldest stimulation technique still in use. The earliest acid treatments of oil wells are believed to have been done as far back as 1895.

By dissolving acid soluble components within underground rock formations, or by removing material at the wellbore face, the rate of oil or gas production or the rate of oil-displacing fluids injection may be increased (Williams, 1979). Because of successes with acid

* Corresponding author. Tel.: +41 32 718 26 95; fax: +41 32 718 26 03.
E-mail address: sandrine.portier@unine.ch (S. Portier).

0375-6505/$ – see front matter © 2009 Elsevier Ltd. All rights reserved.
doi:10.1016/j.geothermics.2009.07.001

treatments in limestone formations, new treatments for sandstone reservoirs were developed. In 1933, Halliburton conducted the first sandstone acidizing treatment using a mixture of hydrochloric (HCl) and hydrofluoric (HF) acids. Numerous matrix acidizing treatments of sandstone formations have been conducted since the mid-1960s. In the 1970s and early-1980s, there was a proliferation of "novel" sandstone acidizing methods to retard HF consumption, stabilize fine particles, and prevent precipitation of HF-rock reaction products such as fluorite (Allen and Roberts, 1989; Kalfayan, 2001).

Despite all the differences between hydrocarbon and geothermal systems, fluid extraction and injection techniques, and reservoir management methods are similar. In both cases formation damage should be minimized to optimize well performance. The acidification of geothermal wells is not as common, but the techniques have been borrowed from the oil and gas industry (Entingh, 1999).

This paper first discusses the various methods used to prevent scaling in oil and gas wells and improve reservoir fracture connectivity and permeability, as well as describe chemical stimulation techniques for sandstone formations. Then, the paper focuses on the chemical treatments performed on geothermal reservoirs, particularly in Soultz-sous-Forêts EGS wells.

2. Chemical stimulation methods developed by the oil and gas industry

Two basic types of stimulation or acidizing operations can be conducted: matrix acidizing and fracture acidizing. Matrix stimulation is accomplished, in sandstones, by injecting a fluid (e.g. acid or solvent) to dissolve and/or disperse materials that impair or reduce well productivity/injectivity.

In carbonate formations, the goal of matrix stimulation is to create new, unimpaired flow channels between the formation and the wellbore. Matrix stimulation, typically called matrix acidizing when the stimulation fluid is an acid, is used generally to treat only the near-wellbore region. In a matrix acidizing treatment, the acid used is injected at a pressure low enough to prevent formation fracturing (Economides and Nolte, 1989). Very often carbonates show low matrix permeability and just creating wormholes around the wellbore may not be sufficient to produce fluids in commercial amounts.

Fracture acidizing is the technique that is used to provide conductive paths deeper into the formation (Burgos et al., 2005). This treatment consists of injecting an acid fluid into the formation at a rate higher than the reservoir matrix will accept. This rapid injection produces a wellbore pressure build-up leading to a fracturing of the rock. Continued fluid injection increases the fracture's length and width.

For years, mixtures of HF and HCl have been the standard in sandstone acidizing operations. HCl is selected to treat limestone, dolomite and calcareous zones, whereas HF is used to dissolve clay minerals and silica. In contrast to carbonate reservoirs, the acidification of a sandstone reservoir requires a specific procedure, which is carried out in three main steps: preflush, main flush and overflush. The preflush is performed most often with an HCl solution (10%). The objective of this first step is to displace the formation brine away from the wellbore, and to dissolve as much of the calcareous material in the formation as possible prior to the injection of the HF solution. The preflush acid minimizes the possibility of forming insoluble precipitates.

The main flush is used to remove the damage; most often, a mixture of 12% HCl–3% HF (called regular mud acid—RMA) is pumped into the well. This mixture is generally prepared by dissolving ammonium bifluoride (NH_4HF_2) in HCl. Finally, the overflush, which usually consists of injecting HCl, KCl, NH_4Cl, or freshwater, is an important part of a successful sandstone acid treatment. It displaces the non-reacted mud acid and the mud acid reaction products into the formation away from the wellbore (Paccaloni and Tambini, 1993).

Variations of this approach to sandstone acidizing include changes in the concentration and ratio of HCl and HF acids, as well as in the volumes pumped into the formation during the different phases; these variations depend mainly on formation mineralogy (McLeod, 1984; Perthuis et al., 1989; Davies et al., 1994). Corrosion inhibition is always necessary to protect well casings, and inhibitors must be added to all acid stages (preflush, main flush, and overflush) (Buijse et al., 2000).

A problem that can limit the effectiveness of matrix acidizing relates to the proper placement of the acid, i.e. ensuring that the acid is delivered to the desired zones. This problem is exacerbated by the intrinsic heterogeneity of the permeability (common in many formations), especially the presence of natural fractures and high-permeability zones. Numerous techniques have been developed to direct the treatment fluid toward selected reservoir zones. Coiled tubing is a very useful tool for improving acid placement (Economides and Frick, 1994). In longer open-hole sections, such placement is important, otherwise treatment will be confined to the interval that breaks down or fractures first. Proper placement of the injected acid can be achieved by installing packers, or by the use of polymers.

The re-precipitation of reaction products is a serious concern in acidizing sandstones containing alumino-silicates; as HF is injected it reacts with sandstone minerals (Walsh et al., 1982; Pournik, 2004). Because of the precipitation of secondary and tertiary reaction products, conventional mud acid has a great chance of failure in formations of high (>120 °C) temperature or rich in clays sensitive to HCl (Crowe, 1986; Gdanski, 1997). Clay swelling can be caused by ion exchange between acidizing fluids and formation minerals or changes in salinity, choking off production by obstructing pores and/or fractures.

Although conventional stimulation fluids such as HCl or mud acid can clean the wellbore and stimulate the matrix, they do not penetrate deep into the formation or stabilize fines. Methods have been developed to slow the acidizing process (Templeton et al., 1975; Thomas and Crowe, 1981). A key issue is not to inject a HF solution at the wellhead, but to use a compound able to generate HF at greater depth of penetration and of longer reaction time for maximum dissolution of fines (Crowe et al., 1992). Most of these chemically retarded acid systems rely on the use of weak organic acids, such as fluoroboric, fluoroaluminic and hexa-fluoro-phosphonic acids, and their secondary reactions to improve rock permeability (Malate et al., 1998). Other types of acid systems can be used, such as gelling agents (polymers and surfactants), emulsified solutions of aqueous acid in oil, acids dissolved in a solvent (e.g. alcohol and gel) or the injection of solutions of methyl acetate, which hydrolyses slowly at high temperatures to produce acetic acid, making it more difficult for the H^+ ions to contact a reactive surface.

An alternative to acid treatment is the use of chelating agents such as ethylenediaminetetraacetic acid (EDTA) or nitrilo-triacetic acid (NTA) (Fredd and Fogler, 1998). Chelant solutions are used in formation cleanup and for stimulating wells, especially in formations that may be damaged by strong acids (Frenier et al., 2001). They act as a solvent, increasing the water-wetting process and dissolving (entirely or partially) some minerals containing Fe, Ca, Mg and Al. Through the process of chelation, a calcium ion would be solvated by the chelating agent, allowing the calcite to be transported either to the surface by discharging the well or further into the formation by injecting into the well. The rate of calcite dissolution using chelating agents is not as fast as is the rate of calcite dissolution using strong mineral acids. The lower dissolution rate means

Please cite this article in press as: Portier, S., et al., Chemical stimulation techniques for geothermal wells: experiments on the three-well EGS system at Soultz-sous-Forêts, France. Geothermics (2009), doi:10.1016/j.geothermics.2009.07.001

Table 1
Results of chemical treatments in selected geothermal fields.

Geothermal field	Chemical agents used	Number of treated wells	Variation of the injectivity index before and after chemical treatment ($kg\,s^{-1}\,bar^{-1}$)	Ref.
Bacman (Philippines)	HCl–HF	2	0.68–3.01 0.99–1.40	Buning et al. (1995)
Leyte (Philippines)	HCl–HF	3	3.01–5.84 0.68–1.77 1.52–10.80	Malate et al. (1997); Yglopaz et al. (1998)
Tiwi (Philippines)	HCl–HF	1	2.52–11.34	Buning et al. (1995)
Mindanao (Philippines)	HCl–HF	1	Successful	Buning et al. (1997)
Salak (Indonesia)	HCl–HF	1	4.70–12.10	Pasikki and Gilmore (2006)
Berlín (El Salvador)	HCl–HF	5	1.60–7.60 1.40–8.60 0.20–1.98 0.90–3.40 1.65–4.67	Barrios et al. (2002)
Las Tres Vírgenes (Mexico)	HCl–HF	2	0.8–2.0 1.2–3.7	Jaimes-Maldonado and Sànchez-Velasco (2003)
Los Azufres (Mexico)	HCl–HF	1	3.3–9.1	Flores et al. (2006)
Beowawe (USA)	HCl–HF	1	Successful	Epperson (1983)
The Geysers (USA)	HCl–HF	1	No effect	Entingh (1999)
Coso (USA)	HCl and NTA[a]	30	24 wells successful	Evanoff et al. (1995); Rose et al. (2007)
Larderello (Italy)	HCl–HF	5	11–54 4–25 1.5–18 Successful 11–54	Cappetti (2006)
Fenton Hill (USA)	Na_2CO_3	1	About 1000 kg of quartz were dissolved and removed from the reservoir but no impedance reduction resulted.	LANL (1977)
Fjällbacka (Sweden)	HCl–HF	1	Efficiency of acid injection in returning rock particles.	Sundquist et al. (1988); Wallroth et al. (1999)

[a] NTA: nitrilotriacetic acid ($C_6H_9NO_6$).

that the chelating agent will be able to take a more balanced path and more evenly dissolve calcite along the wellbore and in all available fractures, rather than following the first fluid entry zone and leaving the rest of the wellbore relatively untouched. Laboratory data also indicate that aqueous solutions at high pH can dissolve wellbore silica and near-wellbore formation silicates and that dissolution capacity increases with temperature (Sarda, 1977; Rose et al., 2007).

3. Present use of chemical stimulation in geothermal wells

Various acidizing treatments have been performed in geothermal wells over the last 30 years (Strawn, 1980; Epperson, 1983; Barelli et al., 1985; Barrios et al., 2002; Serpen and Türeyen, 2000). A summary of the main chemical stimulation experiments carried out in geothermal fields is given in Table 1, showing variable results. To date, only a few chemical stimulation experiments and laboratory tests have been attempted in EGS wells and reservoirs. Only limited amount of data were found on the projects at Fenton Hill, USA (Sarda, 1977) and Fjällbacka, Sweden (Sundquist et al., 1988; Wallroth et al., 1999).

In geothermal wells the strongest indication of formation damage is a sharp drop in production rate. Nearly all geothermal wells that are acidizing candidates have been damaged by either drilling mud solids and drill cuttings lost to the formation or by scaling (Buning et al., 1997; Malate et al., 1998, 1999; Yglopaz et al., 1998; Jaimes-Maldonado and Sànchez-Velasco, 2003; Axelsson et al., 2006).

Production and injection of geothermal brines strongly modifies the natural flow taking place within the fractured reservoir. Consequently, chemical and thermodynamic rock–fluid equilibria are disturbed in the formation. One of the major problems affecting reservoir permeability is scaling (most often, calcium carbonate, amorphous silica, calcium sulfate, and mixtures of them), which leads to a decrease in well injectivity/productivity (Flores et al., 2005). This phenomenon has been observed in many geothermal fields, such as Bacman, Leyte and Tiwi, Philippines (Buning et al., 1995, 1997; Malate et al., 1997; Molina et al., 1998; Amistoso et al., 2005), Berlín, El Salvador (Barrios et al., 2002), Coso and Beowawe, USA (Morris et al., 1984; Evanoff et al., 1995) and Latera and Larderello, Italy (Barelli et al., 1985; Cappetti, 2006). Different methods have been tried to prevent scaling in geothermal wells, including varying pressure, temperature and/or fluid pH, and changing scale inhibitors. Although these inhibitors have solved many problems, one promising alternative is acidizing. Increasingly, geochemical modelling studies help geothermal field operators to anticipate scaling problems and to propose solutions in order to maintain well productivity/injectivity (Xie, 2004; Xu et al., 2004; André et al., 2006).

A very successful method of acidizing geothermal wells has been through high-rate injection of strong mineral acids. Elevated acid concentrations have been shown to be effective in geothermal wells producing from natural fractures and from formations that do not have large carbonate zones. In almost all documented cases, acidification is done following the three usual main steps—preflush (HCl), main flush (HCl–HF mixture) and overflush (HCl, KCl, NH_4Cl solutions or freshwater).

Naturally fractured volcanic formations can withstand high HF concentrations. The HCl–HF stage can be, for example, a 10% HCl–5% HF solution, or an organophosphonic acid added to a 3% HCl–5% HF solution. These acid mixtures have been used successfully in stimulating geothermal wells in Indonesia (Pasikki and Gilmore,

Please cite this article in press as: Portier, S., et al., Chemical stimulation techniques for geothermal wells: experiments on the three-well EGS system at Soultz-sous-Forêts, France. Geothermics (2009), doi:10.1016/j.geothermics.2009.07.001

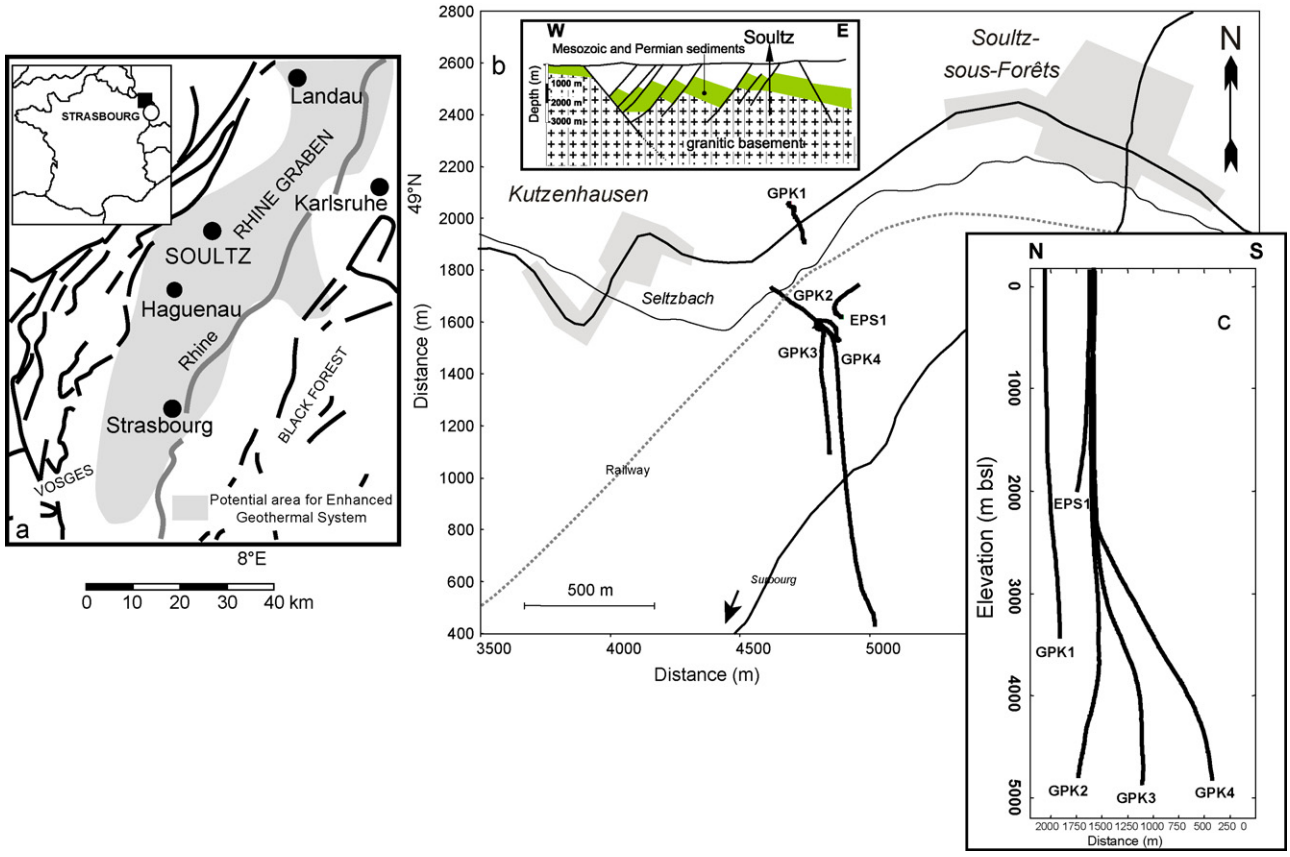

Fig. 1. Schematic geological map of the Rhine Graben and location of the Soultz-sous-Forêts EGS site (a and b). Map view and N–S cross-section of the Soultz deep geothermal wells (b and c); solid lines correspond to well traces (b and c) (after Sausse et al., 2006).

2006), as well as in Mexico (Flores et al., 2006). The only additives needed in a geothermal acid job are the corrosion inhibitor and the inhibitor intensifier that may be used to extend the performance range of the selected corrosion inhibitor at elevated temperatures, as well as a high-temperature iron-control agent. Conventional acid placement techniques are less effective for the long, open-hole or liner-completed intervals typically encountered in geothermal wells. High-temperature foam systems may improve zone coverage.

4. The case of the EGS reservoir at Soultz-sous-Forêts

The Soultz-sous-Forêts Enhanced Geothermal System, located 40 km north of Strasbourg, France, in the Upper Rhine Graben, has been investigated since 1986 (Fig. 1). The final goal of the project is to extract heat for power production from a regional, randomly permeable, natural geothermal reservoir by forced fluid circulation between production and injection boreholes drilled into the granitic basement. This site was chosen because of the large thermal anomaly in the area and because the shallow geology was well known, due to former oil exploitation in this part of the Tertiary Graben.

The shallow geology (0–1400 m depth) consists of sedimentary layers, overlying the crystalline basement of late-Palaeozoic granites that presents hydrothermally altered and fractured zones related to the normal faults of the Rhine Graben (Genter, 1990; Traineau et al., 1991). It has been observed that deep fluid circulation is supported by a network of permeable fractures. Extensive research has been done to characterize the properties of the fractures. Geophysical borehole measurements including image logs and core and cuttings analyses showed nearly vertical, low-permeability fractures that are oriented in an almost North–South direction (Dezayes et al., 1995; Genter et al., 1995). Moreover, it appears that most of the fractures are sealed by hydrothermal deposits, mainly calcite, silica and clays, giving a random character to the overall permeability of the system.

After the successful connection to a 3.6-km deep fractured reservoir in 1997, it was decided to develop a new, deeper and hotter reservoir and to build a pilot geothermal plant. For this purpose, three wells (GPK3 as a central injection well and GPK2 and GPK4 as production wells) were drilled to 5000 m depth in the crystalline basement (Fig. 1). These wells have been stimulated hydraulically and chemically to create the underground reservoir (Gérard et al., 2006). The first implementation phase of the project is the construction of a 1.5 MWe geothermal power plant.

Low-pressure pre-stimulation hydraulic tests were conducted in the wells to characterize the natural permeability of the granite, indicating initial productivity indices of 0.01 L s^{-1} bar^{-1} in GPK4, 0.1 L s^{-1} bar^{-1} in GPK3 and 0.02 L s^{-1} bar^{-1} in GPK2.

The first hydraulic stimulations of the three wells were carried out between 2000 and 2005, and resulted in an improvement of the productivity indices of wells GPK2 and GPK4 by a factor of approximately 20 and of GPK3 by a factor of approximately 1.5 (Nami et al., 2007). The limited performance of the hydraulic stimulation operations, with high costs and public concern about induced seismicity, provided an important set of reasons to carry out chemical treatments as additional or even alternative methods to hydraulic stimulation. The main argument for chemical stimulation based on drill cuttings and cores analyses, as well as on geophysical logs, was that the carbonate and other soluble minerals deposits were filling the fractures.

The results obtained both from tracer (Sanjuan et al., 2006) and pressure interference tests (Dezayes et al., 2005) clearly identified the main pathways the fluid follows during stimulation and showed that some hydraulic connections exist between the boreholes via

Please cite this article in press as: Portier, S., et al., Chemical stimulation techniques for geothermal wells: experiments on the three-well EGS system at Soultz-sous-Forêts, France. Geothermics (2009), doi:10.1016/j.geothermics.2009.07.001

Table 2
Summary of the chemical stimulations performed in the three 5-km deep Soultz-sous-Forêts EGS wells.

Well	Date	Concentration of chemical agents	Stimulation results
GPK2 (production well)	February 2003	One test in two steps: HCl 0.09% and HCl 0.18%	Wellhead pressure drop and productivity increase ($0.5\,L\,s^{-1}\,bar^{-1}$)
GPK3 (injection well)	June 2003	HCl 0.45%	Injectivity: $0.35\,L\,s^{-1}\,bar^{-1}$
	February 2007	OCA HT	Weak impact: $0.4\,L\,s^{-1}\,bar^{-1}$
GPK4 (production well)	February 2005	HCl 0.2%	Productivity: $0.2–0.3\,L\,s^{-1}\,bar^{-1}$
	May 2006	Preflush: HCl 15% RMA (HCl 12%–HF 3%)	Maximum enhancement of injectivity: 35%
	October 2006	NTA 19%	The formation of a plug increased wellhead pressure—Productivity: $0.3–0.4\,L\,s^{-1}\,bar^{-1}$ (after RMA and NTA treatments)
	March 2007	OCA HT	Productivity: $0.4–0.5\,L\,s^{-1}\,bar^{-1}$

RMA: regular mud acid; OCA HT: organic clay acid HT; NTA: nitrilotriacetic acid.

the natural fractures in the granite. The most important fracture zone striking N160°E and dipping 52° toward the W appears as a "direct" connection between GPK2 and GPK3 (Dezayes et al., 2005). However, in GPK2, this fracture zone is thinner and less permeable than in GPK3.

Due to the low productivities of GPK2 and GPK4 and the poor injectivity of GPK3 after successive hydraulic stimulations, it was decided to carry out a chemical stimulation program on all three wells. Chemical treatments with low-concentrations of HCl were performed in the three wells after the hydraulic stimulations (Table 2). Between May 2006 and February 2007, three chemical stimulations were done in GPK4 and one in GPK3. During these operations, solutions of RMA, NTA and organic clay acid (OCA) were successively injected with fresh water into GPK4, but only the OCA treatment was used in GPK3.

Chemical stimulations were performed by injecting acid from the wellhead through the casing string. Therefore, the entire (500–650 m long) open-hole sections of the wells were treated. Corrosion inhibitors were used to protect the inner casing string. The operations were conducted by specialized service companies. Table 2 shows the various chemical treatments conducted in the deep Soultz wells.

Hydraulic tests were performed before and after the chemical stimulations in order to evaluate changes in well productivity or injectivity; the values given in Table 2 are those measured after 3 days of injection or production. The results show that there is no significant difference between injectivity and productivity indices at moderate flows and pressure changes (Nami et al., 2008). In this case, therefore, for the Soultz wells the terms 'injectivity' and 'productivity' can be considered as interchangeable.

Geochemical monitoring was conducted during most of the chemical stimulations. Sanjuan et al. (2007) report on the fluids and deposits collected from GPK4 and GPK3 during the 2006 and 2007 production tests, after the chemical stimulation operations. This work was done in the framework of the research activities accompanying the construction of the European EGS Pilot Plant Project (Baumgärtner et al., 1998; Hettkamp et al., 2004; Baria et al., 2006; Gérard et al., 2006; Genter et al., 2009).

4.1. Soft acidizing: stimulation of the three deep wells using hydrochloric acid

The three deep wells were subjected to chemical stimulation by injection of a low HCl concentration solution. The objective of this dilute but extended stimulation was to dissolve secondary carbonates (calcite and dolomite) deposited in the formation fractures.

4.1.1. GPK2 well

Tests carried out in 2000 on the first deep well (GPK2) after hydraulic stimulation showed an improvement of its injectivity from 0.02 to $0.3\,L\,s^{-1}\,bar^{-1}$. A decision was then made to seek further improvement through soft acidizing. In February 2003, GPK2 was stimulated by injecting 1.5 tons of HCl in two stages. First, 500 kg were injected at a concentration of $1.8\,g\,L^{-1}$ at a rate of $30\,L\,s^{-1}$. The treatment had an immediate and strong impact, showing a significant reduction of near-wellbore friction losses immediately after the acid front reached the open-hole section. The second part of the stimulation, performed at concentrations of 1.8 and $0.9\,g\,L^{-1}$ and flow rates of about 15 and $30\,L\,s^{-1}$, respectively, showed less immediate effects.

Nevertheless, the overall result was impressive for such a small quantity of acid injected. No injectivity test was performed in this well after this chemical stimulation with HCl. However, the increase in injectivity was evident from the circulation tests done in 2003 (between GPK2 and GPK3) and in 2005 (between GPK3 and the two production wells GPK2 and GPK4) (Gérard et al., 2005). The injectivity index of GPK2 increased to approximately $0.5\,L\,s^{-1}\,bar^{-1}$ after this HCl treatment.

4.1.2. GPK3 well

During a circulation test between GPK2 and GPK3 in June 2003, up to 3 tons of HCl were injected into GPK3 over a period of 12 h. A total of $865\,m^3$ of an acid solution with a concentration of about $4.5\,g\,L^{-1}$ of HCl was injected at a rate of $20\,L\,s^{-1}$.

An injection test was carried out in August 2004 after the hydraulic and a HCl chemical stimulation of the well. A total of $7000\,m^3$ of fresh water was injected at flow rates of 12, 18 and $24\,L\,s^{-1}$ for a period of 6 days. The injectivity index for this test was about $0.35\,L\,s^{-1}\,bar^{-1}$ (Gérard et al., 2005). Nevertheless, it is difficult to estimate the impact of the acid treatment on GPK3 injectivity because, unlike GPK4, no injection test was performed under the same conditions before and after the chemical stimulation.

4.1.3. GPK4 well

In February 2005, an acidified water injection experiment was conducted with the objective of improving the injectivity around GPK4. A total of $4700\,m^3$ of an about $2\,g\,L^{-1}$ HCl solution was injected at a flow rate of $27\,L\,s^{-1}$; in this test 11 tons of HCl were used. Despite the fact that the injection was performed in an overpressurized reservoir, the injection pressure was decreasing during the last hours of the acidification test.

The impact of the GPK4 stimulation was evaluated before and after each phase of the operation by performing a step-rate injection test. About $4500\,m^3$ of fresh water were injected at increasing flow rates (9, 18 and $24\,L\,s^{-1}$) in 1-day steps. The first step-rate injection test was carried out in GPK4 after its second hydraulic stimulation in 2005. The analysis of this test gave a productivity index, after 3 days of injection, of $\sim 0.20\,L\,s^{-1}\,bar^{-1}$.

After injecting acid into GPK4 on 13 March 2005, a second step-rate injection test was performed. Results show that the well-

Please cite this article in press as: Portier, S., et al., Chemical stimulation techniques for geothermal wells: experiments on the three-well EGS system at Soultz-sous-Forêts, France. Geothermics (2009), doi:10.1016/j.geothermics.2009.07.001

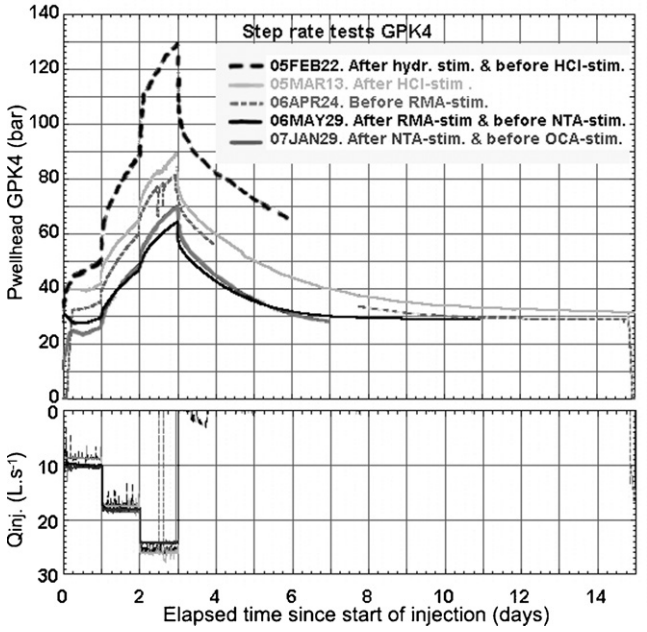

Fig. 2. Comparison of wellhead pressures and injection rates during the GPK4 step-rate tests (modified after Nami et al., 2007).

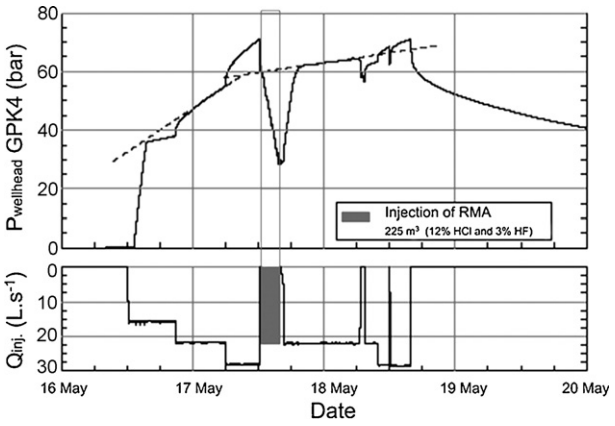

Fig. 3. Impact of the regular mud acid (RMA) acidification test performed on GPK4 in May 2006 (after Nami et al., 2007). The slope change in the pressure (dashed line) for the same flow rate before and after the RMA injection (preflush of 25 m^3 of 15% HCl solution and main flush of 200 m^3 of RMA at 22 $L\,s^{-1}$ during about 3 h) indicates a gain in well injectivity (productivity).

head pressure was about 40 bars below the value observed under the same conditions before acidification (Fig. 2). This represents a decrease in the apparent reservoir impedance, as inferred from the wellhead pressure, by a factor of about 1.5 (Gérard et al., 2005). The productivity index of GPK4 reached 0.30 $L\,s^{-1}$ bar^{-1} after acid injection.

4.2. Stimulation of GPK4 with regular mud acid

Regular mud acid a mixture of HCl and HF, widely used in oil and gas wells, was only injected into GPK4. The purpose of the RMA treatment was to dissolve the hydrothermal minerals (e.g. carbonates, clay, feldspars and micas) deposited in the fractures and pores of the granite, and thus improve its permeability.

To determine the most effective acid mixture to use in the stimulation of the deep reservoir, laboratory tests were performed both in batch and under continuous flowing conditions (Erga, 2000). The batch experiments consisted in testing the reactivity of acid mixtures (HCl/HF) at 50 and 150 °C on core samples of granite composed mainly of feldspars, quartz, micas, phyllosilicates and that presented hydrothermal veins. Batch results indicated that the mixtures 12/3 and 12/6 (by wt%) were the best to attack these rocks and minerals. These two HCl/HF mixtures were then used in a series of tests under flowing conditions and temperatures of up to 90 °C.

The flowing test apparatus can be used on a circular plane sample (0.02 m in diameter) by applying an acid mixture under variable flow rate and temperature conditions. The samples were carefully weighted before and after each test using a precision balance and thus measure the weight loss per unit surface. Scanning electron microscope and quantitative X-ray microanalyses were used in order to determine the minerals affected by the acidification treatment. The most effective acid mixture was found to be 12/3 (wt%) HCl/HF mixture.

In May 2006, the RMA treatment was carried out in four steps and adding a corrosion inhibitor when needed. Before the injection of RMA, 2000 m^3 of cold deoxygenated water were introduced into the well at rates of 12, 22, and, finally, 28 $L\,s^{-1}$. Then, to avoid calcium fluoride (CaF_2) precipitation that can lead to well damage, a preflush of 25 m^3 of a 15% HCl solution in deoxygenated water (3.75 tons of HCl) was pumped ahead of the HCl–HF mixture for 15 min at a rate of 22 $L\,s^{-1}$. A main flush consisting of a total of 200 m^3 of 12/3 (wt%) RMA was then injected for 2.5 h at a rate of 22 $L\,s^{-1}$. Finally, a postflush of 2000 m^3 of cold deoxygenated water was injected after the RMA treatment during 1 day, at flow rates of 22 and 28 $L\,s^{-1}$.

After the RMA stimulation, the wellhead pressure versus time curve for GPK4 was smooth, indicating an efficient clean-up of the fractures and/or pores around the open hole (GEIE, 2006) (Fig. 3). The step-rate test performed later in May 2006 (Fig. 2), following the RMA stimulation, shows that after 3 days of injection the wellhead pressure is about 65 bars, which is about 16 bars lower than before the chemical treatment (i.e. when the April 2006 step-rate test was performed). This represents a 35% reduction in wellhead pressure due to the acidification treatment (GEIE, 2006). Before the RMA treatment, the wellhead pressure increased rapidly with flow rate indicating restricted storage capacity in the vicinity of the well.

It is estimated that the RMA stimulation of GPK4 has resulted in the enhancement of the well's injectivity index by up to 35%. However, no production test was performed after these operations to measure the productivity index.

4.3. Stimulation of GPK4 using chelating agents

After the RMA stimulation, GPK4 was chemically treated with NTA, a chelating agent, in October 2006. While the RMA treatment was used to clean the fractured and porous zones of hydrothermal mineral deposits in the near field around the borehole, the goal of the NTA stimulation was to drive the chelating agent as far as possible into these zones to improve the hydraulic connections in the reservoir.

NTA ($C_6H_9NO_6$) is a weak tri-acid that forms complexes with cations like Fe, Ca, Mg, and Al, and thereby reduces the activity of these cations, leading to an enhanced dissolution of the corresponding minerals (e.g. calcite). Chelants are much less corrosive to steel tubulars than acids.

What prevented geothermal operators from using caustic solutions in the past was the fear of calcite deposition, which is strongly favored at high pH. However, laboratory experiment results have demonstrated the potential for calcite dissolution at high pH in the presence of chelating agents (Mella et al., 2006; Rose et al., 2007). This suggests that thermally stable chelating agents at high

Please cite this article in press as: Portier, S., et al., Chemical stimulation techniques for geothermal wells: experiments on the three-well EGS system at Soultz-sous-Forêts, France. Geothermics (2009), doi:10.1016/j.geothermics.2009.07.001

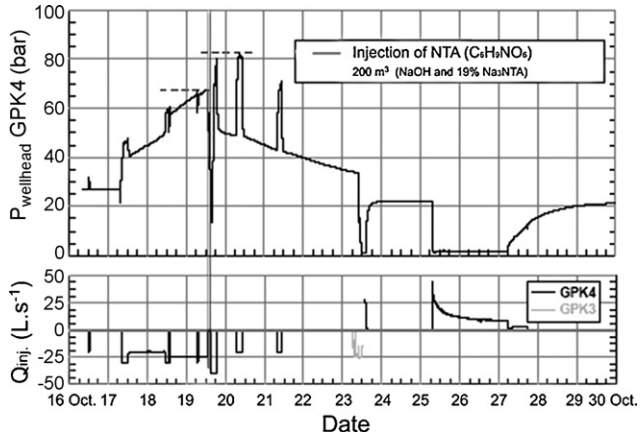

Fig. 4. Impact of the nitrilo-triacetic acid (NTA) treatment performed on GPK4 in October 2006 (after Nami et al., 2007). The wellhead pressure (dashed line) following short water injections is higher than shortly before the injection of 200 m^3 of NTA at 35 L s^{-1}, followed by a postflush injection of 400 m^3 of water at 40 L s^{-1}, and indicates probable plugging of the well. A production test was done on 25 October to remove NTA solution residuals.

pH can provide the basis for an affordable and effective mineral dissolution approach. Although thermal stability studies have not been completed yet, the literature suggests that NTA could be used at temperatures as high as 290 °C, whereas the other two chelating agents, EDTA and hydroxyethylethylenediaminetriacetic acid (HEDTA), are significantly less thermally stable, i.e. up to about 200 °C. Calcite dissolution experiments in a high-temperature flow reactor confirmed the superior performance of NTA above 200 °C (Peter Rose, pers. comm., April, 2008).

Before GPK4 was treated with NTA, the well was cooled by injecting 4150 m^3 of fresh water at an average flow rate of about 24 L s^{-1} for a period of 53 h. After well cooling, 200 m^3 of a basic solution (pH 12) consisting of caustic soda (NaOH) and 19% Na_3NTA (about 38 tons of NTA) were injected at a flow rate of 35 L s^{-1} during 1.6 h period. After the NTA injection, 850 m^3 of fresh water were injected at 20–40 L s^{-1}.

Surprisingly, after these injections the wellhead pressure increased radically (Fig. 4). To prevent any well plugging, a production test was carried out in GPK4 (October 2006) to remove residuals of the NTA solution. During this test about 2600 m^3 of fluid were discharged. At the beginning of the production test, large quantities of magnetite-rich grey sands and drilling grease deposits were produced, followed by a yellow-coloured fluid containing chelant precipitate (GEIE, 2007). At the end of the test, geochemical analysis of the produced water samples showed a neutral pH (7.1–7.4), and thus the almost complete removal of the chelating agents from the borehole and neighbouring fractures and pores (Sanjuan et al., 2007). The mobilization and accumulation of these deposits in the fractured and porous zones were probably due to the significant cleaning of the well itself and of the near-wellbore formation by the basic NTA solution, especially because of the use of NaOH. It is likely that, during the injection of chelating agents – which are also used as cleaning agents – scale deposits were detached from the casing and transported into the surrounding formation. These deposits and the drilling wastes (grease, cuttings) probably blocked some of the flow pathways in the vicinity of the well and resulted in an increase in wellhead pressures.

In January 2007, in the same manner as for the previous RMA stimulation of GPK4, a step-rate test was carried out to assess the effects of the NTA stimulation. The wellhead pressure after the NTA injection was about 7 bars higher than before the chemical treatment (Fig. 2), indicating loss in productivity; i.e. the index dropped to about 0.35 L s^{-1} bar^{-1}.

4.4. Stimulation with chemically retarded acid systems: chemical stimulation of the GPK4 and GPK3 far fields

To complete a series of hydraulic and chemical stimulations to enhance the productivity of the three deep Soultz wells that started in 2000, GPK3 and GPK4 were treated with chemically retarded acid systems (organic clay acid for high temperature; OCA-HT). The main objectives of this operation were to dissolve the remaining solid deposits and to increase as much as possible the hydraulic connectivity between wells and the fractured and porous formation.

The OCA fluid was a mixture of citric, hydrofluoric and borofluoric acids and ammonium chloride. The solution consisted of 5–10% $C_6H_8O_7$, 0.1–1% HF, 0.5–1.5% HBF_4, and 1–5% NH_4Cl (Sanjuan et al., 2007). Its use is especially recommended at temperatures above 180 °C for sandstones or formations with zeolite or chlorite contents greater than 5%, which react with conventional stimulation fluids (i.e. HCl). This solution was at first tested in the laboratory by Schlumberger on GPK3 cutting samples. After 5 h of reaction, the OCA solution dissolved 24% of the cuttings samples at 80 °C and 41% at 180 °C. Other laboratory tests were carried out at BRGM showing that the solution could also dissolve metal–NTA complexes (Sanjuan et al., 2007).

The OCA solution can penetrate deep into the formation and stabilize clays and fines without the adverse effects of conventional acid systems. It attacks mainly calcite, but also silicates, aluminosilicates, iron oxy-hydroxide minerals and Ca–Fe–NTA compounds. This solution is a high-performance acid system designed for sandstone matrix formations that can present the biggest challenge to conventional acidizing treatments. The fluid combines a retardation effect and advanced chelation technology to give a deep stimulation of the reservoir with a minimal precipitation potential. It reduces the risk of diminished production as well as secondary and tertiary mineral precipitation that can block pores, and it also diminishes corrosion. The OCA solution also combats sludging problems that plague conventional acid systems and promotes long-term production by stabilizing formation fines while maintaining the integrity of the sandstone structures.

Chemical OCA stimulations were conducted in GPK3 (on 15 February, 2007) and GPK4 (on 21 February, 2007). In GPK3, 1250 m^3 of fresh water were injected at 35–55 L s^{-1} ahead of the injection of 200 m^3 of OCA at 55 L s^{-1}. The amount of fresh water was reduced to 685 m^3 in GPK4, whereas the amount of injected OCA was identical (200 m^3 at 50 L s^{-1}; density of 1.04 g.cm^{-3}). After the OCA injection, about 1400 and 750 m^3 of fresh water were injected into GPK3 and GPK4, respectively, at 30–45 L s^{-1}.

Wells GPK3 and GPK4 present different storage configurations and capacities around their wellbores. GPK3 is intersected by a large fracture zone (i.e. a sizable near wellbore volume of more than 1000 m^3) that must be filled with the injected fluids before reaching the narrowest flowpaths. On the other hand, GPK4 shows some narrow blocked zones close to the well (i.e. a smaller volume of fluids is needed to saturate its near-well storage capacity).

A nearly similar wellhead pressure trend for the same flow rate was observed in GPK3 before and after the OCA injection (Fig. 5). The impact of the OCA stimulation on this well was evaluated by a step-rate injection test on March 2007. It consisted of a short step of 10 L s^{-1} to slowly cool the well, followed by injection at 24 L s^{-1} for more than 3 days. No significant pressure reduction, compared to previous tests, was observed in GPK3 after the OCA stimulation, indicating that its injectivity had not significantly improved (Fig. 6). The injectivity index after 3 days was about 0.40 L s^{-1} bar^{-1}, very close to that measured before this chemical treatment (i.e. 0.35 L s^{-1} bar^{-1}).

There was a fast increase in GPK4 wellhead pressure during the preflush phase (Fig. 7). The pressure reached about 120 bars just

Please cite this article in press as: Portier, S., et al., Chemical stimulation techniques for geothermal wells: experiments on the three-well EGS system at Soultz-sous-Forêts, France. Geothermics (2009), doi:10.1016/j.geothermics.2009.07.001

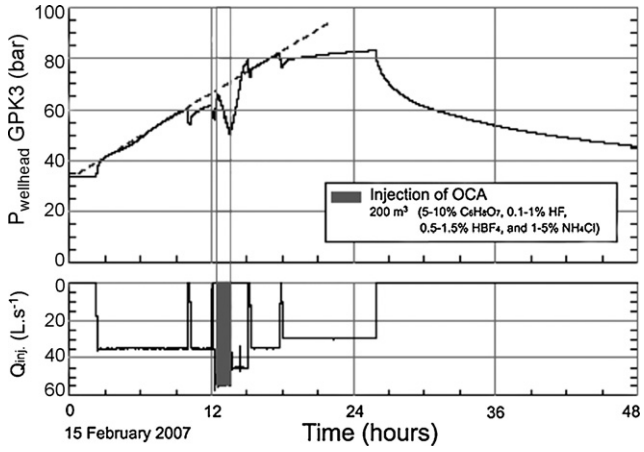

Fig. 5. Impact of the organic clay acid HT (OCA HT) acidification done on GPK3 in February 2007 (after Nami et al., 2007). A nearly similar pressure trend for the same flow rate (dashed line) is observed before and after the injection of 200 m^3 of OCA at 55 $L\,s^{-1}$, and indicates that there was no gain in well productivity.

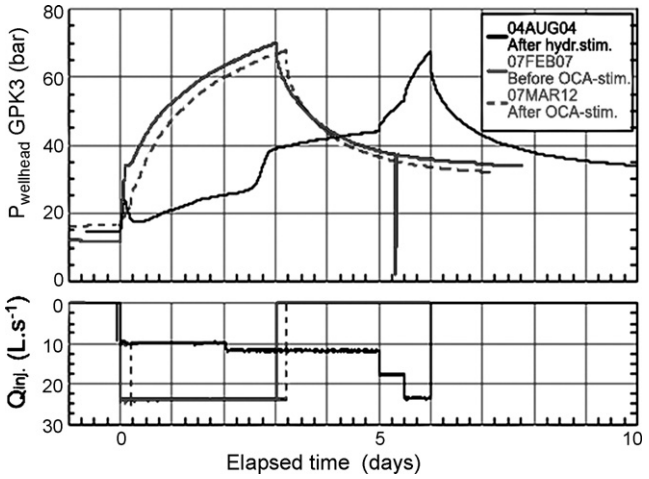

Fig. 6. Injection tests performed in GPK3 (after Nami et al., 2007). The maximum wellhead pressure measured during the injection test done after the OCA stimulation is almost the same as during the injection test performed after the 2004 hydraulic stimulation.

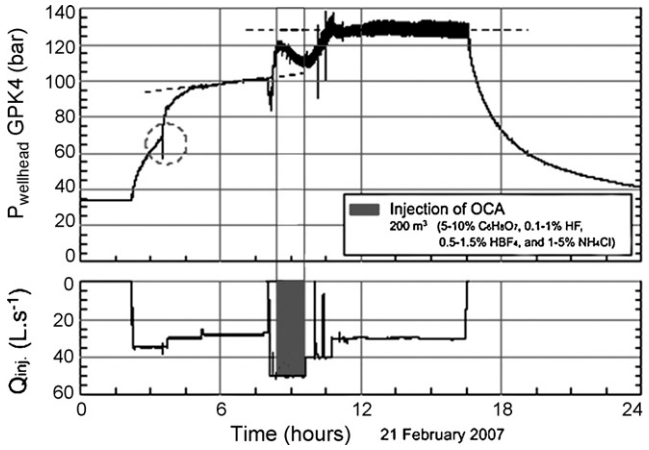

Fig. 7. Impact of the organic clay acid HT (OCA HT) acidification test performed on GPK4 in February 2007 (after Nami et al., 2007). After the injection of 200 m^3 of OCA at 50 $L\,s^{-1}$, a constant pressure (dashed line) is observed during the postflush injection of fresh-water at 35 $L\,s^{-1}$.

before the injection of OCA, and rose to a maximum of 130 bars during the postflush phase until shut-in. The abrupt pressure increase suggests some plugging of the well.

After the displacement of the OCA fluid into the formation, and only 7 h after GPK4 shut-in, the wellhead pressure drastically decreased from 126 to 40 bars (Fig. 7). Part of the increase in injectivity could perhaps be attributed to shear failure, and part to chemical effects. If some feed zones in the well were plugged during injection, as indicated by the pressure versus time curve, the fracturing pressure might have been exceeded, even at the low flow rate of 30 $L\,s^{-1}$ (Nami et al., 2008).

No injection test was performed after the OCA stimulation. However, an assessment of GPK4 was possible, by analyzing the production tests carried out before and after this stimulation. The productivity index increased from 0.4 $L\,s^{-1}\,bar^{-1}$ before the OCA treatment to 0.5 $L\,s^{-1}\,bar^{-1}$ after it. Maybe the most important point is the fact that this index looks stable at 0.5 $L\,s^{-1}\,bar^{-1}$ indicating a good connection to a large reservoir (GEIE, 2007).

4.5. Discussion

The combination of the RMA, NTA and OCA treatments could possibly explain the significant increase in GPK4 productivity. The integration of seismic monitoring, temperature and flow logging results helps in detecting the productive zones in the wells and their changes in response to chemical stimulations (Nami et al., 2008). Minor micro-seismic activity (hundreds of events with magnitudes up to 1.5) was observed around 4100 m true vertical depth (TVD) during the OCA test in GPK4 well (Nami et al., 2008). Flow logs were run and revealed two leak zones in the well casing at 4110 (15–25%) and 4440 m TVD (50 m above the casing shoe 9–15%), respectively. These leaks do not correspond to the joints of the casing, and their origin is not clearly explained, but fracture shearing may be involved. Except for these two fluid loss zones in GPK4, the flow remains constant until a last fluid loss at 4800 m TVD that corresponds to a fracture zone with abundant hydrothermal minerals.

In contrast to the previous production tests, the temperature curve for the production test performed after the OCA stimulation showed a decreasing trend despite the highest fluid production rate (Nami et al., 2008). Apparently, this gain of productivity does not originate only from the open-hole section of the well. The chemical stimulations with RMA, NTA dissolved in caustic soda solution and OCA improved the productivity of the GPK4 well by 30 and 25%, respectively, but part of this gain could be attributed to the hydraulic stimulation of two loss zones in the cemented part of the casing, assuming that they were not generated during or after the initial hydraulic stimulation had ended.

Starting with the step-rate test performed in GPK4, the pressure in GPK3 and GPK2 was monitored throughout the stimulation operations to study the connection between the wells. A clear pressure response was observed in these two wells after the stimulation with RMA. The pressure change in GPK3 is higher than in GPK2 because of its proximity to GPK4. For the same reason, the response time is shorter in GPK3. The propagation of pressures to GPK2 might be explained by the improved hydraulic interconnection between GPK3 and GPK4 and between GPK2 and GPK3. The large fracture zone connecting GPK2 and GPK3 (see Section 4) could form a short circuit and reduce fluid residence times in the reservoir, thereby affecting fluid production temperatures.

Geochemical monitoring of the fluids discharged by GPK3 and GPK4 also indicates that the percent of traced fresh water (injected in large amounts into GPK2, GPK3 and GPK4 in 2000, 2003 and 2005) is always low (<10%) in the produced geothermal brine (Sanjuan et al., 2007). The existence of at least three fluid flow pathways between the wells GPK2 and GPK3 with different effective

Please cite this article in press as: Portier, S., et al., Chemical stimulation techniques for geothermal wells: experiments on the three-well EGS system at Soultz-sous-Forêts, France. Geothermics (2009), doi:10.1016/j.geothermics.2009.07.001

fluid velocities, which contrasts with a poor hydraulic connection between GPK3 and GPK4, was detected during the July–December 2005 fluid circulation loop and the associated fluorescein tracer test (Sanjuan et al., 2006).

4.6. Summary

The chemical stimulation program performed at Soultz improved well injectivities/productivities by factors ranging between 1.12 and 2.5 (Nami et al., 2008). Well GPK2 was the easiest to stimulate, but the largest gain in injectivity was obtained in GPK4 (GEIE, 2007).

Although the chemical well stimulations were not executed with the same comparable protocol, variable but encouraging results were obtained in the Soultz EGS wells. While GPK3 showed small variations in injectivity whatever technique was used (hydraulic or chemical), GPK4 presented a real increase of injectivity and productivity after the treatments, while GPK2 showed significant improvements despite the fact that the acid treatments were limited in terms of time, volume and concentration.

Table 2 summarizes the chemical stimulation methods used in the three deep boreholes of the Soultz EGS Project, as well as the results obtained so far. These results show that the acids have actively reacted with the minerals present in the fractures and pores of the Soultz granite. The injection of NTA into GPK4 dissolved in a caustic soda solution (pH 12) cleaned the borehole and part of the fractures in the granite by eliminating and extracting significant amounts of drilling wastes (grease, cuttings), rock fragments and hydrothermal deposits. In addition, dissolved and solid Ca–Fe–NTA compounds were also formed.

The maximum volumes of calcite dissolved by the RMA and NTA treatments were estimated at about 19.2 and 5.5 m^3, respectively (Sanjuan et al., 2007). The use of a caustic soda solution to clean GPK4 before injecting NTA would have probably allowed NTA to reach deeper into the fractures and, consequently, to be more efficient. The OCA treatment improved GPK4's productivity index from 0.4 to 0.5 $L\,s^{-1}\,bar^{-1}$, but seems not to have made much difference to the injectivity of GPK3.

No major improvement in GPK3 injectivity was observed after successive stimulation operations with HCl and OCA. Even though the distribution and sizes of the fractured areas around GPK3 and GPK4 are probably different, the failure to use a caustic soda solution to clean GPK3 and the neighbouring fractured areas (where the accumulated debris likely blocked the hydraulic connection between the wellbore and the main fracture zones) could partially explain the limited results obtained in this well. It seems that a single chemical stimulation method may not be appropriate for the Soultz wells, but that a combination of treatments might have to be considered.

5. Conclusions

Acid treatments were originally developed by the oil industry to improve the productivity of oil and gas wells. This technology was partially adapted to geothermal wells, most often to remove mineral scales deposited in the wells after several years of exploitation. Nevertheless, these acid treatments also allow the enhancement of fracture networks in the near-wellbore region. They have been successfully performed in granitic geothermal reservoirs like Fjällbacka (Sweden) and Beowawe (USA). In recent years, the reliability of acidizing sandstone intervals has been significantly improved. In the USA, about 90% of treated geothermal wells have responded with a 2- to 4-fold increase in fluid production.

More recently, this technology has been applied to the Soultz-sous-Forêts (France) EGS reservoir after massive hydraulic stimulation operations, which, however, induced several microseismic events of concern to the public. The three 5-km deep Soultz wells (GPK2, GPK3 and GPK4) were treated with different amounts of chemicals in order to dissolve the maximum amount of hydrothermal minerals precipitated in fractures and pores of the granitic reservoir, and to reach as deep as possible into the formation.

The injectivity and productivity of each well was affected differently. While encouraging results were obtained in GPK2 and GPK4, the injectivity improvement in GPK3 was minimal whatever stimulation technique (hydraulic or chemical) was used. At present, GPK2 has a productivity index of about 0.50 $L\,s^{-1}\,bar^{-1}$ in single-well tests.

The injectivity index of GPK3 is about 0.40 $L\,s^{-1}\,bar^{-1}$, which remained almost unchanged after successive stimulation operations with hydrochloric acid (HCl) and OCA. A highly conductive fracture with a large area crosses the open-hole section of the well and prevents further improvements by chemical stimulation. The productivity index of GPK4 reached 0.20 $L\,s^{-1}\,bar^{-1}$ after hydraulic stimulation and has increased to about 0.50 $L\,s^{-1}\,bar^{-1}$ after chemical stimulation. The chemical stimulation with RMA and chelating agents (NTA) further improved the hydraulic communication between GPK3 and GPK4.

Despite the small number of chemical stimulation operations completed at Soultz-sous-Forêts and their limitation in terms of time, volume and concentration, the results suggest that this type of stimulation must be developed further. Combined with moderate hydraulic stimulation, it might reduce the need of carrying out high fluid pressure stimulation operations that may induce micro-seismic events that could raise public concern and negatively impact future geothermal activities.

Acknowledgements

The authors would like to thank the Swiss Federal Office of Education and Science (Project No. 03.0460) and the Swiss Federal Office of Energy (Project No. 150'649) for funding this project. The authors are also grateful to the scientific team of the EEIG "Heat Mining" at Soultz-sous-Forêts and the ENGINE Coordination Action (ENhanced Geothermal Innovative Network for Europe) supported by the 6th Framework Programme of Research and Development of the European Union. We thank the associate editor John Garnish for the numerous suggestions to improve the manuscript.

References

Allen, T.O., Roberts, A.P., 1989. Production Operations, vols. 1 and 2. Well Compilations, Workover and Stimulation. OGCI Inc., Technical Publications, Tulsa, OK, USA, 720 pp.

Amistoso, A.E., Aqui, A.R., Yglopaz, D.M., Malate, R.C.M., 2005. Sustaining steam supply in Palinpinon 1 production field, Southern Negros Geothermal Project, Philippines. In: Proceedings of the 2005 World Geothermal Congress, Antalya, Turkey, pp. 2411–2415.

André, L., Rabemanana, V., Vuataz, F.-D., 2006. Influence of water–rock interactions on fracture permeability of the deep reservoir at Soultz-sous-Forêts, France. Geothermics 35, 507–531.

Axelsson, G., Thórhallsson, S., Björnsson, G., 2006. Stimulation of geothermal wells in basaltic rock in Iceland. In: Proceedings of ENGINE Workshop 3: Stimulation of Reservoir and Microseismicity, Kartausen Ittingen, Zürich, Switzerland, June, 8 pp.

Barelli, A., Cappetti, G., Manetti, G., Peano, A., 1985. Well stimulation in Latera Field. Geothermal Resources Council Transactions 9, 213–219.

Baria, R., Jung, R., Tischner, T., Nicholls, J., Michelet, S., Sanjuan, B., Soma, N., Asanuma, H., Dyer, B., Garnish, J., 2006. Creation of an HDR reservoir at 5000 m depth at the European HDR project. In: Proceedings of the 31st Workshop on Geothermal Reservoir Engineering, Stanford University, Stanford, CA, USA, 8 pp.

Barrios, L.A., Quijano, J.E., Romero, R.E., Mayorga, H., Castro, M., Caldera, J., 2002. Enhanced permeability by chemical stimulation at the Berlin Geothermal Field, El Salvador. Geothermal Resources Council Transactions 26, 73–78.

Baumgärtner, J., Gérard, A., Baria, R., Jung, R., Tran-Viet, T., Gandy, T., Aquilina, L., Garnish, J., 1998. Circulating the HDR reservoir at Soultz; maintaining production and injection flow in complete balance. In: Proceedings of the 23rd Workshop

Please cite this article in press as: Portier, S., et al., Chemical stimulation techniques for geothermal wells: experiments on the three-well EGS system at Soultz-sous-Forêts, France. Geothermics (2009), doi:10.1016/j.geothermics.2009.07.001

on Geothermal Reservoir Engineering, Stanford University, Stanford, CA, USA, 10 pp.
Buijse, M., Maier, R., Casero, A., 2000. Successful high pressure, high temperature acidising with in situ crosslinked acid diversion. In: Proceedings of the SPE International Symposium on Formation Damage Control, Lafayette, LA, USA, February 23–24, 8 pp.
Buning, B.C., Malate, R.C.M., Lacanilao, A.M., Sta Ana, F.X.M., Sarmiento, Z.F., 1995. Recent experiments in acid stimulation technology by PNOC-Energy Development Corporation, Philippines. In: Proceedings of the 1995 World Geothermal Congress, Florence, Italy, pp. 1807–1812.
Buning, B.C., Malate, R.C.M., Austria, J.J.C., Noriega, M.T., Sarmiento, Z.F., 1997. Casing perforation and acid treatment of well SK-2D Mindanao 1 Geothermal project, Philippines. In: Proceedings of the 22nd Workshop on Geothermal Reservoir Engineering, Stanford University, Stanford, CA, USA, pp. 273–277.
Burgos, B., Buijse, M., Fonseca, E., Milne, A., Brady, M., Olvera, R., 2005. Acid fracturing in lake Maracaibo: how continuous improvements kept on raising the expectation bar. In: Schlumberger, Shell Venezuela, S.A. (Eds.), Proceedings of the SPE Annual Technical Conference and Exhibition. Dallas, TX, USA, paper SPE 96531, October 9–12, 9 pp.
Cappetti, G., 2006. How EGS is investigated in the case of the Larderello geothermal field. In: Paper presented at the Engine Launching Conference, February 12–15, 2006, Orléans, France, 32 pp.
Combs, J., Garg, S.K., Pritchett, J.W., 2004. Geothermal well stimulation. Will it work? Geothermal Resources Council Bulletin 33, 245–250.
Correia, H., Sigurdsson, O., Sanjuan, B., Tulinius, H., Lasne, E., 2000. Stimulation of a high-enthalpy geothermal well by cold water injection. Geothermal Resources Council Transactions 24, 129–136.
Crowe, C., 1986. Precipitation of hydrated silica from spent hydrofluoric acid: how much of a problem is it? Journal of Petroleum Technology 38, 1234–1240.
Crowe, C., Masmonteil, J., Thomas, R., 1992. Trends in matrix acidizing. Oilfield Review 4, 24–40.
Davies, D.R., Faber, R., Nitters, G., Ruessink, B.H., 1994. A novel procedure to increase well response to matrix acidizing treatments. SPE Advanced Technology Series 2 (1), 5–14.
Dezayes, C., Villemin, T., Genter, A., Traineau, H., Angelier, J., 1995. Analysis of fractures in boreholes of hot dry rock project at Soultz-sous-Forêts (Rhine Graben, France). Journal of Scientific Drilling 5, 31–41.
Dezayes, C., Genter, A., Hooijkaas, G.R., 2005. Deep-seated geology and fracture system of the HFR Soultz reservoir (France) based on recent 5 km depth boreholes. In: Proceedings of the 2005 World Geothermal Congress, Antalya, Turkey, pp. 1612–1617.
Economides, M.J., Frick, T.P., 1994. Optimization of horizontal well matrix stimulation treatments. SPE Production & Facilities 9 (2), 93–99.
Economides, M.J., Nolte, K.G., 1989. Reservoir Stimulation, 2nd ed. Prentice Hall, Upper Saddle River, NY, USA, 440 pp.
Entingh, D.J., 1999. A review of geothermal well stimulation experiments in the United States. Geothermal Resources Council Transactions 23, 175–180.
Epperson, I.J., 1983. Beowawe acid stimulation. Geothermal Resources Council Transactions 7, 409–411.
Erga, 2006. Esperimenti di acidificazione in flusso continuo di soluzione acida. Erga (Gruppo Enel) Internal Report, Pisa, Italy, 20 pp.
Evanoff, J., Yeager, V., Spielman, P., 1995. Stimulation and damage removal of calcium carbonate scaling in geothermal wells: a case study. In: Proceedings of the 1995 World Geothermal Congress, Florence, Italy, pp. 2481–2485.
Flores, M., Davies, D., Couples, G., Palsson, B., 2005. Stimulation of geothermal wells, can we afford it? In: Proceedings of the 2005 World Geothermal Congress, Antalya, Turkey, pp. 1028–1035.
Flores, M., Barajas, E.N., Rodriguez, M.A., 2006. Productivity analysis and acid treatment of well AZ-9AD at the Los Azufres geothermal field, Mexico. Geothermal Resources Council Transactions 30, 791–796.
Fredd, C.N., Fogler, H.S., 1998. The influence of chelating agents on the kinetics of calcite dissolution. Journal of Colloid and Interface Science 204, 187–197.
Frenier, W.W., Fredd, C.N., Chang, F., 2001. Hydroxyaminocarboxylic acids produce superior formulations for matrix stimulation of carbonates at high temperatures. In: Proceedings of the SPE Annual Technical Conference and Exhibition, New Orleans, LA, 30 September–3 October, 16 pp.
Gdanski, R.D., 1997. Kinetics of the secondary reaction of HF on alumino-silicates. In: Proceedings of the SPE International Symposium on Oilfield Chemistry, Houston, TX, USA, paper SPE 37214, 6 pp.
GEIE, 2006. Results of GPK4 RMA stimulation of May 2006. Groupement Européen d'Intérêt Economique "Exploitation Minière de la Chaleur"(GEIE "EMC"), Internal Report, Soultz-sous-Forêts, France, 5 pp.
GEIE, 2007. Soultz Enhanced Geothermal System pilot plant. Third periodic activity report, project no. SES6-CT-2003-502 706. Groupement Européen d'Intérêt Economique "Exploitation Minière de la Chaleur"(GEIE "EMC"), Internal Report, Soultz-sous-Forêts, France, 53 pp.
Genter, A., 1990. Géothermie roche chaudes sèches. Le granite de Soultz-sous-Forêts (Bas-Rhin, France). Fracturation naturelle, altérations hydrothermales et interaction eau-roche. Bureau de Recherches Géologiques et Minières, Document No. 185, Ed. BRGM, Orléans, France, 201 pp.
Genter, A., Traineau, H., Dezayes, C., Elsass, P., Ledésert, B., Meunier, A., Villemin, T., 1995. Fracture analysis and reservoir characterization of the granitic basement in the HDR Soultz project (France). Geothermal Science and Technology 4, 189–214.
Genter, A., Fritsch, D., Cuenot, N., Baumgärtner, J., Graff, J.-J., 2009. Overview of the current activities of the European EGS Soultz project: from exploration to electricity production. In: Proceedings of the 34th Workshop on Geothermal Reservoir Engineering, Stanford University, Stanford, CA, USA, 7 pp.
Gérard, A., Fritz, B., Vuataz, F.-D., 2005. Results of soft acid injection tests performed at Soultz in wells GPK2, GPK3 and GPK4—extended summary: revised status on 14 March 2005. In: Proceedings of the 2005 EHDRA Scientific Conference, Soultz-sous-Forêts, France, March 17–18, 4 pp.
Gérard, A., Genter, A., Kohl, T., Lutz, P., Rose, P., Rummel, F., 2006. The deep EGS (Enhanced Geothermal System) project at Soultz-sous-Forêts (Alsace, France). Geothermics 35, 473–484.
Hettkamp, T., Baumgärtner, J., Baria, R., Gérard, A., Gandy, T., Michelet, S., Teza, D., 2004. Electricity production from hot rocks. In: Proceedings of the 29th Workshop on Geothermal Reservoir Engineering, Stanford University, Stanford, CA, USA, 10 pp.
Jaimes-Maldonado, J.G., Sànchez-Velasco, R., 2003. Acid stimulation of production wells in Las Tres Vírgenes geothermal field, BCS, México. Geothermal Resources Council Transactions 27, 699–705.
Kalfayan, L., 2001. Production Enhancement with Acid Stimulation. Pennwell Books, Tulsa, OK, USA, 350 pp.
LANL, 1977. Chemical leaching with Na_2CO_3. Hot Dry Rock Geothermal Energy Development Project, Annual report, Fiscal Year 1977, Los Alamos National Laboratory report LA-7109-PR, Los Alamos, NM, USA, pp. 184–192.
Malate, R.C.M., Yglopaz, D.M., Austria, J.J.C., Lacanilao, A.M., Sarmiento, Z.F., 1997. Acid stimulation of injection wells in the Leyte Geothermal power project, Philippines. In: Proceedings of the 22nd Workshop on Geothermal Reservoir Engineering, Stanford University, Stanford, CA, USA, pp. 267–272.
Malate, R.C.M., Austria, J.J.C., Sarmiento, Z.F., DiLullo, G., Sookprasong, A., Francia, E.S., 1998. Matrix stimulation treatment of geothermal wells using sandstone acid. In: Proceedings of the 23rd Workshop on Geothermal Reservoir Engineering, Stanford University, Stanford, CA, USA, pp. 375–378.
Malate, R.C.M., Sookprasong, P.A., Austria, J.J.C., Sarmiento, Z.F., Francia, E.S., 1999. Wellbore soaking: a novel acid treatment of geothermal injection wells. In: Proceedings of the 24th Workshop on Geothermal Reservoir Engineering, Stanford University, Stanford, CA, USA, pp. 336–339.
McLeod, H.O., 1984. Matrix acidizing. Journal of Petroleum Technology 36, 2055–2069.
Mella, M., Rose, P., Kovac, K., Xu, T., Pruess, K., 2006. Calcite dissolution in geothermal reservoirs using chelants. Geothermal Resources Council Transactions 30, 347–352.
Molina, P.O., Malate, R.C.M., Buning, B.C., Yglopaz, D.M., Austria, J.J.C., Lacanilao, A.M., 1998. Productivity analysis and optimization of well SK-2D, Mindanao I geothermal project Philippines. In: Proceedings of the 23rd Workshop on Geothermal Reservoir Engineering, Stanford University, Stanford, CA, USA, pp. 368–374.
Morris, C.W., Verity, R.V., Dasie, W., 1984. Chemical stimulation treatment of a well in the Beowawe geothermal field. Geothermal Resources Council Transactions 8, 269–274.
Nami, P., Schindler, M., Tischner, R., Jung, T., Teza, D., 2007. Evaluation of stimulation operations and current status of the deep Soultz wells prior to power production. In: Proceedings of the EHDRA Scientific Conference, Soultz-sous-Forêts, France, 11 pp.
Nami, P., Schellschmidt, R., Schindler, M., Tischner, R., 2008. Chemical Stimulation operations for reservoir development of the deep crystalline HDR/EGS system at Soultz-sous-Forêts (France). In: Proceedings of the 32nd Workshop on Geothermal Reservoir Engineering, Stanford University, Stanford, CA, USA, 5 pp.
Paccaloni, G., Tambini, M., 1993. Advances in matrix stimulation technology. Journal of Petroleum Technology 45 (3), 256–263.
Pasikki, R.G., Gilmore, T.G., 2006. Coiled tubing acid stimulation: the case of AWI 8-7 production well in Salak Geothermal Field, Indonesia. In: Proceedings of the 31st Workshop on Geothermal Reservoir Engineering, Stanford University, Stanford, CA, USA, 7 pp.
Perthuis, H., Touboul, E., Piot, B., 1989. Acid reactions and damage removal in sandstones. A model for selecting the acid formulation. In: Proceedings of the SPE International Symposium on Oilfield Chemistry, Houston, TX, February 8–10, 11 pp.
Pournik, M., 2004. Evaluation of sandstone acidizing with high strength HF solutions. Master of Science in Engineering Thesis, University of Texas, Austin, TX, USA, 111 pp.
Rose, P., Xu, T., Kovac, K., Mella, M., Pruess, K., 2007. Chemical stimulation in near-wellbore geothermal formations: silica dissolution in the presence of calcite at high temperature and high pH. In: Proceedings of the 32nd Workshop on Geothermal Reservoir Engineering, Stanford University, Stanford, CA, USA, 5 pp.
Sanjuan, B., Pinault, J.-L., Rose, P., Gérard, A., Brach, M., Braibant, G., Crouzet, C., Foucher, J.-C, Gautier, A., Touzelet, S., 2006. Tracer testing of the geothermal heat exchanger at Soultz-sous-Forêts (France) between 2000 and 2005. Geothermics 35, 622–653.
Sanjuan, B., Pinault, J.-L., Rose, P., Gérard, A., Crouzet, C., Touzelet, S., Gautier, A., Charlot, A., 2007. Geochemical monitoring at Soultz-sous-Forêts (France) between October 2006 and March 2007, after the chemical stimulations (RMA, NTA and OCA) carried out in the wells GPK-4 and GPK-3. In: Proceedings of the EHDRA Scientific Conference, Soultz-sous-Forêts, France, June 28–29, 16 pp.
Sarda, J.P., 1977. Chemical leaching. In: Proceedings of the 2nd NATO-CCMS Information Meeting on Hot Dry Rock Geothermal Energy, Los Alamos, NM, USA, June 28–30, 6 pp.
Sausse, J., Fourar, M., Genter, A., 2006. Permeability and alteration within the Soultz granite deduced from geophysical and flow log analysis. Geothermics 35, 544–560.

Please cite this article in press as: Portier, S., et al., Chemical stimulation techniques for geothermal wells: experiments on the three-well EGS system at Soultz-sous-Forêts, France. Geothermics (2009), doi:10.1016/j.geothermics.2009.07.001

Schechter, R.S., 1992. Oil Well Stimulation. Prentice Hall, Englewood Cliffs, NJ, USA, 640 pp.
Serpen, U., Türeyen, O.I., 2000. Acidizing geothermal wells. Geothermal Resources Council Transactions 24, 683–688.
Smith, C.F., Hendrickson, A.R., 1965. Hydrofluoric acid stimulation of sandstone reservoirs. Journal of Petroleum Technology 17, 215–222.
Strawn, J.A., 1980. Results of acid treatment in hydrothermal direct heat experiment wells. Geothermal Resources Council Transactions 4, 427–430.
Sundquist, U., Wallroth, T., Eliasson, T., 1988. The Fjällbacka HDR geothermal energy project: reservoir characterisation and injection well stimulation. Chalmers University of Technology, Report Number Fj-9, Gothenburg, Sweden, 92 pp.
Templeton, C.C., Richardson, E.A., Karnes, G.T., Lybarger, J.H., 1975. Self-generating mud acid. Journal of Petroleum Technology 27, 1199–1203.
Thomas, R.L., Crowe, C.W., 1981. Matrix treatment employs new acid system for stimulation and control of fines migration in sandstone formations. Journal of Petroleum Technology 33 (8), 1491–1500.
Traineau, H., Genter, A., Cautru, J.P., Fabriol, H., Chevremont, P., 1991. Petrography of the granite massif from drill cutting analysis and well log interpretation in the geothermal HDR borehole GPK1 (Soultz, Alsace, France). Geothermal Science and Technology 3, 1–29.
Wallroth, T., Eliasson, T., Sundquist, U., 1999. Hot dry rock research experiments at Fjällbacka, Sweden. Geothermics 28, 617–625.
Walsh, M.P., Lake, L.W., Schechter, R.S., 1982. A description of chemical precipitation mechanisms and their role in formation damage during stimulation by hydrofluoric acid. Journal of Petroleum Technology 34, 2097–2112.
Williams, B.B., 1979. Acidizing fundamentals. New York and Dallas Society of Petroleum Engineers, European Formation Damage Control Conference, May 15–16, The Hague, The Netherlands. SPE Monograph No. 6, 124 pp.
Xie, T., 2004. A parametric study of sandstone acidizing using a fine-scale simulator. Thesis for Master of Science in Engineering, University of Texas, Austin, TX, USA, 85 pp.
Xu, T., Ontoy, Y., Molling, P., Spycher, N., Parini, M., Pruess, K., 2004. Reactive transport modelling of injection well scaling and acidizing at Tiwi field, Philippines. Geothermics 33, 477–491.
Yglopaz, D.M., Buning, B.C., Malate, R.C.M., Sta Ana, F.X.M., Austria, J.J.C., Salera, J.R.M., Lacanilao, A.M., Sarmiento, Z.F., 1998. Proving the Mahanagdong B resource: a case of a large-scale well stimulation strategy, Leyte Geothermal Power Project, Philippines. In: Proceedings of the 23rd Workshop on Geothermal Reservoir Engineering, Stanford University, Stanford, CA, USA, pp. 51–56.

Please cite this article in press as: Portier, S., et al., Chemical stimulation techniques for geothermal wells: experiments on the three-well EGS system at Soultz-sous-Forêts, France. Geothermics (2009), doi:10.1016/j.geothermics.2009.07.001

EC Contract SES6-CT-2003-502706

PARTICIPANT ORGANIZATION NAME: Centre of Geothermal Research – c/o CHYN, University of Neuchâtel, Switzerland

Related with Work Package 1b and 2b

Related with Working Group 6

REACTIVE TRANSPORT MODELLING OF FORCED FLUID CIRCULATION AND SCALING TENDENCIES IN FRACTURED GRANITE AT SOULTZ-SOUS-FORÊTS EGS GEOTHERMAL SITE

Portier Sandrine and Vuataz François-D.

**CREGE c/o CHYN, E. Argand, 11, BP, CH-2009 Neuchâtel*

e-mail: sandrine.portier@unine.ch

ABSTRACT

The coupled hydro-thermo-chemical response of a fractured media to forced fluid flow in a simple EGS system is investigated. The geometry, a single fractured zone in 2D matrix, was chosen in order to better understand the impact of water-rock interaction on permeability evolution of the EGS reservoir. The major issue deals with forced fluid circulation effects on mineral scaling in hot fractured granite at Soultz EGS geothermal site.

INTRODUCTION

Over time, geochemical fluid-rock interactions may impact the performance of an enhanced geothermal system. In order to properly simulate such systems and predict their performance accurately, models will need to include these interactions. Geochemical evolution in geothermal fields occurs through a complex interplay of multiphase fluid and heat flow and chemical transport processes. These complexities include the kinetics of fluid-rock chemical interaction, and heat effects on thermophysical and chemical properties and processes. Reactive fluid flow and geochemical transport modeling is a powerful tool to get insight into these processes, to test conceptual model, and to study the geochemical behavior, mineral alteration, changes in porosity and permeability.

During the stimulation phase, the injected water is composed of formation and surface fluids and will react with the rocks minerals. The composition of the resulting fluids will be controlled by temperature, time, and by the minerals composition and added natural fluids.

Later, during reservoir exploitation, the formation fluid will be most probably dominant in the water-rock reactions, but a heating-cooling cycle will trigger continuous reactions. Dissolution and precipitation will take place along the pathways of these resulting fluids, and open fissures can potentially close by mineral precipitation, restricting fluid flow. Also, mineral precipitation can potentially create clogging problems along the geothermal loop, from the production casing to the surface tubing, the heat exchanger and the reinjection casing, when the hot fluids are cooled down by approximately 100°C at the heat exchanger.

Geochemical models will facilitate the evaluation of the risks of scaling and corrosion in the wells, gathering system and power plant as well as the impact on reservoir performance of increases or decreases in permeability caused by mineral deposition or dissolution in the reservoir (Durst and Vuataz, 2000). The most conductive fractures often show evidence of fluid flow in earlier geologic time such as hydrothermal alteration and secondary mineral deposition (Genter et al., 1995; Hooijkaas et al, 2006; Sausse et al., 2006). This suggests that the most connected pathways will already have experienced some reaction between water and the rock fracture surface. Fresh rock surfaces will not have the protection of a layer of deposited minerals or alteration products. Specific research and field testing goals connected to EGS technology improvement are the prediction of scaling or deposition through better understanding of the fluid-rock geochemistry.

WATER-ROCK INTERACTION AND SCALING POTENTIAL

Water-rock interactions in reservoirs are driven by the state of disequilibrium that persists among solids and solutes due to changing temperature and stress conditions, and advective and diffusive influx of solutes. Water-rock interactions bring about changes to formation composition and texture through a complex chemical reaction network. These reactions can be divided into two types: solid-solute and solute-solute. Reactions of solids and solute are kinetic, i.e., they depend on compositions of solids and water, temperature, pore water pressure, and stress. Speciation among solutes is described by thermodynamic relations that depend on water composition and temperature. Both reaction mechanisms, mediated by formation water, are strongly interdependent. The mass transfer processes are governed by reactive phase compositions, surface areas, water-rock ratios, reaction rates, and fluid residence times. It is the ultimate goal of water-rock modelling to be able to describe quantitatively the evolution of both fluid composition and rock mineralogy in time and space.

The great complexity of the scale formation process results from the large number of species found in a geothermal fluid and from the multiple possible physical mechanisms involved. Furthermore, the diversity of fluid composition from site to site and the variation of processes along the flow path, make the generalization of both the mechanisms responsible for the scale formation and preventive measures difficult. The composition of scales in geothermal plants is commonly very complex and depends on many parameters, such as the temperature and pressure of the fluid, the history of water-rock interactions and the operating conditions (Andritsos and Karabelas, 1991).

Scaling occurs due to interaction of geothermal water with rocks deep in the reservoir, resulting in supersaturated water due to the dissolution of minerals. Dissolution may be accelerated by temperature and, sometimes, it may be retrogressive depending on the solute (Arnorsson, 2000). Calcite, silica and metal pyrite deposition are the most common scales. Calcite scaling occurs when geothermal water becomes supersaturated with calcite due to a decrease in partial pressure of carbon dioxide leading to its precipitation. Calcite deposition is highly controlled by water temperature and pH, according to the equation:

$$Ca^{2+} + 2HCO_3^- \leftrightarrow CaCO_3 + CO_2 + H_2O$$

The solubility of silica in geothermal fluids is very dependent on temperature, the initial degree of super-saturation, salinity, pH, and the presence (or absence) of colloidal particles. Thus, separation temperatures of geothermal fluid need to be carefully chosen so that much of the silica will remain in solution or allow it to come out of solution before injection. Silica is mainly deposited as quartz or amorphous silica. Quartz (controls solubility of hot reservoir fluid) is deposited in the temperature range of 100-250℃ and amorphous silica (controls solubility of low temperature fluid) in the range of 7-250℃ (Gunnarsson and Arnorsson, 2005) depending on saturation. The consequent deposition of amorphous silica, which precipitates relatively fast, in surface installation and in reinjection circuits is a major problem in the use and disposal of geothermal liquids for electrical production. For this reason, it is very important to evaluate the temperature at which saturation with respect to amorphous silica is attained. It is also evident that the operating pressures of well-head steam separators must be decided considering the pH of the fluid to avoid silica scaling. If the salinity of the geothermal liquid is higher than that of seawater, its effect on amorphous silica solubility has to be considered too (Fournier, 1985).

Prevention of calcium carbonate scaling can be achieved by alteration of either the partial pressure of carbon dioxide or the pH, and also by adding chemical scale inhibitors (Evanoff et al., 1995). Acidification is also known to lower the rate of deposition and to prevent silica scaling. Mixing of condensate and brine should always be considered as a possible means of preventing scaling in injection wells. Deposition of amorphous silica from supersaturated water could possibly be reduced, even inhibited, by rapid cooling of the water to 50℃ or less (Gunnarsson and Arnorsson, 2005).

Metal sulphides, silicates and oxides also represent common scaling problems in many geothermal installations. They are deposited in surface equipment due to cooling and pH change accompanying flashing processes leading to the concentrations of metal ions. Iron sulphides identified in production and re-injection wells are pyrite, mackinawite and pyrrhotite (Lichti and Braithwaite, 1980).

Furthermore, physico-chemical conditions determine clay particle stability in fractured granite reservoirs. Thus, even if the fluid velocity in the reservoir is relatively low, changing these conditions can cause clay particle detachment and subsequent formation damage. The permeability of the rock is therefore a function of the hydrodynamic parameters as well as the physico-chemical properties of the permeating fluid and the rock material. Only tests with samples of natural rocks reproducing the maximum number of factors affecting permeability can give reasonably reliable information about the formation reaction to fluid injection. Unfortunately, laboratory experiments and existing reservoir models are not really able to reproduce or take into account the whole variety of the physico-chemical micro- and macro-conditions occurring in reality. Better understanding of the fundamental physico-chemical principles of clay particle stability and transport in fractured porous media will help to develop better techniques and apply more effective existing ones for preventing in-situ clay induced formation damage of geothermal reservoirs (Tchistiakov, 2000).

Chemical thermodynamic methodology should be used to quantitatively assess scaling tendencies from geothermal waters (Vetter and Kandarpa, 1987). Such an assessment should be carried out as a part of any geothermal development program to identify optimum conditions for reinjection of cooled geothermal fluids and, at the same time, minimize the need for using inhibitors. The rate of scale formation depends on temperature, the aqueous concentrations of the scale forming components, the degree of supersaturation and kinetics. Thus, reliable prediction of scale production in geothermal production wells and surface facilities requires both thermodynamic models to indicate the tendency for scaling from solution and kinetic models to predict the rate of scaling and thus the time required for plugging fractures or tubings. Nucleation and depositional kinetics are a function of the degree of supersaturation, pressure, temperature and catalytic or inhibitory effects due to minor elements. The application of such models could contribute to field scale management and in the development of more effective treatments of scale during geothermal production.

Coupled thermal-hydraulic-chemical (THC) codes help in studying the potential permeability reduction of fractured media caused by scaling. Mechanisms by which a precipitate reduces permeability include solids deposition on the fracture walls due to attractive forces between the particles and the surfaces of the fractures. The characteristics of the precipitate influence the extent of formation damage. Conditions such as large degree of supersaturation, presence of impurities, change in temperature, and rate of mixing control the quantity and morphology of the precipitating minerals.

REACTIVE TRANSPORT MODELLING TOOL

As previously pointed out, important consequences of storing and transporting heat and fluids in rocks give rise to significant coupling between thermal, hydraulic and chemical (THC) processes. To be able to predict reservoir performance these coupled processes have to be investigated simultaneously.

In early geothermal reservoir simulations the reservoir fluids were idealized as pure water. Subsequent more realistic representations of geothermal fluids included carbon dioxide, which usually is the most prominent non-condensible gas, and dissolved solids, typically represented as NaCl.

Later developments include interactions between several different dissolved and gaseous chemical species in geothermal flows, and porosity and permeability changes from dissolution and precipitation of minerals. More sophisticated multi-species chemical models, that describe reactions between aqueous, gaseous, and solid species, have usually been limited to zero-dimensional systems in which no flow and transport effects are taken into account. A fully-coupled treatment of 3D fluid flow and mass transport with detailed chemical interactions between aqueous fluids, gases, and primary mineral assemblages is very difficult.

Such treatment can potentially provide a more realistic description of geothermal reservoir processes during natural evolution as well as during exploitation, and can provide added constraints that can help reduce the inherent uncertainty of geothermal reservoir models.

Simulations of THC processes include coupling between heat and water flow; aqueous species transport; kinetic and equilibrium mineral-water reactions; and feedback of mineral precipitation/dissolution on porosity and permeability.

Physical model

We consider a thin non-deformable fracture developed within rock matrix with a significantly lower permeability compared to the fracture such that flow within the rock matrix is negligible. The fractures are assumed to have constant apertures and smooth parallel walls initially. In addition we assume in all cases that the width of the fracture is much smaller than its length and that transverse diffusion and dispersion within the fracture cause complete mixing across the fracture width. These two assumptions are used to justify a one-dimensional treatment of mass transport along the fracture. The rock matrix is assumed to have initially homogeneous physical and chemical properties. A chemical source of constant strength is assumed to exist at the inlet of the fracture. The initial composition of the fluid in the fracture and the mineral composition of the rock must be specified at time t = 0. In addition, the composition of the fluid at the inlet of the fracture must be specified.

We present a formulation which allows for feedback between mineral reactions and the transport properties of the fracture. Simulations include the reaction-induced porosity and permeability change.

Governing processes

Temperature and pressure changes lead to chemical disequilibria in the reservoir, which may result in the precipitation or dissolution of several minerals. These chemical reactions alter the permeability of the fractured host rock and cause changes in fluid properties. The alteration of the permeability and the fluid properties have an impact on thermal transport, pressure field and fluid velocity. Herein, every process is coupled to the other processes and their interactions determine the long-term behaviour of the EGS reservoir.

The following conservation equations illustrate the coupling mathematically. The transient heat transport equation (Sauty, 1981) is:

$$\frac{\partial}{\partial t}\left(\left(\overline{\rho c_p}\right)T\right) = -\nabla.\left(\Phi\rho_f c_{pf} v_f T - \overline{\lambda}\nabla T\right) + q_H \quad (1)$$

where T is temperature, Φ the porosity, ρ_f the fluid density, c_{pf} the fluid heat capacity, v_f the fluid velocity and q_H a heat source. The crossed parameters are the arithmetic means and contain values from the fluid and the solid phase. They are calculated depending on the phase fraction. $\overline{\rho.c_p}$ is the arithmetic mean of the medium density and heat capacity (Pribnow, 1994):

$$\overline{\rho c_p} = (1-\Phi)\rho_m c_{pm} + \Phi\rho_f c_{pf} \quad (2)$$

where ρ_m is the density and c_{pm} the heat capacity of the solid phase (matrix). Accordingly, the arithmetic mean of the thermal conductivity $\overline{\lambda}$ is calculated:

$$\overline{\lambda} = (1-\Phi)\lambda_m + \Phi\lambda_f \quad (3)$$

where λ_m and λ_f are the thermal conductivities of the matrix and the fluid, respectively.

Following Clauser (1988), the thermal dispersion terms can be neglected in the above equations for two reasons: 1) it is difficult to obtain reliable diffusivity parameters and 2) in most of the cases diffusivity effects are negligible in comparison to other processes.

The transient hydraulic equation (Bear, 1979) is:

$$\frac{\partial}{\partial t}\left(S_c P\right) = -\nabla.\left(K\left(\nabla P + \rho_0 g\nabla z\left(1-\beta_f\Delta T\right)\right)\right) \quad (4)$$

where S_c is the storativity, P is pressure, K is hydraulic conductivity, ρ_0 is initial fluid density, g is gravity, z is depth and β_f is thermal expansion coefficient. The first expression in the right represents diffusion and the second term buoyancy effects.

The formulation of the transient chemical equation (Steefel and MacQuarrie, 1996) in terms of an equivalent porous media in the case where the fractures form a parallel set is:

$$\frac{\partial}{\partial t}\left(\Phi C_i\right) = -\nabla\left(vC_i - \Phi\tau D_i\nabla C_i\right) - \sum_{s=1}^{N_s}\nu_{is}r_s \text{ , (i=1,..., } N_c) \quad (5)$$

where Ci is the total dissolved concentration of a species i, Φ is fracture porosity, v is fluid velocity, τ is tortuosity of the medium, Di is diffusion coefficient, N_s is the number of reacting minerals in the system, N_c is the number of independent chemical species in the system, ν_{is} is the stoechiometric reaction coefficient and r_s the reaction rate of mineral s. The first term describes advective transport of chemical species and the second diffusive transport of chemical species. It is assumed that mechanical dispersion can be neglected because a simple fracture system is considered.

In this formulation, the total dissolved concentrations, Ci, in the fracture are defined by assuming equilibrium among the individual aqueous species in the system (Reed, 1982):

$$C_i = c_i + \sum_{j=1}^{N\,sec}\nu_{ji}c_j \quad (6)$$

where c_i refers to the concentration of the i^{th} primary or basis species, and c_j refers to the concentration of the j^{th} secondary species, of N_{sec} in number.

The numerical modelling of transient problems requires discretisation not only in space but also in time. Transport and reaction are coupled using a sequential non-iterative approach (SNIA) approach, simpler to implement. In this method, first the reaction equations are solved, then the fluid flow between the elements is calculated and finally the chemical species are transported from element to element. This method can lead to numerical instabilities, since the reaction rates calculated at time t are supposed to stay constant until t+Δt without considering further chemical reactions due to changes in fluid composition and temperature during the interval Δt. To reduce such instabilities, time steps have to be small.

Fracture permeability and flow

The effect of water-rock chemical interaction on permeability can be estimated by the change of flow rate, since mineral dissolution or deposition in the fractured medium results in a widening or narrowing of the fracture aperture and this inevitably causes a change to flow rate.

We assume that fracture permeability is described by the cubic law which states that rate of fluid flow across a section of the fracture is proportional to the applied pressure gradient and the cube of fracture aperture. The permeability for a set of parallel fractures with smooth walls is given by (Snow, 1968):

$$k = \frac{\Phi.b^2}{12} = \frac{nb^3}{12} \quad (7)$$

where n is the number of fractures per unit distance across the rock (L^{-1}), b is the fracture aperture (b = 2δ), and the fracture porosity, Φ, is related to the fracture density and aperture.

A distinction is made between the local porosity of the fracture which is assumed to be unity and the bulk rock (continuum) fracture porosity which in general is not equal to one. The situation is more complicated in a system, as considered here, where local changes in the fracture aperture due to mineral dissolution and precipitation reactions are included. Although clearly an approximation, for practical purposes, the cubic law is assumed to hold locally over the length of a numerical grid cell along the fracture. The Darcian flux in a unit volume of porous medium is given by:

$$u = -\frac{k}{\mu}\left(\nabla P + \rho_f g\nabla z\right) \quad (8)$$

where μ is the fluid viscosity, ρ_f is the fluid density, g is the gravitational constant, and ∇P is the pressure gradient in the fracture plane (de Marsily, 1986). Since the mean flow velocity v is related to the Darcian flux by:

$$v = \frac{u}{\Phi} = \frac{u}{nb} \quad (9)$$

the mean flow velocity can be written as:

$$v = -\frac{b^2}{12\mu}\left(\nabla P + \rho_f g\nabla z\right) \quad (10)$$

Kinetic formulation

We use a kinetic rate law based on the assumption that attachment and detachment of ions from mineral surfaces are ruled by a rate-limiting step (a surface reaction-controlled rate law). The rate laws used for mineral precipitation and dissolution are based on transition state theory (Lasaga et al., 1994; Aagaard and Helgeson, 1982). This formulation gives the dependence of the rate on the saturation state of the solution with respect to a particular mineral as a function of the ion activity product, Qs, defined by:

$$Q_s = \prod_{i=1}^{N_c} a_i^{V_{is}} \quad (11)$$

where the a_j are the activities of the primary species used in writing the dissolution reaction for the mineral. The overall reaction rate law for a particular mineral is:

$$r_s = k_s A_s \left[1 - \left(\frac{Q_s}{K_s} \right)^p \right]^o \quad (12)$$

where k_s is the kinetic constant of the reaction and depends on temperature, K_s the equilibrium constant of the reaction, p and o, determined experimentally, are positive values, not always equal to one and A_s refers to the surface area of individual minerals in the fracture. Positive values of r_s correspond to dissolution rates, whereas negative values refer to precipitation rates. The kinetic constant k_s can be expressed as (Krauskopf, 1995):

$$k_s = k_{s0} f\left(a_i^*\right) \exp\left(\frac{-E_a}{RT} \right) \quad (13)$$

Where E_a is the activation energy needed for the formation of the activated complex, $f(a_i^*)$ a function of the activity of the species involved in the creation and the destruction of the activated complex, k_{s0} is the rate constant independent of the conditions at 25℃, R is the gas constant and T is the absolute temperature in Kelvin.

The highly nonlinear nature of the kinetic equations describing the coupled geochemical and physical processes involved in enhanced fluid circulation has posed serious questions about the predictability of the EGS productivity.

Mineral surface area formulations based on grain size like that presented by Lasaga (1984) cannot be used to describe the mineral surface area in contact with fluid as the porosity goes to zero. We use the expression:

$$A_s(t) = A_s^0 \left(\frac{\Phi(t)}{\Phi_0} \right) \quad (14)$$

where A_s^0 and Φ_0 refer to the initial surface area and initial porosity, respectively.

Surface area is important in quantifying mineral-water reaction rates. Models of complex systems should require kinetic data on mineral surface processes during dissolution and growth. Therefore, we need measured reaction rates of specific surface features in order to distinguish the role of reactive versus total surfaces area. The determination of reactive surface area is known to be a central problem in fluid-solid interactions.

Mineral alteration

The mineral alteration equation for the fracture has the form:

$$\frac{\partial \phi_s}{\partial t} = \overline{V_s} . r_s \quad (15)$$

where $\overline{V_s}$ refers to the mineral molar volume. The porosity can be calculated directly from Eq. (14), (assuming no other processes result in a change in porosity) since:

$$\Phi = 1 - \sum_{s=1}^{N_s} \phi_s \quad (16)$$

The rate of change of the fracture aperture can be related to the rate of change of the mineral volume fractions in the fracture by applying Eq. (14) to the fracture to yield:

$$\frac{\partial \delta}{\partial t} = -\delta \sum_{s=1}^{Ns} \frac{\partial \phi_s}{\partial t} = -\delta \sum_{s=1}^{Ns} \overline{V_s} r_s \quad (17)$$

where Φ_s refers to the mineral volume fractions in the fracture. In finite difference form, this equation becomes

$$\delta(x, t+\Delta t) = \delta(x,t) . \left(1 - \Delta t . \sum_s \overline{V}_s . r_s \right) \quad (18)$$

This equation is used when updating the fracture aperture as a function of time and space.

APPLICATION TO THE SOULTZ RESERVOIR

The evolution of fluid chemistry and mineral alteration in Soultz geothermal reservoir has been evaluated using FRACHEM simulator.

Specificity of FRACHEM simulator

FRACHEM is a THC simulator that has been developed specially for the granitic reservoir of Soultz-sous-Forêts (Durst, 2002; Bächler, 2003; Kohl and Hopkirk, 1995; Bächler and Kohl, 2005; Rabemana et al., 2003; André et al., 2006). The model considers the flow of water and heat, plus reactions between minerals, and aqueous species, and porosity–permeability coupling for a dual permeability (fractures and matrix) medium. The model deals solely with chemical interactions as a function of flow rate and temperature, and takes no account of fracture aperture variation as a result of thermoelastic effects.

The model is composed of 1250 fractured zones. Each fractured zone has an aperture of 0.1 m, a depth of 10 m, a porosity of 10%, and contains 200 fractures. Initially the temperature was set to the reservoir temperature of 200℃. One of these fractured zones is modelled with the assumption that the fluid exchange with the surrounding low permeability matrix is insignificant. Due to the symmetrical shape of the model, only the upper part of the fractured zone is considered in the simulation. The fractured zone is assumed to be well connected (Fig 1).

The principal input variable held constant is the hydraulic injection pressure. Thus, changes in system impedance will be manifest as changes in production rates. The fluid velocity in the fracture between injection and production wells is of the order of 10^{-2} m.s^{-1} whereas the maximum flow velocity in the matrix near the wells is of the order of 10^{-11} m.s^{-1}. Heat transport in the fracture is found to take place almost entirely by advection, and that in the matrix by conduction. The calculated temperature distribution in the reservoir, at each calculation time step, is in turn used to model the effect of water-rock interaction during circulation. The rate of change of the fracture aperture can be related to the rate of change of the mineral volume fractions in the fracture.

The reservoir at Soultz, at a depth of 5000 m, contains a brine with total dissolved solids (TDS) about 100 g.kg^{-1}H_2O and a temperature of 200℃ (Tab. 1). Partial equili brium conditions occur between fluids and secondary minerals in the Soultz geothermal system. Considering the high salinity of the geothermal fluid, the Pitzer activity model is used to determine the activity coefficients of the species. Aqueous species included in the model are H^+, Ca^{2+}, Na^+, Mg^{2+}, K^+, H_4SiO_4(aq), Mg^{2+}, Al^{3+}, Fe^{2+}, SO_4^{2-}, HCO_3^-, Cl^-, OH^-, HS^-, CO_3^{2-}, $CaHCO_3^+$, $CaCO_3$(aq), $CaSO_4$(aq) and CO_2(aq). The activity coefficients calculations are carried out using the Harvie-Moller-Weare database (Harvie et al., 1984; Moller et al., 1998; Wolery, 1992). Presently, a limited number of minerals are considered which correspond to the minerals constituting the Soultz granite (Tab. 2). The determination of kinetic parameters of each mineral is deduced from published experiments, conducted at high temperature in NaCl brines. Detailed kinetic data for calcite, dolomite, pyrite, quartz, amorphous silica, K-feldspar, albite and illite can be found in Durst (2002) and André et al. (2006). It is assumed that all dissolution reactions are congruent. Thermodynamic data (equilibrium constants) are taken mostly from SUPCRT92 (Johnson et al., 1992) and Helgeson et al. (1978) and are function of temperature and pressure.

At last, a supplementary module allows the determination of porosity and permeability variations linked with chemical processes occurring in the reservoir. Several alternative models for the porosity–permeability relationship are included (Norton and Knapp, 1977; Steefel and Lasaga, 1994; Bolton et al., 1996).

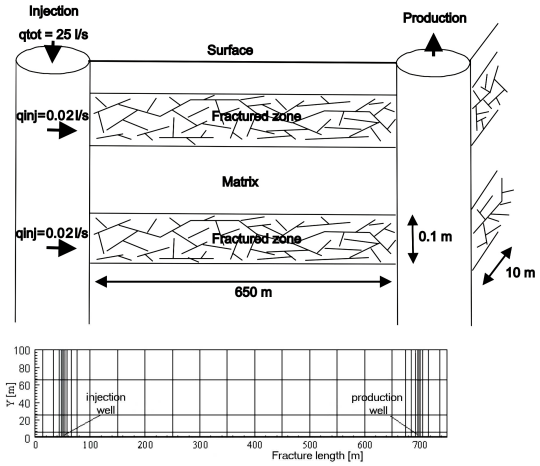

Figure 1: Simplified model and spatial discretization.

Table 1: Characteristics of the formation fluid used for the numerical simulations (after Durst, 2002)

Species	Concentration [mmol/kg]
Na+	1148.00
K+	73.40
Ca2+	169.50
Mg2+	3.21
Cl-	1648.00
S	1.77
C	42.76
Fe2+	2.61
SiO2	6.06

Table 2: Mean composition (in volume percent) of the different facies of granite in the Soultz reservoir (Jacquot, 2000).

	Healthy granite	Hydrothermalised granite	Vein of alteration
Quartz	24.2	40.9	43.9
K-Feldspar	23.6	13.9	
Plagioclases	42.5		
Illite		24.6	40.2
Smectite		9.7	9.6
Micas	9.4		
Calcite	0.3	3.3	4.3
Dolomite		0.8	0.7
Pyrite		0.7	1.0
Galena		1.3	0.3
Chlorite		4.8	

Table 3: Values of the thermo-hydraulic parameters for fracture, matrix and fluid.

Parameters		Fracture	Matrix	Fluid
Hydraulic conductivity	[m^2/Pas]	7.44 10^{-8}	9.5 10^{-15}	-
Thermal conductivity	[W/m.K]	2.9	3	0.6
Density	[kg/m^3]	-	2650	1000
Heat capacity	[J/kg.K]	-	1000	4200
Porosity	[%]	10	0	-

Model results

The values of the thermo-hydraulic parameters considered in the simulations are listed in Table 3. Results in terms of porosity evolution and amount of dissolved or precipitated minerals along the fractured zone are in Figure 2.

The cooled injection water is over-saturated with quartz and under-saturated with respect to calcite because this water was in equilibrium with reservoir rock at 200 °C. T herefore, significant calcite dissolves close to the injection well because calcite solubility increases with decreasing temperature. Calcite has a higher solubility at the injection temperature of 65 °C. As temperatures increase away from the injection well, calcite becomes over-saturated and precipitation occurs. Areas of calcite dissolution and precipitation move gradually away from the injection well due to changes in temperature along the flow path. A maximum of 5% volume of calcite has been precipitated after 5 years. Dolomite also dissolves close to the injection well. The amounts of dolomite dissolution are about one order of magnitude smaller than calcite.

Amorphous silica is gradually precipitating due to kinetics, wich is different from calcite. A precipitation peak can be observed in the vicinity of the injection well. Quartz, which is a major mineral in granite, has a reaction rate three order of magnitude smaller than the one of amorphous silica. Quartz precipitation is observed for this range of temperatures.

Some pyrite and K-Feldspar precipitation, and very slight illite precipitation occur near the injection well. When increasing circulation time, the precipitation zone of pyrite and K-Feldspar extends towards the production well, but this process decreases when temperature increases. It is interesting to note the weak dissolution of illite close to the production well. Siderite precipitation concerns, after 5 years, the entire length of the fracture. However, the reaction rate of these minerals stays one or two orders of magnitude smaller than for calcite.

Calcite is the most reactive mineral (Fig. 2). Including dolomite, more than 6000 kg of carbonates are dissolved in the fracture within 5 years, whereas about 5000 kg precipitate. We can also observe that the amounts of other reactive minerals stay far below the carbonates. The only significant amount concerns the amorphous silica, with about 1900 kg, which precipitate close to the injection well (Fig. 2).

Impact of water-rock interaction during enhanced circulation

The current study comprised a series of coupled 2D simulations of circulation trough a single horizontal fracture zone over 5 years. Several simulations were performed using different combinations of overpressure at the injection well, fluid temperature at the injection well, well spacing, porosity–permeability relationship and injection water chemistry. The aim of this study is to forecast chemical changes under water flow in fractured granite, changes in pH, effects of dissolution and precipitation on hydrological characteristics.

The trends in fluid composition and mineral alteration are controlled by various coupled mechanisms. For example, by increasing the over-pressure at the injection point from 50 to 80 bars, the injection rate is proportionally increased initially. After 5 years, the temperature at the production well decreases to below 150 °C due to the larger injecti on rate (Fig. 3). By increasing the pH of injected water, results indicate that illite precipitates near the mixing front of neutral surface fluids and formation fluids. The changes in porosity and permeability due to precipitation of illite are small compared with that of calcite, quartz and pyrite. However, the illite precipitation is likely to fill open fractures and to form an impermeable barrier. Numerical simulations could provide useful insight into geochemical behavior and formation of impermeable barriers from fluid mixing. We also do not know how much surface water (which cannot be in equilibrium with the reservoir rock) will be needed to add to the system over

the years. Simulation of diluted water injection by mixing with fresh water causes dissolution effects and enhances injectivity (if clay swelling is neglected, which otherwise could cause a slight porosity decrease).
Simulated results showed that fluid chemistry, initial rock temperature, magnitude of flow rate and well spacing have a major effect on water-rock interactions. The simulations also indicate that the choice of functional form for the specific surface area plays an important role in controlling porosity patterns. As specific surface area is currently one of the least constrained parameters in models of porosity evolution, these results highlight the need for future experimental studies.

Effect of permeability distribution along the fractured zone

The effects of permeability distributions along the fractured zone on fluid flow and water-rock interactions have been investigated. Examples of results are in Figures 4, 5 and 6. For the uniform permeability model, an average hydraulic conductivity value (7.44.10-8 $m^2.Pa.s^{-1}$) is assigned all along the fractured zone. For the probabilistic model, the distribution of permeability along the fracture zone follows a lognormal distribution, where hydraulic conductivity is distributed between 10^{-6} and 10^{-9} $m^2.Pa.s^{-1}$, with an average value of 7.44.10-8 $m^2.Pa.s^{-1}$. In our models, the permeability has a decreasing tendency with distance from wells in general but it varies widely; thus fracture zones could remain permeable far from well.
In Figures 2 and 4, porosity distributions can be compared for a uniform fracture zone permeability, and for probabilistically distributed permeability. The uniform and probabilistic permeability models share a similar pattern in porosity distribution, even though the distribution is less uniform at the vicinity of the wells and towards the production well when the initial permeability contrast is higher. Porosity of the fractured zone is notably increased for the probabilistic permeability cases because the fracture zone permeability becomes higher in the vicinity of the injection well. Several permeability models were developed to test the relationship between distance from wells and fractured zone permeability, on the basis of the conceptual model (Gérard et al., 2006). A change in the width and transmissivity of the fractured zone results in a change in fluid flow along the fracture zone and then impacts the water-rock chemical interaction.
Similarly, flow of reactive fluids through variable-aperture fractures can lead to geochemical alteration of the fracture surfaces resulting in localized changes in fracture permeability. For a pore fluid that is undersaturated with respect to the minerals forming the fracture surfaces, chemical reactions lead to dissolution and increases in local fracture apertures. Local dissolution rates tend to be positively correlated with fracture aperture, meaning that larger flow rates lead to locally higher flow rates and faster dissolution.

CONCLUSION

The reactive transport modelling may be useful in the exploration and management of geothermal reservoirs, including chemical evolution, mineral alteration, mineral scaling, and changes in porosity and permeability.
A two-dimensional (2-D) thermo-hydro-chemical coupled model has been developed to examine the effect of water-rock chemical interaction on the long-term performance of EGS reservoirs. The model can predict the influence of water-rock interactions on the overall fractured reservoir. Factors affecting water-rock interactions and the effect of water-rock interactions on deep reservoir behaviour at Soultz have been modelled. The major issue deals with injectivity effects on mineral scaling in a fractured geothermal reservoir.

To test a conceptual model, to model forced fluid circulation and the chemical and physical reactions between the injected fluid and geothermal reservoir minerals and to study the geochemical behavior due to mixing of surface and formation fluids, reactive geothermal transport simulations under both natural and production conditions can be carried out using the code FRACHEM. This model should allow identifying critical reactions controlling scaling and changes in permeability, and investigate possible intervention techniques.
Ongoing research is exploring different approximations for coupled processes with vastly different intrinsic time scales, and is addressing uncertainties in thermodynamic parameters, reactive surface areas and kinetic rate constants. Besides theoretical and computational limitations, a lack of adequate data to calibrate again limits the applicability of the models.
Also, monitoring changes in the chemistry of the circulating fluid in an engineered reservoir over time can provide data that will be highly valuable to characterize the reservoir and predict its performance over time.

REFERENCES

Aagaard, P., Helgeson, H.C., (1982), Thermodynamic and kinetic constraints on reaction rates among minerals and aqueous solutions. I: Theoretical considerations, *Amer. J. Sci*., **282**, 237–285.

André, L., Rabemanana, V. and Vuataz, F.-D., (2006), Influence of water-rock interactions on fracture permeability of the deep reservoir at Soultz-sous-Forêts, France. *Geothermics*, **35**, 507-531.

Andritsos, N. and Karabelas, A.J., (1991), Sulphide scale formation and control: the case of lead sulphide. *Geothermics*, **20**, 343–353.

Arnorsson S. (ed.), (2000), Isotopic and chemical techniques in geothermal exploration, development and use. International Atomic Energy Agency, Vienna, 351 pp.

Bächler, D. and Kohl, T., (2005), Coupled thermal-hydraulic-chemical modelling of enhanced geothermal systems. *Geophys. J. Int.*, **161** (2), 533–548.

Bächler, D., (2003), Coupled Thermal-Hydraulic-Chemical modelling at the Soultz-sous-Forêts HDR reservoir (France). *PhD thesis*, ETH-Zürich, Switzerland, 151 p.

Bear, J., (1979), Hydraulics of Groundwater. McGraw-Hill, New York, p. 569.

Bolton, E.W., Lasaga, A.C. and Rye, D.M., (1996), A model for the kinetic control of quartz dissolution and precipitation in porous media flow with spatially variable permeability; formulation and examples of thermal convection. *J. Geophys. Res. Part B. Solid Earth Planets*, **101** (10), 22157–22187.

Clauser, C., (1988), Untersuchungen zur Trennung der konduktiven und konvektiven Anteile im Wärmetransport in einem Sedimentbecken am Beispiel des Oberrheintalgrabens. *PhD thesis*. Fortschritts-Berichte VDI, Reihe 19, Nr. 28, VDI Verlag, Düsseldorf.

de Marsily, G., (1986), Quantitative Hydrogeology. Academic Press, New York, p. 440.

Dezayes, C., Valley, B., Maqua, E., Sysen, G. and Genter, A., (2005), Natural fracture system of the Soultz granite based on UBI data in the GPK3 and GPK4 wells. *Proceedings of the EHDRA Scientific Meeting. Soultz-sous-Forêts, France*.

Durst, P., Vuataz, F.D., (2000), Fluid-rock interactions in hot dry rock reservoirs - a review of the HDR sites and detailed investigations of the Soultz-sous-Forêts

system. *Proc. World Geothermal Congress 2000, Beppu-Morioka, Japan,* 3677-3682.

Durst, P., (2002), Geochemical modelling of the Soultz-sous-Forêts Hot Dry Rock test site: coupling fluid-rock interactions to heat and fluid transport. *PhD thesis*, University of Neuchâtel, Switzerland, 127 p.

Evanoff, J., Yeager, V. and Spielman, P., (1995), Stimulation and damage removal of calcium carbonate scaling in geothermal wells: a case study. *Proceedings of the World Geothermal Congress, Florence, Italy,* **95**, 2481–2485.

Fournier R.O., (1985), The behavior of silica in hydrothermal solutions. *In Geology and Geochemistry of Epithermal Systems (B.R. Berger and P.M. Bethke, Eds) Rev. Econ. Geol.*, **2**, 45-61.

Genter, A., Traineau, H., Dezayes, C., Elsass, P., Ledesert, B., Meunier, A. and Villemin, T., (1995), Fracture analysis and reservoir characterization of the granitic basement in the HDR Soultz project (France). *Geotherm. Sci. Tech*., **4** (3), 189-214.

Gérard, A., Genter, A., Kohl, T., Lutz, P., Rose, P. and Rummel, F., (2006), The deep EGS (Enhanced Geothermal System) project at Soultz-sous-Forêts (Alsace, France). *Geothermics*, **35** (5-6), 473-483.

Gunnarsson I. and Arnorsson S., (2005), Impact of silica scaling on the efficiency of heat extraction from high-temperature geothermal fluids. *Geothermics*, **34**, 320-329.

Harvie, C.E., Moller, N., Weare, J.H., (1984), The prediction of mineral solubilities in natural waters: the Na-K-Mg-Ca-H-Cl-SO_4-OH-HCO_3-CO_3-CO_2-H_2O system to high ionic strengths at 25℃. *Geochimica et Cosmochimica Acta*, **48**, 723-751.

Helgeson, H.C., Delany, J.M., Nesbitt, H.W. and Bird, D.K., (1978), Summary and critique of the thermodynamic properties of rock-forming minerals. *Am. J. Sci.*, **278**-A, 1-229.

Hooijkaas, G. R., Genter, A. and Dezayes, C., (2006), Deep-seated geology of the granite intrusions at the Soultz EGS site based on data from 5km deep boreholes. *Geothermics*, **35** (5-6), 484-506.

Jacquemont B., (2002), Etude des interactions eau-roche dans le granite de Soultz-sous-Forêts. Quantification et modélisation des transferts de matière par les fluides. *PhD thesis*, Univ. Louis Pasteur, Strasbourg, France.

Jacquot, E., (2000), Modélisation thermodynamique et cinétique des réactions géochimiques entre fluides de bassin et socle cristallin: application au site expérimental du programme européen de recherche en géothermie profonde (Soultz-sous-Forêts, Bas-Rhin, France). *PhD thesis*, Univ. Louis Pasteur, Strasbourg, 202 p.

Johnson, J.W., Oelkers, E.H. and Helgeson, H.C., (1992), SUPCRT92: A software package for calculating the standard molal thermodynamic properties of minerals, gases, aqueous species, and reactions from 1 to 5000 bar and 0 to 1000℃. *Computers and Geosciences*, **18** (7), 899-947.

Kohl, T. and Hopkirk, R.J., (1995), "FRACTure" – a simulation code for forced fluid flow and transport in fractured, porous rock. *Geothermics*, **24** (3), 333–343.

Krauskopf, K.B., Bird, D.K., (1995), Introduction to geochemistry. McGraw-Hill, Inc. New York, America, 647p.

Lasaga, A.C., (1984), Chemical kinetics of water–rock interactions. *J. Geophys. Res*., **89**, 4009–4025.

Lasaga, A.C., Soler, J.M., Ganor, J., Burch, T.E., Nagy, K.L., (1994), Chemical weathering rate laws and global geochemical cycles. *Geochim. Cosmochim. Acta*, **58**, 2361-2386.

Lichti, K.A. and Braithwaite, W.R., (1980), Surface corrosion of metals in geothermal fluids at Broadlands, New Zealand. *Geothermal Scaling and Corrosion*, **717**, 97-105.

Lichtner, P.C., (1984), Contiuum model for simultaneous chemical reactions and mass transport in hydrothermal systems. *Geochimica et Cosmochimica Acta*, **49**.

Moller, N., Greenberg, J.P. and Weare, J.H., (1998), Computer modeling for geothermal systems: predicting carbonate and silica scale formation, CO_2 breakout and H_2S exchange. *Transp. porous media*, **33**, 173-204.

Norton, D. and Knapp, R., (1977), Transport phenomena in hydrothermal systems; the nature of porosity. *Am. J. Sci.*, **277** (8), 913–936.

Pitzer, K.S., (1973), Thermodynamic of electrolytes. I. Theoretical basis and general equations. *J. Phys. Chem.*, **12**, 268–277.

Pribnow, D., (1994), Ein Vergleich von Bestimmungsmethoden der Wärmeleitfähigkeit unter Berücksichtigung von Gesteinsgefügen und Anisotropie. Fortschritt-Berichte VDI. Reihe 19, Wärmetechnik/Kältetechnik, Nr. 75. *PhD thesis*. Düsseldorf.

Rabemanana, V., Durst, P., Bächler, D., Vuataz, F.-D. and Kohl, T., (2003), Geochemical modelling of the Soultz-sous-Forêts Hot Fractured Rock system: comparison of two reservoirs at 3.8 and 5 km depth. *Geothermics*, **32** (4–6), 645–653.

Reed M.H., (1982), Calculation of multicomponent chemical equilibria and reaction processes in systems involving minerals, gases and an aqueous phase. *Geochim. Cosmochim. Acta*, **46**, 513-528.

Rimstidt, J.D. and Barnes, H.L., (1980), The kinetics of silica-water reactions. *Geochim. Cosmochim. Acta*, **44** (11), 1683–1699.

Sanjuan, B., Pinault, J.L., Rose, P., Gérard, A., Brach, M., Braibant, G., Crouzet, C., Foucher, J.-C., Gautier, A. and Touzelet, S., (2006), Tracer testing of the geothermal heat exchanger at Soultz-sous-Forêts (France) between 2000 and 2005. *Geothermics*, **35**, 622-653.

Sausse, J., Fourar, M. and Genter, A., (2006), Permeability and alteration within the Soultz granite inferred from geophysical and flow log analysis. *Geothermics*, **35** (5-6), 544-560.

Sauty, J.P., (1981), Du comportement thermique des réservoirs aquifères exploités pour le stockage d'eau chaude ou la géothermie basse enthalpie. *Thèse d'état*, Grenoble.

Snow, D.T., (1968), Rock fracture spacings, openings, and porosities. *J. Soil Mech., Found Div., Proc. Amer. Soc. Civil Engrs*., **94**, 73–91.

Steefel, C.I., Lasaga, A.C., (1994), A coupled model for transport of multiple chemical species and kinetic precipitation/dissolution reactions with application to reactive flow in single phase hydrothermal system. *Am. J. Sci.*, **294** (5), 529-592.

Steefel, C.I., MacQuarrie, K.T.B., (1996), Approaches to modeling of reactive transport in porous media. In: Lichtner, P.C., Steefel, C.I., Oelkers, E.H. (EDS.), Reactive transport in porous media. *Reviews in Mineralogy*, **34**, 83-129.

Tchistiakov, A.A., (2000), Physico-chemical aspects of clay migration and injectivity decrease of geothermal clastic reservoir. *Proceedings of the World Geothermal Congress 2000, Kyushu-Tohoku, Japan*, 3087–3095.

Vetter O.J. and Kandarpa V., (1987), Chemical thermodynamics in geothermal operations. *In: Applied Geothermics. (J. Economides and P.O. Ungemach, Eds), J. Wiley & Sons*, 125-135.

White, S.P., (1995), Multiphase nonisothermal transport of systems of reacting chemicals. *Water Resour. Res*., **31** (7), 1761–1772.

Wolery, T.J., (1992), EQ3nr, a computer program for geochemical aqueous speciation solubility calculations: theoretical manual, user's guide and related documentation (Version 7.0). *Report, UCRL-MA-110662 PT III, Lawrence Livermore National Laboratory, Livermore, California, USA*, 246 p.

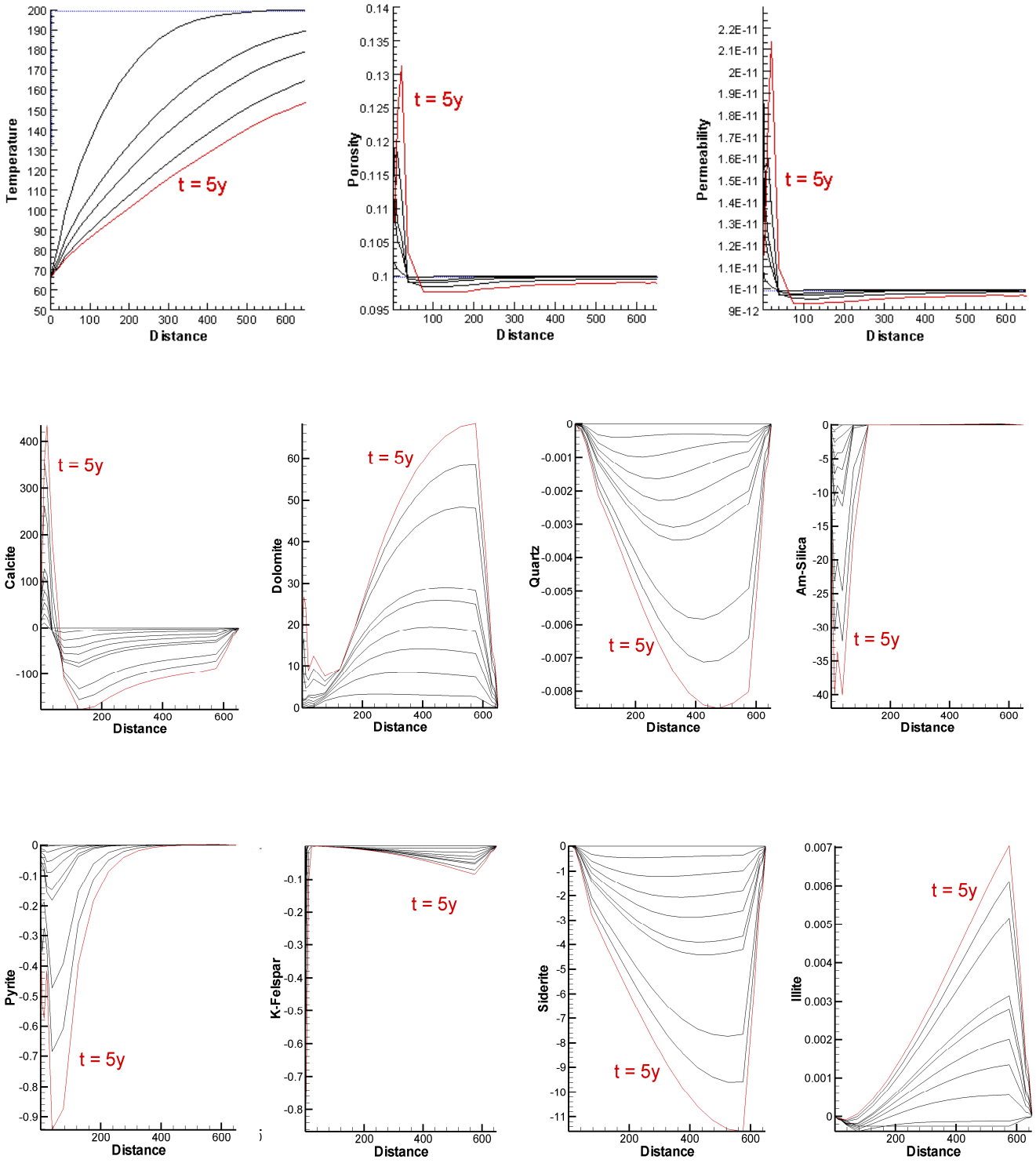

Figure 2. Simulated evolution of temperature, porosity, permeability and dissolved or precipitated amount of minerals in kilogram along one fractured zone during 5 years, assuming uniform initial permeability (hydraulic conductivity of $7.44.10^{-8}$ $m^2.Pa^{-1}.s^{-1}$) in the fractured zone, injection overpressure of 80 bar and injected fluid temperature of 65°C. Positive values of the amount of minerals indicate the dissolved and negative ones the precipitated amount.

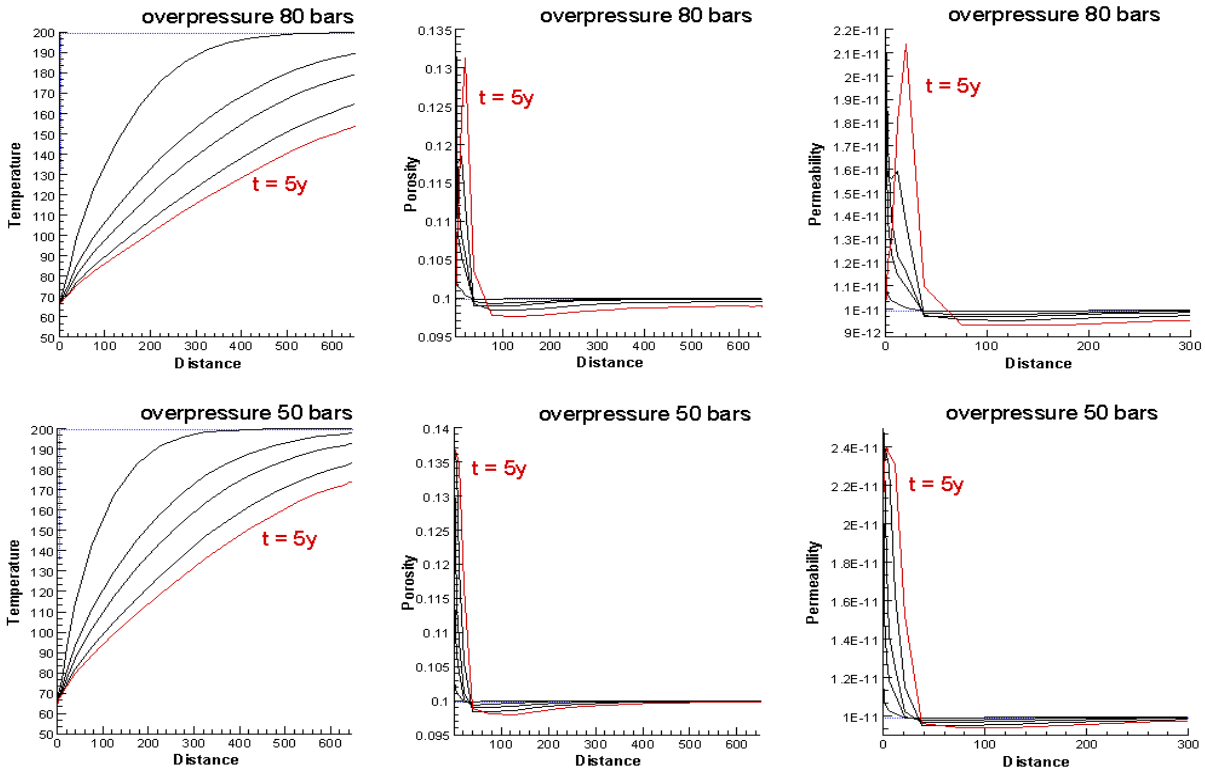

Figure 3. Effect of overpressure injection on simulated evolution of temperature, porosity and permeability along one fractured zone during 5 years, assuming uniform initial permeability distribution in the fractured zone and injected fluid temperature of 65℃.

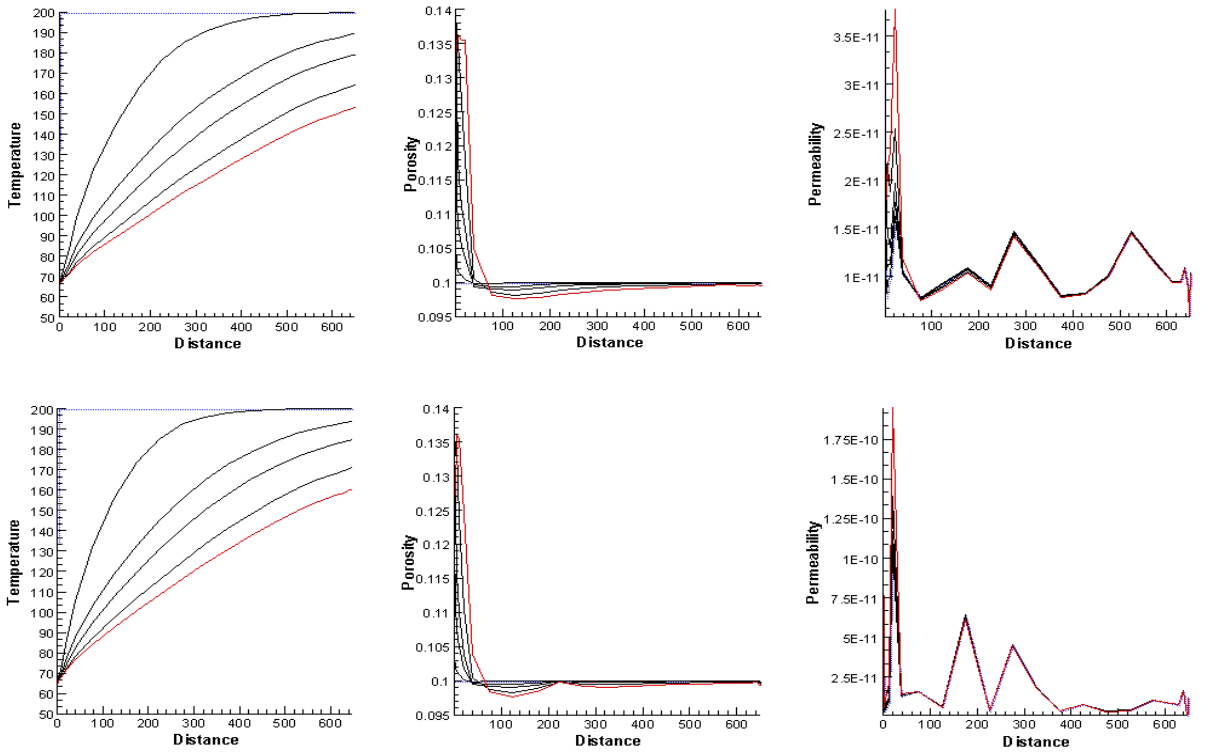

Figure 4. Examples of simulated evolution of temperature, porosity and permeability along one fractured zone during 5 years, assuming probabilistic initial permeability distribution (with different contrast) in the fractured zone.

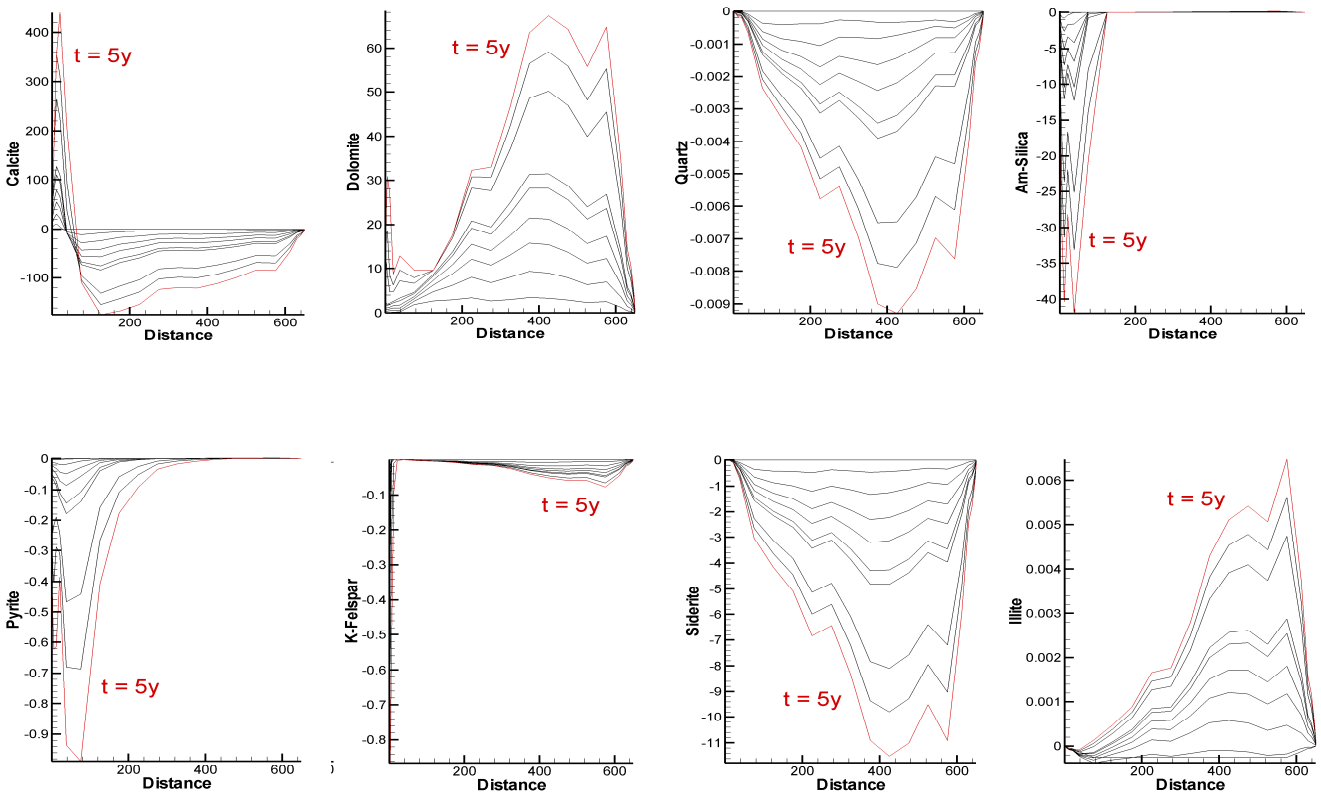

Figure 5. Example of simulated evolution of dissolved or precipitated amounts of minerals (in kg) along one fractured zone during 5 years, assuming weak standard deviation of initial permeability distribution in the fractured zone.

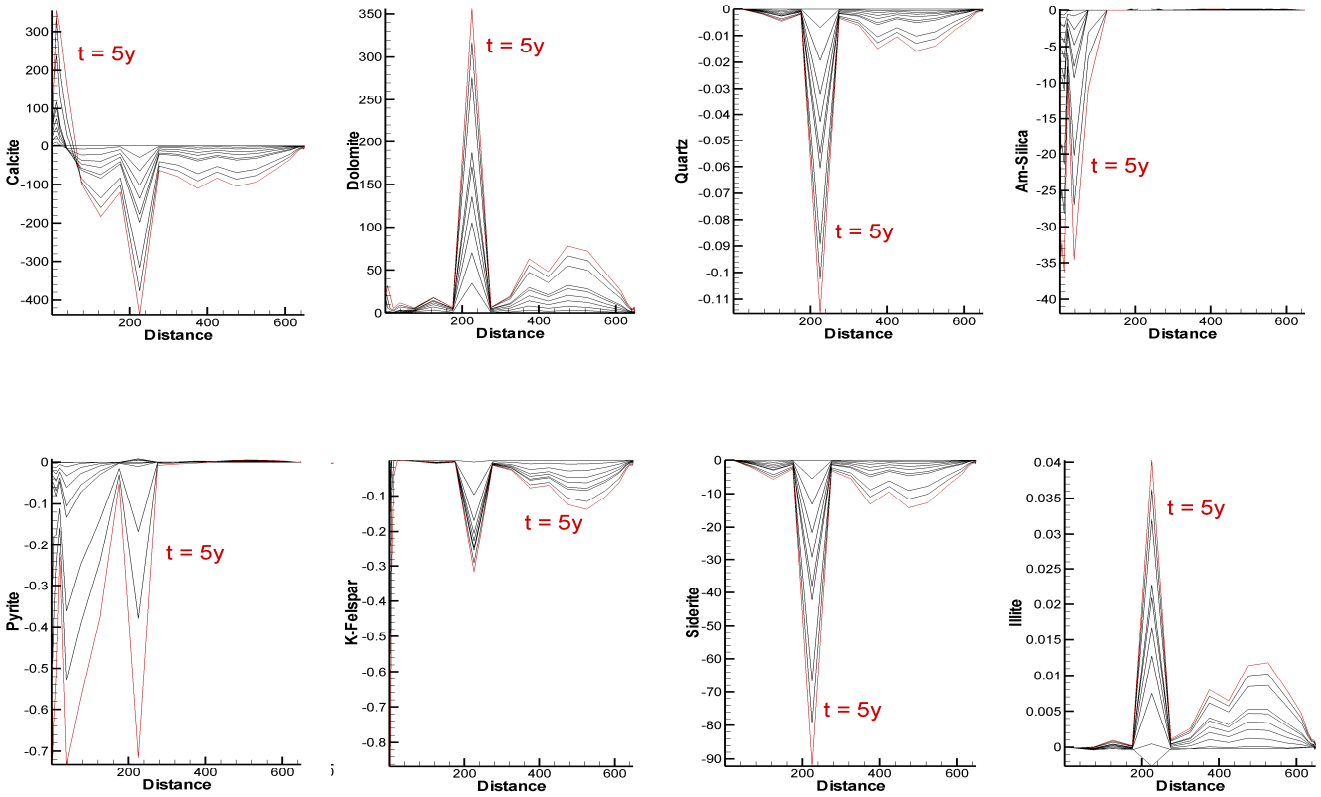

Figure 6. Example of simulated evolution of dissolved or precipitated amounts of minerals (in kg) along one fractured zone during 5 years, assuming probabilistic high contrasting initial permeability distribution in the fractured zone.

DHMA
Deep Heat Mining Association

ENhanced Geothermal Innovative Network for Europe
Work Package 4 :
Drilling, stimulation and reservoir assessment
Participant No 28:
Deep Heat Mining Association – DHMA, Switzerland

v.9

Technical report

Review on chemical stimulation techniques in oil industry and applications to geothermal systems

by Sandrine Portier, Laurent André & François-D. Vuataz

CREGE – Centre for Geothermal Research, Neuchâtel, Switzerland

January 2008

CENTRE DE RECHERCHE EN GEOTHERMIE
c/o CHYN
CH-2009 Neuchâtel, Suisse
www.crege.ch

Table of contents

Review on chemical stimulation techniques in oil industry and applications to geothermal systems

Sandrine [1] Portier, Laurent André [2] & François-D. Vuataz [1]

[1] CREGE – Centre for Geothermal Research, c/o CHYN, CH-2009 Neuchâtel, Switzerland

e-mail : sandrine.portier@crege.ch; francois.vuataz@crege.ch

[2] Present address : BRGM, Bureau de Recherches Géologiques et Minières, EAU/M2H, F-45060 Orléans Cedex, France

e-mail: l.andre@brgm.fr

Summary

Introduction and background

The Enhanced Geothermal Systems (EGS) are dedicated to the exploitation of the heat present in deep hot rocks of limited permeability. But this extraction is only feasible if the reservoir permeability is sufficient to ensure a fluid circulation between injection and production wells. Economic exploitation of enhanced geothermal systems is strongly dependant on natural or induced mineral precipitation and associated decrease in permeability of the system. One solution to this problem consists in injecting a reacting fluid into the wells, in order to dissolve the secondary minerals scaled on the casing or sealing fractures, to increase the permeability.

A study of the literature on acidification of high temperature geothermal reservoirs has been attempted, but the number of references is very limited and apparently, experiments in geothermal fields are by far not all published. On the other hand, a wealth of research and publications is available on these topics in the oil industry literature. Indeed, since the early 20th century, chemical stimulation techniques were originally developed to increase or to recover the production rates of oil and gas wells to commercial levels.

Acid stimulation jobs intend to clean fractures by dissolving filling materials and mobilizing them for an efficient removal by flow transport. Acidizing is probably the most widely used work-over and stimulation practice in the oil industry. By dissolving acid soluble components within reservoir formations, or by removing material at the wellbore face, the flow rate from oil or gas production wells may be increased.

Within this review, the role and the impact of different reactants used for the chemical treatments (acids, chelating agents and mixed compounds) are explained and some examples of acidizing treatments in geothermal wells are described. First, various methods used to prevent scaling in oil, gas and geothermal wells or to improve the reservoir fracturation are presented. The second part of this review is focused on chemical stimulation of sandstone reservoirs. Finally, the third part is concentrated on cleaning of geothermal wells and the experiments of chemical stimulation at the Soultz EGS reservoir.

Acidizing may, in fact, be the oldest stimulation technique still in modern use. The earliest acid treatments of oil wells are believed to have occurred as far back as 1895. Because of the growing interest surrounding acid treatments of limestone formations, new treatments for sandstone formations began to appear. In 1933, Halliburton conducted the first sandstone acidizing treatment using a mixture of hydrochloric and hydrofluoric acid. Numerous matrix acidizing treatments of sandstone formations have been conducted since the mid-1960s. In the 1970s and early 1980s there was a proliferation of “novel” sandstone acidizing systems, in order to provide certain benefits such as retarding HF spending, stabilizing fine particles, and preventing precipitation of HF-rock reaction products.

Technology review

Two basic types of acidizing operations can be conducted: *Matrix acidizing* and *Fracture acidizing*. *Matrix acidizing* is performed below fracturing rate and pressure. Acid flows through the matrix with reactions taking place in existing pores and natural fractures. and is normally used for the removal of skin damage associated with work-over, well killing or injection fluids and to increase formation permeability in undamaged wells. A number of different acids are used in conventional acidizing treatments, such as HCl, HF, CH_3COOH, HCOOH, H_2NSO_3H, etc. Choice of the acid and any additives for a given situation depends on the underground reservoir characteristics and on the specific intention of the treatment, for example near wellbore damage removal, dissolution of scale in fractures. HCl and HF are two acids reacting quickly with carbonates and silicates. However, the objectives of acid treatment are to increase porosity and permeability of the medium, deeply in the formation. Methods, which have been developed to slow the acidizing process. Besides acids, the chelating agents are solutions used as formation cleanup and for stimulating wells especially in formations that may be damaged by strong acids.

The second main technique, *Fracture acidizing* is performed above fracturing rates and pressures. Etching of the created fractures provides well stimulation, not just damage removal. The aim is to change the future flow pattern of the reservoir from radial to linear to effectively stimulate the reservoir and increase production. The key to success is the penetration of reactive acid along the fracture. To achieve deeper penetration in fracture acidizing, it is often desirable to retard acid reaction rate. This can be done by gelling (polymers and surfactants), emulsifying, or chemically-retarding the acid, in effect, making it more difficult for the H^+ ions to contact a reactive surface.

Compared to carbonate reservoirs, the acidification of a sandstone reservoir, requires a specific procedure. The objective of acidizing sandstone wells is to increase permeability by dissolving clays and other pore plugging materials near the wellbore. Clays may be naturally occurring formation clays or those introduced from drilling, completion or workover fluids.

Three sequences are needed for the treatment of a sandstone reservoir: preflush, main flush and overflush. The preflush is performed most often with a HCl solution, first to displace the formation brines, away from the wellbore so there will be no mixing with HF acids. This decreases the probability of forming alkali-fluorosilicates. Second, to dissolve as much of the calcareous material as possible, prior to injection of the HF acid to minimize calcium fluoride precipitation. The main flush is used to remove the damage and most often, a mixture of HF and HCl or organic acids is pumped into the well. Finally the overflush is an important part of a successful sandstone acid treatment. It performs the displacement of the nonreacted mud acid into the formation and of the mud acid reaction products away from the wellbore. It also removes potential oil-wet relative permeability problems caused by some corrosion inhibitors. Large overflushes help prevent the near wellbore precipitation of amorphous silica.

Current practices of sandstone acidizing are linked to concentration and ratio of HCl and HF acids, as well as the volumes pumped into the formation during the different phases, which are dependant on the formation rock mineralogy. Corrosion inhibitor is always necessary and it must be added to all acid stages (preflush, mainflush, and overflush). It is the rather dilute acid mixtures, like 15% HCl, that have a lot of water present that present the most corrosive effect.

Coiled tubing is a very useful tool for improving acid placement. Coiled tubing is of less use in fracturing acidizing because of pumping rate limitations. It is still best to pump fracturing treatments through larger strings, such as production tubing. In larger open hole, acid diversion is important, otherwise only the interval, which breaks down or fractures first will be treated. Diversion can be achieved with packers.

The re-precipitation of reaction products is a serious concern in sandstone acidizing containing alumino-silicates. Many reactions take place in the formation as HF injection proceeds. The chemical reactions between sandstone minerals and HF acids have been extensively described in the literature.

Chemical stimulation in geothermal wells

Acidizing geothermal wells is related to sandstone acidizing in that most geothermal reservoirs produce from volcanic rocks. Formation conditions are often conducive to large-volume, high-rate acid treatments. In geothermal wells, the strongest indication of acid-removable formation damage is a sharp drop in production rate. Nearly all geothermal wells that are acidizing candidates have been damaged by either drilling mud solids and drill cuttings lost to the formation fractures or by scale (calcium carbonate, silica, calcium sulphate, and mixtures). Various methods have been tried to

prevent scaling in geothermal wells, including varying pressure, temperature or pH changes and scale inhibitors. If scale inhibitors have solved many problems, one promising alternative method is the acidizing.

A very successful method of acidizing geothermal wells has been a basic, high-rate, brute-force method. High acid concentrations have been shown to be effective in geothermal wells producing from natural fractures not containing separate, large carbonate zones. Hydrochloric acid (HCl), hydrofluoric acid (HF) or both have been used since the 1980's in hydrothermal wells. The only acid additives necessary in a geothermal acid job are corrosion inhibitor and inhibitor intensifier, as well as high-temperature iron-control agent.

Conventional acid placement techniques are less effective for the long, open-hole or liner-completed intervals typically encountered in geothermal wells. High-temperature foam systems may improve zone coverage. During the 1990's, the acidification technique has been used more often, principally for the reservoir development or to treat formation damage caused by drilling mud and scaling in geothermal wells. In all documented cases, acidification occurred in the three usual main steps, preflush (HCl), main flush (HCL-HF mixture) and overflush (HCl, or KCl, NH_4Cl or freshwater).

In geothermal well acidizing, more acid often is better. Naturally fractured volcanic formations can withstand high HF concentration. The HCl-HF stage can be for example 10% HCl - 5% HF, or 3% HCl - 5% HF and an organophosphonic acid. These acid mixtures have been used rather successfully in stimulating geothermal wells in Southeast Asia, as well as in South and North America. A summary of the main chemical stimulation experiments carried out in geothermal fields is given in Table 1, showing variable results.

Table 1 : Results of HCl-HF treatments for scaling removal and connectivity development

Geothermal field	Number of treated wells	Improvement factor of injectivity
Bacman (Philippines)	2	1.4 - 4.4
Leyte (Philippines)	3	1.9 – 7.1
Tiwi (Philippines)	1	2.6
Mindanao (Philippines)	1	2.8
Salak (Indonesia)	1	2.6
Berlín (El Salvador)	5	2.8 – 9.9
Las Tres Virgenes (Mexico)	2	2.5 - 3.1
Los Azufres (Mexico)	1	2.8
Beowawe (USA)	1	2.2
The Geysers (USA)	1	no effect
Coso (USA)	30	24 wells successful
Larderello (Italy)	5	4 - 12

Experiments in EGS systems

Only few chemical stimulation experiments and laboratory tests have been attempted until now in enhanced geothermal systems (EGS) wells and reservoirs. Limited reported data were found at the projects of Fenton Hill (USA) and Fjällbacka (Sweden).

At the EGS reservoir of Soultz-sous-Forêts however, several consistent and documented chemical stimulation tests have been carried out since 2003. Different techniques were consecutively used in the three 5-km deep wells: soft acidizing, Regular Mud Acid (RMA), chelating agents (NTA) and Organic Clay Acid (OCA). Although they were not executed with the same comparable protocol, various but encouraging results were observed after this first series of tests using chemical stimulation methods in a fractured granitic EGS reservoir (Table 2).

Table 2 : Summary of the chemical stimulation operations carried out in the three 5-km deep wells at Soultz-sous-Forêts

Well	Date	Concentration of chemical agents	Results: Injectivity/Productivity increase
GPK2	February 2003	HCl 0.09 + 0.18 %	Wellhead pressure drop, but no productivity increase observed.
GPK3	June 2003	HCl 0.45 %	No increase: 0.35 $L.s^{-1}.bar^{-1}$
	February 2007	Organic Clay Acid OCA	No increase: 0.35 $L.s^{-1}.bar^{-1}$
GPK4	February 2005	HCl 0.2 %	Productivity: 0.2 to 0.3 $L.s^{-1}.bar^{-1}$
	May 2006	HCl 15 % (3 tons) HCl 12 % + HF 3 %	Productivity: 0.3 to 0.4 $L.s^{-1}.bar^{-1}$
	October 2006	Chelant: NTA 19 %	The formation of a plug increased wellhead pressure.
	March 2007	Organic Clay Acid OCA	Productivity: 0.4 to 0.5 $L.s^{-1}.bar^{-1}$

Conclusions

From this literature review on the chemical stimulation in oil and gas wells, it is apparent that these technological advances will affect many different portions of this industry, from old, mature fields, where significant reserves have previously been economically unattractive, to the new, major ultradeep projects that are being evaluated today. New and innovative stimulation technologies are emerging that will modify some of previous tried and more or less proven methods. It appears that well stimulation will remain a dynamic part of the petroleum industry.

Challenges in sandstone acidizing still exist, although great improvements have been made in the last decade. Factors that contribute to these challenges include: multiple types of co-existing formation damage; uncertain rock mineralogy; multiple fluids and pumping stages; complex chemical reactions between fluids and formation minerals; and fast reaction kinetics at elevated temperatures.

This technology was partially adapted to the geothermal wells, most often to remove the mineral scaling deposited in the wells after several years of exploitation. Nevertheless, acid treatments also allow the enhancement of the fractures network. They have been successfully performed in geothermal granitic reservoirs like Fjällbacka (Sweden) or Beowawe (USA). In recent years, the reliability of acidizing sandstone intervals has been significantly improved. In the USA, about 90 percent of wells treated have responded with two- to four-fold production increases.

Recently, some aspects of this technology have been applied to the Soultz-sous-Forêts granitic reservoir. The three 5-km deep wells were treated with different types and amounts of chemical compounds and the injectivity of each well was differently affected. If encouraging results were obtained with GPK2 and GPK4, the injectivity improvement of GPK3 well is apparently less marked.

1 Introduction

The Enhanced Geothermal Systems (EGS) are dedicated to the exploitation of the heat present in deep hot rocks of limited permeability. But this extraction is only feasible if the reservoir permeability is sufficient to ensure a fluid circulation between injection and production wells. Economic exploitation of enhanced geothermal systems is dependant on natural or induced mineral precipitation and associated decrease in permeability of the system. This may inhibit fluid flow in well casings or in rock fractures and therefore decrease the heat extraction from the system. One solution to this problem consists in injecting a reacting fluid into the wells, in order to dissolve the secondary minerals scaled on the casing or partially sealing the fractures, to increase the permeability and hence to develop the reservoir.

A study of the literature on acidification of geothermal reservoirs has been attempted mainly based on the Proceedings of the annual Stanford Workshop on Geothermal Reservoir Engineering, the annual Transactions of the Geothermal Resources Council and the last three World Geothermal Congress. Surprisingly, the number of references is very limited, with few recent papers and most of the studies were carried out by a team from the Philippines. Apparently, experiments in geothermal fields are not all published. On the other hand, a wealth of research and publications is mainly available on these topics in the oil industry literature.

Chemical stimulation techniques were originally developed to increase or to recover oil and gas wells production rates to commercial levels. This technology, developed for more than one century by oil industry for the stimulation of oil and gas wells, has also been used in geothermal wells for the last 20 years.

Acid stimulation jobs intend to clean (pre-existing) fractures by dissolving filling materials (secondary minerals or drilling mud) and mobilizing them for an efficient removal by flow transport. Acid treatments have been applied to wells in oil and gas bearing rock formations for many years. Acidizing is probably the most widely used work-over and stimulation practice in the oil industry. By dissolving acid soluble components within underground rock formations, or removing material at the wellbore face, the rate of flow of oil or gas out of production wells or the rate of flow of oil-displacing fluids into injection wells may be increased.

The role and the impact of the different reactants used for the chemical treatments (hydrochloric acid (HCl), hydrofluoric acid (HF), chelating agents and mixed compounds) will be explained and some examples of acidizing treatments in geothermal wells will be described. First, various methods used to prevent scaling in oil, gas and geothermal wells or to improve the reservoir fracturation will be presented in this note. The second part of this note will be focused on the chemical stimulation of sandstone reservoirs. Acidizing geothermal wells can be related to sandstone acidizing techniques, because most geothermal reservoirs produce from silicated magmatic or volcanic rocks. Finally, the third part of this technical note is more focused on the cleaning of geothermal wells and the experiments of chemical stimulation at the Soultz EGS reservoir.

2 Brief history and experience acquired with acidizing

The main objective of a stimulation treatment is to increase the rate at which the formation delivers hydrocarbons naturally. Acid treatments have been applied to wells in oil and gas bearing rock formations for many years. Acidizing is a widely used work-over and stimulation practice in the oil industry. By dissolving acid soluble components within underground rock formations or removing material at the wellbore face, the flow rate of oil or gas out of production wells or the flow rate of oil-displacing fluids into injection wells may be increased.

Acidizing predates just about all well stimulation techniques. Other techniques, such as hydraulic fracturing, were developed much more recently. Acidizing may, in fact, be the oldest stimulation technique still in modern use. The earliest acid treatments of oil wells are believed to have occurred as far back as 1895. The Standard Oil Company used concentrated hydrochloric acid (HCl) to stimulate oil wells producing from carbonate formations in Lima, Ohio, at their Solar Refinery. The acidizing process was applied with great success in the Lima, Ohio wells. Many wells were acidized with remarkable results in the short term. However, the first acid treatment in 1895 was probably considered a novel idea that would not last very long, and acidizing was used very infrequently during the next 30 years probably due to the lack of an effective method for limiting acid corrosion. However, throughout its history, acidizing has a repeating record of quickly and inexplicably losing popularity, seemingly independent of results at times.

Because of the growing interest surrounding acid treatments of limestone formations, new treatments for sandstone formations began to appear. In 1933, Halliburton conducted the first sandstone acidizing treatment using a mixture of hydrochloric and hydrofluoric acid (HF), in a test well belonging to the King Royalty Co., near Archer City, Texas. Unfortunately, the results of first attempt were very discouraging. Dowell did introduce a mixture of 12% HCl – 3% HF, called “Mud acid”, in 1939. Successful wellbore treatments were pumped in the Gulf Coast area. This acid mixture is still quite common and is now known as “regular strength” mud acid.

In 1947, the first hydraulic fracturing treatment was completed in the Hugoton Field (Kansas) and fraccing has also become a standard treatment to improve production. Since that time, hydraulic fracturing has increased recoverable reserves more than any other technique. Historically, carbonate fracture acidizing has experienced limited success in geologic reservoirs characterized by high-closure stress or temperatures above 120° C. Although many formations in North America are sandstone and require the use of granular propping agents, acid fracturing is more commonly used in Europe and the Middle East, especially in Bahrain and Saudi Arabia.

Numerous matrix acidizing treatments of sandstone formations have been conducted since the mid-1960s. In the 1970s and early 1980s there was a proliferation of “novel” sandstone acidizing systems, in order to provide certain benefits such as retarding HF spending, stabilizing fine particles, preventing precipitation of HF-rock reaction products. In the 1980s and into the 1990s, developments in sandstone acidizing addressed treatment execution more than fluid chemistry. More recently, fluid chemistry has again stepped to the forefront (twists on old systems are developed).

Recent years have seen a marked increase in well stimulation activity (acid and frac jobs) with the number of treatments performed more than doubling through the 1990s. In 1994, 79% of the jobs were acid jobs, but since they are lower cost than hydraulic fracturing treatments, they only consumed 20% of the money spent for well stimulation. For acid jobs, the observed failure rate was 32%. Failure rate for the less frequent but more expensive hydraulic fracturing treatments was much lower, only 5%. In analyzing the reasons for job failure, one-third was due to incorrect field procedures, while two-thirds were attributed to incorrect design or improperly identifying well damage.

Except for some high temperature hydrothermal fields, the acidification of geothermal wells is not frequently used on a routine basis. Originally, the operative modes were borrowed from the treatments performed on oil or gas wells.

3 Technology overview

Advances in oil and gas well stimulation—matrix acidizing, fracture acidizing, hydraulic fracturing, extreme overbalance operations—enable operators to optimally increase well/reservoir productive capacity. Two basic types of acidizing operations can be conducted:

(1) **Matrix acidizing** is performed below fracturing rate and pressure. Acid flows through the matrix with reactions taking place in existing pores and natural fractures.

(2) **Fracture acidizing** is performed above fracturing rates and pressures. Etching of the created fractures provides well stimulation, not just damage removal.

Acid fracturing treatments can be a solution for wells with impaired production. Not only would acid fracturing increase well productivity, but it also would help retain the generated hydraulic conductivity for a longer time period.

The design of any acid-stimulation treatment should begin with a thorough evaluation of the characteristics of the targeted formation. The composition, structure, permeability, porosity, and strength of the rock must be determined, along with formation temperature and pressure and the properties of reservoir fluids.

Furthermore, understanding reservoir mineralogy is essential to designing truly effective acidizing treatments. For most of the 20th century, acidizing oil and gas wells to optimize production gave unacceptably erratic results in primary and remedial applications. The reliability and effectiveness of acid-stimulation technology began to change for the better in the mid-1990s, driven by improved understanding of the complex chemical and physical reactions of minerals with acidizing fluids. Both fundamental and applied research, and results of field work all have confirmed that—whether in a sandstone or carbonate reservoir, a mature field, deepwater environment, or high-temperature reservoir—reliably achieving long-term production increases from acidizing requires a thorough understanding of the formation mineralogy.

Essentially, the productivity of a given well may be impaired either by the natural characteristics of the reservoir rock and fluids or by damage resulting from drilling, completion or production operations. Fracture acidizing treatments can be designed that penetrate deep into lower permeability rock.

3.1 Matrix acidizing

This process is performed below fracturing flow rate and pressure and is normally used for the removal of skin damage associated with work-over, well killing or injection fluids and to increase formation permeability in undamaged wells.

3.1.1 Protocol

It is in the removal of near-wellbore formation damage that acidizing find its primary application. With respect to acidizing, especially sandstone acidizing, assessment of formation damage is perhaps the single most important factor in treatment design. To assess formation damage, it is first necessary to know the skin term in the Darcy's law equation defining well production rate, and its effect on production rate. The production rate is directly proportional to permeability and inversely proportional to skin. Skin damage is a mathematical representation of the degree of damage present. Permeability and skin can be measured with a pressure transient well test. Formation damage can occur during any well operation, including:

- drilling;
- cementing;
- perforating;
- production;
- workover;
- stimulation.

Therefore, in assessing formation damage, all aspects of a well and its history should be investigated, including:

- reservoir geology and mineralogy;
- reservoir fluids;
- offset well production;
- production history;
- drilling history (including fluids used);
- cementing program (including cement bond logs);
- completion and perforation reports (including fluids used);
- workover history;
- stimulation history.

In order to make the most of acidizing, acid treatment design must be approached as a process. The general approach is as follows:

1- select an appropriate stimulation candidate well;
2- design an effective treatment;
3- monitor the treatment for subsequent improvement.

Treatment volumes for matrix acidizing range from 120 to 6,000 liters per meter (L/m) of targeted interval, pumped at the highest rate possible without fracturing the formation.

3.1.2 Conventional acid systems

A number of different acids are used in conventional acidizing treatments. The most common are:

- Hydrochloric, HCl
- Hydrofluoric, HF
- Acetic, CH_3COOH
- Formic, HCOOH
- Sulfamic, H_2NSO_3H
- Chloroacetic, $ClCH_2COOH$.

These acids differ in their characteristics. Choice of the acid and any additives for a given situation depends on the underground reservoir characteristics and the specific intention of the treatment, for example near well bore damage removal, dissolution of scale in fractures, etc.

Factors controlling the reaction rate of acid are: area of contact per unit volume of acid; formation temperature; pressure; acid concentration; acid type; physical and chemical properties of formation rock and flow velocity of acid. These factors are strongly interrelated.

Reaction time of a given acid is indirectly proportional to the surface area of carbonates in contact with a given volume of acid. Extremely high area-volume ratios are the general rule in matrix acidizing. Therefore it is very difficult to obtain a significant acid penetration before spending during matrix treatments.

As temperature increases, acid spends faster on carbonates. It is often necessary to increase pumping rate during acid fracturing to place acid effectively before it is spent. Pre-cooling the formation, or alternating stages of acid and water is another approach.

An increase in pressure up to 500 psi will increase spending time for HCl. Above this pressure, only a very small increase in spending time can be expected with increases in pressure.

As concentration of HCl increases, acid spending time increases because the higher strength acid dissolves a greater volume of carbonate rocks. This reaction releases greater volumes of $CaCl_2$ and CO_2, which further retards HCl.

Physical and chemical composition of the formation rock is a major factor in determining spending time. Generally, the reaction rate of limestone is more than twice that of dolomite; however, at high temperatures reaction rates tend to be nearly equal.

Velocity has a large effect on reaction rate. Retarded acids should be evaluated under flowing conditions since static tests often yield misleading results. In fracture acidizing, an increase in pumping rate increases fracture width. This decreases area-volume ratio, thereby increasing acid reaction time.

The majority of acidizing treatments carried out utilize hydrochloric acid (HCl). However, the very fast reaction rate of hydrochloric acid, and other acids listed above, can limit their effectiveness in a number of applications. All conventional acids including HCl and organic acids react very rapidly on contact with acid sensitive material in the wellbore or formation. Wormholing is a common phenomenon. The rapid reaction means the acid does not penetrate very far into the formation before it is spent. Conventional acid systems are therefore of limited effectiveness in treatments where deep acid penetration is needed. There was an early recognition that it was desirable to delay the rate of reaction of the acid and a variety of techniques have been developed to achieve this. Patents relating to several of these techniques have been issued. Further information on these retarded acid systems is given below.

3.1.3 Retarded Acid Systems

HCl and HF are two acids reacting quickly with carbonates and silicates. However, the objectives of acid treatment are to increase porosity and permeability of the medium, deeply in the formation. Methods, which have been developed to slow the acidizing process, include:

- Emulsifying the aqueous acid solutions in oil (or solvents such as kerosene or diesel fuel) to produce an emulsion, which is reacting slower.

- Dissolving the acids in a non-aqueous solvent (alcohol, gel,...).

- The use of non-aqueous solutions of organic chemicals which release acids only on contact with water.

- The injection of solutions of methyl acetate, which hydrolyses slowly at very high temperatures to produce acetic acid.

In addition to these methods, of which emulsifying the acid is probably the most important, some retardation of the reaction rate can be achieved by gelling the acid or oil wetting the formation solids. Gelled acids are used to retard acid reaction rate in treatments such as acid fracturing. Retardation results from the increased fluid viscosity reducing the rate of acid transfer to the fracture wall. However, use of the gelling agents (normally water soluble polymers) is limited to lower temperature formations as most gelling agents degrade rapidly in acid solution at temperatures above 55°C.

Some retardants can be added to the mud acid (HCl-HF mixture) to slow the reaction rate of acid with the minerals. A key is to inject a solution not containing HF explicitly but a compound able to generate HF at greater depth of penetration and longer reaction time for maximum dissolution of fines (Crowe et al., 1992). This retardant hydrolyzes in water when it enters in the reservoir to form HF according to the reaction:

$HBF_4 + H_2O \rightarrow HBF_3OH + HF$

Other retardant systems can be used as the emulsifying of the aqueous acid solutions in oil, the dissolving of the acids in a solvent (alcohol, gel…) or the injection of solutions of methyl acetate, which hydrolyses slowly at very high temperatures to produce acetic acid.

Malate et al. (1998) also proposed an acid system applicable for moderate to deep penetrations. They used a phosphonic acid complex (HEDP) to hydrolyse NH_4HF_2 instead of HCl. HEDP has 5 hydrogens available that dissociate at different stochiometric conditions. Mixture of HEDP acid with NH_4HF_2 produces an ammonium phosphonate salt and HF.

3.1.4 Other compounds: Chelating agents

Besides acids, the chelating agents are solutions used as formation cleanup and for stimulating wells especially in formations that may be damaged by strong acids (Frenier et al., 2001). If these compounds are applied in gas and oil wells, this is not yet the case in a routine mode for the development of geothermal reservoirs. They act as a solvent, increasing the water-wetting operations and dissolving (entirely or partially) some minerals containing Fe, Ca, Mg and Al.

The chelating agents are mainly used in oil and gas wells and they present as advantage to have very low corrosion rates, much lower than the one observed with HCl solutions, in the same conditions. As a consequence, the use of chelating agents needs small amounts of inhibitor to protect the casings.

Among the chelating agents, the most used are compounds of the EDTA family (EDTA: Ethylenediaminetetraacetic acid; HEDTA: Hydroxyethylenediaminetriacetic acid; HEIDA: Hydroxyethyliminodiacetic acid; NTA: Nitrilotriacetic acid). The disadvantages of using chelating agents are their high cost compared to acids and for some of them, their impact on the environment.

3.2 Fracture acidizing

Fracturing treatments are defined as treatments in which the injection rate of the fluid is larger than the fluid leakoff into the matrix of the formation. Pressure in the wellbore will therefore buildup and eventually lead to tensile failure of the rock, creating a conductive channel. Because of the reactive nature of the fluid, the addition of acid in treatments can dissolve and remove primary and secondary minerals (scales) sealing the fractures. The aim is to change the future flow pattern of the reservoir from radial to linear to effectively stimulate the reservoir and increase production.

In fracture acidizing, the ideal, but rarely achieved outcome is a fracture plane that is continuously conductive from the wellbore all the way to the tip to provide maximum production enhancement from the surrounding rock. To be effective, etched fracture surfaces must retain sufficient conductivity for production enhancement after fracture closure.

Although a large mass of rock may be dissolved, if the resultant fracture face dissolution does not render the surfaces with sufficient differential relief, the fracture conductivity under closure stress will be low at least for sedimentary rocks. If the acid spends too quickly, excessive spending and acid leakoff near the wellbore will result in little or no conductivity toward the fracture tip. Lack of active acid penetration deep along the fracture plane will result in very short conductive fractures.

Sometimes, acid fracturing was preferred to hydraulic fracturing because proppant cleanout in a well with coiled tubing required operational and safety resources. Additionally, the high conductivity of an acid-etched fracture made acid fracturing a more attractive technique if comparable fracture lengths could be achieved. After several acid fracturing treatments were experienced, it became clear that a normal response of the treated wells was a sharp production increase followed by a slight gain in average production.

Also called acid fraccing, this technique is widely used for stimulating limestone, dolomite formations or formations presenting above 85 % acid solubility. It consists to inject first a viscous fluid at a rate higher than the reservoir matrix could accept leading to the cracking of the rock. Continued fluid injection increases the fracture's length and width and injected HCl acid reacts all along the fracture to create a flow channel that extends deep into the formation. The key to success is the penetration of reactive acid along the fracture. However, the treatment volumes for fracture acidizing are much larger than the matrix acidizing treatment, being as high as 12 000 - 25 000 L/m of open hole.

Three geometric quantities are needed for proper treatment design:

- Acid penetration: distance travelled by acid at end of pumping.
- Live acid penetration: farthest point reached by live acid at end of given pumping stage (live HCl strength > 0.10%).
- Etching distance: maximum distance that etching has occurred. For a one acid stage treatment this is the same as live acid penetration.

3.2.1 Techniques

Acid fracturing is a stimulation technique where acid, usually HCl, is injected into the reservoir at fracturing pressures. Fracture acidizing is also called acid fracturing, acid-fraccing or acid-fracture treatment.

Acid (normally 15% HCl) is then injected into the fracture to react with the formation and create a flow channel (by etching of the fracture surface) that extends deep into the formation. This allows more reservoir fluid to be drained into the wellbore along the new fractures once the well is put back to production.

As the acid flows along the fracture, the fracture face is dissolved in a nonuniform manner, creating conductive or etched channels that remain open when the fracture closes. The effective fracture length is a function of the type of acid used, the acid reaction rate, and the fluid loss from the fracture into the formation. The length of the etched fracture limits the effectiveness of an acid-fracture treatment. The fracture length depends on acid leakoff and acid spending. If acid fluid-loss characteristics are poor, excessive leakoff will terminate fracture extension. Similarly, if the acid spends too rapidly, the etched portion of the fracture will be too short. The major problem in fracture acidizing is the development of wormholes in the fracture face; these wormholes increase the reactive surface area and cause excessive leakoff and rapid spending of the acid. To some extent, this problem can be overcome by using inert fluid-loss additives to bridge wormholes or by using viscosified acids.

The effective length of an acidized fracture is limited by the distance that acid travels along the fracture before it is spent. This is controlled by the acid fluid loss, the reaction rate and the fracture flow rate. This problem is more difficult to solve when the acid reaction rate is high, owing to high formation temperature.

The acid fluid-loss mechanism is more complex than that of non-reactive fluids. In addition to diffusive leak off into the formation, flowing acid leaks off dynamically by dissolving the rock and producing wormholes. Wormholes are very detrimental in fracture acidizing. They greatly increase the effective surface area from which leak off occurs and are believed to affect acid fluid loss adversely. Acid leaks off predominantly from wormhole tips rather than the fracture face. As wormholing and excessive leak-off occur, the leak-off rate exceeds the pump rate, and a positive net fracturing pressure cannot be maintained to keep the fracture open. At this point in the treatment, this may be as soon as 6 minutes after starting to pump acid, the fracture extension slows or stops.

Acid fluid loss control has long been a problem in fracture acidizing. The most common techniques involve use of viscous pads. The principle behind these is to lay an impermeable filter cake on the fracture face and minimize wormholing. In practice these filter cakes are relatively ineffective in controlling acid fluid loss because of the quick penetration in wormholes and the constant erosion of fracture faces during treatment.

The key to success is penetration of reactive acid along the fracture. This is more difficult to achieve in acid fraccing than in propped fractures (the other main form of frac treatment). Acid penetration is particularly important in low permeability formations which are frequently subject to scaling where small fractures meet larger fractures. Acid fracturing methods, which can achieve deep acid penetration, offer large potential to solve scaling problems.

3.2.2 Fluids used

To achieve deeper penetration in fracture acidizing, it is often desirable to retard acid reaction rate. This can be done by gelling (polymers and surfactants), emulsifying, or chemically-retarding the acid, in effect, making it more difficult for the H^+ ions to contact a reactive surface. Also HCl can be retarded by adding $CaCl_2$ or CO_2. Another approach is to use naturally retarded acetic or formic acid.

An ideal fracture acidizing fluid is able to penetrate long distances, etch fracture faces, increase the permeability of the matrix where the fluid enters the formation by diffusion, and remove any existing formation damage (Table 1). In addition the low viscosity of the fluid means that maximum production rate should be attained quickly following the treatment. The pad fluid used in conventional treatments would probably be needed.

Table 1: Fluid properties required from an acid fracturing fluid

Acid fracturing fluid properties required	Low viscosity
	Etches fracture face by dissolution
	Leaks off into formation mainly by diffusion
	Causes minimal formation damage
	No wormholing

Fluids used in the fracture acidizing process (pad fluid, acid or additives) can be detrimental to well performance following the job. This can be due to clean up problems or a reduction in the formation permeability adjacent to the fracture. A particular problem is the removal of high viscosity fluids. The time required to achieve cleanup increases significantly as fluid viscosity increases. Similar increases in cleanup time are seen as fracture length increases.

Ideally the best acid system for fracturing is one that only etches the fracture face by dissolution and leaks off into the formation mainly by diffusion. It is also very desirable to be able to obtain deep penetration along fractures without resorting to the use of high viscosity components.

3.2.3 Typical treatment modes

Acid solubility of the formation is a key factor influencing whether fracture acidizing or proppant treatments should be employed. If the formation is less than 75% acid soluble, proppant treatments should be used. For acid solubilities between 75 and 85%, special laboratory work can help define which approach should be used. Above 85% acid solubility, fracture acidizing would be the most effective approach.

There are four primary fracture acidizing processes:

- Fluid-loss control strives to contain the acid in natural/ created fractures.
- Conductivity enhancement pumps a viscous fluid padpumped ahead of the acid to generate a fracture geometry. Subsequent acid injection then fingers through the viscous pad. The process results in longer acid penetration distances and more effective conductivity at a greater distance along the induced fracture.
- Etched height control uses fluid density differences to control fluid placements, such as avoiding water-producing zones or gas caps.
- Tailored treatments may include foamed acids, heated acids, zonal coverage acid, and closed-fracturing acid.

Fluid-loss control is critical for achieving a good fracture acidizing treatment. Acid leakoff can be controlled by viscosifying the acid, adding solid particulates or using alternate stages of acid and nonacid fluids. Methods for thickening acid include emulsified acid, foamed acid, polymer gelled acid, and surfactant gelled acid. Silica flour and 100-mesh sand are common solid particulates.

In larger open hole, acid diversion is important, otherwise only the interval, which breaks down or fractures first will be treated. Diversion can be achieved with packers.

The following techniques have been developed:

- Viscous preflush in fracture acidizing.
- Chemically retarded acid for selective etching.
- Combination of density and viscosity controlled fracture acidizing.

Various acid combinations are employed. However, a frequent mixture is 15% HCl and 10% acetic acid. A typical treatment consists of pumping the acid mixture at pressures of 0.1 to 0.3 bar per meter. When acid is pumped at high rates, over 1000 liters per minute, it is called fracture acidizing. Several services companies offer some or the whole series of chemical treatments for oil, gas or geothermal wells as shown on figure 1.

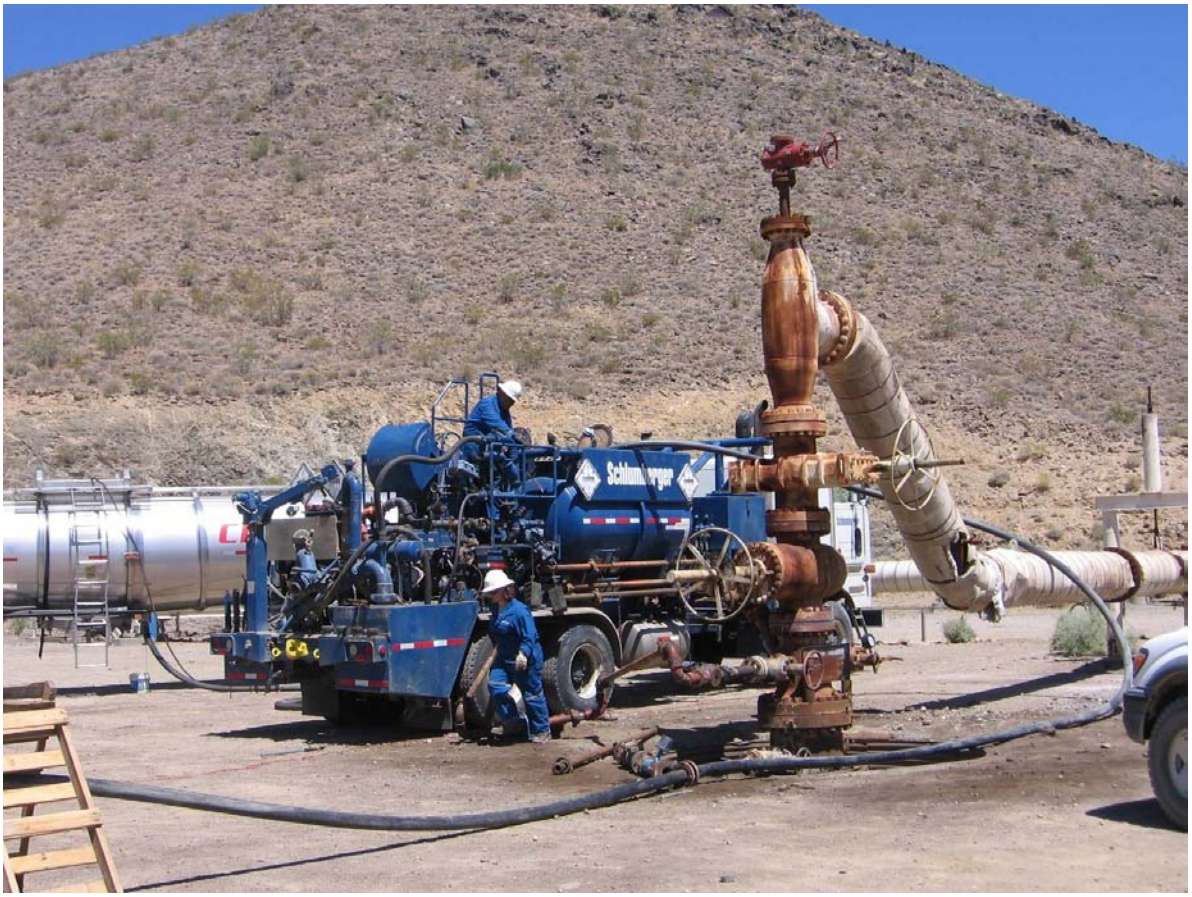

Figure 1: Installation of a pumping unit for injection of chemical compounds at Coso geothermal field (photo P. Rose, EGI, Univ. of Utah)

4 Chemical stimulation in sandstone reservoirs

The objective of acidizing sandstone wells is to increase permeability by dissolving clays and other pore plugging materials near the wellbore. Clays may be naturally occurring formation clays or those introduced from drilling, completion or workover fluids.

Treatment fluid selection in sandstone formations is highly dependent on the mineralogy of the rock as well as the damage mechanism. Hydrofluoric (HF) acid is typically used to dissolve the damaging silicate particles. Nonacid systems are sometimes used to disperse whole mud and allow it to be produced with the treating fluid. The criteria for selecting the treating fluid are mineralogy, formation damage mechanism, petrophysics and well conditions.

The treating fluid, therefore, must remove existing damage without creating additional damage through interactions with the formation rock or fluids. A formation is sensitive if the reaction between the rock minerals and a given fluid induces damage to the formation. The sensitivity of a formation to a given fluid includes all the detrimental reactions that can take place when this fluid contacts the rock. These detrimental reactions include the deconsolidation and collapse of the matrix, the release of fines or the formation of precipitates. The precipitation of some damaging compounds cannot be avoided. Treating and overflush fluid stages are sized; so, there is sufficient volume to push potential precipitates deep enough into the reservoir to minimize their effects because of the logarithmic relationships between pressure drop and distance from the wellbore.

Sandstones can be sensitive to acid depending on temperature and mineralogy. Ions of silicon, aluminum, potassium, sodium, magnesium and calcium react with acid and can form precipitates at downhole temperatures, once their solubility product is exceeded. If these precipitates occur in the near wellbore area, they can damage the formation. Sensitivity depends on the overall reactivity of the formation minerals with the acid. Reactivity depends on the structure of the rock and the distribution of minerals within the rock, i.e., the probability of the acid reaching the soluble minerals.

The sensitivity of sandstone will also depend on the permeability of the formation. Low permeability sandstones are more sensitive than high-permeability sandstones for a given mineralogy. Acid formulations should be optimized on the basis of a detailed formation evaluation (Davies *et al.*, 1992, Nitters and Hagelaars, 1990).

4.1 Sandstone acidizing process (treatment design)

There are a limited number of reasons why sandstone acidizing treatments do not succeed.

The six-step process to successful sandstone acidizing is as follows:

1. determine the presence of acid-removal skin damage;
2. determine appropriate fluids, acid types, concentrations, and treatment volumes;
3. determine proper treatment additive program;
4. determine treatment placement method;
5. ensure proper treatment execution and quality control;
6. evaluate the treatment.

All sandstone acid treatments are variations of the following maximum step procedure:

1. formation water displacement;
2. acetic acid stage;
3. HCl preflush stage;
4. main acid (HF) stage;
5. overflush stage;
6. diverter stage;
7. repeat steps 2-7 (as necessary);
8. final displacement stage.

Sandstone acidizing reactions occur where the fluids meet minerals. As fluid is injected, the position of the zone where reactions take place moves radially outward from the wellbore. As the acid moves through the near wellbore region where all acid soluble minerals have been dissolved, it retains its full

strength. Acid spending takes place in the reaction front. The radial width of this zone depends on the minerals present and the temperature of the reservoir at the point of contact, which is affected by any residual cool down effects due to difference between fluid and rock temperature. When the injected fluid is totally spent, it moves through the unreacted minerals.

The primary reactions occur when fresh acid contacts fresh reservoir. This typically happens in the near wellbore region. As spent acid moves through this same matrix, the secondary and tertiary reactions occur with the reaction products precipitating further away from the wellbore. It is important to keep the injected fluid moving to carry reaction products past the critical matrix region of the well.

Proper treatment design can be very effective in decreasing the negative effects of pumping acids into sandstone through the use of multiple injection stages and correct fluid selection. A typical matrix treatment in a sandstone will include a preflush, a main fluid and an overflush. When long intervals are treated, diversion stages are pumped after the overflush and before the next stage of preflush.

4.1.1 Preflush

The sequence of fluids used in a sandstone treatment is largely dependent on the damage type(s) being addressed.

A preflush is a fluid stage pumped ahead of the main treating fluid. Multiple preflush stages are sometimes used to address multiple damage mechanisms and prepare the surface for the main treatment fluids. In sandstone reservoirs, the acid preflush, performed most often with a HCl solution, serves two purposes:

- To displace the formation brines, usually containing K, Na, or Ca ions, away from the wellbore so there will be no mixing with HF acids. This decreases the probability of forming alkali-fluorosilicates such as potassium hexafluorosilicate.

- To dissolve as much of the calcareous material as possible, prior to injection of the HF acid to minimize calcium fluoride precipitation.

Due to reservoir heterogenities, it is unlikely that the acid preflush will remove all of the calcite. However, it has been shown that reducing calcite below 6% is sufficient to avoid precipitation (Figure 2). This has been investigated and confirmed by fieldwork done by McLeod (1984) and others. Strength and volume guidelines are based on this criterium (Economides and Nolte, 1987).

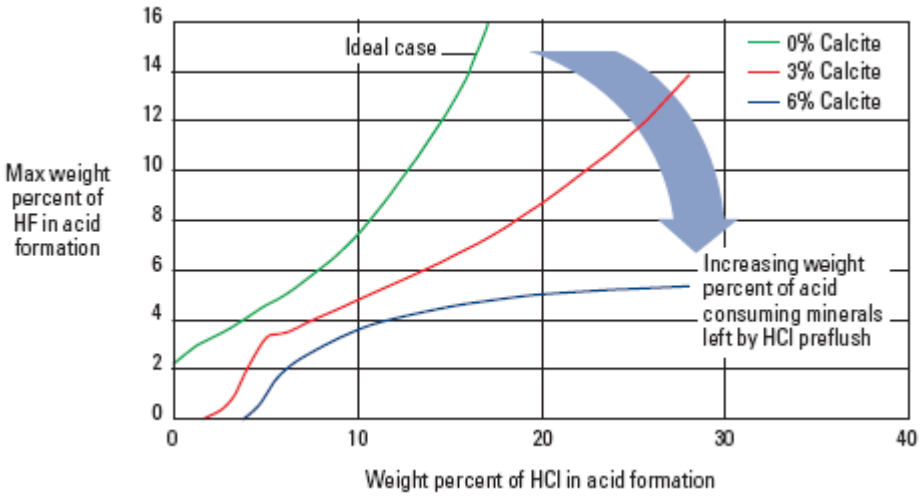

Figure 2: HCl/HF ratio to avoid precipitation, based on AlF_3 and CaF_2 precipitation (Schlumberger, 2003)

HCl can shrink hydrated clays, however, most clays have very little solubility in HCl. One possible exception is chlorite, an iron-rich, three-layer clay. Strong HCl can leach Fe^{2+} iron (and possibly aluminium and magnesium) from chlorite, leaving an amorphous silica residue. HCl does not dissolve sand. However, HCl can dissolve carbonates present in sandstone formations.

Using an additional ammonium chloride (NH4Cl) brine preflush for sandstone acid treatments is an emerging practice. This preflush conditions the formation clays as it moves formation water away from the near wellbore area. The $NH4^+$ ions in the brine exchange with the alkali (Na, K, or Ca) ions on the

clay particles; so, they will be displaced from contact with the mud acid. The effectiveness of this procedure appears to be controlled by the brine concentration at a radial distance of 0.75 m from the wellbore. This preflush is pumped at the start of the job to establish injectivity before the regular mud acid treatment is pumped. It is only pumped once and is not a part of the regular treating sequence.

4.1.2 Main flush

The main fluid in a sandstone acid treatment is the fluid used to remove the damage. It is typically a mixture of hydrofluoric (HF) and hydrochloric (HCl) or organic acids. HF acid is used because it is the only common, inexpensive mineral acid able to dissolve siliceous minerals. It is mixed with HCl or organic acid to keep the pH low when it spends to aid in prevention of detrimental precipitates. These mixtures are called mud acids because they were originally developed to treat siliceous drilling mud damage. HF acid should not be used in sandstone formations with high carbonate content. The risk of forming calcium fluoride precipitates is too great, since it is unlikely that a sufficient amount of HCl acid preflush can be pumped. The accepted cutoff point for the use of hydrofluoric acid is 20% calcite + dolomite based on the guidelines developed by McLeod in 1984.

Hydrofluoric acid (HF) can dissolve carbonates, clays felspars, micas, chert and quartz. However, the primary reason to use HF acid is to remove clay. If any carbonates are present in a sandstone, these should be removed with a preflush of HCl. If a sandstone formation contains more than 20% carbonate, the well should be acidizied with HCl only. Table 2 shows the chemical composition of minerals that are typically present in sandstones and generalizes the solubility of these minerals in HCl and HCl-HF.

Table 2: Solubility of sandstone minerals

Minerals	**Solubility**	
	HCl	**HCl-HF**
Quartz	No	Very low
Felspars	No	Low to moderate
Micas	No	Low to moderate
Kaolinite	No	High
Illite	No	High
Smectite	No	High
Chlorite	Low to moderate	High
Calcite	High	High, but CaF_2 precipitation
Dolomite	High	High
Ankerite	High	High
Siderite	High	High

During the mainflush, the HF acid reacts mainly with the associated minerals of sandstones (clays, feldspars and micas), rather than with quartz. The reaction rates of HF with clays or feldspars are 100 to 200 times faster than the one with quartz. It results from these reactions an enlargement and interconnections of the pores in the matrix, facilitating fluid flow. The risk of using HF acid is the strong affinity of Si and Al with F, which can cause the precipitation of silicium or aluminum complexes (SiF_6^{2-}, AlF^{2+}, AlF_2^{+}, AlF_3, AlF_4^{-}), then damaging the formation by plugging. This is why HCl is added to HF: hydrochloric acid keeps a low pH and prevents the formation of fluorosilicates, fluoroaluminates, and fluoride salts.

The trend in HF acid concentration is away from the previous standard 3% HF + 12% HCl.

1.5% HF + 13.5% HCl is becoming the normal choice and Table 3 shows general recommandations for specific well conditions.

Table 3: Alternate sandstone acid procedures for specific formation conditions

Well and formation conditions	Treatment fluid recommandation
Bottomhole treating temperatures > 100°C	1.5% HF + 13.5% HCl
Permeability < 5 md	1.5% HF + 13.5% HCl
Quartz content: Over 90% 50 to 90%	 3% HF + 12% HCl 3% HF + 12% HCl or retarded HF
Feldspar, 15 to 30%	1.5% HF + 13.5% HCl
Chlorite clay: 1 to 5% > 5%	 3% HF + 10% Acetic 1.5% HF + 10% Acetic or Formic

4.1.3 Overflush

The overflush is an important part of a successful sandstone acid treatment. It performs the following functions:

- Displacement of the nonreacted mud acid into the formation.
- Displacement of the mud acid reaction products away from the wellbore.
- Removal of potential oil-wet relative permeability problems caused by some corrosion inhibitors.

The overflush fluid must be miscible with the acid in order to displace it. Therefore, aqueous base liquids should be considered as the first displacing and flushing fluid. This may be followed by other fluid systems depending on the concerns and well conditions. Studies of displacement fronts indicate that the reactivity and fluid character of the overflush have a major influence on the volume required to displace the spent mud acid. Recent experience indicates the advantage of including HCl or acetic acid in the first part of the overflush to maintain a low-pH environment for the displaced spent mud acid stage. The minimum total overflush volume should provide at least 0.9 m of radial penetration into the formation to move potential problems past the critical matrix where the greatest pressure drop occurs. Damage effects are minimized beyond the critical matrix because of the logarithmic relationship between pressure drop and distance from the wellbore. Volumes that are less than twice the mud acid stage volume should be considered inappropriate. Formation permeability anisotropy may require doubling or even tripling this volume, if the reservoir pressure is sufficient to unload the injected fluid.

Large overflushes help prevent the near wellbore precipitation of amorphous silica. At formation temperatures of 93°C or greater, amorphous silica precipitation occurs while the mud acid is being pumped into the formation. The precipitate is somewhat mobile at first, but it can set up as a gel after flow stops. If this potentially damaging material is kept moving by the overflush fluid, it will be diluted and moved beyond the critical matrix.

4.2 Acid strength versus composition of the formation

The acid used as a preflush or an overflush to a main treatment containing hydrofluoric acid depends on the silt and clay content of the formation, its permeability and the presence of HCl sensitive minerals, like chlorite, glauconite and zeolites. For operational simplicity, the same acid is used for both pre- and overflush. Organic acids are recommended for use in conjunction with, or instead of, HCl in sensitive formations. Although they will dissolve the carbonate, they work more slowly. When pumping organic acids as stand-alone fluids, they should be mixed in ammonium chloride rather than fresh water. Organic acids also act as a low-pH buffer and complexing agent that helps minimize the tendency of iron compounds to precipitate as the acid spends. However, they do not dissolve iron scale or prevent clay swelling.

Determining the proper blend of HCl and HF to use in a mud acid mixture, and whether HCl or organic acid is used, is a complex process. The selection depends on the silt and clay content of the formation, its permeability and the presence of HCl sensitive clays. The criteria are similar to those for choosing the acid preflush or overflush concentration.

For the preflush operation in acidizing treatments, a solution of hydrochloric acid at a concentration of 10 to 15 % is most often used. For the mainflush, the mud acids generally range from 10 % HCl – 5 % HF to 12 % HCl – 3 % HF. Some examples of mud acids are given in Table 4 for the treatment of sandstones.

Table 4: Acid guidelines for the chemical treatment of sandstones according to the composition of the formation (after Crowe et al., 1992)

Temp. (°C)	Rock mineralogy (%)	Rock permeability (milliDarcy [md])					
		> 100 md		20 to 100 md		< 20 md	
		HCl (%)	HF (%)	HCl (%)	HF (%)	HCl (%)	HF (%)
< 100	High quartz (> 80), low clay (< 10)	12	3	10	2	6	1.5
	High clay (> 10), low silt (< 10)	7.5	3	6	1	4	0.5
	High clay (> 10), high silt (> 10)	10	1.5	8	1	6	0.5
	Low clay (< 10), high silt (> 10)	12	1.5	10	1	8	0.5
> 100	High quartz (> 80), low clay (< 10)	10	2	6	1.5	6	1
	High clay (> 10), low silt (< 10)	6	1	4	0.5	4	0.5
	High clay (> 10), high silt (> 10)	8	1	6	0.5	6	0.5
	Low clay (< 10), high silt (> 10)	10	1	8	0.5	8	0.5

The cleaner the sandstone (lower silt and clay content) and the higher the permeability, the lower the HCl/HF ratio, and the more aggressive the treatment can be. Typically, the HCl/HF ratio is either 4/1, 6/1, or 9/1. A higher volume of weak acid must be pumped to attain the same results as a smaller volume of a stronger acid. This is an important consideration when designing treatments for environmentally sensitive areas, where disposing spent acids can create problems. The ratio of HCl/HF should be increased if the formation contains clay rather than calcite cementing materials. If the HCl/HF ratio is less than 9/1, change the recommendation to the 9/1 ratio that contains a lower HF content. For example, if a 6% HCl + 1% HF fluid is normally used, change to a 4.5% HCl + 0.5% HF mixture. Mud acids should only be used in formations with less than 20% carbonate (calcite + dolomite) because of the increased risk of forming damaging calcium fluoride precipitates at higher carbonate content. HCl or acetic acids are used for these formations. The specific acid used is dependent upon reservoir temperature and the presence of HCl sensitive clays as shown in Table 4.

4.3 Review of current practices to successful sandstone acidizing

The rate of acid injection is dictated by allowable injection pressure. Selection of acid concentrations must be based on the formation characteristics. Knowledge of permeability, porosity and mineralogy is imperative. Amounts and types of clays and felspars are especially important to ascertain. This information can be obtained trough X-ray diffraction analysis. However, the location of minerals is of greatest importance. SEM (scanning electron microscopy) and thin-section analysis are additionally useful in identifying locations of quartz, clays, feldspars, carbonates, and other minerals.

For HCl-HF mixtures, a small amount of acetic acid (e.g., 3%) may be added to reduce precipitation of aluminium fluoride compounds, as the pH of the HCl-HF mixture rises with acid spending, by buffering the acid mixture and by complexing with aluminium, chelating effect.

Corrosion inhibitor is always necessary. It must be added to all acid stages (acid preflush, main acid, and acid overflushes). It is the “dilute” acid mixtures, like 15% HCl, that have a lot of water present that are corrosive. If concentrated HCl (37% solution) is pumped, corrosion inhibitor is not necessary. That is water present (more than 63% by weight) in acid mixture that causes corrosion.

Iron control is required in any acidizing treatment. Therefore, an iron-control agent is almost always needed. Products exist in two general categories: iron-complexing or iron-sequestering agents, and iron-reducing agents. One or more of these can be used in an acid mixture. Combinations can be

effective, especially at higher temperatures, where dissolved iron contents may be high. Iron-control agents react with dissolved iron and other dissolved metal ions to inhibit solids precipitation by maintaining iron cations in solution, as acid spends and pH increases.

A clay stabilizer is often recommended but not necessary for the purpose of preventing migration and/or swelling of clays following an acid treatment. Common clay stabilizers are either polyquaternary amines (PQA) or polyamines (PA), at 0.1-0.4%. Clay stabilizer seems to be most effective when added to the overflush only.

It may be advisable to include a calcium sulphate ($CaSO_4$) scale inhibitor in the acid stages or the overflush if treating a well containing high sulphate concentration (>1000 ppm) in the formation water. $CaSO_4$ scale inhibitors are typically phosphoric acid or polyacrylate polymers.

Coiled tubing (CT) is a very useful tool for improving acid placement. Coiled tubing utility is versatile. However, when applied properly, it is an excellent tool. Coiled tubing is of less use in fracturing acidizing because of rate limitations. It is still best to pump fracturing treatments through larger strings, such as production tubing. Coiled tubing is most useful in matrix and wellbore treatment. It offers some major advantages in acidizing, including:

- Ease with which an acid injection can be terminated, if it appears that continuing injection is not doing any further good, and switch to flush.
- Ease with which treatment displacement with nitrogen can be achieved quickly to push reactive fluids away from the wellbore, energizing the near-wellbore fluid zone, thereby enhancing flowback.

Disadvantages include:

- Pump rate limitations.
- Depth limitations in openhole sections of very deep deviated wells. But some experiments report coil tubing applications up to a depth of 4000 m.
- If solids are needed (perhaps for diversion), there may be problems pumping them through smaller diameter CT strings.
- Acid mixtures must be very thoroughly mixed and must remain that way prior to and during injection. Corrosion in a CT string is especially disastrous.

Overall, coiled tubing is very effective in placing acid, especially in smaller treatments, and treatments for damage very near the wellbore. Treatment evaluation involves the following:

- Pressure monitoring during injection will indicate diverter effectiveness and possibly evolution of skin removal. These methods for evaluating pressure responses are based on interpreting recorded wellhead pressure values and corresponding injection rates as treatment progresses.
- Flowback sample analysis is important for observation of sludge, emulsion, solids production, and related problems.
- Production rate comparison and analysis (before and after) is the most obvious and simple measure of success. Rate comparison should only be made seriously after all spent acid has been returned and well production has returned to formation fluids only.
- Well test analysis (skin removal). Post-stimulation well testing is the truest indicator of success or failure.
- Payout and ROI (return on investment) are among the bottom-line factors to the operator. Relative low-cost formation damage removal treatments, such as acidizing, are unrivaled in their potential financial significance.

Recently, there have been advancements with unconventional methods introduced to the industry by creative, reasonable risk-taking, stimulation design engineers. Some examples of such interesting methods are:

- Maximum rate/maximum pressure HF acidizing.
- High-concentration HF acidizing.
- CO_2-enhanced HF acidizing.
- On-the-fly minimum volume HF acidizing.

4.4 Acidizing damage

Acidizing damage mechanisms include:

- Inadvertent injection of solids.
- Use of incompatible additives or improper mixing procedures.
- Reprecipitation of acid reaction products.
- Loss of near-wellbore formation compressive strength.
- Formation of emulsions.
- Formation of sludge.
- Water blocking.
- Wettability alteration.
- Post-treatment fines migration.

The reprecipitation of reaction products is a serious concern in sandstone acidizing containing alumino-silicates. Many reactions take place in the formation as HF injection proceeds.

The chemical reactions between sandstone minerals and HF acids have been extensively described in the literature. There are three classes of HF reactions: primary, secondary and tertiary.

Primary reactions describe the action of the unspent acid with the various minerals. The presence of calcium (Ca^{2+}) will cause calcium fluoride (CaF_2^+) to precipitate. Sodium (Na^+) and potassium (K^+) can create alkali-fluorosilicates and alkali-fluoaluminates when formation minerals, or sodium or potassium brines, react with the hexafluorosilicic acid produced by this reaction. The fluosilicate and fluoaluminate compounds are more likely to form during the initial phases of the dissolution, since a high concentration of HF relative to the clay enhances the reaction. Precipitation of these compounds will occur when the amount present increases above the solubility limit.

Secondary reactions result from the action of the hexafluorosilicic acid with remaining acid and the rock. The driving force for this reaction is the greater affinity of fluorine for aluminum than for silicon. Silica gel precipitation is well documented. This precipitation occurs when the initial HF is nearly consumed. An exchange reaction occurs on the surface of the clays and fines to generate fluoaluminates and silica gel. The silica is deposited on the surface of the mineral particles, and the fluoaluminates remain in solution. This precipitate is more like to occur when fast-reacting aluminosilicates, such as clays, are present. The damaging effect of silica gel precipitates is still a point of debate; however, it does appear that they are more damaging at higher than lower temperatures.

Tertiary reactions are the reactions of the aluminum fluorides and aluminosilicates. The reaction is insignificant at temperatures below 90°C. At higher temperature, the reaction can be considerable depending on the stability of the formation clays with HCl. As the reaction drives on, and HF is spent, complex aluminofluorides may be precipitated out deep in the matrix. Kalfayan (2001) recommendations of 9% HCl + 1% HF are based on these observations.

Post-treatment fines migration is quite common in sandstone acidizing. It may be difficult to avoid in many cases. The reaction of HF with clays and other aluminosilicates minerals, and quartz, can release undissolved fines. Also, new fines may be generated as a result of partial reaction with high-surface-area minerals, particularly the clays. Postacidizing fines migration problems can be reduced by bringing a well on slowly after acidizing, and increasing rate step-wise over time (e.g., one to two weeks), rather than maximizing return production right away.

Besides that, dissolved iron precipitate as iron compounds when acid spends. Iron is another potential source of precipitation during sandstone acidizing. Precipitation is due to the formation of colloidal ferric hydroxide as the acid spends (pH > 2). Sources of ferric iron (Fe^{3+}) include some minerals (chlorite and glauconite clays) and tubing rust (iron oxide). These reactions begin to precipitate gelatinous ferric hydroxide at a pH of 2.2. The nature of the precipitate (crystalline or amorphous) varies as a function of the anions present (Smith *et al.*, 1969). Precipitation of ferric hydroxide during acid injection is normally not a problem, if an adequate HCl tubing wash was used to remove most of the soluble FeO_2. All acids used for matrix treatments should also contain iron control additives, either sequestering or reducing agents or both. Ferrous iron (Fe^{2+}) is typically not problematic, since ferrous hydroxide precipitates at a pH between 7.7 and 9.

The main sources and causes of precipitates formed during sandstone matrix acidizing are summarized in Table 5. The formation of these potentially damaging precipitates is affected by the complex mineralogy of many sandstones.

Damage can be caused during hydraulic fracturing operations too.

Table 5: Possible precipitates in sandstone acidizing (Schlumberger, 2003)

Precipitate	Origin
Calcium fluoride (CaF_2)	Carbonate-HF reaction CaF_2 can be caused by an inadequate HCl preflush to remove calcium ions from calcite cementing materials or to flush calcium chloride completion fluids away from the near wellbore.
Amorphous silica	Clay and silicate dissolution in HF. Amorphous silica results from both secondary and tertiary HF acidizing reactions.
Sodium and potassium fluorosilicates	Feldspar and illite clay dissolution in HF produce these primary reaction products. They can also form if seawater or sodium or potassium brines are mixed with spent HF.
Sodium and potassium fluoaluminates	Silico-aluminate dissolution in HF. Fluoaluminates, like fluorosilicates, occur when spent mud acid (H_2SiF_6) reacts with the formation. They can also form if seawater or sodium or potassium brines are mixed with spent HF.
Aluminium hydroxides and fluorides	Clay and feldspar dissolution in HF can cause these precipitates.
Iron compounds	Iron minerals or iron oxides (rust) can react with HCl-HF to produce these compounds.

4.5 Completions versus composition

To help improve completions for reservoirs rich in one or more of the minerals listed in Table 6 special consideration should be given to drilling procedures and to treatments/stimulants with the aim of minimizing damage or considering remedial treatments.

Table 6: Mineral – related procedures for completions

Mineral	Potential Effect	Maximizes Damage	Minimizes Damage	Remedy
Smectite	swelling	fresh water, HF	air, KCl, oil-based mud drilling	HCl; re-perforate. & fracturing
Mixed Layer Clay	swelling; mobile fines	fresh water, HF	air, KCl, oil-based mud drilling	HCl; re-perforate. & fracturing
Kaolinite	mobile fines	HF	air, foam drilling	clay stabilized; low flow rates
Chlorite	iron gel precipitate	high pH muds; O_2 rich	air, foam; HCl sequestered	HCl sequestered, low strength
Carbonate minerals	complex CaF precipitates	HF	salt muds; oil-based mud	HCl
Quartz, Feldspar Glass (silt)	mobile fines; gel precipitate	high pH muds	air, foam; bland fluids	clay stabilized; foam fracturing

5 Geothermal wells acidizing procedures

Acidizing geothermal wells is related to sandstone acidizing in that most geothermal reservoirs produce from volcanic rocks (andesite). Formation conditions are often conducive to large-volume, high-rate acid treatments. In geothermal wells, the strongest indication of acid-removable formation damage is a sharp drop in production rate. Nearly all geothermal wells that are acidizing candidates have been damaged by:

- Drilling mud solids and drill cuttings lost to the formation fractures.
- Scale (calcium carbonate, silica, calcium sulphate, and mixtures).

Various methods have been tried to prevent scaling in geothermal wells, including varying pressure, temperature or pH changes and scale inhibitors. If scale inhibitors have solved many problems, one promising alternative method is the acidizing.

One thing geothermal wells have in their favour is that complete damage removal is not necessary. Partial removal of damage with acid treatment may eventually result in complete damage removal when the treated well produces back. The high-rate and high-energy backflow from geothermal wells can blow out damage that was not dissolved by acid. Damage that was softened, broken up, or detached from downhole tubulars and fracture channels can be produced back through a large diameter casing completion. Erosion of production lines may occur if drill cuttings are produced back during blow down of a well after stimulation. Care must be taken in this regard. A temporary flow line may be required until solids production has stopped.

A very successful method of acidizing geothermal wells has been a basic, high-rate, brute-force method. High acid concentrations have been shown to be effective in geothermal wells producing from natural fractures not containing separate, large carbonate zones.

Hydrochloric acid (HCl), hydrofluoric acid (HF) or both have been used since the 1980's in hydrothermal wells. Strawn (1980) listed yet these two acids as the most effective ones. HCl was selected to treat limestone, dolomite and calcareous zones whereas HF was used to dissolve clay minerals and silica.

The only acid additives necessary in a geothermal acid job are:

- Corrosion inhibitor and inhibitor intensifier (often required).
- High-temperature iron-control (reducing) agent.

Water-wetting surfactants, necessary in oil well stimulation, are not needed in geothermal wells because of the absence of hydrocarbons. Suspending agents (nonemulsifier surfactants) are also not needed, although they seem to be included often in geothermal well stimulation job proposals. Clay stabilizer is not needed.

Conventional acid placement techniques are less effective for the long, open-hole or liner-completed intervals typically encountered in geothermal wells. High-temperature foam systems may improve zone coverage. Gelling agents for thickening acid have been shown to be ineffective in geothermal liner completions. The best way to maximize acid coverage in geothermal wells is by pumping at maximum injection rates.

During the 1990's, the acidification technique has been used more often, principally for the reservoir development or to treat formation damage caused by drilling mud and scaling (mineral deposits) in geothermal wells (Buning et al, 1995; Buning et al, 1997; Malate et al., 1997; Yglopaz et al., 1998; Malate et al., 1999, Barrios et al., 2002, Jaime-Maldonado and Sánchez-Velasco, 2003). This protocol has not really evolved since these years. In each of the experiments proposed by the authors, the same technique is used. The acidification occurred in three main steps:

1. A preflush, usually with hydrochloric acid (10%). The objective of this preflush is to displace the formation brine and to remove calcium and carbonate materials in the formation. The preflush acid minimizes the possibility of insoluble precipitates.
2. A main flush with hydrochloric – hydrofluoric acid mixture. A mixture of 10% HCl – 5% HF (called Mud acid) is generally prepared by dissolving ammonium bifluoride (NH_4HF_2) in HCl. A mixture of 1% of HCl and 56 kilos of NH_4HF_2 will generate 1% HF solution. Regular mud acid (12% HC l- 3% HF) is made from 15% HCl, where 3% HCl is used to hydrolyse the fluoride salts.
3. A postflush/overflush usually by either HCl, KCl, NH_4Cl or freshwater.

Concerning the injected amounts for the cleaning out of the geothermal wells, the mainflush volume was based on a dosing rate of 900 liters per meter of target payzone. The preflush volume was based on a dosing rate of 600 liters per meter of target zone (Malate et al., 1997; Barrios et al., 2002).

In geothermal well acidizing, more acid often is better. Naturally fractured volcanic formations can withstand high HF concentration. The HCl-HF stage can be 10% HCl - 5% HF, or 10% HCl - 7% HF, for example. These acid mixtures have been used successfully in stimulating geothermal wells in Southeast Asia (the Philippines), where a large number of acid treatments have taken place. Acid volumes can vary quite a bit. These acidizing treatments have also employed an acid formulation containing 3% HCl - 5% HF and an organophosphonic acid. The mixture is less corrosive and may help slow scale reprecipitation, as the phosphonic acid complexes with certain cations in spent acid.

HCl-HF mixture dissolves clays originating from drilling mud and reacts with most constituents of the sandstone formation. It results from these reactions an enlargement and interconnections of the pores in the matrix, facilitating the fluid flow. But, it seems that rapid acid consumption with clays and silicates, matrix disintegration in near wellbore and subsequent precipitation of various reaction byproducts (i.e. complex fluorosilicates, fluoaluminates, and fluoride salts) have somewhat restricted the usefulness of mud acid for matrix stimulation treatment. A new acid treatment system (called sandstone acid) is used in treating sandstone formations at some geothermal wells in the Philippines. The new HF acid compared with the usual mud acid systems has a lower reaction rate and a limited solubility action on clays but higher reaction rate and dissolving power with quartz (Malate et al., 1998).

Some retarded or slow reacting HF acid such as fluoroboric, fluoroaluminic and hexa-fluoro-phosphonic were developed to improve rock permeability. Most of these acid systems rely on the use of weak organic acids and their secondary reactions to slowly generate HF acid. Malate et al. (1998) proposed a new acid system applicable for moderate to deep penetrations. They used a phosphonic acid complex (HEDP) to hydrolyse NH_4HF_2 instead of HCl. HEDP has 5 hydrogens available that dissociate at different stochiometric conditions. Mixture of HEDP acid with NH_4HF_2 produces an ammonium phosphonate salt and HF. 76 liters of HEDP acid per 3785 liters of water are required to react with approximately 56 kilos of NH_4HF_2 to produce a 1% HF solution.

The advantages of sandstones acid are:

- Limiting clays dissolution and preventing disintegration of pore matrix by coating them with a film blocking reactions.
- Sandstone acid has better dispersing properties and is an excellent antiscalant inhibiting precipitates formation in the vicinity of the well.
- Excess HCl are not needed to avoid the fluoride salt precipitates. As a consequence, sandstone acid aids in reduction of corrosion.

All these protocols are listed in Schlumberger (2003). However, these properties of acid mixtures should be investigated if one wishes to influence the fractures properties beyond a radius of 5 meters around the wells.

Treatment volumes, injection rates, acid placement techniques, acid system selection and evaluation of the results when stimulating geothermal wells, all follow the same criteria as for oil wells. The important difference is the formation temperature. High temperature reduces the efficiency of corrosion inhibitors (and increase their cost) as well as increasing the acid/rock reaction rate. The high acid rock reaction rate requires the use of a retarded acid system to ensure acid will not all be spent immediately next to the wellbore, but will penetrate deeper into the formation. Protecting the tubulars against corrosion is another serious challenge. This requires careful selection of acid fluids and inhibitors (Buijse et al., 2000), while cooling the well by injecting a large volume of water preflush may reduce the severity of the problem.

6 Review of the chemical treatments in geothermal reservoirs

A study of the literature on acidification of geothermal reservoirs has been attempted. The majority of the papers concern the cleaning out of geothermal wells.

The cleaning out of geothermal wells to increase their productivity after scaling deposits constitutes the main application of the acid treatments. This technique has been used extensively in some geothermal fields in the Philippines (Buning et al, 1995; Buning et al, 1997; Malate et al., 1997; Yglopaz et al., 1998; Malate et al., 1999, Jaime-Maldonado and Sánchez-Velasco, 2003, Amistoso et al., 2005), in El Salvador (Barrios et al., 2002) and in USA (Morris et al., 1984; Entingh, 1999). It presents interesting results, such as the well injectivity increasing by 2 to 10-folds according to the studied reservoirs.

At the Larderello geothermal field (Italy), several stimulation methodologies have been used successfully by ENEL (Capetti, 2006). Among them, chemical stimulation operations were carried out by injection of acid mixtures. First, various laboratory tests were realised on reservoir rock samples to optimize the HCl/HF ratios and the effect on mineral dissolution. Field tests have shown impressive results on five deep wells for reservoir rocks composed of phyllites, hornfels and granites: the improvement of injectivity, respectively productivity ranged from a factor 4 to 10.

In the field of EGS, few chemical treatments have been applied to stimulate fractured reservoirs. Since 1976, some experiments have been tried with more or less of success at Fenton Hill (USA) and Fjällbacka (Sweden). At Coso geothermal field however, 24 wells were successfully treated.

A summary of the chemical stimulation experiments carried out on geothermal fields and EGS reservoirs are presented in Table 7.

Table 7: Results of HCl-HF treatments for scaling removal and connectivity development

Geothermal field	Number of treated wells	Variation of the injectivity index before and after acid treatment (kg/s/bar)	Improvement factor
Bacman (Philippines)	2	0.68 → 3.01 0.99 → 1.4	4.4 1.4
Leyte (Philippines)	3	3.01 → 5.84 0.68 → 1.77 1.52 → 10.8	1.9 2.6 7.1
Tiwi (Philippines)	1	2.52 → 11.34	2.6
Mindanao (Philippines)	1		2.8
Salak (Indonesia)	1	4.7 → 12.1	2.6
Berlín (El Salvador)	5	1.6 → 7.6 1.4 → 8.6 0.2 → 1.98 0.9 → 3.4 1.65 → 4.67	4.8 6.1 9.9 3.8 2.8
Las Tres Virgenes (Mexico)	2	0.8 → 2.0 1.2 → 3.7	2.5 3.1
Los Azufres (Mexico)	1	3.3 → 9.1	2.8
Beowawe (USA)	1	-	2.2
Coso (USA)	30	24 wells	successful
Larderello (Italy)	5	11 → 54 4 → 25 1.5 → 18 - 11 → 54	4.9 6.3 12 4 4.9

6.1 Salak geothermal field (Indonesia)

An acid treatment was carried out to improve the production characteristics of a geothermal well in the Salak geothermal field following an accurate analysis of the possible causes for the initial poor performance of the well. Despite promising indications, the initial steam flow rate from the Awi 8-7 well, drilled during 2004, was below expectations (Pasikki, R. G. and Gilmore, T. G., 2006). An acid stimulation treatment was designed and carried out to improve well performance. The treatment used a hydrofluoric acid system known as Sandstone Acid. The acid was placed to the target interval zone with a two-inch coiled tubing unit to maximize control over the treatment. Well test results before and after stimulation demonstrate that the acid stimulation has successfully produced improvements in overall well characteristics such as reduction of skin, increase of injectivity and permeability-thickness product, and production output. Based on the positive results obtained in this case, further application of this method is envisaged for other poor-performing wells with similar characteristics.

6.2 Las Tres Virgenes and Los Azufres geothermal fields (Mexico)

In Las Tres Virgenes geothermal field, the steam is supplied by four wells located near the power plants, but LV-11 and LV-13 recorded low wellhead pressure and marginal steam production. LV-11 is a deviated well and was drilled in September 2000 to a total depth of 2081 m. LV-13 was drilled to a total depth of 2200 m. An acidizing job was performed in order to improve the production characteristics of these wells. Acid treatment included a pre, post and over flush using chloride acid (HCl) and a chloride acid-fluoride acid (10% HCl- 5% HF). The acid was injected using a coiled tubing unit. Matrix acid stimulation job for production well LV-11 and LV-13 was successfully conducted without major problems. Post-acid completion tests results indicated major improvements in the injectivity index where a considerable drop in wellbore pressures of the two wells (~30 bars) were recorded that indicated a reduction in the pressure resistance inside the wellbore. The post-acid pressure falloff data also confirmed the improvement in the well where a negative skin (-5.8) was obtained in LV-13 and similar for LV-11 (Jaimes-Maldonado and Sánchez-Velasco, 2003). The post-acidizing discharge tests also showed substantial improvement compared with the previous well production characteristics to the acid job. As a result, within less than a month the field steam production increased from 3.2 MW_e to 7.3 MW_e.

The Los Azufres geothermal field is located in the northern portion of the transmexican volcanic belt, 250 km of Mexico city. Currently, 78 wells have been drilled at depths ranging between 700 and 3500 meters. Well Az-9AD is located in the northern zone of Los Azufres geothermal field and it was drilled from January 7 to April 22 on 2003, to a total depth of 1500 m. Early testing and survey analysis indicated that the low output of Az-9AD was caused by considerable drilling induced wellbore damage in its open hole section, where 1326 m^3 of mud were lost. Skin factor of 16 was causing additional pressure drop equivalent to 41 bars, reducing its optimal flow rate. The success of earlier acid treatment jobs in Mexico and the analysis of the available information encouraged the company to apply the same technique for this well during 2005. Acid treatment of well Az-9AD introduced very significant improvement in the wellbore showing 174% increase in production capacity (Flores et al., 2006). The results of this job have been used for encouraging new stimulation programs, such as those in wells Az-56R and Az-9A located in the north zone of Los Azufres geothermal field.

6.3 Beowawe geothermal field (Nevada, USA)

The Beowawe geothermal field is composed of a production zone within a volcanic and sedimentary rocks sequence. The geothermal fluid contained in the formation is of $NaHCO_3$ type with a very low salinity (1000-1200 ppm of total dissolved solids).

A first acid stimulation was performed in November 1982 on the Batz well (Epperson, 1983). The acid amounts consisted of about 18.9 m^3 of 15 % HCl acid for the preflush followed by a mainflush composed of 37.8 m^3 of 12% HCl - 3% HF. Then, a Beowawe fluid injection of 35 m^3 was performed to displace the acid farther in the formation. As a consequence, the acidification impact modified the acid displacement pressure from 27.5 bars to about 13.8 bars.

In August 1983, a second acidification test was performed on another well, Rossi 21-19 (Morris et al., 1984). Firstly, 79.5 m^3 of a 14.5% HCl solution was pumped at rates of 40-42 $L.s^{-1}$ and was displaced deeper in the formation by injecting 389 m^3 of water. A water injection test followed this first acidification but no significant change was noted in the injectivity of the well. Secondly, a new reservoir acidification was performed, using 156 m^3 of a 12% HCl - 3% HF acid solution. A total of 480 m^3 of

water were injected to displace the acid solution in the formation. The following water injection test then showed a 2.2 fold increase of the injectivity.

6.4 The Geysers geothermal field (California, USA)

An acid stimulation was performed in January 1981 on the OS-22 well (Entingh, 1999). An amount of 75.7 m^3 of 5 % HCl and 10% HF were pumped and 70 m^3 of fresh water were injected to displace the acid mixture deeper into the formation. But, no effect on the well productivity was recorded.

6.5 Coso geothermal field (California, USA)

The Coso Geothermal Field, located in east central California, hosts a world-class power-generating project that has been in continuous operation for the past 15 years. A field experiment was designed for dissolving calcite in a wellbore at the Coso field. The most promising mineral dissolution agent to emerge from the laboratory studies was the chelating agent nitrilotriacetate (NTA) (Rose et al., 2007). The well that was selected was producer 32A-20, which had recently failed due to calcite deposition. A total of 57 m^3 of a 10 wt% solution of NTA was injected into the well in a series of three injections. The solutions were each injected at 13.5-16 $L.s^{-1}$. The total volume of fluid injected (57 m^3) was calculated to be approximately the volume of the open-hole section of the well. Upon completion of the injection of the NTA solution, the well was shut in for approximately four hours, giving the chelating agent time to dissolve the calcite scale.

Once the well was opened, at first the brine was clear, but soon turned to milky white, indicating the presence of the calcium-NTA complex. The concentration of the unreacted NTA dropped from about 34'000 ppm to approximately 2'000 ppm during the experiment. The final value of 2'000 ppm indicated that the milky white NTA solution being produced was nearly completely complexed with calcium. These experiments indicate that NTA can be an effective dissolution agent for the dissolution of wellbore calcite. The production of unreacted NTA early in the production cycle indicated that a longer shut-in period may have resulted in a more complete reaction of the NTA solution and more wellbore calcite dissolution.

A total of 30 wells were treated with HCl and 24 gave successful results (Evanoff et al., 1995).

6.6 Baca geothermal field (New Mexico, USA)

For the development of the fracture network in the Baca Union Project, different methods of reservoir stimulation were compared. Acid stimulation had not been selected because of the filling of the natural fractures. Composed of authigenic material such as quartz, feldspar and pyrite (Pye and Allen, 1982). Therefore the acid stimulation should require substancial amounts of hydrochloric acid with uncertain results. A hydraulic fracturation was selected and performed on Baca-20 well in October 1981 utilizing a cooling water followed by a high viscosity frac fluid (Morris and Bunyak, 1981). Different compounds were used to do this hydraulic stimulation as proppant (sintered bauxite), hydroxypropyl polymer gel (stable at high temperature) and calcium carbonate added to act as a fluid-loss additive.

Nevertheless, all these treatments have not allowed a significant increase of the injectivity. It was also thought that the calcium carbonate has plugged the natural fractures and flow paths in the formation. As a consequence, an acid treatment was performed. A volume of 166 m^3 of hydrochloric acid at a concentration of 11.9% was used but this acidizing treatment has not allowed the development of the well productivity (Entingh, 1999).

6.7 Fenton Hill HDR project (New Mexico, USA)

This HDR reservoir, located in north-central New Mexico, is composed at a depth of 3-4 km of a highly jointed Precambrian plutonic and metamorphic complex, basically of granitic composition. This HDR project was operated by Los Alamos National Laboratory. Many experiments, in the laboratory and on the field, were performed to study the impact of a chemical treatment on this rock.

Different works were performed on cuttings and granite cores at the laboratory scale to study the impact of chemical treatments on permeability increases. Aqueous solutions of Na_2CO_3, NaOH and HCl were investigated on well-known crystalline rocks. Sarda (1977) reported the results (Table 8).

Table 8: Impact of three chemical treatment at 100 °C and 100 bars during 144 h (Sarda, 1977)

Chemical Treatment	Weight Loss	Permeability increase
Na_2CO_3	-0.3 %	2-fold
HCl	- 6 %	negligible
NaOH	- 6 %	20-fold

Those laboratory experiments have demonstrated that Na_2CO_3 dissolves SiO_2 primarily by attacking the quartz component of the granite. Holley et al. (1977) showed that the amount of dissolved silica increased with increasing sodium carbonate concentration and with increasing time.

Field experiments were attempted in November 1976 to reduce the impedance of the deep enhanced reservoir by a chemical leaching treatment. Na_2CO_3 was used to dissolve quartz from the formation. A total of 190 m^3 of 1 N Na_2CO_3 solution was injected. About 1000 kg of quartz were dissolved and removed from the reservoir but no impedance reduction resulted.

6.8 Fjällbacka HDR project (Sweden)

The experimental HDR reservoir of Fjällbacka is made of a granite composed of two main facies, the predominant variety being a greyish-red, biotite monzogranite. This granite contains abundant fractures and minor fractures zones, which showed an evidence of being hydraulically conductive and which were filled with calcite, chlorite and clay minerals (Sundquist et al., 1988; Wallroth et al., 1999). Most of the stimulation experiments were hydraulic fracturing but an acid treatment was performed in 1988. An amount of 2 m^3 of HCl-HF acid was injected in Fjb3 to leach fracture filling. The results have shown the efficiency of acid injection in returning rock particles.

6.9 Experiments at EGS reservoir of Soultz-sous-Forêts (Alsace, France)

The Soultz-sous-Forêts Enhanced Geothermal System (EGS), established in the Rhine Graben, North of Strasbourg (France), has been investigated since the mid 1980's. The final goal of this project is to extract energy for power production from a regional randomly permeable natural geothermal reservoir with the complementary resource coming from a forced fluid circulation between injection and production boreholes within a granitic basement.

Recently chemical treatments were performed at Soultz-sous-Forêts (France). This deep granitic reservoir contains fractures partially filled with a mixture of secondary carbonates (calcite and dolomite), various kinds of clay minerals (Illite, chlorite….) and silica. In order to dissolve these carbonates and to enhance productivity around the wells, each of the three 5-Km deep boreholes (GPK2, 3 and 4) were treated with different amounts of hydrochloric acid. If GPK3 has shown weak variations of its injectivity, GPK4 presented a real increase of its injectivity and productivity after the treatments and GPK2 presented also a very sensible improvement despite the fact that the treatment was only a very little test.

6.9.1 Preliminary tests on cores

In order to define the most effective acid mixture to be used in the stimulation of the deep reservoir, laboratory test were performed both in batch and in the continuous flowing conditions (Erga, 2000). The batch experiments consisted to test the reactivity of acid mixtures (HCl/HF) on core samples of granite formed by micas, phylites, hydrothermal veins, quartz and feldspars at 50°C and 150°C. Batch results indicated the mixtures 12/3 and 12/6 (in weight %) as the best one to attack these rocks and minerals. These 12/3 (wt%) and 12/6 (wt%) mixtures were then used in a series of tests in flowing conditions at 30, 50, 70 and 90°C. The evolution of the weight losses were followed by electronic scanning microscope analyses to determine the mineralogical phases influenced by acidification treatment. On a core coming from a depth of 1996 m in EPS1, weight losses of about 80-100 $mg.cm^{-2}$ were measured and the most effective acid mixture was the ratio 12/3 percent by weight.

6.9.2 GPK2 well

The first injection tests performed on GPK2 on January 23 and February 12, 2003, with water injection volumes of 9214 m^3 and 5814 m^3 respectively, showed an injectivity in GPK2 estimated to about 0.3 $L.s^{1}.bar^{-1}$. It was then decided to improve the well injectivity by a soft acidizing. During this test,

only 1.5 tons of HCl were injected. First, 500 kg of HCl were injected at a concentration of 1.8 $g.L^{-1}$ and with a flow of 30 $L.s^{-1}$.

It showed an immediate and strong impact (see "A" on Figure 3), demonstrating that part of the injection pressure required to inject the total flow was due to very near well bore scaling. The second part of the test, performed at concentrations of 1.8 $g.L^{-1}$ and 0.9 $g.L^{-1}$ for flows of about 15 and 30 $L.s^{-1}$ respectively, showed less immediate impacts but nevertheless the global result was impressive (see differences between "D" and "E" on Figure 3) for such a little quantity of acid injected, the injectivity has increased up to approximately 0.5 $L.s^{-1}.bar^{-1}$.

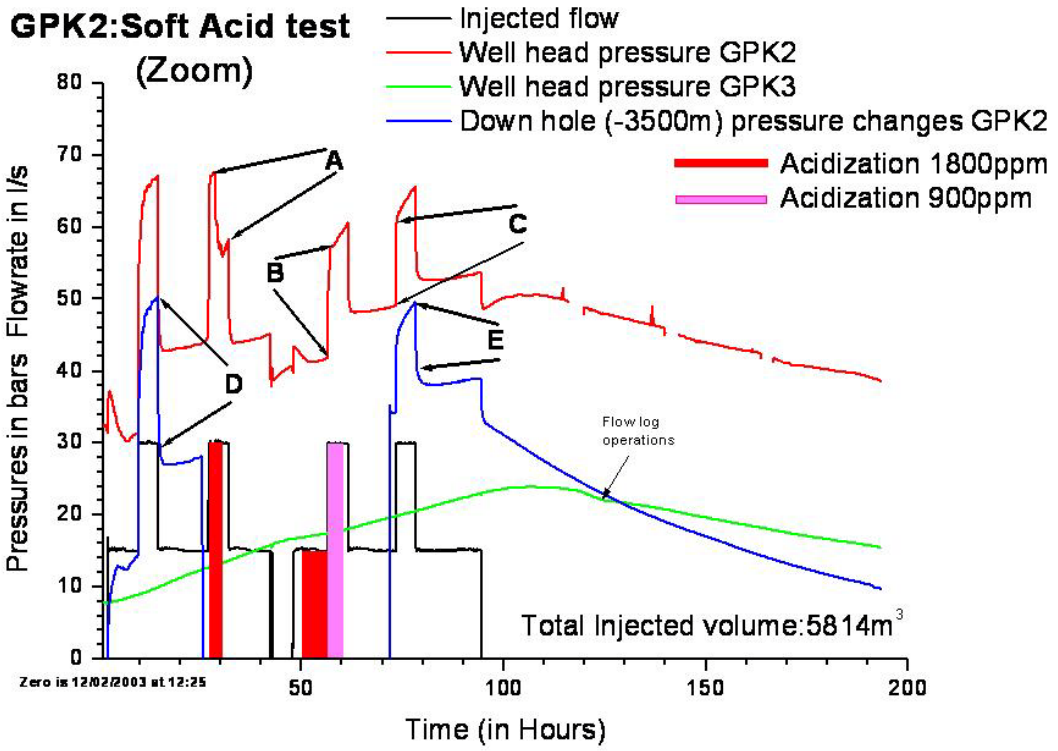

Figure 3: Impact of soft acidification test on GPK2 (Gérard et al, 2005).

6.9.3 GPK3 well

The second acidification test was run in GPK3 in June 2003 during a circulation test between GPK3, the injection well, and GPK2, the producer. A total of 950 m^3 of an acid solution, with a concentration of about 3.2 $g.L^{-1}$, were injected at a flow of 21.3 $L.s^{-1}$. Up to 3 tons of HCl were used in GPK3. The results are shown on Figure 4. Figure 4 shows a sudden drop of the wellhead pressure of GPK3 (slope break at 240 h) after the injection of about 4000 m^3 of acid and fresh water. This break could be caused by acidic water and its action in the reservoir, in particular in the large fault identified at 4750 m and able to absorb more than 75 % of the injected fluid (Gérard et al, 2005). Nevertheless, it is difficult to estimate the real improvement of the GPK3 injectivity due to acid treatment, because no water injection test was performed in the same conditions before and after acid injection, unlike for GPK4 well.

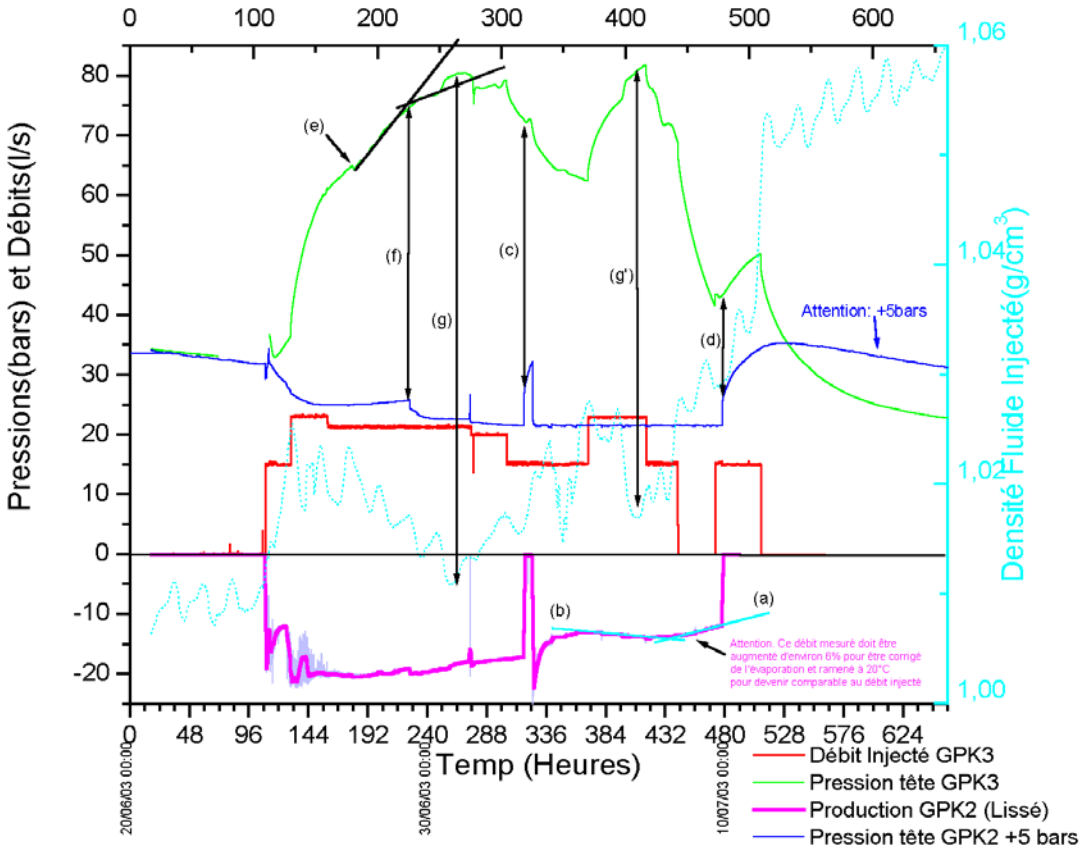

Figure 4: Impact of acidification test on GPK3 (Gérard et al, 2005).

6.9.4 GPK4 well

In February 2005, an acidified (HCl) water injection was tested to improve the injectivity around GPK4 well. The experiment began on 22 February 2005 with an injectivity test of the well before soft acidification. It consisted of the injection of 4'500 m^3 of water at increasing flow rates (9 $L.s^{-1}$, 18 $L.s^{-1}$, 25 $L.s^{-1}$) in 24-hour steps. The injection of water acidified by the addition of approximately 2 $g.L^{-1}$ of hydrochloric acid started on 2 March 2005 at a flow rate of 27 $L.s^{-1}$. It lasted 2 days, followed by one day of injecting fresh water at much lower rates in decreasing steps. A total volume of 5'200 m^3 was injected; with a total weight of acid (HCl) of 11 tons. When the wellhead pressure was back to the value observed during the previous injectivity test, an identical test was repeated on 13 March 2005, that is injection of 4'500 m^3 of water in flow rate steps of 24 hours at 9 $L.s^{-1}$, 18 $L.s^{-1}$ and 25 $L.s^{-1}$.

The impact of the acidified water on the wellhead pressure during the first acid injection in GPK4 well is shown on Figure 5. Despite the fact that the injection was performed in an over-pressurised reservoir, the injection pressure was decreasing during the last hours of the acidification test. Moreover, it is interesting to compare the data from two tests of water injection performed in the same conditions before (February 22, 2005) and after (March 13, 2005) the acid injection. Results (Gérard et al., 2005) show that after some 72 hours of water injection in the second test (24 hours at 9 $L.s^{-1}$, 24 hours at 18 $L.s^{-1}$ and 24 hours at 26 $L.s^{-1}$), the GPK4 wellhead pressure was about 40 bars below the value observed in the same conditions before acidification. This represents a decrease of the apparent reservoir impedance seen from the wellhead by a factor ~1.5 (0.20 to 0.30 $L.s^{-1}.bar^{-1}$).

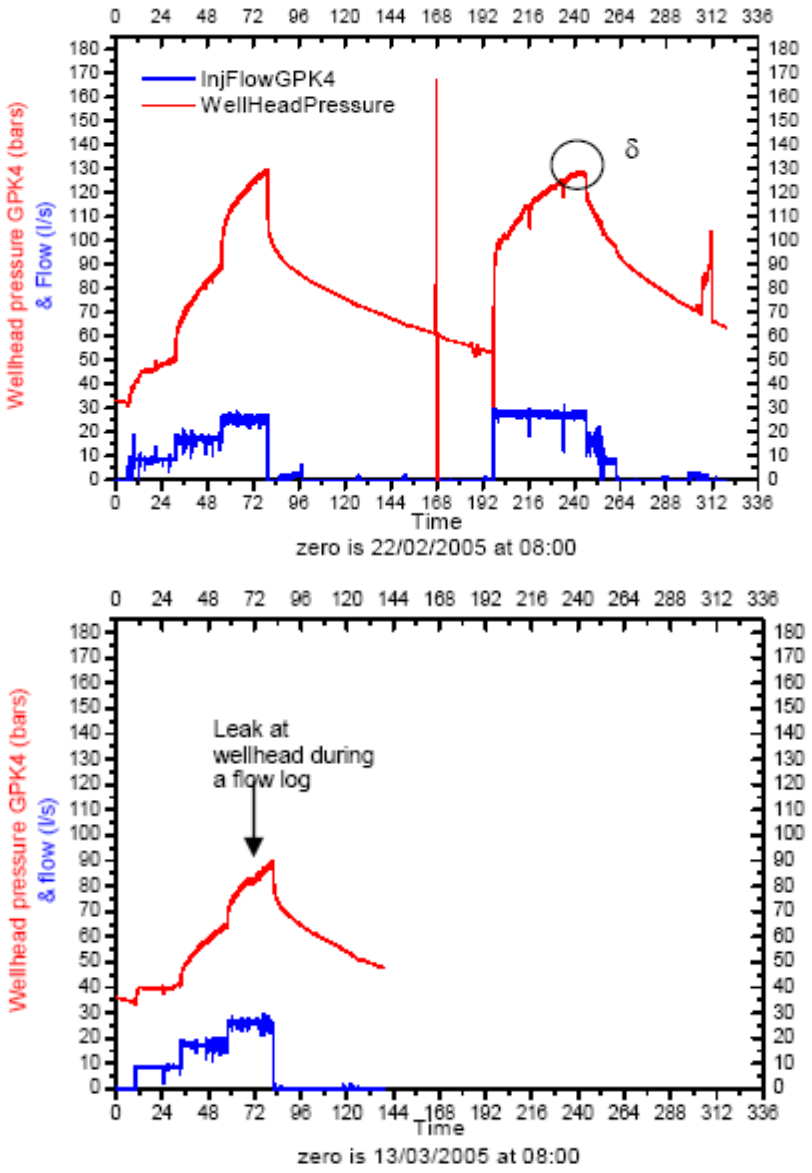

Figure 5: Impact of acidification test on GPK4; above, before and during acidification injection, below, after acidification (Gérard et al, 2005).

In May 2006, new tests began with a test of the well injectivity before acidification. The acid treatment was performed in four stages:

- Injection of 2000 m^3 of cold water deoxygenized at 12 $L.s^{-1}$, 22 $L.s^{-1}$ then finally at 28 $L.s^{-1}$.

- A preflush of 25 m^3 HCl diluted at 15% (3 tons) (with deoxygenized water) was pumped ahead of the HCl-HF acid mixture during 15 minutes at 22 $L.s^{-1}$.

- A main flush consisted of the injection of 200 m^3 of Regular Mud Acid (RMA), (12% hydrochloric (HCl) - 3% Hydrofluoric (HF) acid mixture treatment), with addition of a corrosion inhibitor, at a flow rate of 22 $L.s^{-1}$ during 2,5 hours.

- A postflush by injection of 2'000 m^3 cold water deoxygenized without inhibitor at a flow rate of 22 $L.s^{-1}$ then 28 $L.s^{-1}$ during 1 day.

When the wellhead pressure was back to a value identical to that observed in the previous injectivity test, a 3-day test identical to that of March 13, 2005 was repeated. Figure 6 shows the impact of RMA acid job on the wellhead pressure by comparison before and after the second acid injection in GPK4 well. The repetition of the injectivity test showed that the difference in the over pressure values at the wellhead between the beginning of the test and the end were 16 bars. This represents a 35% reduction of the wellhead pressure due to the acidification treatment. After some preliminary

evaluation of downhole pressure changes, performed by GEOWATT, this leads to a provisional estimate of GPK4 injectivity after chemical treatment slightly lower than 0.40 $L.s^{-1}.bar^{-1}$.

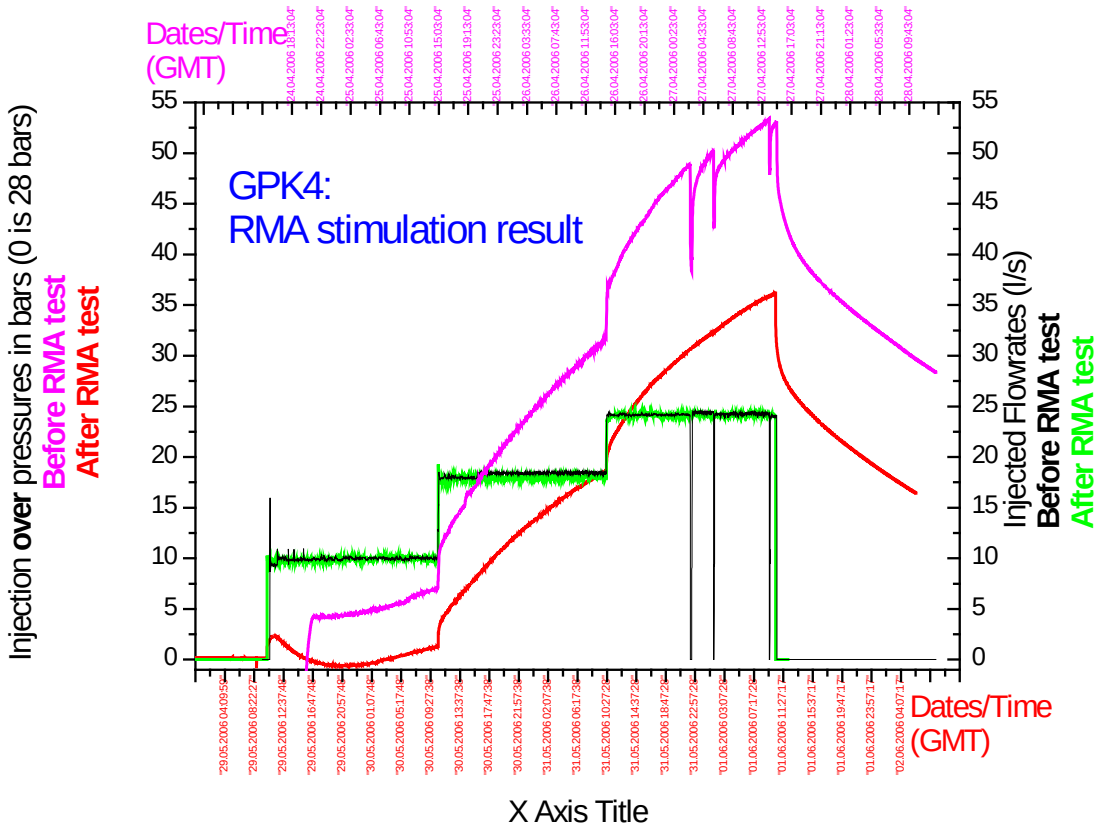

Figure 6: Impact of the RMA acidification test on the wellhead measured by comparison before and after the acidification test on GPK4 well (May 2006) (GEIE, 2006).

6.9.5 Chemical stimulation with chelating agents

An alternative to acid treatment is the use of chelating agents such as ethylenediaminetetraacetic acid (EDTA) or nitrilotriacetic acid (NTA). Such chelating agents have the ability to chelate, or bind, metals such as calcium. Through the process of chelation, a calcium ion would be solvated by the chelating agent, allowing the calcite to be transported either to the surface by flowing the well or further into the formation by injecting into the well. The rate of calcite dissolution using chelating agents is not as fast as is the rate of calcite dissolution using strong mineral acids. The lower dissolution rate means that the chelating agent will be able to take a more balanced path and more evenly dissolve calcite along the wellbore and in all available fractures, rather than following the first fluid entry zone and leaving the rest of the wellbore relatively untouched.

The current state-of-the-art method for chemically removing wellbore silica scale is through HF treatments, which are expensive and hazardous. Laboratory data indicate, however, that aqueous solutions at high pH can dissolve wellbore silica and near-wellbore formation silica and quartz reasonably well and at much lower cost than HF treatments. What has prevented geothermal operators from using caustic solutions in the past is the fear of calcite deposition, which is strongly favored at high pH. Laboratory studies have indicated that calcite is dissolved rather than precipitated at high pH in the presence of chelating agents. This suggests that thermally stable chelating agents at high pH can provide the basis for an affordable and effective mineral dissolution approach.

Although thermal stability studies have not been completed, the literature suggested that NTA could be used at temperatures as high as 290°C, whereas the other two chelating agents, EDTA and HEDTA, were significantly less thermally stable with maximum use temperatures in the range of 200°C. The calcite dissolution experiments in the high temperature flow reactor confirmed the superior

performance of NTA above 200°C. Therefore, a field experiment was designed for dissolving calcite and other minerals with a high pH solution of NTA in GPK4 well.

In October 2006, the chelating agents stimulation was performed (Figure 7). About 38 tons of NTA were injected with 200 m^3 of cold water at a flow rate of 35 $L.s^{-1}$. A total of 850 m^3 of water were injected to displace the chelating agent in the formation. Figures 7 and 8 show the impact of the chelating agents stimulation after the production test on the wellhead pressure and flow rate.

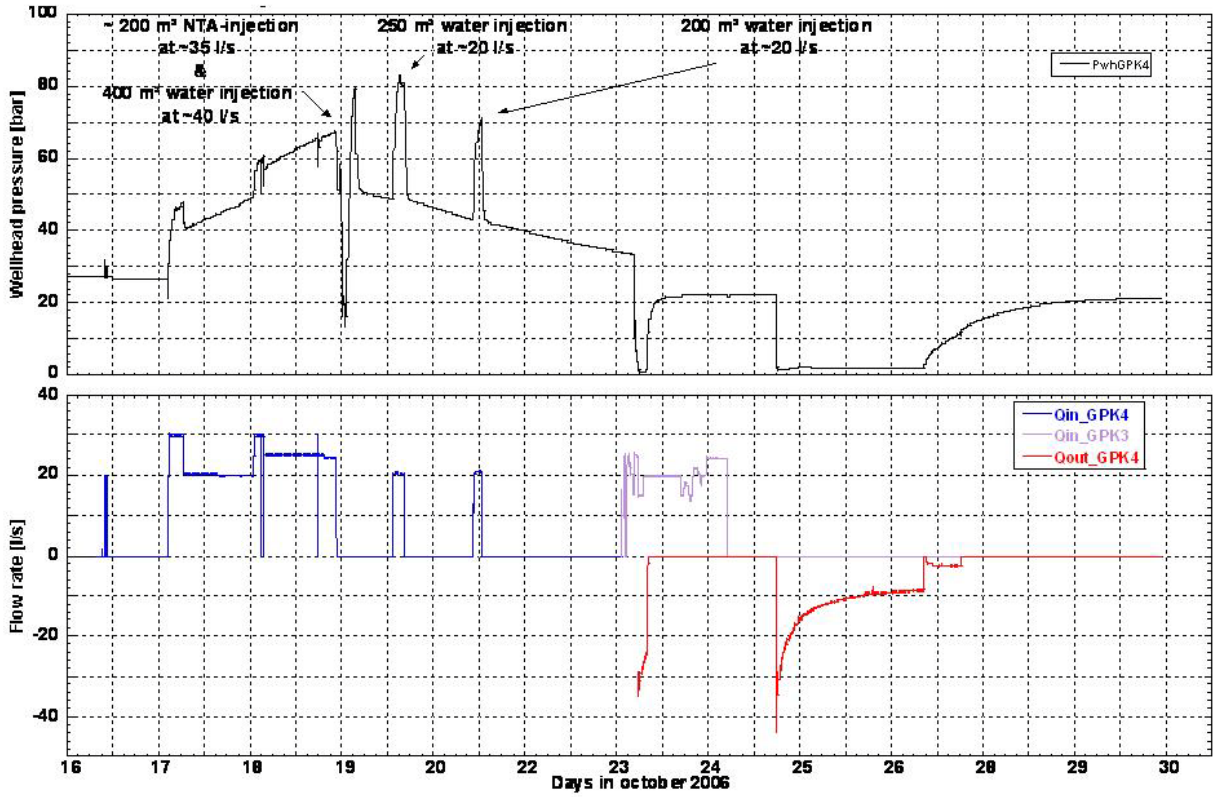

Figure 7: History plot of the chelating agents stimulation 06OCT16 and production test 06OCT23 in GPK4 well (GEIE, 2006).

6.9.6 Chemical stimulation of the farfield of the wells GPK4 and GPK3

Although conventional stimulation fluids, such as hydrochloric (HCl) or mud acid, can clean up the wellbore and stimulate the matrix, they do not penetrate deep into the formation nor stabilize fines. Conventional acids can also have adverse effects in formations with certain types of clays, or alumino-silicates like zeolite and chlorite, that are unstable in HCl acid. Consequently it was decided to develop the expected result of the NTA treatment in GPK4 by using Organic Clay Acid for High Temperature (OCA-HT). This stimulation fluid penetrates deep into the sensitive formation and stabilizes clays and fines without the adverse effects of conventional acid systems. OCA fluid is a high-performance acid system designed for sensitive sandstone matrix formations that can present the biggest challenge to conventional acidizing treatments. Because of the damaging precipitation of secondary and tertiary reaction products, conventional mud acid has the highest chance of failure in formations with very high temperature or a high clay content that is sensitive to HCl. OCA fluid combines a retardation effect and advanced chelation technology for stimulation deep into the reservoir with minimal precipitation. It reduces the risk of diminished production as well as secondary and tertiary mineral precipitation that can block pores. Its retarded properties allow a reduced corrosivity. OCA fluid also combats sludging problems that plague conventional acid systems and stabilizes formation fines while maintaining the integrity of the sandstone structures to promote long-term production.

New tests were run in February 2007. The operation consisted in cooling the GPK4 well and only stimulating it with 200 m³ of "Organic Clay Acid HT". The operation was also performed on well GPK3. Organic Clay Acid is a delayed acid proposed in its high temperature version (OCA HT). Its maximum temperature of use is slightly higher than 200°C, while the inhibition of corrosion can be efficiently ensured until 177°C. In fact, it was considered as being safe enough to use a corrosion inhibitor to guarantee a protection during 4 hours with 80°C for steels.

Figure 8 illustrates the impact of the successive chemical treatments on the productivity of GPK4 well. One can remark that now (March 2007) the productivity of GPK4 after few days only reached a stable value of 5l/s/MPa despite the fact that the produced fluid was stored in a lined lagoon and not reinjected in the well GPK3 during that test. One can also observe on figure 8 that during that production test of March 2007 the pressure in the reservoir at the impact of GPK3 dropped at a rate of around 1 bar/day. That implies a possible higher productivity of GPK4 when some reinjection in GPK3 will be performed.

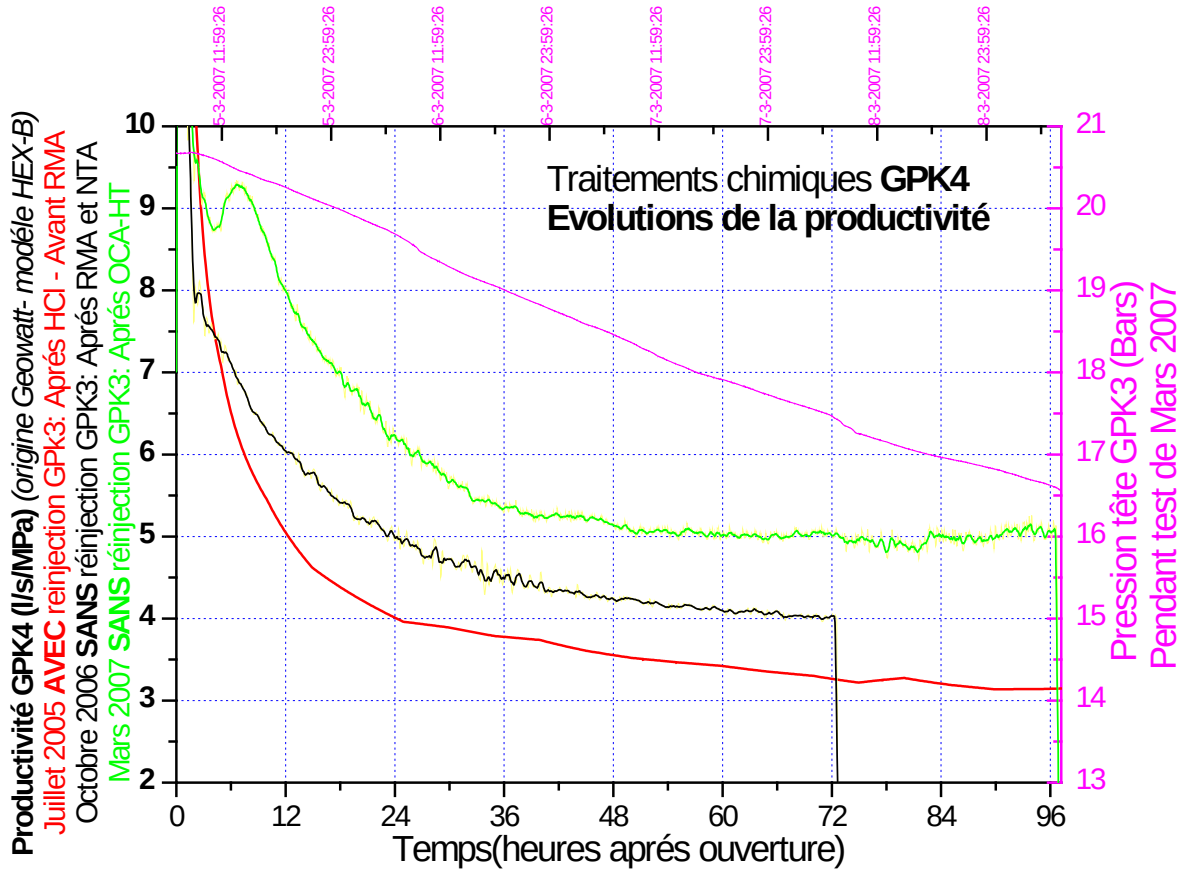

Figure 8: GPK4 productivity evolution with time during chemical treatments (GEIE, 2007).

As a summary of the chemical stimulation tested in the three deep wells of the Soultz EGS programme, the table 9 gives a synthesis of the principal results.

Table 9 : Summary of the chemical stimulation operations carried out in the three 5-km deep wells at Soultz-sous-Forêts (Nami et al. 2007)

Well	Date	Injected chemicals	Concentration of chemical agents	Results: Injectivity/Productivity increase
GPK2	Febr. 2003	1.5 tons (0.5 + 1)	HCl 0.09 + 0.18 %	Wellhead pressure drop, but no productivity increase observed.
GPK3	June 2003	3 tons	HCl 0.45 %	No increase: 0.35 $L.s^{-1}.bar^{-1}$
	Febr. 2007	250 m^3	Organic Clay Acid OCA	No increase: 0.35 $L.s^{-1}.bar^{-1}$
GPK4	Febr. 2005	11 tons	HCl 0.2 %	Productivity: 0.2 to 0.3 $L.s^{-1}.bar^{-1}$
	May 2006	Preflush: 25 m^3 Main flush: 200 m^3 Postflush: 2000 m^3	HCl 15 % (3 tons) HCl 12 % + HF 3 % water + inhibitor	Productivity: 0.3 to 0.4 $L.s^{-1}.bar^{-1}$
	Oct. 2006	38 tons	Chelant: NTA 19 %	The formation of a plug increased wellhead pressure; no production test to clean this plug afterwards.
	March 2007	200 m^3	Organic Clay Acid OCA	Productivity: 0.4 to 0.5 $L.s^{-1}.bar^{-1}$

7 Conclusions

Current economic conditions dictate that oil field operators maximize well/reservoir productivity or injectivity. Achieving the goal of long-term, low-cost sources of hydrocarbons will require significant technology advances in the area of well stimulation. From this papers review, it is apparent that these technological advances will affect many different portions of this industry, from old, mature fields, where significant reserves have previously been economically unattractive, to the new, major ultradeepwater projects that are being evaluated today. The challenge will be to increase productivity, and then to maintain that increased productivity throughout the life of the field to provide improved ultimate recovery.

New and innovative stimulation technologies are emerging that will modify some of previous tried and more or less proven methods. Still, in other cases, we see enhancements to improve the performance of existing technologies. It appears that the future challenge will be for the petroleum industry to find more-cost-effective ways to improve well productivity. It appears that well stimulation will remain a dynamic part of the petroleum industry.

Challenges in sandstone acidizing still exist, although great improvements have been made in the last decade. Factors that contribute to these challenges include: multiple types of co-existing formation damage; uncertain rock mineralogy; multiple fluids and pumping stages; complex chemical reactions between fluids and formation minerals; and fast reaction kinetics at elevated temperatures. Others are: inadequate zonal coverage; limited active acid penetration; rock deconsolidation due to acid-rock interactions; acid emulsion and sludge tendencies; corrosion; and health, safety and environmental (HSE) concerns. These factors contribute to the low success rate of sandstone acidizing treatments especially in acid-sensitive, and clay- and carbonate-rich sandstone formations at high temperatures.

Deleterious side-effects of acidizing in sandstone formations—such as clay swelling, fines migration, gel formation or particle precipitation—may be minimized or avoided altogether by designing hydrofluoric acid (HF) stimulation treatments with compatible chemical and physical properties. Smectite and mixed illite-smectite clays are among the most water-sensitive clays, while illites and chlorites are less prone to ion exchange. Also of concern when acidizing sandstone in the presence of illite, potassium feldspars, sodium feldspars, and zeolites, because these compounds can contribute to the formation of matrix-blocking precipitates.

Clay swelling can occur when acidizing fluids exchange ions with formation minerals, choking off production by obstructing the matrix, unless care is taken to sustain the salinity of the injected fluid after ion exchange. Many water-sensitive clays contain potassium chloride (KCl) and sodium chloride (NaCl) ions that can be exchanged with ions in injected fluids to lower the salinity of the fluid. For example, when a 3% ammonium chloride (NH_4Cl) acidizing fluid flows across a typical ion-exchanging clay, the fluid becomes 3.3% NaCl, a brine too weak to prevent clay swelling, thus requiring a 5% NH_4Cl or equivalent solution.

The acid treatments were developed by oil industry for improving the productivity of oil and gas wells. This technology was partially adapted to the geothermal wells, most often to remove the mineral scaling deposited in the wells after several years of exploitation. Nevertheless, acid treatments also allow the enhancement of the fractures network. They have been successfully performed in geothermal granitic reservoirs like Fjällbacka or Beowawe. In recent years, the reliability of acidizing sandstone intervals has been significantly improved. In the USA, about 90 percent of wells treated have responded with two- to four-fold production increases.

Recently, this technology has been applied to the Soultz reservoir. The three 5-Km deep wells (GPK2, GPK3 and GPK4) were treated with different amounts of chemicals and the injectivity of each well was differently affected. If encouraging results were obtained with GPK2 and GPK4, the injectivity improvement of GPK3 well is apparently less marked but the diagnostic for this well was not really performed[1].

[1] *It can be also noted that the likely origins of the very limited efficiency of all the methods (including hydraulic stimulation) used for trying to improve the injectivity of GPK3 well seem rather specific and are still a subject of discussion.*

Nevertheless, the high reactivity and a weak flow prevent the penetration of acid in the far field between the wells. This high reactivity also involves the risk of creating wormholes, able to increase the porosity but not always the permeability of the medium.

The increase of acid concentration augments the reactivity in the vicinity of the injection well and creates a new porosity. But the high acidity of the solution has also the disadvantage to decrease the solution pH and to augment the risk of damaging the casing.

The answer could be an increase of the flow to force the acid transport farther in the formation or the use of another acid (e.g. HF), which will dissolve silicates minerals. The result will be an enhancement of the fractures network and of the fractures connectivity.

Finally, simulators have been developed to track the propagation of reaction fronts and to gain insight into the effectiveness of acid injection as a well stimulation technique. Reactive transport modelling was used to simulate injectivity recovery by acid injection (Xu et al., 2004; André et al., 2006). The predicted amount of scaling minerals dissolved by acid was consistent with the estimal amount.

8 References

Allen, T.O. and Roberts A.P. (1989). Production Operations Vol 1 & 2. Well Compilations, Workover and Stimulation. OGCI Inc. Technical Publications, Tulsa, Oklahoma.

Almond, S.W., Harris, R.E. and Penny, G.S.(1995). Utilization of biologically generated acid for drilling fluid damage removal and uniform acid placement across long formation intervals. Proc. European Formation Damage Control Conference, 15-16 May, 1995, The Hague, the Netherlands, SPE 30123, pp.465-478.

André, L., Rabemanana, V. and Vuataz, F.-D. (2006). Influence of water-rock interactions on fracture permeability of the deep reservoir at Soultz-sous-Forêts, France. Geothermics 35, 507-531.

André, L., Rabemanana, V. and Vuataz, F.-D. (2005). Geochemical modelling of water-rock interactions and implications on the properties of the Soultz fractured reservoir. Proc. EHDRA Scientific Conference, March 17-18, 2005, Soultz-sous-Forêts, France.

Amistoso, A.E., Aqui, A.R., Yglopaz, D.M. and Malate, R.C.M. (2005). Sustaining steam supply in Palinpinon 1 production field, Southern Negros Geothermal Project, Philippines. World Geothermal Congress, Antalya, Turkey, 24-29 April, 2005.

Barrelli, A., Cappetti, G., Manetti, G. and Peano, A. (1985). Well stimulation in Latera Field. Geothermal resources Council Transactions, vol. 9(2), pp. 213-219.

Barrios, L.A., Quijano, J.E., Romero, R.E., Mayorga, H., Castro, M. and Caldera, J. (2002). Enhanced permeability by chemical stimulation at the Berlin Geothermal Field, El Salvador. Geothermal Resources Council Transactions, vol. 26, September 22-25, 2002.

Buning, B.C., Malate, R.C.M., Lacanilao, A.M., Sta Ana, F.X.M. and Sarmiento, Z.F. (1995). Recent experiments in acid stimulation technology by PNOC-Energy development corporation, Philippines. Proc. World Geothermal Congress, vol. 3, pp. 1807-1812.

Buning, B.C., Malate, R.C.M., Austria, J.J.C., Noriega, M.T. and Sarmiento, Z.F. (1997). Casing perforation and acid treatment of well SK-2D Mindanao 1 Geothermal project, Philippines. Proc. 22nd Workshop on Geothermal Reservoir Engineering, January 27-29, 1997, Stanford, California, USA.

Burgos, B., Buijse, M., Fonseca, E., Milne, A., Brady, M., and Olvera, R. (2005). Acid Fracturing in Lake Maracaibo: How Continuous Improvements Kept on Raising the Expectation Bar. Schlumberger and Shell Venezuela S.A, 2005 SPE Annual Technical Conference and Exhibition, 9-12 October, Dallas,Texas, USA, SPE 96531.

Crowe, C., Masmonteil, J. and Thomas, R. (1992). Trends in Matrix Acidizing. Oilfield Review, pp. 24-40.

Erga, F. (2000). Esperimenti di acidificazione in flusso continuo di soluzione acida. Erga, Gruppo Enel, 20 p.

Entingh, D.J. (1999). A review of geothermal well stimulation experiments in the United States. Geothermal Resources Council Transactions, October 17-20, 1999, vol. 23, pp. 175-180.

Evanoff, J., Yeager, V. and Spielman, P. (1995). Stimulation and damage removal of calcium carbonate scaling in geothermal wells: a case study. World Geothermal Congress, Florence, Italy, pp. 2481-2485.

Epperson, I.J. (1983). Beowawe acid stimulation. Geothermal Resources Council Transactions, pp. 409-411.

Flores, M., Barajas, E.N. and Rodriguez, M.A. (2006). Productivity analysis and acid treatment of well AZ-9AD at the Los Azufres Geothermal field, Mexico. Geothermal Resources Council Transactions, vol. 30.

Flores, M., Davies, D., Couples, G. and Palsson, B. (2005). Stimulation of geothermal wells, can we afford it? World Geothermal Congress, Antalya, Turkey, 24-29 April, 2005.

Frenier, W.W., Fredd, C.N. and Chang, F. (2001). Hydroxyaminocarboxylic Acids produce superior formulations for matrix stimulation of carbonates at high temperatures. SPE 71696.

Gérard, A., Fritz, B. and Vuataz, F.-D. (2005). Results of soft acid injection tests performed at Soultz in wells GPK2, GPK3 and GPK4 – Extended summary: revised status on 14 March 2005. Proc. EHDRA Scientific Conference, March 17-18, 2005, Soultz-sous-Forêts, France.

Holley, C.E., Blatz, L.A., Tester, J.W. and Grigsby, C.O. (1977). The interaction of granite with aqueous sodium carbonate. Geothermal Resources Council Transactions, vol. 1, pp. 147-148.

Jacquot, E. (2000). Modélisation thermodynamique et cinétique des réactions géochimiques entre fluides de bassin et socle cristallin: application au site expérimental du programme européen de recherche en géothermie profonde (Soultz-sous-Forêts, Bas-Rhin, France). PhD thesis, Université Louis Pasteur, Strasbourg, France.

Jaimes-Maldonado, J.G. and Sánchez-Velasco, R. (2003). Acid stimulation of production wells in Las Tres Vírgenes Geothermal field, BCS, México. Geothermal Resources Council Transactions, vol. 27.

Kalfayan, L. (2001). Production Enhancement With Acid Stimulation. Pennwell Books.

Leschi, P., Demarthon, G., Davidson, E., and Clinch, D. (2006). Delayed-Release Acid System for Cleanup of Al Khalij Horizontal Openhole Drains. Total E&P and Halliburton, 2006 SPE International Symposium and Exhibition on Formation Damage Control, 15-17 February, Lafayette, Louisiana, USA, SPE 98164.

Malate, R.C.M., Yglopaz, D.M., Austria, J.J.C., Lacanilao, A.M., and Sarmiento, Z.F. (1997). Acid stimulation of injection wells in the Leyte Geothermal power project, Philippines. Proc. 22nd Workshop on Geothermal Reservoir Engineering, January 27-29, 1997, Stanford, California, USA.

Malate, R.C.M., Austria, J.J.C., Sarmiento, Z.F., DiLullo, G., Sookprasong, A. and Francia, E.S. (1998). Matrix Stimulation Treatment of Geothermal Wells Using Sandstone Acid. Proc. 23rd Workshop on Geothermal Reservoir Engineering, January 26-28, 1998, Stanford, California, USA.

Malate, R.C.M., Sookprasong, P.A., Austria, J.J.C., Sarmiento, Z.F. and Francia, E.S. (1999). Wellbore Soaking: a Novel Acid Treatment of Geothermal Injection Wells. Proc. 24th Workshop on Geothermal Reservoir Engineering, January 25-27, 1999, Stanford, California, USA.

Mendez, A., Neumann, L.F., de Almeida Pinto, E., Torres, R., Farias, R., and Acosta, M. (2005). Achieving True Sandstone-Reservoir Stimulation in Deepwater Horizontal Wells. BJ Services Co. and Petrobras, 2005 SPE Annual Technical Conference and Exhibition, 9-12 October, Dallas, Texas, USA, SPE 95826.

Molina, P.O., Malate, R.C.M., Buning, B.C., Yglopaz, D.M., Austria, J.J.C. and Lacanilao, A.M. (1998). Productivity Analysis and Optimization of Well SK-2D, Mindanao I Geothermal Project Philippines. Proc. 23rd Workshop on Geothermal Reservoir Engineering, January 26-28, 1998, Stanford, California, USA.

Morris, C.W. and Bunyak, M.J. (1981). Fracture stimulation experiments at the Baca Project Area. Proc. 7th Workshop on Geothermal Reservoir Engineering, Stanford, California, USA, pp. 53-60.

Morris, C.W., Verity, R.V. and Dasie, W. (1984). Chemical stimulation treatment of a well in the Beowawe Geothermal Field. Geothermal Resources Council Transactions, pp. 269-274.

Mukherjee, H. and Cudney, G. (1993). Extension of acid fracture penetration by drastic fluid loss control. Journal of Petroleum Technology, pp 102-105.

Nami, P., Schindler, M., Tischner, R. Jung and T., Teza, D. (2007). Evaluation of stimulation operations and current status of the deep Soultz wells prior to power production. EHDRA Scientific Conference, June 2007.

Nguyen, P.D. (2006). Controlling Formation Fines at Their Sources To Maintain Well Productivity. Halliburton. SPE 97659.

Pasikki, R.G. and Gilmore, T.G. (2006). Coiled Tubing Acid Stimulation: The Case of AWI 8-7 Production Well in Salak Geothermal Field, Indonesia. Proc. 31st Workshop on Geothermal Reservoir Engineering, January 30-February 1, 2006, Stanford, California, USA.

Pauwels, H., Fouillac, C. and Fouillac, A.M. (1993). Chemistry and isotopes of deep geothermal saline fluids in the Upper Rhine Graben: origin of compounds and water-rock interactions. Geochim. Cosmochim. Acta, 57, pp. 2737-2749.

Pournik, M. (2004). Evaluation of sandstone acidizing with high strength HF solutions. Master of Science in Engineering, University of Texas, Austin, USA.

PTTC (2000). Well stimulation advances. Workshop co-sponsored by PTTC's North Midcontinent Region and the Wichita Chapter of Society of Petroleum Engineers, February 9, 2000, Wichita, KS, 3 p.

Pye, D.S. and Allen, W.C. (1982). Hydraulic fracturing at the Baca Project New Mexico. Geothermal Resources Council, Special Reports, pp. 127-136.

Rose, P., Xu, T., Kovac, K., Mella, M. and Pruess, K. (2007). Chemical Stimulation in near-wellbore geothermal formations: silica dissolution in the presence of calcite at high temperature and high pH. Proc. 32st Workshop on Geothermal Reservoir Engineering, January 22-24, 2007, Stanford, California, USA.

Sarda, J.P. (1977). Chemical leaching. Proc. 2nd NATA-CCMS Information Meeting on Hot Dry Rock Geothermal Energy, June 28-30, 1977, Los Alamos, New Mexico, USA.

Schlumberger (2003). Sand Control Pumping Services. pp. 37-70.

Serpen, U. and Türeyen, O.I. (2000). Acidizing geothermal wells. Geothermal Resources Council Transactions, vol. 24, September 24-27, 2000.

Strawn, J.A. (1980). Results of acid treatment in hydrothermal direct heat experiment wells. Geothermal Resources Council Transactions, vol. 4, September 1980.

Sullivan, R.B. (2006). Evaluation of Nonlinear Fracture Relative Permeabilities and Their Impact on Waterfrac Performance in Tight Gas Sands. Anadarko Petroleum Corp. SPE 98329.

Sundquist, U., Wallroth, T. and Eliasson, T. (1988). The Fjällbacka HDR Geothermal Energy project: reservoir characterisation and injection well stimulation. Chalmers University of Technology, Report Number Fj-9.

Tuedor, F.E. (2006). A Breakthrough Fluid Technology in Stimulation of Sandstone Reservoirs. Schlumberger. SPE 98314.

Ventre, A-V. and Ungemach, P. (1998). Soft Acidizing of Damaged Geothermal Injection Wells. Discussion of Results Achieved in the Paris Basin, Proc. 23rd Workshop on Geothermal Reservoir Engineering, January 26-28, 1998, Stanford, California, USA.

Wallroth, T., Eliasson, T. and Sundquist, U. (1999). Hot Dry Rock research experiments at Fjällbacka, Sweden. Geothermics, 28(4), pp. 617-625.

Williams, B.B. et al,. (1979). Acidizing Fundamentals. New York and Dallas Society of Petroleum Engineers, European Formation Damage Control Conference, 15-16 May, The Hague, the Netherlands. SPE Monograph No. 6.

Xie, T. (2004). A parametric study of sandstone acidizing using a fine-scale simulator. Master of Science in Engineering, University of Texas, Austin, USA.

Xu, T., Ontoy, Y., Molling, P., Spycher, N., Parini, M. and Pruess, K. (2004). Reactive transport modeling of injection well scaling and acidizing at Tiwi field, Philippines. Geothermics, 33 (4), pp. 477–491.

Yglopaz, D.M., Buning, B.C., Malate, R.C.M., Sta Ana, F.X.M., Austria, J.J.C., Salera, J.R.M., Lacanilao, A.M. and Sarmiento, Z.F. (1998). Proving the Mahanagdong B Resource: A Case of a Large-Scale Well Stimulation Strategy, Leyte Geothermal Power Project, Philippines. Proc. 23rd Workshop on Geothermal Reservoir Engineering, January 26-28, 1998, Stanford, California, USA.

Selected websites

Guides to acid stimulation for improving productivity in oil, gas, injection and disposal wells: outlines the purposes and benefits of acidizing, and shows how to design and execute successful acid treatments.

http://www.bjservices.com/

http://www.cleansorb.com/

http://www.corelab.com/

http://www.halliburton.com/

http://www.slb.com/content/services/stimulation/

NB: This list is not exhaustive and does not represent any recommendation for specific services companies.

EC Contract SES6-CT-2003-502706

PARTICIPANT ORGANIZATION NAME: Centre of Geothermal Research – c/o CHYN, University of Neuchâtel, Switzerland

Related with Work Package 8 - Thermo-Hydro-Mechanical modelling of reservoir / heat exchanger

Related with Working Group 6.

EVOLUTION OF AN EGS RESERVOIR SIMULATED BY MODELLING THE GEOCHEMICAL EFFECTS OF FORCED FLUID CIRCULATION AT SOULTZ-SOUS-FORETS.

Sandrine Portier[1,2], Laurent André[3] and François-D. Vuataz[1]

[1] Centre of Geothermal Research – CHYN, University of Neuchâtel, E.-Argand 11, CP 158, CH-2009 Neuchâtel, Switzerland
[2] Centre of Hydrogeology – University of Neuchâtel, E.-Argand 11, CP 158, CH-2009 Neuchâtel, Switzerland
[3] BRGM, Service EAU/M2H, BP 6009, F-45060 Orléans cedex, France

e-mail: sandrine.portier@unine.ch l.andré@brgm.fr francois.vuataz@crege.ch

ABSTRACT

Operations exploiting little known, deep geothermal sources and low permeability reservoirs face new problems involving high temperature and pressure brine-rock interactions. FRACHEM code has been developed to forecast the long-term evolution of fractured reservoirs in order to determine how forced fluid circulation within a reservoir can modify the rock properties. FRACHEM code has been applied to simulate fluid circulation in the fractured hydrothermalised granite of Soultz-sous-Forêts. A complex geometry has been shaped to represent a realistic reservoir model. This model includes fractured zones of different widths following different paths with the dimension of the Soultz reservoir. Depending on their distance and the relative exposure, these fractured zones interact on each other. These fluid-rock interactions have been investigated over time to predict where dissolution and deposition occur in the reservoir. Goals are to forecast if mineral dissolution is going to create short circuits or improve pressure drop and also if long term circulation will result in some equilibrium being reached with the fluid and reservoir rocks.

Economic exploitation of enhanced geothermal systems is dependent to mineral precipitation and associated decrease in permeability of the system. This inhibits fluid flow and associated heat extraction from the system. One solution to this problem consists in injecting a reacting fluid into the wells, in order to dissolve the secondary minerals sealing the fractures, to increase the permeability and hence to stimulate the reservoir. Recent acid treatments were performed on the Soultz wells. FRACHEM simulations have been tested to forecast the impact of reacting fluid injection, such as acidizing, on amounts of carbonates dissolved and precipitated and resulting porosity developments.

INTRODUCTION

Abundant geothermal resources sound like a great deal, but in addition to the extraction costs, there are numerous geological problems associated with its exploitation. The heat is extracted by conduction and convection. As a consequence, circulating hot water in the crust inevitably leads to dissolution, transport and re-deposition of minerals. In the case of heat extraction projects, the pores and the fractures in the water-bearing rocks may become clogged by mineral deposition, eventually stemming flow. This can limit the productive lifetime of an engineered geothermal system, even though heat may still be available at depth. Current research into water–rock interaction in geothermal reservoirs is directed at ways to enhance energy production and to avoid clogging of the rock openings.

The principle of an Enhanced Geothermal System (EGS) is to inject cold water into a hot fractured rock reservoir, to extract the heated water by one or several production wells, and to transfer its energy to a working fluid via a surface heat exchanger close to the wells. The feasibility and characteristics of this process rely ultimately on the fact that the natural fissures, opened and/or widened artificially by injection of water at high pressures through the borehole, remain open. However, during the stimulation phase, the injected water is composed of formation and surface fluids and will react with the rocks minerals. The composition of the resulting fluids will be controlled by temperature, time, and by the minerals composition and added natural fluids.

Later, during reservoir exploitation, the formation fluid will be most probably dominant in the water-rock reactions, but a heating-cooling cycle will trigger continuous reactions. Dissolution and precipitation will take place along the pathways of these resulting fluids, and open fissures can potentially close by mineral precipitation. Also, mineral precipitation can potentially create problems along the geothermal loop, from the production casing to the surface tubing, the heat exchanger and the reinjection casing, when the hot fluids are cooled down by approximately 100°C at the heat exchanger.

Evidently, at an EGS site, it is necessary to understand and quantify fluid circulation and composition with time and to predict the dissolution-precipitation behaviour of the fluids along their pathways. Our main goal is to comprehend and quantify fluid circulation and composition with time and to predict the dissolution-precipitation behaviour of the fluids along their pathways. This will be achieved by geochemical modelling.

The proposed study consists of modelling fluid–rock interaction and scale formation during geothermal heat extraction with application to Soultz project. FRACHEM code has been developed to realistically simulate the long-term (years to decades) evolution of permeability and heat-exchange efficiency in an EGS reservoir. The latter are dependent on the interaction of chemical processes (mineral

dissolution and precipitation in rock fractures and technical installations) with the flow of the reactive fluids through a geometrically complex, and changing fracture network.

A great deal of specific and detailed information is required to assess the chemical impact of an injection operation. The present study is intended to represent the granitic fractured reservoir of Soultz-sous-Forêts and consequently, wells configuration as well as data of chemical and mineralogical composition were taken from the European Enhanced Geothermal System at Soultz-sous-Forêts (Jacquot, 2000; Durst, 2002; Bächler, 2003).

MODELLING APPROACH

The main task of the research on THC coupled modelling has been to forecast the evolution of reservoir porosity and permeability. Different researchers (Durst, 2002, Bächler, 2003, Rabemanana et al. 2003, André et al., 2005) have incrementally built a reactive transport simulator, FRACHEM, able to simulate the main characteristics of the Soultz reservoir.

FRACHEM is a THC simulator issued from the combination of two existing codes: FRACTure and CHEMTOUGH2. FRACTure is a 3-D finite-element code for modelling hydrological, transport and elastic processes. It was developed originally for the study of flow-driven interactions in fractured rock (Kohl & Hopkirk, 1995). CHEMTOUGH2 (White, 1995) is a THC code developed after the TOUGH2 simulator (Pruess, 1991), a 3-D numerical model for simulating the coupled transport of water, vapor, noncondensable gas, and heat in porous and fractured media. CHEMTOUGH2 presents the possibility to transport chemical species and to model the chemical water-rock interactions as well as the chemical reactions driven by pressure and temperature changes. The transport and reaction are coupled using a one-step approach. FRACHEM has been built by introducing geochemical subroutines from CHEMTOUGH2 (White, 1995) into the framework of the code FRACTure (Bächler, 2003; Bächler and Kohl, 2005). After an initialization phase, FRACTure calculates, over each time step, the thermal and hydrological conditions within each element volume and determines the advective flow between each of them. Resulting thermal and hydrological variables are stored in arrays common to FRACTure and the geochemical modules. At this point, the program calculates the chemical reactions using a mass balance/mass action approach, the advective transport of chemical species, and the variations of porosity and permeability. Once this calculation is performed, the porosity and permeability are updated and fed into the FRACTure part of the code. The program then returns to the start of the loop until the end of the simulation time (sequential noniterative approach, SNIA).

FRACHEM has been developed specially for the granitic reservoir of Soultz-sous-Forêts and consequently, specific implementations have been added to the chemical part of this code. Considering the high salinity of the geofluid, the Debye-Hückel model, initially implemented in the CHEMTOUGH2 routines to determine the activity coefficients, has been replaced by a Pitzer activity model. It should be mentioned here that the activity coefficients calculations are carried out in an indirect manner by means of another code, TEQUIL model of the Na-K-H-Ca-Cl-SO_4-HCO_3-CO_3-CO_2-H_2 system for 0 to 250℃ (Moller et al., 1998). The TEQUIL application package includes chemical models based on the Pitzer formalism, and calculates liquid-solid-gas equilibria in complex brine systems by globally minimizing the free energy of a system at constant temperature and pressure.

Presently, a limited number of minerals are considered, which correspond to the minerals constituting the Soultz granite. The precipitation/dissolution reactions of carbonates (calcite, dolomite), quartz, amorphous silica, pyrite, and some aluminosilicates (K-feldspar, albite, illite) can be modeled under kinetic constraints. Rate laws follow more or less the transition state theory (TST)-derived equation (e.g., Lasaga et al., 1994). The implemented kinetic-rate laws are specific to each mineral and taken from published experiments conducted at high temperature in NaCl brines.

Thermodynamic data (equilibrium constants) are taken mostly from SUPCRT92 (Johnson et al., 1992) and Helgeson et al. (1978) and are functions of temperature and pressure. The effect of pressure on equilibrium constants is explicitly taken into account. The equilibrium constants input into FRACHEM were initially computed along the water-saturation pressure curve, however, these constants are recomputed with changes in pressure during run time.

Finally, a supplementary module allows the determination of porosity and permeability variations linked with chemical processes occurring in the reservoir. Considering the alteration of the Soultz granite, the flow is assumed to circulate in a medium composed of fractures and grains. Therefore, a combination of fracture model (Norton and Knapp, 1977; Steefel and Lasaga, 1994) and grain model (Bolton et al., 1996) is used to determine the permeability evolution. In this model, we assume that the fracture aperture and the thickness of the mineral layer follow Gaussian distributions (Durst, 2002).

SIMULATION SETUP

Three wells (GPK2, GPK3 and GPK4) drilled at a depth of about 5,000 m in the granite (T ≈ 200℃) will constitute the heat exchanger for electricity generation at the site of Soultz-sous-Forêts.

Several production tests have been conducted between 1999 and 2005, after the GPK-2 drilling and the hydraulic stimulation tests carried out in the wells GPK-2, GPK-3 and GPK-4, or during the fluid circulation test in 2005, between the injection well GPK-3 and the production wells GPK-2 and GPK-4. A tracer test using fluorescein and a geochemical fluid monitoring accompanied this operation in 2005. This work gave major results in terms of geochemistry (chemical and isotopic composition, fluid origin, reservoir temperature, water-rock-gas interaction processes) and circulation (natural fluid convection flux, existence of more permeable areas and different circulation paths in the heat exchanger, fluid velocities), (Sanjuan et al., 2006).

The very important fluid-flow data obtained from tracer tests conducted since 2000 and especially in 2005 should be confirmed by further tracer testing and other techniques (hydraulic tests, numerical modelling, geophysical monitoring, etc.). Nevertheless, the tracer test shows the presence of different circulation paths in the deep reservoir.

The simulations will use data for the Soultz reservoir derived from petrological and geochemical studies, and supplied by the site developers.

Mineralogical conditions

The geothermal reservoir at Soultz is made up of three types of granite (Jacquot, 2000; Hooijkaas et al., André et al., 2006) (Table 1). The first is non-altered (fresh) granite that is characterized by a predominance of feldspar, plagioclase and quartz, and by an extremely low fracture density. Consequently, its porosity is close to zero and does not contain significant amounts of water. The properties of this

granite are that of the impermeable rock matrix. Fluid exchange, by advection or diffusion processes, will be disregarded for this granite; it will only act as a good heat convector.

Table 1: Mean composition (in volume percent) of the different types of granite in the Soultz reservoir (Jacquot, 2000).

Minerals	Healthy granite	Hydrothermalised granite	Vein of alteration
Quartz	24.2	40.9	43.9
K-Feldspar	23.6	13.9	
Plagioclases	42.5		
Illite		24.6	40.2
Smectite		9.7	9.6
Micas	9.3		
Calcite	0.3	3.3	4.3
Dolomite		0.8	0.7
Pyrite		0.7	1.0
Galena		1.3	0.3
Chlorite		4.8	

The second rock facies is a fractured, hydrothermally altered granite, with quartz as the major mineral component; because of alteration the amount of feldspar decreases and some secondary minerals such as galena, pyrite, smectite or illite are present. This facies is the most porous (porosity ranging from 5 to 10%) and contains most of the formation fluid. The third rock facies is the most altered; it corresponds to alteration veins that present minerals such as illite, smectite and quartz. Precipitated secondary minerals (clays, carbonates) fully cement the fractures, resulting in a decrease of porosity and permeability. As a consequence, fluid circulation within the rock mass takes place through the second facies only (Genter et al., 1998).

Brine chemistry

The formation fluid circulating through the fracture network is a sodium-chloride brine with a total mineralization close to 100 $g.L^{-1}$. Its pH is approximately 4.9 and its temperature (200°C) is in equilibrium with that of the rock at 5'000-m depth. The composition of the formation brine extracted during a 1999 production test is given in Table 2. The chemistry of the deep fluid is not very different from that of the fluid produced from the shallower reservoir (Durst, 2002). Its silica and carbon concentrations are higher because of the elevated temperatures and CO_2 partial pressures.

Total concentrations obtained from chemical analyses (Table 2) were input into TEQUIL, which then computed speciation and corresponding activity coefficients. Computations were done using a typical Soultz fluid at a temperature of 200°C. This fluid was initially equilibrated with calcite and anhydrite at 200°C, which resulted in a decrease of Ca^{2+} and SO_4^{2-} concentrations (compared to input concentrations) due to precipitation of calcite and anhydrite. The pH value of 4.9 at 200°C was calculated from the equilibration with calcite and input total aqueous carbonate concentration. Using the fluid composition at 200°C, TEQUIL was then used to numerically cool the solution, recompute pH, and determine activity coefficients at temperatures down to 20°C. It should be noted that the cooling simulation was performed without allowing reactions with gases or minerals. Mg, Fe, and Al are not included in the TEQUIL database. For this reason, the geochemical program EQ3nr (Wolery, 1992) was applied to determine the activity coefficients of Mg^{2+}, Fe^{2+} and Al^{3+} by using the Pitzer model and the EQ3nr thermodynamic database data0.hmw (Harvie et al. 1984). Activity coefficients determined in this way were then input into FRACHEM as polynomial functions of temperature, for the specific ionic strength of the fluid. This approach works well for the case of Soultz simulations because the ionic strength of the circulated fluid remains more or less constant.

Table 2: Representative chemical analysis of the fluid sampled at the wellhead of GPK2 after being deepened to 5000 m in 1999 (Durst, 2002)

Species	Concentration (mmol/kg)
Na^+	1148.00
K^+	73.40
Ca^{2+}	169.50
Mg^{2+}	3.21
Cl^-	1648.00
S	1.77
C	42.76
Fe^{2+}	2.61
SiO_2	6.06
Al^{3+}	$3.7.10^{-3}$

Mesh geometry, fluid and heat flow conditions

This paper describes the application of the model to two cases: a single 1-D fractured zone and two 1-D connected fractured zones models. First, mesh discretization, geometrical model, models parameters and initial- and boundary conditions are described. Then, results of simulations are described to test if the fracture geometry has an impact on the chemical model results. Thermal and chemical processes were coupled and the porosity and permeability changes affect the hydraulic field. The simulations time was 600 days.

The model consists of a 750*300 m granitic matrix zone (Fig. 1). An injection and a production well separated by 650 m have been set. Because of symmetry, only half (the upper part) of fractured zones and of the adjacent porous matrix is modelled, by subdividing them into 502 elements (Fig. 1). The size of the elements ranges from a minimum of 0.5 m × 0.05 m near the injection and the production wells to a maximum of 50 m × 35 m. The fractured zones are located between 50 and 700 m; injection is made at 50 m and production occurs at point 750m (Fig. 1).

The first complete application of FRACHEM code was a single fracture model. The model consists of a single 650 m long, 0.1 m wide and 10 m deep fractured zone surrounded by rock matrix.
The second application consisted in a more complex model with two fractured zones of different widths. In this case, the two wells are linked by two types of fracture: a 0.1 m wide fracture going directly from injection to production and a set of 0.05 m wide fracture traversing 1050 m between the two wells. The model set up represents only the upper half of the overall model. The lower part of the model, not set up, is mirror-inverted along the x-axis. Therefore only half of the fracture (0.05 m) along the x-axis is taken into the model. The model is discretized finer along the fractures as shown in Figure 1 which illustrates the mesh discretization. The fluid is injected at the beginning of both fracture, and produced at the end of both fractures.

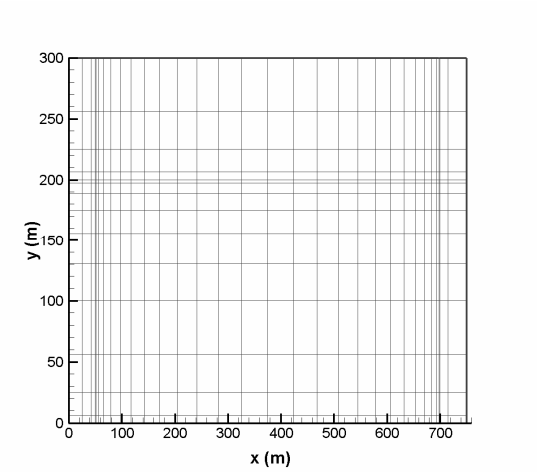

Figure 1. Whole model spatial discretization (distances are in m). The y-axis represents model width and the x-axis is along the fractured zone between injection and production wells, located at x=50m and x=700m, respectively.

The initial temperature in the model was set to 200℃, which corresponds to the temperature at 5000 m depth in the reservoir. The pressure at the production point was held constant at 50 MPa (bottom well pressure at GPK2). A constant over-pressure of 8 MPa was assumed at the injection well. In each of the fractured zones, fluid was injected at qinj= $2*10^{-2}$ $L.s^{-1}$ in the first volume element of the fractured zones. The injection rate for each fracture was based on the fluid production rate qtot= 25 $L.s^{-1}$ and assuming 1250 fractured zones (qtot/qinj= 1250 fractured zones) consisting of 200 fractures. The fluid flowing out of the last volume element is reinjected in the first one through a buffer of 2000 m^3 representing the fluid volume contained in wells and surface installation.

The fluid density is 1000 $kg.m^{-3}$ (at 200 ℃), the rock density 2650 $kg.m^{-3}$, the heat capacity of the rock is 1000 $J.kg^{-1}.K^{-1}$ and the heat capacity of the fluid is 4200 $J.kg^{-1}.K^{-1}$. No radiogenic heat production was integrated in the model. Only heat transfer between the matrix and the fractured zones is allowed.

The fluid flow in the matrix is negligible due to low hydraulic conductivity and zero matrix porosity. Thus, all chemical reactions happen in the fractures, whereas in the matrix no reactions take place. Though, we assume that major circulation occurs in hydrothermally altered granite. Cooled brine interacts with quartz, carbonates, K-feldspars, sulfides and clays. Secondary precipitation of amorphous silica was considered.

Initial reservoir water chemistry was obtained by equilibrating the sample water of formation fluid (Table 2) with the corresponding mineral compositions (Table 1) at 200℃. In each of the fractured zones fluid was injected at a temperature of 65℃.

Finally, three types of injection waters were considered, and were held constant over time. The first is the produced reservoir water (base case). The second was obtained by mixing one unit of reservoir water with one unit of fresh water (mixing case). The third was obtained by the addition of concentrated HCl in formation brine (acidification case).

RESULTS

Fracture geometry effect

Reservoir temperature

Before fluid circulation in the fractured zone, all the system (rock and brine) is chemically and thermally at equilibrium. The brine is in chemical equilibrium with the granite and these two components are at a constant temperature of 200℃. But, during the injection of cold fluid at 65℃ in the reservoir, the system is disturbed and the rock progressively cools down (Figs. 2 and 3).

For the first application, all along the fractured zone, we observe a global decrease of temperature, especially near the injection well, due to the temperature of the re-injected fluid (Fig. 2). After one year of fluid circulation, the temperature in the vicinity of the production well is close to 180℃. The development of this thermal front due to the thermal diffusion from rock to fluid affects a zone of 10 to 20 meters around the fractured zone (Figure 2). This temperature decrease of the produced fluid is particularly important but it is strongly dependent of the geometric model.

In the second application, we consider two parallel pathways. The temperature distribution in the fracture and the matrix after one year is shown in Figure 3. The temperature was decreased from 200℃ to 65℃ near the injection well. Along the fractured zones it increases to 190℃ towards the production point. Due to thermal diffusion, the temperature of the matrix is decreased around the fractured zones.

As a consequence, the cooling effect on the produced fluid modelled, when we consider a straight line flow between injection and production wells, without taking in consideration parallel pathways, is most probably overvalued compared to the real reservoir.

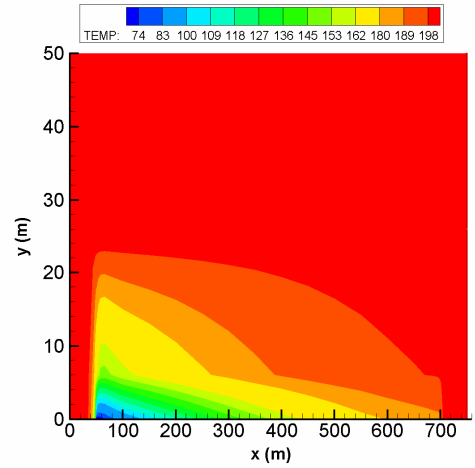

Figure 2: Temperature of rock around the single fractured zone after one year of forced fluid circulation.

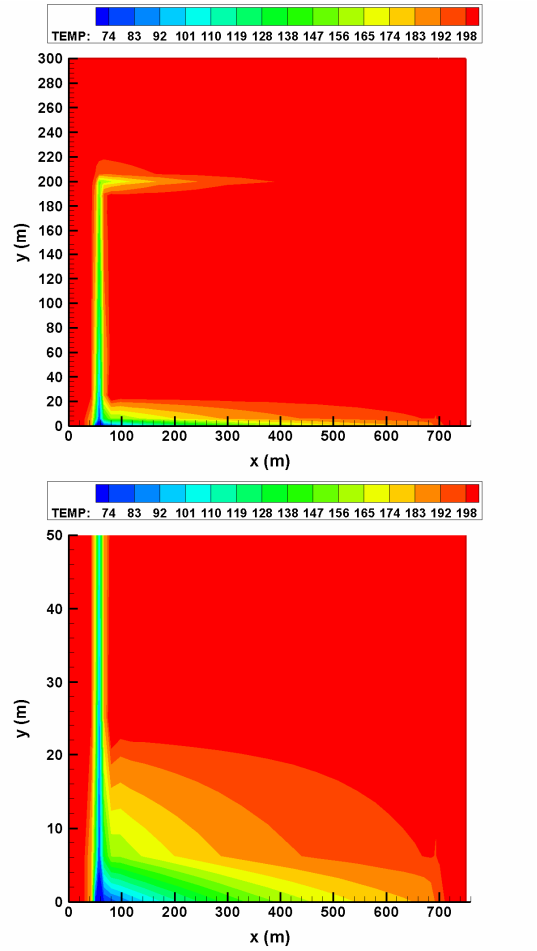

*Figure 3: Temperature of rock around the two fractured zones after one year of fluid circulation. a) Whole model. b) 50*750 m zone around the injection point.*

Mineral-brine interactions

The two-fracture simulation results are concordant to those of the single fracture simulation. Calcite dissolves at the vicinity of the injection zone and reprecipitates when the temperature rises. With time, the calcite dissolution rate in the injection elements decreases due to the diminution of available calcite that is almost totally dissolved after one year. Dolomite shows a similar dissolution trend but is removed faster at the injection point. The quartz precipitates in the low temperature zone and dissolves when the fluid warms up. Due to the relatively low reaction rates both precipitation and dissolution occur on a wide portion of the fracture. The pyrite does not present significant variations.

The injection of cold fluid creates a chemical disequilibrium, which induces dissolution of calcite and dolomite as well as precipitation of quartz and pyrite. The results show that the main chemical process are the fluid-calcite reactions that lead to porosity and permeability increases near the injection point, due to calcite dissolution. Because of the progressive temperature increase along the fracture, precipitation of calcite occurs towards the production point.

Calcite dissolves near the injection point at a maximum rate of $2.7.10^{-4}$ mol.m^{-3}.s^{-1} and precipitates at maximum $7.6.10^{-6}$ mol.m^{-3}.s^{-1} at the production well (Fig. 4). With increasing simulation time, the dissolution zone moves towards the production point. Near the injection well all calcite has dissolved after one year with a reaction rate reducing correspondingly to zero. In contrast, dolomite never precipitates (Fig. 5). At the beginning of the simulation, dissolution only takes place near the injection point at a maximum rate of 6.10^{-6} mol.m^{-3}.s^{-1}. After one year, the dissolution zone moves slightly towards the production point and the reaction rate increases to $1.4.10^{-5}$ mol.m^{-3}.s^{-1}.

These results show the interdependence of pH, temperature and carbonate behaviour: the cold fluid at low pH dissolves calcite and dolomite near the injection well at a high rate (Fig. 6). Reheating the fluid causes the calcite to precipitate and the pH to rise. Since the calcite precipitation rate is higher than that of dolomite, calcite precipitation prevents the precipitation of dolomite. According to the temperature evolution in the fracture, this process moves towards the production well and the reaction rates decrease. With increasing reaction time, the reaction rates reduce strongly due to the decrease of available carbonates. At the beginning, the dissolution of dolomite is controlled by temperature, whereas with time it depends more on calcite precipitation.

The most reactive of the silicates are amorphous silica. It precipitates near the injection well at a maximum rate of $2.8.10^{-5}$ mol.m^{-3}.s^{-1} (Fig. 7). With increasing circulation time, the zone of amorphous silica precipitation spreads towards the production well. Quartz precipitates all along the fracture at a maximum rate of $5.5.10^{-10}$ mol.m^{-3}.s^{-1} (Fig. 8). Depending on the temperature evolution, with time the maximum reaction rate moves towards the production point and decreases. K-feldspar and pyrite present a similar behaviour. Precipitation of K-feldspar occurs close to the injection point. Unlike quartz, some punctual dissolution events of pyrite occur. These differences are due to the fact that even if the pyrite reaction depends on the temperature evolution, there is still an influence from the pH.

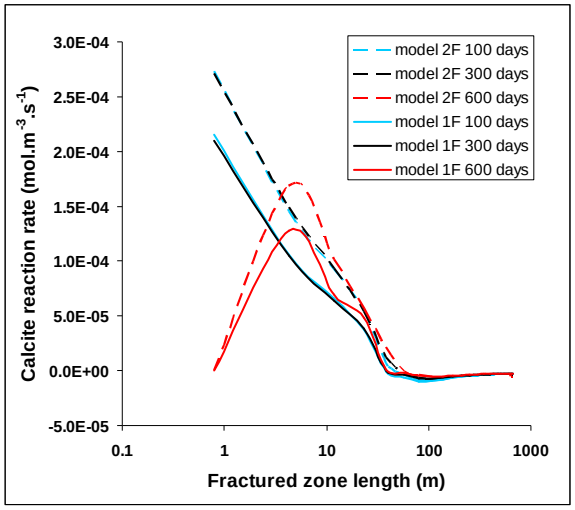

Figure 4: Calcite reaction rate along the fractured zone at different times (positive values indicate dissolution).

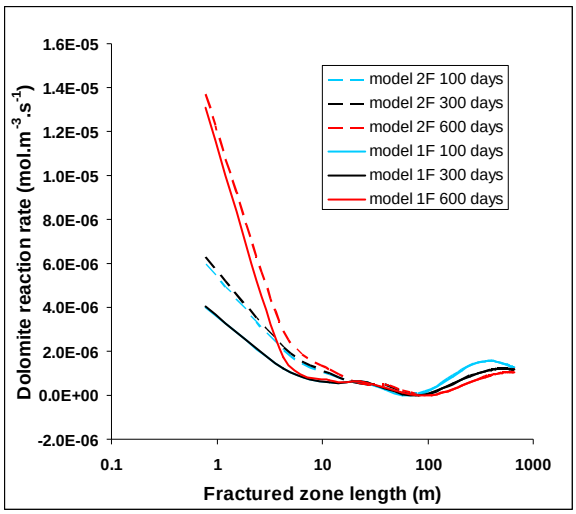

Figure 5: Dolomite reaction rate along the fractured zone at different times (positive values indicate dissolution).

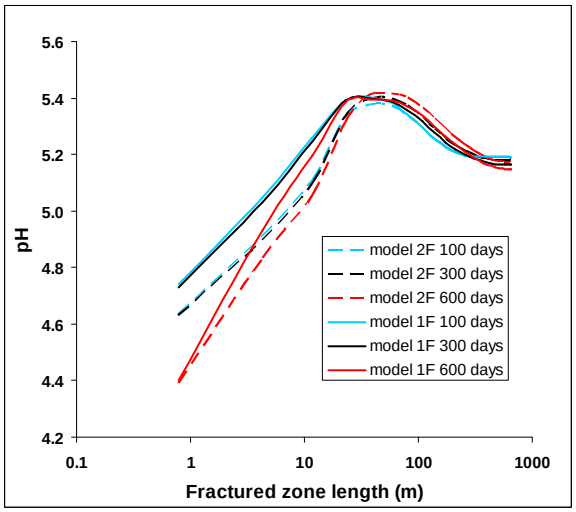

Figure 6: pH evolution along the fractured zone at different times.

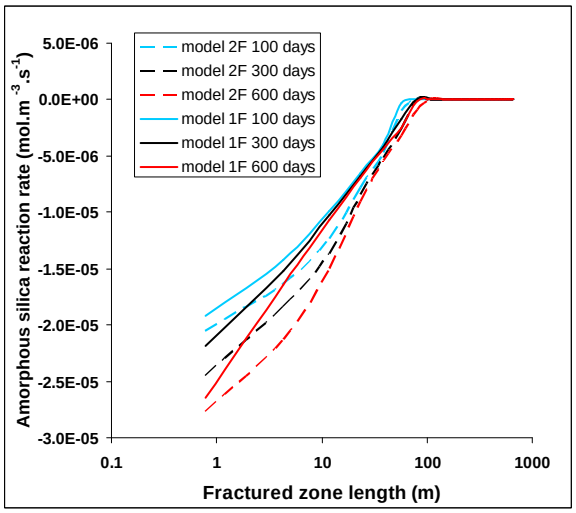

Figure 7: Amorphous silica reaction rate along the fractured zone at different times.

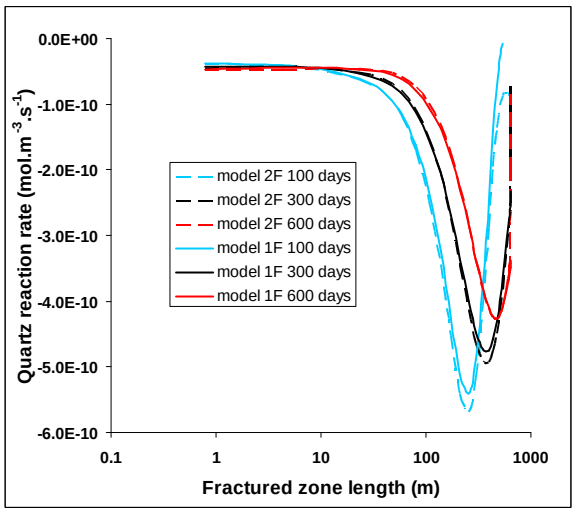

Figure 8: Quartz reaction rate along the fractured zone at different times (negative values indicate precipitation).

Evolution of reservoir properties

The differences in the reaction rates result in varying porosities. This difference is expected to increase further when calculating more than one year.

In both cases, porosity and permeability increase near the injection point due to dissolution of carbonates and decrease near the production point due to calcite precipitation (Fig. 9).

After one year the porosity at the injection point reaches 0.13 and goes down to 0.09 and 0.1 respectively in the large and thin fracture. The more porous zone extends up to 20 m in the large fracture and 10 m in the thin fracture. After 600 days, the area affected by the porosity reduction is wider.

Considering that there are only two fluid pathways and that the value of the permeability reduction in these two paths are small and close to each other, the geochemical reactions do not significantly modify the thermal-hydraulic parameter in the model.

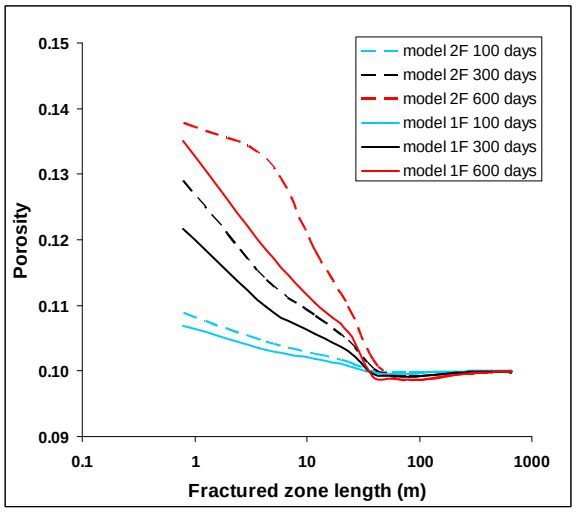

Figure 9: Porosity evolution along the fractured zone at different times. Initial porosity was 0.1.

Effect of fluid chemistry on fracture porosity

Recently chemical treatments were performed at Soultz-sous-Forêts (France). This deep granitic reservoir contains fractures partially filled with a mixture of secondary carbonates (calcite and dolomite), various kinds of clay minerals (Illite, chlorite….) and silica. In order to dissolve these carbonates and to enhance productivity around the wells, each of the three 5-Km deep boreholes (GPK2, 3 and 4) were treated with different amounts of hydrochloric acid. If GPK3 has shown weak variations of its injectivity, GPK4 presented a real increase of its injectivity and productivity after the treatments and GPK2 presented also a very sensible improvement despite the fact that the treatment was only a very small preliminary test.

Reactive transport modelling can be used to track the propagation of reaction fronts and to gain insight into the effectiveness of acid injection as a well stimulation technique.

To explore chemically-induced effects of fluid circulation in the system, we examine ways in which the chemical composition of reinjected waters can be modified to improve reservoir performance.

Modifying the injection water could avoid mineral scaling and enhance injectivity. Chemical manipulations considered here include pH modification and dilution with fresh water.

Two types of injection waters were considered, and were held constant over time. The first was obtained by mixing one unit of reservoir water with one unit of fresh water (mixing case). The second was obtained by the addition of concentrated HCl in formation brine (acidification case). The pH of the acidified injected solution was close to 3.2. In each of the fractured zones fluid was injected at a temperature of 65°C.

Chemistry evolution of the produced fluid

Concerning the evolution of the fluid concentration in the whole model, one major evolution appears (Figures 10 and 11). In the mixing case, pH of the produced fluid increases and the total calcium concentration of the produced fluid decreases from its initial 0.12 mol.kg^{-1} and stabilizes at 0.09 mol.kg^{-1} after 20 days. In the acidification case, pH of the produced fluid decreases from 5 to 4.65 and consequently, the total calcium concentration of the produced fluid slightly increases. This illustrates the dissolution of calcite.

Calcite can also be precipitated at surface during the raise of the geothermal brine and CO_2 degassing. However, in the case of the Soultz site, the alkalinity measurements tend to increase in solution with decreasing well depth and temperature. Two assumptions can explain this evolution: dissolution of carbonate minerals (calcite, for instance) and/or dissolution of organic compounds present in the granite, during the raise and the cooling of the deep geothermal brine (Sanjuan et al., 2006).

Generally, the cooling of hot fluid during its raise causes silicate mineral precipitation (amorphous silica at surface, quartz in deeper areas). The risk of silica precipitation is increased when the fluid raise is slow.

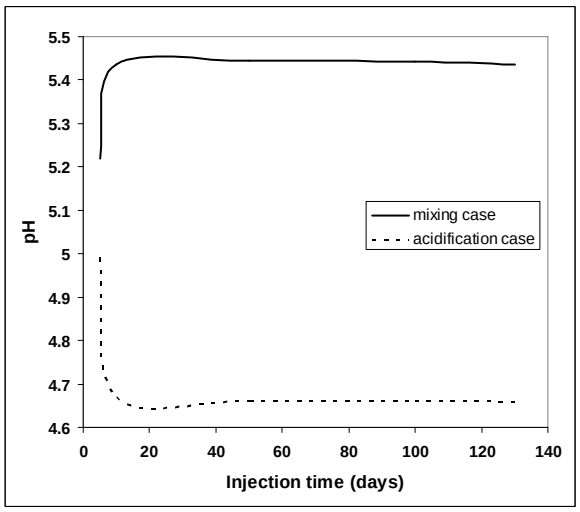

Figure 10: pH evolution in the produced fluid as a function of injection time.

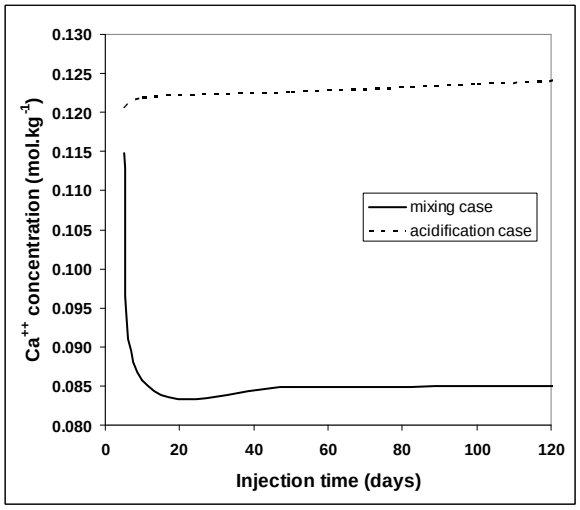

Figure 11: Calcium concentration evolution in the produced fluid as a function of injection time.

Evolution of fracture porosity

The mixing water is less prone to precipitating calcite (Fig. 12), and therefore is favorable for porosity development and maintaining injectivity. Though, alteration of injection water chemistry, for example by dilution with fresh water, can greatly alter precipitation and dissolution effects along the entire flow paths, and can offer a powerful tool for operating EGS reservoirs in a sustainable manner.

Another possible means to reduce the tendency towards calcite precipitation is to add HCl acid to injection water. Variations of the initial pH (3.2) have a significant effect on the reaction rates of carbonates (Fig. 12), but this effect should disappear during the first months of simulation, when the system will tend to recover equilibrium and will not have significant effects for long time simulations. The acidified brine injection water contributes to a porosity increase of about 0.035 in the vicinity of injection well (Fig. 13). Short injection of acidified water is favorable for porosity development and maintaining injectivity.

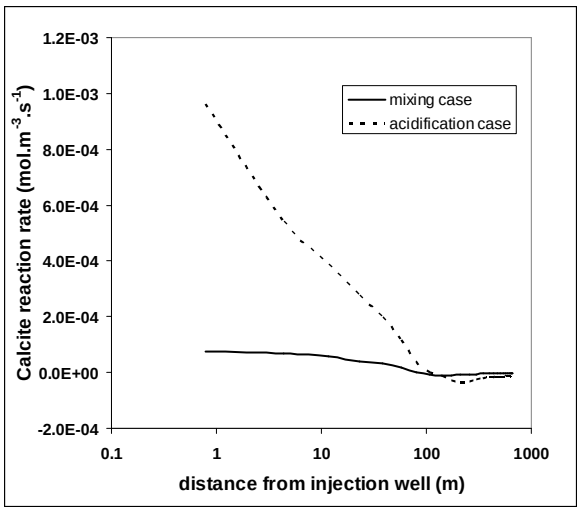

Figure 12: Calcite reaction rate along the fractured zone after 100 days of injection.

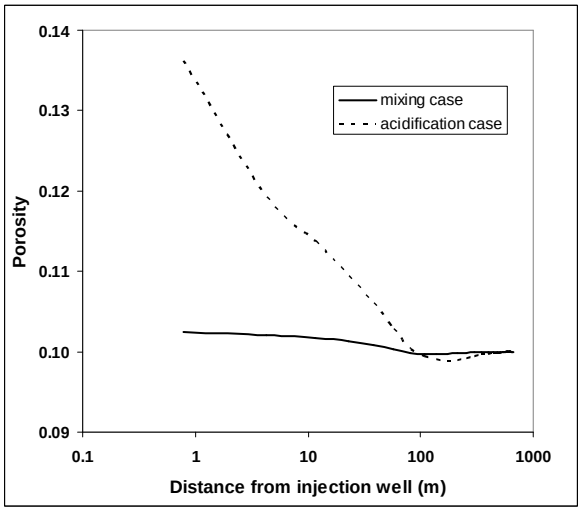

Figure 13: Porosity evolution along the fractured zone after 100 days of injection. Initial porosity was 0.1.

FRACHEM has been used to simulate injectivity recovery by acid injection (André et al., 2006). The predicted amount of scaling minerals dissolved by acid is consistent with the estimal amount.

Temperature, chemical composition and pH of injection fluid, host rock and fracture mineralogies can all have a great impact on the fate of injection. These parameters will be examined more closely trough sensitivity studies in future work. For instance, the relatively large amount of SiO_2(aq) in the injection fluid appears to be a factor that could potentially have a significant impact on porosity and permeability.

CONCLUSIONS

The first application of the new code FRACHEM consisted of the modelling of a simplified system, including a cooled fluid reinjected in a hot reservoir composed of a 650-m long by 0.1-m wide fracture surrounded by an impermeable matrix. The results show that at the beginning of the simulation, calcite and dolomite are rapidly dissolved near the injection point. Then, warming up induces carbonates precipitation on a wider zone. Later, the carbonates being less available in the injection area, reactions rates decrease significantly. Amorphous silica, K-feldspar, quartz and pyrite precipitate in the fracture. Moreover, some exceptional events of pyrite dissolution are also observed. Porosity evolution mainly shows a high increase near the injection point, due to carbonates dissolution. On the other hand, a small decrease of porosity is observed later, due to calcite re-precipitation. The second application was a 2-D model with the dimension of the upper Soultz reservoir. This model includes two fractures of different widths following two different paths. The geochemical evolution is similar to the previous simulation with carbonates dissolving near the injection point and re-precipitating further in the fracture. During the first 600 days this lead to a porosity increase of 0.04 followed by a decrease of 0.005. The variations are similar in both fractures and affected the first 10 m of the thin fracture and the first 20 m of the large one.

Both models are still simple and clearly do not represent the complex and heterogeneous situation at Soultz. However, fully coupled models of the Soultz EGS reservoir were developed and the model sensitivity can be tested. No true sensitivity analysis has been made concerning the spatial discretization and fracture network density, but the comparison between the results of the two simulation models indicates that the permeability variation depends principally on the evolution of the temperature field calculated by FRACTure and not much on the spatial discretization or the fluid flow rate. But changes in the porosity/permeability, and thus in the hydraulic conductivity, impact the fluid velocity and the pressure distribution in the fracture: mineral precipitation causes the porosity and therefore also the permeability and the hydraulic conductivity to decrease. Lower hydraulic conductivity results in lower fluid velocities. Since the fluid velocities are smaller, the rate of temperature decrease in the fractured zone is lower

In the mixing and acidification cases presented, the results differ much from the basic model: the largest porosity difference in the fractured zone is 0.015. This is more than 15% of the initial porosity. Various reacting fluids can be injected to enhance fracture permeability in the vicinity of the wells. FRACHEM code could be used to identify the most efficient ways in which the chemical composition of reinjected waters can be modified to improve EGS reservoir performance (pH modification or dilution with fresh water).

Finally, fluid-rock interactions may have a long-term effect on reservoir operation. While more or less detailed studies of the initial interaction of the reservoir rock with the injected fluid have been made at most of the EGS sites, there is still a good deal to learn about how the injected fluid will interact with the rock over the long term. The most conductive fractures often show evidence of fluid flow in earlier geologic time such as hydrothermal alteration and secondary mineral deposition. This is encouraging in that it suggests that the most connected pathways will already have experienced some reaction between water and the rock fracture surface. Fresh rock surfaces will not have the protection of a layer of deposited minerals or alteration products. The amount of surface or shallow water, which cannot be in equilibrium with the reservoir rock, required to add to the system over the long term is although unknown. The longest field tests have seen some evidence for dissolution of rock leading to development of preferred pathways and possible short-circuits. Moreover, the produced fluid will be cooled through a heat exchanger, in the surface equipment, possibly resulting in precipitation of scale or corrosion. To conclude, despite efforts to model fluid-rock interactions, there are still major questions to be answered.

ACKNOWLEDGEMENTS

The authors would like to thank the Swiss Federal Office of Education and Science (Project N° 03.0460) and the Swiss Federal Office of Energy (Project N° 150'649) for f unding this project. The authors are also grateful to André Gérard of the GEIE at Soultz and Thomas Kohl of GEOWATT AG (Zürich).

REFERENCES

André, L., Rabemanana, V. and Vuataz, F.-D., 2006. Influence of water-rock interactions on fracture permeability of the deep reservoir at Soultz-sous-Forêts, France. Geothermics 35, 507-531.

André, L. and Vuataz, F.-D., 2005. Simulated evolution of reservoir properties for the Enhanced Geothermal System at Soultzsous-Forêts: the role of hot brine-rock interactions. In: Proceedings of the 30th Workshop on Geothermal Reservoir Engineering. Stanford University, 283–290.

André, L., Spycher, N., Xu, T., Pruess, K. and Vuataz, F.-D., 2006. Comparing FRACHEM and TOUGHREACT for reactive transport modeling of brine-rock interactions in Enhanced Geothermal Systems (EGS). In: Proceedings of the 31st Workshop on Geothermal Reservoir Engineering. Stanford University, 350–358.

Bächler, D. and Kohl, T., 2005. Coupled thermal-hydraulic-chemical modelling of enhanced geothermal systems. Geophys. J. Int. 161 (2), 533–548.

Bächler, D., Kohl, T. and Rybach, L., 2003. Impact of graben-parallel faults on hydrothermal convection – Rhine Graben case study. Physics and Chemistry of the Earth 28, 431-441.

Bächler, D., 2003. Coupled Thermal-Hydraulic-Chemical Modelling at the Soultz-sous-Forêts HDR reservoir (France). PhD thesis, ETH-Zürich, Switzerland, 151 p.

Baria, R., Jung, R., Tischner, T., Teza, D., Baumgaertner, J., Dyer, B., Hettkamp, T., Nicholls, J., Michelet, S., Sanjuan, B., Soma, N., Asanuma, H. and Garnish, J., 2006. Creation of an HDR/EGS reservoir at 5000 m depth at the European HDR project. Proc. 31st Workshop on Geothermal Reservoir Engineering, Stanford University, California, USA.

Barrett, T.J. and Anderson, G.M., 1988. The solubility of sphalerite and galena in 1–5m NaCl solutions to 300℃. Geochim. Cosmochim. Acta 52 (4), 813–820.

Bartels, J., Kühn, M. and Clauser, C., 2003. Numerical simulation of reactive flow using SHEMAT. In: Clauser C. (ed) Numerical simulation of reactive flow in hot aquifers - SHEMAT and Processing SHEMAT, Springer Publishers, Heidelberg, 5-74.

Blum, A.E. and Stillings, L.L., 1995. Feldspar dissolution kinetics. In: White, A.F., Brantley, S.L. (Eds.), ChemicalWeathering Rates of Silicate Minerals, 31. Mineralogical Society of America, 291–351, Reviews in Mineralogy.

Bolton, E.W., Lasaga, A.C. and Rye, D.M., 1996. A model for the kinetic control of quartz dissolution and precipitation in porous media flow with spatially variable permeability; formulation and examples of thermal convection. J. Geophys. Res. Part B. Solid Earth Planets 101 (10), 22157–22187.

Brown, D.W., 2000. A Hot Dry Rock geothermal energy concept utilizing supercritical CO_2 instead of water. Proc. 25th Workshop on Geothermal Reservoir Engineering, Stanford University, California, USA.

Carroll, S., Mroczek, E., Alai, M. and Ebert, M., 1998. Amorphous silica precipitation (60 to 120℃): comparison of laboratory and field rates. Geochim. Cosmochim. Acta 62 (8), 1379–1396.

Dezayes, C., Valley, B., Maqua, E., Sysen, G. and Genter, A., 2005. Natural fracture system of the Soultz granite based on UBI data in the GPK3 and GPK4 wells. In: Proceedings of the EHDRA Scientific Meeting. Soultz-sous-Forêts, France.

Durst, P., 2002. Geochemical modelling of the Soultz-sous-Forêts Hot Dry Rock test site: coupling fluid-rock interactions to heat and fluid transport. PhD thesis, University of Neuchˆatel, Switzerland, 127 p.

Evanoff, J., Yeager, V. and Spielman, P., 1995. Stimulation and damage removal of calcium carbonate scaling in geothermal wells: a case study. In: Proceedings of the World Geothermal Congress '95, Florence, Italy, 2481–2485.

Evans, K.F. , Moriya, H., Niitsuma, H., Jones, R.H., Phillips, W.S., Genter, A., Sausse, J., Jung, R. and Baria, R., 2005. Microseismicity and permeability enhancement of hydrogeologic structures during massive fluid injections into granite at 3 km depth at the Soultz HDR site, Geophys. J. Int., 160, 388-412.

Genter, A., Traineau, H., Dezayes, C., Elsass, P., Ledesert, B., Meunier, A. and Villemin, T., 1995. Fracture analysis and reservoir characterization of the granitic basement in the HDR Soultz project (France). Geotherm. Sci. Tech., 4 (3), 189-214.

Gérard, A., Fritz, B. and Vuataz, F.-D., 2005. Results of soft acid injection tests performed at Soultz in wells GPK2, GPK3 and GPK4—extended summary: revised status on 14 March 2005. In: Proceedings of the EHDRA Scientific Conference, Soultz-sous-Forêts, France.

Gérard, A., Genter, A., Kohl, T., Lutz, P., Rose, P. and Rummel, F., 2006. The deep EGS (Enhanced Geothermal System) project at Soultz-sous-Forêts (Alsace, France). Geothermics, 35 (5-6), 473-483.

Hellmann, R., 1994. The albite-water system. Part I. The kinetics of dissolution as a function of pH at 100, 200 and 300 ◦C. Geochim. Cosmochim. Acta 58 (2), 595–611.

Hooijkaas, G. R., Genter, A. and Dezayes, C., 2006. Deep-seated geology of the granite intrusions at the Soultz EGS site based on data from 5 km-deep boreholes. Geothermics, 35 (5-6), 484-506.

Icenhower, J.P. and Dove, P.M., 2000. The dissolution kinetics of amorphous silica into sodium chloride solutions: effects of temperature and ionic strength. Geochim. Cosmochim. Acta 64 (24), 4193–4203.

Jacquemont B., 2002. Etude des interactions eau-roche dans le granite de Soultz-sous-Forêts. Quantification et modélisation des transferts de matière par les fluides. Thèse Univ. Louis Pasteur, Strasbourg, France.

Jacquot, E., 2000. Modélisation thermodynamique et cinétique des réactions géochimiques entre fluides de bassin et socle cristallin: application au site expérimental du programme européen de recherche en

géothermie profonde (Soultz-sous-Forêts, Bas-Rhin, France). PhD thesis, Université Louis Pasteur, Strasbourg, 202 p.

Kohl, T. and Hopkirk, R.J., 1995. “FRACTure” – a simulation code for forced fluid flow and transport in fractured, porous rock. Geothermics 24 (3), 333–343.

Kohl, T. and Rybach, L., 2001. Assessment of HDR reservoir geometry by inverse modelling of non-laminar hydraulic flow. In: Proceedings of the 26th Workshop on Geothermal Reservoir Engineering. Stanford University, 259–265.

Moller, N., Christov, C. and Weare, J., 2006. Thermodynamic models of aluminum silicate mineral solubility for application to enhanced geothermal systems. Proc. 31st Workshop on Geothermal Reservoir Engineering, Sanford University, California, USA.

Monnin, C., 1989. An ion interaction model for the volumetric properties of natural waters: density of the solution and partial molal volume of electrolytes to high concentrations at 25 ◦C. Geochim. Cosmochim. Acta 53, 1177–1188.

Nagy, K.L., Blum, A.E. and Lasaga, A.C., 1991. Dissolution and precipitation kinetics of kaolinite at 80 ◦C and pH 3: the dependence on solution saturation state. Am. J. Sci. 291 (7), 649–686.

Norton, D. and Knapp, R., 1977. Transport phenomena in hydrothermal systems; the nature of porosity. Am. J. Sci. 277 (8), 913–936.

Pitzer, K.S., 1973. Thermodynamic of electrolytes. I. Theoretical basis and general equations. J. Phys. Chem. 12, 268–277.

Pokrovskii, V.A. and Helgeson, H.C., 1995. Thermodynamic properties of aqueous species and the solubilities of minerals at high pressures and temperatures: the system Al2O3-H2O-NaCl. Am. J. Sci. 295, 1255–1342.

Portier, S., André, L. and Vuataz, F.-D., 2006. Modelling geochemical effects of acid treatments and comparison with field observations at Soultz-sous-Forêts geothermal site. Proc. ENGINE Scientific Workshop 3, « Stimulation of reservoir and microseismicity », Kartause Ittingen, Zürich, Switzerland.

Portier, S., André, L. and Vuataz, F.-D., 2006. Review of chemical stimulation techniques and results of acid injection experiments at Soultz-sous-Forets. Proc. EHDRA Scientific Conference, Soultz-sous-Forêts, France.

Pruess, K. and Azaroual, M., 2006. On the feasibility of using supercritical CO_2 as heat transmission fluid in an engineered Hot Dry Rock geothermal system. Proc. 30th Workshop on Geothermal Reservoir Engineering, Stanford University, California, USA.

Rabemanana, V., Durst, P., Bächler, D., Vuataz, F.-D. and Kohl, T., 2003. Geochemical modelling of the Soultz-sous-Forêts Hot Fractured Rock system: comparison of two reservoirs at 3.8 and 5 km depth. Geothermics 32 (4–6), 645–653.

Rimstidt, J.D. and Barnes, H.L., 1980. The kinetics of silica-water reactions. Geochim. Cosmochim. Acta 44 (11), 1683–1699.

Sanjuan, B., Pinault, J.L., Rose, P., Gérard, A., Brach, M., Braibant, G., Crouzet, C., Foucher, J.-C., Gautier, A. and Touzelet, S., 2006. Tracer testing of the geothermal heat exchanger at Soultz-sous-Forêts (France) between 2000 and 2005. Geothermics 35, 622-653.

Sausse, J. and Genter, A., 2005. Types of permeable fractures in granite, Special Publication of the Geological Society of London, 240, 1-14.

Sausse, J., Fourar, M. and Genter, A., 2006. Permeability and alteration within the Soultz granite inferred from geophysical and flow log analysis. Geothermics, 35 (5-6), 544-560.

Tchistiakov, A.A., 2000. Physico-chemical aspects of clay migration and injectivity decrease of geothermal clastic reservoir. In: Proceedings of the World Geothermal Congress 2000, Kyushu-Tohoku, Japan, 3087–3095.

Tenzer, H., 2001. Development of hot dry rock technology. Bulletin GeoHeat Center, 32 (4), 14-22.

Tester, J. W. and al., 2007. The future of geothermal energy: The impact of Enhanced Geothermal Systems (EGS) on the United States in the 21st century. An assessment by an MIT-led interdisciplinary panel, Massachusetts Institute of Technology Report, 372 p.

Vuataz, F.-D., 2000. Review of the papers on HDR and Enhanced Geothermal Systems. World Geothermal Congress 2000, Kyushu, Tohoku, Japan, unpubl. report.

White, S.P., 1995. Multiphase nonisothermal transport of systems of reacting chemicals. Water Resour. Res. 31 (7), 1761–1772.

Wolery, T.J., 1992. EQ3nr, a computer program for geochemical aqueous speciation solubility calculations: theoretical manual, user’s guide and related documentation (Version 7.0). Report, UCRL-MA-110662 PT III, Lawrence Livermore National Laboratory, Livermore, California, USA, 246 p.

Xu, T., Ontoy, Y., Molling, P., Spycher, N., Parini, M. and Pruess, K., 2004. Reactive transport modeling of injection well scaling and acidizing at Tiwi field, Philippines. Geothermics 33 (4), 477–491.

Proceedings European Geothermal Congress 2007
Unterhaching, Germany, 30 May-1 June 2007

Modelling the impact of forced fluid-rock interactions on reservoir properties at Soultz-sous-Forêts EGS geothermal site.

Portier Sandrine[*], André Laurent[**], Vuataz François-David[*] and Kohl Thomas[***]

[*] Centre for Geothermal Research - CREGE, c/o CHYN, University of Neuchâtel, E.-Argand 11, CP158

CH-2009 Neuchâtel, Switzerland.

[**] BRGM - Service EAU/M2H - BP 6009 - F-45060 Orléans cedex, France.

[***] GEOWATT AG – Dohlenweg 28, CH-8050 Zürich, Switzerland.

Keywords: Geothermal reservoir, brine, granite, secondary minerals, thermo-hydraulic-chemical coupled code, fluid-rock interactions, mineral reaction rates, porosity, permeability, acidizing treatments, Enhanced Geothermal System (EGS), Soultz-sous-Forêts.

ABSTRACT

The development of Enhanced Geothermal Systems (EGS) depends on the creation of permeable fractures. Once the fractures network is created, the success of the long-term exploitation depends on maintaining and enhancing permeability. Sustaining fracture permeability will depend on many variables including rock mineralogy, fluid chemistry, temperature, local stress field, fracture strain rate, and the proximity of natural fractures to the wellbore. Operations exploiting little known, deep heat sources and low permeability reservoirs face new problems involving high temperature and pressure brine-rock interactions. In order to forecast the behaviour of an enhanced geothermal reservoir under exploitation, interaction between flow, heat transfer, transport and chemical reactions must be evaluated. For this purpose, coupled reactive transport modelling can provide useful information, by simulating chemical reactions likely to occur in the system coupled to reactive transport, at large time and space scales.

FRACHEM, a thermo-hydraulic-chemical coupled code, was developed especially to forecast the evolution of the EGS project at Soultz-sous-Forêts, Alsace (France). FRACHEM can simulate thermal, hydraulic and fluid-rock interactions within the fractures connecting the injection and the production wells, and determine the dissolution/precipitation reactions of nine minerals in the Soultz granite (carbonates, pyrite, silicated minerals). In the first application, the coupled processes of a single fractured zone between two wells were investigated. In the second application, a more complex geometry has been shaped to represent a realistic reservoir model. This model includes two fractured zones of different widths following two different paths with the dimension of the Soultz reservoir. Depending on their distance and the relative exposure, these fractured zones interact on each other. These interactions have been investigated to predict the geochemical evolution and to quantify the impact on the reservoir. Results of numerical simulations for a long-term circulation confirm the role played by carbonates on the evolution of reservoir porosity and permeability. Due to their fast reaction rates, carbonate minerals are responsible for most of the reservoir evolution. Indeed, occurrence of calcite precipitation near the production well tends to decrease the reservoir porosity and permeability, induced by the decrease of the fractures aperture. Silicates and pyrite behaviour is also simulated between two wells, but their influence on the fractures aperture is minor.

Economic exploitation of enhanced geothermal systems is dependent to mineral precipitation and associated decrease in permeability of the system. This inhibits fluid flow and associated heat extraction from the system. One solution to this problem consists in injecting a reacting fluid into the wells, in order to dissolve the secondary minerals sealing the fractures, to increase the permeability and hence to stimulate the reservoir. Recent acid treatments were performed on the Soultz wells. FRACHEM simulations have been tested to forecast the impact of reacting fluid injection, such as acidizing, on amounts of carbonates dissolved and precipitated and resulting porosity developments.

1. INTRODUCTION

Enhanced (or engineered) Geothermal Systems (EGS) are defined as engineered reservoirs that have been created to extract economical amounts of heat from low permeability and/or porosity geothermal resources. EGS concepts would recover thermal energy contained in subsurface rocks by creating or accessing a system of open, connected fractures through which water can be circulated down injection wells, heated by contact with the rocks, and returned to the surface in production wells to form a closed loop. This large renewable energy resource can be exploited in a sustainable mode in the sense that different reservoir rock volumes can be developed successively from the same surface installation by extending or deviating existing boreholes, and they have practically zero CO_2 emissions.

Abundant geothermal resources sound like a great deal, but in addition to the extraction costs, there are numerous geological problems associated with its exploitation. The heat is extracted by conduction and convection. As a consequence, circulating hot water in the crust inevitably leads to dissolution, transport and re-deposition of minerals. In the case of heat extraction projects, the pores and the fractures in the water-bearing rocks may become clogged by mineral deposition, eventually stemming flow. This can limit the productive lifetime of an engineered geothermal system, even though heat may still be available at depth. Current research into water–rock interaction in geothermal reservoirs is directed at ways to enhance energy production and to avoid clogging of the rock openings.

The principle of an Enhanced Geothermal System (EGS) is to inject cold water into a hot fractured rock reservoir, to extract the heated water by one or several production wells, and to transfer its energy to a working fluid via a surface heat exchanger close to the wells. The feasibility and characteristics of this process rely ultimately on the fact that the natural fissures, opened and/or widened artificially by injection of water at high pressures through the borehole, remain open. However, during the stimulation phase, the

injected water is composed of formation and surface fluids and will react with the rocks minerals. The composition of the resulting fluids will be controlled by temperature, time, and by the minerals composition and added natural fluids.

Later, during reservoir exploitation, the formation fluid will be most probably dominant in the water-rock reactions, but a heating-cooling cycle will trigger continuous reactions. Dissolution and precipitation will take place along the pathways of these resulting fluids, and open fissures can potentially close by mineral precipitation. Also, mineral precipitation can potentially create problems along the geothermal loop, from the production casing to the surface tubing, the heat exchanger and the reinjection casing, when the hot fluids are cooled down by approximately 100°C at the heat exchanger.

Evidently, at an EGS site, it is necessary to understand and quantify fluid circulation and composition with time and to predict the dissolution-precipitation behaviour of the fluids along their pathways. Our main goal is to comprehend and quantify fluid circulation and composition with time and to predict the dissolution-precipitation behaviour of the fluids along their pathways. This will be achieved by geochemical modelling.

The proposed study consists of modelling fluid–rock interaction and scale formation during geothermal heat extraction with application to Soultz project. FRACHEM code has been developed to realistically simulate the long-term (years to decades) evolution of permeability and heat-exchange efficiency in an EGS reservoir. The latter are dependent on the interaction of chemical processes (mineral dissolution and precipitation in rock fractures and technical installations) with the flow of the reactive fluids through a geometrically complex, and changing fracture network.

A great deal of specific and detailed information is required to assess the chemical impact of an injection operation. The present study is not intended to represent any specific site. However, well configuration and data for mineralogical composition were taken from the European Enhanced Geothermal System at Soultz-sous-Forêts (Soultz project; Jacquot, 2000; Durst, 2002; Bächler, 2003). The simulations will use data for the Soultz reservoir derived in petrological and geochemical studies, and supplied by the site developers.

2. SOULTZ-SOUS-FORETS EGS PROJECT

The Soultz-sous-Forêts EGS is located in Alsace, about 50 km north of Strasbourg (France). The Soultz area was selected as the European EGS pilot site because of its strong temperature gradient in the sedimentary cover (up to 100°C/km) and its high heat flow, locally reaching 0.15 W/m^2 (Kohl and Rybach, 2001). The geology of the Soultz region is characterized by a graben structure affected by several N-S striking faults. The crystalline basement, covered by 1'400 m of Triassic and Tertiary sediments, is composed of three facies in granitic rocks: (1) an unaltered granite in which fracture density is close to zero; (2) a hydrothermally altered granite facies and (3) altered veins within the hydrothermally altered granite (Jacquot, 2000). The hydrothermally altered granite is the most porous facies (Genter et al., 1997) and altered veins are highly fractured. Natural circulation of formation fluid and fluid-rock interaction processes take place mainly within the hydrothermally altered granite, and to a lesser extent within altered veins. Flow in the unaltered granite is essentially nil. To extract the heat from the Soultz reservoir, three deviated wells have been installed to a depth of 5'000 m, with lower ends separated by 600 m. The reservoir encountered at this depth presents an initial temperature of 200°C. One well (GPK3) will be dedicated to the injection of cold water in the granitic reservoir at a rate of about 50 $L.s^{-1}$, whereas the two other wells (GPK2 and GPK4), located on both sides of the injector, will be used to produce about 25 $L.s^{-1}$ each of the formation fluid. At Soultz, the injection–production system has been designed as a closed loop. The fluid used is a formation fluid existing in the altered granite, namely a brine with a total dissolved solids value of around 100'000 ppm. Injection of cooled brine disturbs the equilibrium between the formation fluid and reactive minerals. The resulting change in temperature and pressure in the reservoir, and the forced circulation in fractured granite, will drive geochemical reactions able to affect the physical properties of the reservoir through mineral precipitation and dissolution.

2.1 Fractured granitic reservoir

The geothermal reservoir at Soultz is made up of three types of granite (Jacquot, 2000; Hooijkaas et al., André et al., 2006) (Table 1). The first is non-altered (fresh) granite that is characterized by a predominance of feldspar, plagioclase and quartz, and by an extremely low fracture density. Consequently, its porosity is close to zero and does not contain significant amounts of water. The properties of this granite are that of the impermeable rock matrix. Fluid exchange, by advection or diffusion processes, will be disregarded for this granite; it will only act as a good heat convector.

Table 1: Mean composition (in %) of the different types of granite in the Soultz reservoir (Jacquot, 2000).

	Fresh granite	**Hydrothermally altered granite**	**Alteration veins**
Quartz	24.2	40.9	43.9
K-feldspar	23.6	13.9	
Plagioclase	42.5		
Illite		24.6	40.2
Smectite		9.7	9.6
Mica	9.4		
Calcite	0.3	3.3	4.3
Dolomite		0.8	0.7
Pyrite		0.7	1.0
Galena		1.3	0.3
Chlorite		4.8	

The second rock facies is a fractured, hydrothermally altered granite, with quartz as the major mineral component; because of alteration the amount of feldspar decreases and some secondary minerals such as galena, pyrite, smectite or illite are present. This facies is the most porous (porosity ranging from 5 to 10%) and contains most of the formation fluid. The third rock facies is the most altered; it corresponds to alteration veins that present minerals such as illite, smectite and quartz. Precipitated secondary minerals (clays, carbonates) fully cement the fractures, resulting in a decrease of porosity and permeability. As a consequence, fluid circulation within the rock mass takes place through the second facies only (Genter et al., 1998).

2.2 Geofluid chemistry

The formation fluid circulating through the fracture network is a sodium-chloride brine with a total mineralization close to 100 g L^{-1}. Its pH is approximately 4.9 and its temperature (200°C) is in equilibrium with that of the rock at 5'000-m depth. The composition of the formation brine extracted during a 1999 production test is given in Table 2. The chemistry of the deep fluid is not very different from that of the fluid produced from the shallower reservoir (Durst, 2002). Its silica and carbon concentrations are higher because of the elevated temperatures and CO_2 partial pressures.

Table 2: Representative chemical analysis of the fluid sampled at the wellhead of GPK2 after being deepened to 5000 m in 1999 (Durst, 2002)

Species	Concentration (mmol/kg)
Na^+	1148.00
K^+	73.40
Ca^{2+}	169.50
Mg^{2+}	3.21
Cl^-	1648.00
S	1.77
C	42.76
Fe^{2+}	2.61
SiO_2	6.06
Al^{3+}	$3.7.10^{-3}$

3. NUMERICAL MODEL

The main task of the research on THC coupled modeling for this site has been to forecast the evolution of reservoir porosity and permeability. Different researchers (Durst, 2002, Bächler, 2003, Rabemanana et al. 2003, André et al., 2005) have incrementally built a reactive transport simulator, FRACHEM, able to simulate the main characteristics of the Soultz reservoir.

FRACHEM is a THC simulator issued from the combination of two existing codes: FRACTure and CHEMTOUGH2. FRACTure is a 3-D finite-element code for modelling hydrological, transport and elastic processes. It was developed originally for the study of flow-driven interactions in fractured rock (Kohl & Hopkirk, 1995). CHEMTOUGH2 (White, 1995) is a THC code developed after the TOUGH2 simulator (Pruess, 1991), a 3-D numerical model for simulating the coupled transport of water, vapor, noncondensable gas, and heat in porous and fractured media. CHEMTOUGH2 presents the possibility to transport chemical species and to model the chemical water-rock interactions as well as the chemical reactions driven by pressure and temperature changes. The transport and reaction are coupled using a one-step approach. FRACHEM has been built by introducing geochemical subroutines from CHEMTOUGH2 (White, 1995) into the framework of the code FRACTure (Bächler, 2003; Bächler and Kohl, 2005). After an initialization phase, FRACTure calculates, over each time step, the thermal and hydrological conditions within each element volume and determines the advective flow between each of them. Resulting thermal and hydrological variables are stored in arrays common to FRACTure and the geochemical modules. At this point, the program calculates the chemical reactions using a mass balance/mass action approach, the advective transport of chemical species, and the variations of porosity and permeability. Once this calculation is performed, the porosity and permeability are updated and fed into the FRACTure part of the code. The program then returns to the start of the loop until the end of the simulation time (sequential noniterative approach, SNIA).

FRACHEM has been developed specially for the granitic reservoir of Soultz-sous-Forêts and consequently, specific implementations have been added to the chemical part of this code. Considering the high salinity of the geofluid, the Debye-Hückel model, initially implemented in the CHEMTOUGH2 routines to determine the activity coefficients, has been replaced by a Pitzer activity model. It should be mentioned here that the activity coefficients calculations are carried out in an indirect manner by means of another code, TEQUIL model of the Na-K-H-Ca-Cl-SO_4-HCO_3-CO_3-CO_2-H_2 system for 0 to 250°C (Moller et al., 1998). The TEQUIL application package includes chemical models based on the Pitzer formalism, and calculates liquid-solid-gas equilibria in complex brine systems by globally minimizing the free energy of a system at constant temperature and pressure. Using this model, total concentrations obtained from chemical analyses (Table 2) were input into TEQUIL, which then computed speciation and corresponding activity coefficients. Computations were done using a typical Soultz fluid at a temperature of 200°C. This fluid was initially equilibrated with calcite and anhydrite at 200°C, which resulted in a decrease of Ca^{2+} and SO_4^{2-} concentrations (compared to input concentrations) due to precipitation of calcite and anhydrite. The pH value of 4.9 at 200°C was calculated from the equilibration with calcite and input total aqueous carbonate concentration. Using the fluid composition at 200°C, TEQUIL was then used to numerically cool the solution, recompute pH, and determine activity coefficients at temperatures down to 20°C. It should be noted that the cooling simulation was performed without allowing reactions with gases or minerals. Mg, Fe, and Al are not included in the TEQUIL database. For this reason, the geochemical program EQ3nr (Wolery, 1992) was applied to determine the activity coefficients of Mg^{2+}, Fe^{2+} and Al^{3+} by using the Pitzer model and the EQ3nr thermodynamic database data0.hmw (Harvie et al. 1984). Activity coefficients determined in this way were then input into FRACHEM as polynomial functions of temperature, for the specific ionic strength of the fluid. This approach works well for the case of Soultz simulations because the ionic strength of the circulated fluid remains more or less constant.

Presently, a limited number of minerals are considered, which correspond to the minerals constituting the Soultz granite. The precipitation/dissolution reactions of carbonates (calcite, dolomite), quartz, amorphous silica, pyrite, and some aluminosilicates (K-feldspar, albite, illite) can be modeled under kinetic constraints. Rate laws follow more or less the transition state theory (TST)-derived equation (e.g., Lasaga et al., 1994). The implemented kinetic-rate laws are specific to each mineral and taken from published experiments conducted at high temperature in NaCl brines.

Thermodynamic data (equilibrium constants) are taken mostly from SUPCRT92 (Johnson et al., 1992) and Helgeson et al. (1978) and are functions of temperature and pressure. The effect of pressure on equilibrium constants is explicitly taken into account. The equilibrium constants input into FRACHEM were initially computed along the water-saturation pressure curve, however, these constants are recomputed with changes in pressure during run time.

Finally, a supplementary module allows the determination of porosity and permeability variations linked with chemical processes occurring in the reservoir. Considering the alteration of the Soultz granite, the flow is assumed to circulate in a medium composed of fractures and grains. Therefore, a combination of fracture model (Norton and Knapp, 1977; Steefel and Lasaga, 1994) and grain model (Bolton et al., 1996) is used to determine the permeability evolution. In this model, we assume that the fracture aperture and the thickness of the mineral layer follow Gaussian distributions (Durst, 2002).

4. SIMULATION RESULTS

This paper describes the application of the model to two simple cases: single 1-D fracture and two 1-D fractures models. First, mesh discretization, geometrical model, models parameters and initial- and boundary conditions are described. Then, results of simulations are described to test if the fracture geometry has an impact on the chemical model results. Thermal and chemical processes were coupled and the porosity and permeability changes affect the hydraulic field. The simulations time was 600 days.

The model consists of a 750*300 m granitic matrix zone (Fig. 1). An injection and a production well separated by 650 m have been set. Because of symmetry, only half (the upper part) of fractured zones and of the adjacent porous matrix is modelled, by subdividing them into 502 elements (Fig. 1). The size of the elements ranges from a minimum of 0.5 m × 0.05 m near the injection and the production wells to a maximum of 50 m × 35 m. The fractured zones are located between 50 and 700 m; injection is made at 50 m and production occurs at point 750m (Fig. 1).

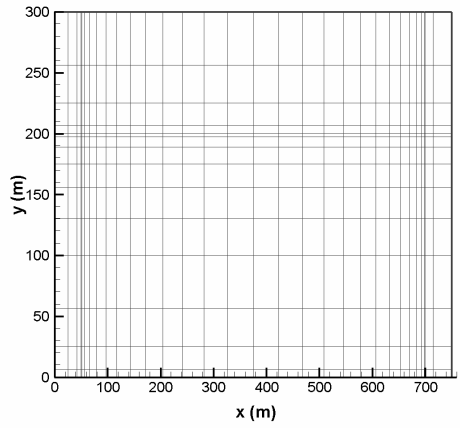

Figure 1. Whole model spatial discretization (distances are in m). The y-axis represents model width and the x-axis is along the fractured zone between injection and production wells, located at x=50m and x=700m, respectively.

The initial temperature in the model was set to 200°C, which corresponds to the temperature at 5000 m depth in the reservoir. The pressure at the production point was held constant at 50 MPa (bottom well pressure at GPK2). A constant over-pressure of 8 MPa was assumed at the injection well. In each of the fractured zones, fluid was injected at qinj= $4*10^{-2}$ $L.s^{-1}$ in the first volume element of the fractured zones. The injection rate for each fracture was based on the fluid production rate qtot= 50 $L.s^{-1}$ and assuming 1250 fractured zones (qtot/qinj= 1250 fractured zones) consisting of 200 fractures. The fluid flowing out of the last volume element is reinjected in the first one through a buffer of 2000 m^3 representing the fluid volume contained in wells and surface installation.

The fluid density is 1000 $kg.m^{-3}$, the rock density 2650 $kg.m^{-3}$, the heat capacity of the rock is 1000 $J.kg^{-1}.K^{-1}$ and the heat capacity of the fluid is 4200 $J.kg^{-1}.K^{-1}$. No radiogenic heat production was integrated in the model. Only heat transfer between the matrix and the fractured zones is allowed.

The fluid flow in the matrix is negligible due to low hydraulic conductivity and zero matrix porosity. Thus, all chemical reactions happen in the fractures, whereas in the matrix no reactions take place. Though, we assume that major circulation occurs in hydrothermally altered granite. Cooled brine interacts with quartz, carbonates, K-feldspars, sulfides and clays. Secondary precipitation of amorphous silica was considered.

Initial water chemistry was obtained by equilibrating the sample water of formation fluid (Table 2) with the corresponding mineral compositions (Table 3) at 200°C. The initial fluid pH computed with the code, assuming saturation with respect to calcite, was 4.95. In each of the fractured zones fluid was injected at a temperature of 65°C.

Finally, three types of injection waters were considered, and were held constant over time. The first is the produced reservoir water (base case). The second was obtained by mixing one unit of reservoir water with one unit of fresh water (mixing case). The third was obtained by the addition of concentrated HCl in formation brine (acidification case).

4.1 Fracture geometry effect

4.1.1 Models description

The first complete application of FRACHEM code was a single fracture model. The model consists of a single 650 m long, 0.1 m wide and 10 m deep fractured zone surrounded by rock matrix.

The second application consisted in a more complex model with two fractured zones of different widths. The two wells are linked by two types of fracture: a 0.1 m wide fracture going directly from injection to production and a set of 0.05 m wide fracture traversing 1050 m between the two wells. The model set up represents only the upper half of the overall model. The lower part of the model, not set up, is mirror-inverted along the x-axis. Therefore only half of the fracture (0.05 m) along the x-axis is taken into the model. The model is discretized finer along the fractures as shown in Figure 1 which illustrates the mesh discretization. The fluid is injected at the beginning of both fracture, and produced at the end of both fractures.

4.1.2 Reservoir temperature

Before fluid circulation in the fractured zone, all the system (rock and brine) is chemically and thermally at equilibrium. The brine is in chemical equilibrium with the granite and these two components are at a constant temperature of 200°C. But, during the injection of cold fluid at 65°C in the reservoir, the system is disturbed and the rock progressively cools down (Figs. 2 and 3).

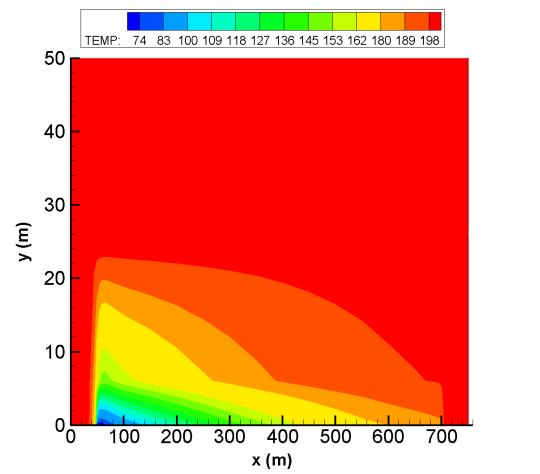

Figure 2: Temperature of rock around the single fractured zone after one year of forced fluid circulation.

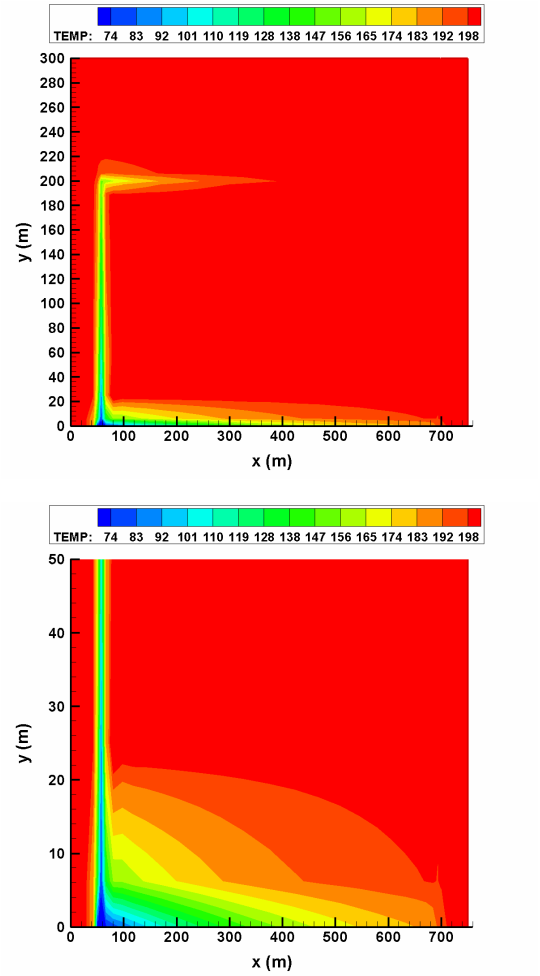

Figure 3: Temperature of rock around the two fractured zones after one year of fluid circulation. a) Whole model. b) 50*750 m zone around the injection point.

For the first application, all along the fractured zone, we observe a global decrease of temperature, especially near the injection well, due to the temperature of the re-injected fluid (Fig. 2). After one year of fluid circulation, the temperature in the vicinity of the production well is close to 180°C. The development of this thermal front due to the thermal diffusion from rock to fluid affects a zone of 10 to 20 meters around the fractured zone (Figure 2). This temperature decrease of the produced fluid is particularly important but it is strongly dependent of the geometric model.

In the second application, we consider two parallel pathways. The temperature distribution in the fracture and the matrix after one year is shown in Figure 3. The temperature was decreased from 200°C to 65°C near the injection well. Along the fractured zones it increases to 190°C towards the production point. Due to thermal diffusion, the temperature of the matrix is decreased around the fractured zones.

As a consequence, the cooling effect on the produced fluid modeled, when we consider a straight line flow between injection and production wells, without taking in consideration parallel pathways, is most probably overvalued compared to the real reservoir.

4.1.3 Mineral-brine interactions

The two-fracture simulation results are concordant to those of the single fracture simulation. Calcite dissolves at the vicinity of the injection zone and reprecipitates when the temperature rises. With time, the calcite dissolution rate in the injection elements decreases due to the diminution of available calcite that is almost totally dissolved after one year. Dolomite shows a similar dissolution trend but is removed faster at the injection point. The quartz precipitates in the low temperature zone and dissolves when the fluid warms up. Due to the relatively low reaction rates both precipitation and dissolution occur on a wide portion of the fracture. The pyrite does not present significant variations.

The injection of cold fluid creates a chemical non-equilibrium, which induces dissolution of calcite and dolomite as well as precipitation of quartz and pyrite. The results show that the main chemical process are the fluid-calcite reactions that lead to porosity and permeability increases near the injection point, due to calcite dissolution. Because of the progressive temperature increase along the fracture, precipitation of calcite occurs towards the production point.

Calcite dissolves near the injection point at a maximum rate of $2.7.10^{-4}$ $mol.m^{-3}.s^{-1}$ and precipitates at maximum $7.6.10^{-6}$ $mol.m^{-3}.s^{-1}$ at the production well (Fig. 4). With increasing simulation time, the dissolution zone moves towards the production point. Near the injection well all calcite has dissolved after one year with a reaction rate reducing correspondingly to zero. In contrast, dolomite never precipitates (Fig. 5). At the beginning of the simulation, dissolution only takes place near the injection point at a maximum rate of 6.10^{-6} $mol.m^{-3}.s^{-1}$. After one year, the dissolution zone moves slightly towards the production point and the reaction rate increases to $1.4.\ 10^{-5}$ $mol.m^{-3}.s^{-1}$.

These results show the interdependence of pH, temperature and carbonate behaviour: the cold fluid at low pH dissolves calcite and dolomite near the injection well at a high rate (Fig. 6). Reheating the fluid causes the calcite to precipitate and the pH to rise. Since the calcite precipitation rate is higher than that of dolomite, calcite precipitation prevents the precipitation of dolomite. According to the temperature evolution in the fracture, this process moves towards the production well and the reaction rates decrease. With increasing reaction time, the reaction rates reduce strongly due to the decrease of available carbonates. At the beginning, the dissolution of dolomite is controlled by temperature, whereas with time it depends more on calcite precipitation.

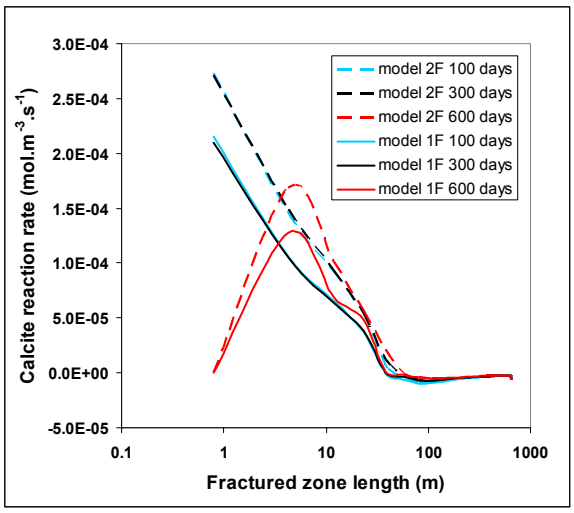

Figure 4: Calcite reaction rate along the fractured zone at different times (positive values indicate dissolution).

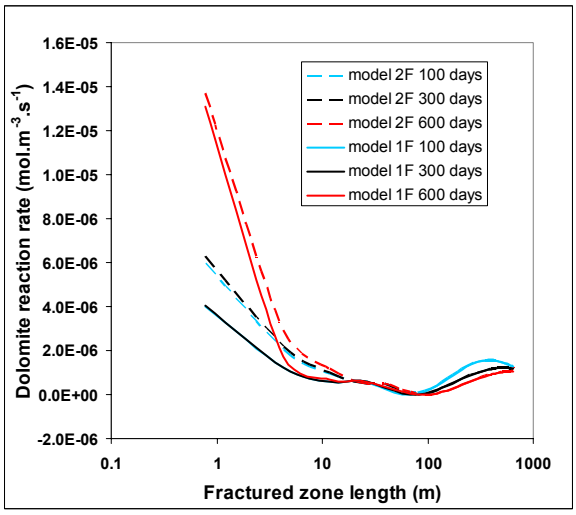

Figure 5: Dolomite reaction rate along the fractured zone at different times (positive values indicate dissolution).

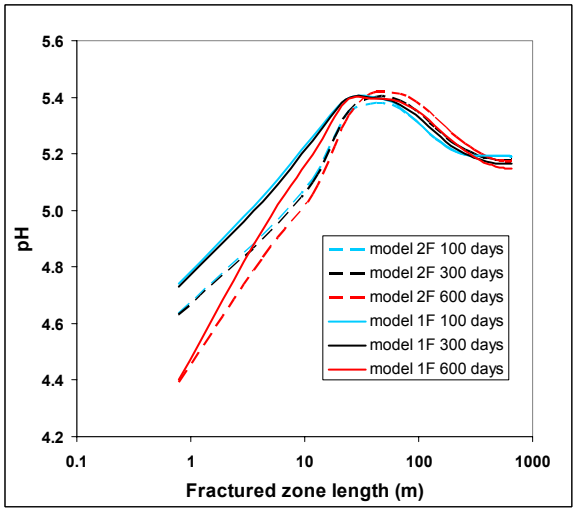

Figure 6: pH evolution along the fractured zone at different times.

The most reactive of the silicates are amorphous silica. It precipitates near the injection well at a maximum rate of $2.8.10^{-5}$ mol.m^{-3}.s^{-1} (Fig. 7). With increasing circulation time, the zone of amorphous silica precipitation spreads towards the production well. Quartz precipitates all along the fracture at a maximum rate of $5.5.10^{-10}$ mol.m^{-3}.s^{-1} (Fig. 8). Depending on the temperature evolution, with time the maximum reaction rate moves towards the production point and decreases. K-feldspar and pyrite present a similar behaviour. Precipitation of K-feldspar occurs close to the injection point. Unlike quartz, some punctual dissolution events of pyrite occur. These differences are due to the fact that even if the pyrite reaction depends on the temperature evolution, there is still an influence from the pH.

The differences in the reaction rates result in varying porosities. This difference is expected to increase further when calculating more than one year.

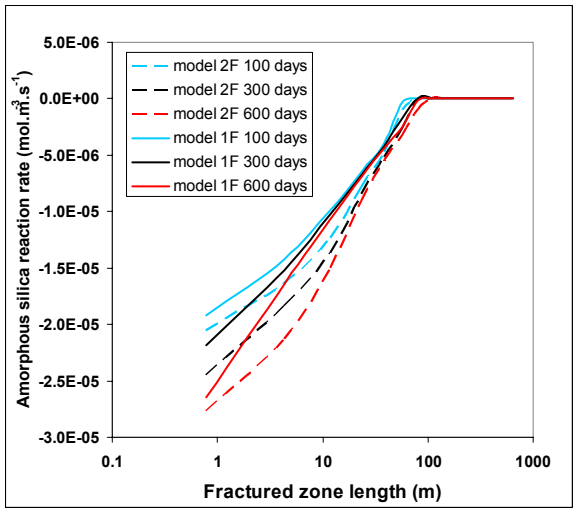

Figure 7: Amorphous silica reaction rate along the fractured zone at different times (negative values indicate precipitation).

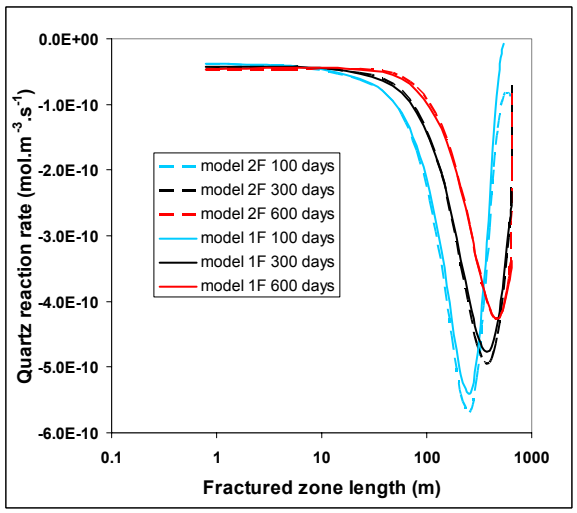

Figure 8: Quartz reaction rate along the fractured zone at different times (negative values indicate precipitation).

4.1.4 Evolution of reservoir properties

In both cases, porosity and permeability increase near the injection point due to dissolution of carbonates and decrease near the production point due to calcite precipitation (Fig. 9).

After one year the porosity at the injection point reaches 0.13 and goes down to 0.09 and 0.1 respectively in the large and thin fracture. The more porous zone extends up to 20 m in the large fracture and 10 m in the thin fracture. After 600 days, the area affected by the porosity reduction is wider.

The differences in the reaction rates result in varying porosities. This difference is expected to increase further when calculating more than one year.

Considering that there are only two fluid pathways and that the value of the permeability reduction in these two paths are small and close to each other, the geochemical reactions do not significantly modify the thermal-hydraulic parameter in the model.

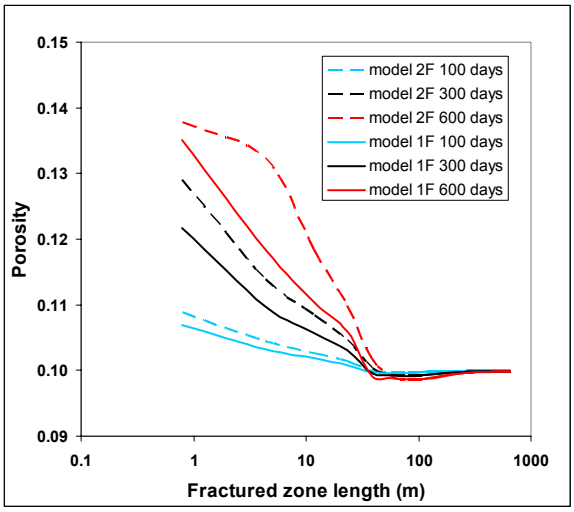

Figure 9: Porosity evolution along the fractured zone after five years of forced fluid circulation.
Initial porosity was 0.1.

4.2 Effect of fluid chemistry on fracture porosity

To explore chemically-induced effects of fluid circulation in the system, we examine ways in which the chemical composition of reinjected waters can be modified to improve reservoir performance.

Two types of injection waters were considered, and were held constant over time. The first was obtained by mixing one unit of reservoir water with one unit of fresh water (mixing case). The second was obtained by the addition of concentrated HCl in formation brine (acidification case). The pH of the acidified injected solution was close to 3.2. In each of the fractured zones fluid was injected at a temperature of 65°C.

4.2.1 Chemistry evolution of the produced fluid

Concerning the evolution of the fluid concentration in the whole model, one major evolution appears (Figures 10 and 11). In the mixing case, pH of the produced fluid increases and the total calcium concentration of the produced fluid decreases from its initial 0.12 mol.kg^{-1} and stabilizes at 0.09 mol.kg^{-1} after 20 days. In the acidification case, pH of the produced fluid decreases from 5 to 4.65 and consequently, the total calcium concentration of the produced fluid slightly increases. This illustrates the dissolution of calcite.

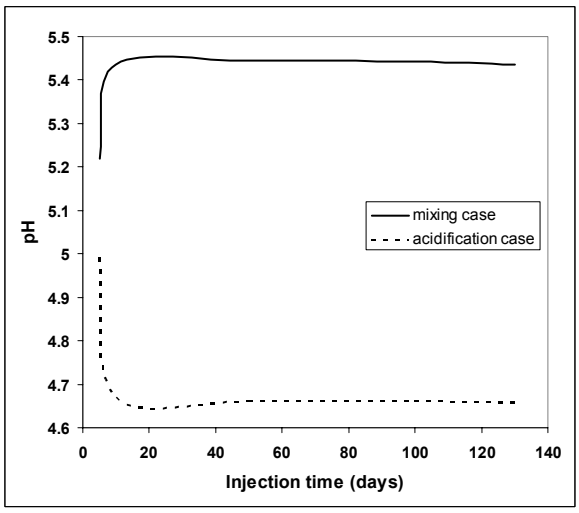

Figure 10: pH evolution in the produced fluid as a function of injection time.

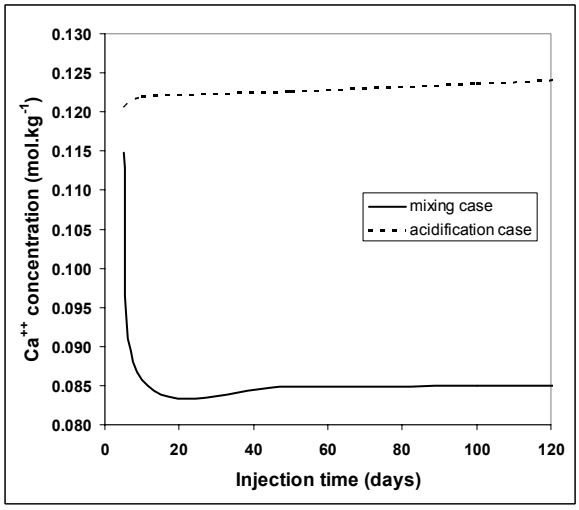

Figure 11: Calcium concentration evolution in the produced fluid as a function of injection time.

4.2.2 Evolution of fracture porosity

The mixing water is less prone to precipitating calcite (Fig. 12), and therefore is favorable for porosity development and maintaining injectivity. Though, alteration of injection water chemistry, for example by dilution with fresh water, can greatly alter precipitation and dissolution effects along the entire flow paths, and can offer a powerful tool for operating EGS reservoirs in a sustainable manner.

Another possible means to reduce the tendency towards calcite precipitation is to add HCl acid to injection water. Variations of the initial pH (3.2) have a significant effect on the reaction rates of carbonates (Fig. 12), but this effect should disappear during the first months of simulation, when the system will tend to recover equilibrium and will not have significant effects for long time simulations. The

acidified brine injection water contributes to a porosity increase of about 0.035 in the vicinity of injection well (Fig. 13). Short injection of acidified water is favorable for porosity development and maintaining injectivity.

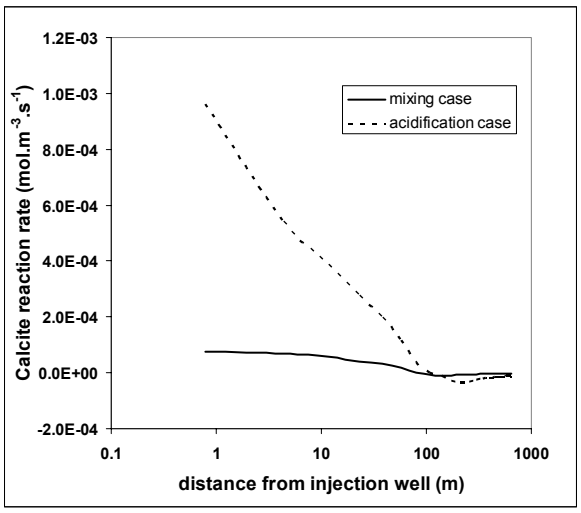

Figure 13: Calcite reaction rate along the fractured zone after 100 days of injection.

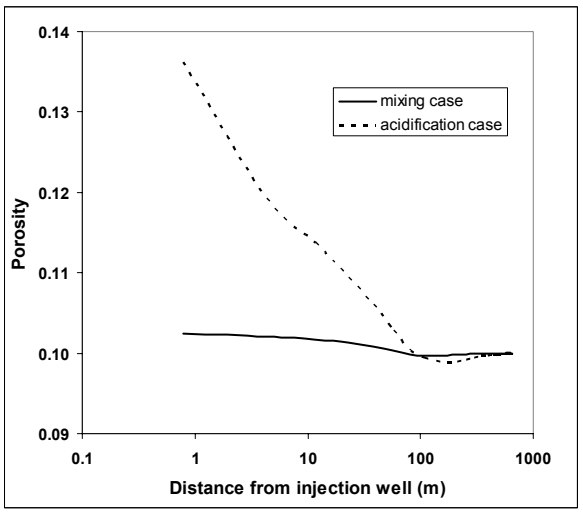

Figure 13: Porosity evolution along the fractured zone after 100 days of injection. Initial porosity was 0.1.

5. CONCLUSIONS

The first application of the new code FRACHEM consisted of the modelling of a simplified system, including a cooled fluid reinjected in a hot reservoir composed of a 650-m long by 0.1-m wide fracture surrounded by an impermeable matrix. The results show that at the beginning of the simulation, calcite and dolomite are rapidly dissolved near the injection point. Then, warming up induces carbonates precipitation on a wider zone. Later, the carbonates being less available in the injection area, reactions rates decrease significantly. Amorphous silica, K-feldspar, quartz and pyrite precipitate in the fracture. Moreover, some exceptional events of pyrite dissolution are also observed. Porosity evolution mainly shows a high increase near the injection point, due to carbonates dissolution. On the other hand, a small decrease of porosity is observed later, due to calcite re-precipitation. The second application was a 2-D model with the dimension of the upper Soultz reservoir. This model includes two fractures of different widths following two different paths. The geochemical evolution is similar to the previous simulation with carbonates dissolving near the injection point and re-precipitating further in the fracture. During the first 600 days this lead to a porosity increase of 0.04 followed by a decrease of 0.005. The variations are similar in both fractures and affected the first 10 m of the thin fracture and the first 20 m of the large one.

Both models are still simple and clearly do not represent the complex and heterogeneous situation at Soultz. However, fully coupled models of the Soultz EGS reservoir were developed and the model sensitivity can be tested. No true sensitivity analysis has been made concerning the spatial discretization and fracture network density, but the comparison between the results of the two simulations indicates that the permeability variation depends principally on the evolution of the temperature field calculated by FRACTure and not much on the spatial discretization or the fluid flow rate. But changes in the porosity/permeability, and thus in the hydraulic conductivity, impact the fluid velocity and the pressure distribution in the fracture: mineral precipitation causes the porosity and therefore also the permeability and the hydraulic conductivity to decrease. Lower hydraulic conductivity results in lower fluid velocities. Since the fluid velocities are smaller, the rate of temperature decrease in the fractured zone is lower

In the mixing and acidification cases presented, the results differ much from the basic model: the largest porosity difference in the fractured zone is 0.015. This is more than 15% of the initial porosity. Various reacting fluids can be injected to enhance fracture permeability in the vicinity of the wells. the FRACHEM code could be used to identify the most efficient chemical stimulation for EGS projects.

Finally, fluid-rock interactions may have a long-term effect on reservoir operation. While more or less detailed studies of the interaction of the reservoir rock with the injected fluid have been made at most of the EGS sites, there is still a good deal to learn about how the injected fluid will interact with the rock over the long term. The most conductive fractures often show evidence of fluid flow in earlier geologic time such as hydrothermal alteration and secondary mineral deposition. This is encouraging in that it suggests that the most connected pathways will already have experienced some reaction between water and the rock fracture surface. Fresh rock surfaces will not have the protection of a layer of deposited minerals or alteration products. The amount of surface or shallow water, which cannot be in equilibrium with the reservoir rock, required to add to the system over the long term is although unknown. The longest field tests have seen some evidence for dissolution of rock leading to development of preferred pathways and short-circuits. Moreover, the produced fluid will be cooled through a heat exchanger, in the surface equipment, possibly resulting in precipitation of scale or corrosion. To conclude, despite efforts to model fluid-rock interactions, there are still major questions to be answered.

6. ACKNOWLEDGEMENTS

The authors would like to thank the Swiss Federal Office of Education and Science (Project N° 03.0460) and the Swiss Federal Office of Energy (Project N° 150’649) for funding this project.

7. REFERENCES

André, L., Rabemanana, V. and Vuataz, F.-D., 2006. Influence of water-rock interactions on fracture permeability of the deep reservoir at Soultz-sous-Forêts, France. Geothermics 35, 507-531.

André, L. and Vuataz, F.-D., 2005. Simulated evolution of reservoir properties for the Enhanced Geothermal System at Soultzsous-Forêts: the role of hot brine-rock interactions. In: Proceedings of the 30th Workshop on Geothermal Reservoir Engineering. Stanford University, 283–290.

André, L., Spycher, N., Xu, T., Pruess, K. and Vuataz, F.-D., 2006. Comparing FRACHEM and TOUGHREACT for reactive transport modeling of brine-rock interactions in Enhanced Geothermal Systems (EGS). In: Proceedings of the 31st Workshop on Geothermal Reservoir Engineering. Stanford University, 350–358.

Bächler, D. and Kohl, T., 2005. Coupled thermal-hydraulic-chemical modelling of enhanced geothermal systems. Geophys. J. Int. 161 (2), 533–548.

Bächler, D., Kohl, T. and Rybach, L., 2003. Impact of graben-parallel faults on hydrothermal convection – Rhine Graben case study. Physics and Chemistry of the Earth 28, 431-441.

Bächler, D., 2003. Coupled Thermal-Hydraulic-Chemical Modelling at the Soultz-sous-Forêts HDR reservoir (France). PhD thesis, ETH-Zürich, Switzerland, 151 p.

Baldeyrou, A., Vidal, O. and Fritz, B., 2003. Etude expérimentale des transformations de phases dans un gradient thermique : application au granite de Soultz-sous-Forêts, France. Comptes rendus Acad. Sci., Sér. II, Fasc. A, Paris, France, 335, 371-380.

Baria, R., Jung, R., Tischner, T., Teza, D., Baumgaertner, J., Dyer, B., Hettkamp, T., Nicholls, J., Michelet, S., Sanjuan, B., Soma, N., Asanuma, H. and Garnish, J., 2006. Creation of an HDR/EGS reservoir at 5000 m depth at the European HDR project. Proc. 31st Workshop on Geothermal Reservoir Engineering, Stanford University, California, USA.

Barrett, T.J. and Anderson, G.M., 1988. The solubility of sphalerite and galena in 1–5m NaCl solutions to 300°C. Geochim. Cosmochim. Acta 52 (4), 813–820.

Bartels, J., Kühn, M. and Clauser, C., 2003. Numerical simulation of reactive flow using SHEMAT. In: Clauser C. (ed) Numerical simulation of reactive flow in hot aquifers - SHEMAT and Processing SHEMAT, Springer Publishers, Heidelberg, 5-74.

Blum, A.E. and Stillings, L.L., 1995. Feldspar dissolution kinetics. In: White, A.F., Brantley, S.L. (Eds.), ChemicalWeathering Rates of Silicate Minerals, 31. Mineralogical Society of America, 291–351, Reviews in Mineralogy.

Bolton, E.W., Lasaga, A.C. and Rye, D.M., 1996. A model for the kinetic control of quartz dissolution and precipitation in porous media flow with spatially variable permeability; formulation and examples of thermal convection. J. Geophys. Res. Part B. Solid Earth Planets 101 (10), 22157–22187.

Brown, D.W., 2000. A Hot Dry Rock geothermal energy concept utilizing supercritical CO_2 instead of water. Proc. 25th Workshop on Geothermal Reservoir Engineering, Stanford University, California, USA.

Carroll, S., Mroczek, E., Alai, M. and Ebert, M., 1998. Amorphous silica precipitation (60 to 120°C): comparison of laboratory and field rates. Geochim. Cosmochim. Acta 62 (8), 1379–1396.

Dezayes, C., Valley, B., Maqua, E., Sysen, G. and Genter, A., 2005. Natural fracture system of the Soultz granite based on UBI data in the GPK3 and GPK4 wells. In: Proceedings of the EHDRA Scientific Meeting. Soultz-sous-Forêts, France.

Durst, P., 2002. Geochemical modelling of the Soultz-sous-Forêts Hot Dry Rock test site: coupling fluid-rock interactions to heat and fluid transport. PhD thesis, University of Neuchˆatel, Switzerland, 127 p.

Evanoff, J., Yeager, V. and Spielman, P., 1995. Stimulation and damage removal of calcium carbonate scaling in geothermal wells: a case study. In: Proceedings of the World Geothermal Congress ’95, Florence, Italy, 2481–2485.

Evans, K.F. , Moriya, H., Niitsuma, H., Jones, R.H., Phillips, W.S., Genter, A., Sausse, J., Jung, R. and Baria, R., 2005. Microseismicity and permeability enhancement of hydrogeologic structures during massive fluid injections into granite at 3 km depth at the Soultz HDR site, Geophys. J. Int., 160, 388-412.

Genter, A., Traineau, H., Dezayes, C., Elsass, P., Ledesert, B., Meunier, A. and Villemin, T., 1995. Fracture analysis and reservoir characterization of the granitic basement in the HDR Soultz project (France). Geotherm. Sci. Tech., 4 (3), 189-214.

Gérard, A., Fritz, B. and Vuataz, F.-D., 2005. Results of soft acid injection tests performed at Soultz in wells GPK2, GPK3 and GPK4—extended summary: revised status on 14 March 2005. In: Proceedings of the EHDRA Scientific Conference, Soultz-sous-Forêts, France.

Gérard, A., Genter, A., Kohl, T., Lutz, P., Rose, P. and Rummel, F., 2006. The deep EGS (Enhanced Geothermal System) project at Soultz-sous-Forêts (Alsace, France). Geothermics, 35 (5-6), 473-483.

Hellmann, R., 1994. The albite-water system. Part I. The kinetics of dissolution as a function of pH at 100, 200 and 300 ◦C. Geochim. Cosmochim. Acta 58 (2), 595–611.

Hooijkaas, G. R., Genter, A. and Dezayes, C., 2006. Deep-seated geology of the granite intrusions at the Soultz EGS site based on data from 5 km-deep boreholes. Geothermics, 35 (5-6), 484-506.

Icenhower, J.P. and Dove, P.M., 2000. The dissolution kinetics of amorphous silica into sodium chloride solutions: effects of temperature and ionic strength. Geochim. Cosmochim. Acta 64 (24), 4193–4203.

Jacquemont B., 2002. Etude des interactions eau-roche dans le granite de Soultz-sous-Forêts. Quantification et modélisation des transferts de matière par les fluides. Thèse Univ. Louis Pasteur, Strasbourg, France.

Jacquot, E., 2000. Modélisation thermodynamique et cinétique des réactions géochimiques entre fluides de bassin et socle cristallin: application au site expérimental du programme européen de recherche en géothermie profonde (Soultz-sous-Forêts, Bas-Rhin, France). PhD thesis, Université Louis Pasteur, Strasbourg, 202 p.

Kohl, T. and Hopkirk, R.J., 1995. "FRACTure" – a simulation code for forced fluid flow and transport in fractured, porous rock. Geothermics 24 (3), 333–343.

Kohl, T. and Rybach, L., 2001. Assessment of HDR reservoir geometry by inverse modelling of non-laminar hydraulic flow. In: Proceedings of the 26th Workshop on Geothermal Reservoir Engineering. Stanford University, 259–265.

Moller, N., Christov, C. and Weare, J., 2006. Thermodynamic models of aluminum silicate mineral solubility for application to enhanced geothermal systems. Proc. 31st Workshop on Geothermal Reservoir Engineering, Sanford University, California, USA.

Monnin, C., 1989. An ion interaction model for the volumetric properties of natural waters: density of the solution and partial molal volume of electrolytes to high concentrations at 25 ◦C. Geochim. Cosmochim. Acta 53, 1177–1188.

Nagy, K.L., Blum, A.E. and Lasaga, A.C., 1991. Dissolution and precipitation kinetics of kaolinite at 80 ◦C and pH 3: the dependence on solution saturation state. Am. J. Sci. 291 (7), 649–686.

Norton, D. and Knapp, R., 1977. Transport phenomena in hydrothermal systems; the nature of porosity. Am. J. Sci. 277 (8), 913–936.

Pitzer, K.S., 1973. Thermodynamic of electrolytes. I. Theoretical basis and general equations. J. Phys. Chem. 12, 268–277.

Pokrovskii, V.A. and Helgeson, H.C., 1995. Thermodynamic properties of aqueous species and the solubilities of minerals at high pressures and temperatures: the system Al2O3-H2O-NaCl. Am. J. Sci. 295, 1255–1342.

Portier, S., André, L. and Vuataz, F.-D., 2006. Modelling geochemical effects of acid treatments and comparison with field observations at Soultz-sous-Forêts geothermal site. Proc. ENGINE Scientific Workshop 3, « Stimulation of reservoir and microseismicity », Kartause Ittingen, Zürich, Switzerland.

Portier, S., André, L. and Vuataz, F.-D., 2006. Review of chemical stimulation techniques and results of acid injection experiments at Soultz-sous-Forets. Proc. EHDRA Scientific Conference, Soultz-sous-Forêts, France.

Pruess, K. and Azaroual, M., 2006. On the feasibility of using supercritical CO_2 as heat transmission fluid in an engineered Hot Dry Rock geothermal system. Proc. 30th Workshop on Geothermal Reservoir Engineering, Stanford University, California, USA.

Rabemanana, V., Durst, P., Bächler, D., Vuataz, F.-D. and Kohl, T., 2003. Geochemical modelling of the Soultz-sous-Forêts Hot Fractured Rock system: comparison of two reservoirs at 3.8 and 5 km depth. Geothermics 32 (4–6), 645–653.

Rimstidt, J.D. and Barnes, H.L., 1980. The kinetics of silica-water reactions. Geochim. Cosmochim. Acta 44 (11), 1683–1699.

Sausse, J. and Genter, A., 2005. Types of permeable fractures in granite, Special Publication of the Geological Society of London, 240, 1-14.

Sausse, J., Fourar, M. and Genter, A., 2006. Permeability and alteration within the Soultz granite inferred from geophysical and flow log analysis. Geothermics, 35 (5-6), 544-560.

Tchistiakov, A.A., 2000. Physico-chemical aspects of clay migration and injectivity decrease of geothermal clastic reservoir. In: Proceedings of the World Geothermal Congress 2000, Kyushu-Tohoku, Japan, 3087–3095.

Tenzer, H., 2001. Development of hot dry rock technology. Bulletin GeoHeat Center, 32 (4), 14-22.

Tester, J. W. and al., 2007. The future of geothermal energy: The impact of Enhanced Geothermal Systems (EGS) on the United States in the 21st century. An assessment by an MIT-led interdisciplinary panel, Massachusetts Institute of Technology Report, 372 p.

Vuataz, F.-D., 2000. Review of the papers on HDR and Enhanced Geothermal Systems. World Geothermal Congress 2000, Kyushu, Tohoku, Japan, unpubl. report.

White, S.P., 1995. Multiphase nonisothermal transport of systems of reacting chemicals. Water Resour. Res. 31 (7), 1761–1772.

Wolery, T.J., 1992. EQ3nr, a computer program for geochemical aqueous speciation solubility calculations: theoretical manual, user's guide and related documentation (Version 7.0). Report, UCRL-MA-110662 PT III, Lawrence Livermore National Laboratory, Livermore, California, USA, 246 p.

Xu, T., Ontoy, Y., Molling, P., Spycher, N., Parini, M. and Pruess, K., 2004. Reactive transport modeling of injection well scaling and acidizing at Tiwi field, Philippines. Geothermics 33 (4), 477–491.

Proceedings European Geothermal Congress 2007
Unterhaching, Germany, 30 May-1 June 2007

Comparing FRACHEM and SHEMAT for the modelling of brine-rock interactions in Enhanced Geothermal Systems.

Portier Sandrine[*], Kühn Michael[**] and Vuataz François-David[*]

[*] Centre for Geothermal Research - CREGE, c/o CHYN, University of Neuchâtel, E.-Argand 11, CP158

CH-2009 Neuchâtel, Switzerland.

[**] Applied Geophysics - RWTH Aachen University - Lochnerstr. 4-20 - D-52056 Aachen, Germany.

Keywords: Geothermal reservoir, FRACHEM, SHEMAT, brine-rock interactions, geochemical modelling, Pitzer activity coefficients model, thermodynamic, kinetic reaction rate, porosity-permeability relationship, Enhanced Geothermal System (EGS), Soultz-sous-Forêts.

ABSTRACT

Coupled numerical simulations of heat transfer, fluid flow and chemical reactions in geothermal systems are complex because of the highly heterogeneous geology, high temperatures, elevated pressures and often high salinity of the formation fluids. Codes such as FRACHEM and SHEMAT have been developed to forecast the long-term evolution of exploited geothermal reservoirs in order to determine how fluid circulation within geothermal reservoirs can modify the rock properties.

FRACHEM is a thermo-hydraulic-chemical coupled program developed from the combination of two existing codes: FRACTure, a 3D finite element code for modelling hydraulic, fluid and heat transport and elastic processes, that was developed originally for the study of flow-driven interactions in fractured rock; and CHEMTOUGH2, a modified version of the TOUGH2 simulator able to simulate the coupled transport of water, vapour, non-condensable gas and heat in porous and fractured media. FRACHEM has been developed especially to simulate the behaviour of the fractured granitic EGS reservoir at Soultz-sous-Forêts (Alsace).

SHEMAT, the "Simulator for HEat and MAss Transport", has been developed in several phases and is today a general purpose reactive transport code for a wide variety of thermal and hydrogeological problems in two and three dimensions. SHEMAT solves coupled problems involving fluid flow, heat transfer, species transport and chemical water-rock interaction. SHEMAT is particularly well suited to quantify the effect on flow and transport of chemically induced changes in the pore space of deep sandstone aquifers and was successfully employed for the prediction of the 30-year behaviour of geothermal fluid production systems.

The Soultz-sous-Forêts Enhanced Geothermal System (EGS), established in the Rhine Graben, North of Strasbourg (France), has been investigated since the mid 1980's. The final goal of this project is to extract energy from a forced fluid circulation between injection and production boreholes within a granitic basement rock. The two codes have been applied to simulate fluid circulation in the enhanced geothermal system of Soultz-sous-Forêts. The same geometrical model and identical thermodynamic and kinetic input data have been used. The specific features of each code concerning calculation schemes and coupling mechanisms are presented. Such differences could typically lead to differences in numerical simulation results. Focus has been on the evolution of reservoir temperature, calcite and quartz reaction rates and porosity evolution. Even though the simulators show significant differences with regard to the quantities of minerals precipitated and dissolved it is determined that changes of the hydraulic system are equally well described by both models. FRACHEM and SHEMAT calculate the same temperature development and fluid velocities as well as resulting porosities from the mineral reactions.

1. INTRODUCTION

A major concern in EGS reservoirs is maintaining adequate injectivity, while avoiding the development of preferential short-circuiting flow paths. Past analyses have focused primarily on the coupling between fluid flow, heat transfer and rock mechanics. Recent studies suggest that chemical interactions between rocks and fluids and associated mineral dissolution and precipitation effects, could have a major impact on the performance of EGS.

Prediction of long-term evolution of geothermal reservoirs is of primary interest, in particular for maintaining optimised injectivity and productivity. However, modelling of fluid flow and reactive transport in geothermal systems is challenging because of reservoir conditions such as high temperatures, elevated pressures and sometimes high salinities of the formation fluids. Reactive transport codes coupling thermal, hydrological, and chemical (THC) processes have been developed and used in Enhanced Geothermal Systems to predict permeability evolution by modelling the behaviour of hot, hypersaline brines and their interactions with reservoir minerals.

In this study, two THC simulators were applied using identical thermodynamic and kinetic input data to forecast geothermal reservoir evolution: FRACHEM, a multi-component reactive transport code (Durst, 2002; Bächler, 2003), designed to use the Pitzer activity coefficient model and SHEMAT (Simulator for HEat and MAss Transport), a multi-component reactive transport code for the simulation of the stationary and transient processes in geothermal reservoirs in two and three dimensions, which allows to use the Pitzer activity coefficient model (Clauser, 2003).

2. PROBLEM SETUP

A great deal of specific and detailed information is required to assess the chemical impact of an injection operation. The present study is intended to represent the granitic reservoir of Soultz-sous-Forêts. Consequently, well configuration data as well as chemical and mineralogical composition were taken from the European Enhanced Geothermal System at Soultz-sous-Forêts (Jacquot, 2000; Durst, 2002; Bächler, 2003).

The Soultz-sous-Forêts EGS is located in Alsace, about 50 km north of Strasbourg (France). The Soultz area was selected as the European EGS pilot site because of its high temperature gradient in the sedimentary cover (up to 100 °C km^{-1}) and its high heat flow, locally up to 0.15 W m^{-2} (Kohl and Rybach, 2001). The geology of the Soultz region is characterized by a graben structure affected by several N-S striking faults. The crystalline basement, covered by 1400 m of Triassic and Tertiary sediments, is composed of three facies in granitic rocks: (1) an unaltered granite; (2) a hydrothermally altered granite facies and (3) altered veins within the hydrothermally altered granite (Jacquot, 2000). The hydrothermally altered granite is the most porous facies (Genter et al., 1997) and altered veins are highly fractured. Natural circulation of formation fluid and fluid-rock interaction processes take place mainly within the hydrothermally altered granite and to a lesser extent within altered veins. Flow in the unaltered granite is essentially nil. To extract the heat from the Soultz reservoir, three deviated wells have been installed to a depth of 5,000 m, with lower ends separated by 600 m. The reservoir temperature at this depth is initially 200 °C. One well (GPK3) will be dedicated to the injection of cold water in the granitic reservoir at a rate of about ~50 $L.s^{-1}$, whereas the two other wells (GPK2 and GPK4), located on both sides of the injector, will be used to produce ~25 $L.s^{-1}$ of the formation fluid each. At Soultz, the injection–production system has been designed as a closed loop. The fluid used in this loop is the formation fluid abundant in the altered granite, namely a brine with total dissolved solids of around 100,000 ppm. Injection of cooled brine disturbs the equilibrium between the formation fluid and reactive minerals. The resulting change in temperature and pressure in the reservoir and the forced circulation in fractured granite will drive geochemical reactions able to affect the physical properties of the reservoir through mineral precipitation and dissolution. The main task of the research on THC coupled modelling for this site has been to forecast the evolution of reservoir porosity and permeability.

However, the highly heterogeneous and complicated structure of the Soultz reservoir has been simplified to the following concept.

2.1 Conceptual model and hydraulic parameters

Benchmark simulations described below were performed with the same simplified, horizontal, confined 2D model with a geometry that is close to that of the Soultz system. Injection and production wells are linked by 650 m long fractured zones in the granite rock mass. If we consider that the granitic Soultz reservoir can be represented by a series of alternating fractured and impermeable matrix zones (Dezayes et al., 2005) only one of these fractured zones needs to be modelled; it would be 10 cm thick, have a horizontal width of 10 m (Fig. 1a) and a mean porosity of 10 %. The fractured zones are separated by 100-m thick rock matrix zones, this being the distance required to assume a semi-infinite matrix for heat transfer purposes.

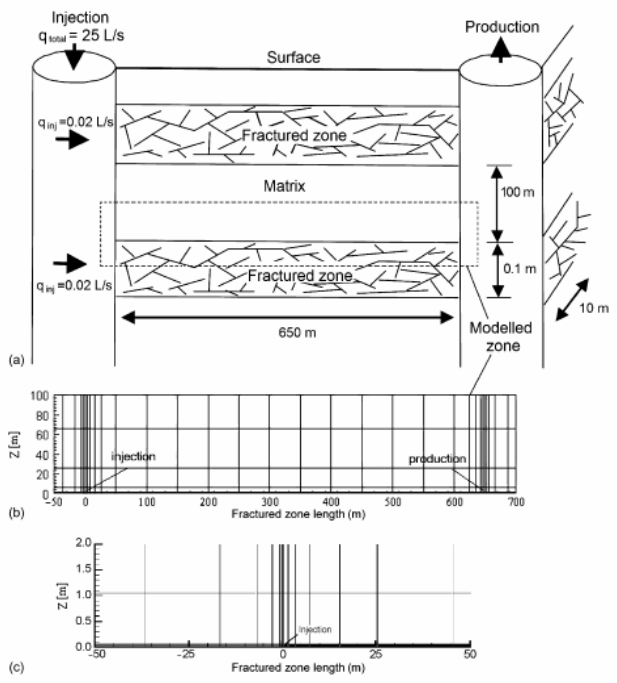

Figure 1: (a) Simplified, vertical 2D model of the Soultz system (dimensions are not shown to scale); (b) spatial discretization of the model; (c) finer mesh discretization near the injection zone. The black bar near the bottom corresponds to the fractured zone.

We consider that the fluid exchange between fractured zones and the surrounding low-permeability matrix is insignificant and thus can be neglected. Only heat transfer between the matrix and the fractured zones is allowed, following the model of Sauty (1981). Because of symmetry, only half (the upper part) of a fractured zone and of the adjacent porous matrix is modelled, by subdividing them into 222 elements (Fig. 1b). The size of the elements ranges from a minimum of 0.5 m × 0.05 m near the injection and the production wells to a maximum of 50 m × 35 m. The fractured zone is located between 0 and 650 m; injection is made at 0 m and production occurs at point 650m (Fig. 1c).

The initial temperature throughout the modelled area was set to 200 °C, the natural-state reservoir temperature. During the simulations, the fluid was injected into the modelled fractured zone at a constant temperature of 65 °C. In FRACHEM hydrostatic pressure distribution was assumed in the production well, while a constant overpressure of 8 MPa was set at the injection well. The pressure gradient between the two wells does not change during the injection period, resulting in an initial flow of 0.02 L s^{-1} into the modelled fractured zone. In SHEMAT the injection well was recharged with 0.02 L s^{-1} and at the production well the same amount of fluid was produced throughout the simulation. Mineral dissolution and precipitation bring about changes in the porosity and permeability of the modelled fractured zone affecting the flow rates through the mesh elements. Therefore the hydraulic rock properties were updated/recalculated after each time step. Dirichlet boundary conditions (i.e. constant temperature and pressure conditions) were applied to the upper, left and right boundaries of the modelled zone. The values of the thermo-hydraulic parameters considered in the simulations are listed in Table 1.

Table 1: Values of the thermo-hydraulic parameters used in benchmark simulations.

Parameter	Fracture	Matrix	Fluid
Hydraulic conductivity ($m\ s^{-1}$)	$7.03.10^{-4}$	$9.5.10^{-12}$	-
Thermal conductivity ($W\ m^{-1}\ K^{-1}$)	2.9	3	0.6
Density ($kg\ m^{-3}$)	-	2650	1000
Heat capacity ($J\ kg^{-1}\ K^{-1}$)	-	1000	4200
Porosity (%)	10	0	-

2.2 Initial mineralogical composition

The geothermal reservoir at Soultz is made up of three types of granite (Jacquot, 2000; Hooijkaas et al., André et al., 2006) (Table 2). The first is non-altered (fresh) granite that is characterized by a predominance of feldspar, plagioclase and quartz, and by an extremely low fracture density. Consequently, its porosity is close to zero and does not contain significant amounts of water. The properties of this granite are that of the impermeable rock matrix. Fluid exchange, by advection or diffusion processes, will be disregarded for this granite; it will only act as a good heat conductor.

The second rock facies is a fractured, hydrothermally altered granite with quartz as the major mineral component; because of alteration the amount of feldspar decreases and some secondary minerals such as galena, pyrite, smectite or illite are present. This facies is the most porous (porosity ranging from 5 to 10 %) and contains most of the formation fluid. The third rock facies is the most altered; it corresponds to alteration veins that contain minerals such as illite, smectite and quartz. Precipitated secondary minerals (clays, carbonates) fully cement the fractures, resulting in a decrease of porosity and permeability. As a consequence, fluid circulation within the rock mass takes place through the second facies only (Genter et al., 1998).

Table 2: Mean composition (in %) of the different types of granite in the Soultz reservoir (Jacquot, 2000).

	Fresh granite	Hydrothermally altered granite	Alteration veins
Quartz	24.2	40.9	43.9
K-feldspar	23.6	13.9	
Plagioclase	42.5		
Illite		24.6	40.2
Smectite		9.7	9.6
Mica	9.4		
Calcite	0.3	3.3	4.3
Dolomite		0.8	0.7
Pyrite		0.7	1.0
Galena		1.3	0.3
Chlorite		4.8	

2.3 Water chemistry

The formation fluid circulating through the fracture network is a sodium-chloride brine with total mineralization close to 100 $g\ L^{-1}$. Its pH is approximately 4.9. The water is in thermal equilibrium (200 °C) with the rock at 5000 m depth. The composition of the formation brine extracted during a 1999 production test is given in Table 3. The chemistry of the deep fluid is similar to that of the fluid produced from the shallower reservoir at 3000 m depth (Durst, 2002). Its silica and carbon concentrations are higher because of the elevated temperatures and CO_2 partial pressures, respectively.

Table 3: Representative chemical analysis of the fluid sampled at the wellhead of GPK2 after being deepened to 5000 m in 1999 (Durst, 2002)

Species	Concentration (mmol/kg)
Na^+	1148.00
K^+	73.40
Ca^{2+}	169.50
Mg^{2+}	3.21
Cl^-	1648.00
S	1.77
C	42.76
Fe^{2+}	2.61
SiO_2	6.06
Al^{3+}	$3.7.10^{-3}$

3. NUMERICAL SIMULATORS

This description of the codes is a brief overview of the computation capabilities of the two simulators. For more details, the reader can consult the SHEMAT User's Guide (Clauser, 2003), as well as the different FRACHEM studies on the Soultz system (Durst, 2002; Bächler et al., 2005; André et al., 2006).

The methods for calculating activity coefficients are described for each code below. A Pitzer ionic interaction model has been introduced into both codes for solving non-isothermal reactive transport problems under conditions of high ionic strength, as encountered in typical EGS systems.

Applied thermodynamic data and equilibrium constants have been chosen to be consistent for both codes.

3.1 FRACHEM code

Different researchers (Durst, 2002, Bächler, 2003, Rabemanana et al. 2003, André et al., 2006) have incrementally built a reactive transport simulator, FRACHEM, able to simulate the main characteristics of the Soultz reservoir at 5 km below the surface, 200 °C, 500 bar, and a fluid salinity of around 100,000 ppm.

FRACHEM is a THC simulator issued from the combination of two existing codes: FRACTure and CHEMTOUGH2. FRACTure is a 3D finite-element code for modelling hydrological, transport and elastic processes. It was developed originally for the study of flow-driven interactions in fractured rock (Kohl & Hopkirk, 1995). CHEMTOUGH2 (White, 1995) is a THC code developed based on the TOUGH2 simulator (Pruess, 1991), a 3D numerical model for simulating the coupled transport of water, vapour, non-condensable gas, and heat in porous and

fractured media. CHEMTOUGH2 represents the possibility to transport chemical species and to model the chemical water-rock interactions as well as the chemical reactions driven by pressure and temperature changes. Transport and reactions are coupled in a one-step approach. FRACHEM has been built by introducing geochemical subroutines from CHEMTOUGH2 (White, 1995) into the framework of the code FRACTure (Bächler, 2003; Bächler and Kohl, 2005). After an initialization phase, FRACTure calculates, over each time step, the thermal and hydrological conditions within each element volume and determines the advective flow between each of them. Resulting thermal and hydrological variables are stored in arrays common to FRACTure and the geochemical modules. At this point, the program calculates the chemical reactions using a mass balance/mass action approach, the advective transport of chemical species, and the variations of porosity and permeability. Once this calculation is performed, porosity and permeability are updated and fed into the FRACTure part of the code. The program then returns to the start of the loop until the end of the simulation time (sequential non-iterative approach, SNIA).

FRACHEM has been developed especially for the granitic reservoir of Soultz-sous-Forêts and consequently, specific implementations have been added to the chemical part of this code. Considering the high salinity of the fluid, the Debye-Hückel model, initially implemented in the CHEMTOUGH2 routines to determine the activity coefficients, has been replaced by a Pitzer activity model. It should be mentioned here that the activity coefficient calculations are carried out indirectly using the code TEQUIL for the Na-K-H-Ca-Cl-SO_4-HCO_3-CO_3-CO_2-H_2 system from 0 to 250 °C (Moller et al., 1998). Using this model, total concentrations obtained from chemical analyses (Table 3) are used in TEQUIL to compute speciation and corresponding activity coefficients. Presently, a limited number of minerals are considered, which correspond to the minerals constituting the Soultz granite. The precipitation/dissolution reactions of carbonates (calcite, dolomite), quartz, amorphous silica, pyrite, and some aluminosilicates (K-feldspar, albite, illite) can be modelled under kinetic constraints. Rate laws follow the transition state theory (e.g., Lasaga et al., 1994). The implemented kinetic rate laws are specific to each mineral and taken from published experiments conducted at high temperature in NaCl brines.

Thermodynamic data (equilibrium constants) are taken mostly from SUPCRT92 (Johnson et al., 1992) and Helgeson et al. (1978) and are functions of temperature and pressure. The effect of pressure on equilibrium constants is explicitly taken into account with regard to the mineral reactions.

Finally, a supplementary module allows the determination of porosity and permeability variations linked with chemical processes occurring in the reservoir. Considering the alteration of the Soultz granite, the flow is assumed to circulate in a medium composed of fractures and grains. Therefore, a combination of a fracture model (Norton and Knapp, 1977; Steefel and Lasaga, 1994) and a grain model (Bolton et al., 1996) is used to determine the permeability evolution.

3.2 SHEMAT code

The Simulator for HEat and MAss Transport (SHEMAT, Bartels et al., 2003) is in combination with its graphical user interface "Processing SHEMAT" (Kühn and Chiang, 2003) an easy-to-use, general purpose reactive transport code for a wide variety of thermal and hydrogeological problems in two and three dimensions. SHEMAT solves coupled problems involving fluid flow, heat transfer, species transport and chemical water-rock interaction. It is a finite difference code that solves the flow and transport equations on a Cartesian grid. The "IAPWS Industrial Formulation" (Wagner et al. 2000) is the equation of state used for water. In SHEMAT, the different flow, transport and reaction processes can be selectively coupled. Flow and heat transport are coupled in that the fluid parameters density, viscosity, compressibility, thermal conductivity and thermal capacity are functions of temperature and pressure. Flow and salt transport are coupled via fluid density implemented by a linear approximation.

The current version of SHEMAT offers the user two choices for calculating the activity-concentration relationships underlying the mineral reaction processes: (1) Pitzer's equations (best suited for concentrated brines) or (2) Debye-Hückel's theory (useful for more dilute solutions).

SHEMAT's first chemical speciation module CHEMEQ is a modification of the geochemical modeling code, PHRQPITZ (Plummer et al. 1988). It permits calculations of geochemical reactions in brines and other highly concentrated electrolyte solutions using the Pitzer virial-coefficient approach for activity-coefficient corrections. Reaction-modeling capabilities include calculation of aqueous speciation and mineral-saturation as well as mineral solubility.

To extend the applicability of SHEMAT with a second chemical speciation module, for example to enable re-engineering ore deposits or simulate permeable reactive barriers, the program has now been interfaced additionally to the chemical code PHREEQC (Parkhurst and Appelo 1999). PHREEQC is based on the Debye Hückel ion association approach. Compared to PHRQPITZ and due to the considerably larger thermodynamic data set for the chemistry of dilute aqueous solutions, it allows to study chemical reactions between much more elements.

4. RESULTS AND DISCUSSION

The two codes were applied to a geometrical model representing the granitic reservoir at Soultz. We assume that major circulation occurs in the hydrothermally altered granite. Injected cooled brine mainly interacts with carbonates and quartz. Secondary precipitation of amorphous silica was considered.

FRACHEM and SHEMAT simulations have been compared in order to determine how fluid circulation within fractured granitic rock modifies fracture porosity. Total simulations time lasted 1800 days.

4.1 Reservoir temperature

The circulation of cooled fluid in the porous zone affects the temperature of the reservoir. But considering the flow rate (about 0.02 $L.s^{-1}$ during five years), the temperature decrease is only effective in the first 100 m of the porous zone. Obviously, the most important decrease concerns the near vicinity around the injection well with a temperature of about 65 °C. The predicted general trend of temperature with distance from injection well after roughly 5 years of fluid circulation is similar for the two codes. These results show that model conceptualizations regarding heat transport are almost identical (Fig. 2).

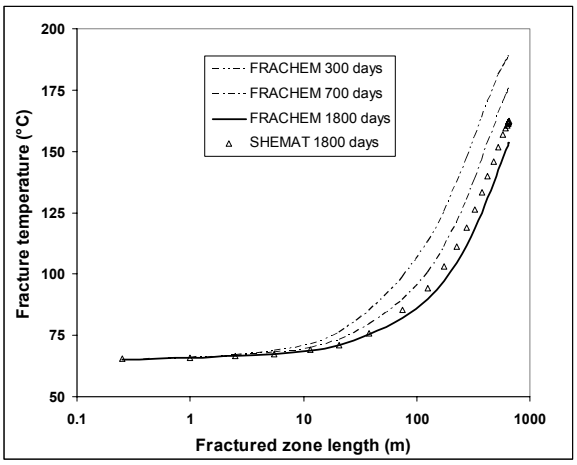

Figure 2: Temperature evolution along the fractured zone at different times.

4.2 Mineral-brine interactions

Results of numerical simulations for a long-term circulation confirm the major role of the carbonates on the evolution of reservoir porosity. Due to their fast reaction rates, carbonate minerals are responsible for most of the evolution. Silicates and pyrite behaviour is also simulated between the two wells, but their influence is minor.

The reservoir water has a ionic strength of about 1.8. The Debye-Hückel model does not account for any ionic interaction terms and generally is only applicable to solutions with $I < 1$. At high ionic strength and temperature, γCa^{2+} calculated from the Pitzer model is much larger than from Debye-Hückel. This means a lower Ca^{2+} concentration is needed to maintain calcite equilibrium or calcite is less soluble. The effect of increased Ca^{2+} activity coefficients on calcite solubility in this case is similar to the "salting out" effects for dissolution of non-condensible gases such as CO_2.

In both FRACHEM and SHEMAT models, the 65°C injection water is under-saturated with respect to calcite because calcite solubility increases with decreasing temperature. Calcite then dissolves close to the injection point. As temperature increases away from the injection point, calcite precipitation occurs (Fig. 3). Figure 4 shows that dolomite dissolves within the first ten meters from the injection well. The general dissolution and precipitation behaviour of dolomite is similar to calcite. Among silicates, quartz and K-feldspar are major minerals in granite. Contrary to calcite, the solubility of these minerals improves with decreasing temperature. As a consequence, these minerals precipitate near the injection well, but less so further away where temperature increases. Thus, quartz precipitates close to the injection point, and as temperature increases away from the injection point, quartz dissolution occurs (Fig. 5). Amorphous silica precipitates near the injection well at a maximum rate of 4.10^{-5} $mol.m^{-3}.s^{-1}$ (Fig. 6). After 25–30 m from the injection well, towards the production well and along the fracture, the reactions between the fluid and the minerals fade away because the injected brine comes close to thermodynamic equilibrium with regard to these minerals.

With FRACHEM, the observation of the mineral behaviour shows that all the reactions occur in the first 20 m of the injection zone. Calcite, a secondary mineral present within granite fractures in relatively small proportions, shows the highest reactivity. In the vicinity of the injection well, calcite dissolves, whereas it precipitates from about 2 to 20 m, because of the retrograde solubility of calcite (solubility decrease with temperature increase). At the onset of fluid circulation within the reservoir, calcite dissolves mainly within the first two meters of the injection well. This dissolution releases calcium in solution, which is then available for calcite precipitation further away from the injection well, where the temperature increases. With increasing simulation time and decreasing rock temperatures the calcite dissolution zone moves towards the production well and stops as soon as the mineral has been consumed completely in a specific area around the injection well.

Although the two codes yield similar results, in a qualitative sense, quantitative results differ significantly. These differences are primarily caused by differences in implemented kinetic models. Concerning the mineral reaction rates, significant differences were observed for calcite, dolomite and quartz. The largest differences in reaction rates were observed for calcite and dolomite.

With SHEMAT, after 1800 days of fluid circulation, calcite dissolves near the injection point at a maximum rate of two order of magnitude less than with FRACHEM (5.10^{-7} $mol.m^{-3}.s^{-1}$ compared to 5.10^{-5} $mol.m^{-3}.s^{-1}$), and then precipitates further in the fracture at a rate smaller than with FRACHEM (Fig. 3).

With FRACHEM, dissolution and precipitation of dolomite and quartz are about one order of magnitude smaller than calcite. In contrary, with SHEMAT, reaction rates of quartz and dolomite are one order of magnitude higher than calcite. Dolomite, a secondary mineral present within granite fractures in relatively small proportions, shows the highest reactivity (Fig. 4).

The diverging amount of dissolved and precipitated calcite has to be traced back to different chemical kinetic calculations in FRACHEM and SHEMAT. The equilibrium constants for minerals and activity coefficients of solutes used with FRACHEM and SHEMAT have been mostly issued from the same sources. But, kinetic rate laws do not take exactly the same form in both codes. The rate laws and parameters implemented into FRACHEM were specifically developed for each mineral and specifically established for high-salinity and/or high-temperature fluids most relevant to the reservoir conditions at Soultz. In SHEMAT, one generic equation is used for all minerals using varying initial reaction rates, activation energies and initial surface reaction areas to differentiate between the minerals. For calcite, the spread between models can reach 5 orders of magnitude, for dissolution and precipitation, respectively, regardless of the type of calcite considered (hydrothermal or sedimentary).

4.3 Effects on porosity

Evolution of the reservoir porosity is determined by the mineral reactions occuring in the fractured zone. With SHEMAT, as with FRACHEM, the porosity is enhanced in the first 10 meters from the injection well, due to the dissolution of carbonates (Fig. 7). Carbonates then precipitate between about 10 and 100 meters, yielding a maximum porosity decrease in this zone.

The two codes give generally similar trends. Consequently, the porosity-permeability models implemented in FRACHEM and SHEMAT result in similar porosities.

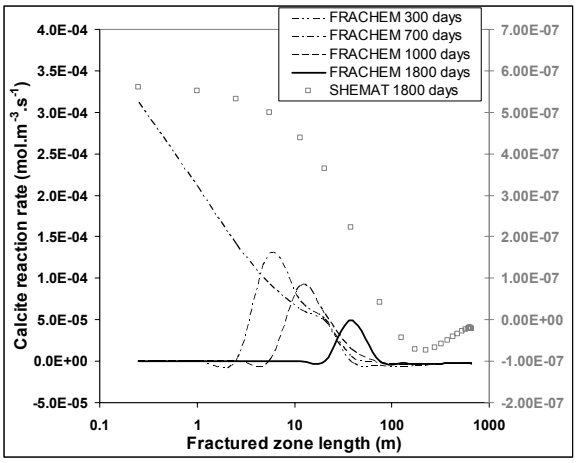

Figure 3: Calcite reaction rate along the fractured zone at different times (positive values indicate dissolution). Left and right y-axis correspond to FRACHEM and SHEMAT plots respectively.

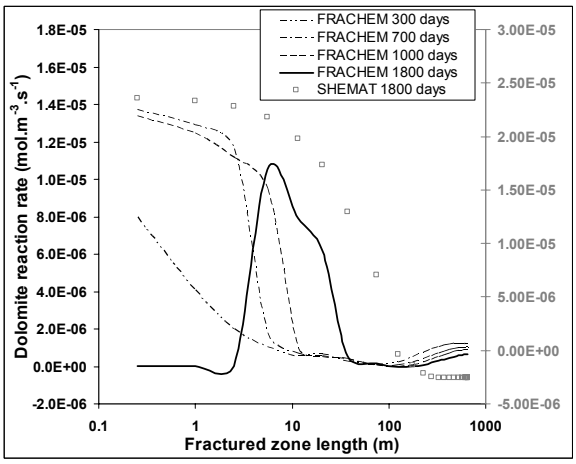

Figure 4: Dolomite reaction rate along the fractured zone at different times (positive values indicate dissolution).

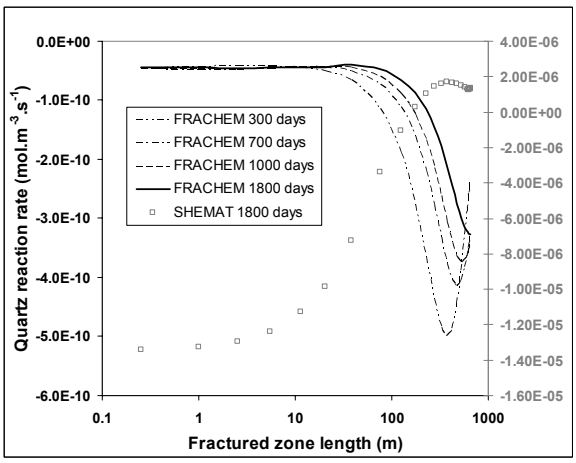

Figure 5: Quartz reaction rate along the fractured zone at different times (positive values indicate dissolution).

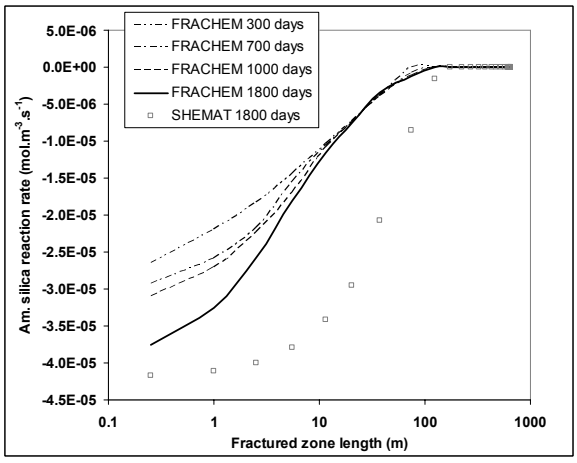

Figure 6: Amorphous silica reaction rate along the fractured zone at different times.

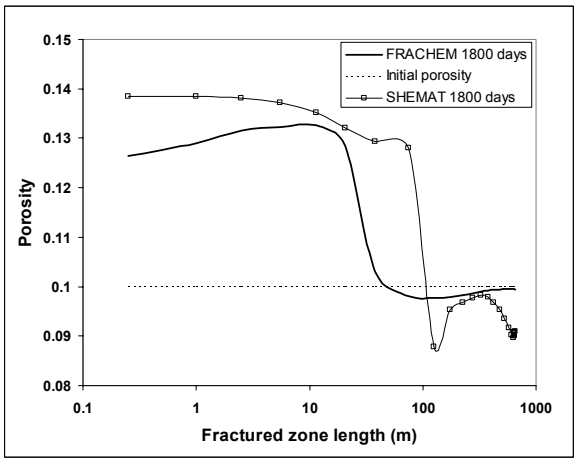

Figure 7: Porosity evolution for the two models along the fractured zone after five years of forced fluid circulation.

5. CONCLUSIONS

The goals of this work were to compare two geochemical transport codes, FRACHEM and SHEMAT (with similar databases), and to model complex systems like Enhanced Geothermal systems.

The two codes were applied to simulate reactive transport processes in the Soultz reservoir, using essentially identical conceptual model and input chemical and hydraulic data. Three main processes were investigated for a forced fluid circulation of 5 years: the evolution of reservoir temperature, mineral precipitation/dissolution behaviour and the evolution of reservoir porosity. Significant differences in models results were found, primarily due to differences in the kinetic models and their parameters. This study highlights the importance of these models in reactive transport simulations, in particular for systems involving brines.

Nevertheless, it can be seen from the porosity evolution that the results of FRACHEM and SHEMAT are very similar. Even though the simulators show significant differences with regard to the quantities of minerals precipitated and dissolved it is determined that changes of the hydraulic system are equally well described by both models. The fact

that both models yield similar results is of great importance, since no reliable measured data nor adequate laboratory experiments are available for comparison. FRACHEM and SHEMAT calculate the same temperature development and fluid velocities as well as resulting porosities from the mineral reactions. Thermodynamic equilibrium modelling resulted in comparable species and mineral concentrations in both models (applied activity coefficients and equilibrium constants have been chosen to be consistent for both codes). Thus, the Pitzer approach is well implemented. Finally, assuming an adequate calcite reaction rate in the SHEMAT code should result in a better fit of calcite amounts precipitated and dissolved.

6. ACKNOWLEDGEMENTS

The authors would like to thank the Swiss State Secretariat for Education and Research (Project N° 03.0460) and the Swiss Federal Office of Energy (Project N° 150'649) for funding this project. The authors are also grateful to Laurent André of BRGM (Orléans) and Thomas Kohl of Geowatt AG (Zürich) for their help in building and improving the FRACHEM chemical-thermo-hydraulic model and for numerous fruitful discussions.

7. REFERENCES

André, L., Rabemanana, V. and Vuataz, F.-D., 2006. Influence of water-rock interactions on fracture permeability of the deep reservoir at Soultz-sous-Forêts, France. Geothermics 35, 507-531.

André, L. and Vuataz, F.-D., 2005. Simulated evolution of reservoir properties for the Enhanced Geothermal System at Soultzsous-Forêts: the role of hot brine-rock interactions. In: Proceedings of the 30th Workshop on Geothermal Reservoir Engineering. Stanford University, 283–290.

André, L., Spycher, N., Xu, T., Pruess, K. and Vuataz, F.-D., 2006. Comparing FRACHEM and TOUGHREACT for reactive transport modeling of brine-rock interactions in Enhanced Geothermal Systems (EGS). In: Proceedings of the 31st Workshop on Geothermal Reservoir Engineering. Stanford University, 350–358.

Bächler, D. and Kohl, T., 2005. Coupled thermal-hydraulic-chemical modelling of enhanced geothermal systems. Geophys. J. Int. 161 (2), 533–548.

Bächler, D., Kohl, T. and Rybach, L., 2003. Impact of graben-parallel faults on hydrothermal convection – Rhine Graben case study. Physics and Chemistry of the Earth 28, 431-441.

Bächler, D., 2003. Coupled Thermal-Hydraulic-Chemical Modelling at the Soultz-sous-Forêts HDR reservoir (France). PhD thesis, ETH-Zürich, Switzerland, 151 p.

Baria, R., Jung, R., Tischner, T., Teza, D., Baumgaertner, J., Dyer, B., Hettkamp, T., Nicholls, J., Michelet, S., Sanjuan, B., Soma, N., Asanuma, H. and Garnish, J., 2006. Creation of an HDR/EGS reservoir at 5000 m depth at the European HDR project. Proc. 31st Workshop on Geothermal Reservoir Engineering, Stanford University, California, USA.

Barrett, T.J. and Anderson, G.M., 1988. The solubility of sphalerite and galena in 1–5m NaCl solutions to 300°C. Geochim. Cosmochim. Acta 52 (4), 813–820.

Bartels, J., Kühn, M. and Clauser, C., 2003 Numerical simulation of reactive flow using SHEMAT. In: Clauser C. (ed) Numerical simulation of reactive flow in hot aquifers - SHEMAT and Processing SHEMAT, Springer Publishers, Heidelberg, 5-74.

Blum, A.E. and Stillings, L.L., 1995. Feldspar dissolution kinetics. In: White, A.F., Brantley, S.L. (eds.), ChemicalWeathering Rates of Silicate Minerals, 31. Mineralogical Society of America, 291–351, Reviews in Mineralogy.

Bolton, E.W., Lasaga, A.C. and Rye, D.M., 1996. A model for the kinetic control of quartz dissolution and precipitation in porous media flow with spatially variable permeability; formulation and examples of thermal convection. J. Geophys. Res. Part B. Solid Earth Planets 101 (10), 22157–22187.

Carroll, S., Mroczek, E., Alai, M. and Ebert, M., 1998. Amorphous silica precipitation (60 to 120°C): comparison of laboratory and field rates. Geochim. Cosmochim. Acta 62 (8), 1379–1396.

Clauser, C. (ed.), 2003. Numerical simulation of reactive flow in hot aquifers. SHEMAT and Processing SHEMAT. Springer Verlag, Heidelberg, 332 p.

Debye, P. and Hückel, E., 1923a. Zur Theorie der Elektrolyte I: Gefrierpunktserniedrigung und verwandte Erscheinungen. Phys. Zeitsch. 24, 185–207.

Debye, P. and Hückel, E., 1923b. Zur Theorie der Elektrolyte II: das Grensgesetz f˙ur die elektrische Leitf˙ahigkeit. Phys. Zeitsch. 24, 305–325.

Dezayes, C., Valley, B., Maqua, E., Sysen, G. and Genter, A., 2005. Natural fracture system of the Soultz granite based on UBI data in the GPK3 and GPK4 wells. In: Proceedings of the EHDRA Scientific Meeting. Soultz-sous-Forêts, France.

Durst, P., 2002. Geochemical modelling of the Soultz-sous-Forêts Hot Dry Rock test site: coupling fluid-rock interactions to heat and fluid transport. PhD thesis, University of Neuchˆatel, Switzerland, 127 p.

Genter, A., Dezayes, C., Gentier, S., Ledésert, B. and Sausse, J., 1998. Conceptual fracture model at Soultz based on geological data. In: Proceedings of the 4th HDR Forum. Strasbourg, France.

Genter, A., Traineau, H., Dezayes, C., Elsass, P., Ledesert, B., Meunier, A. and Villemin, T., 1995. Fracture analysis and reservoir characterization of the granitic basement in the HDR Soultz project (France). Geotherm. Sci. Tech., 4 (3), 189-214.

Gérard, A., Genter, A., Kohl, T., Lutz, P., Rose, P. and Rummel, F., 2006. The deep EGS (Enhanced Geothermal System) project at Soultz-sous-Forêts (Alsace, France). Geothermic, 35 (5-6), 473-483.

Gérard, A., Fritz, B. and Vuataz, F.-D., 2005. Results of soft acid injection tests performed at Soultz in wells GPK2, GPK3 and GPK4—extended summary: revised status on 14 March 2005. In: Proceedings of the EHDRA Scientific Conference, Soultz-sous-Forêts, France.

Gérard, A. and Kappelmeyer, O., 1991. European HDR Project at Soultz-sous-Forêts, Geothermal Sc. & Tech. 3(1–4), Gordon & Breach Science Publishers, New York, USA, 308 p.

Hellmann, R., 1994. The albite-water system. Part I. The kinetics of dissolution as a function of pH at 100, 200

and 300°C. Geochim. Cosmochim. Acta 58 (2), 595–611.

Hettkamp, T., Baumgärtner, J., Baria, R., Gérard, A., Gandy, T., Michelet, S. and Teza, D., 2004. Electricity production from hot rocks. In: Proceedings of the 29thWorkshop on Geothermal Reservoir Engineering. Stanford University, 184-193.

Hooijkaas, G. R., Genter, A. and Dezayes, C., 2006. Deep-seated geology of the granite intrusions at the Soultz EGS site based on data from 5 km-deep boreholes. Geothermics 35 (5-6), 484-506.

Icenhower, J.P. and Dove, P.M., 2000. The dissolution kinetics of amorphous silica into sodium chloride solutions: effects of temperature and ionic strength. Geochim. Cosmochim. Acta 64 (24), 4193–4203.

Jacquemont B., 2002. Etude des interactions eau-roche dans le granite de Soultz-sous-Forêts. Quantification et modélisation des transferts de matière par les fluides. Thèse Univ. Louis Pasteur, Strasbourg.

Jacquot, E., 2000. Modélisation thermodynamique et cinétique des réactions géochimiques entre fluides de bassin et socle cristallin: application au site expérimental du programme européen de recherche en géothermie profonde (Soultz-sous-Forêts, Bas-Rhin, France). PhD thesis, Université Louis Pasteur, Strasbourg, France, 202 p.

Kohl, T. and Hopkirk, R.J., 1995. "FRACTure" – a simulation code for forced fluid flow and transport in fractured, porous rock. Geothermics 24 (3), 333–343.

Kohl, T. and Rybach, L., 2001. Assessment of HDR reservoir geometry by inverse modelling of non-laminar hydraulic flow. In: Proceedings of the 26th Workshop on Geothermal Reservoir Engineering. Stanford University, 259–265.

Köhler, S.J., Dufaud, F. and Oelkers, E.H., 2003. An experimental study of illite dissolution kinetics as a function of pH from 1.4 to 12.4 and temperature from 5 to 50°C. Geochim. Cosmochim. Acta 67 (19), 3583–3594.

Kühn, M., 2003. Chemical equilibrium speciation for brines at high temperatures and ionic strength. In: Clauser C (ed) Numerical simulation of reactive flow in hot aquifers - SHEMAT and Processing SHEMAT, Springer Publishers, Heidelberg, 75-170.

Kühn, M. and Chiang, W.-H., 2003. Pre- and post processing with "Processing SHEMAT". In: Clauser C (ed) Numerical simulation of reactive flow in hot aquifers - SHEMAT and Processing SHEMAT, Springer Publishers, Heidelberg, 75-151.

Lasaga, A.C., Soler, J.M., Ganor, J., Burch, T.E. and Nagy, K.L., 1994. Chemical weathering rate laws and global geochemical cycles. Geochim. Cosmochim. Acta 58, 2361–2386.

Moller, N., Christov, C. and Weare, J., 2006. Thermodynamic models of aluminum silicate mineral solubility for application to enhanced geothermal systems. Proc. 31st Workshop on Geothermal Reservoir Engineering, Sanford University, California, USA.

Moller, N., Greenberg, J.P. and Weare, J.H., 1998. Computer modeling for geothermal systems: predicting carbonate and silica scale formation, CO2 breakout and H2S exchange. Transp. Porous Media 33, 173–204.

Monnin, C., 1989. An ion interaction model for the volumetric properties of natural waters: density of the solution and partial molal volume of electrolytes to high concentrations at 25°C. Geochim. Cosmochim. Acta 53, 1177–1188.

Nagy, K.L., Blum, A.E. and Lasaga, A.C., 1991. Dissolution and precipitation kinetics of kaolinite at 80°C and pH 3: the dependence on solution saturation state. Am. J. Sci. 291 (7), 649–686.

Norton, D. and Knapp, R., 1977. Transport phenomena in hydrothermal systems; the nature of porosity. Am. J. Sci. 277 (8), 913–936.

Parkhurst, D.L. and Appelo, C.A.J., 1999. User's guide to PHREEQC (version 2) -A computer program for speciation, batch-reaction, one-dimensional transport, and inverse geochemical calculations: U.S. Geological Survey Water-Resources Investigations Report 99-4259, Reston Va.

Pitzer, K.S., 1973. Thermodynamic of electrolytes. I. Theoretical basis and general equations. J. Phys. Chem. 12, 268–277.

Plummer, L.N., Parkhurst, D.L., Fleming, G.W. and Dunkle, S.A., 1988. A computer program incorporating Pitzer's equations for calculation of geochemical reactions in brines: U.S. Geological Survey Water Resources Investigations Report 88-4153, Reston Va.

Pokrovskii, V.A. and Helgeson, H.C., 1995. Thermodynamic properties of aqueous species and the solubilities of minerals at high pressures and temperatures: the system Al2O3-H2O-NaCl. Am. J. Sci. 295, 1255–1342.

Portier, S., André, L. and Vuataz, F.-D., 2006. Modelling geochemical effects of acid treatments and comparison with field observations at Soultz-sous-Forêts geothermal site. Proc. ENGINE Scientific Workshop 3, « Stimulation of reservoir and microseismicity », Kartause Ittingen, Zürich, Switzerland.

Portier, S., André, L. and Vuataz, F.-D., 2006. Review of chemical stimulation techniques and results of acid injection experiments at Soultz-sous-Forets. Proc. EHDRA Scientific Conference, Soultz-sous-Forêts, France.

Rabemanana, V., Durst, P., Bächler, D., Vuataz, F.-D. and Kohl, T., 2003. Geochemical modelling of the Soultz-sous-Forêts Hot Fractured Rock system: comparison of two reservoirs at 3.8 and 5 km depth. Geothermics 32 (4–6), 645–653.

Rimstidt, J.D. and Barnes, H.L., 1980. The kinetics of silica-water reactions. Geochim. Cosmochim. Acta 44 (11), 1683–1699.

Sausse, J. and Genter, A., 2005. Types of permeable fractures in granite, Special Publication of the Geological Society of London, 240, 1-14.

Sausse, J., Fourar, M. and Genter, A., 2006. Permeability and alteration within the Soultz granite inferred from geophysical and flow log analysis. Geothermics, 35 (5-6), 544-560.

Sauty, J.P., 1981. Du comportement thermique des réservoirs aquifères exploités pour le stockage d'eau

chaude ou la géothermie basse enthalpie. Thèse d'état, Grenoble, 207 p.

Steefel, C.I. and Lasaga, A.C., 1994. A coupled model for transport of multiple chemical species and kinetic precipitation/dissolution reactions with application to reactive flow in single-phase hydrothermal system. Am. J. Sci. 294 (5), 529–592.

Stillings, L.L. and Brantley, S.L., 1995. Feldspar dissolution at 25°C and pH 3: reaction stoichiometry and the effect of cations. Geochim. Cosmochim. Acta 59 (8), 1483–1496.

Vuataz, F.-D., 2000. Review of the papers on HDR and Enhanced Geothermal Systems. World Geothermal Congress 2000, Kyushu, Tohoku, Japan, unpubl. report.

Wagner, W., Cooper, J.R., Dittmann, A., Kijima, J., Kretzschmar, H.-J., Kruse, A., Mares, R., Oguchi, K., Sato, H., Stöcker, I., Sifner, O., Takaishi, Y., Tanishita, I., Trübenbach, J. and Willkommen, Th., 2000. The IAPWS Industrial Formulation 1997 for the Thermodynamic Properties of Water and Steam. Journal of Engineering for Gas Turbines and Power 122, 150-182.

White, S.P., 1995. Multiphase nonisothermal transport of systems of reacting chemicals. Water Resour. Res. 31 (7), 1761–1772.

Wolery, T.J., 1992. EQ3nr, a computer program for geochemical aqueous speciation solubility calculations: theoretical manual, user's guide and related documentation (Version 7.0). Report, UCRL-MA-110662 PT III, Lawrence Livermore National Laboratory, Livermore, California, USA, 246 p.

ENGINE – **EN**hanced **G**eothermal **I**nnovative **N**etwork for **E**urope
Workshop 3, "Stimulation of reservoir and microseismicity"
Kartause Ittingen, Zürich, June 29 – July 1, 2006, Switzerland

Modelling geochemical effects of acid treatments and comparison with field observations at Soultz-sous-Forêts geothermal site.

Sandrine Portier*, Laurent André** and François-D. Vuataz*

* Centre for Geothermal Research - CREGE, c/o CHYN - University of Neuchâtel,
E.-Argand 11, CP158 - CH-2009 Neuchâtel, Switzerland
** BRGM - Service EAU/M2H - BP 6009 – 45060 Orléans cedex, France

e-mail: sandrine.portier@unine.ch, l.andré@brgm.fr, francois.vuataz@crege.ch

Abstract

Acid treatments have been successfully applied in many cases to increase or to recover geothermal wells production rates to commercial levels. Chemical stimulation techniques were originally developed to address similar problems in oil and gas production wells. The applicability of these stimulation techniques to a hot and fractured reservoir is less well known. High temperatures increase the acid-rock reaction rate. The development of Enhanced Geothermal Systems (EGS) depends on the creation of permeable and connected fractures. Acid stimulation jobs intend to clean (pre-existing) fractures by dissolving filling materials (secondary minerals or drilling mud) and mobilizing them for an efficient removal by flow transport. Recent acid treatments were performed on the EGS wells at Soultz-sous-Forêts (France). This 200°C and 5-km deep granitic reservoir contains fractures partially filled with secondary carbonates (calcite and dolomite). In order to dissolve these carbonates and to enhance the productivity around the wells, each of the three boreholes (GPK2, 3 and 4) were successively treated with various amounts of hydrochloric acid. The FRACHEM code, a Thermo-Hydraulic-Chemical coupled code, has been developed especially to forecast the evolution of the Soultz reservoir. Reactive transport modelling with FRACHEM code has been used to simulate acid injection and its impact on brine-rock interactions. Comparisons between FRACHEM simulations and field observations have been tested to forecast the impact of acid treatments on reservoir properties. The main goal is to simulate the effect of acid injection on permeability evolution in fractures at pressure and temperature conditions of the Soultz geothermal site.

Keywords: Enhanced Geothermal Systems ; chemical stimulation ; acid injection ; brine-rock interactions ; coupled modelling ; reactive transport ; Soultz-sous-Forêts.

1. Introduction

The Enhanced Geothermal Systems (EGS) are dedicated to the exploitation of the heat present in low productivity reservoirs. A geothermal resource is quite different from an oil or gas reservoir or even a ground water reservoir. In an oil reservoir, once the oil has been extracted, the reservoir is exhausted. By contrast, in a geothermal reservoir the water or steam originally present in the reservoir can be replaced by surrounding cooler water or re-injected fluid that is heated by the reservoir rock, becoming again available for production (O'Sullivan and McKibbin, 1993). Despite all the differences between hydrocarbon and geothermal reservoir, the techniques used for extraction of fluids are similar; as are the exploration techniques and reservoir management approaches. Techniques comparable to those used in the oil industry are employed to drill and complete well in the productive reservoir. In both cases formation damage should be minimized in order to optimize well performance. A well may encounter multiple, widely spaced, fracture zones, resulting in flow rates that are too low. Stimulation techniques have the potential to remediate such causes for low flow-rate wells. Different techniques can be used to enhance the fracture network but the main ones are hydraulic fracturation and chemical treatment. The present paper will be focused on the chemical stimulation of geothermal wells. This technology, developed for more than one century by oil industry for the stimulation of oil and gas wells, is also used in

geothermal wells. After a reminding of the different chemical stimulations performed on the GPK4 well at Soultz-sous-Forêts, numerical simulations using FRACHEM code have been carried out to estimate the impact of the acidizing treatments on carbonates and reservoir properties.

2. Cleaning of geothermal wells

2.1 Well stimulation techniques

Resources exploitation of gas, oil and heat from deep reservoirs needs sometimes a permeability development around the production wells to ensure an efficient flow. The aim of this technology is to enhance the well productivity and to reduce the skin factor by removing near-wellbore damage and by dissolving scales in natural fractures. It consists to pump into the reservoir reactants such as strong acids (hydrochloric acid, HCl-HF mixture), organic acids (acetic acid, chloroacetic acid, formic acid, sulfamic acid) or chelatants (EDTA family). Besides the traditional acids, the chelatants are solutions used as formation cleanup and for stimulating wells especially in formations that may be damaged by strong acids (Frenier et al., 2001). They act as a solvent, increasing the water-wetting operations and dissolving (entirely or partially) some minerals containing Fe, Ca, Mg and Al.

These reactants can be pumped into the reservoir according to two procedures: below the fracturing flow rate and pressure of the reservoir (matrix acidizing) or above the fracturing flow rate and pressure (fracture acidizing). The main disadvantage of acid treatments is linked to the corrosion risk of the casing in particular with strong acids. Nevertheless, this risk can be reduced by addition of corrosion inhibitors or by using less-corrosive agents as chelatants, but their use increases the treatment cost.

Matrix acidizing

This process is performed below fracturing flow rate and pressure and is normally used for the removal of skin damage associated with work-over, well killing or injection fluids and also for to increasing formation permeability in undamaged wells.

The protocol of matrix acidizing has not really evolved since the beginning of the 1980's and is composed of three main steps: a preflush, with hydrochloric acid ; a mainflush with a hydrochloric – hydrofluoric acid mixture ; a postflush / overflush with soft HCl acid solutions or with KCl, NH_4Cl solutions and freshwater.

Treatment volumes, injection rates, acid placement techniques, acid system selection and evaluation of the results when stimulating geothermal wells, all follow the same criteria as for oil wells. The important difference is the formation temperature. High temperature reduces the efficiency of corrosion inhibitors (and increase their cost) as well as increasing the acid/rock reaction rate. The high acid rock reaction rate requires the use of a retarded acid system to ensure acid will not all be spent immediately next to the wellbore, but will penetrate deeper into the formation. Protecting the tubulars against corrosion is another serious challenge. This requires careful selection of acid fluids and inhibitors (Buijse et al., 2000), while cooling the well by injecting a large volume of water preflush may reduce the severity of the problem.

Fracture acidizing

Also called acid fraccing, this technique is widely used for stimulating limestone and dolomite formations or formations presenting above 85 % acid solubility. It consists to inject first a viscous fluid at a rate higher than the reservoir matrix could accept leading to the cracking of the rock. Continued fluid injection increases the fracture's length and width and injected HCl acid reacts all along the fracture to create a flow channel that extends deep into the formation. The key to success is the penetration of reactive acid along the fracture. However, the treatment volumes for fracture acidizing are much larger than the matrix acidizing treatment, being as high as 12'000 – 25'000 l/m of open hole (Economides and Nolte, 1987).

Chemical mechanisms involved in acidizing

The preflush, performed most often with a HCl solution, has to allow the displacement of the formation brine and the removing of calcium and carbonate materials in the formation. Acid reacts rapidly with carbonate rocks when it reaches the grain surface according to reactions:

$$CaCO_3 + HCl \rightarrow Ca^{2+} + Cl^- + HCO_3^-$$

$$CaMg(CO_3)_2 + 2HCl \rightarrow Ca^{2+} + Mg^{2+} + 2Cl^- + 2HCO_3^-$$

By dissolving calcite and dolomite, acid may create wormholes (Crowe et al., 1992) and new pathways. If the reaction rate is too quick, acid is immediately consumed in the vicinity of the

fracture, forming wormholes but preventing the aperture of new pathways and connection to other fractures.

The role of the preflush, by dissolving carbonates, also prevents their contact and their reaction with HF injected with the mainflush and therefore minimizes the risk of precipitation of calcium fluoride CaF_2, highly insoluble in water:

$$CaCO_3 + 2\ HF \rightarrow CaF_2 + 2\ HCO_3^-$$

During the mainflush, the HF acid reacts mainly with the associated minerals of sandstones (clays, feldspars and micas), rather than with quartz. The reaction rates of HF with clays or feldspars are 100 to 200 times faster than the one with quartz. It results from these reactions an enlargement and interconnections of the pores in the matrix, facilitating fluid flow. The risk of using HF acid is the strong affinity of Si and Al with F, which can cause the precipitation of silicium or aluminum complexes (SiF_6^{2-}, AlF^{2+}, AlF_2^+, AlF_3, AlF_4^-), then damaging the formation by plugging. This is why HCl is added to HF: hydrochloric acid keeps a low pH and prevents the formation of fluorosilicates, fluoroaluminates, and fluoride salts.

For the preflush operation in acidizing treatments, a solution of hydrochloric acid at a concentration of 10 to 15 % is most often used. For the mainflush, the mud acids generally range from 10% HCl – 5% HF to 12% HCl – 3% HF. Acidification of geothermal wells is not as frequent as of oil and gas wells, but the operations are borrowed from this industry.

Concerning the injected amounts, in the majority of the cases, the preflush volume was based on a dosing rate of 600 litres per metre of open hole (Malate et al., 1997; Barrios et al., 2002). The cleaning out of the geothermal wells needs about 900 litres per metre of target zone.

HCl and HF are two acids reacting quickly with carbonates and silicates. However, the objective of acid treatment is to increase porosity and permeability of the medium, deeply in the formation. Some retardants can be added to the mud acid to slow the reaction rate of acid with the minerals.

A key point is to inject a solution not containing HF explicitly but a compound able to generate HF at greater depth of penetration for a longer reaction time and a maximum dissolution of fines (Crowe et al., 1992). This retardant hydrolyzes in water when it enters in the reservoir to form HF according to the reaction:

$$HBF_4 + H_2O \rightarrow HBF_3OH + HF$$

Other retardant systems can be used as an emulsifier of the aqueous acid solutions in oil, the dissolving of the acids in a solvent (alcohol, gel…) or the injection of solutions of methyl acetate which hydrolyses slowly at very high temperatures to produce acetic acid.

Malate et al. (1998) also proposed an acid system applicable for moderate to deep penetrations. They used a phosphonic acid complex (HEDP) to hydrolyse NH_4HF_2 instead of HCl. HEDP has five hydrogens available that dissociate at different stochiometric conditions. Mixture of HEDP acid with NH_4HF_2 produces an ammonium phosphonate salt and HF.

2.2 Experiments of acid injection

The cleaning out of geothermal wells to increase their productivity after scaling deposits constitutes the main application of the acid treatments. This technique has been used extensively in some geothermal fields in the Philippines (Buning et al, 1995; Buning et al, 1997; Malate et al., 1997; Yglopaz et al., 1998; Malate et al., 1999, Jaime-Maldonado and Sánchez-Velasco, 2003, Amistoso et al., 2005), in El Salvador (Barrios et al., 2002) and in USA (Morris et al., 1984, Entingh, 1999). It presents interesting results, such as the well injectivity increasing by 2 to 12-folds according to the studied reservoirs (Table 1).

At the Larderello geothermal field (Italy), several stimulation methodologies have been used successfully by ENEL (Capetti, 2006). Among them, chemical stimulation operations were carried out by injection of acid mixtures. First, various laboratory tests were realised on reservoir rock samples to optimize the HCl/HF ratios and the effect on mineral dissolution. Field tests have shown impressive results on five deep wells for reservoir rocks composed of phyllites, hornfels and granites: the improvement of injectivity, respectively productivity ranged from a factor 4 to 12.

In the field of EGS, few chemical treatments have been applied to stimulate reservoirs. In 1976, at the Fenton Hill Hot Dry Rock site (USA), 190’000 l of 1 N carbonate sodium base solution was injected to dissolve quartz from the formation and to reduce the impedance of the existing system. About 1’000 kg of silica were dissolved and removed from the reservoir but without impedance reduction. In 1988, a matrix acidizing was performed on the Fjällbacka

reservoir (Sweden): major and minor fractures of the granitic reservoir were filled with calcite, chlorite and clay minerals. About 2'000 l of HCl-HF acid were injected in Fjb3 to leach fracture filling. Returning rock particles showed some efficiency of this acid injection (Wallroth et al., 1999). Several wells at Coso field, affected by calcium carbonate scaling, were treated by acid methods. A total of 30 wells were treated with HCl and 24 gave successful results (Evanoff et al., 1995).

Geothermal Fields	Number of treated wells	Injectivity Index (kg/s/bar)	Improvement factor
Bacman (Philippines)	2	0.68 → 3.01	4.4
		0.99 → 1.4	1.4
Leyte (Philippines)	3	3.01 → 5.84	1.9
		0.68 → 1.77	2.6
		1.52 → 10.8	7.1
Salak (Indonesia)	1	4.7 → 12.1	2.6
Larderello (Italy)	5	11 → 54	5
		4 → 25	7
		1.5 → 18	12
		-	4
		11 → 54	5
Berlín (El Salvador)	5	1.6 → 7.6	4.8
		1.4 → 8.6	6.1
		0.2 → 1.98	9.9
		0.9 → 3.4	3.8
		1.65 → 4.67	2.8
Beowawe (USA)	1	-	2.2
Coso (USA)	30	24 wells	successful

Table 1: Results of HCl-HF treatments for scaling removal and connectivity development

2.3 The case of the EGS reservoir at Soultz

The geothermal research program for the extraction of energy from a Hot Fractured Rock at the Soultz-sous-Forêts site began in 1987 (Hettkamp et al., 2004). The project aims to convert heat to electricity from a deep fractured and granitic reservoir. To extract the heat from the reservoir, three deviated wells have been drilled at a depth of 5'000 m and their bottoms are separated by 650 m. The fractured reservoir encountered at this depth presents a temperature of 200°C. One well (GPK3) is dedicated to injection of cold water in the granitic reservoir whereas the two others (GPK2 and GPK4), located on both sides of injector, are used to pump hot water.

Stimulation experiments and injection tests

Recently acid treatments were performed at Soultz-sous-Forêts (France). This deep granitic reservoir contains fractures partially filled with secondary carbonates (calcite and dolomite). In order to dissolve these carbonates and to enhance productivity around the wells, each of the three boreholes (GPK2, 3 and 4) were treated with different amounts of hydrochloric acid. If GPK2 and GPK3 have shown weak variations of their injectivity, GPK4 presented a real increase of its injectivity after the treatments.

GPK4 well

In February 2005, an acid injection was tested to improve the injectivity around GPK4 well. The experiment began on 22 February 2005 with an injectivity test of the well before soft acidification. It consisted of the injection of 4'500 m^3 of water at increasing flow rates (9 l/s, 18 l/s, 25 l/s) in 24-hour steps. The injection of water acidified by the addition of approximately 2 g/l of hydrochloric acid started on 2 March 2005 at a flow rate of 27 l/s. It lasted 2 days, followed by one day of injecting fresh water at much lower rates in decreasing steps. A total volume of 5'200 m^3 was injected; with a total weight of acid (HCl) of 11 tons. When the wellhead pressure was back to the value observed during the previous injectivity test, an identical test was repeated on 13 March 2003: injection of 4'500 m^3 of water in flow rate steps of 24 hours at 9 l/s, 18 l/s and 25 l/s.

In May 2006, new tests began with a test of the well injectivity before acidification. The acid treatment was performed in four stages :

- Injection of 2000 m^3 of cold water deoxygenized at 12 l/s, 22 l/s then finally at 28 l/s.

- A preflush of 25 m^3 HCl diluted at 15 % (3 tons) (with deoxygenized water) was pumped ahead of

the HCl-HF acid mixture during 15 minutes at 22 l/s.

- A main flush consisted of the injection of 200 m^3 of Regular Mud Acid (RMA), (12 % hydrochloric (HCl)-3 % Hydrofluoric (HF) acid mixture treatment), with addition of a corrosion inhibitor, at a flow rate of 22 l/s during 2,5 hours.

- A postflush by injection of 2'000 m^3 cold water deoxygenized without inhibitor at a flow rate of 22 l/s then 28 l/s during 1 day.

When the wellhead pressure was back to a value identical to that observed in the previous injectivity test, a 3-day test identical to that of March 13, 2005 was repeated.

Results of acid stimulation treatments

Figure 1 shows the impact of the acidified water on the wellhead pressure during the first acid injection in GPK4 well. Despite the fact that the injection was performed in an over-pressurised reservoir, the injection pressure was decreasing during the last hours of the acidification test. Moreover, it is interesting to compare the data from two tests of water injection performed in the same conditions before (February 22, 2005) and after (March 13, 2005) the acid injection (Figure 1). Results (Gérard et al., 2005) show that after some 72 hours of water injection in the second test (24 hours at 9 l/s, 24 hours at 18l/s and 24 hours at 26 l/s), the GPK4 wellhead pressure was about 40 bars below the value observed in the same conditions before acidification. This represents a decrease of the apparent reservoir impedance seen from the wellhead by a factor ~1.5 (0.20 to 0.30 l/s/bar).

Figure 2 shows the impact of RMA acid job on the wellhead pressure by comparison before and after the second acid injection in GPK4 well. The repetition of the injectivity test showed that the difference in the over pressure values at the wellhead between the beginning of the test and the end were 16 bars. This represents a 35 % reduction of the wellhead pressure due to the acidification treatment. After some preliminary evaluation of downhole pressure changes, performed by Geowatt, this leads to a provisional estimate of GPK4 injectivity after chemical treatment of ~0.40 l/s/bar.

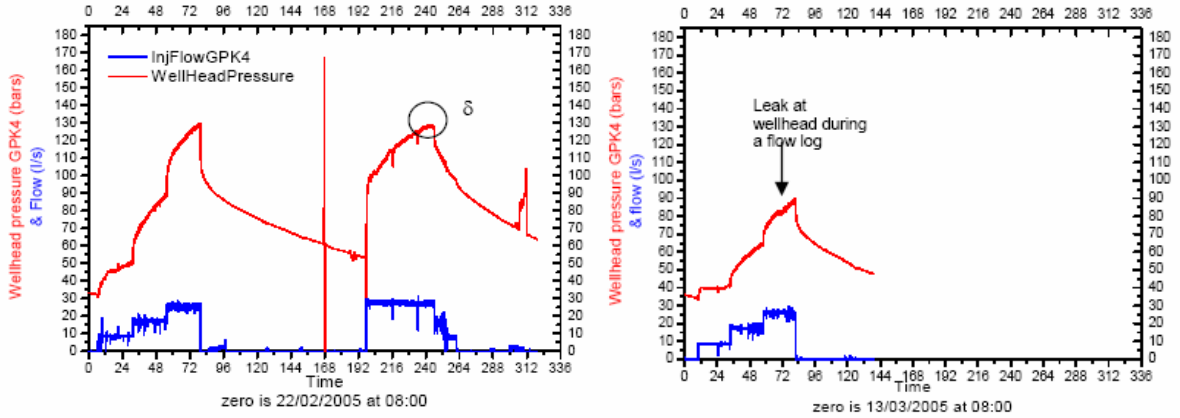

Figure 1: Impact of acidification test on GPK4; on the left, wellhead pressure before and during acidification injection, on the right, after acidification (Gérard et al, 2005).

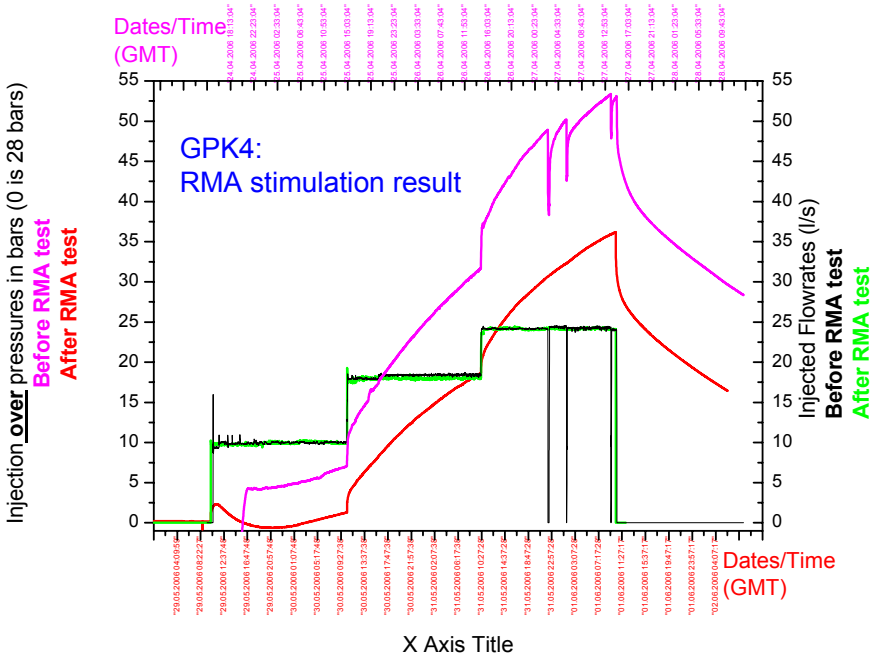

Figure 2: Impact of the RMA acidification test on the wellhead over pressure measured before and after the acidification test on GPK4 well (May 2006). (GEIE, 2006).

3. Modelling acidification impact on geothermal reservoir

The objective of the numerical simulation is to determine the impact of acid on the fracture minerals and on the reservoir properties.

3.1 Numerical modelling approach

To predict the impact of the acid treatment on the Soultz reservoir, the Thermo-Hydraulic and Chemical (THC) coupled code FRACHEM has been utilized. This THC code was built for the Soultz reservoir conditions. Instead of creating a totally new modelling programme, two existing codes, FRACTure and CHEMTOUGH2, have been combined in a new code called FRACHEM (Durst, 2002; Bächler, 2003; Rabemanana et al., 2003; André and Vuataz, 2005). FRACTure is a 3-D finite elements code and it determines thermal and hydraulic processes in fractured and porous rocks (Kohl and Hopkirk, 1995). CHEMTOUGH2 is a 3-D finite volumes code (White, 1995); it simulates the reactive transport and allows the variation of permeability according to chemical reactions occurring between fluid and rock of the reservoir. Considering the strong mineralization of brine and the high temperature of the reservoir, this last code has been modified by several implementations: thermodynamic model and computation of the activity coefficients of selected species in solution, kinetic model for dissolution and precipitation of minerals, as well as the relationship between porosity and permeability.

Knowing the high salinity of the brine of the Soultz system, The Pitzer formalism has been implemented in FRACHEM code to calculate the activity coefficients of selected chemical species; then, the precipitation/dissolution reactions of some minerals can be estimated. For the present time, the behaviour of eight minerals (calcite, dolomite, pyrite, quartz, amorphous silica, K-feldspars, albite and illite) is investigated. Detailed information on the determination of the reaction laws can be found in Durst (2002). At last, a supplementary module allows the determination of porosity and permeability variations linked with chemical processes occurring in the reservoir (André et al., 2005). The porosity variations are calculated and a combination of a fracture model and a grain model is used to determine the permeability evolution.

3.2 Simulation setup

Geometry

The same geometrical model as that presented in previous papers has been considered (André and Vuataz, 2005). The present application of FRACHEM is the modelling of a 2-D simplified model with a geometry close to the Soultz system. Injection and production wells are linked by fractured zones and surrounded by the impermeable granite matrix. The model is composed of 1250 fractured zones. Each fractured zone has an aperture of 0.1 m, a depth of 10 m, a porosity of 10%, and contains 200 fractures. This model allows an effective open thickness of about 125 m, while the mean openhole section of each well is about 600 m. Initially the temperature was set to the reservoir temperature of 200°C and the fractured zone contains the formation fluid.

One of these fractured zones is modelled with the assumption that the fluid exchange with the surrounding low permeability matrix is insignificant. Due to the symmetrical shape of the model, only the upper part of the fractured zone is considered in the simulation. The area is discretized into 222 2D elements (Figure 3).

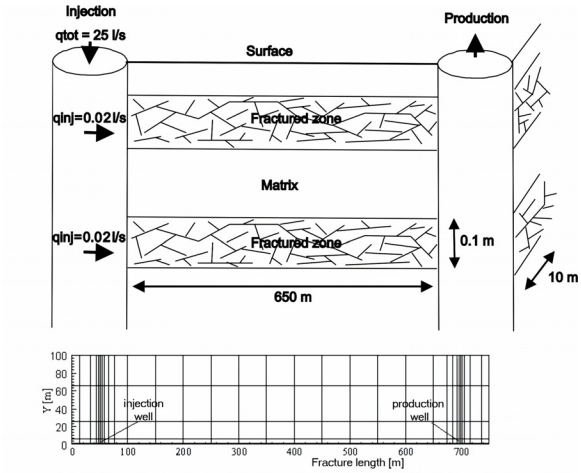

Figure 3: Simplified model and spatial discretization.

Considering a production rate of 25 l/s, the fluid was re-injected in each of the fractured zones at a rate of 2.10^{-2} l/s at a constant temperature of 65°C. During this simulation a constant overpressure of 8 MPa was assumed at the injection well and a hydrostatic pressure at the production well. Dirichlet boundary conditions were applied to the upper, left and right side of the model. The values of thermo-hydraulic parameters considered in the simulation are listed in Table 2.

Table 2: Thermo-hydraulic model parameters.

Parameters	Units	Fracture	Matrix	Fluid
Hydraulic conductivity	[m^2/Pa]	7.4 10^{-8}	10^{-15}	-
Thermal conductivity	[W/m.K]	2.9	3	0.6
Density	[kg/m^3]	-	2650	1000
Heat capacity	[J/kg.K]	-	1000	4200
Porosity	[%]	10	0	-

Rock composition

The mineralogical composition of Soultz granite given by Jacquot (2000) on GPK2 is assumed to be the same for the three wells (GPK2, GPK3 and GPK4) (Table 3). In the following simulations, the fluid is assumed to circulate within the hydrothermalised granite containing about 3.3 % of calcite and 0.8 % of dolomite.

Fluids composition

The fluid present in the formation is a NaCl brine with a pH of 4.9, a total dissolved solids of about 100 g/l and a temperature at the beginning of the simulation of 200 °C. The main characteristics of this fluid are given in Table 4.

The HCl solutions used to acidize the circulation fluid are highly diluted solutions (a fresh water) acidified to 2 g/l and to 15 g/l with concentrated HCl. These solutions are injected in the fractured zone at a temperature of 65 °C.

Table 3: Mean composition (in volume percent) of the different facies of granite in the Soultz reservoir (Jacquot, 2000).

Minerals	Healthy granite	Hydrothermalised granite	Vein of alteration
Quartz	**24.2**	**40.9**	**43.9**
K-Feldspar	**23.6**	**13.9**	
Plagioclases	**42.5**		
Illite		**24.6**	**40.2**
Smectite		**9.7**	**9.6**
Micas	**9.3**		
Calcite	**0.3**	**3.3**	**4.3**
Dolomite		**0.8**	**0.7**
Pyrite		**0.7**	**1.0**
Galena		**1.3**	**0.3**
Chlorite		**4.8**	

Table 4: Characteristics of the fluids used for the numerical simulations

Fluid		HCl solutions	Formation brine
Temperature (°C)		65	200
pH		1.3 to 0.4	4.9
Concentration (mg/kg)	Na^+	26.40	26400
	K^+	2.90	2870
	Ca^{2+}	4.75	6160
	Mg^{2+}	0.10	112
	Fe^{2+}	0.13	134
	SiO_2	0.36	364
	Cl^-	1455	54205
	SO_4^{2-}	0.07	63
	HCO_3^-	0.09	58

3.3 Simulation results of acid injections

We have been studying the impact of acid treatments on the Soultz reservoir properties near the injection well. The FRACHEM simulator is used to inject the adequate volume of acid in the model. The solutions are expected to circulate in a fractured zone composed of hydrothermally altered granite and their behaviour with respect to the minerals present in this granite is observed. When the desired volume is reached, the injection is stopped and the return to chemical equilibrium of the injected fluid is modelled. In the reservoir, a total pressure of 500 bars is assumed and the CO_2 partial pressure is fixed to 5 bars.

Concerning the acid solution used in the simulations, it should be noted that, for the time being, the code is not able to make the difference between the type of injected acid. It means that FRACHEM does not make the difference between hydrochloric and hydrofluoric acids. In this condition, the injection of an acid solution and the acid concentration are fixed by the H^+ concentration and by the total volume injected. Concentrated solutions are characterised by low pH solutions.

At last, it should be noted that the code calculates phases equilibrium between fluid and rock without taking into account the specific reaction rate of acid on carbonates. We suppose here that the reaction between acid and carbonates is instantaneous which is not a real disadvantage considering the high reactivity of HCl with carbonates and in particular with calcite.

Soft acidification

The duration of the numerical simulation was determined in order to simulate the real amount of acid injected in GPK4 in February 2005. The interpretation presented here are given for HCl injection of 60 hours at a flow rate of 25 l/s and at a concentration of 2g/l, equivalent to the 11 tons of HCl injected in GPK4 in February 2005.

The action of acid on carbonates has been investigated. Results show that acid solution dissolves carbonates in the first metres of the fractured zone. Around GPK4 (60 hours injection), the injected amount of HCl affects the first 3.5 metres around the injection well (Figure 4). Due to the respective reaction rate of each mineral, it should be noted that dolomite has dissolution rates two orders of magnitude smaller than calcite (Figure 5). Comparatively to a normal brine injection, after 60 h, the acid injection involves an increase of dissolved calcite and dolomite.

HCl acidification has a weak impact on other minerals: it only decreases the precipitation rate of K-feldspar, albite, illite and amorphous silica (Figure 6). Finally, quartz is not affected by this type of acidification (Figure 6).

All these dissolution processes cause an increase of about 2.0 % of rock porosity in the short interval of 0.5 m around the injection well and 0.1 % in the interval 0.5-1.5 m. This estimation of the reservoir changes is linked to the choice of the porosity model used in FRACHEM, namely the double fracture and grain model.

In conclusion, we can suppose that the volume of injected acid in the first soft acidizing test on GPK4 had only an impact on the first 4 metres around the injection well. With these rather small acid amounts, the impact on the reservoir properties seems to be limited, although the porosity increases in the close vicinity of the wells due to carbonates dissolution.

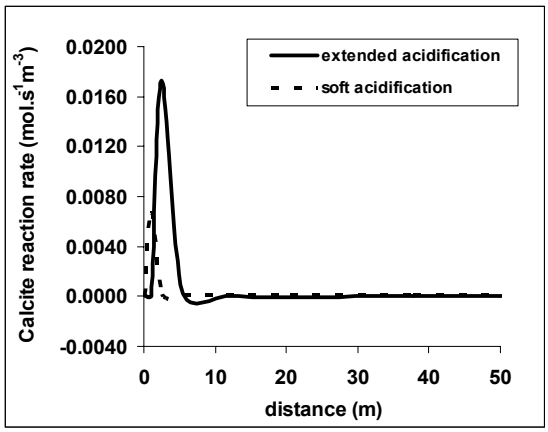

Figure 4: Variation of calcite reaction rate after acid injection.

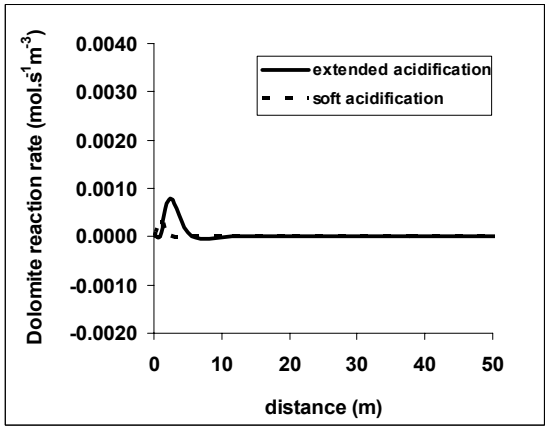

Figure 5: Variation of dolomite reaction rate after acid injection.

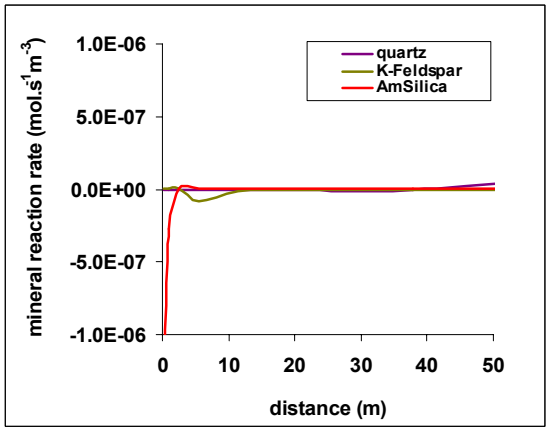

Figure 6: Variations of quartz, K-Feldspar and amorphous silica reaction rate after soft acid injection.

Influence of injection flow

The chemical stimulation of an EGS reservoir is effective if the acid can reach fractures distant from the injection well. In order to simulate this process, the flow was doubled meaning that the acid solution, at a concentration of 2 g/l, was pumped at 50 l/s. In these conditions, the 11 tons of acid are injected in 30 hours, compared to the 60 hours of the previous simulation. We observed that doubling the flow allows a farther transport of acid within the fracture. Less calcite is dissolved near the well but the impact of acid is visible up to 7.5 metres (Table 5). The same phenomenon applies to dolomite. Dissolution rate of this mineral is two orders of magnitude smaller than calcite. Consequently the impact of acid is still active beyond 15 metres along the fracture.

Table 5: Variation of the proportion of carbonates around the injection well according to variable transport flow

Distance from injection well (m)	Injection at 25 L.s^{-1}		Injection at 50 L.s^{-1}	
	Calcite (%)	Dolomite (%)	Calcite (%)	Dolomite (%)
0 0.5	- 19.70	- 5.73	- 18.80	- 6.00
0.5 1.5	- 1.40	- 0.12	- 1.02	- 0.10
1.5 3.5	- 0.15	- 0.15	- 0.37	- 0.06
3.5 7.5	0	- 0.10	- 0.10	- 0.05
7.5 15	0	0	0	- 0.05

Extended acidification

In May 2006, GPK4 well was stimulated by injecting 98 tons of HCl during a period of 2.5 hours. This second acidizing treatment used hydrochloric acid at a concentration of 12 % and hydrofluoric acid at a concentration of 3 %. After this injection, the acid is displaced within the formation by injecting about 2'000 m^3 of fresh water. The results showed a decrease of the injection pressure in the vicinity of the injection well, as the calcite was dissolved and progressively carried away. The response of the model to the acid addition has been examined.

Influence of high acid concentration

Knowing that the code is not able to make the difference between the type of injected acid, a numerical simulation was carried out to investigate the impact of this acid injection at a

concentration of 15 g/l. This simulation was performed with fresh water. Its pH was lowered to 0.4, whereas the injection rate within the fractured zone was maintained to 2.10^{-2} l/s. Therefore, the flow was fixed at 25 l/s and the duration of the injection was 70 hours. The total amount of injected acid is equal to 98 tons. The results indicate that calcite is as usual, the most affected mineral by the acid injection. Respectively to the extended acidification, the increase of acid concentration seems to augment the dissolution processes in the first meter around the injection well, and the impact of acid is also noticeable farther in the formation (Figures 4, 5 and Table 6). The porosity increases mainly in the vicinity of the injection well of about 4.5 % (Figure 7) instead of the 2.0 % estimated with a soft acidification. This increase of porosity is expressed by an injectivity rise in the zones affected by acidizing treatment.

In conclusion, the extended acidification amplifies the amount of dissolved calcite of about 70 % around the injection well. We can also suppose that the volume of injected acid in the second test on GPK4 had an impact on the first 10 metres around the injection well. The simulation results were consistent with those of the experiment. The additional H^+ ions significantly modify the calcite reaction rate around the injection well. The additional acid reaction leads to significantly drop the pressure around the injection well (Figure 8). This brine acidification implies a decrease of about 4 bars near the injection well, corresponding to a reduction of about 5 % of the pressure in 70 hours. This result is linked to the enhanced dissolution of calcite within the fractured zone. As the reservoir permeability and porosity are controlled by the occurrence of mineral precipitation and dissolution, this stronger calcite dissolution implies an improvement of the reservoir properties, namely the hydraulic impedance of the injection well.

Table 6: Variation of the amounts of carbonates and quartz near the injection well according to the amount of acid injected.

Amounts of minerals (kg)	Calcite	Dolomite	Quartz
Soft acidification	-15.4	-13.8	+0.0207
Extended acidification	-145	-35.6	+0.0129

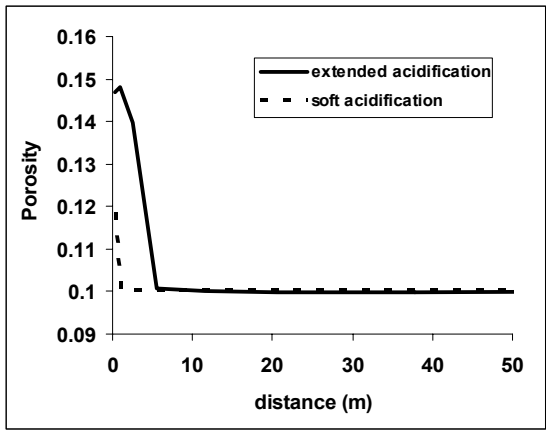

Figure 7: Porosity variation at different distance from the injection well after acid injection.

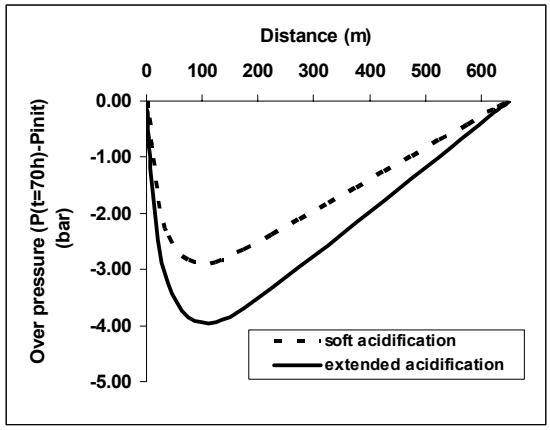

Figure 8: Variation of the pressure at different distance from the injection well after acid injection.

3.4 New improvements of the simulation

In order to improve simulation of the acidification processes, some new results of acid injections simulations using FRACHEM code are presented here. Porosity evolution resulting of acid injection has been observed according to three main parameters:

- acid concentration, varying from 2 to 15 g/l of HCl.

- flow imposed to the system, ranging from 10 to 50 l/s.

- duration of acid injection / circulation fluid in the fractured zone, reaching 0.5 to 10 days.

For a limited acid injection (10 l/s at 2 g/l), acid effect on dissolved carbonates and on penetration within the reservoir is very restricted. At this flow, a real impact on reservoir properties is only obtained for extended injections of many days and for high

acid concentrations. After an injection of 10 days of a solution at 15 g/l, all carbonates are dissolved in the first 0.5 metres around the injection well but only 65 % in the range 0.5 – 1.5 m. The relative weak effect of a small flow is shown here.

Nevertheless, for the other simulations at this flow, it seems that acid concentrations of about 7 to 15 g/l could have a positive impact up to 7.5 metres away from the injection well, and for a relatively limited injection time (5 days).

Injected acid reacts of course with carbonates (calcite and dolomite). According to mineralogical data, these compounds represent more or less 5 % of the hydrothermally altered granite. From this proportion and in case of a massive acid injection, all carbonates can be dissolved by acid solution leading to a porosity of about 0.15.

Obviously, the best results are obtained for long-term injections of high-concentration acid solutions. In these conditions, the impact radius can reach 15 metres around the injection well. Considering these conditions (for example 15 g/l and 50 l/s), it should be noted that the important amount of injected acid is able to dissolve carbonates (calcite + dolomite) up to 7 metres from the injection well, even for very limited injection times (2.5 days), (Figure 9).

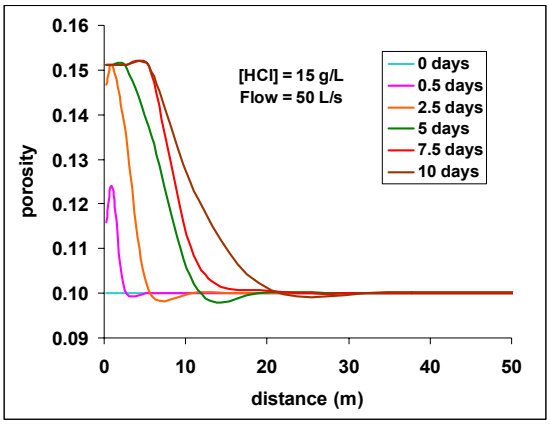

Figure 9: Porosity evolution of the fractured zone according to acid concentration and time of acid circulation and for a flow in the fractured zone of 50 L/s.

Finally, the increase of acid concentration involves an augmentation of dissolution processes but always in the first 5 metres around the injection well. Due to the high reactivity of HCl, the rock volume affected by acid is relatively small. An increase of the flow should allow a better dispersion of acid within the formation. The increase of the acid injection pressure to simulate a fracture acidizing allows a farther acid transport trough the fractures (Figure 10).

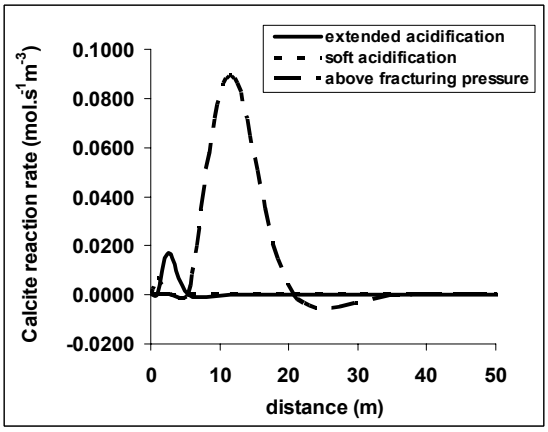

Figure 10: Variation of calcite reaction rate after acid injection below and above fracturing pressure.

4. Conclusions

Recent acid treatments have been successfully performed in geothermal granitic reservoirs such as at Soultz and encouraging results were obtained on GPK4 well.

Some numerical simulations using FRACHEM code were performed to better understand the acid behaviour within the reservoir. Considering the geometrical model used for the simulations and the different assumptions about fluid and rock compositions, some estimations have been proposed.

Simulations result indicate that carbonates are the most dissolved minerals by hydrochloric acid.

For GPK4 well, the first acid injection lasted 3 days at a concentration of 2 g/l (about 11 tons of acid injected in the reservoir). According to the simulation of this test, the amount of acid is just sufficient to dissolve half of the carbonates initially present in the range of 0 – 0.5 metres. Farther in the fracture, the impact is quasi nil.

Simulation of extended acid injection performed in May 2006 (about 98 tons of acid injected in the reservoir) seem to show a significant dissolution of carbonates around the injection well. The increase of acid concentration augments the reactivity in the vicinity of the injection well and enhances the porosity.

Nevertheless, the high reactivity and a weak flow prevent the penetration of acid in the far field between the wells. This high reactivity also involves the risk of creating wormholes, able to increase the porosity but not always the permeability of the fractured medium.

Finally, we have demonstrated that acid injection can play a significant role in the development of porosity around injection wells. It was shown that HCl acid has the possibility to react with carbonates, dissolving them and opening new pores within the reservoir. The positive effect of acid injection on porosity is proportional to the amount of injected acid.

Looking for commercial production rates of the wells, other chemical stimulation techniques should be considered, such as fracture acidizing, more complex acid compounds and chemical retardants. These types of acid jobs should have a more pronounced effect on the fracture network of the far field and eventually connect injection to production wells.

Acknowledgements

The authors thank the State Secretariat for Education and Research and the Swiss Federal Office of Energy for funding this project (OFES-N° 03.04.60). The authors are also grateful to André Gérard of the GEIE at Soultz and Thomas Kohl of GEOWATT AG (Zürich) for their scientific support.

References

André, L., Vuataz, F.-D. (2005), "Simulated evolution of reservoir properties for the Enhanced Geothermal System at Soultz-sous-Forêts: the role of hot brine-rock interactions". Proceedings 30th Workshop on Geothermal Reservoir Engineering, January 31- February 2, 2005, Stanford University, Stanford, California.

André, L., Vuataz, F.-D. (2006), "Simulated evolution of reservoir properties for the Enhanced Geothermal System at Soultz-sous-Forêts: the role of hot brine-rock interactions". Geothermics, in press.

André, L., Rabemanana, V. and Vuataz, F.-D. (2005), "Geochemical modelling of water-rock interactions and implications on the properties of the Soultz fractured reservoir". Proceedings EHDRA Scientific Conference, March 17-18, 2005, Soultz-sous-Forêts, France

Amistoso, A.E., Aqui, A.R., Yglopaz, D.M. and Malate, R.C.M. (2005), "Sustaining steam supply in Palinpinon 1 production field, Southern Negros Geothermal Project, Philippines". World Geothermal Congress, Antalya, Turkey, 24-29 April, 2005.

Bächler, D. (2003), "Coupled Thermal-Hydraulic-Chemical Modelling at the Soultz-sous-Forêts HDR reservoir (France)", PhD Thesis, ETH-Zürich, Switzerland, 150 p.

Barrelli, A., Cappetti, G., Manetti, G. and Peano, A. (1985), "Well stimulation in Latera Field". Geothermal resources Council Transactions, Vol. 9- Part II, pp. 213-219.

Barrios, L.A., Quijano, J.E., Romero, R.E., Mayorga, H., Castro, M. and Caldera, J. (2002), "Enhanced permeability by chemical stimulation at the Berlin Geothermal Field, El Salvador". Geothermal Resources Council Transactions, Vol. 26, September 22-25, 2002.

Buijse, M., Maier, R. and Casero, A. (2000), "Successful high pressure, high temperature acidising with in situ crosslinked acid diversion". SPE paper 58804.

Buning, B.C., Malate, R.C.M., Lacanilao, A.M., Sta Ana, F.X.M. and Sarmiento, Z.F. (1995), "Recent experiments in acid stimulation technology by PNOC-Energy development corporation, Philippines". Proceedings World Geothermal Congress, Vol. 3, p. 1807-1812.

Buning, B.C., Malate, R.C.M., Austria, J.J.C., Noriega, M.T. and Sarmiento, Z.F. (1997), "Casing perforation and acid treatment of well SK-2D Mindanao 1 Geothermal project, Philippines". Proceedings 22nd Workshop on Geothermal Reservoir Engineering, January 27-29, 1997.

Capetti, G. (2006), "How EGS is investigated in the case of the Larderello geothermal field ?". Engine Launching Conferente, Orleans 12-15 February 2006, unpubl. presentation.

Crowe, C., Masmonteil, J. and Thomas, R. (1992), "Trends in Matrix Acidizing". Oilfield Review, October 1992, pp. 24-40.

Durst, P. (2002), "Geochemical modelling of the Soultz-sous-Forêts Hot dry Rock test site: Coupling fluid-rock interactions to heat and fluid transport". PhD thesis, University of Neuchâtel, Switzerland, 127p.

Economides, M. and Nolte, K. (1987), "Reservoir stimulation". Schlumberger Educational Services.

Entingh, D.J. (1999), "A review of geothermal well stimulation experiments in the United States". Geothermal Resources Council Transactions, October 17-20, 1999, vol. 23, pp. 175-180.

Evanoff, J., Yeager, V. and Spielman, P. (1995), "Stimulation and damage removal of calcium carbonate scaling in geothermal wells: a case study". World Geothermal Congress, Florence, Italy, pp. 2481-2485.

Frenier, W.W., Fredd, C.N. and Chang, F. (2001), "Hydroxyaminocarboxylic Acids produce superior formulations for matrix stimulation of carbonates at high temperatures". SPE 71696.

GEIE. (2006), "Results of GPK4 RMA stimulation of May 2006". Unpublished data.

Gérard, A., Fritz, B. and Vuataz, F.-D. (2005), "Results of soft acid injection tests performed at Soultz in wells GPK2, GPK3 and GPK4 – Extended summary: revised status on 14 March 2005- Proceedings EHDRA Scientific Conference", March 17-18, 2005, Soultz-sous-Forêts, France.

Hettkamp, T., Baumgärtner, J., Baria, R., Gérard, A., Gandy, T., Michelet, S. and Teza, D. (2004), "Electricity production from hot rocks". Proceedings, 29th Workshop on Geothermal Reservoir Engineering, Stanford University, Stanford, California, January 26-28, 2004, 184-193.

Jacquot, E. (2000), "Modélisation thermodynamique et cinétique des réactions géochimiques entre fluides de bassin et socle cristallin: application au site expérimental du programme européen de recherche en géothermie profonde (Soultz-sous-Forêts, Bas-Rhin, France)". PhD thesis, Université Louis Pasteur-Strasbourg I, France.

Jaime-Maldonado, J.G. and Sánchez-Velasco, R. (2003), "Acid stimulation of production wells in Las Tres Vírgenes Geothermal field, BCS, México". Geothermal Resources Council Transactions, Vol. 27, October 12-15, 2003.

Kohl, T. and Hopkirk, R. J. (1995), "FRACTURE" – A simulation code for forced fluid flow and transport in fractured, porous rock", Geothermics, 24, 333-343.

Malate, R.C.M., Yglopaz, D.M., Austria, J.J.C., Lacanilao, A.M., and Sarmiento, Z.F. (1997), "Acid stimulation of injection wells in the Leyte Geothermal power project, Philippines". Proceedings 22nd Workshop on Geothermal Reservoir Engineering, January 27-29, 1997.

Malate, R.C.M., Austria, J.J.C., Sarmiento, Z.F., DiLullo, G., Sookprasong, A. and Francia, E.S. (1998), "Matrix Stimulation Treatment of Geothermal Wells Using Sandstone Acid". Proceedings 23rd Workshop on Geothermal Reservoir Engineering, January 26-28, 1998.

Malate, R.C.M., Sookprasong, P.A., Austria, J.J.C., Sarmiento, Z.F. and Francia, E.S. (1999), "Wellbore Soaking: a Novel Acid Treatment of Geothermal Injection Wells". Proceedings 24th Workshop on Geothermal Reservoir Engineering, January 25-27, 1999.

Morris, C.W., Verity, R.V. and Dasie, W. (1984), "Chemical stimulation treatment of a well in the Beowawe Geothermal Field". Geothermal Resources Council, Transactions, pp. 269-274.

O'Sullivan, M. and McKibbin, R. (1993), "Geothermal reservoir engineering". Course notes, Institute of geothermal Engineering, University of Auckland, New Zealand.

Rabemanana, V., Durst, P., Bächler, D., Vuataz, F.-D., and Kohl, T. (2003), "Geochemical modelling of the Soultz-sous-Forêts Hot Fractured Rock system: comparison of two reservoirs at 3.8 and 5 km depth". Geothermics, 32(4-6), 645-653.

Wallroth, T., Eliasson, T. and Sundquist, U. (1999), "Hot Dry Rock research experiments at Fjällbacka, Sweden". Geothermics, 28(4), 617-625.

White, S.P. (1995), "Multiphase nonisothermal transport of systems of reacting chemicals". Water Resources Research, 31, 1761-1772.

Yglopaz, D.M., Buning, B.C., Malate, R.C.M., Sta Ana, F.X.M., Austria, J.J.C., Salera, J.R.M., Lacanilao, A.M. and Sarmiento, Z.F. (1998), "Proving the Mahanagdong B Resource: A Case of a Large-Scale Well Stimulation Strategy, Leyte Geothermal Power Project, Philippines". Proceedings 23rd Workshop on Geothermal Reservoir Engineering, January 26-28, 1998.

EC Contract SES6-CT-2003-502706

PARTICIPANT ORGANIZATION NAME: Centre of Hydrogeology, University of Neuchâtel, Switzerland

Synthetic 2nd year report

Related with Work Package 8 - Thermo-Hydro-Mechanical modelling of reservoir / heat exchanger

REVIEW OF CHEMICAL STIMULATION TECHNIQUES AND RESULTS OF ACID INJECTION EXPERIMENTS AT SOULTZ-SOUS-FORETS.

Sandrine Portier[1,2], Laurent André[3] and François-D. Vuataz[2]

[1] Centre of Hydrogeology – University of Neuchâtel, E.-Argand 11, CH-2007 Neuchâtel, Switzerland
[2] Centre of Geothermal Research – CHYN, University of Neuchâtel, E.-Argand 11, CH-2007 Neuchâtel, Switzerland
[3] BRGM - Service EAU/M2H - BP 6009 – 45060 Orléans cedex, France

e-mail: sandrine.portier@unine.ch l.andré@brgm.fr francois.vuataz@crege.ch

ABSTRACT

Acid treatments have been successfully applied in many cases to increase or to recover geothermal wells production rates to commercial levels. Chemical stimulation techniques were originally developed to address similar problems in oil and gas production wells. The applicability of these stimulation techniques to a hot and fractured reservoir is less well known. High temperatures increase the acid-rock reaction rate. The development of Enhanced Geothermal Systems (EGS) depends on the creation of permeable and connected fractures. Acid stimulation jobs intend to clean (pre-existing) fractures by dissolving filling materials (secondary minerals or drilling mud) and mobilizing them for an efficient removal by flow transport. Recent acid treatments were performed on the EGS wells at Soultz-sous-Forêts (France). This 200°C and 5-km deep granitic reservoir contains fractures partially filled with secondary carbonates (calcite and dolomite). In order to dissolve these carbonates and to enhance the productivity around the wells, each of the three boreholes (GPK2, 3 and 4) were successively treated with various amounts of hydrochloric acid. The FRACHEM code, a Thermo-Hydraulic-Chemical coupled code, has been developed especially to forecast the evolution of the Soultz reservoir. Reactive transport modelling with FRACHEM code has been used to simulate acid injection and its impact on brine-rock interactions. Comparisons between FRACHEM simulations and field observations have been tested to forecast the impact of acid treatments on reservoir properties. The main goal is to simulate the effect of acid injection on permeability evolution in fractures at pressure and temperature conditions of the Soultz geothermal site.

INTRODUCTION

The Enhanced Geothermal Systems (EGS) are dedicated to the exploitation of the heat present in low productivity reservoirs. A geothermal resource is quite different from an oil or gas reservoir or even a ground water reservoir. In an oil reservoir, once the oil has been extracted, the reservoir is exhausted. By contrast, in a geothermal reservoir the water or steam originally present in the reservoir can be replaced by surrounding cooler water or re-injected fluid that is heated by the reservoir rock, becoming again available for production (O'Sullivan and McKibbin, 1993). Despite all the differences between hydrocarbon and geothermal reservoir, the techniques used for extraction of fluids are similar; as are the exploration techniques and reservoir management approaches. Techniques comparable to those used in the oil industry are employed to drill and complete well in the productive reservoir. In both cases formation damage should be minimized in order to optimize well performance. A well may encounter multiple, widely spaced, fracture zones, resulting in flow rates that are too low. Stimulation techniques have the potential to remediate such causes for low flow-rate wells. Different techniques can be used to enhance the fracture network but the main ones are hydraulic fracturation and chemical treatment. The present paper will be focused on the chemical stimulation of geothermal wells. This technology, developed for more than one century by oil industry for the stimulation of oil and gas wells, is also used in geothermal wells. The second part of this paper is more focused on the case of Soultz-sous-Forêts. After a reminding of the different chemical treatments performed on the GPK4 well, numerical simulations using FRACHEM code have been carried out to estimate the impact of the acidizing treatments on carbonates and reservoir properties.

WELL STIMULATION TECHNIQUES

Resources exploitation of gas, oil and heat from deep reservoirs needs sometimes a permeability development around the production wells to ensure an efficient flow. The aim of this technology is to enhance the well productivity and to reduce the skin factor by removing near-wellbore damage and by dissolving scales in natural fractures. It consists to pump into the reservoir reactants such as strong acids (hydrochloric acid, HCl-HF mixture), organic acids (acetic acid, chloroacetic acid, formic acid, sulfamic acid) or chelatants (EDTA). These reactants can be pumped into the reservoir according to two procedures: below the fracturing flow rate and pressure of the reservoir (matrix acidizing) or above the fracturing flow rate and pressure (fracture acidizing). The main disadvantage of acid treatments is linked to the corrosion risk of the casing in particular with strong acids. Nevertheless, this risk can be reduced by addition of corrosion inhibitors or by using less-corrosive agents as chelatants, but their use increases the treatment cost.

Matrix acidizing

This process is performed below fracturing flow rate and pressure and is normally used for the removal of skin damage associated with work-over, well killing or injection fluids and also for to increasing formation permeability in undamaged wells.
The protocol of matrix acidizing has not really evolved since the beginning of the 1980's and is composed of three main steps: a preflush, with hydrochloric acid ; a mainflush with a hydrochloric – hydrofluoric acid mixture ; a postflush / overflush with soft HCl acid solutions or with KCl, NH_4Cl solutions and freshwater.
Treatment volumes, injection rates, acid placement techniques, acid system selection and evaluation of the results when stimulating geothermal wells, all follow the same criteria as for oil wells. The important difference is the formation temperature. High temperature reduces the efficiency of corrosion inhibitors (and increase their cost) as well as increasing the acid/rock reaction rate. The high acid rock reaction rate requires the use of a retarded acid system to ensure acid will not all be spent immediately next to the wellbore, but will penetrate deeper into the formation. Protecting the tubulars against corrosion is another serious challenge. This requires careful selection of acid fluids and inhibitors (Buijse et al., 2000), while cooling the well by injecting a large volume of water preflush may reduce the severity of the problem.

Chemical mechanisms involved in acidizing

The preflush, performed most often with a HCl solution, has to allow the displacement of the formation brine and the removing of calcium and carbonate materials in the formation. Acid reacts rapidly with carbonate rocks when it reaches the grain surface according to reactions:

$$CaCO_3 + HCl \rightarrow Ca^{2+} + Cl^- + HCO_3^-$$

$$CaMg(CO_3)_2 + 2\ HCl \rightarrow Ca^{2+} + Mg^{2+} + 2Cl^- + 2HCO_3^-$$

By dissolving calcite and dolomite, acid may create wormholes (Crowe et al., 1992) and new pathways. If the reaction rate is too quick, acid is immediately consumed in the vicinity of the fracture, forming wormholes but preventing the aperture of new pathways and connection to other fractures.
The role of the preflush, by dissolving carbonates, also prevents their contact and their reaction with HF injected with the mainflush and therefore minimizes the risk of precipitation of calcium fluoride CaF_2, highly insoluble in water:

$$CaCO_3 + 2\ HF \rightarrow CaF_2 + 2\ HCO_3^-$$

During the mainflush, the HF acid reacts mainly with the associated minerals of sandstones (clays, feldspars and micas), rather than with quartz. The reaction rates of HF with clays or feldspars are 100 to 200 times faster than the one with quartz. It results from these reactions an enlargement and interconnections of the pores in the matrix, facilitating fluid flow. The risk of using HF acid is the strong affinity of Si and Al with F, which can cause the precipitation of silicium or aluminum complexes (SiF_6^{2-}, AlF^{2+}, AlF_2^+, AlF_3, AlF_4^-), then damaging the formation by plugging. This is why HCl is added to HF: hydrochloric acid keeps a low pH and prevents the formation of fluorosilicates, fluoroaluminates, and fluoride salts.
For the preflush operation in acidizing treatments, a solution of hydrochloric acid at a concentration of 10 to 15 % is most often used. For the mainflush, the mud acids generally range from 10% HCl – 5% HF to 12% HCl – 3% HF. Acidification of geothermal wells is not as frequent as of oil and gas wells, but the operations are borrowed from this industry.
Concerning the injected amounts, in the majority of the cases, the preflush volume was based on a dosing rate of 600 litres per metre of target zone (Malate et al., 1997; Barrios et al., 2002). The cleaning out of the geothermal wells needs about 900 litres per metre of target payzone.
HCl and HF are two acids reacting quickly with carbonates and silicates. However, the objective of acid treatment is to increase porosity and permeability of the medium, deeply in the formation. Some retardants can be added to the mud acid to slow the reaction rate of acid with the minerals.
A key point is to inject a solution not containing HF explicitly but a compound able to generate HF at greater depth of penetration for a longer reaction time and a maximum dissolution of fines (Crowe et al., 1992). This retardant hydrolyzes in water when it enters in the reservoir to form HF according to the reaction:

$$HBF_4 + H_2O \rightarrow HBF_3OH + HF$$

Other retardant systems can be used as an emulsifier of the aqueous acid solutions in oil, the dissolving of the acids in a solvent (alcohol, gel…) or the injection of solutions of methyl acetate which hydrolyses slowly at very high temperatures to produce acetic acid.
Malate et al. (1998) also proposed an acid system applicable for moderate to deep penetrations. They used a phosphonic acid complex (HEDP) to hydrolyse NH_4HF_2 instead of HCl. HEDP has five hydrogens available that dissociate at different stochiometric conditions. Mixture of HEDP acid with NH_4HF_2 produces an ammonium phosphonate salt and HF.

Fracture acidizing

Also called acid fraccing, this technique is widely used for stimulating limestone and dolomite formations or formations presenting above 85 % acid solubility. It consists to inject first a viscous fluid at a rate higher than the reservoir matrix could accept leading to the cracking of the rock. Continued fluid injection increases the fracture's length and width and injected HCl acid reacts all along the fracture to create a flow channel that extends deep into the formation. The key to success is the penetration of reactive acid along the fracture. However, the treatment volumes for fracture acidizing are much larger than the matrix acidizing treatment, being as high as 12' 000 – 25' 000 l/m of open hole (Economides and Nolte, 1987).

Chelatants

Besides the traditional acids, the chelatants are solutions used as formation cleanup and for stimulating wells especially in formations that may be damaged by strong acids (Frenier et al., 2001). If these compounds are applied in gas and oil wells, this is not yet the case for the development of geothermal reservoirs. They act as a solvent, increasing the water-wetting operations and dissolving (entirely or partially) some minerals containing Fe, Ca, Mg and Al. The chelatants are mainly used in oil and gas wells and they present as advantage to have very low corrosion rates, much lower than the one observed with HCl solutions, in the same conditions. As a consequence, the use of chelatants needs small amounts of inhibitor to protect the casings. Among the chelatants, the most used are compounds of the EDTA family (EDTA: Ethylene-diaminetetraacetic acid; HEDTA: Hydroxyethylene-diaminetriacetic acid; HEIDA: Hydroxyethyliminodiacetic acid). The disadvantages of using chelatants are their high cost compared to acids and their impact on the environment.

CLEANING OF GEOTHERMAL WELLS

The cleaning out of geothermal wells to increase their productivity after scaling deposits constitutes the main application of the acid treatments. This technique has been used extensively in some geothermal fields in the Philippines (Buning et al, 1995; Buning et al, 1997; Malate et al., 1997; Yglopaz et al., 1998; Malate et al., 1999, Jaime-Maldonado and Sánchez-Velasco, 2003, Amistoso et al., 2005), in El Salvador (Barrios et al., 2002) and in USA (Morris et al., 1984, Entingh, 1999). It presents interesting results, such as the well injectivity increasing by 2 to 10-folds according to the studied reservoirs.

At the Larderello geothermal field (Italy), several stimulation methodologies have been used successfully by ENEL (Capetti, 2006). Among them, chemical stimulation operations were carried out by injection of acid mixtures. First, various laboratory tests were realised on reservoir rock samples to optimize the HCl/HF ratios and the effect on mineral dissolution. Field tests have shown impressive results on five deep wells for reservoir rocks composed of phyllites, hornfels and granites: the improvement of injectivity, respectively productivity ranged from a factor 4 to 10.

In the field of EGS, few chemical treatments have been applied to stimulate reservoirs. In 1976, at the Fenton Hill Hot Dry Rock site (USA), 190'000 l of 1 N carbonate sodium base solution was injected to dissolve quartz from the formation and to reduce the impedance of the existing system. About 1'000 kg of silica were dissolved and removed from the reservoir but without impedance reduction. In 1988, a matrix acidizing was performed on the Fjällbacka reservoir (Sweden): major and minor fractures of the granitic reservoir were filled with calcite, chlorite and clay minerals. About 2'000 l of HCl-HF acid were injected in Fjb3 to leach fracture filling. Returning rock particles showed some efficiency of this acid injection (Wallroth et al., 1999). Several wells at Coso field, affected by calcium carbonate scaling, were treated by acid methods. A total of 30 wells were treated with HCl and 24 gave successful results (Evanoff et al., 1995).

The case of the EGS reservoir at Soultz

The geothermal research program for the extraction of energy from a Hot Fractured Rock at the Soultz-sous-Forêts site began in 1987 (Hettkamp et al., 2004). The project aims to convert heat to electricity from a deep fractured and granitic reservoir. To extract the heat from the reservoir, three deviated wells have been drilled at a depth of 5'000 m and their bottoms are separated by 650 m. The fractured reservoir encountered at this depth presents a temperature of 200°C. One well (GPK3) is dedicated to injection of cold water in the granitic reservoir whereas the two others (GPK2 and GPK4), located on both sides of injector, are used to pump hot water.

Stimulation experiments and injection tests

Recently acid treatments were performed at Soultz-sous-Forêts (France). This deep granitic reservoir contains fractures partially filled with secondary carbonates (calcite and dolomite). In order to dissolve these carbonates and to enhance productivity around the wells, each of the three boreholes (GPK2, 3 and 4) were treated with different amounts of hydrochloric acid. If GPK2 and GPK3 have shown weak variations of their injectivity, GPK4 presented a real increase of its injectivity after the treatments.

GPK4 well

In February 2005, an acid injection was tested to improve the injectivity around GPK4 well. The experiment began on 22 February 2005 with an injectivity test of the well before soft acidification. It consisted of the injection of 4'500 m^3 of water at increasing flow rates (9 l/s, 18 l/s, 25 l/s) in 24-hour steps. The injection of water acidified by the addition of approximately 2 g/l of hydrochloric acid started on 2 March 2005 at a flow rate of 27 l/s. It lasted 2 days, followed by one day of injecting fresh water at much lower rates in decreasing steps. A total volume of 5'200 m^3 was injected; with a total weight of acid (HCl) of 11 tons. When the wellhead pressure was back to the value observed during the previous injectivity test, an identical test was repeated on 13 March 2003, that is injection of 4'500 m^3 of water in flow rate steps of 24 hours at 9 l/s, 18 l/s and 25 l/s.

In May 2006, new tests began with a test of the well injectivity before acidification. The acid treatment was performed in four stages :

- Injection of 2000 m^3 of cold water deoxygenized at 12 l/s, 22 l/s then finally at 28 l/s.
- A preflush of 25 m^3 HCl diluted at 15 % (3 tons) (with deoxygenized water) was pumped ahead of the HCl-HF acid mixture during 15 minutes at 22 l/s.
- A main flush consisted of the injection of 200 m^3 of Regular Mud Acid (RMA), (12 % hydrochloric (HCl)-3 % Hydrofluoric (HF) acid mixture treatment), with addition of a corrosion inhibitor, at a flow rate of 22 l/s during 2,5 hours.
- A postflush by injection of 2'000 m^3 cold water deoxygenized without inhibitor at a flow rate of 22 l/s then 28 l/s during 1 day.

When the wellhead pressure was back to a value identical to that observed in the previous injectivity test, a 3-day test identical to that of March 13, 2005 was repeated.

Results of acid stimulation treatments

Figure 1 shows the impact of the acidified water on the wellhead pressure during the first acid injection in GPK4 well. Despite the fact that the injection was performed in an over-pressurised reservoir, the injection pressure was decreasing during the last hours of the acidification test. Moreover, it is interesting to compare the data from two tests of water injection performed in the same conditions before (February 22, 2005) and after (March 13, 2005) the acid injection (Figure 1). Results (Gérard et al., 2005) show that after some 72 hours of water injection in the second test (24 hours at 9 l/s, 24 hours at 18l/s and 24 hours at 26 l/s), the GPK4 wellhead pressure was about 40 bars below the value observed in the same conditions before acidification. This represents a decrease of the apparent reservoir impedance seen from the wellhead by a factor ~1.5 (0.20 to 0.30 l/s/bar).

Figure 2 shows the impact of RMA acid job on the wellhead pressure by comparison before and after the second acid injection in GPK4 well. The repetition of the injectivity test showed that the difference in the over pressure values at the wellhead between the beginning of the test and the end were 16 bars. This represents a 35 % reduction of the wellhead pressure due to the acidification treatment. After some preliminary evaluation of downhole pressure changes, performed by Geowatt, this leads to a provisional estimate of GPK4 injectivity after chemical treatment of ~0.40 l/s/bar.

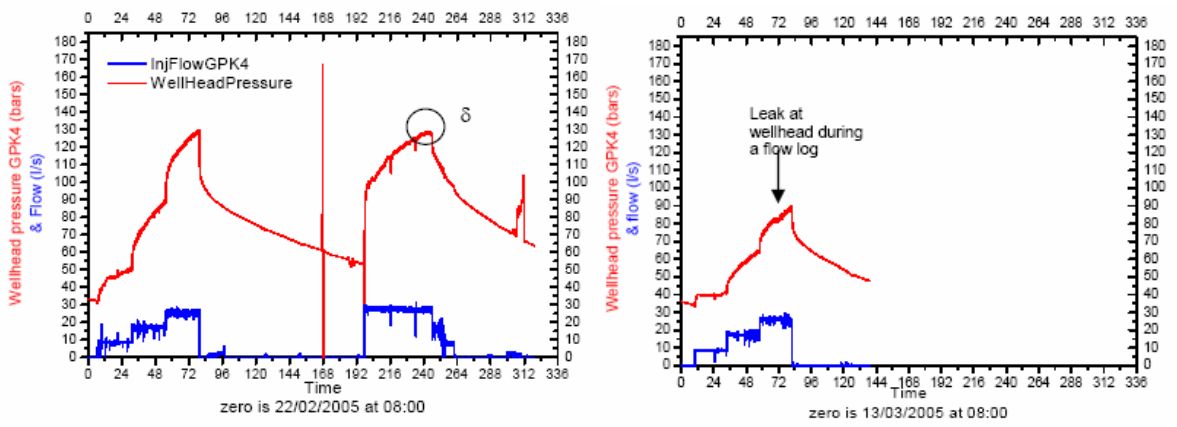

Figure 1: Impact of acidification test on GPK4; on the left, before and during acidification injection, on the right, after acidification (Gérard et al, 2005).

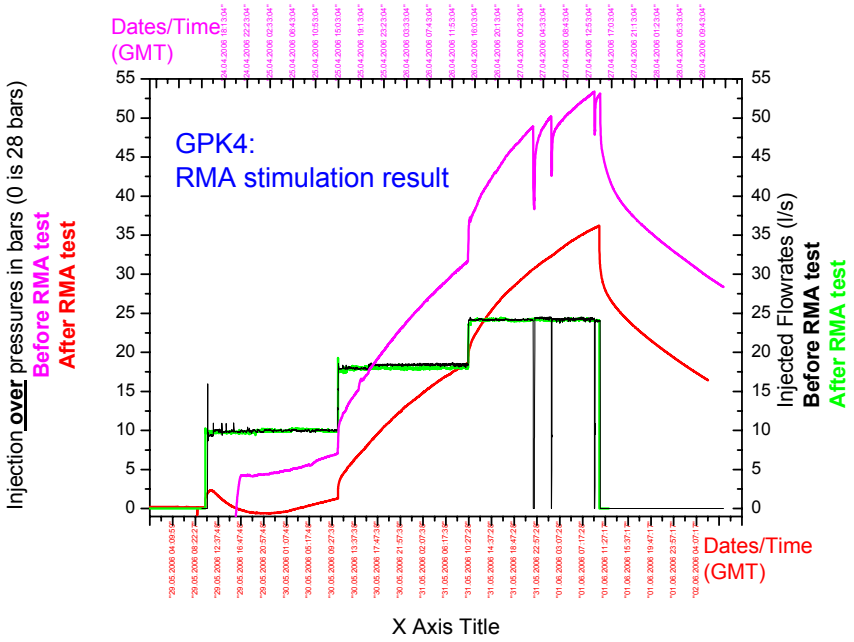

Figure 2: Impact of the RMA acidification test on the wellhead measured by comparison before and after the acidification test on GPK4 well (May 2006). (GEIE, 2006).

MODELLING OF THE ACIDIFICATION IMPACT ON THE SOULTZ RESERVOIR

The objective of the numerical simulation is to determine the impact of acid on the fracture minerals and on the reservoir properties.

Numerical modelling approach

To predict the impact of the acid treatment on the Soultz reservoir, the Thermo-Hydraulic and Chemical (THC) coupled code FRACHEM has been utilized. This THC code was built for the Soultz reservoir conditions. Instead of creating a totally new modelling programme, two existing codes, FRACTure and CHEMTOUGH2, have been combined in a new code called FRACHEM (Durst, 2002; Bächler, 2003; Rabemanana et al., 2003; André and Vuataz, 2005). FRACTure is a 3-D finite elements code and it determines thermal and hydraulic processes in fractured and porous rocks (Kohl and Hopkirk, 1995). CHEMTOUGH2 is a 3-D finite volumes code (White, 1995); it simulates the reactive transport and allows the variation of permeability according to chemical reactions occurring between fluid and rock of the reservoir. Considering the strong mineralization of brine and the high temperature of the reservoir, this last code has been modified by several implementations: thermodynamic model and computation of the activity coefficients of selected species in solution, kinetic model for dissolution and precipitation of minerals, as well as the relationship between porosity and permeability.
Knowing the high salinity of the brine of the Soultz system, The Pitzer formalism has been implemented in FRACHEM code to calculate the activity coefficients of selected chemical species; then, the precipitation/dissolution reactions of some minerals can be estimated. For the present time, the behaviour of eight minerals (calcite, dolomite, pyrite, quartz, amorphous silica, K-feldspars, albite and illite) is investigated. Detailed information on the determination of the reaction laws can be found in Durst (2002). At last, a supplementary module allows the determination of porosity and permeability variations linked with chemical processes occurring in the reservoir (André et al., 2005). The porosity variations are calculated and a combination of a fracture model and a grain model is used to determine the permeability evolution.

Simulation setup

Geometry

The same geometrical as that presented in previous papers has been considered (André and Vuataz, 2005). The present application of FRACHEM is the modelling of a 2-D simplified model with a geometry close to the Soultz system. Injection and production wells are linked by fractured zones and surrounded by the impermeable granite matrix. The model is composed of 1250 fractured zones. Each fractured zone has an aperture of 0.1 m, a depth of 10 m, a porosity of 10%, and contains 200 fractures. This model allows an effective open thickness of about 125 m, while the mean openhole section of each well is about 600 m. Initially the temperature was set to the reservoir temperature of 200°C and the fractured zone contains the formation fluid.
One of these fractured zones is modelled with the assumption that the fluid exchange with the surrounding low permeability matrix is insignificant. Due to the symmetrical shape of the model, only the upper part of the fractured zone is considered in the simulation. The area is discretized into 222 2D elements (Figure 3).

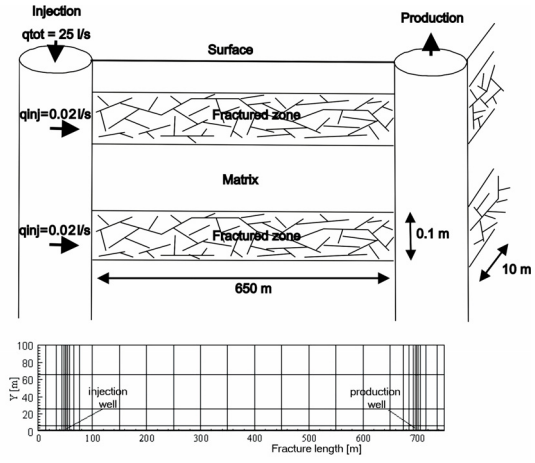

Figure 3: Simplified model and spatial discretization.

Considering a production rate of 25 l/s, the fluid was re-injected in each of the fractured zones at a rate of 2.10^{-2} l/s at a constant temperature of 65°C. During this simulation a constant overpressure of 8 MPa was assumed at the injection well and a hydrostatic pressure at the production well. Dirichlet boundary conditions were applied to the upper, left and right side of the model. The values of thermo-hydraulic parameters considered in the simulation are listed in Table 1.

Table 1: Thermo-hydraulic model parameters.

Parameters	Units	Fracture	Matrix	Fluid
Hydraulic conductivity	[m^2/Pa]	7.4 10^{-8}	10^{-15}	-
Thermal conductivity	[W/m.K]	2.9	3	0.6
Density	[kg/m^3]	-	2650	1000
Heat capacity	[J/kg.K]	-	1000	4200
Porosity	[%]	10	0	-

Rock composition

The mineralogical composition of Soultz granite given by Jacquot (2000) on GPK2 is assumed to be the same for the three wells (GPK2, GPK3 and GPK4) (Table 2). In the following simulations, the fluid is assumed to circulate within the hydrothermalised granite containing about 3.3 % of calcite and 0.8 % of dolomite.

Fluid compositions

The fluid present in the formation is a NaCl brine with a pH of 4.9, a total dissolved solids of about 100 g/l and a temperature at the beginning of the simulation of 200 °C. The main characteristics of this fluid are given in Table 3.
The HCl solutions used to acidize the circulation fluid are highly diluted solutions (a fresh water) acidified to 2 g/l and to 15 g/l with concentrated HCl. These solutions are injected in the fractured zone at a temperature of 65 °C.

Table 2: Mean composition (in volume percent) of the different facies of granite in the Soultz reservoir (Jacquot, 2000).

Minerals	Healthy granite	Hydrothermalised granite	Vein of alteration
Quartz	24.2	40.9	43.9
K-Feldspar	23.6	13.9	
Plagioclases	42.5		
Illite		24.6	40.2
Smectite		9.7	9.6
Micas	9.3		
Calcite	0.3	3.3	4.3
Dolomite		0.8	0.7
Pyrite		0.7	1.0
Galena		1.3	0.3
Chlorite		4.8	

Table 3: Characteristics of the fluids used for the numerical simulations

Fluid		HCl solutions	Formation brine
Temperature (°C)		65	200
pH		1.3 to 0.4	4.9
Concentration (mg/kg)	Na^+	26.40	26400
	K^+	2.90	2870
	Ca^{2+}	4.75	6160
	Mg^{2+}	0.10	112
	Fe^{2+}	0.13	134
	SiO_2	0.36	364
	Cl^-	1455	54205
	SO_4^{2-}	0.07	63
	HCO_3^-	0.09	58

Simulation results of acid injections

We have been studying the impact of acid treatments on the Soultz reservoir properties near the injection well. The FRACHEM simulator is used to inject the adequate volume of acid in the model. The solutions are expected to circulate in a fractured zone composed of hydrothermally altered granite and their behaviour with respect to the minerals present in this granite is observed. When the desired volume is reached, the injection is stopped and the return to chemical equilibrium of the injected fluid is modelled. In the reservoir, a total pressure of 500 bars is assumed and the CO_2 partial pressure is fixed to 5 bars.

Concerning the acid solution used in the simulations, it should be noted that, for the time being, the code is not able to make the difference between the type of injected acid. It means that FRACHEM does not make the difference between hydrochloric and hydrofluoric acids. In this condition, the injection of an acid solution and the acid concentration are fixed by the H^+ concentration and by the total volume injected. Concentrated solutions are characterised by low pH solutions.

At last, it should be noted that the code calculates phases equilibrium between fluid and rock without taking into account the specific reaction rate of acid on carbonates. We suppose here that the reaction between acid and carbonates is instantaneous which is not a real disadvantage considering the high reactivity of HCl with carbonates and in particular with calcite.

Soft acidification

The duration of the numerical simulation was determined in order to simulate the real amount of acid injected in GPK4 in February 2005. The interpretation presented here are given for HCl injection of 60 hours at a flow rate of 25 l/s and at a concentration of 2g/l, equivalent to the 11 tons of HCl injected in GPK4 in February 2005.

The action of acid on carbonates has been investigated. The figure 4 compares the influence of HCl injection on calcite and dolomite minerals with respect to the reinjection of the original brine. These results show that acid solution dissolves carbonates in the first metres of the fractured zone. Around GPK4 (60 hours injection), the injected amount of HCl affects the first 3.5 metres around the injection well (Figure 4). Due to the respective reaction rate of each mineral, it should be noted that dolomite has dissolution rates two orders of magnitude smaller than calcite (Figure 5). Consequently the impact of acid is still active farther in the fractured zone (Figure 4).

Comparatively to a normal brine injection, after 60 h, the acid injection involves an increase of dissolved calcite and dolomite.

HCl acidification has a weak impact on other minerals: it only decreases the precipitation rate of K-feldspar, albite, illite and amorphous silica. Finally, quartz is not affected by this type of acidification.

All these dissolution processes cause an increase of about 2.0 % of rock porosity in the short interval of 0.5 m around the injection well and 0.1 % in the interval 0.5-1.5 m. This estimation of the reservoir changes is linked to the choice of the porosity model used in FRACHEM, namely the double fracture and grain model.

In conclusion, we can suppose that the volume of injected acid in the first soft acidizing test on GPK4 had only an impact on the first 4 metres around the injection well. With these rather small acid amounts, the impact on the reservoir properties seems to be limited, although the porosity increases in the close vicinity of the wells due to carbonates dissolution.

Influence of injection flow

The chemical stimulation of an EGS reservoir is effective if the acid can reach fractures distant from the injection well. In order to simulate this process, the flow was doubled meaning that the acid solution, at a concentration of 2 g/l, was pumped at 50 l/s. In these conditions, the 11 tons of acid are injected in 30 hours, compared to the 60 hours of the previous simulation. We observed that a double flow allows a farther transport of acid within the fracture. Less calcite is dissolved near the well but the impact of acid is visible up to 7.5 metres. The same phenomenon applies to dolomite. Dissolution rate of this mineral is two orders of magnitude smaller than calcite. Consequently the impact of acid is still active beyond 15 metres along the fracture.

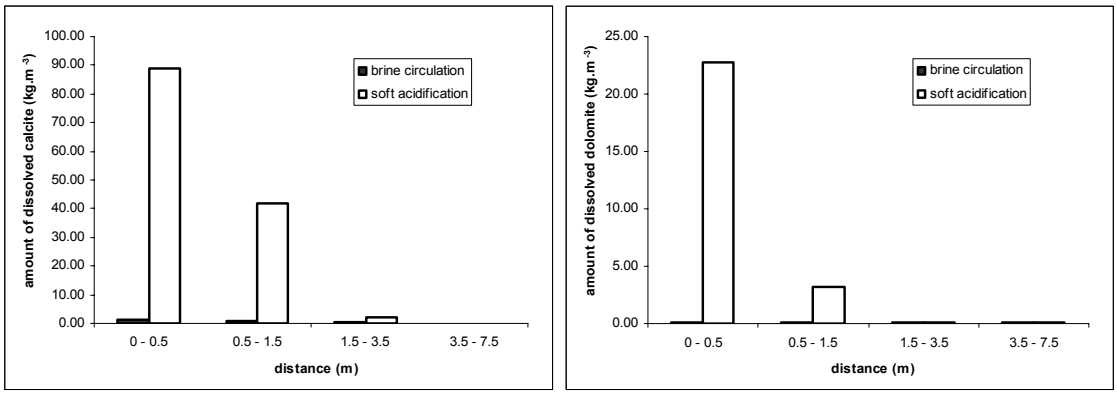

Figure 4: Amounts of dissolved calcite and dolomite at different distance from the injection well according to the type of injected fluid after 60 hours of injection.

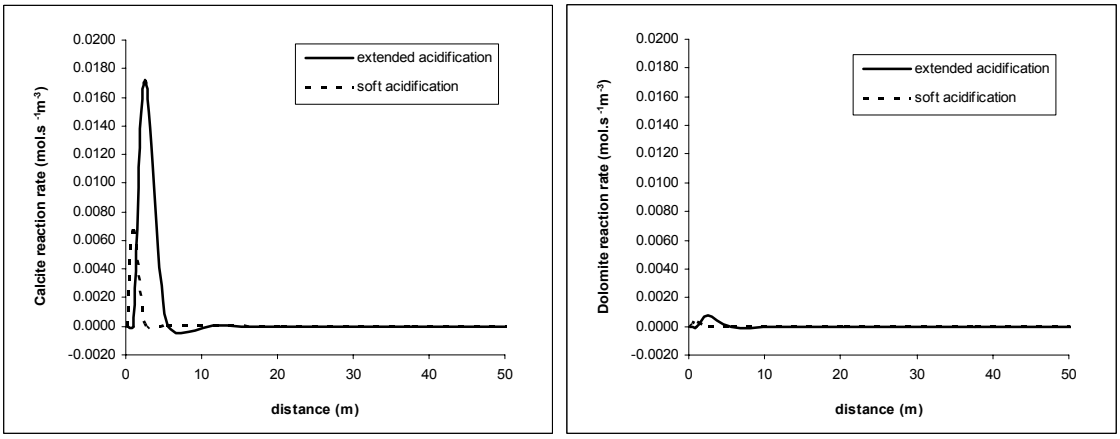

Figure 5: Variation of calcite and dolomite reaction rates after acid injection.

Extended acidification

In May 2006, GPK4 well was stimulated by injecting 98 tons of HCl during a period of 2.5 hours. This second acidizing treatment used hydrochloric acid at a concentration of 12 % and hydrofluoric acid at a concentration of 3 %. After this injection, the acid is displaced within the formation by injecting about 2'000 m^3 of fresh water. The results showed a decrease of the injection pressure in the vicinity of the injection well, as the calcite was dissolved and progressively carried away. The response of the model to the acid addition has been examined.

Influence of high acid concentration

Knowing that the code is not able to make the difference between the type of injected acid, a numerical simulation was carried out to investigate the impact of this acid injection at a concentration of 15 g/l. This simulation was performed with fresh water. Its pH was lowered to 0.4, whereas the injection rate within the fractured zone was maintained to 2.10^{-2} l/s. Therefore, the flow was fixed at 25 l/s and the duration of the injection was 70 hours. The total amount of injected acid is equal to 98 tons. The results indicate that calcite is as usual, the most affected mineral by the acid injection. Respectively to the extended acidification, the increase of acid concentration seems to augment the dissolution processes in the first 0.5 m around the injection well, and the impact of acid is also noticeable farther in the formation (Figure 6). The porosity increases mainly in the vicinity of the injection well of about 4.5 % (Figure 7) instead of the 2.0 % estimated with a soft acidification. This increase of porosity is expressed by an injectivity rise in the zones affected by acidizing treatment.

In conclusion, the extended acidification amplifies the amount of dissolved calcite of about 70 % around the injection well. We can also suppose that the volume of injected acid in the second test on GPK4 had an impact on the first 10 metres around the injection well. The simulation results were consistent with those of the experiment. The additional H^+ ions significantly modify the calcite reaction rate around the injection well. The additional acid reaction leads to significantly drop the pressure around the injection well (Figure 8). This brine acidification implies a decrease of about 4 bars near the injection well, corresponding to a reduction of about 5 % of the pressure in 70 hours. This result is linked to the enhanced dissolution of calcite within the fractured zone. As the reservoir permeability and porosity are controlled by the occurrence of mineral precipitation and dissolution, this stronger calcite dissolution implies an improvement of the reservoir properties, namely the hydraulic impedance of the injection well.

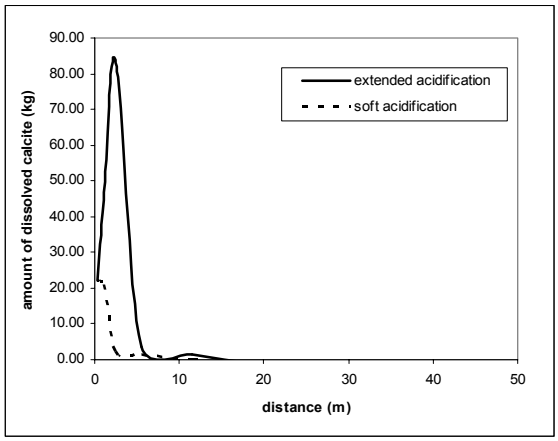

Figure 6: Amounts of dissolved calcite at different distance from the injection well according to the type of injected acidified fluid after acid injection.

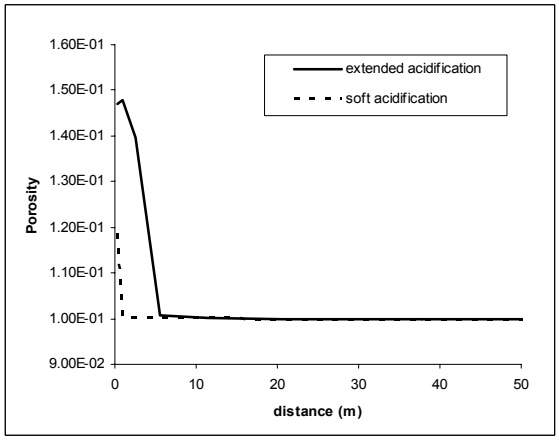

Figure 7: Porosity variation at different distance from the injection well after acid injection.

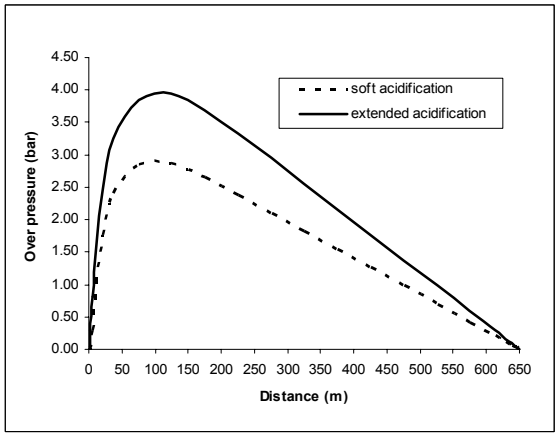

Figure 8: Variation of the pressure at different distance from the injection well after acid injection.

DISCUSSION

Some new results of acid injections simulations using FRACHEM code are presented here. Porosity evolution resulting of acid injection has been observed according to three main parameters:

- acid concentration, varying from 2 to 10 g/l of HCl.
- flow imposed to the system, ranging from 10 to 50 l/s.
- duration of acid injection / circulation fluid in the fractured zone, reaching 0.5 to 10 days.

For a limited acid injection (10 l/s at 2 g/l), acid effect on dissolved carbonates and on penetration within the reservoir is very restricted. At this flow, a real impact on reservoir properties is only obtained for extended injections of many days and for high acid concentrations. After an injection of 10 days of a solution at 10 g/l, all carbonates are dissolved in the first 0.5 metres around the injection well but only 65 % in the range 0.5 – 1.5 m. The relative weak effect of a small flow is shown here.

Nevertheless, for the other simulations at this flow, it seems that acid concentrations of about 7 to 10 g/l could have a positive impact up to 7.5 metres away from the injection well, and for a relatively limited injection time (5 days).

Injected acid reacts of course with carbonates (calcite and dolomite). According to mineralogical data, these compounds represent more or less 5 % of the hydrothermally altered granite. From this proportion and in case of a massive acid injection, all carbonates can be dissolved by acid solution leading to a porosity of about 0.15.

Obviously, the best results are obtained for long-term injections of high-concentration acid solutions. In these conditions, the impact radius can reach 15 metres around the injection well. Considering these conditions (for example 10 g/l and 50 l/s), it should be noted that the important amount of injected acid is able to dissolve carbonates (calcite + dolomite) up to 7 metres from the injection well, even for very limited injection times (2.5 days).

Finally, the increase of acid concentration involves an augmentation of dissolution processes but always in the first 5 metres around the injection well. Due to the high reactivity of HCl, the rock volume affected by acid is relatively small. An increase of the flow should allow a better dispersion of acid within the formation.

CONCLUSIONS

Recently, acid treatments have been successfully performed in geothermal granitic reservoirs such as at Soultz and encouraging results were obtained on GPK4 well.

Some numerical simulations using FRACHEM code were performed to better understand the acid behaviour within the reservoir. Considering the geometrical model used for the simulations and the different assumptions about the fluid and rock compositions, some estimations have been proposed.

The simulations results indicate that the carbonates are the most dissolved minerals by hydrochloric acid.

For GPK4 well, first acid injection lasted 3 days at a concentration of 2 g/l (more or less 11 tons of acid injected in the reservoir). According to the simulations of this test, the amount of acid is just sufficient to dissolve half of the carbonates initially present in the range 0 – 0.5 metres. Farther in the fracture, the impact is quasi nil.

Simulations of extended acid injection performed in May 2006 (more or less 98 tons of acid injected in the reservoir) seem to show a significant dissolution of carbonates around the injection well. The increase of acid concentration augments the reactivity in the vicinity of the injection well and enhances the porosity.

Nevertheless, the high reactivity and a weak flow prevent the penetration of acid in the far field between the wells. This high reactivity also involves the risk of creating wormholes,

able to increase the porosity but not always the permeability of the fractured medium.
Finally, we have demonstrated that acid injection can play a significant role in the development of porosity around injection wells. It was shown that acid has the possibility to react with carbonates, dissolving them and opening new pores within the reservoir. The positive effect of acid injection on porosity is proportional to the amount of injected acid.
Looking for commercial production rates of the wells, other chemical stimulation techniques should be considered such as fracture acidizing. This type of acid job should reach the fracture network of the far field and connect the injection and production wells.

Acknowledgements

The authors thank the State Secretariat for Education and Research and the Swiss Federal Office of Energy for funding this project (OFES-N° 03.04.60). The authors are also grateful to André Gérard of the GEIE at Soultz and Thomas Kohl of GEOWATT AG (Zürich).

REFERENCES

André L., Vuataz F.-D., 2005. Simulated evolution of reservoir properties for the Enhanced Geothermal System at Soultz-sous-Forêts: the role of hot brine-rock interactions. Proceedings 30th Workshop on Geothermal Reservoir Engineering, January 31- February 2, 2005, Stanford University, Stanford, California.

André L., Vuataz F.-D., 2005. Simulated evolution of reservoir properties for the Enhanced Geothermal System at Soultz-sous-Forêts: the role of hot brine-rock interactions. Submitted to Geothermics, December 2005, in press.

André L., Rabemanana V. and Vuataz F.-D. (2005). Geochemical modelling of water-rock interactions and implications on the properties of the Soultz fractured reservoir. Proceedings EHDRA Scientific Conference, March 17-18, 2005, Soultz-sous-Forêts, France

Amistoso, A.E., Aqui, A.R., Yglopaz, D.M. and Malate, R.C.M. (2005). Sustaining steam supply in Palinpinon 1 production field, Southern Negros Geothermal Project, Philippines, World Geothermal Congress, Antalya, Turkey, 24-29 April, 2005.

Bächler, D. (2003), "Coupled Thermal-Hydraulic-Chemical Modelling at the Soultz-sous-Forêts HDR reservoir (France)", PhD Thesis, ETH-Zürich, Switzerland, 150 p.

Barrelli, A., Cappetti, G., Manetti, G. and Peano, A. (1985). Well stimulation in Latera Field, Geothermal resources Council Transactions, Vol. 9- Part II, pp. 213-219.

Barrios, L.A., Quijano, J.E., Romero, R.E., Mayorga, H., Castro, M. and Caldera, J. (2002). Enhanced permeability by chemical stimulation at the Berlin Geothermal Field, El Salvador. Geothermal Resources Council Transactions, Vol. 26, September 22-25, 2002.

Buijse, M., Maier, R. and Casero, A. (2000). Succesful high pressure, high temperature acidising with in situ crosslinked acid diversion. SPE paper 58804.

Buning, B.C., Malate, R.C.M., Lacanilao, A.M., Sta Ana, F.X.M. and Sarmiento, Z.F. (1995). Recent experiments in acid stimulation technology by PNOC-Energy development corporation, Philippines. Proceedings World Geothermal Congress, Vol. 3, p. 1807-1812.

Buning, B.C., Malate, R.C.M., Austria, J.J.C., Noriega, M.T. and Sarmiento, Z.F. (1997). Casing perforation and acid treatment of well SK-2D Mindanao 1 Geothermal project, Philippines. Proceedings 22nd Workshop on Geothermal Reservoir Engineering, January 27-29, 1997.

Capetti G., 2006. How EGS is investigated in the case of the Larderello geothermal field ? Engine Launching Conferente, Orleans 12-15 February 2006, unpubl. presentation.

Crowe, C., Masmonteil, J. and Thomas, R. (1992). Trends in Matrix Acidizing. Oilfield Review, October 1992, pp. 24-40.

Durst, P. (2002), "Geochemical modelling of the Soultz-sous-Forêts Hot dry Rock test site: Coupling fluid-rock interactions to heat and fluid transport", PhD thesis, University of Neuchâtel, Switzerland, 127p.

Economides, M. and Nolte, K. (1987). Reservoir stimulation. Schlumberger Educational Services.

Entingh, D.J. (1999). A review of geothermal well stimulation experiments in the United States,. Geothermal Resources Council Transactions, October 17-20, 1999, vol. 23, pp. 175-180.

Evanoff, J., Yeager, V. and Spielman, P. (1995). Stimulation and damage removal of calcium carbonate scaling in geothermal wells: a case study, World Geothermal Congress, Florence, Italy, pp. 2481-2485.

Frenier, W.W., Fredd, C.N. and Chang, F. (2001). Hydroxyaminocarboxylic Acids produce superior formulations for matrix stimulation of carbonates at high temperatures, SPE 71696.

GEIE. (2006). Results of GPK4 RMA stimulation of May 2006, unpublished data.

Gérard, A., Fritz. B. and Vuataz, F.-D. (2005). Results of soft acid injection tests performed at Soultz in wells GPK2, GPK3 and GPK4 – Extended summary: revised status on 14 March 2005- Proceedings EHDRA Scientific Conference, March 17-18, 2005, Soultz-sous-Forêts, France.

Hettkamp, T., Baumgärtner, J., Baria, R., Gérard, A., Gandy, T., Michelet, S. and Teza, D. (2004), Electricity production from hot rocks, Proceedings, 29th Workshop on Geothermal Reservoir Engineering, Stanford University, Stanford, California, January 26-28, 2004, 184-193.

Jacquot, E. (2000). Modélisation thermodynamique et cinétique des réactions géochimiques entre fluides de bassin et socle cristallin: application au site expérimental du programme européen de recherche en géothermie profonde (Soultz-sous-Forêts, Bas-Rhin, France), PhD thesis, Université Louis Pasteur-Strasbourg I, France.

Jaime-Maldonado, J.G. and Sánchez-Velasco, R. (2003). Acid stimulation of production wells in Las Tres Vírgenes Geothermal field, BCS, México. Geothermal Resources Council Transactions, Vol. 27, October 12-15, 2003.

Kohl, T. and Hopkirk, R. J. (1995), ""FRACTURE" – A simulation code for forced fluid flow and transport in fractured, porous rock", Geothermics, 24, 333-343.

Malate, R.C.M., Yglopaz, D.M., Austria, J.J.C., Lacanilao, A.M., and Sarmiento, Z.F. (1997). Acid stimulation of injection wells in the Leyte Geothermal power project, Philippines. Proceedings 22nd Workshop on Geothermal Reservoir Engineering, January 27-29, 1997.

Malate, R.C.M., Austria, J.J.C., Sarmiento, Z.F., DiLullo, G., Sookprasong, A. and Francia, E.S. (1998). Matrix Stimulation Treatment of Geothermal Wells Using Sandstone Acid. Proceedings 23rd Workshop on Geothermal Reservoir Engineering, January 26-28, 1998.

Malate, R.C.M., Sookprasong, P.A., Austria, J.J.C., Sarmiento, Z.F. and Francia, E.S. (1999). Wellbore Soaking: a Novel Acid Treatment of Geothermal Injection Wells, Proceedings 24th Workshop on Geothermal Reservoir Engineering, January 25-27, 1999.

Morris, C.W., Verity, R.V. and Dasie, W. (1984). Chemical stimulation treatment of a well in the Beowawe Geothermal Field, Geothermal Resources Council, Transactions, pp. 269-274.

O'Sullivan, M. and McKibbin, R. (1993). Geothermal reservoir engineering, Course notes, Institute of geothermal Engineering, University of Auckland, New Zealand.

Rabemanana, V., Durst, P., Bächler, D., Vuataz, F.-D., and Kohl, T. (2003), "Geochemical modelling of the Soultz-sous-Forêts Hot Fractured Rock system: comparison of two reservoirs at 3.8 and 5 km depth", Geothermics, 32(4-6), 645-653.

Wallroth, T., Eliasson, T. and Sundquist, U. (1999). Hot Dry Rock research experiments at Fjällbacka, Sweden. Geothermics, 28(4), 617-625.

White, S.P. (1995), "Multiphase nonisothermal transport of systems of reacting chemicals", Water Resources Research, 31, 1761-1772.

Yglopaz, D.M., Buning, B.C., Malate, R.C.M., Sta Ana, F.X.M., Austria, J.J.C., Salera, J.R.M., Lacanilao, A.M. and Sarmiento, Z.F. (1998). Proving the Mahanagdong B Resource: A Case of a Large-Scale Well Stimulation Strategy, Leyte Geothermal Power Project, Philippines. Proceedings 23rd Workshop on Geothermal Reservoir Engineering, January 26-28, 1998.

Proceedings World Geothermal Congress 2005
Antalya, Turkey, 24-29 April 2005

Simulation of Mineral Precipitation and Dissolution in the 5-km Deep Enhanced Geothermal Reservoir at Soultz-sous-Forêts, France

Vero Rabemanana[1], François-D. Vuataz[1], Thomas Kohl[2] and Laurent André[1]

[1] Centre of Hydrogeology, University of Neuchâtel, Emile Argand, 11 – CH-2007 Neuchâtel, Switzerland

[2] GEOWATT AG, Dohlenweg 28, CH-8050 Zürich, Switzerland

E-mails: Vero.Rabemanana@unine.ch, Francois.Vuataz@unine.ch, Kohl@geowatt.ch, Laurent.Andre@unine.ch

Keywords: brine, enhanced geothermal system, EGS, thermo-hydraulic-chemical modelling, Soultz-sous-Forêts.

ABSTRACT

The long-term behaviour of the Soultz-sous-Forêts enhanced geothermal reservoir has been investigated. Major processes susceptible to modify the properties of the reservoir were taken into account. Heat, fluid transport and geochemical reactions are coupled for modelling the reactive flow. As the fluid is a hot brine, a new code was built to simulate the Thermo-Hydraulic and Chemical effects (THC) within the fractures connecting the injection and production wells. The results revealed that re-injection of the formation brine after cooling changes the chemical equilibrium states between the formation fluid and different minerals present in the host rock. Due to their fast reaction rates, carbonate minerals are responsible for most of the reservoir evolution. Amounts of quartz and pyrite deposited are negligible during the period of simulation. In order to improve the hydraulic performance of the reservoir, the effects of acid addition and temporary reverse circulation of fluid were also investigated.

1. INTRODUCTION

In order to forecast the long term behaviour of an enhanced geothermal reservoir under exploitation, interaction between flow, heat transfer, transport and chemical reactions must be considered. This study aims to the coupled modelling of these processes applied to the Soultz-sous-Forêts enhanced geothermal system (EGS), located in Alsace, about 50 km north of Strasbourg (France). The Soultz area was selected as the European EGS pilot site because of its strong temperature gradient in the sedimentary cover (up to 100°C km^{-1}) and its high heat flow reaching locally 0.15 W m^{-2} (Kohl and Rybach, 2001).

The project has started in 1987 with the final goal to produce electricity by conversion of heat extracted from a fractured reservoir. The geology of the Soultz region is characterized by a graben structure affected by several N-S striking faults. The crystalline basement is composed of granitic rocks covered by 1400 m of Triassic and Tertiary sediments. Three facies of the granitic host rock are identified: unaltered granite in which fracturation density is close to zero, hydrothermally altered granite facies and veins of alteration (Jacquot, 2000). Hydrothermally altered granite facies is the most porous one (Genter et al., 1997) and veins of alteration are highly fractured. Circulation of fluid takes place mainly within these two last facies, but only the hydrothermalized facies plays the major role in the fluid-rock interaction processes.

The planned arrangement of boreholes is 3-well system with one well for cooled water re-injection, and two wells, on both sides of injector, are used for hot water production. The bottom of each well is separated by around 650 m from the other ones. Cooled water will be reinjected in the system at a rate of about 100 l s^{-1}. Currently, the three deep boreholes GPK2, GPK3 and GPK4 were drilled at a depth of 5000 m. A temperature of 200°C was measured at the bottom hole. GPK3 should be the injection well, while GPK2 and GPK4 will serve as the production wells. At Soultz, the injection – production system is a closed loop. The fluid used is the formation fluid existing in the granite, namely a brine with a total dissolved solids of 100 g kg^{-1}. The re-injection of the cooled brine disturbs the equilibrium between fluid and reactive minerals. Temperature and pressure in the reservoir will also be changed. In a previous study, a first modelling of deep reservoir at Soultz was presented (Rabemanana et al., 2003).

In the present paper, influence of water-rock interaction on the fluid flow and the reservoir properties is investigated for a longer simulation period.

2. NUMERICAL MODELLING

To predict the long term behaviour of an enhanced geothermal reservoir, it is necessary to understand the chemical phenomena occurring during exploitation. However, the chemical behaviour of a hot brine system is very complex, depending on the fluid composition, the temperature and the pressure. For the case of the formation fluid at Soultz, application of Debye-Hückel theory is not accurate, and existing geochemical codes are not adapted to its temperature. A new numerical simulation model called FRACHEM (Durst, 2002; Bächler, 2003) based on the Pitzer formalism to calculate aqueous speciation has been developed. It is a combination of two existent codes FRACTure (Kohl et al., 1995) and CHEM-TOUGH2 (White, 1995). FRACTure calculates the thermal and hydraulic processes whereas CHEM-TOUGH2 simulates the reactive transport. Some modifications have been implemented to the geochemical module of CHEM-TOUGH2. These modifications consist of the calculation of the activity of the aqueous species, the kinetic laws, the permeability and porosity changes as well as the re-injection process.

2.1 Thermodynamic model

The original CHEM-TOUGH2 code uses Debye-Hückel model for the calculation of the activity coefficient. Taking into account the high salinity of Soultz fluid, Pitzer formalism was implemented in the geochemical module of CHEM-TOUGH2. According to some assumptions about the Soultz fluid, such as no boiling, no degassing, no condensation, no mixing with a different fluid and conservation of major species such as chloride, the activity a_i of each aqueous species is assumed to be only function of the temperature T (°C) and the molality m_i (mol kg^{-1}) (Durst, 2002).

$$a_i = \gamma_i(T) * m_i \quad (1)$$

$$\gamma_i = B_0 + B_1 T + B_2 T^2 + B_3 T^3 + B_4 T^4 \quad (2)$$

where B_i are the coefficients of the activity coefficient of the specie i (γ_i).

2.2 Kinetic model

For the kinetic model, a simplified model based on one kinetic law accounting, the temperature, the reaction surface and the distance from equilibrium is proposed to describe each dissolution and precipitation reaction for each mineral.

$$v = k_m(T).s_m.\left(1 - \left(\frac{Q_m}{K_m}\right)^{\mu}\right)^n \quad (3)$$

where m is the mineral index, s_m (m^2) is the surface area, k_m (mol s^{-1} m^{-2}) is the rate constant, K_m is the equilibrium constant, Q_m is the ionic activity product and the exponents μ and n are positive empirical factors. Positive values of the reaction rate v (mol s^{-1}) indicate dissolution and negative values precipitation.

The kinetic laws of the Soultz system are derived from published experiments conducted in NaCl brines. Detailed information on the determination of the reaction laws can be found in Durst (2002).

2.3 Permeability and porosity relationships

As the circulation at Soultz mainly occurs in clusters of fractures and in highly altered granite, two porosity and permeability relationships were considered. The first one is a simple cubic Kozeny - Carman grain model based on spheres that relates the permeability k (m^2) to the porosity ϕ by:

$$k = \frac{R_0^2}{45} * \left[\frac{\phi^3}{(1-\phi)^2}\right] \quad (4)$$

where R_0 (m) is the initial spherical close-pack radius.

The second one is the porosity-permeability model for fractured rock after Norton and Knapp (1977). In this model, the permeability for a single set of parallel fracture is given by:

$$k = \frac{\phi * \delta^2}{12} \quad (5)$$

where δ (m) is the fracture aperture and ϕ is the fracture porosity.

This last relation assumes that reactions occur exclusively along the fracture walls and do not within the matrix around the fractures.

2.4 Re-injection process

The last modification implemented in CHEM-TOUGH2 consists of the modelling of the re-injection process. The original version of CHEM-TOUGH2 did not adjust automatically the concentration changes of the injected fluid. This was manually made after each time step. In the modified version, the re-injection of the cooled produced fluid is now possible. The concentration of each species in the volume element where the re-injection takes place is determined in function of the mass of the fluid injected and of the concentration in the production volume element.

3. APPLICATION OF FRACHEM

3.1 Model set up

The present application of FRACHEM is the modelling of a 2D simplified model with a geometry close to the real Soultz system. The injection and the production wells are linked by fractured zones and surrounded by the granite matrix. The model is composed of 125 fractured zones. Each fractured zone has an aperture of 0.1 m, a depth of 200 m, a porosity of 10%, and contains 100 fractures. Initially the temperature was set to the reservoir temperature of 200°C. One of these fractured zones is modelled with the assumption that the fluid exchange with the surrounding low permeability matrix is insignificant. Due to the symmetrical shape of the model, only the upper part of the fractured zone is considered in the simulation. The area is discretized into 222 2D elements (Figure 1).

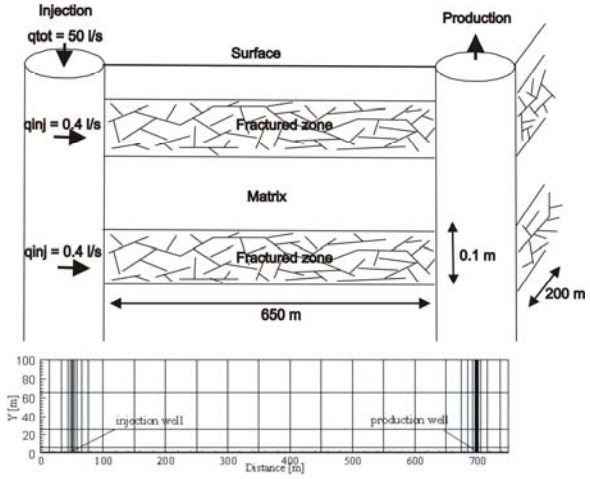

Figure 1: Simplified model and spatial discretization

The size of the elements ranges from a minimum of 0.5 m x 0.5 m near the injection and the production wells to a maximum of 50 m x 35 m. Considering a production rate of 50 l s^{-1}, the fluid was re-injected in each of the fractured zones at a rate of 4 x 10^{-1} l s^{-1} and at a constant temperature of 65°C. In this simulation a constant overpressure of 8 MPa was assumed at the injection well and a hydrostatic pressure at the production well. Dirchlet boundary conditions were applied to the upper, left and right side of the model. Due to the sensitivity of the sequential non iterative approach (SNIA) method on the time discretization, the time step used for this simulation is limited to 10^2 s, meaning that long-term simulations take several days of computer time. The values of thermo-hydraulic parameters considered in the simulation are listed for the Table 1.

Table 1: Thermo-hydraulic model parameters

Parameters			Fracture	Matrix	Fluid
Hydraulic conductivity	K	[m^2/Pa]	7.4 10^{-8}	10^{-15}	-
Thermal conductivity	λ	[W/m.K]	2.9	3	0.6
Density	ρ	[kg/m^3]	-	2650	1000
Heat capacity	C_p	[J/kg.K]	-	1000	4200
Porosity	Φ	[%]	10	0	-

Table 2 contains the mean composition of the fluid which is derived from the chemistry of the fluid produced during the production test in 1999. The fluid has a pH of 4.9 and a temperature of 200°C. This composition was recalculated assuming an equilibrium between the fluid and the mineral assemblage of the fracture. Initial mineral abundances are based on the synthetically identification of host rock facies (Jacquot, 2000).

Table 2: Mean fluid composition of the 5-km reservoir

Species	Concentration [mmol kg^{-1}]
Na^+	1079
K^+	68.5
Ca^{2+}	157
Mg^{2+}	3
Cl^-	1452
S	1.6
C	19
Fe^{2+}	2.4
SiO_2	5.7

3.2 Results

3.2.1 Temperature distribution

At first, the reservoir fluid is considered to be in thermal equilibrium at 200°C with the host granite. Re-injection of fluid at 65°C will disturb this equilibrium and will cause mineral dissolution and precipitation. The temperature distribution after 5 years of exploitation is illustrated. For clarity, Figure 2 shows only the half model extension in Y direction. Around the injection well, a thermal front is progressively developed. The temperature decreases due to the thermal diffusion. The front has reached the production well after a simulation period of 5 years and a temperature decrease of 15°C is observed at the production well.

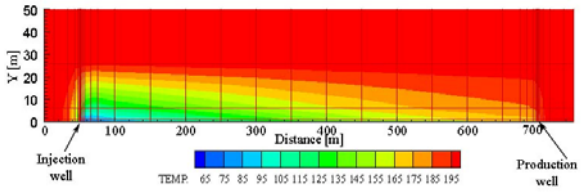

Figure 2: Temperature distribution after 5 years of circulation

3.2.2 Simulation of fluid-rock interaction

Evolution of the fluid-rock interaction is investigated by studying the reaction rate of minerals. For this simulation, only calcite, quartz, dolomite and pyrite have been considered. Other minerals are assumed to be non-reactive because of the lack of their Pitzer coefficients. Figure 3 illustrates the calcite reaction rate. During the first year of simulation, calcite dissolution occurs exclusively in a 300 m wide zone near the injection well. This dissolution process leads to an enrichment of the Ca^{2+} content in the fluid. With the increase of the temperature, calcite starts to precipitate towards the production well. A maximun precipitation rate of 1.59 x 10^{-4} mol s^{-1} m^{-3} is reached after 3 months of circulation. With increasing the simulation time, the dissolution zone extends towards the production well and the dissolution reaction rate decreases near the equilibrium state.

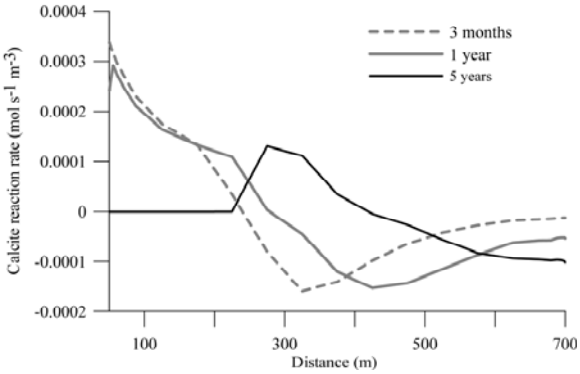

Figure 3: Evolution of calcite reaction rate

Compared to calcite, the behaviour of dolomite is slightly different and the reaction rate is much lower. Over the simulation period, no precipitation of dolomite is observed (Figure 4). Dolomite dissolves all along the fracture zone. After one year of circulation, the dissolution rate reaches 1.60 x 10^{-5} mol s^{-1} m^{-3} and then decreases during all the simulation.

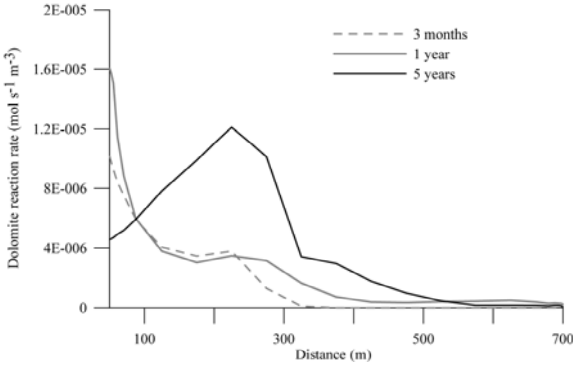

Figure 4: Evolution of dolomite reaction rate

Figures 5 and 6 show that during all simulation period, quartz and pyrite do not dissolve along the fracture zone. Compared to those of carbonates, their reaction rates are much lower. The maximum quartz precipitation rate is observed towards the production well but with increasing of simulation time, this tends towards zero, which is the rate at thermodynamic equilibrium.

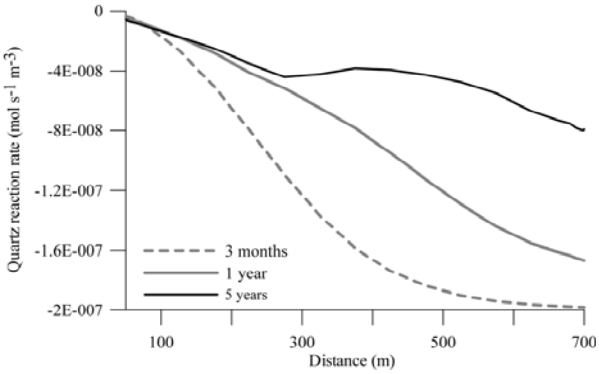

Figure 5: Evolution of quartz reaction rate

Among the minerals taken into account for this simulation, pyrite has the lowest magnitude rate, which can be considered as negligible. A maximum precipitation rate of 3.05 x 10^{-17} mol s^{-1} m^{-3} is observed and remains constant during all the simulation period. However, with increasing

time, the zone maximum of precipitation moves towards the production well.

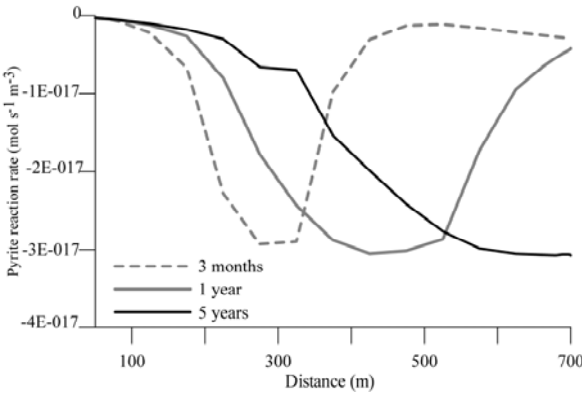

Figure 6: Evolution of pyrite reaction rate

3.2.3 Forecast of secondary mineral transfer

Knowing the reaction rate of each mineral, the amount of dissolved and precipitated minerals per element at the time t was calculated from the following expression:

$$m_{i,E} = mw_i * v_E * \phi_E * \sum_{j=t_0}^{t} (r_{i,j} * \Delta t) \quad (6)$$

$m_{i,E}$ (kg): the amount of mineral i within element E
mw (kg mol^{-1}): the molecular weight of the mineral
v_E(m^{-3}): the volume of element, ϕ_E is the porosity
$r_{i,j}$ (mol s^{-1} m^{-3}): the reaction rate of the mineral i
Δt (s): the time interval.

Table 3 gives the amounts of precipitated and dissolved mineral after 5 years of exploitation. As the calcite reaction is very fast, a significant amount of calcite dissolved and precipitated all along the fractured zone. Due to the retrograde solubility of calcite, amounts of dissolved calcite are most pronounced around the injection well. Quartz and pyrite precipitate in very small quantities.

Table 3: Amounts of precipitated and dissolved minerals within the simulated fractured zone after 5 years of circulation

Mineral	Dissolved amount (kg)	Precipitated amount (kg)
Calcite	2’740	1’330
Dolomite	510	0
Quartz	0	1.74
Pyrite	0	0.74

3.2.4 Changes of permeability and porosity

One of key questions in reservoir exploitation is how do the reservoir properties evolve with time? In this section, the evolution of the porosity and the permeability is coupled to the reactions taking place along the fractured zone. According to the amount of precipitated and dissolved calcite, porosity and permeability of the reservoir are changing (Figure 7). Occurrence of calcite precipitation results in a decrease of fracture void volume by 40%.The corresponding permeability decrease towards the production well. In contrast, due to the mineral dissolution, an increase of porosity and permeability are observed along the first 350 m from the injection well.

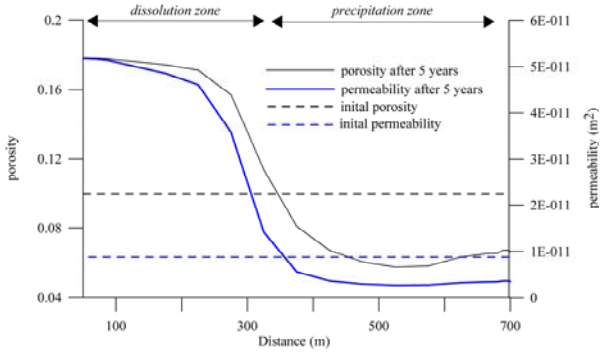

Figure 7: Evolution of porosity and permeability after 5 years of exploitation

3.2.5 Simulation of acid injection

The porosity and permeability are expected to evolve with time during exploitation. A decrease of these parameters values is the result of calcite precipitation and may alter the performance of the fluid circulation after a long-term exploitation. In this simulation, the effect of acid (HCl) injection is examined in order to reduce calcite deposit. To this end, the pH of the brine is changed to 3.7. Figure 8 compares the amount of dissolved calcite near the injection well and all along the fractured zone obtained with the original brine and acidified brine. The result shows that the additional H^+ ions significantly increased the amount of dissolved calcite. As the permeability and porosity of reservoir are controlled by the occurrence of mineral precipitation and dissolution, this increase of dissolved calcite mirrors an improvement of the reservoir properties.

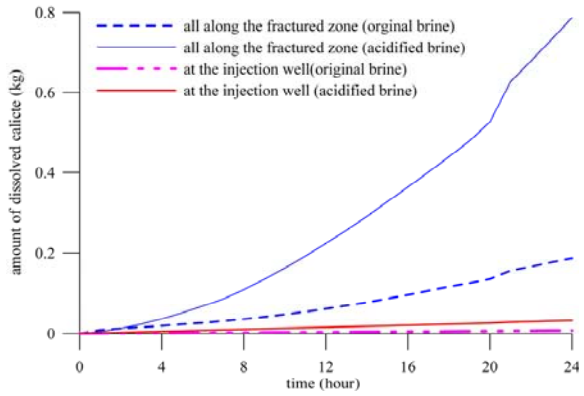

Figure 8: Evolution of amount of dissolved calcite after acid addition

3.2.6 Effect of a temporary reverse circulation

Another scenario has been tested with a temporary reverse fluid circulation after a given period of exploitation. The simulation of fluid-rock interaction showed that calcite is more soluble around the injection well and that an increase of temperature favours calcite deposits. In order to improve porosity and permeability around the production well, the fluid circulation has been reversed during one month after one year of exploitation. This means the production well is used for injection and vice versa during this period. The fluid chemistry and mineral components are updated and the boundary conditions are inverted to this configuration. Figure 9 shows a comparison of the porosity simulation with and without reverse circulation after 2 years of exploitation.

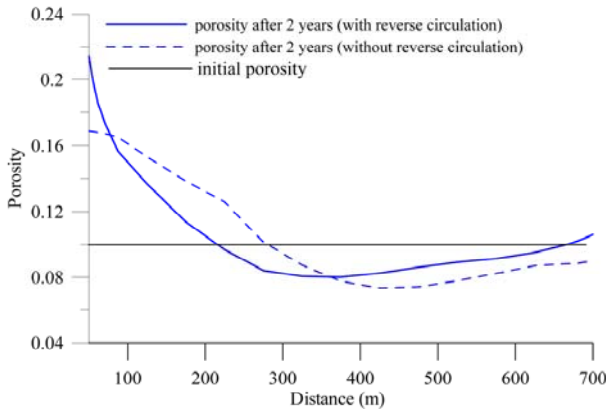

Figure 9: Evolution of the porosity by temporary reversing the fluid circulation

The porosity evolution is different for these two scenarios of exploitation. Calcite reaction rate is significantly important for the forward circulation as confirmed by the observed greater amount of calcite deposited and dissolved (Table 4). However, by including a reverse circulation of the fluid during a period of one month, the porosity changes are significantly improved around the wells. The porosity is slightly increased of 6% at the production well and the decrease of the porosity caused by calcite precipitated is less pronounced, compared to that obtained without reverse circulation.

Table 4: Comparison of amount of calcite deposited and dissolved after 2 years of circulation

Weight of calcite (kg)	Forward circulation	Reverse circulation (1 month) after 1 year of forward circulation
precipitated	917	825
dissolved	1'412	975

4. CONCLUSION

A Thermo-hydraulic and chemical (THC) coupled model has been developed and applied for the Soultz-sous-Forêts enhanced geothermal system. This study is focused on the prediction of the long-term behaviour of reservoir properties. It has been shown that re-injection of the cooled formation brine changes the chemical equilibrium states between the formation fluid and different minerals in the host rock. At the beginning of the simulation, carbonates are quickly dissolved near the injection well. With increasing simulation time, the carbonates are progressively consumed and the reaction rates decrease significantly. Small amounts of quartz and pyrite precipitate during the simulation period. Compared to those of carbonates, their reaction rates are much lower. It can be concluded that carbonates reaction predominate, especially the calcite reaction. As a consequence of calcite precipitation, permeability is reduced from its initial value of 9×10^{-12} m^2 to 2×10^{-12} m^2 at the production well. This alteration of the hydraulic performance of the reservoir could be improved by carrying out a temporary reverse circulation of the fluid between the injection and production wells or by injecting acid to dissolve calcite deposited around the production well.

Acknowledgements

The authors thank the Swiss Federal Office for Education and Science for funding this project (OFES-N° 00.0453). The EEIG Heat Mining at Soultz is acknowledged for kindly providing data from the Soultz project (EC: ENK5-CT2000-00301).

REFERENCES

Bächler, D.: Coupled Thermal-Hydraulic-Chemical Modelling at the Soultz-sous-Forêts HDR reservoir (France), *PhD Thesis*, (2003), ETH- Zürich.

Durst, P.: Geochemical modelling of the Soultz-sous-Forêts Hot Dry Rock test site: Coupling fluid-rock interactions to Heat and Fluid Transport, *PhD Thesis*, (2002), University of Neuchâtel.

Genter, A., Traineau, H., and Artignan, D.: Synthesis of geological and geophysical data at Soultz-sous-Forêts (France), *BRGM Report*, (1997), R 39440.

Jacquot, E.: Modélisation thermodynamique et cinétique des réactions géochimiques entre fluides de bassin et socle cristallin: application au site expérimental du programme européen de recherche en géothermie profonde (Soultz-sous-Forêts, Bas-Rhin, France), *PhD thesis*, (2000), Université Louis Pasteur-Strasbourg I, France.

Kohl, T., and Hopkirk, R.: "FRACTURE"- a simulation code for forced fluid flow and transport in fractured, porous rock, *Geothermics*, **24**, (1995), 333-343.

Kohl, T., and Rybach, L.: Assessment of HDR reservoir geometry by inverse modelling of non-laminar hydraulic flow, *Proceedings*, 26th Workshop on Geothermal Reservoir Engineering, Stanford University, Stanford, CA, (2001), 259-265.

Norton, D., and Knapp, R.: Transport phenomena in hydrothermal systems; the nature of porosity, *American Journal of Science*, **277**, (1977), 1447-1460.

Rabemanana, V., Durst, P., Bächler, D., Vuataz, F-D., and Kohl, T.: Geochemical modelling of Soultz-sous-Forêts Hot Fractured Rock system: comparison of two reservoirs at 3.8 and 5 km depth, *Geothermics*, **32**, (2003), 645-653.

White, S.P.: Multiphase nonisothermal transport of systems of reacting chemicals, *Water Resource Research*, **31**, (1995), 1761-1772.